

Understanding extreme wheat production failures through modeling

Rogério de Souza Nóia Júnior

Vollständiger Abdruck der von der TUM School of Life Sciences der Technischen Universität München zur Erlangung eines
Doktors der Naturwissenschaften (Dr. rer. nat.)
genehmigten Dissertation.

Vorsitz: Prof. Dr. Mariana Rufino

Prüfer*innen der Dissertation:

1. Prof. Dr. Senthold Asseng
2. Dr. Pierre Martre
3. Dr. Jean-Charles Deswarte

Die Dissertation wurde am 27.07.2023 bei der Technischen Universität München eingereicht und durch die TUM School of Life Sciences am 25.10.2023 angenommen.

Acknowledgements

This is the end of a journey of studies that started in 2006, with a strong encouragement from my mother to register myself in a selection process to study at an agricultural school, and a ride from my father to take the exam. But I was not approved in this selection process. After the exam, I returned home and started reviewing my answers with my uncle Romário, who quickly pointed out my mistakes, making it evident that I wouldn't be approved. But of course, I wasn't going to give up, the following year I took the same exam and was finally approved to study at the Federal Institute of Espírito Santo (or Escola Agrotécnica Federal de Alegre). In 2008, I embarked on a technical course in agriculture at one of the top technical schools in my state. It was three intense years of studies, work and particularly of many friendships. I thank the school, professors, friends but particularly to my great friends Abraão, Alan, Carlos Eduardo, Guilherme, Priscilla, Karen, Joelly, Holiver, Roni, Tamires who, together with me, have changed and matured in these 3 years of technical school in agriculture.

In 2011, after finishing the technical course, I lived for 6 months in Vitória, capital of Espírito Santo state, to prepare myself for the university entrance exam. During this period, I must thank my friends Ângelo, Cássio, Guilherme, Gustavo Cenoura and Thales for their partnership always, from studies to parties. After this period, I returned to Alegre where I could realize my dream of studying agronomy at the Federal University of Espírito Santo. My undergraduate years were marked by my unwavering dedication to my studies, and I owe that to my friend Bruno Fardim, who was a great friend and encourager from the first day of class. I also lived in the best fraternity in town, Recanto do Guerreiro. There I lived memorable moments of friendship with my friends Caião, Cássio, Hugo, Joaquim, Junior Karatê e Kaio. I thank them for every minute spent in the Recanto do Guerreiro. I must also thank my friends Adonis, Felipe Menine, Jorge Tadeu, Matheus baiano and Martins. And my sister Luana, who was a great friend during my graduation.

During my undergraduate years I had professors who supervised me during periods when I was Trainee professor assistant and Trainee research assistant. I would like to thank Professor Leandro Pin Dalvi for the great supervision during my first scientific experiments. I must thank Professor Afrânio that gave me the opportunity to help him as a trainee assistant of Genetics in Agriculture for more than a year. And a special thanks to my friend Professor José Eduardo Macedo Pezzopane, who introduced me to agrometeorology, supervised me in experiments

to calibrate soil moisture measurement sensors and in controlled experiments to quantify the impact of drought and heat on the physiology of various agricultural and forestry crops. Professor Pezzopane also encouraged me to learn about the operation mechanisms of various equipment for measuring meteorological variables such as rain, temperature, net radiation and others, and he encouraged and helped me to pursue science as a professional career.

In 2013, in the middle of my undergraduate years, I had the opportunity to study for a year the graduation course Agri-environmental Sciences at University of Milan, Italy. I still remember my parents' happiness when I shared with them that I was going to live outside Brazil for a year. They threw a huge celebration party with over 200 guests to celebrate my achievement. I would like to thank the Coordination for the Improvement of Higher Education Personnel (CAPES) for the one-year scholarship that allowed me to live in Italy. In Italy, I had the company of great friends that I could not fail to thank, Cheila, Selles, Diego, Giovanni, Paulo, Neiva, Fernandão and Luiz.

After completing my undergraduate studies, I pursued a Master's degree in Agricultural Systems Engineering at the "Gloriosa" ESALQ, University of São Paulo. There, I had the privilege of working with Professor Paulo Cesar Sentelhas, a renowned agrometeorology researcher in Brazil. Sadly, Professor Sentelhas passed away in 2021. His personal and professional teachings left a lasting impact, making him an exemplary professional and an outstanding teacher. I am grateful to all the professors at ESALQ for shaping my scientific perspective, and I extend my thanks to my friends André Dotto, Lucas Butina, José Lucas, Felipão Schwerz, Elvão, Paulo André, Vinícius, Tiago, Pinão, Silvana, Juliana and Paola who made my time at ESALQ enjoyable.

I continued my journey and from November 2018 to December 2020, I worked for two years at the University of Florida, USA. I must express my gratitude to Professor Clyde Fraisse for welcoming me to UF, in the Agroclimate team. Despite facing difficulties in expressing myself in English, Prof. Clyde provided me with the opportunity to learn and grow. Working with him, I also gained valuable knowledge in different cropping systems and agrometeorology. During my time in Florida, I had the privilege of collaborating with great scientists, Prof. Ken Boote and Prof. Mike Mulvaney, to whom I am grateful. I also want to extend my appreciation to Joseph and Mahesh for their partnership and friendship during the three months I spent living in Jay, on an experimental campus of the University of Florida.

In Gainesville, I was fortunate to have the friendship of Maurício and Fábio, which made my life much easier during that period. I also want to express my sincere gratitude to my dear roommates Juliana and Felipe, who not only shared their apartment with me but also taught me a lot about the benefits of being a good person. I would also like to thank Luc, Vinícius and Daniel Perondi and other friends for the partnership during my time in Florida.

While in Florida, I had the opportunity to meet and work with Professor Senthold Asseng, who supervised my PhD. Senthold provided me with the opportunity to pursue my doctoral studies at the prestigious TUM School of Life Sciences at the Technical University of Munich, in Freising. Senthold exemplifies professionalism. I will always take pride in saying that I was supervised by my friend Senthold, from whom I learned to be a better professional and, above all, a better person. I extend my sincere gratitude to him and his family. I must also express my gratitude to Jean-Charles Deswarte, Jean-Pierre Cohan from ARVALIS, and Pierre Martre from INRAE for their invaluable scientific support throughout my PhD. The work during my doctoral studies would not have been possible without all of you. I also had the privilege of working with renowned researchers who provided valuable support during important phases of my doctoral studies, for this I thank Marijn van der Velde, Tamara Ben-Ari, Frank Ewert, Heidi Webber, Gustavo A. Slafer, Alex C. Ruane, Robert Finger, Vakhtang Shelia, Benoît Piquemal, Alain Dutertre, Yean-Uk Kim, Taru Palosuo, Ke Liu, Matthew T. Harrison, Gerrit Hoogenboom, Thomas W. Hertel and Martin K. van Ittersum. I would like to express my gratitude for the significant contribution of Valentina Stocca in the analysis of this thesis and for her friendship. I would also like to thank my officemates Maximilian Zachow, Malte von Bloh, Sebastian Eichelsbacher and my friend Zenthao Zhang, as well as my colleagues from the chair and HEF Vijay Varanasi, Vanesa Calvo-Baltanas, Anand Kumar Inthiram, Benjamin Leroy, David Gackestetter, Margit von Lützow, Desiree Bienert, Claudia Luksch, Talissa Stadler, Verona Bekteshi Sylva, Sylvia Heinrich, and Petra Weinmann for their support and collaboration.

Finally, I would like to thank my family, starting with my love, Maria Carolina Safanelli (Carolzinha). Carolzinha was essential throughout my doctorate, giving me support and especially love in all these moments. Thanks, Carolzinha, for being by my side. I would like to thank my parents Liziane and Rogério and my sister Luana, to whom I dedicate this thesis. Despite the challenges faced during these more than 15 years of journey, my family has always

provided me with friendship, love, and the necessary financial and emotional support. I would also like to express my gratitude to my aunts Rosean, Reni, Rosimere and my uncle Djalma for their constant encouragement. As a fortunate teenager, I was blessed with the presence of five grandmothers: my great-great-grandmother Didi, great-grandmothers Maria (on my mother's side) and Maria (on my father's side), and grandmothers Zita and Idis. These incredible women have shown me the strength to persevere in life. I thank my grandfather Dimas for his friendship and teachings, which have had a profound impact on me. I would also like to extend my thanks to all my cousins and uncles, who have always been a source of encouragement and support for me.

I would like to thank ARVALIS for performing all the field experiments and for the financial support of this study. I also acknowledge support from the Prince of Albert II of Monaco foundation through the IPCC Scholarship Program. The contents of this thesis are solely the liability of the authors and under no circumstances may be considered as a reflection of the position of the Prince Albert II of Monaco Foundation and/or the IPCC.

I am grateful to everyone mentioned here for their invaluable support, which made my achievements possible. I deeply appreciate all of you. As one journey ends, another begins, and I feel prepared for the next phase of my life thanks to each of you.

Zusammenfassung

Diese Dissertation untersucht die Verwundbarkeiten und Herausforderungen, mit denen der Weizen als entscheidende Kulturpflanze für die globale Ernährungssicherheit konfrontiert ist. Sie untersucht reale Fallstudien über extreme Missernten bei Weizen weltweit unter Verwendung von prozessbasierten Modellen zur Simulation des Pflanzenwachstums und statistischen Modellen zur Ertragsvorhersage. Die Forschung untersucht die Ursachen und Folgen dieser Missernten, wobei ein besonderer Schwerpunkt auf extremen Wetterereignissen und Konflikten liegt.

Die Ergebnisse dieser Studie weisen auf mehrere wichtige Erkenntnisse hin. Erstens stellt der Krieg in der Ukraine eine erhebliche Bedrohung für den Weizenexport dar, was koordinierte Lagerfreigaben und eine erhöhte Produktion erfordert, um die Versorgung zu stabilisieren. Dabei treten jedoch Herausforderungen aufgrund steigender Düngerpreise und durch klimawandelbedingte Missernten auf, die die Ernährungssicherheit weiter beeinträchtigen.

In Brasilien wird die unzureichende Weizenproduktion durch ungünstige Klimaereignisse verschärft, was zu einer zunehmenden Häufigkeit von extrem niedrigen Ernteerträgen führt. Dieser Trend stellt nicht nur eine ernsthafte Bedrohung für die Ernährungssicherheit in Brasilien dar, sondern auch für andere Länder, die auf Weizenimporte angewiesen sind. Die Prognosen zeigen, dass das Ausmaß dieser Erntemängel weiter zunehmen wird, wodurch die bestehenden Extremsituationen verstärkt und die Herausforderungen für die globale Ernährungssicherheit intensiviert werden.

Der erhebliche Rückgang der Weizenerträge in Frankreich im Jahr 2016 dient als ein weiteres bedeutendes Fallbeispiel. Dieser Rückgang wurde auf eine Kombination von Faktoren zurückgeführt, darunter reduzierte Sonneneinstrahlung aufgrund von langanhaltendem Regen, Schädigung der Blüten durch starke Niederschläge, Bodenversauerung und Pilzkrankheiten. Der Klimawandel wird voraussichtlich solche extreme Ertragsrückgänge in der Zukunft weiter verschärfen und damit zusätzliche Risiken für die Weizenproduktion darstellen. Die Ergebnisse zeigen auch die zunehmende Variabilität der Weizenerträge aufgrund von kombinierten Wetterextremen und Krankheiten auf und unterstreichen die Notwendigkeit von Anpassungsstrategien zur Bewältigung zukünftiger klimatischer Bedingungen.

Um unser Verständnis für die komplexen Auswirkungen des Klimawandels auf die Weizenproduktion zu verbessern, wurde ein neues Modul zur Bodenvernässung in das DSSAT-NWheat-Modell eingeführt. Dieses Modul simuliert die Auswirkungen von Bodenvernässung auf den Weizenertrag, die Anzahl der Körner und die Größe der Körner. Durch seine Integration werden Unsicherheiten in Klimawandelstudien reduziert, insbesondere in Regionen mit zunehmender Regenintensität. Die Forschung betont die Notwendigkeit weiterer Untersuchungen zu den Auswirkungen von Bodenvernässung auf das Pflanzenwachstum und fordert kontrollierte Feldexperimente, um diese Effekte zu quantifizieren und Bodenvernässungsalgorithmen für Kulturpflanzenmodelle zu entwickeln. Solche Fortschritte werden die Prognosen der Auswirkungen des Klimawandels auf die Ernährungssicherheit verbessern und die Entwicklung effektiver Anpassungsstrategien erleichtern.

Zusätzlich schlägt die Dissertation eine einfache Methodik vor, die globale Klimadaten verwendet, um nationale Weizenerträge abzuschätzen. Dieser Ansatz wurde erfolgreich angewendet und in drei wichtigen Weizen produzierenden Ländern, nämlich Brasilien, Frankreich und Russland, evaluiert. Die Methodik basiert auf statistischen Modellen unter Verwendung repräsentativer Klimagitterzellen und ermöglicht Vorhersagen der Weizenerträge auf nationaler Ebene. Diese Echtzeit-Ertragsschätzungen sind entscheidend für fundierte Entscheidungsfindung und effektive Planung während einer Anbausaison.

Zusammenfassend untersucht diese Dissertation umfassend wichtige Aspekte der Weizenproduktion, der Auswirkungen des Klimawandels und der Ertragsprognosestrategien. Sie schlägt Lösungen vor, um die Widerstandsfähigkeit der globalen Weizenproduktion zu stärken und die Ernährungssicherheit zu gewährleisten. Durch die Bewältigung dieser Herausforderungen kann sie zu sichereren und nachhaltigeren Weizenproduktionssystemen beitragen

Schlüsselwörter: Weizenproduktion, Versorgungsengpässe, Klimawandel, extreme Wetterereignisse, globale Ernährungssicherheit, Anpassungsstrategien.

Summary

This thesis explores the vulnerabilities and challenges faced by wheat, a crucial crop for global food security. It examines real-life case studies of extreme wheat production failures worldwide, utilizing process-based crop simulation models and statistical models for yield simulation. The research investigates the causes and consequences of these failures, with a specific emphasis on extreme weather events and conflicts.

The results of this study indicate several critical findings. Firstly, the war in Ukraine poses a significant threat to wheat exports, necessitating coordinated stock releases and increased production to stabilize supplies. However, challenges arise due to rising fertilizer prices and climate change-induced failures, which further compromise food security.

In Brazil, insufficient wheat production is exacerbated by adverse climate events, leading to an increasing frequency of extreme low crop production. This trend poses a severe threat to food security not only in Brazil but also in other countries reliant on wheat imports. The projections indicate that the magnitude of these shortfalls will continue to increase, amplifying the existing extremes and intensifying the challenges faced by global food security. The severe wheat yield decline observed in France in 2016 serves as another significant case study. This decline yield was attributed to a combination of factors, including reduced solar radiation from extended rainfall, floret damage from intense rainfall, soil anoxia, and fungal diseases. Climate change is anticipated to exacerbate such extreme yield declines in the future, posing additional risks to wheat production. The findings also highlight the increased variability in wheat yield caused by compound weather extremes and diseases, underscoring the need for adaptation strategies to address future climate change conditions.

To enhance our understanding of the complex impacts of climate change on wheat production, a new waterlogging module was introduced in the DSSAT-NWheat model. This module simulates the effects of waterlogging on wheat yield, grain number, and grain size. Its inclusion reduces uncertainties in climate change studies, particularly in regions experiencing increased rainfall intensity. The research emphasizes the necessity of further investigation into the effects of waterlogging on plant growth, calling for controlled field experiments to quantify these effects and develop waterlogging algorithms for crop models. Such advancements will enhance projections of climate change impacts on food security and facilitate the development of effective adaptation strategies.

Additionally, the thesis proposes a simple methodology that uses global climate data to estimate national wheat yields. This approach has been successfully applied and evaluated in three major wheat-producing countries, namely Brazil, France, and Russia. The methodology, based on statistical models using representative climate grid cells, enables predictions of wheat yields at the national level. These real-time yield estimations are crucial for informed decision-making and effective planning during a crop season.

In conclusion, this thesis comprehensively examines critical aspects of wheat production, climate change impacts, and yield forecasting strategies. It proposes solutions to enhance global wheat production resilience and ensure food security. By addressing these challenges, it may contribute to more secure and sustainable wheat production systems.

Keywords: Wheat production, supply failures, climate change, extreme weather events, global food security, adaptation strategies.

Scientific Communication

Published studies

1. **Nóia Júnior**, R. de S., Ewert, F., Webber, H., Martre, P., Hertel, T.W., van Ittersum, M.K., Asseng, S. (2022). Needed global wheat stock and crop management in response to the war in Ukraine. *Global Food Security* 35, 100662. DOI: [10.1016/j.gfs.2022.100662](https://doi.org/10.1016/j.gfs.2022.100662)
2. **Nóia Júnior**, R. de S., Martre, P., Finger, R., van der Velde, M., Ben-Ari, T., Ewert, F., Webber, H., Ruane, A.C., Asseng, S. (2021). Extreme lows of wheat production in Brazil. *Environmental Research Letters* 16, 104025. DOI: [10.1088/1748-9326/ac26f3](https://doi.org/10.1088/1748-9326/ac26f3)
3. **Nóia Júnior**, R. de S., Deswarte, J.-C., Cohan, J.-P., Martre, P., van der Velde, M., Lecerf, R., Webber, H., Ewert, F., Ruane, A.C., Slafer, G.A., Asseng, S. (2023). The extreme 2016 wheat yield failure in France. *Global Change Biology*. DOI: [10.1111/gcb.16662](https://doi.org/10.1111/gcb.16662)
4. **Nóia Júnior**, R. de S., Asseng, S., García-Vila, M., Liu, K., Stocca, V., dos Santos Vianna, M., Weber, T.K.D., Zhao, J., Palosuo, T., Harrison, M.T. (2023). A call to action for global research on the implications of waterlogging for wheat growth and yield. *Agricultural Water Management* 284, 108334. DOI: [10.1016/j.agwat.2023.108334](https://doi.org/10.1016/j.agwat.2023.108334)
5. **Nóia Júnior**, R. de S., Olivier, L., Wallach, D., Mullens, E., Fraisse, C.W., Asseng, S. (2023). A simple procedure for a national wheat yield forecast. *European Journal of Agronomy* 148, 126868. DOI: [10.1016/j.eja.2023.126868](https://doi.org/10.1016/j.eja.2023.126868)

To-be-published studies

6. **Nóia Júnior**, R. de S., Martre, P., Deswarte, J.-C., Cohan, J.-P., van der Velde, M., Webber, H., Ewert, F., Ruane, A.C., Ben-Ari, T., Asseng, S.: Past and future wheat yield losses in France. *Under review in Agricultural and Forest Meteorology*, submitted on 8 December 2022.
7. **Nóia Júnior**, R. de S., Stocca, V., Shelia, V., Martre, P., Deswarte, J.-C., Cohan, J.-P., Piquemal, B., Dutertre, A., Slafer, G., van der Velde, M., Kim, Y., Webber, H., Ewert, F., Palosuo, T., Liu, K., Harrison, M.T., Hoogenboom, G., Asseng, S.: Enabling modeling of waterlogging impact on wheat. *To be submitted in Journal of Experimental Botany*. Currently, waiting for the approval of the authors to proceed with the submission.

Contents

Part I: Introduction and Methods	11
1. General Introduction	12
1.1. Vulnerabilities of global wheat production and supply	14
1.2. Modeling extreme wheat production failures	17
1.2.1. Process-based crop simulation models.....	17
1.2.2. Statistical models.....	20
2. Aim and structure of this thesis	21
3. Methods	23
3.1. Needed global wheat stock and crop management in response to the war in Ukraine.....	23
3.2. Extreme lows of wheat production in Brazil	23
3.3. The extreme 2016 wheat yield failure in France.....	24
3.4. Past and future wheat yield losses in France	25
3.5. Enabling modeling of waterlogging impact on wheat.....	26
3.6. A call to action for global research on the implications of waterlogging for wheat growth and yield	27
3.7. A simple procedure for a national wheat yield forecast.....	27
Part II: Empirical Studies	29
4. Summaries of the Empirical Studies.....	30
4.1. Needed global wheat stock and crop management in response to the war in Ukraine.....	30
4.2. Extreme lows of wheat production in Brazil	32
4.3. The extreme 2016 wheat yield failure in France.....	34
4.4. Past and future wheat yield losses in France	36
4.5. Enabling modeling of waterlogging impact on wheat.....	38
4.6. A call to action for global research on the implications of waterlogging for wheat growth and yield	41
4.7. A simple procedure for a national wheat yield forecast.....	43
Part III: Discussion and Conclusions	45
5. Discussion and Conclusions.....	46
5.1. Policy implications	48
5.2. Research recommendations.....	49
6. References.....	52
Part IV: Appendix with Full Publications	59

Part I: Introduction and Methods

1. General Introduction

Wheat has been cultivated for thousands of years, with its origins traced back to the Fertile Crescent in the Middle East (de Sousa et al., 2021). Over time, it became a global crop, spreading across continents through trade and exploration, and adapting to various climates and growing conditions (Bonjean et al., 2011).

China, India, Russia, the United States, Canada, and Australia are significant contributors to global wheat production (FAO, 2023). In 2021, Russia and India exceeded 25 million hectares (Mha) of wheat planted area (Figure 1). China and India, with a combined annual production of over 200 million tonnes (Mt), are major wheat producers. However, due to significant domestic demand fueled by their large populations, China and India are not major exporters of wheat (FAO, 2023).

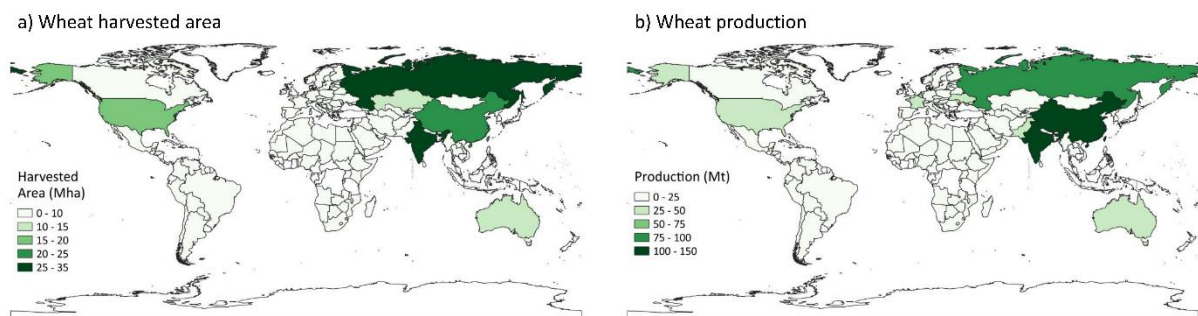


Figure 1. Global wheat planted area and production. Wheat (a) harvested area and (b) production in all wheat production countries in the world in 2021, according to FAO (2023).

Wheat production in the European Union (EU) holds considerable significance both within the region and globally, with several member states contributing to its production. The EU is one of the world's largest wheat-producing regions, and its collective output plays a crucial role in meeting both domestic and international demand (FAO, 2023). Among the EU member states, France stands out as a key wheat producer. Renowned for its favorable growing conditions and stability in wheat production, France possesses vast agricultural lands and utilizes advanced farming techniques, resulting in high wheat yields. The country's expertise in wheat cultivation, positions it as a leading supplier in the EU and global wheat markets. France's expertise in wheat cultivation positions it as a leading supplier in the EU and global wheat

markets. With over 4 million hectares (Mha) of wheat cultivation, France produces more than 40 million tonnes (Mt) of wheat annually (FAO, 2023).

Countries such as Egypt, Indonesia, Algeria, Nigeria, and Brazil are prominent importers of wheat due to their large populations and growing economies, leading to increased consumption of wheat-based products (USDA, 2023). Importing wheat is crucial for these nations to ensure food security and meet the food demands of their populations. However, fluctuations in global wheat prices, supply disruptions, and climate-related challenges can greatly influence their import and food security strategies (Glauben et al., 2022).

Wheat production is influenced by several factors, such as climate and weather conditions (Asseng et al., 2019, 2011), agricultural practices (Le Gouis et al., 2020), pest and disease management (te Beest et al., 2009), government policies and subsidies (Alston and Gray, 2019), and market demand and trade dynamics (Bentley et al., 2022; Glauben et al., 2022). These factors can vary across regions and have a significant impact on production levels and global supply of wheat. Climate change, with its impact on weather patterns, has resulted in more frequent and extreme events like droughts and floods (IPCC, 2021), which can adversely affect crop growth and yield. Additionally, water scarcity, pests, diseases, and land degradation pose additional constraints on wheat production, necessitating the development and implementation of innovative and sustainable solutions to ensure the continued production of this essential crop (Carr et al., 2021; Trnka et al., 2019).

The future of global wheat production is indeed influenced by various trends and challenges, including the growing population and changing dietary preferences (Erenstein et al., 2022). However, the impact of extreme weather events and conflicts, such as wars (Bentley et al., 2022; Glauben et al., 2022), on wheat production and supply is a critical aspect that needs to be addressed. This thesis aims to explore real-life cases of failures in wheat production and supply, considering the causes of these events and suggesting alternative approaches to mitigate their impact. By understanding the underlying causes and identifying potential solutions, we can work towards ensuring a more secure and resilient global wheat production system for the future.

1.1. Vulnerabilities of global wheat production and supply

Wheat is a crucial crop, providing essential nutrients and supporting global food security. With an annual production and consumption of over 700 million tons (FAO, 2023), wheat is a staple food for billions of people worldwide. However, only six countries dominate global wheat exports, accounting for almost 70% of the total exports. These countries are Russia, Australia, United States, Canada, Ukraine, and France (FAO, 2023). The concentration of exports exposes wheat prices to speculation and risks associated with production disruptions, conflict and war, and export blockages.

Already in the past, wheat exports were highly concentrated among a few countries, with the six largest wheat exporters accounting for 97% of world exports in 1961 (FAO, 2023). The United States and Canada alone represented 70% of these exports at this time. Despite recent efforts to distribute production among countries, wheat prices have become more volatile in recent decades. From 1959 to mid-2007, the wheat price mainly fluctuated between \$100 and \$200 per ton, with only two instances of prices surpassing \$200 per ton in 1974 and 1996 (Figure 2). However, in 2008, the price of wheat surpassed \$250 for the first time, reaching \$466 in February of this year due to low wheat production caused by simultaneous unfavorable weather conditions in several of the world's largest wheat exporters. This highlighted how extreme weather events can destabilize food availability, leading to ongoing discussions about the need for climate-resilient agriculture.

The possibility of multiple wheat-producing countries experiencing failures simultaneously underscores the need for more resilient agricultural practices. Studies on the likelihood of such failures have been carried out, indicating the potential for a more frequent occurrence in the future (Gaupp et al., 2020). The impacts of climate change have been shown to significantly affect wheat production (Asseng et al., 2015; Zhao et al., 2017), with the crop's yield and quality decreasing in regions where temperatures are rising, precipitation patterns are changing, and extreme weather events are becoming more frequent (Battisti and Naylor, 2009).

Since 2008, extreme events have been affecting world wheat production more frequently, leading to significant production losses and increased wheat prices. For example, prolonged

heatwaves in Russia in 2010 and 2012 caused up to 20 million tonnes of wheat production losses in each year, resulting in the wheat prices exceeding \$300 per ton. The beginning of the COVID-19 pandemic in 2020 led to uncertainty about world wheat production, leading to increased speculation of possible low production due to limited human labor, causing prices to rise again to \$300 per ton. In February 2022, when Russia invaded Ukraine, prices reached unprecedented heights, surpassing for the first time \$470 per ton, due to the potential of low exports from Ukraine. These events highlight the vulnerability of global wheat supply chains to external shocks, including geopolitical events and extreme weather events.

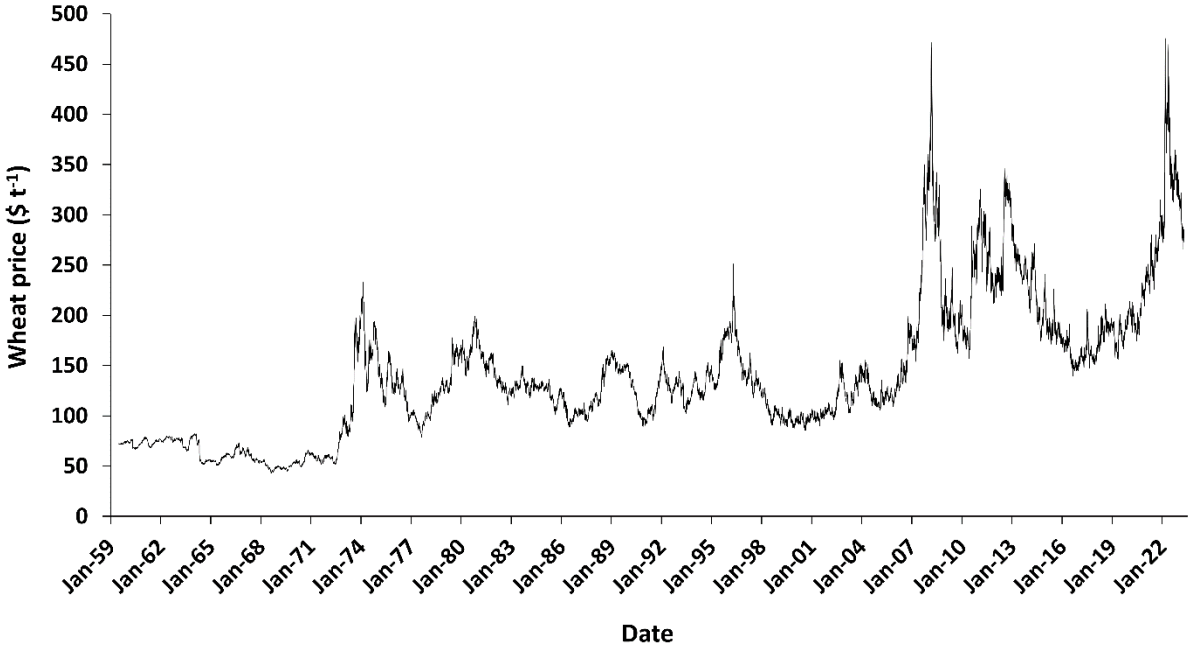


Figure 2. The wheat price. Historical world wheat commodities price from 1959 to 2023. (Macrotrends, <https://www.macrotrends.net/2534/wheat-prices-historical-chart-data#:~:text=The%20current%20price%20of%20wheat,2022%20is%20%2410.7075%20per%20bushel.>)

Shortages in wheat production stem from various factors, including high costs, commodity prices fluctuations (Nóia Júnior et al., 2021), wars (Bentley et al., 2022; Glauben et al., 2022), and increasingly, extreme weather events (Iizumi and Ramankutty, 2016; Senapati et al., 2021; Webber et al., 2020). In particular, recent extreme weather events leading to low wheat production stand out due to the combination of factors (Beillouin et al., 2020; Ben-Ari et al.,

2018; Zscheischler et al., 2018). In 2016, France experienced the most extreme wheat yield decline since 1960, with a 27% drop in national wheat yield, causing a trade balance shortfall of approximately 2.3 billion US\$. The combination of a warm, wet winter and extended spring precipitation led to simultaneous or consecutive factors, including heavy rainfall, crop diseases, low solar radiation, and anoxia, affecting grain set and filling. The extreme 2016 wheat yield failure resulted from a compound of temporally and multivariate events (Ben-Ari et al., 2018). Most crop modeling approaches neglect the compound nature of extreme climate and weather-related events, limiting the predictive ability of crop forecast systems, especially for extreme weather (van der Velde et al., 2020). The inability to predict the low 2016 wheat yield suggests underestimation of climate change impacts on agriculture. This event demonstrates the damaging effects of climate change, including excesses of precipitation, on crop production and reveals vulnerabilities in stable cropping systems. It also highlights the failure of current crop forecasting methods to predict yield losses, even shortly before harvest.

In 2006, Brazil experienced a compound of negative events, including low planting incentives, drought, frost damage, and additional drought during winter, resulting in a 46% drop in wheat production (CONAB, 2023). This was the lowest production recorded in the last 20 years, leading to a 60% increase in wheat price in Brazil and a significant increase in wheat imports the following year (FAO, 2023). Although such country-specific production failures may not affect global wheat prices, they can have significant domestic consequences. The local price increase in wheat negatively impacted investments, retail spending, and the overall economy of Brazil due to the inelastic demand for wheat as an essential food. In years with low wheat production, domestic wheat prices in Brazil can be up to 80% higher than the world market (CEPEA, 2023), leading to potential inflation and economic growth slowdown.

These events highlight global wheat production systems' vulnerability and their consequences for global food security. The alarming rates of hunger affecting over 820 million people globally and the limited access to nutritious food by approximately 2 billion individuals are urgent challenges (REF). These issues will worsen due to population growth, increased affluence and associated demands for food. Furthermore, the impact of climate change and

extreme events on food production and agricultural productivity exacerbates the vulnerability of our food systems.

1.2. Modeling extreme wheat production failures

With the projected increase in extreme weather events and the recent record yield failures witnessed across various regions, there is a growing demand to assess the impacts of these events and the risks of yield failure. It is essential to understand the underlying factors that drive the risk of yield failure in order to develop effective adaptation strategies for risk management. These strategies may include insurance solutions to address specific weather risks, planning for investments in irrigation infrastructure, or tailored crop breeding. Consequently, modeling wheat production failures has become a critical aspect of agricultural research and planning to enhance resilience and ensure food security.

To quantify the impact of climate change and weather extremes on agriculture, models are employed to translate climate changes into agricultural outcomes. This is necessary because direct observations of impacts are limited due to simultaneous changes in other agricultural factors, such as technology and government policy. As a result, two main approaches have emerged for developing such models, process-based crop simulation models and statistical models. The two approaches used for modeling wheat production failures are briefly described below.

1.2.1. Process-based crop simulation models

The first approach involves process-based crop simulation models, commonly known as crop models. These models aim to represent the key processes that govern crop growth and yield formation. They operate on a daily or hourly time step and dynamically simulate various crop and soil process. By simulating physiological processes leading to grain yield, crop models provide valuable insights. Although they have a long history and were initially developed for field-level cropping system decisions, they have been increasingly used to evaluate climate change scenarios. However, concerns have been raised regarding their ability to fully account for extreme climate conditions due to their original design. Crop models primarily focus on

individual impacts like drought and nitrogen deficiency and usually do not consider other factors such as pests, diseases, frost, hail, high windspeeds, and waterlogging. Consequently, simulating yield in complex environments influenced by multiple weather extremes becomes challenging with crop simulation models.

Guarin et al. (2020) assessed the ability of the DSSAT-NWheat crop model to simulate extreme low-yielding years at global locations. The crop model reproduced some extreme low yields but not others due to factors not considered, such as frost, hail, pests, and diseases. Additionally, limitations in historical district yield records were identified. Therefore, it is not recommended to rely solely on such records for testing the ability of crop models to simulate extreme low yields. Instead, it is advisable to conduct carefully designed experiments with on-site observations of crop yield components, soil, and weather, which are scarce and not readily available to the public. However, a study that had access to such data indicated that the DSSAT-NWheat model tended to underestimate yield losses caused by extremely wet conditions during heavy rainfall and waterlogging (Nóia Júnior et al., 2023). Additionally, Heinicke et al. (2022) showed that most global gridded crop models underestimate yield declines from extreme droughts and heatwaves, indicating potential underestimation of future wheat production failures.

Through a comprehensive review of wheat response mechanisms across 31 crop models, this thesis has revealed a significant limitation in their representation of key factors (Figure 3). While some models consider heat impacts on wheat yield, frost, ozone, pests, and weeds are only accounted for in a fraction of them. When it comes to wet conditions, around one-third of the models address waterlogging and diseases, yet none effectively simulate the combined detrimental impacts of heavy rainfall, plant diseases, and waterlogging on wheat growth and development. This finding underscores the urgent need for refining our modeling approaches.

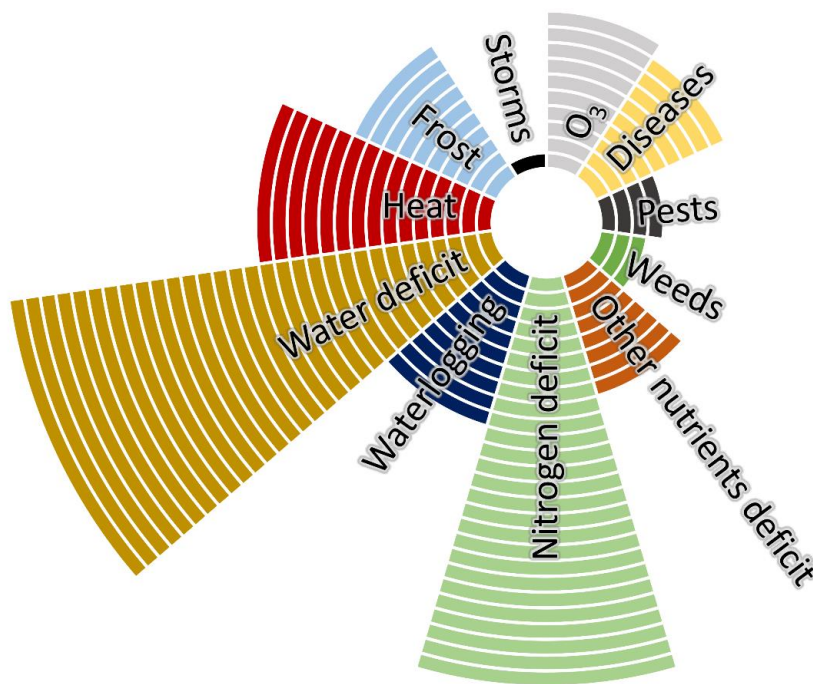


Figure 3. Plant stress mechanisms in wheat crop simulation models. Analysis based on the review of 34 wheat crop simulation models frameworks. Within each color, the bars represent the number of crop simulation models that consider the specified plant stress mechanism. Processes of 31 crop simulation models were reviewed, namely APSIM-Wheat (Zheng et al., 2015), AQUACROP (Raes et al., 2018), CropSyst (Stockle et al., 1994), DAISY (Hansen, n.d.), DSSAT-CERES (Godwin et al., 1990), DSSAT-CropSim (Thorp et al., 2010), DSSAT-Nwheat (Kassie et al., 2016), EPIC (Sharpley and J.R. Williams, 1990), EXPERT-N-CERES (Priesack, 2019), EXPERT-N-CropSim (Priesack, 2019), EXPERT-N-SPASS (Priesack, 2019), EXPERT-N-SUCROS (Priesack, 2019), FASSET (Mette Laegdsmand, 2011), GLAM (Challinor et al., 2004), HERMES (Kersebaum, 2011), InproCrop (Krishnan et al., 2016), LINTUL (Wolf, 2011), LPJmL (Schaphoff et al., 2018), MCWLA-Wheat (Tao et al., 2009), MONICA (Nendel et al., 2022), SALUS (Dzotsi et al., 2013), SIMPLACE (Gaiser et al., 2013), Sirius (Jamieson et al., 1998), Sirius-Quality (Martre et al., 2006), STICS (Brisson et al., 2003), WheatGrow (Guo et al., 2018), WOFOST (Wit, 2022), SIMPLE (Zhao et al., 2019), JULES-Crop (Osborne et al., 2015), AFRCWHEAT2-O3 (Porter, 1993) and BioMA (JRC, 2022).

The crucial importance of accurately capturing the various factors is acknowledged and their compounded effects that profoundly influence wheat production. Enhancing crop models to better incorporate these adverse conditions allows for an improved understanding and prediction of wheat crop resilience and productivity. By continuously advancing modeling techniques, stakeholders in the agricultural sector can gain valuable insights to manage and mitigate risks associated with extreme weather events. The incorporation of new routines and approaches in crop models enables the development of more robust strategies for ensuring

food security and sustaining agricultural productivity in the face of evolving environmental challenges.

1.2.2. Statistical models

A second approach involves statistical models that establish functional relationships between weather observations and crop yields. These models rely on historical data obtained from field measurements, farmer surveys, government statistics, and other sources. The availability of comprehensive weather and crop databases has led to an increased use of statistical models. However, challenges arise in disentangling the effects of highly correlated weather variables, such as temperature and rainfall. It is important to note that while statistical models can provide valuable insights, they do not simulate the underlying physiological processes of crop yields unless specifically designed to do so. Understanding these physiological processes is crucial for comprehensively explaining simulation results and gaining insights into crop production dynamics. For this reason, some authors argue that while statistical models are a powerful tool, they should not be considered a surrogate for science (Lischeid et al., 2022).

Lobell and Marshall (2010) revealed the capability of statistical models to replicate important aspects of process-based model responses to temperature and precipitation changes. Moreover, statistical models exhibited improved performance with broader spatial analyses using growing season average temperature and precipitation. Paudel et al. (2022) applied statistical models to forecast crop yields across various spatial levels, demonstrating lower errors and uncertainty in regional forecasts compared to trend forecasts. While statistical models effectively capture spatial patterns for average harvests, they encountered challenges in predicting extreme low yields (Paudel et al., 2022). The difficulty in simulating and forecasting extreme lows in crop production due to adverse weather is a well-known challenge (Ben-Ari et al., 2018; van der Velde et al., 2020; van der Velde and Nisini, 2019). In France, the 2016 winter-wheat harvest experienced a significant decline, with yields in the breadbasket region dropping by 27% compared to trend expectations and 39% compared to the previous year. However, none of the public forecasting systems predicted the magnitude of this loss. Forecasts just before the harvest overestimated average yields by about 2 t ha^{-1} , indicating a

lack of accuracy. However, Ben Ari et al. (2018) developed a binomial logistic regression technique that considers fall and spring conditions. This approach successfully captured key yield loss events, including extreme losses, in France since 1959 (Ben-Ari et al., 2018). For climate change scenarios, statistical models can predict more severe impacts of weather extremes compared to the crop models (Roberts et al., 2017).

The use of statistical models for estimating national crop yield faces several challenges. One key obstacle is the requirement for a substantial amount of climate and crop data to develop and utilize these models. In contrast, crop simulation models, while able to predict growth and development, often face hindrances at the national level due to the need for detailed information on initial conditions, soils, cultivars, and crop management (Boote et al., 2013). The considerable variability in agricultural systems across a country further complicates capturing the full range of conditions through agricultural experiments. Consequently, statistical and crop models may encounter limitations in accurately incorporating the intricate interactions between climate factors and crop performance at a national scale.

Despite their limitations, both statistical models and crop simulation models are essential tools for quantifying future risks of wheat production failures under climate change. By combining these modeling techniques with projected climate data, a more accurate understanding of future risks can be obtained. This knowledge is needed to assist the development of appropriate adaptation strategies to address the challenges posed by climate change on agricultural systems.

In summary, modeling is indispensable in mitigating extreme wheat production failures and enhancing resilience. By utilizing crop simulation models and statistical models, along with historical data and climate projections, we will better understand the impact of climate change on agriculture. These models allow us to quantify future risks and develop effective adaptation strategies to safeguard wheat production and global food security.

2. Aim and structure of this thesis

This thesis aims to explore real-life cases of failures in wheat production and supply, focusing on the causes of these events and suggesting alternative approaches to mitigate their impact.

This thesis explores key threats to global food security, identifies factors contributing to wheat production failures, quantifies their future likelihood under climate change, proposes advanced forecasting methods, and suggests improvements for crop simulation models. This aligns with research priorities for global food security under extreme events (Mehrabi et al., 2022), emphasizing the complexity and systemic impacts of wheat production failures.

The topics addressed in this thesis include threats to global food security, factors contributing to wheat production failures, quantification of future risks under climate change, improvements for crop simulation models, and forecasting methods for better planning for wheat production variability and failures.

The thesis comprises seven scientific studies, with four specifically focused on identifying the causes and proposing mitigation strategies for wheat production and supply failures in Brazil, Ukraine, and France. Excessive water, specifically waterlogging, was identified as a significant factor, prompting the need for further research on its impact. In response, we developed a new waterlogging module in the DSSAT-NWheat model to accurately simulate these effects, reducing uncertainties in climate change studies with intensified rainfall. Additionally, we called for global research to examine the implications of waterlogging on wheat growth and yield, emphasizing the importance of controlled field experiments and waterlogging algorithms for crop models. Lastly, we proposed a simple methodology that utilizes global climate data for national wheat yield forecasting. More detailed information can be found below.

1. ***Needed global wheat stock and crop management in response to the war in Ukraine:*** The war in Ukraine threatened global wheat exports. Coordinated stock releases and increased production are needed to compensate, but rising fertilizer prices and climate change-induced failures pose challenges to stabilizing supplies and ensuring food security.
2. ***Extreme lows of wheat production in Brazil:*** Insufficient wheat production in Brazil is exacerbated by adverse climate events. Regression models combined with climate projections indicate a drastic increase in extreme low crop production frequency, posing a threat to food security and hunger eradication in Brazil and other countries.
3. ***The extreme 2016 wheat yield failure in France:*** In 2016, France experienced the most severe wheat yield decline in recent history, attributed to a combination of factors including reduced solar radiation, floret damage, soil anoxia, and fungal diseases. Future climate change may increase the frequency of such extreme yield declines.
4. ***Past and future wheat yield losses in France:*** Compound weather extremes and diseases have led to increased wheat yield variability in France. Projections indicate

more frequent extreme low yields, with double losses from drought and heat waves, increased disease damage, and a need for adaptation to future conditions.

5. ***Enabling modeling of waterlogging impact on wheat:*** Waterlogging significantly affects wheat yield, grain size, and grain number. A new waterlogging module in the DSSAT-NWheat model accurately simulates these impacts, reducing uncertainties in climate change studies with increased rainfall intensity.
6. ***A call to action for global research on the implications of waterlogging for wheat growth and yield:*** Existing literature lacks research on the effects of waterlogging on plant growth. We emphasize the need for controlled field experiments to quantify these effects and develop waterlogging algorithms for crop models, enhancing projections of climate change impacts on food security.
7. ***A simple procedure for a national wheat yield forecast:*** A simple methodology using global climate data was developed to estimate national crop yields. Statistical models based on the most representative climate grid cell showed accurate predictions for wheat yields in Brazil, France, and Russia, enabling real-time yield estimations during the crop season.

3. Methods

Following, an brief overview is provided on methodology, while detailed information can be found in the attached full articles.

3.1. Needed global wheat stock and crop management in response to the war in Ukraine

The methods utilized in this study involved analyzing the effects of the war in Ukraine on global wheat exports. Measures needed to compensate for the export shortage were estimated, including quantifying the required increase in wheat yields or expansion of cropping areas in other exporting countries. The study also considered the impacts of climate change-induced crop failures. The importance of managing stocks and improving yields to ensure food and national security on a global scale was emphasized.

3.2. Extreme lows of wheat production in Brazil

A multi-model regression analysis was conducted using 20 years of data from 776 municipalities representing 90% of Brazilian wheat production. The study examined wheat

planted area, non-harvested area, trend-corrected yield, and production. Yield anomalies were calculated by comparing observed and average trend-corrected yields. These anomalies were used in a hierarchical clustering analysis to define four main wheat regions based on agroclimatic conditions. Monthly temperature and rainfall data from weather stations in each region were then used. Wheat prices, and for two regions, wheat and maize prices, were considered to estimate wheat planted area. Statistical models were developed separately for each region, taking into account climate records and commodity prices. Stepwise selection and LASSO methods were used to identify the best combination of input variables. Five global climate models were employed to estimate future wheat production under different scenarios. CO₂ growth stimulus effects on yield were included. Wheat production was estimated by multiplying yield with harvested area. Extreme low national wheat production was defined as the 5th percentile during 1850-2020, using the low national wheat price. Three contrasting wheat price scenarios were applied, and the results were aggregated to estimate national wheat production.

3.3. The extreme 2016 wheat yield failure in France

The study utilized wheat field trial data from 3,512 experimental unit treatments of 221 cultivars over a period of six cropping seasons (2014-2019 harvests) across eight locations in the breadbasket region of France. The objective was to quantify the individual contribution of various factors such as nitrogen leaching, plant diseases, low solar radiation, anoxia, and high rainfall to the variation in wheat yield in France in 2016.

The study involved different types of experiments:

- Growth performance experiments: These experiments compared the growth of different wheat cultivars. Measurements of various parameters such as wheat ear emergence date, grain number per unit area, average single grain size, grain nitrogen concentration, and grain yield were performed.
- Nitrogen response experiments: These experiments tested the response of wheat cultivars to different nitrogen fertilizer rates.

- Plant disease experiments: These experiments recorded plant disease types and tested the efficiency of fungicides in controlling the diseases. Measurements of wheat yield were performed.

All the experiments were rainfed and conducted from late September to November, with harvests taking place between the beginning of July and the end of August. The crop protection practices followed local farm practices, including the use of fungicides, herbicides, and insecticides. Nitrogen fertilizers were applied during specific periods, and phosphorous and potassium fertilizers were applied if needed.

The study analyzed anomalies in wheat yield components based on the growth performance trials. It calculated the wheat yield component anomalies relative to a reference period (2014-2019). The study also analyzed the climatic anomalies, such as excessive rainfall, low solar radiation, and anoxia, that occurred across the research stations during the critical periods of wheat growth. The incidence of plant diseases, including wheat Fusarium ear blight, Septoria leaf blotch, and leaf rust, was also analyzed.

To determine the impact of nitrogen leaching, the study calculated the nitrogen nutrition index (NNI) and assessed crop nitrogen uptake and translocation. The study also developed weather-based indices for analyzing the effects of low solar radiation, heavy rainfall, anoxia, and plant diseases on grain number per unit area and average single grain size.

Statistical models were built using the anomalies and weather-based indices as input variables to identify the factors influencing grain number and grain size anomalies. The models were trained using data from the experimental unit treatments and validated using out-of-sample analysis.

Overall, the study aimed to understand the causes of the 2016 wheat yield failure in France by analyzing various factors, including climatic anomalies, nitrogen leaching, and plant diseases.

3.4. Past and future wheat yield losses in France

In the breadbasket of France, which is responsible for a significant portion of the country's wheat production, we conducted a study to understand the factors influencing wheat yields. We selected eight representative locations based on the geographical distribution of research stations and collected long-term weather data from 1984 to 2020. To remove the effects of technological improvements, we removed the long-term yield trends for each department independently. We identified 11 climate and disease indices that affect wheat yield, including drought, heat, flooding, low solar radiation, ear blight, and foliar fungal diseases. Using a random forest machine learning approach, we developed a statistical model to predict wheat yield anomalies based on these indices. We validated the model through cross-validation and evaluated its performance using various statistical indices. Additionally, we quantified the impacts of individual yield-limiting factors by modifying the input variables. For future projections, we used climate data from the CMIP6 models and estimated the frequency of extreme weather events during wheat anthesis and grain filling. We also projected the occurrence of ear blight and foliar fungal diseases. Our findings provide insights into the potential causes of wheat yield losses and the future risks associated with climate change.

3.5. Enabling modeling of waterlogging impact on wheat

In this study, we analyzed 17 research articles published between 2008 and 2021 to understand how waterlogging affects wheat grain yield, grain number, and grain size. We collected data from various experiments conducted at different stages of wheat growth and with different durations of waterlogging. To improve the DSSAT-NWheat model, we developed a waterlogging module that considers the direct impact of waterlogged soil on carbohydrate accumulation and grain size. We also incorporated the effects of waterlogging on root growth and rooting depth. This updated module was integrated into the DSSAT-NWheat software. We introduced the aeration deficit factor (AF) to quantify waterlogging conditions in the soil and its impact on root growth. We also developed the wheat roots aeration index (AF_{root}) to assess carbohydrate accumulation under waterlogged conditions. By establishing parameters like wheat cultivar sensitivity to AF_{root} (WLSI) and maximum reduction of carbohydrate accumulation under waterlogging (WLM_I), we determined the wheat cultivar's tolerance or sensitivity to waterlogging. Additionally, we examined the

influence of waterlogging on grain size and grain number per unit area using data from experiments in France. We created four groups based on different grain yield and grain number characteristics. To validate our waterlogging module, we simulated an experiment conducted by Marti et al. (2015) using the DSSAT-NWheat model. The simulation involved varying durations of waterlogging before anthesis. Overall, our study gave insights into how waterlogging affects wheat grain yield, grain number, and grain size. With the updated waterlogging module in DSSAT-NWheat, we can now better simulate and understand the impact of waterlogging on wheat growth and development.

3.6. A call to action for global research on the implications of waterlogging for wheat growth and yield

This review article employed methods that involved assessing the existing literature and process-based frameworks pertaining to waterlogging simulation. Through this analysis, it was revealed that there is a scarcity of field experiments examining the effects of waterlogging on plant growth.

3.7. A simple procedure for a national wheat yield forecast

The estimation of national wheat yield for Brazil, France, and Russia was conducted using a four-step process. First, the trend in increased yield due to technology advancements was removed from historical data. Second, a representative grid cell was identified based on temperature and rainfall correlations. Third, a regression model was developed using climate variables and national wheat yield data. Fourth, the model was validated using independent data from France and Russia. Climate data were obtained from the CRU Time-Series database, and yield data were from the FAO Corporate Statistical Database. The performance of the model was evaluated using cross-validation and measures such as coefficient of determination and agreement index. A sensitivity analysis was performed, and in-season analysis was conducted to assess forecasting performance. Spring and winter wheat were not distinguished.

Part II: Empirical Studies

4. Summaries of the Empirical Studies

4.1. Needed global wheat stock and crop management in response to the war in Ukraine

The war in Ukraine has posed a significant threat to global wheat exports, resulting in unprecedented price hikes and potential food security risks. This paper emphasizes the need for short-term measures to compensate for the export shortage, such as coordinated release of wheat stocks, while also highlighting the long-term necessity of increasing wheat yields and expanding cropping areas. However, several challenges, including rising fertilizer prices, climate change-induced crop failures, and year-to-year variability, further strain global wheat markets. The repercussions extend beyond Ukraine, as many countries heavily rely on Ukrainian wheat for staple food supplies, making them vulnerable to the escalating wheat prices. To address this crisis, effective management of stocks and continual yield improvements are vital for both food and national security worldwide.

The study underscores the significance of Ukrainian wheat exports, which accounted for 9% of global wheat exports in 2020. However, the war in Ukraine has severely disrupted wheat trade, with a significant portion of exports blocked. This disruption, coupled with lower wheat planting areas in Ukraine, has major implications for the Ukrainian economy and global food security. The export block has led to a surge in wheat prices, threatening food security in importing countries like Brazil, Algeria, and many sub-Saharan African nations.

To mitigate the export shortage, compensatory measures are required. Coordinated release of wheat stocks is recommended in the short term, as the top 13 wheat-exporting countries possess significant reserves. However, in the medium and long term, increasing wheat production becomes imperative. The study suggests that an 8% increase in wheat grain yields, primarily through closing the yield gap, would be necessary to compensate for the missing Ukrainian exports. Achieving this yield increase would require additional nitrogen fertilizer of around half a million tons.

Alternatively, expanding wheat cropping areas by 5.5 million hectares could be considered, but this would have environmental consequences and potentially reduce future crop productivity. Moreover, year-to-year variability and climate change-induced crop failures

could lead to additional export reductions of 5 to 7 million tons annually, exacerbating the strain on global markets. These challenges highlight the importance of proactive measures to stabilize wheat supplies, including prudent management of stocks and investments in yield improvements.

While this study focuses on wheat, it is important to note that Ukraine and the Russian Federation are major exporters of other crops, such as sunflower, rapeseed, maize, and barley. Disruptions in the supply of these commodities further contribute to the global food market disruption. Actions must be taken to enhance the resilience and reduce the vulnerability of agricultural systems, reducing reliance on a limited number of countries for food exports.

In conclusion, the war in Ukraine has caused a significant disruption to global wheat markets, necessitating immediate measures to compensate for the export shortage. Long-term strategies focused on improving wheat production and managing stocks are essential for stabilizing supplies and mitigating the risks associated with climate change-induced crop failures.

Authors' contributions: RSNJ and SA, FE and PM conceptualized the study, all co-authors contributed to the methodology, RSNJ developed the statistical models and analyzed data, ACR assisted with climate data, TBA assisted with statistical models and statistical analysis, RF assisted with economic analysis, all co-authors contributed to data evaluation and interpretation, RSNJ wrote initial draft, all co-authors assisted with writing and reviewed the manuscript.

This article is published as: *Nóia Júnior R. de S., Ewert, F., Webber, H., Martre, P., Hertel, T.W., van Ittersum, M.K., Asseng, S. (2022): Needed global wheat stock and crop management in response to the war in Ukraine in Global Food Security in 2022, following peer review. It is available at <https://doi.org/10.1016/j.gfs.2022.100662>*

4.2. Extreme lows of wheat production in Brazil

This study examines the impact of climate change on wheat production in Brazil and its implications for food security. The research combines multiple regression models to estimate national wheat production based on climate data, cropping area, yield trends, and commodity prices. Projections using climate change models suggest that extreme low wheat production events, which historically occurred once every 20 years, could become up to 90% more frequent by the end of the century. These projections, influenced by representative concentration pathway scenarios and price fluctuations, indicate a threat to Brazil's progress towards food security.

The analysis focuses on four major wheat-growing regions in Brazil, developing regression impact models for planting area, non-harvested area, and grain yield. These models successfully reproduce historical data and capture the compound effects of adverse weather events on wheat production. The study highlights the vulnerability of wheat farms, primarily family-owned and of relatively small size, to market signals and weather conditions during the planting season. Climate change is expected to increase drought events during the crucial planting period, leading to a decline in wheat planting area.

Furthermore, the study projects a decline in national mean wheat yield due to rising temperatures during flowering and grain filling stages. The absolute decline in yield is anticipated to be larger in warmer regions, such as Brazil, compared to other parts of the world. The combination of projected decreases in planted area, non-harvested area, and grain yield leads to a decline in national wheat production, regardless of commodity price signals. This decline is projected to continue until 2100 under different representative concentration pathways, with potential production losses reaching 60% compared to historical averages.

The research also highlights the increasing frequency of extreme low wheat production years, which will become the norm in Brazil by 2100. The magnitude of these shortfalls is expected to intensify, with the extreme years becoming even lower in wheat production than in the past. Such extreme low production years pose a challenge to national food security and can have global implications, as demonstrated by previous food crises caused by wheat production failures in exporting countries.

The study emphasizes the need to understand the drivers of extreme production losses and their frequency to adapt agriculture to climate change and ensure future food availability. It suggests that alternative crops like sugarcane, maize, and pasture may be better suited to a warmer climate and highlights the importance of diversifying agricultural strategies to mitigate the impact of climate change on food security.

Authors' contributions: RSNJ and SA conceptualized the study, all co-authors contributed to the methodology, RSNJ developed the statistical models and analyzed data, ACR assisted with climate data, TBA assisted with statistical models and statistical analysis, RF assisted with economic analysis, all co-authors contributed to data evaluation and interpretation, RSNJ wrote initial draft, all co-authors assisted with writing and reviewed the manuscript.

This article is published as: **Nóia Júnior, R. de S., Martre, P., Finger, R., van der Velde, M., Ben-Ari, T., Ewert, F., Webber, H., Ruane, A.C., Asseng, S. (2021) : Extreme lows of wheat production in Brazil in Environmental Research Letters in 2023 following peer review. It is available at <https://doi.org/10.1088/1748-9326/ac26f3>**

4.3. The extreme 2016 wheat yield failure in France

The production of wheat, which is crucial for global food security, is being threatened by climate change-induced climatic extremes. Europe, responsible for 35% of global wheat production, has experienced crop failures due to droughts and heatwaves, as seen in northern European countries in 2018. These adverse weather conditions are expected to worsen with climate change. To understand the impact of climate events on wheat yield, various modeling approaches have been developed, but they often overlook the compound nature of multiple factors affecting crop growth.

In 2016, France, the fourth largest wheat-exporting country, faced a significant decline in wheat yield. The yield dropped by 27%, resulting in a substantial trade balance deficit. The failure to predict this yield loss highlighted the complexity of the events that caused it. Multiple factors such as heavy rainfall, crop diseases, low solar radiation, and anoxia (lack of oxygen) during grain development contributed to the decline. Existing crop forecast systems often neglect the interconnectedness of these factors, limiting their predictive ability, especially for extreme weather events.

The inability to predict the 2016 wheat yield decline suggests that the projected impacts of climate change on agriculture might be underestimated. To improve seasonal forecasting, we used detailed datasets and modeling techniques to quantify the impacts of various climate factors on wheat yield components in 2016. We found that the decline in grain yield resulted from drops in both grain number and average grain size, influenced by adverse climate events.

The study revealed that low solar radiation and heavy rainfall around anthesis (flowering) directly affected grain number and increased the likelihood of flower abortion and lodging. Waterlogging and fungal diseases further reduced average grain size. The projections for future climate change scenarios indicated that drought, heat stress, diseases, and heavy rainfall during anthesis and grain filling would become more frequent in Europe. This raises concerns about the occurrence of future episodes of extremely low wheat production, potentially leading to global breadbasket failures and threatening food security.

The complex nature of multiple limiting impacts makes it challenging to forecast extremely low-yielding seasons. Existing models often fail to adequately represent waterlogging and

plant diseases. Therefore, the development and integration of new routines into crop simulation models are necessary to capture the extent of these compounding factors.

The study's modeling approach had certain limitations, such as the simplified separation of factors affecting grain number and average grain size and assumptions about anthesis dates and grain filling duration. However, the framework provided insights into the physiological impacts of climate factors and can be extended to other European countries that faced similar weather anomalies in 2016.

Improving the prediction capacity of crop simulation models and yield forecast systems, as well as developing wheat cultivars with enhanced resilience to complex environments, are crucial for mitigating future instability in grain production under more extreme climates. By forecasting and planning for compound yield-reducing events, it may be possible to alleviate the impacts of climate change on wheat production and ensure global food security.

Authors' contributions: All co-authors conceptualized the study. RSNJ performed the formal analysis. SA, TP and MTH supervised the study. RSNJ wrote initial draft, all co-authors assisted with writing and reviewed the manuscript.

This article is published as: **Nóia Júnior, R. de S., Deswarte, J.-C., Cohan, J.-P., Martre, P., van der Velde, M., Lecerf, R., Webber, H., Ewert, F., Ruane, A.C., Slafer, G.A., Asseng, S. (2023): The extreme 2016 wheat yield failure in France in *Global Change Biology* in 2023 following peer review. It is available at <https://doi.org/10.1111/qcb.16662>**

4.4. Past and future wheat yield losses in France

The study focuses on the impact of compounding weather extremes and plant diseases on wheat yield variability in France, the largest wheat producer in the European Union. We combined historical data on wheat yields, disease prevalence, and climate indices from 1984 to 2020 with machine learning algorithms to estimate grain yields. We found that these factors explained approximately 60% of the historical yield variability.

The findings suggest that extreme low wheat yields, defined as yields below the 10th percentile of the historical period, are expected to occur more frequently in the future. Projections using climate models indicate that such extreme lows will occur once every 10 years. However, the study also reveals some variations in the frequency of extreme lows across different regions of France.

The analysis highlights the importance of considering multiple interacting factors, such as climate extremes and crop diseases, in assessing agricultural risks. Previous crop failures in France have been attributed to compound events involving the simultaneous occurrence of climate extremes and plant diseases. For example, in 2016, a combination of a warm, wet winter and extended spring precipitation led to heavy rainfall, high incidence of crop diseases, low solar radiation, and anoxia, resulting in a 27% decline in national wheat yield compared to the previous five years' average.

The study identifies excess water, reduced solar radiation, and plant diseases as the main factors affecting wheat production in France. While excessive precipitation historically had the most significant impact on wheat yields, the correlation between heavy rainfall and yield has decreased in recent decades due to increased heat and drought events. The analysis suggests that heat and drought, combined with the occurrence of ear blight disease, will become increasingly damaging to wheat yield in the future. Rising temperatures and reduced precipitation during wheat flowering and grain filling periods are projected to exacerbate heat and drought stress on crops. The study estimates that ear blight will cause twice as much yield loss in the future compared to current levels.

Although the average amount of solar radiation reaching wheat canopies is expected to increase due to warmer and wetter summers, low solar radiation events are projected to

continue impacting wheat yield due to the continued frequency of heavy rainfall. The study also notes that the potential interaction between elevated carbon dioxide (CO₂) levels and other factors, such as plant diseases and extreme weather conditions, requires further investigation.

The results emphasize the need for adaptation strategies in French wheat production systems to address future challenges posed by droughts, heatwaves, and increased disease pressure. The discussion highlights the importance of wheat breeding programs in developing new cultivars that are more tolerant to drought, heat, and resistant to plant diseases.

In conclusion, the study provides insights into the causes of historical wheat yield failures in France and projects how these drivers might affect future wheat production. It underscores the importance of considering compounding factors such as climate extremes and plant diseases in assessing agricultural risks and highlights the need for adaptive measures to ensure the resilience of wheat production systems in the face of changing climatic conditions.

Authors' contributions: All co-authors conceptualized the study. RSNJ performed the formal analysis. SA, TP and MTH supervised the study. RSNJ wrote initial draft, all co-authors assisted with writing and reviewed the manuscript.

This article is being prepared to be submitted as: **Nóia Júnior, R. de S., Martre, P., Deswarte, J.-C., Cohan, J.-P., van der Velde, M., Webber, H., Ewert, F., Ruane, A.C., Ben-Ari, T., Asseng, S.: Past and future wheat yield losses in France.**

4.5. Enabling modeling of waterlogging impact on wheat

Most crop simulation models do not consider the effect of waterlogging despite its importance for crop performance. Waterlogging occurs when a soil is saturated with water for an extended period, depriving plant roots of oxygen. It is a major cause of crop yield losses globally, affecting an estimated 15-20% of the global wheat cropping area each year. Regions such as southern Asia, Europe, Russia, China, and southern Brazil are particularly vulnerable to waterlogging compared to drought.

Excessive rainfall leading to waterlogging has resulted in significant damage to agricultural crops. For example, in India, 33.9 million hectares of arable land were affected by waterlogging between 2015 and 2022. In France, where only 9% of arable land has drainage systems, excessive precipitation and waterlogging have been the primary factors impacting wheat yields since the early 20th century. Similarly, southern Brazil experienced a 40% drop in wheat yield in 2017 due to waterlogging and increased plant diseases. The Pampas Region of Argentina has also faced extensive waterlogging over the past two decades. Despite the widespread damage caused by waterlogging, studies on its impact on grain production are limited.

To address this gap, crop simulation models play a crucial role in understanding crop growth processes and predicting the impacts of abiotic stresses like waterlogging. However, most existing crop models do not consider waterlogging, leading to underestimation of climate change impacts on agriculture. Only a few crop models account for waterlogging effects on parameters such as carbohydrate accumulation, radiation use efficiency, transpiration, root activity, and leaf area index. However, these models have been tested in limited situations and lack comprehensive understanding of the impact of waterlogging on grain yield and its components.

In this study, we aimed to improve the representation of waterlogging in the wheat crop simulation model DSSAT-NWheat. To achieve this, we reviewed published articles on the impact of waterlogging at different wheat phenological stages, including grain number per unit area, average grain size, and grain yield. Based on the findings, we developed a new

waterlogging module that considers its effects on wheat root growth, carbohydrate accumulation, and potential average grain size.

The new waterlogging module was tested using data from controlled experiments, including an outdoor experiment in Lleida, Spain, and wheat field trials in France. The module demonstrated reasonable performance in simulating wheat yield in response to waterlogging, with good agreement between simulated and observed data. Sensitivity analysis revealed that the impact of waterlogging on above-ground biomass, roots, leaf area index, grain number, and grain yield varied with different phenological stages. Notably, the simulated crop was most sensitive to waterlogging shortly before anthesis, consistent with experimental studies.

Moreover, the relationship between grain number per unit area and average grain size was studied, and an equation was implemented in the model to limit potential grain size when waterlogging occurs before anthesis. This improvement in simulating grain size accounted for observations of fewer but heavier grains under waterlogging conditions. The process of grain size determination around anthesis is critical, as it influences both grain number per unit area and average grain size.

While the new waterlogging-enabled crop model shows promising results in simulating the impact of excess rainfall and waterlogging on crop growth and grain yield, further studies are needed to consider other factors such as air temperature, soil type, mineral nutrition, and genotype. Additionally, the combined effects of waterlogging with other abiotic stresses, including heat, drought, ozone, and nitrogen deficit, require investigation. Enhancements in crop models to accurately simulate extreme climate events and their impacts on crop growth will improve the robustness of future projections.

In conclusion, the incorporation of a waterlogging module into the DSSAT-NWheat crop simulation model represents a significant advancement in understanding and predicting the impacts of waterlogging on wheat production. By accounting for the complex interactions between waterlogging and crop growth processes, these models can contribute to more accurate yield projections and assist in agricultural decision-making under changing climate conditions. Furthermore, this study emphasizes the need for considering waterlogging in crop simulation models, as neglecting its impact may lead to underestimating the potential negative effects of climate change on crop productivity. By improving our understanding of

how waterlogging and other extreme climate events will affect future crop production, we can better prepare and adapt to ensure global food security.

Authors' contributions: All co-authors conceptualized the study. JCD, JPC, PM and SA supervised the study. VSt and VSh implemented the waterlogging module in DSSAT-NWheat. GS made available the data from the outdoor controlled waterlogging experiment in Lleida in Spain, and BP and AD the wheat data from field trials with side-by-side drained and undrained soils in France. The grain number per unit area and average grain size data in France, was made available by JCD and JPC. RSNJ and VSt performed the formal analysis. RSNJ wrote initial draft, all co-authors assisted with writing and reviewed the manuscript.

This article is being prepared to be submitted as: *Nóia Júnior, R. de S., Stocca, V., Shelia, V., Martre, P., Deswarte, J.-C., Cohan, J.-P., Piquemal, B., Dutertre, A., Slafer, G., van der Velde, M., Kim, Y., Webber, H., Ewert, F., Palosuo, T., Liu, K., Harrison, M.T., Hoogenboom, G., Asseng, S.: Enabling modeling of waterlogging impact on wheat.*

4.6. A call to action for global research on the implications of waterlogging for wheat growth and yield

Waterlogging has a significant impact on agricultural land used for food production, affecting millions of hectares every year. However, there is a lack of research and frameworks for simulating waterlogging, limiting our understanding of its effects. Particularly, field experiments that quantify the impact of waterlogging on plant growth are sparse, highlighting the need for further investigation in this area.

To address these knowledge gaps, it is essential to conduct more research on waterlogging, particularly in controlled field conditions with well-defined soil properties and continuous monitoring of soil moisture. By studying the effects of waterlogging on plant phenology, root development, and the uptake of water and nutrients, researchers can gain a better understanding of its impact on crop productivity. This research should also explore the interactions between waterlogging and other environmental factors such as atmospheric CO₂ concentration, temperature, and biotic/abiotic stresses.

The data obtained from these experiments could be used to develop waterlogging algorithms for crop models, enabling more accurate predictions of how climate change will impact global food security. Wheat, for example, is a vital crop with a global annual consumption of over 780 million tonnes. Waterlogging-induced wheat production failures can lead to increasing wheat commodity prices, affecting seed, food, and industry needs. Therefore, understanding the detrimental effects of waterlogging on wheat production is crucial for ensuring food availability and affordability.

Waterlogging occurs due to intense or sustained rainfall, poor soil drainage, rising water tables, or lateral water flows. It creates anoxic soil conditions and negatively affects root growth, nutrient absorption, and transport to the shoot. In extreme cases, waterlogging can even lead to partial root death. The reduction of root front velocity and increased nutrient leaching further exacerbate the nutrient deficit stress caused by waterlogging. Moreover, waterlogging limits root water conductivity, resulting in stomatal closure, reduced CO₂ concentration within the leaves, and restricted photosynthesis and crop growth. It also promotes the occurrence of plant diseases and plant lodging.

The impact of waterlogging is not limited to specific regions; it has global implications. For instance, regions in southern Asia and western Europe are more prone to waterlogging than drought. Increased occurrences of extreme rainfall have intensified waterlogging in the Indus river basins, which are crucial for crop production in Pakistan and India. Central China has also experienced declining wheat yields due to frequent extreme weather events, including waterlogging. In countries like France, waterlogging caused by excessive spring precipitation has been a major factor affecting wheat yields. These examples illustrate the urgent need to study the effects of waterlogging in different regions and climatic conditions.

To improve crop simulation models and effectively address the impacts of waterlogging, it is crucial to bridge the existing knowledge gaps. Future research should focus on understanding root morphology changes under waterlogging stress, the interaction between waterlogging and other stresses, the combined effects of waterlogging and atmospheric CO₂ concentration, the impact of partial waterlogging, cultivar resilience, spatial implications of waterlogging, nutrient availability, and the effectiveness of engineering management practices. Conducting controlled experiments in the field and greenhouse, along with field validation experiments, will provide valuable insights and data to enhance crop simulation models.

Overall, it is essential to prioritize and intensify research efforts on waterlogging to ensure the development of sustainable agricultural practices and mitigate the potential threats it poses to global food security.

Authors' contributions: All co-authors conceptualized the study. RSNJ performed the formal analysis. SA, TP and MTH supervised the study. RSNJ wrote initial draft, all co-authors assisted with writing and reviewed the manuscript.

This article is published as: **Nóia Júnior, R. de S., Asseng, S., García-Vila, M., Liu, K., Stocca, V., dos Santos Vianna, M., Weber, T.K.D., Zhao, J., Palosuo, T., Harrison, M.T. (2023): A call to action for global research on the implications of waterlogging for wheat growth and yield in Agricultural Water Management in 2023 following peer review. It is available at <https://doi.org/10.1016/j.aqwat.2023.108334>**

4.7. A simple procedure for a national wheat yield forecast

The study proposes a simple methodology to estimate national wheat yields that can be easily applied to any country and crop. The study correlated 20 years of global gridded monthly climate data with national wheat production-weighted mean climate indices to determine the most representative climate grid cell for the entire wheat region of a country. They then used the climate data from this representative grid cell to build statistical models for estimating trend-corrected national wheat yields.

Three different models were tested: Stepwise Regression with the Bayesian information criterion (BIC), the least absolute shrinkage and selection operator algorithm (Lasso), and the Random Forest machine-learning algorithm. The Random Forest model performed the best, with a relative root mean square error (rRMSE) of 9.1% for estimating wheat yields in Brazil. The same approach was then applied to estimate wheat yields in France and Russia, resulting in rRMSE values of 6.7% and 6.4%, respectively.

The methodology presented in the study offers a simpler and more accessible approach to estimate national crop yields, compared to traditional methods that rely on field surveys or remote sensing. By using a single representative grid cell within a nation-wide crop area and readily available monthly climate data, the proposed method provides accurate and replicable yield estimates. It allows for early yield forecasting during the cropping season, which can assist policymakers, agricultural commodity traders, and growers in planning and adjusting strategies to ensure food supply.

However, it's important to note that the methodology has some limitations. It may miss extreme high and low yields, and its performance depends on the country and specific climatic conditions. The use of a single representative grid cell can lead to over or underestimation of yields in certain years, particularly in large countries with significant spatial variability. To address this, dividing the country into homogeneous crop production zones and selecting representative points within each zone could improve the accuracy of the method. Additionally, combining the approach with other estimation and forecasting techniques, such as remote sensing or crop simulation models, could enhance its predictability.

Overall, the study highlights the potential of a simple and accessible method for national crop yield estimation, which can be valuable for policymakers, traders, and growers in planning and managing agricultural production.

Authors' contributions: RSNJ, LO, SA conceptualized the study, all co-authors contributed to the methodology, RSNJ and LO developed the statistical models and analyzed data, DW assisted with statistical models and statistical analysis, all co-authors contributed to data evaluation and interpretation, RSNJ wrote initial draft, all co-authors assisted with writing and reviewed the manuscript.

This article is published as: **Nóia Júnior**, R. de S., Olivier, L., Wallach, D., Mullens, E., Fraisse, C.W., Asseng, S. (2023): A simple procedure for a national wheat yield forecast in *European Journal of Agronomy* in 2023, following peer review. It is available at <https://doi.org/10.1016/j.eja.2023.126868>

Part III: Discussion and Conclusions

5. Discussion and Conclusions

This thesis addresses several crucial aspects related to wheat production and supply failures, adaptation strategies, and global threats to food security. It begins by quantifying the risks posed by climate change, offering advanced forecasting methods, and suggesting improvements for crop simulation models. The research highlights extreme yield declines in France, waterlogging implications, challenges in Brazil, and the impact of the Ukraine war. These findings significantly contribute to our understanding of the causes behind production failures, potential mitigation approaches, and the need for improved models to ensure food security.

The disruption of Ukraine's grain production and export capacities, combined with climate and environmental challenges, underscores the importance of coordinated efforts to stabilize wheat markets and enhance agricultural resilience. It is crucial to manage national stocks effectively and diversify food exports to mitigate global market disruptions. Previous calls for action have highlighted the necessity of implementing additional policies, such as preventing export bans and supporting emergency relief efforts by organizations like the World Food Programme, to address these challenges effectively (Ben Hassen and El Bilali, 2022; Bentley et al., 2022; Calder, 2022; Glauben et al., 2022)..

Furthermore, Brazil is projected to experience more frequent extreme low production years for crops like wheat, beans, and maize (Antolin et al., 2021; Figueiredo Moura da Silva et al., 2021; Nória Júnior et al., 2021). These events, caused by a combination of extreme weather conditions, pose a significant threat to global food security. While previous climate impact studies have mainly focused on average effects (Antolin et al., 2021; Liu et al., 2016), our projections indicate that the magnitude of shortfalls will increase, exacerbating the already existing extremes.

The 2016 wheat yield decline in France was the most extreme in recent history and resulted from adverse climate events (Ben-Ari et al., 2018). Prolonged cloud cover, heavy rainfall, soil anoxia, fungal foliar diseases, and ear blight collectively contributed to a reduction in grain number and lighter grain size (Nória Júnior et al., 2023). It is anticipated that these compound effects will occur with greater frequency in the future, posing risks to wheat production.

Although losses related to flooding may decrease, losses resulting from combined drought and heat waves during critical growth stages are projected to double. Additionally, ear blight is estimated to cause 35% of the total expected average yield losses. European wheat-growing regions are expected to face increasing challenges, such as drought, heat stress, diseases, and heavy rainfall, potentially leading to episodes of severely low wheat production (Trnka et al., 2014; Vogel et al., 2019). The occurrence of similar crop failures worldwide further emphasizes the potential dangers associated with simultaneous failures in major wheat-exporting countries and the implications for global food security (Gaupp et al., 2020). To address these concerns, enhancing crop simulation models to account for waterlogging and diseases, while concurrently developing resilient cultivars, is imperative for accurately predicting and mitigating the impacts of compound yield-reducing events under future extreme climates.

In order to enhance wheat production forecasting and reduce uncertainties in future impact studies, we introduced a waterlogging module into the DSSAT-NWheat model. This addition addresses the previous limitations of crop models in accurately simulating decreased wheat yields caused by excessive rainfall (Nóia Júnior et al., 2023). By incorporating the waterlogging module, our model can provide a more precise representation of such events. Notably, in the case of the 2016 extreme event, waterlogging was responsible for 26% of France's significant yield decline, which existing seasonal forecasting systems and crop simulation models failed to anticipate. These extreme events, encompassing waterlogging, crop diseases, and heavy rainfall, are often overlooked by conventional crop simulation models (Rötter et al., 2018). Therefore, continuous improvements aimed at incorporating the impacts of extreme climate events in crop models are crucial for more reliable simulations in the future. These advancements will significantly contribute to our understanding of the complex effects of climate change on future crop production, ultimately facilitating the development of effective adaptation strategies.

Additionally, the presented research endeavours have resulted in the development and testing of a method for estimating national yields using a single representative point within a country's crop area. This method has been applied and evaluated in three wheat-producing countries, with its primary objective being to provide valuable support to policymakers and agricultural commodity traders. By offering reliable estimates of national crop production, this

approach enables informed decision-making and effective planning. Despite the challenges associated with predicting extreme years, the method has demonstrated a relative error of up to 6%, indicating its potential as a robust tool for estimating national yields.

5.1. Policy implications

This thesis highlights the pressing need for immediate action to address climate change and its impact on wheat systems. It emphasizes the importance of national and international cooperation in developing resilient farming practices, enhancing crop diversity, and improving food storage and distribution networks.

One key policy implication is the need for coordinated actions to stabilize wheat markets in the face of disruptions. The case study of Ukraine's grain production and export capacities demonstrates the importance of effectively managing national stocks and diversifying food exports to mitigate global market disruptions. Policymakers should consider implementing policies that prevent export bans and support emergency relief efforts, as advocated by previous research, to address these challenges effectively.

Another critical policy implication is the need for climate change adaptation strategies. Brazil and France are projected to experience more frequent extreme low production years for wheat. Policymakers should prioritize investments in research and development of climate-resilient crop varieties, improved irrigation systems, and sustainable agricultural practices to mitigate the threats posed by extreme weather conditions. Additionally, implementing policies that promote sustainable land management and conservation practices can enhance agricultural resilience and contribute to long-term sustainability.

Furthermore, the integration of climate models, disease impact assessments, and advanced crop simulation techniques is vital for accurate predictions and informed decision-making. Policymakers should support research and development efforts aimed at incorporating the impacts of extreme climate events, such as waterlogging, diseases, and heavy rainfall, into crop and statistical models. This will enable more reliable simulations, enhance our understanding of climate change effects on crop production, and inform the development of effective adaptation strategies.

Moreover, the development and testing of a method for estimating national yields using a single representative point within a country's crop area have significant policy implications. Policymakers and agricultural commodity traders can leverage this approach to make informed decisions and effectively plan for national crop production. Despite the challenges associated with predicting extreme years, the method has shown promising results with a relative error of up to 6%. Policymakers should consider integrating this method into their decision-making processes to enhance agricultural planning and support strategies for addressing crop production impacts on a national scale.

In summary, this research highlights the urgency of combating climate change and protecting global food systems. It underscores the significance of supporting farmers, fostering agricultural innovation, and advocating for policies that mitigate climate risks while ensuring access to nutritious food for all. Despite the challenges ahead, proactive global collaboration can help navigate the complexities of climate change and secure our food systems for future generations. Policymakers must prioritize these policy implications to address the risks and uncertainties associated with climate change and ensure sustainable food security.

5.2. Research recommendations

Based on the presented findings and contributions, several recommendations for future research can be made:

- ***Further investigate and refine mitigation strategies:*** While the thesis addresses adaptation strategies for wheat production failures, there is room for additional research to explore and refine these strategies. This could involve assessing the effectiveness of specific interventions, such as adopting climate-resilient crop varieties, implementing sustainable agricultural practices, or improving irrigation systems.
- ***Explore the impact of weather extremes on other crop types:*** Although the thesis focuses on wheat production, it would be valuable to extend the research to other major crops, such as maize, rice, or soybeans. Investigating the specific climate change

risks, potential mitigation strategies, and the need for improved models in these contexts could provide a comprehensive understanding of food security challenges.

- ***Assess the effectiveness of policy interventions:*** The thesis emphasizes the importance of coordinated efforts and policy interventions to stabilize wheat markets and enhance agricultural resilience. Future research can delve deeper into evaluating the impact and effectiveness of specific policies, such as export bans prevention or emergency relief programs, in addressing food security threats. This could involve examining case studies from different regions and evaluating the outcomes of policy interventions.
- ***Consider socio-economic factors in food security analysis:*** While the thesis mostly focuses on climate-related challenges, it is essential to recognize the influence of socio-economic factors on food security. Future research can explore the interaction between climate change and socio-economic variables, such as poverty levels, market dynamics, and access to resources. Understanding these interconnections can provide a more comprehensive understanding of food security vulnerabilities and inform targeted interventions.
- ***Improve models for extreme climate events:*** The thesis highlights the need to enhance crop simulation models to accurately simulate the impacts of extreme climate events, such as waterlogging, diseases, and heavy rainfall. Future research can focus on developing and refining these models, incorporating additional variables and refining the methodologies used. This could involve integrating more extensive datasets, improving model parameterization, and validating the models against observed data from extreme events.
- ***Expand the application of yield estimation methods:*** The thesis introduces a method for estimating national yields using a single representative point within a country's crop area. Further research can explore the applicability of this method in other regions and for different crops. Evaluating its performance in diverse agro-climatic conditions and comparing it with existing yield estimation approaches would enhance its robustness and reliability.

By addressing these areas of research, the insights have further advanced our understanding of food security, develop more effective adaptation strategies, and improve our capacity to predict and manage the impacts of climate change on crop production.

6. References

- Alston, J., Gray, R., 2019. Export Subsidies and State Trading: Theory and Application to Canadian Wheat. pp. 281–298. <https://doi.org/10.4324/9780429268168-15>
- Antolin, L.A.S., Heinemann, A.B., Marin, F.R., 2021. Impact assessment of common bean availability in Brazil under climate change scenarios. *Agricultural Systems* 191, 103174. <https://doi.org/https://doi.org/10.1016/j.agsy.2021.103174>
- Asseng, S., Ewert, F., Martre, P., Rötter, R.P., Lobell, D.B., Cammarano, D., Kimball, B.A., Ottman, M.J., Wall, G.W., White, J.W., Reynolds, M.P., Alderman, P.D., Prasad, P.V. V., Aggarwal, P.K., Anothai, J., Basso, B., Biernath, C., Challinor, A.J., De Sanctis, G., Doltra, J., Fereres, E., Garcia-Vila, M., Gayler, S., Hoogenboom, G., Hunt, L.A., Izaurralde, R.C., Jabloun, M., Jones, C.D., Kersebaum, K.C., Koehler, A.-K., Müller, C., Naresh Kumar, S., Nendel, C., O’Leary, G., Olesen, J.E., Palosuo, T., Priesack, E., Eyshi Rezaei, E., Ruane, A.C., Semenov, M.A., Shcherbak, I., Stöckle, C., Stratonovitch, P., Streck, T., Supit, I., Tao, F., Thorburn, P.J., Waha, K., Wang, E., Wallach, D., Wolf, J., Zhao, Z., Zhu, Y., 2015. Rising temperatures reduce global wheat production. *Nature Climate Change* 5, 143–147. <https://doi.org/10.1038/nclimate2470>
- Asseng, S., Foster, I., Turner, N.C., 2011. The impact of temperature variability on wheat yields. *Global Change Biology* 17, 997–1012. <https://doi.org/https://doi.org/10.1111/j.1365-2486.2010.02262.x>
- Asseng, S., Martre, P., Maiorano, A., Rötter, R.P., O’Leary, G.J., Fitzgerald, G.J., Girousse, C., Motzo, R., Giunta, F., Babar, M.A., Reynolds, M.P., Kheir, A.M.S., Thorburn, P.J., Waha, K., Ruane, A.C., Aggarwal, P.K., Ahmed, M., Balkovič, J., Basso, B., Biernath, C., Bindi, M., Cammarano, D., Challinor, A.J., De Sanctis, G., Dumont, B., Eyshi Rezaei, E., Fereres, E., Ferrise, R., Garcia-Vila, M., Gayler, S., Gao, Y., Horan, H., Hoogenboom, G., Izaurralde, R.C., Jabloun, M., Jones, C.D., Kassie, B.T., Kersebaum, K.-C., Klein, C., Koehler, A.-K., Liu, B., Minoli, S., Montesino San Martin, M., Müller, C., Naresh Kumar, S., Nendel, C., Olesen, J.E., Palosuo, T., Porter, J.R., Priesack, E., Ripoche, D., Semenov, M.A., Stöckle, C., Stratonovitch, P., Streck, T., Supit, I., Tao, F., Van der Velde, M., Wallach, D., Wang, E., Webber, H., Wolf, J., Xiao, L., Zhang, Z., Zhao, Z., Zhu, Y., Ewert, F., 2019. Climate change impact and adaptation for wheat protein. *Global Change Biology* 25, 155–173. <https://doi.org/https://doi.org/10.1111/gcb.14481>
- Battisti, D.S., Naylor, R.L., 2009. Historical Warnings of Future Food Insecurity with Unprecedented Seasonal Heat. *Science* 323, 240–244. <https://doi.org/10.1126/science.1164363>
- Beillouin, D., Schauburger, B., Bastos, A., Ciais, P., Makowski, D., 2020. Impact of extreme weather conditions on European crop production in 2018. *Philosophical Transactions of the Royal Society B: Biological Sciences* 375, 20190510. <https://doi.org/10.1098/rstb.2019.0510>
- Ben-Ari, T., Boé, J., Ciais, P., Lecerf, R., Van der Velde, M., Makowski, D., 2018. Causes and implications of the unforeseen 2016 extreme yield loss in the breadbasket of France. *Nature Communications* 9, 1627. <https://doi.org/10.1038/s41467-018-04087-x>

- Ben Hassen, T., El Bilali, H., 2022. Impacts of the Russia-Ukraine War on Global Food Security: Towards More Sustainable and Resilient Food Systems? *Foods*. <https://doi.org/10.3390/foods11152301>
- Bentley, A.R., Donovan, J., Sonder, K., Baudron, F., Lewis, J.M., Voss, R., Rutsaert, P., Poole, N., Kamoun, S., Saunders, D.G.O., Hodson, D., Hughes, D.P., Negra, C., Ibba, M.I., Snapp, S., Sida, T.S., Jaleta, M., Tesfaye, K., Becker-Reshef, I., Govaerts, B., 2022. Near- to long-term measures to stabilize global wheat supplies and food security. *Nature Food* 3, 483–486. <https://doi.org/10.1038/s43016-022-00559-y>
- Bonjean, A., Angus, W., Ginkel, M. van, 2011. *History of Wheat Breeding*, 2nd ed. Lavoisier, Paris.
- Boote, K.J., Jones, J.W., White, J.W., Asseng, S., Lizaso, J., 2013. Putting mechanisms into crop production models. *Plant, Cell & Environment* 36, 1658–1672. <https://doi.org/https://doi.org/10.1111/pce.12119>
- Brisson, N., Gary, C., Justes, E., Roche, R., Mary, B., Ripoche, D., Zimmer, D., Sierra, J., Bertuzzi, P., Burger, P., Bussi re, F., Cabidoche, Y.M., Cellier, P., Debaeke, P., Gaudill re, J.P., H nault, C., Maraux, F., Seguin, B., Sinoquet, H., 2003. An overview of the crop model stics. *European Journal of Agronomy* 18, 309–332. [https://doi.org/https://doi.org/10.1016/S1161-0301\(02\)00110-7](https://doi.org/https://doi.org/10.1016/S1161-0301(02)00110-7)
- Calder, N., 2022. What the war in Ukraine means for energy, climate and food. *Nature* 244, 187. <https://doi.org/10.1038/244187a0>
- Carr, T.W., Balkovi , J., Dodds, P.E., Folberth, C., Skalsk , R., 2021. The impact of water erosion on global maize and wheat productivity. *Agriculture, Ecosystems & Environment* 322, 107655. <https://doi.org/https://doi.org/10.1016/j.agee.2021.107655>
- CEPEA, 2023. Center for Advanced Studies in Applied Economics: Commodities prices [WWW Document]. Agricultural series. URL <https://www.cepea.esalq.usp.br/en> (accessed 3.4.23).
- Challinor, A.J., Wheeler, T.R., Craufurd, P.Q., Slingo, J.M., Grimes, D.I.F., 2004. Design and optimisation of a large-area process-based model for annual crops. *Agricultural and Forest Meteorology* 124, 99–120. <https://doi.org/https://doi.org/10.1016/j.agrformet.2004.01.002>
- CONAB, 2023. National Supply Company: Agricultural information system [WWW Document]. URL <https://portaldeinformacoes.conab.gov.br/index.php/safras/safra-serie-historica> (accessed 2.2.23).
- de Sousa, T., Ribeiro, M., Saben a, C., Igrejas, G., 2021. The 10,000-Year Success Story of Wheat! *Foods*. <https://doi.org/10.3390/foods10092124>
- Dzotsi, K.A., Basso, B., Jones, J.W., 2013. Development, uncertainty and sensitivity analysis of the simple SALUS crop model in DSSAT. *Ecological Modelling* 260, 62–76. <https://doi.org/https://doi.org/10.1016/j.ecolmodel.2013.03.017>
- Erenstein, O., Jaleta, M., Mottaleb, K.A., Sonder, K., Donovan, J., Braun, H.-J., 2022. Global Trends in Wheat Production, Consumption and Trade BT - Wheat Improvement: Food

Security in a Changing Climate, in: Reynolds, M.P., Braun, H.-J. (Eds.), . Springer International Publishing, Cham, pp. 47–66. https://doi.org/10.1007/978-3-030-90673-3_4

FAO, 2023. FAOSTAT Statistical Database [WWW Document].

Figueiredo Moura da Silva, E.H., Silva Antolin, L.A., Zanon, A.J., Soares Andrade, A., Antunes de Souza, H., dos Santos Carvalho, K., Aparecido Vieira, N., Marin, F.R., 2021. Impact assessment of soybean yield and water productivity in Brazil due to climate change. *European Journal of Agronomy* 129, 126329. <https://doi.org/https://doi.org/10.1016/j.eja.2021.126329>

Gaiser, T., Perkons, U., Küpper, P.M., Kautz, T., Uteau-Puschmann, D., Ewert, F., Enders, A., Krauss, G., 2013. Modeling biopore effects on root growth and biomass production on soils with pronounced sub-soil clay accumulation. *Ecological Modelling* 256, 6–15. <https://doi.org/10.1016/j.ecolmodel.2013.02.016>

Gaupp, F., Hall, J., Hochrainer-Stigler, S., Dadson, S., 2020. Changing risks of simultaneous global breadbasket failure. *Nature Climate Change* 10, 54–57. <https://doi.org/10.1038/s41558-019-0600-z>

Glauben, T., Svanidze, M., Götz, L., Prehn, S., Jamali Jaghdani, T., Đurić, I., Kuhn, L., 2022. War in Ukraine and the challenge to global food security. *Nature* 57, 157–163.

Godwin, D., Ritchie, J., Singh, U., Hunt, L., 1990. A User's Guide to CERES".

Guarin, J.R., Asseng, S., Martre, P., Bliznyuk, N., 2020. Testing a crop model with extreme low yields from historical district records. *Field Crops Research* 249, 107269. <https://doi.org/10.1016/j.fcr.2018.03.006>

Guo, C., Zhang, L., Zhou, X., Zhu, Y., Cao, W., Qiu, X., Cheng, T., Tian, Y., 2018. Integrating remote sensing information with crop model to monitor wheat growth and yield based on simulation zone partitioning. *Precision Agriculture* 19, 55–78. <https://doi.org/10.1007/s11119-017-9498-5>

Hansen, S., n.d. Daisy , a flexible Soil-Plant-Atmosphere system Model.

Heinicke, S., Frieler, K., Jägermeyr, J., Mengel, M., 2022. Global gridded crop models underestimate yield responses to droughts and heatwaves. *Environmental Research Letters*.

Iizumi, T., Ramankutty, N., 2016. Changes in yield variability of major crops for 1981-2010 explained by climate change. *Environmental Research Letters* 11. <https://doi.org/10.1088/1748-9326/11/3/034003>

IPCC, 2021. Technical Summary. Contribution of Working Group I to the Sixth Assessment Report of the Intergovernmental Panel on Climate Change, *Climate Change 2021: The Physical Science Basis*.

Jamieson, P.D., Semenov, M.A., Brooking, I.R., Francis, G.S., 1998. Sirius: a mechanistic model of wheat response to environmental variation. *European Journal of Agronomy* 8, 161–179. [https://doi.org/https://doi.org/10.1016/S1161-0301\(98\)00020-3](https://doi.org/https://doi.org/10.1016/S1161-0301(98)00020-3)

- JRC, 2022. BioMA Framework [WWW Document]. SOFTWARE RESOURCES. URL <https://agri4cast.jrc.ec.europa.eu/DataPortal/Index.aspx?o=s> (accessed 9.20.22).
- Kassie, B.T., Asseng, S., Porter, C.H., Royce, F.S., 2016. Performance of DSSAT-Nwheat across a wide range of current and future growing conditions. *European Journal of Agronomy* 81, 27–36. <https://doi.org/10.1016/j.eja.2016.08.012>
- Kersebaum, K.C., 2011. Special Features of the HERMES Model and Additional Procedures for Parameterization, Calibration, Validation, and Applications, in: *Methods of Introducing System Models into Agricultural Research, Advances in Agricultural Systems Modeling*. pp. 65–94. <https://doi.org/https://doi.org/10.2134/advagriscystmodel2.c2>
- Krishnan, P., Sharma, R.K., Dass, A., Kukreja, A., Srivastav, R., Singhal, R.J., Bandyopadhyay, K.K., Lal, K., Manjaiah, K.M., Chhokar, R.S., Gill, S.C., 2016. Web-based crop model: Web InfoCrop – Wheat to simulate the growth and yield of wheat. *Computers and Electronics in Agriculture* 127, 324–335. <https://doi.org/https://doi.org/10.1016/j.compag.2016.06.008>
- Le Gouis, J., Oury, F.-X., Charmet, G., 2020. How changes in climate and agricultural practices influenced wheat production in Western Europe. *Journal of Cereal Science* 93, 102960. <https://doi.org/https://doi.org/10.1016/j.jcs.2020.102960>
- Lischeid, G., Webber, H., Sommer, M., Nendel, C., Ewert, F., 2022. Machine learning in crop yield modelling: A powerful tool, but no surrogate for science. *Agricultural and Forest Meteorology* 312, 108698. <https://doi.org/https://doi.org/10.1016/j.agrformet.2021.108698>
- Liu, B., Asseng, S., Müller, C., Ewert, F., Elliott, J., Lobell, D.B., Martre, P., Ruane, A.C., Wallach, D., Jones, J.W., Rosenzweig, C., Aggarwal, P.K., Alderman, P.D., Anothai, J., Basso, B., Biernath, C., Cammarano, D., Challinor, A., Deryng, D., Sanctis, G.D., Doltra, J., Fereres, E., Folberth, C., Garcia-Vila, M., Gayler, S., Hoogenboom, G., Hunt, L.A., Izaurrealde, R.C., Jabloun, M., Jones, C.D., Kersebaum, K.C., Kimball, B.A., Koehler, A.-K., Kumar, S.N., Nendel, C., O’Leary, G.J., Olesen, J.E., Ottman, M.J., Palosuo, T., Prasad, P.V.V., Priesack, E., Pugh, T.A.M., Reynolds, M., Rezaei, E.E., Rötter, R.P., Schmid, E., Semenov, M.A., Shcherbak, I., Stehfest, E., Stöckle, C.O., Stratonovitch, P., Streck, T., Supit, I., Tao, F., Thorburn, P., Waha, K., Wall, G.W., Wang, E., White, J.W., Wolf, J., Zhao, Z., Zhu, Y., 2016. Similar estimates of temperature impacts on global wheat yield by three independent methods. *Nature Climate Change* 6, 1130–1136. <https://doi.org/10.1038/nclimate3115>
- Lobell, D.B., Burke, M.B., 2010. On the use of statistical models to predict crop yield responses to climate change. *Agricultural and Forest Meteorology* 150, 1443–1452. <https://doi.org/https://doi.org/10.1016/j.agrformet.2010.07.008>
- Marti, J., Savin, R., Slafer, G.A., 2015. Wheat Yield as Affected by Length of Exposure to Waterlogging During Stem Elongation. *Journal of Agronomy and Crop Science* 201, 473–486. <https://doi.org/https://doi.org/10.1111/jac.12118>
- Martre, P., Jamieson, P.D., Semenov, M.A., Zyskowski, R.F., Porter, J.R., Triboi, E., 2006. Modelling protein content and composition in relation to crop nitrogen dynamics for

- wheat. *European Journal of Agronomy* 25, 138–154.
<https://doi.org/10.1016/j.eja.2006.04.007>
- Mette Laegdsmand, 2011. FASSET - Crop Simulation Model.
- Nendel, C., Specka, X., Berg, M., 2022. MONICA [WWW Document]. International Soil Modeling Consortium. URL <https://soil-modeling.org/resources-links/model-portal/monica> (accessed 9.20.22).
- Nóia Júnior, R. de S., Deswarte, J.-C., Cohan, J.-P., Martre, P., van der Velde, M., Lecerf, R., Webber, H., Ewert, F., Ruane, A.C., Slafer, G.A., Asseng, S., 2023. The extreme 2016 wheat yield failure in France. *Global Change Biology* n/a.
<https://doi.org/https://doi.org/10.1111/gcb.16662>
- Nóia Júnior, R. de S., Asseng, S., García-Vila, M., Liu, K., Stocca, V., dos Santos Vianna, M., Weber, T.K.D., Zhao, J., Palosuo, T., Harrison, M.T., 2023. A call to action for global research on the implications of waterlogging for wheat growth and yield. *Agricultural Water Management* 284. <https://doi.org/10.1016/j.agwat.2023.108334>
- Nóia Júnior, R. de S., Martre, P., Finger, R., van der Velde, M., Ben-Ari, T., Ewert, F., Webber, H., Ruane, A.C., Asseng, S., 2021. Extreme lows of wheat production in Brazil. *Environmental Research Letters* 16, 104025. <https://doi.org/10.1088/1748-9326/ac26f3>
- Osborne, T., Gornall, J., Hooker, J., Williams, K., Wiltshire, A., Betts, R., Wheeler, T., 2015. JULES-crop: a parametrisation of crops in the Joint UK Land Environment Simulator. *Geoscientific Model Development* 8, 1139–1155. <https://doi.org/10.5194/gmd-8-1139-2015>
- Paudel, D., Boogaard, H., de Wit, A., van der Velde, M., Claverie, M., Nisini, L., Janssen, S., Osinga, S., Athanasiadis, I.N., 2022. Machine learning for regional crop yield forecasting in Europe. *Field Crops Research* 276, 108377.
<https://doi.org/https://doi.org/10.1016/j.fcr.2021.108377>
- Porter, J.R., 1993. AFRCWHEAT2: A model of the growth and development of wheat incorporating responses to water and nitrogen. *European Journal of Agronomy* 2, 69–82. [https://doi.org/https://doi.org/10.1016/S1161-0301\(14\)80136-6](https://doi.org/https://doi.org/10.1016/S1161-0301(14)80136-6)
- Priesack, E., 2019. EXPERT -N Model Library Documentation. Munich.
- Raes, D., Steduto, P., HSIAO, T.C., FERERES, E., 2018. AquaCrop - Reference manual. Rome.
- Roberts, M.J., Braun, N.O., Sinclair, T.R., Lobell, D.B., Schlenker, W., 2017. Comparing and combining process-based crop models and statistical models with some implications for climate change. *Environmental Research Letters* 12, 095010.
<https://doi.org/10.1088/1748-9326/aa7f33>
- Rötter, R.P., Hoffmann, M.P., Koch, M., Müller, C., 2018. Progress in modelling agricultural impacts of and adaptations to climate change. *Current Opinion in Plant Biology* 45, 255–261. <https://doi.org/https://doi.org/10.1016/j.pbi.2018.05.009>
- Schaphoff, S., von Bloh, W., Rammig, A., Thonicke, K., Biemans, H., Forkel, M., Gerten, D., Heinke, J., Jägermeyr, J., Knauer, J., Langerwisch, F., Lucht, W., Müller, C., Rolinski, S.,

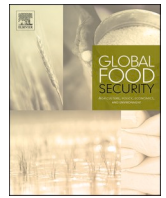
- Waha, K., 2018. LPJmL4 -- a dynamic global vegetation model with managed land -- Part 1: Model description. *Geoscientific Model Development* 11, 1343–1375. <https://doi.org/10.5194/gmd-11-1343-2018>
- Senapati, N., Halford, N.G., Semenov, M.A., 2021. Vulnerability of European wheat to extreme heat and drought around flowering under future climate. *Environmental Research Letters* 16, 24052. <https://doi.org/10.1088/1748-9326/abd3f3>
- Sharpley, A., J.R. Williams, 1990. EPIC — Erosion / Productivity.
- Stockle, C.O., Martin, S.A., Campbell, G.S., 1994. CropSyst, a cropping systems simulation model: Water/nitrogen budgets and crop yield. *Agricultural Systems* 46, 335–359. [https://doi.org/10.1016/0308-521X\(94\)90006-2](https://doi.org/10.1016/0308-521X(94)90006-2)
- Tao, F., Yokozawa, M., Zhang, Z., 2009. Modelling the impacts of weather and climate variability on crop productivity over a large area: A new process-based model development, optimization, and uncertainties analysis. *Agricultural and Forest Meteorology* 149, 831–850. <https://doi.org/10.1016/j.agrformet.2008.11.004>
- te Beest, D.E., Shaw, M.W., Pietravalle, S., van den Bosch, F., 2009. A predictive model for early-warning of Septoria leaf blotch on winter wheat. *European Journal of Plant Pathology* 124, 413–425. <https://doi.org/10.1007/s10658-009-9428-0>
- Thorp, K.R., Hunsaker, D.J., French, A.N., White, J.W., Clarke, T.R., 2010. EVALUATION OF THE CSM-CROPSIM-CERES WHEAT MODEL AS A TOOL FOR CROP WATER MANAGEMENT. *Transactions of the ASABE* 53, 87–102.
- Trnka, M., Feng, S., Semenov, M.A., Olesen, J.E., Kersebaum, K.C., Rötter, R.P., Semerádová, D., Klem, K., Huang, W., Ruiz-Ramos, M., Hlavinka, P., Meitner, J., Balek, J., Havlík, P., Büntgen, U., 2019. Mitigation efforts will not fully alleviate the increase in water scarcity occurrence probability in wheat-producing areas. *Science Advances* 5, eaau2406. <https://doi.org/10.1126/sciadv.aau2406>
- Trnka, M., Rötter, R.P., Ruiz-Ramos, M., Kersebaum, K.C., Olesen, J.E., Žalud, Z., Semenov, M.A., 2014. Adverse weather conditions for European wheat production will become more frequent with climate change. *Nature Climate Change* 4, 637–643. <https://doi.org/10.1038/nclimate2242>
- USDA, F.A.S., 2023. Downloadable Data Sets [WWW Document]. Foreign Agricultural Service. URL <https://apps.fas.usda.gov/psdonline/app/index.html#/app/home> (accessed 5.4.23).
- van der Velde, M., Lecerf, R., d’Andrimont, R., Ben-Ari, T., 2020. Chapter 8 - Assessing the France 2016 extreme wheat production loss—Evaluating our operational capacity to predict complex compound events, in: Sillmann, J., Sippel, S., Russo, S.B.T.-C.E. and T.I. for I. and R.A. (Eds.), . Elsevier, pp. 139–158. <https://doi.org/10.1016/B978-0-12-814895-2.00009-4>
- van der Velde, M., Nisini, L., 2019. Performance of the MARS-crop yield forecasting system for the European Union: Assessing accuracy, in-season, and year-to-year improvements

- from 1993 to 2015. *Agricultural Systems* 168, 203–212.
<https://doi.org/https://doi.org/10.1016/j.agsy.2018.06.009>
- Vogel, E., Donat, M.G., Alexander, L. V, Meinshausen, M., Ray, D.K., Karoly, D., Meinshausen, N., Frieler, K., 2019. The effects of climate extremes on global agricultural yields. *Environmental Research Letters* 14, 54010. <https://doi.org/10.1088/1748-9326/ab154b>
- Webber, H., Lischeid, G., Sommer, M., Finger, R., Nendel, C., Gaiser, T., Ewert, F., 2020. No perfect storm for crop yield failure in Germany. *Environmental Research Letters* 15, 104012. <https://doi.org/10.1088/1748-9326/aba2a4>
- Wit, A. de, 2022. Principles of WOFOST [WWW Document]. URL <https://www.wur.nl/en/research-results/research-institutes/environmental-research/facilities-tools/software-models-and-databases/wofost/principles-of-wofost.htm> (accessed 9.20.22).
- Wolf, J., 2011. LINTUL-3, a simple crop growth model for both potential, water limited and nitrogen limited growing conditions [WWW Document]. Models and Data Library. URL <https://models.pps.wur.nl/lintul-3-simple-crop-growth-model-both-potential-water-limited-and-nitrogen-limited-growing> (accessed 9.20.22).
- Zhao, C., Liu, B., Piao, S., Wang, X., Lobell, D.B., Huang, Y., Huang, M., Yao, Y., Bassu, S., Ciais, P., Durand, J.-L., Elliott, J., Ewert, F., Janssens, I.A., Li, T., Lin, E., Liu, Q., Martre, P., Müller, C., Peng, S., Peñuelas, J., Ruane, A.C., Wallach, D., Wang, T., Wu, D., Liu, Z., Zhu, Y., Zhu, Z., Asseng, S., 2017. Temperature increase reduces global yields of major crops in four independent estimates. *Proceedings of the National Academy of Sciences* 114, 9326 LP – 9331. <https://doi.org/10.1073/pnas.1701762114>
- Zhao, C., Liu, B., Xiao, L., Hoogenboom, G., Boote, K.J., Kassie, B.T., Pavan, W., Shelia, V., Kim, K.S., Hernandez-Ochoa, I.M., Wallach, D., Porter, C.H., Stockle, C.O., Zhu, Y., Asseng, S., 2019. A SIMPLE crop model. *European Journal of Agronomy* 104, 97–106.
<https://doi.org/https://doi.org/10.1016/j.eja.2019.01.009>
- Zheng, B., Chenu, K., Doherty, A., Chapman, S., 2015. The APSIM-Wheat Module (7.5 R3008).
- Zscheischler, J., Westra, S., van den Hurk, B.J.J.M., Seneviratne, S.I., Ward, P.J., Pitman, A., AghaKouchak, A., Bresch, D.N., Leonard, M., Wahl, T., Zhang, X., 2018. Future climate risk from compound events. *Nature Climate Change* 8, 469–477.
<https://doi.org/10.1038/s41558-018-0156-3>

Part IV: Appendix with Full Publications

List of Contents of the Appendix

Study I:	Needed global wheat stock and crop management in response to the war in Ukraine	4 Pages
	Supplementary Material for Study I	9 Pages
Study II:	Extreme lows of wheat production in Brazil	8 Pages
	Supplementary Material for Study II	36 pages
Study III:	The extreme 2016 wheat yield failure in France.	17 Pages
	Supplementary Material for Study III	44 Pages
Study IV:	Past and future wheat yield losses in France	23 Pages – not published
	Supplementary Material for Study IV	26 pages
Study V:	A call to action for global research on the implications of waterlogging for wheat growth and yield	8 Pages
	Supplementary Material for Study V	7 Pages
Study VI:	Enabling modeling of waterlogging impact on wheat	33 Pages – not published
	Supplementary Material for Study VI	12 Pages
Study VII:	A simple procedure for a national wheat yield forecast	9 Pages
	Supplementary Material for Study VII	6 Pages



Needed global wheat stock and crop management in response to the war in Ukraine

Rogério de S. Nóia Júnior^a, Frank Ewert^{b,c}, Heidi Webber^{b,d}, Pierre Martre^e, Thomas W. Hertel^f, Martin K. van Ittersum^g, Senthold Asseng^{a,*}

^a Technical University of Munich, Department of Life Science Engineering, Digital Agriculture, Freising, Germany

^b Leibniz-Centre for Agricultural Landscape Research (ZALF), Müncheberg, Germany

^c Crop Science Group, INRES, University of Bonn, Bonn, Germany

^d Brandenburg Technical University (BTU), Cottbus, Germany

^e LEPSE, Univ Montpellier, INRAE, Institut Agro Montpellier, Montpellier, France

^f Agricultural Economics, Purdue University, West Lafayette, IN, USA

^g Plant Production Systems Group, Wageningen University, Wageningen, the Netherlands

ARTICLE INFO

Keywords:

Food security

Hunger

Ukraine

War

Wheat export

ABSTRACT

The war in Ukraine threatened to block 9% of global wheat exports, driving wheat prices to unprecedented heights. We advocate, that in the short term, compensating for such an export shortage will require a coordinated release of wheat stocks, while if the export block persists, other export countries will need to fill the gap by increasing wheat yields or by expanding wheat cropping areas by 8% in aggregate. We estimate that a production increase would require an extra half a million tons of nitrogen fertilizer, yet fertilizer prices are at record levels, driven by rising energy prices. Year-to-year variability plus more frequent climate change-induced crop failures could additionally reduce exports by another 5 to 7 million tons in any given year, further stressing global markets. Without stabilizing wheat supplies through judicious management of stocks and continuing yield improvements, food and national security are at risk across many nations in the world.

1. Main

Ukraine contributes to 9% of the world's wheat exports (in 2020). In 2020, the country produced 26 million tons (Mt) of which they exported 72%, which was valued at more than 3.5 billion dollars (FAO stat, 2022). The war in Ukraine threatened to block most of Ukrainian wheat exports (FAO stat, 2022). Even if part of this wheat would be exported (FAO, 2022), the areas in Ukraine sown with crops are estimated to be significantly lower than those in recent years (W et al., 2022). It is a crisis for the Ukrainian national economy and a threat to global food security. Several African and Asian countries depend on Ukrainian wheat to provide staple foodstuffs for their population. Indonesia and Egypt consume together more than 5 Mt of Ukrainian wheat per year, which corresponds to more than 20% of their annual imports. Ukraine supplies more than 40% of the wheat imported by Pakistan, and 51% by Lebanon (USDA PSD). Consequently, the risk of food insecurity and civil unrest may increase in these Ukrainian-wheat dependent countries, and potentially beyond. For example, other wheat importing countries like

Brazil and Algeria, and particularly those in sub-Saharan Africa will also feel the impact from the wheat price hike caused by the export block. Wheat was priced at US\$281 per ton in the beginning of February 2022 and reached US\$490 per ton early March 2022 (Supplementary Fig. S3), a week after the Russian Federation invaded the Ukraine. The wheat price has remained high for several weeks and recently decreased again, but it remains exceptionally high compared to the last five years (Supplementary Fig. S3), threatening food insecurity in many importing countries.

Ninety percent of wheat exports in 2020 (the most recent year for which reliable data are available from FAO) are supplied by the world's 13 largest wheat exporting countries (Fig. 1). Across exporting countries, wheat areas have remained steady over the last two decades at about 105 million ha (Mha), even as total arable area has grown in these countries (Fig. 1). Over the same period, wheat production of the top-13 wheat exporters has increased to 325 Mt by producing more yield per unit area (mostly in the Russian Federation), with most of the additional wheat being exported (FAO stat, 2022). Global wheat exports have

* Corresponding author.

E-mail address: senthold.asseng@tum.de (S. Asseng).

increased from about 100 Mt in 2000 to 178 Mt in 2020 (Fig. 1).

Sudden wheat price hikes have occurred in the past with devastating consequences across the world. For example, in 2007 (with less stocks available than in 2020, Supplementary Fig. S2a), late spring frosts occurred simultaneously with heat waves and droughts in central Europe causing a widespread decline in wheat yields (USDA, 2007). Combined with a prolonged drought in Australia, low yields in Ukraine and demand for biofuels (Headey, 2011), resulted in tripled wheat prices (FAO, 2008), contributing to food riots in at least 14 countries (Berazneva and Lee, 2013). Similarly, in 2010, a heatwave and fires destroyed one third of Russia's national production, causing its government to ban wheat exports. This sudden wheat export shortage caused a 50% spike in wheat commodity prices, which, in turn, has contributed to the Arab Spring unrest (Perez, 2013), followed by a migration wave affecting many countries across the world (Van Mol et al., 2016).

A short-term solution for such a food crisis would be to release wheat stocks, which in recent years have been between 50 and 80 MT and dropped in recent years to about 60 Mt (as of 2022 USDA report (USDA, 2022): Supplementary Fig. S2a). The Russian Federation, the world's largest wheat exporter has a large wheat stock but is not seen currently as a reliable supplier and may have an incentive to withhold stocks or to use them as a geo-political instrument. With no Ukrainian wheat being exported due to the current war, the other top-13 wheat exporters countries should increase exports. These countries have the necessary infrastructure for wheat exportation, with capacity to transport, sell and store grains, and additional efforts to export more wheat is most likely to come from these countries. However, in the short-term, this export boost will have to come mainly from available stocks in these countries. But in the mid- and long-term, these extra demands on wheat need to be met through higher wheat production.

The top-13 wheat export countries (omitting the Russian Federation and Ukraine) produced 214 Mt of wheat on 67 Mha, with an average yield of 3.3 t ha^{-1} in 2020 (FAO stat, 2022). To compensate for the missing Ukrainian wheat export, without contributions from the Russian Federation, will need to increase wheat grain yields by at least 8% (slightly less than the 9% export share of Ukraine as the mean yield level in the Ukraine is lower compared to the mean of the other countries) by closing the yield gap (difference between exploitable yield potential

[80% of yield potential] (van Ittersum et al., 2013) and actual farmers' yield) (Fig. 2b). As an annual yield increase of 8% is far beyond the average trend in wheat yields (Grassini et al., 2013; Fischer et al., 2014), such an abrupt change in wheat yield is not likely in the short and medium-term and will require long-term preparation through research and development in yield improvements. Also, increasing yields towards the exploitable yield potential would require about half a million tons of additional N fertilizer in these countries to offset the 18 Mt lost from the Ukrainian wheat export block (Fig. 2d; Supplementary Table S4). For example, USA and Canada together would need more than 0.2 Mt of N fertilizer to achieve this goal (Fig. 2d). However, considering fertilizer prices have increased dramatically during COVID19 and more since the Russian invasion of Ukraine (Supplementary Fig. S4), high fertilizer use is a significant contributor to nutrient pollution of the environment (Foley et al., 2011) and is extremely energy intensive, such an increase in fertilizer use might not be possible or desirable (Union, 2020). Although, the increase in N fertilizer price may result in a reduction in N fertilizer applications by farmers, which would further accelerate the wheat shortage.

Alternatively, the additional wheat could come from expanding wheat production to another 5.5 Mha of cultivated area, displacing other crops or expanding into non-cultivated, less fertile areas. For example, The European Commission and several Member States are discussing a roll-back of The Green Deal – allowing farmers to sow wheat on ecologically protected areas established to meet the target of 10% ecologically protected areas by 2035 in response to the environmental crisis, in particularly the biodiversity crisis, to increase wheat production for export (Anghel, 2022). However, this would accelerate the environmental crisis and likely further reduce crop productivity in the future. And, the required area would be even larger due to low yield levels on these marginal lands (Beyer et al., 2022) (Fig. 2).

Year-to-year variability and an increase in the frequency of climate change-induced production failures could reduce exports by up to another 5 to 7 Mt in any year, further stressing global markets. This stems from the fact that total average wheat export of the top-13 wheat exporting countries normally varies by up to 5 Mt (standard deviation of time series; Fig. 1a), which is largely caused by year-to-year-climate variability (Ray et al., 2015). In addition, we estimate that crop

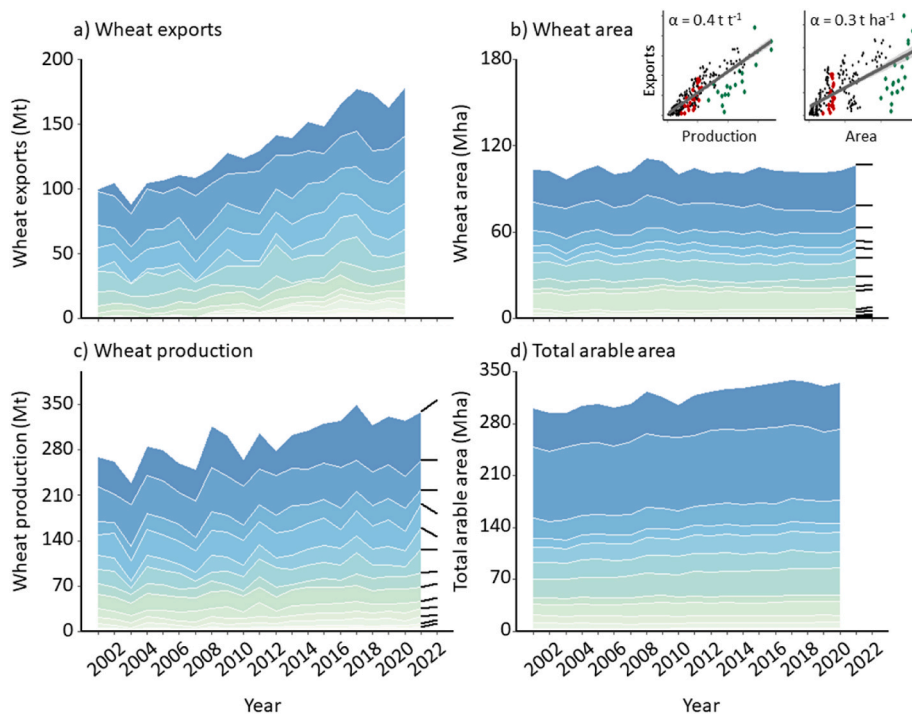


Fig. 1. Top-13 wheat exporters of the world. Reported cumulative wheat (a) exports, (b) harvested area, (c) production and (d) total arable area of the top-13 wheat export countries, accounting for 90% of recent global wheat exports. In (b) insets show exports versus production (left) and exports versus wheat harvest area (right) in last 20 years (FAO stat, 2022). α is the slope of a linear regression. Data were obtained from FAO Stats (FAO stat, 2022) and expanded with estimates from USDA (USDA, 2022) for 2021 and estimates for 2022 (black lines in (b) and (c)). All stacked lines are in order from largest to smallest top-13 wheat exporter, from dark blue to light green. Top-13 wheat exporters in 2020 (most recent FAO report) were (in order of exported tons per year) the Russian Federation, United States of America, Canada, France, Ukraine, Australia, Argentina, Germany, Kazakhstan, Poland, Romania, Lithuania, and Bulgaria. (For interpretation of the references to colour in this figure legend, the reader is referred to the Web version of this article.)

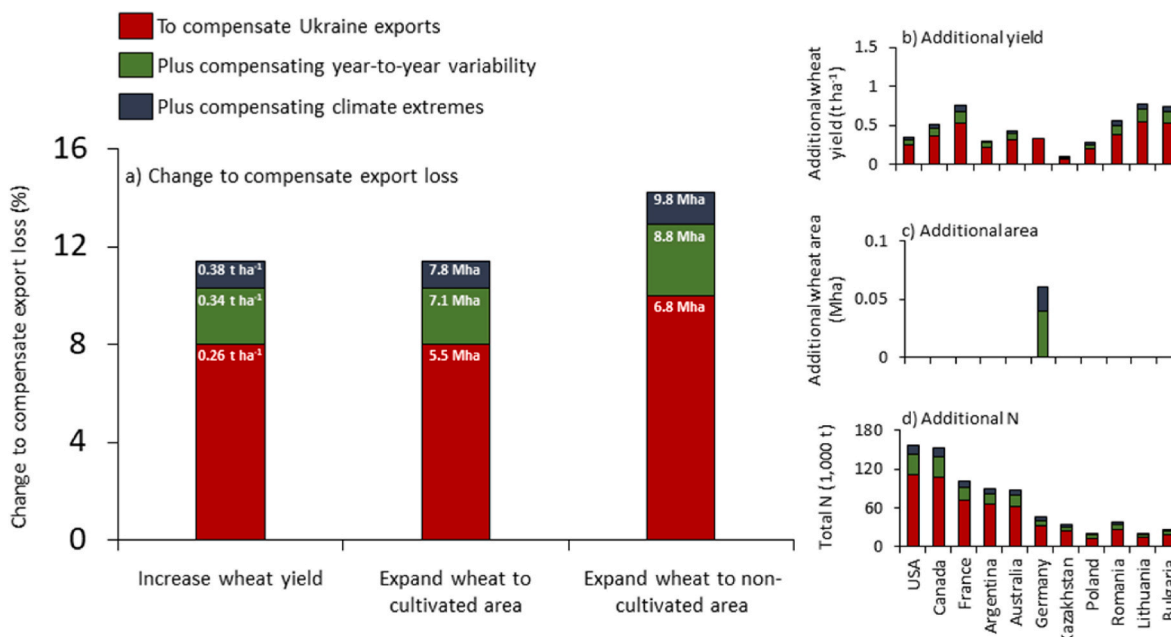


Fig. 2. Required change in wheat yield or wheat area by top-13 wheat exporting countries (excluding Russia and Ukraine) to compensate export loss by Ukraine, plus additional possible wheat export losses from year-to-year variability or climate change induced extreme losses. (a) Average required increase in wheat grain yield and in wheat area expanded to cultivated and non-cultivated areas. Additional required wheat (b) grain yield, (c) cultivated area and (d) N fertilizer for each of the top-13 exporting countries (excluding Russia and Ukraine). Wheat yield in Germany is already close to the exploitable yield level (van Ittersum et al., 2013), therefore the increase in wheat production in Germany would need to come mostly from additional wheat area. Nitrogen requirements were calculated by using 30 kg of N fertilizer being required to produce one ton of wheat grain yield (Ladha et al., 2016). An additional export decline due to year-to-year-variability was calculated as the standard deviation of the linear regression line of top-13 country total exports during FAO reported years 2001–2020 (Fig. 1). When expanding wheat to other cropped areas (i.e. replacing other crops) similar to current yield levels were assumed. When expanding wheat into currently not-cropped areas, a 20% lower yield was assumed due to less fertile land (Beyer et al., 2022).

production failures due to extreme adverse weather events in these countries in the wake of climate change could further lower exports by another 2 Mt, resulting in potential export declines of up to 7 Mt compared to an average year. An export drop of more than 7 Mt occurred in 2003 during the widespread European drought and heat-wave (Battisti and Naylor, 2009), a climate pattern also observed in 2018 and projected to become more frequent in the future with climate change (Trnka et al., 2014). Such shocks to crop production are possible in 2022 and with an increasing frequency of occurrence any year in the future with climate change (Nóia Júnior, 2021). Hence, to also account for additional wheat export losses due to year-to-year variability and possible climate extremes induced crop failures in wheat exports would require short, medium- and long-term preparations. In the short-term, this means being prepared for even more wheat stock releases.

Recent national crop yield projections indicate that the loss of Ukrainian exports is unlikely to be compensated this year. A pronounced rainfall deficit has been reported for parts of France and Germany, and their national wheat productions are not expected to exceed that of previous years (Baruth et al., 2022). In addition, Kazakhstan has declared restrictions to wheat exports during the crisis (FAS-Nur-Sultan, 2022), further stressing the global wheat export market. The projected wheat production of India and China, the two largest wheat producers and consumers, were also expected to decrease due to adverse weather conditions (Sowell and Swearingen, 2022). The consequences of such supply disruptions for the world market could be devastating as indicated in recent years. For example, the Ukrainian droughts of both 2018 and 2019, which caused its national wheat exports to drop, by 10 and 5% respectively (FAO stat, 2022), likely contributed to the decline of the per capita wheat consumption in Pakistan, a major wheat importer from Ukraine, and accelerated the number of undernourished people by 2.7 M during this period. Other wheat importing countries like Morocco, Egypt and Tunisia with limited fresh water resources to

support their own crop production (Asseng et al., 2018) are also highly vulnerable to global wheat commodities prices (FAO stat, 2022).

While in the medium to long-term, Ukraine exports, which have slowly started again and crop production may be compensated elsewhere through gradual yield increases and area expansion, short-term impacts are likely to be severe for many countries across the globe and will require a better management of national stocks. Controlling part of the stocks by coordinating existing national stockholdings, currently not available, would be a way forward. Even if the war ends in the next few months and/or exports from the Ukraine become normal again, the disruption of Ukraine's grain storage and processing infrastructure, and maritime shipping capacity will have consequences on Ukraine's wheat production and export capacities beyond the 2022/2023 marketing season (FAO, 2022). Therefore, medium-to long-term wheat production improvement will be required, calling for a concerted global effort in conjunction with improved management of the climate and environmental crisis to stabilize future wheat markets (Koning, 2017). Our analysis has focused on wheat, as the main staple food in many countries, but Ukraine and the Russian Federation are also top global exporters of sunflower, rapeseed, maize and barley. The reduced supply of these commodities is adding to the global food market disruption. Actions should be taken to make agriculture less vulnerable and more resilient to the concentration of food exports in a handful of countries.

Declaration of competing interest

The authors declare that they have no known competing financial interests or personal relationships that could have appeared to influence the work reported in this paper.

Data availability

Data will be made available on request.

Acknowledgements

R.S.N.J. acknowledges support from the Prince of Albert II of Monaco foundation through the IPCC Scholarship Program. The contents of this manuscript are solely the liability of R.S.N.J. and under no circumstances may be considered as a reflection of the position of the Prince Albert II of Monaco Foundation and/or the IPCC. FE acknowledges support from the Deutsche Forschungsgemeinschaft (DFG, German Research Foundation) under Germany's Excellence Strategy – EXC 2070 – 390732324. P.M. acknowledge support from the metaprogram Agriculture and forestry in the face of climate change: adaptation and mitigation (CLIMAE) of the French National Research Institute for Agriculture, Food and Environment (INRAE). T.H. acknowledges support from the National Science Foundation: NSF-OISE-2020635. M.K.v.I. acknowledges the Senior Expert Programme of NWO-WOTRO Strategic Partnership NL-CGIAR.

Appendix A. Supplementary data

Supplementary data to this article can be found online at <https://doi.org/10.1016/j.gfs.2022.100662>.

References

- Anghel, I., 2022. Germany Rolls Back Environmental Rules to Boost Domestic Crops Threatened by Russia's War in Ukraine. *Time - Climate*. Food & Agriculture.
- Asseng, S., et al., 2018. Can Egypt become self-sufficient in wheat? *Environ. Res. Lett.* 13, No 5. [https://doi.org/10.2760/908536\(online\)](https://doi.org/10.2760/908536(online)).
- Battisti, D.S., Naylor, R.L., 2009. Historical warnings of future food insecurity with unprecedented seasonal heat. *Science* 323, 240–244.
- Berazneva, J., Lee, D.R., 2013. Explaining the African food riots of 2007–2008: an empirical analysis. *Food Pol.* 39, 28–39.
- Beyer, R.M., Hua, F., Martin, P.A., Manica, A., Rademacher, T., 2022. Relocating croplands could drastically reduce the environmental impacts of global food production. *Communications Earth & Environment* 3, 49.
- FAO, 2008. Global Cereal Supply and Demand Brief. *Crop Perspectives and Food Situation*. <https://www.fao.org/3/ah881e/ah881e04.htm>.
- FAO stat, 2022. FAOSTAT: FAO statist. databases. [http://www.fao.org/faostat/en/#home%20\(2022\)](http://www.fao.org/faostat/en/#home%20(2022)).
- FAS-Nur-Sultan, 2022. Kazakhstan Announces Wheat and Wheat Flour Export Restrictions.
- Fischer, R.A., Byerlee, D., Edmeades, G., 2014. Crop Yields and Global Food Security: Will Yield Increase Continue to Feed the World? ACIAR Monograph No. 158. Australian Centre for International Agricultural Research, Canberra.
- Foley, J.A., et al., 2011. Solutions for a cultivated planet. *Nature* 478, 337–342.
- Grassini, P., Eskridge, K.M., Cassman, K.G., 2013. Distinguishing between yield advances and yield plateaus in historical crop production trends. *Nat. Commun.* 4, 2918.
- Headey, D., 2011. Causes of the 2007-2008 Global Food Crisis Identified, p. 1.
- Koning, N., 2017. Food Security, Agricultural Policies and Economic Growth. Routledge.
- Ladha, J.K., et al., 2016. Global nitrogen budgets in cereals: a 50-year assessment for maize, rice and wheat production systems. *Sci. Rep.* 6, 19355.
- Nóia Júnior, R.S., et al., 2021. Extreme lows of wheat production in Brazil. *Environ. Res. Lett.* 16, 104025.
- Perez, I., 2013. Climate Change and Rising Food Prices Heightened Arab Spring. *Scientific American: Sustainability*.
- Ray, D.K., Gerber, J.S., Macdonald, G.K., West, P.C., 2015. Climate variation explains a third of global crop yield variability. *Nat. Commun.* 6, 1–9.
- Sowell, A., Swearingen, B., 2022. Wheat Outlook : May 2022. USDA.
- Trnka, M., et al., 2014. Adverse weather conditions for European wheat production will become more frequent with climate change. *Nat. Clim. Change* 4, 637–643.
- Union, European, 2020. Farm to fork strategy. DG SANTE/Unit 'Food inf. compos. food waste'' 23.
- USDA, F.A.S., 2007. Spring Dryness and Freeze Lowers Europe's 2007/08 Winter Crop Prospects. *Commodity Intelligence Report*. https://ipad.fas.usda.gov/highlights/2007/05/EU_21May07/.
- USDA, F.A.S., 2022. Downloadable Data Sets. Foreign Agricultural Service. <https://apps.fas.usda.gov/psdonline/app/index.html#/app/home>.
- FAO, 2022. Information Note - The importance of Ukraine and the Russian Federation for global agricultural markets and the risks associated with the current conflict, pp. 1–41. <chrome-extension://efaidnbmnnnibpcajpcglclefindmkaj/viewer.html?pdfurl=https%3A%2F%2Fwww.fao.org%2F3%2Fcb9013en%2Fcb9013en.pdf&clen=1680551> (2022).
- USDA PSD. Trade Data Monitor. <https://apps.fas.usda.gov/psdonline/app/index.html#/app/home>.
- van Ittersum, M.K., et al., 2013. Yield gap analysis with local to global relevance—a review. *Field Crop. Res.* 143, 4–17.
- Van Mol, C., de Valk, H., 2016. In: Garcés-Masareñas, B., Penninx, R. (Eds.), Migration and Immigrants in Europe: A Historical and Demographic Perspective BT - Integration Processes and Policies in Europe: Contexts, Levels and Actors, vols. 31–55. Springer International Publishing. https://doi.org/10.1007/978-3-319-21674-4_3.
- W, B.A., et al., 2022. JRC MARS Bulletin - Global Outlook - Crop Monitoring European Neighbourhood - Ukraine - June 2022. [https://doi.org/10.2760/796337\(online\)](https://doi.org/10.2760/796337(online)).

Supplementary material for

Needed global wheat stock and crop management in response to the war in Ukraine

Table S1: Top-13 wheat exporting countries (excluding Russia and Ukraine), ranked from top by export in 2020. Current and additional yield and area required to compensate for Ukraine export stop, plus potential additional export losses due to year-to-year variability (standard deviation of time series from 2001 to 2020) and climate change induced extreme production failures (for instance the European drought and heat wave in 2003, combined with crop failures in Australia and Ukraine and increase biofuel demand REF). *Note: expansion to none-cultivated area is not shown here but would be 1.2 times larger due to less soil fertility of this land*¹. Wheat yield, area and production are averages (avg) for five cropping-seasons from 2016 to 2020.

Country	Avg. Wheat yield (t/ha)	Avg. Wheat area (M ha)	Avg. Wheat production (M t)	Additional yield to compensate Ukraine exports (t/ha)	Yield plus compensating year-to-year-variability (t/ha)	Yield plus compensating climate extremes (t/ha)	Additional Area to compensate Ukraine exports (t/ha)	Additional Area plus compensating year-to-year-variability (M ha)	Area plus compensating climate extremes (M ha)
USA	3.33	15.80	52.76	0.25	0.07	0.03	1.16	0.33	0.15
Canada	3.43	9.50	32.54	0.35	0.10	0.05	0.98	0.29	0.13
France	6.75	5.17	34.83	0.52	0.15	0.07	0.40	0.12	0.05
Australia	1.93	10.93	21.42	0.22	0.06	0.03	1.25	0.32	0.15
Argentina	3.10	5.62	17.49	0.31	0.09	0.04	0.56	0.16	0.07
Germany	7.43	3.08	22.89	0.37	0.11	0.05	0.15	0.04	0.02
Kazakhstan	1.18	11.80	13.89	0.07	0.02	0.01	0.66	0.19	0.09
Poland	4.60	2.41	11.07	0.19	0.06	0.03	0.10	0.03	0.01
Romania	4.27	2.15	9.13	0.38	0.12	0.05	0.19	0.06	0.03
Lithuania	4.51	0.85	3.85	0.55	0.15	0.07	0.10	0.03	0.01
Bulgaria	4.87	1.19	5.78	0.52	0.15	0.07	0.13	0.04	0.02
Total for area and production and mean for yield	3.30	67.60	214.60	0.26	0.08	0.04	5.48	1.59	0.73

Table S2: Top-13 wheat exporting countries (excluding Russia and Ukraine), ranked from top by export in 2020. Potential, exploitable, current yield and yield gap, and additional yield and area required to compensate for Ukraine export stop, plus year-to-year variability, plus climate change induced export loss. A positive yield gap indicates scope for yield increase, a close to zero or negative yield gap indicates no potential for further yield increase. The yield gap was calculated as the difference between exploitable yield potential, defined as 80% of the potential yield (as mean of ca. 15 years, without a technology trend, established by the Global Yield Gap Atlas² and the country mean yield of 2016 to 2020.

	A	B	C	D	E	F	G	H	
Country	Potential yield (t/ha)	Exploitable yield (t/ha)	Avg. Wheat yield (t/ha)	Yield Gap B-C (t/ha)	Additional yield to compensate Ukraine exports (t/ha)	Yield plus compensating year-to-year-variability (t/ha)	Yield plus compensating climate extremes (t/ha)	Total yield compensation E+F+G (t/ha)	Difference between total yield gap and total yield compensation (t/ha)
USA	5.40	4.32	3.33	0.99	0.25	0.07	0.03	0.35	0.64
Canada	5.00	4.00	3.43	0.57	0.35	0.10	0.05	0.51	0.07
France	9.80	7.84	6.75	1.09	0.52	0.15	0.07	0.75	0.35
Australia	3.60	2.88	1.93	0.95	0.22	0.06	0.03	0.30	0.65
Argentina	5.20	4.16	3.10	1.06	0.31	0.09	0.04	0.43	0.63
Germany	9.70	7.76	7.43	0.33	0.37	0.11	0.05	0.53	-0.20
Kazakhstan	2.40	1.92	1.18	0.74	0.07	0.02	0.01	0.09	0.65
Poland	9.40	7.52	4.60	2.92	0.19	0.06	0.03	0.27	2.65
Romania	8.40	6.72	4.27	2.45	0.38	0.12	0.05	0.55	1.90
Lithuania	9.00	7.20	4.51	2.69	0.55	0.15	0.07	0.77	1.92
Bulgaria	8.10	6.48	4.87	1.61	0.52	0.15	0.07	0.74	0.87

Table S3: Top-13 wheat exporting countries (excluding Russia and Ukraine), ranked from top by export in 2020. Exploitable and current average wheat yield and required yield to compensate for Ukraine export stop, year-to-year variability and additional climate change induced extreme exports loss. Forecasted wheat yield for the 2022 wheat harvested. Yields in blue indicate that the forecasted wheat yield would be above the wheat yield required to compensate for Ukraine export stop. The yield gap was calculated as the difference between exploitable yield (as mean of ca. 15 climate seasons, without a technology trend, established by the Global Yield Gap Atlas (<https://www.yieldgap.org/>)) and the country mean yield of 2016 to 2020.

Country	Exploitable yield (t/ha)	Avg. Wheat yield (t/ha)	Wheat yield to compensate Ukraine exports (t/ha)	Yield plus compensating year-to-year-variability (t/ha)	Yield plus compensating climate extremes (t/ha)	Forecasted wheat yield for cropping season harvested in 2022	References
USA	4.32	3.33	3.58	3.65	3.68	3.20	3
Canada	4.00	3.43	3.78	3.88	3.93	3.50	3
France	7.84	6.75	7.27	7.42	7.49	6.96	4
Australia	2.88	1.93	2.15	2.21	2.23	2.52	3
Argentina	4.16	3.10	3.41	3.49	3.53	3.11	3
Germany	7.76	7.43	7.80	7.91	7.96	7.37	4
Kazakhstan	1.92	1.18	1.24	1.26	1.27	1.02	3
Poland	7.52	4.60	4.79	4.84	4.87	4.93	4
Romania	6.72	4.27	4.65	4.77	4.82	4.27	4
Lithuania	7.20	4.51	5.06	5.21	5.28	4.92	4
Bulgaria	6.48	4.87	5.39	5.54	5.61	5.24	4

Table S4: Top-13 wheat exporting countries (excluding Russia and Ukraine), ranked from top by export in 2020. Additional nitrogen fertilizer required to compensate for Ukraine export stop, year-to-year variability and climate change induced extreme export reductions. Nitrogen requirements were calculated using 30 kilogram of N fertilizer applied per ton of grain yield. This assumes a mean grain protein content of 12% (at 13% grain moisture), which is 2% of nitrogen in grains, with a fertilizer N use efficiency of about 67%⁵. Note, as Germany is already close to the exploitable yield potential, additional yield compensations due to year-to-year variability and due to climate change induced extreme yield loss are not possible via yield increase and the additional N for Germany refers to the additional area needed to grow more wheat. Note, the additional required N is about 8% more than currently used in these countries.

Country	Additional N to compensate Ukraine export loss (1,000 t)	Additional N to compensating for year-to-year year-to-year-variability (1,000 t)	Additional N to compensate for climate extremes (1,000 t)	Total N to compensate all three losses combined (1,000 t)
USA	111	31	15	157
Canada	108	31	14	153
France	71	21	10	102
Australia	66	17	8	90
Argentina	63	18	8	88
Germany	32	9	4	45
Kazakhstan	24	7	3	34
Poland	14	4	2	20
Romania	26	8	4	38
Lithuania	15	4	2	21
Bulgaria	19	6	3	27
Total	548	156	72	776

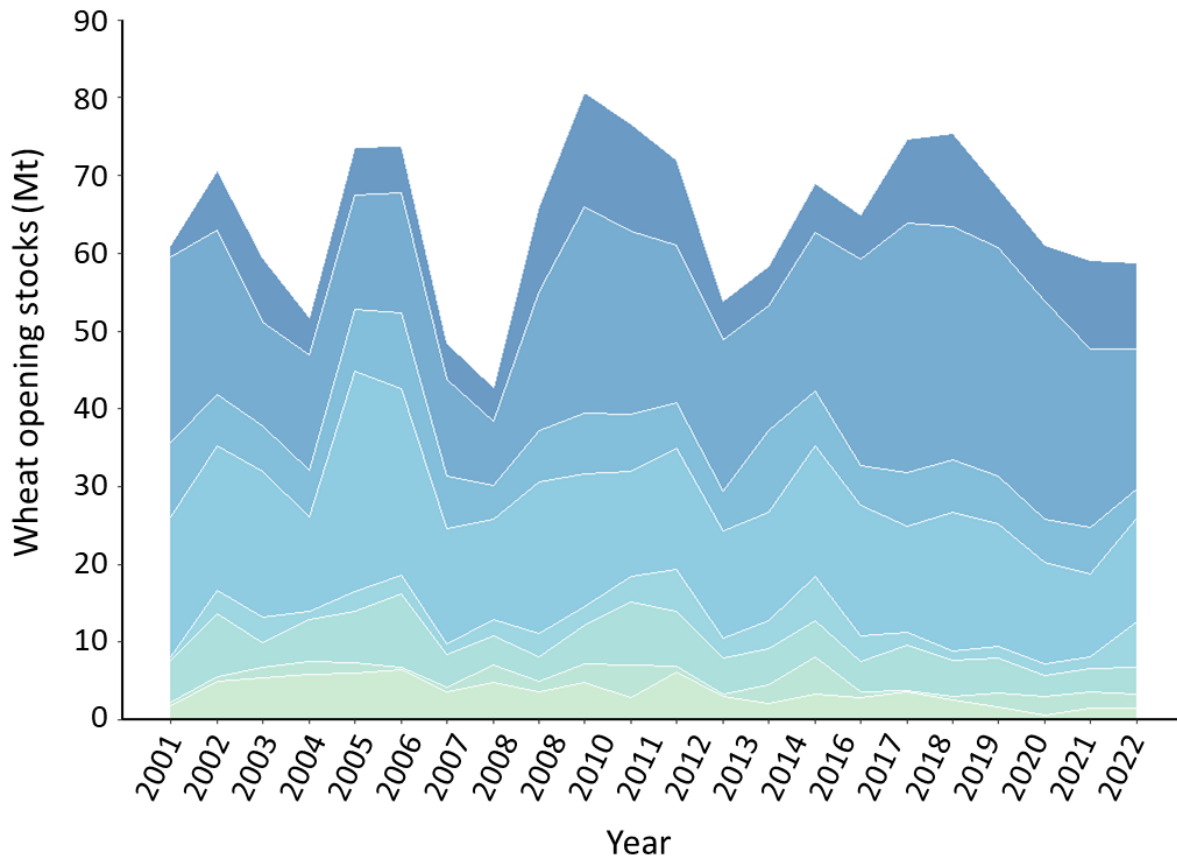


Figure S2. Wheat stocks of the top-13 wheat exporters of the world. Reported wheat opening stocks at first of January 2001 to 2022 of the top wheat export countries and the European Union, accounting for 90% of global wheat exports in 2020. Black line is total, green line is Russia, red line is Ukraine, gray lines are all other countries. Data were obtained from USDA³. Top wheat exporters in 2020 are (in order of exported tons per year) Russia, United States of America, Canada, European Union, Ukraine, Australia, Argentina, Kazakhstan. Opening stocks is the initial quantity of wheat held by a country at the start of any year. Data only available from 2001 to 2022, USDA³. The USDA reports wheat opening stocks for the European Union and not for the individual member countries.

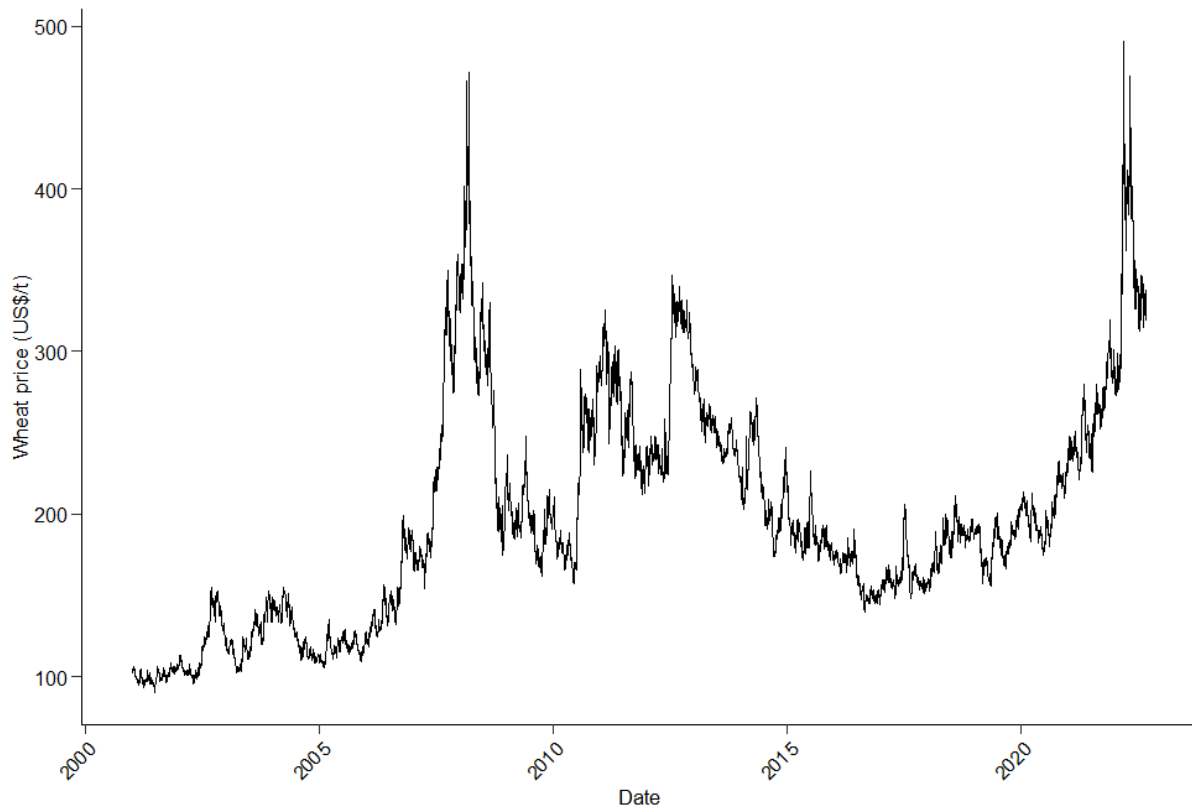


Figure S3. Wheat commodity price. Historical world wheat commodities price, from 2001 to 2022, (Macrotrends, <https://www.macrotrends.net/2534/wheat-prices-historical-chart-data#:~:text=The%20current%20price%20of%20wheat,2022%20is%20%2410.7075%20per%20bushe> !.)

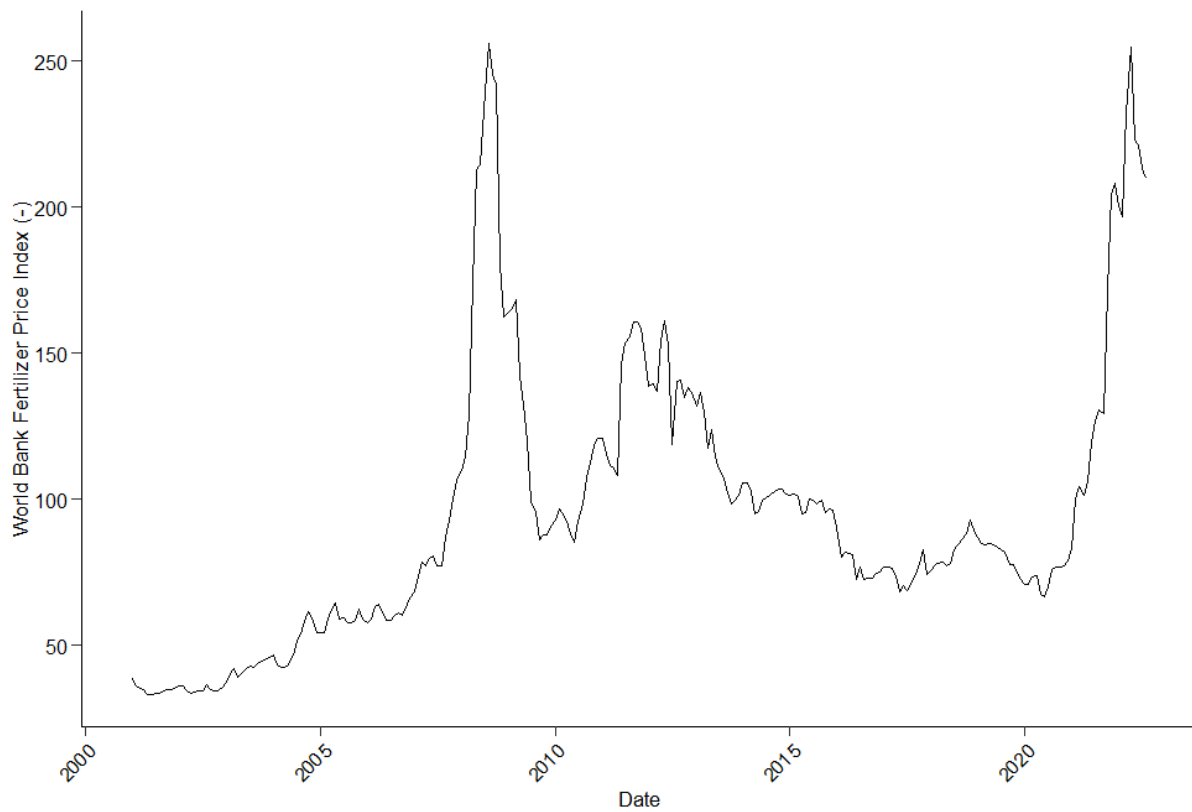


Figure S4. World Bank Fertilizer Commodity Price Index. Historical World Bank Fertilizer Commodity Price Index, from 2001 to 2022, (The World Bank, <https://www.worldbank.org/en/research/commodity-markets>).

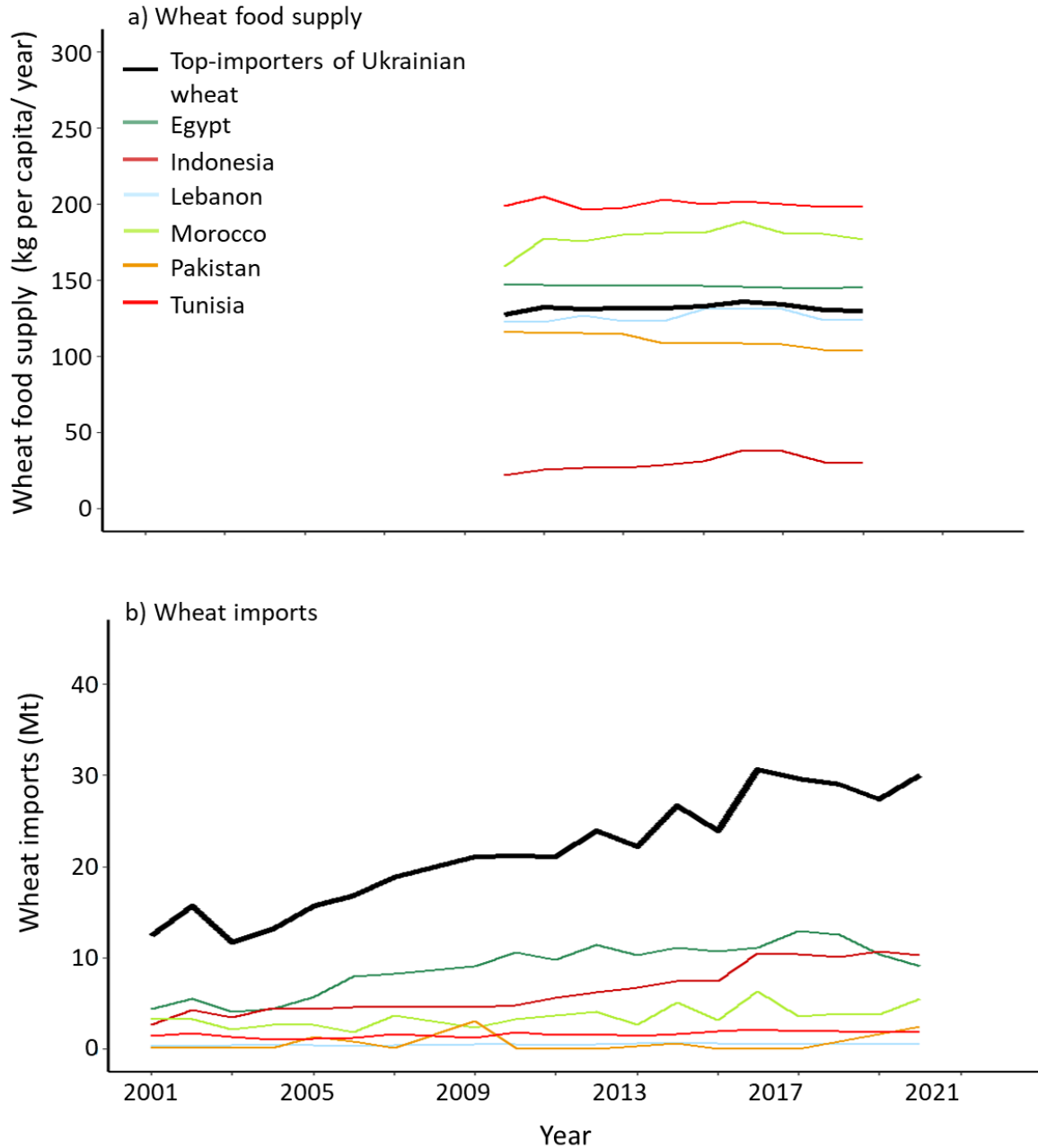


Figure S5. Wheat imports of major wheat importers from the Ukraine. Wheat (a) food supply per capita from 2010 to 2019 and (b) wheat imports of major importers from the Ukraine for the period 2010 – 2020. Black line is the average food supply per capita in (a) and total wheat imports of the top-5 wheat importers from the Ukraine in (b). Data are from FAO Stats ⁶. Top-5 wheat exports in 2020 from the Ukraine are (in order of imported tons per year) Indonesia, Egypt, Pakistan, Morocco, Tunisia and Lebanon.

Table S4. Top wheat importers in 2021. Data source: USDA PSD ⁷

Importing Country	Imports from world including Ukraine (Mt)	Imports from Ukraine (Mt)	Import share from Ukraine (%)
Indonesia	10,450	2,700	26
Egypt	12,149	2,405	20
Pakistan	3,617	1,456	40
Bangladesh	7,200	1,127	16
Morocco	5,444	1,009	19
Turkey	8,081	810	10
Tunisia	1,771	653	37
Lebanon	1,210	611	51
Libya	1,455	565	39

References

1. Beyer, R. M., Hua, F., Martin, P. A., Manica, A. & Rademacher, T. Relocating croplands could drastically reduce the environmental impacts of global food production. *Communications Earth & Environment* **3**, 49 (2022).
2. van Ittersum, M. K. *et al.* Yield gap analysis with local to global relevance—A review. *Field Crops Research* **143**, 4–17 (2013).
3. USDA, F. A. S. Downloadable Data Sets. *Foreign Agricultural Service* <https://apps.fas.usda.gov/psdonline/app/index.html#/app/home> (2022).
4. Baruth, B. *et al.* *JRC MARS Bulletin - Crop monitoring in Europe - August 2022 - Vol. 30 No 8.* (2022) doi:10.2760/908536 (online).
5. Lassaletta, L., Billen, G., Grizzetti, B., Anglade, J. & Garnier, J. 50 year trends in nitrogen use efficiency of world cropping systems: the relationship between yield and nitrogen input to cropland. *Environmental Research Letters* **9**, 105011 (2014).
6. FAO stat. FAOSTAT: FAO statistical databases. <http://www.fao.org/faostat/en/#home> (2022).
7. USDA PSD. Trade Data Monitor. <https://apps.fas.usda.gov/psdonline/app/index.html#/app/home>.

LETTER • OPEN ACCESS

Extreme lows of wheat production in Brazil

To cite this article: Rogério de Souza Nóia Júnior *et al* 2021 *Environ. Res. Lett.* **16** 104025

View the [article online](#) for updates and enhancements.

You may also like

- [Wheat yield loss attributable to heat waves, drought and water excess at the global, national and subnational scales](#)
M Zampieri, A Ceglar, F Dentener *et al.*
- [Evaluating the effects of climate change on US agricultural systems: sensitivity to regional impact and trade expansion scenarios](#)
Justin S Baker, Petr Havlík, Robert Beach *et al.*
- [Construction and experiment of phenotyping system based on field wheat](#)
ZANG Hecang, ZHANG Jie, ZHAO Qing *et al.*

ENVIRONMENTAL RESEARCH
LETTERS

LETTER

Extreme lows of wheat production in Brazil

OPEN ACCESS

RECEIVED
14 June 2021REVISED
6 September 2021ACCEPTED FOR PUBLICATION
15 September 2021PUBLISHED
30 September 2021

Original content from
this work may be used
under the terms of the
[Creative Commons
Attribution 4.0 licence](#).

Any further distribution
of this work must
maintain attribution to
the author(s) and the title
of the work, journal
citation and DOI.

Rogério de Souza Nóia Júnior¹ , Pierre Martre² , Robert Finger³, Marijn van der Velde⁴ ,
Tamara Ben-Ari⁵, Frank Ewert^{6,7}, Heidi Webber⁶, Alex C Ruane⁸ and Senthold Asseng^{1,*} ¹ Technical University of Munich, Department of Life Science Engineering, Freising, Germany² LEPSE, Univ Montpellier, INRAE, Institut Agro, Montpellier, France³ ETH Zurich, Agricultural Economics and Policy Group, Zurich, Switzerland⁴ European Commission, Joint Research Centre, Ispra, Italy⁵ Centre International de Recherche sur l'Environnement et le Développement, Nogent-sur-Marne, France⁶ Leibniz-Centre for Agricultural Landscape Research (ZALF), Müncheberg, Germany⁷ Crop Science Group, INRES, University of Bonn, Bonn, Germany⁸ NASA Goddard Institute for Space Studies, New York, NY, United States of America

* Author to whom any correspondence should be addressed.

E-mail: senthold.asseng@tum.de**Keywords:** climate change, extreme weather, food price and food securitySupplementary material for this article is available [online](#)**Abstract**

Wheat production in Brazil is insufficient to meet domestic demand and falls drastically in response to adverse climate events. Multiple, agro-climate-specific regression models, quantifying regional production variability, were combined to estimate national production based on past climate, cropping area, trend-corrected yield, and national commodity prices. Projections with five CMIP6 climate change models suggest extremes of low wheat production historically occurring once every 20 years would become up to 90% frequent by the end of this century, depending on representative concentration pathway, magnified by wheat and in some cases by maize price fluctuations. Similar impacts can be expected for other crops and in other countries. This drastic increase in frequency in extreme low crop production with climate change will threaten Brazil's and many other countries progress toward food security and abolishing hunger.

Brazil's wheat production is insufficient to meet domestic demand (Conab 2020). Despite being the fourth largest producer of grains in the world, the country imports up to 6 million tons of wheat annually, particularly after years when national wheat production is extremely low (FAO 2021). Instability in crop production can threaten regional and global food security (Wheeler and von Braun 2013, Raymond *et al* 2020).

Understanding what has driven extreme production losses in the past and the frequency of those losses is a critical step in finding ways to adapt agriculture to climate change with the aim of ensuring future food availability in Brazil and elsewhere. For four major agro-climatological zones of the main wheat growing regions of Brazil (Groups I–IV, (available online at stacks.iop.org/ERL/16/104025/mmedia) supplementary figures S2 and S3), multiple regression impact models were developed to estimate wheat planting area, non-harvested area

and grain yield, based on reported sub-regional wheat cropping areas, non-harvested areas, trend-corrected grain yields, monthly regional climate data, and national commodity grain prices during the period 2001–2019, as described in supplementary figures S1, S8–S11 and supplementary tables S1–S3. Wheat non-harvested area is defined as the wheat planted area destroyed by adverse weather, i.e. crop damaging weather (Trnka *et al* 2014), particularly frost and drought, and consequently not harvested. The regression results from each sub-component model (i.e. separate impact models for sub-regional wheat cropping areas, non-harvested areas and grain yield) were combined within each sub-region and then aggregated to national scale (figure 1(d)). The regression impact models, shown in supplementary table S3, reproduced regional and national planting area ($r^2 = 0.75$), harvested area ($r^2 = 0.97$), and trend-corrected yield satisfactorily ($r^2 = 0.98$), in particular the extremely poor harvest of 2006

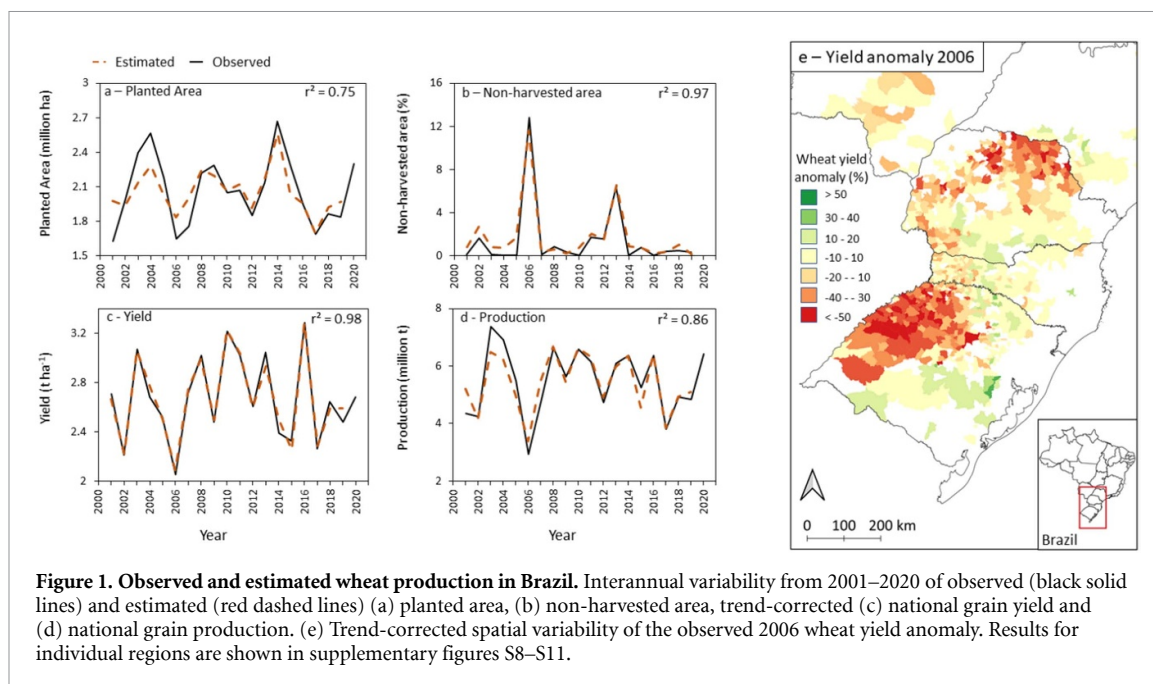
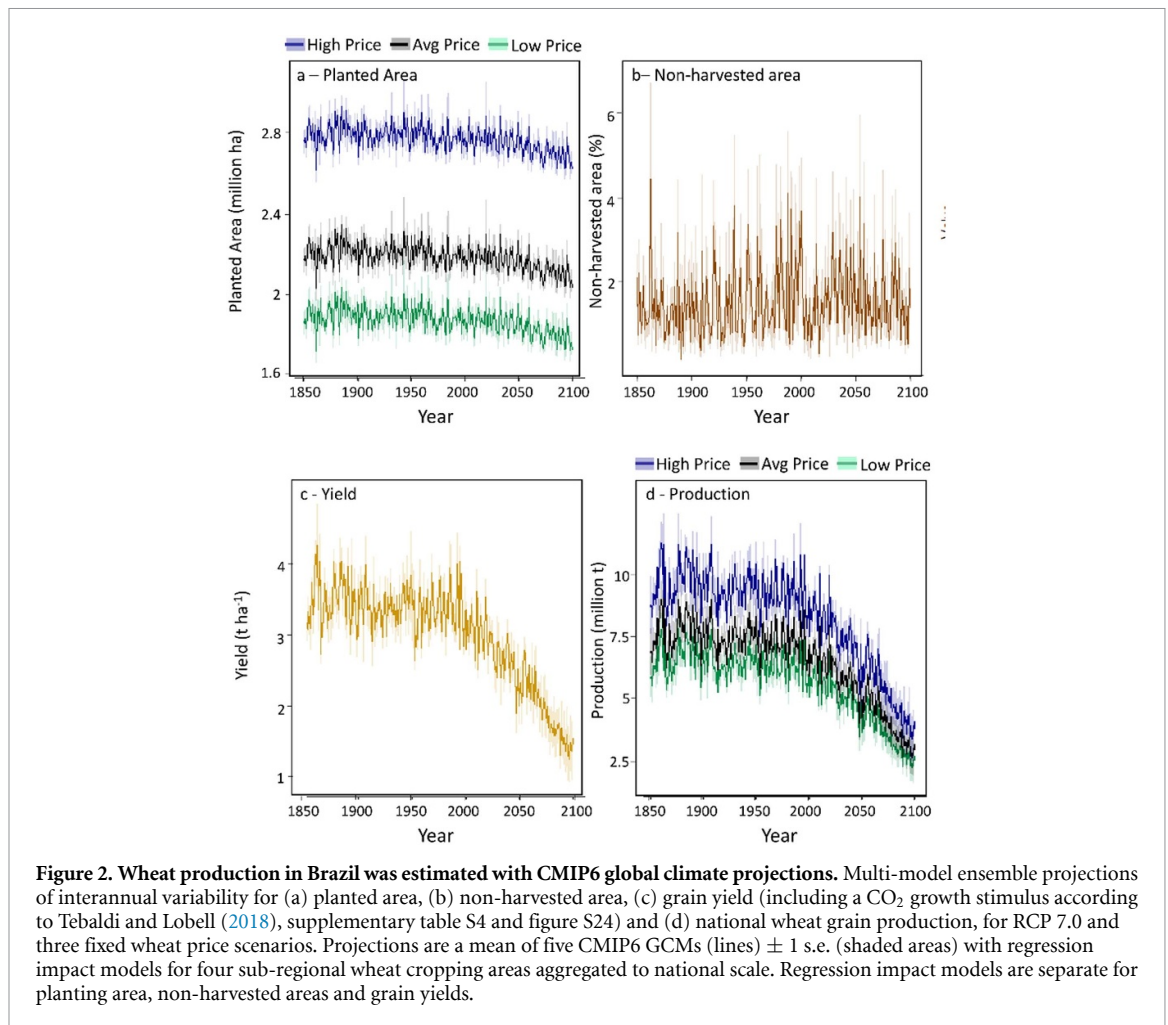


Figure 1. Observed and estimated wheat production in Brazil. Interannual variability from 2001–2020 of observed (black solid lines) and estimated (red dashed lines) (a) planted area, (b) non-harvested area, trend-corrected (c) national grain yield and (d) national grain production. (e) Trend-corrected spatial variability of the observed 2006 wheat yield anomaly. Results for individual regions are shown in supplementary figures S8–S11.

(figures 1(a)–(d), supplementary table S3). In 2006, observed low planting incentives due to low wheat prices before the cropping season and a drought during April and May, the main wheat planting period, reduced the wheat crop area by 15% (figure 1(a) and supplementary figure S5). In addition, frost damage and a drought in early spring destroyed wheat on about 12% of the cropping area (figure 1(b)). An additional drought during winter combined with low temperatures in early spring (during grain filling) reduced the remaining wheat grain yield in average by 23% (figure 1(c)), with some regional yields dropping by 50% (figure 1(e)). This compound of negative events in 2006 caused wheat production in Brazil to drop by 46%, the lowest production recorded in the last 20 years (figure 1(d)), resulting in a 60% increase of wheat price and one of the largest wheat imports in the following year (CEPEA 2020, FAO 2021).

Wheat farms in Brazil are mostly family-owned with an average size of 47 ha. The wheat planting area in Brazil is pre-determined by farmers' expectations from market signals and weather conditions during the planting period in April and May. Initially, planting decisions are driven by the wheat price before the crop season (supplementary table S2, figures S8–S11), and in the two regions, in Paraná state (Group II and III, supplementary figure S3), also by maize prices (supplementary figure S7). Subsequently, low or excessive rainfall during the planting season can further influence the decision to limit the wheat planting area (supplementary table S2, supplementary figure S20). As a result, the wheat planted area in Brazil as a whole varied by up to 0.9 million ha each year, 45% of the average 2 million ha planted yearly since 2001 (figure 1(a)). The national non-harvested area has been as large as 12% (figure 1(b)) and average

national trend-corrected yields have been ranging from 3.2 t ha^{-1} down to 2.0 t ha^{-1} (figure 1(c)), which contribute to variation in national wheat production of between 3.0 and 7.5 million t year^{-1} from 2001 to 2019 (figures 1(d) and (e)). Given the ability of the multi-regression impact models in estimating planted area, non-harvested area, trend-corrected grain yield, and national production in the last two decades (figures 1(a)–(d)), we extended the analysis with long-term climate change scenarios from the recent CMIP6 ensemble for the period 1850–2100, thus considering retrospective and prospective components of climate trends. Results indicated that the wheat planted area varies from year to year, with notably more planted area when wheat prices are above average (figure 2(a)). The wheat planted area is projected to decline after 2020 because of a projected increase of up to 70% of drought events frequency during April to May, affecting wheat planting (supplementary tables S1–S2, and figures S20–S22). The projected non-harvested area fluctuates widely without a clear trend between 1% and 6% from 1850 to 2100 (figure 2(b)), with historical (1850–2000) wheat planted area losses mostly caused by frost, changing to future losses due to frequent heat, drought and excess water from high rainfall events (supplementary S21 and S22). The projected national mean yield varies between 1 to 4 t ha^{-1} with a steep declining trend after 2020 (figure 2(c)). This is mostly due to the projected future increase of up to $3 \text{ }^{\circ}\text{C}$ of maximum monthly mean temperature during wheat flowering and grain filling in July and August, on top of an already warm climate with relatively low yields, leading to heat stress and drought, further reducing grain yields (supplementary figures S20–S22) and despite the projected increase in atmospheric



CO₂ concentration stimulating crop growth and yield (supplementary figure S24). Asseng *et al* (2017) have suggested a linear decline in absolute wheat grain yield with increasing seasonal temperatures above 20 °C, which means that the absolute yield decline is larger in warm wheat cropping regions, such as Brazil. The projected decline of wheat yields in Brazil tend to be higher than wheat yield impacts reported in other regions of the world with lower base temperatures and higher yield levels (Rosenzweig *et al* 2014, Webber *et al* 2018, Liu *et al* 2019). Estimated wheat grain yield decreases by 48 (1.5%), 75 (3.3%) and 83 (3.5%) kg ha⁻¹ decade⁻¹ (supplementary figure S18) for Representative Concentration Pathway (RCP) 2.6, RCP 7.0, and RCP 8.5, respectively (supplementary figure S16) which would result in 20%, 50%, and 60% lower grain yields by 2100 (compared to the 1850–2020 period), assuming no adaptation is undertaken. When the projected wheat planted areas and non-harvested areas are combined in the model with projected grain yield, the national wheat production of Brazil is relatively stable under the past climate (1850–2000), but declines with climate change from 2000 onwards, regardless of commodity price signals (figure 2(d)), and again assuming there is no adaptation.

National wheat production at an average wheat price continues to decrease until 2100 by 110 000 t decade⁻¹ (1.5%) under RCP 2.6 and by about 180 000 t decade⁻¹ (2.5%) under RCP 7.0 and RCP 8.5 (figure 3). The effect of this would be an up to 60% production loss by 2100 compared to mean of the historical period 1850–2020 (supplementary figure S16), in agreement with a recent study that indicates a future decline of suitable areas for wheat in south of Brazil by up to 59% (Santi *et al* 2018). In addition, the interannual variability in national wheat production is projected to increase toward 2100 under RCP 7.0 and 8.5 (supplementary figure S19). In these scenarios, wheat production in Brazil would become more unstable and more variable before the end of the century.

Extreme low wheat production years are statistically defined as the 5th percentile of occurrence (Vogel *et al* 2021) of simulated wheat production during 1850–2020, with a low wheat price scenario, thus with a probability which occurred once every 20 years in the past. The frequency of extreme low wheat production years is projected to increase by the end of the century, regardless of RCP or wheat price (figure 4). However, extreme poor wheat harvests are projected to become even more frequent under high RCPs

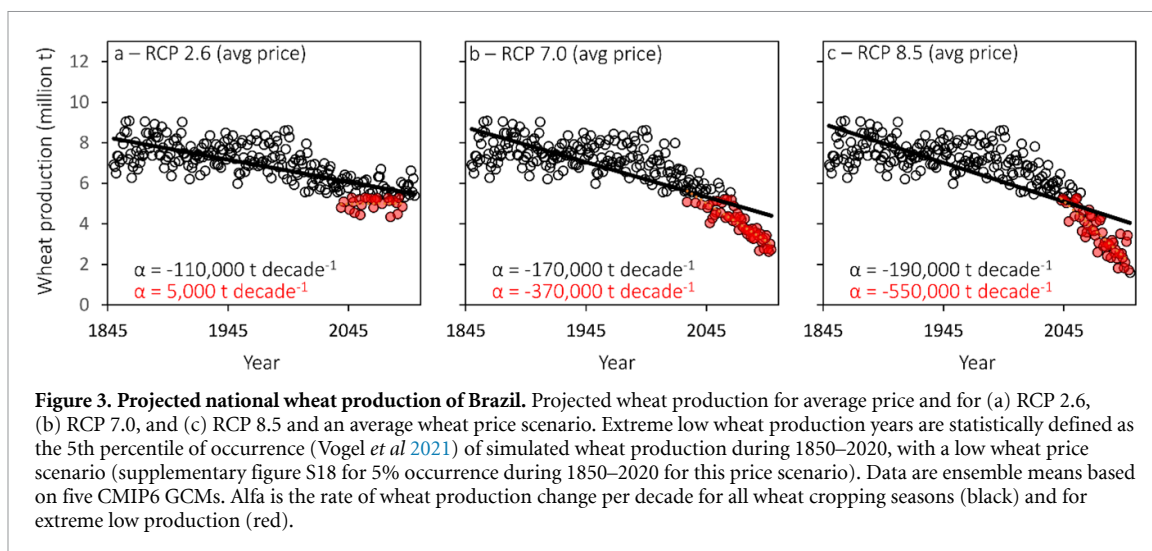


Figure 3. Projected national wheat production of Brazil. Projected wheat production for average price and for (a) RCP 2.6, (b) RCP 7.0, and (c) RCP 8.5 and an average wheat price scenario. Extreme low wheat production years are statistically defined as the 5th percentile of occurrence (Vogel *et al* 2021) of simulated wheat production during 1850–2020, with a low wheat price scenario (supplementary figure S18 for 5% occurrence during 1850–2020 for this price scenario). Data are ensemble means based on five CMIP6 GCMs. Alfa is the rate of wheat production change per decade for all wheat cropping seasons (black) and for extreme low production (red).

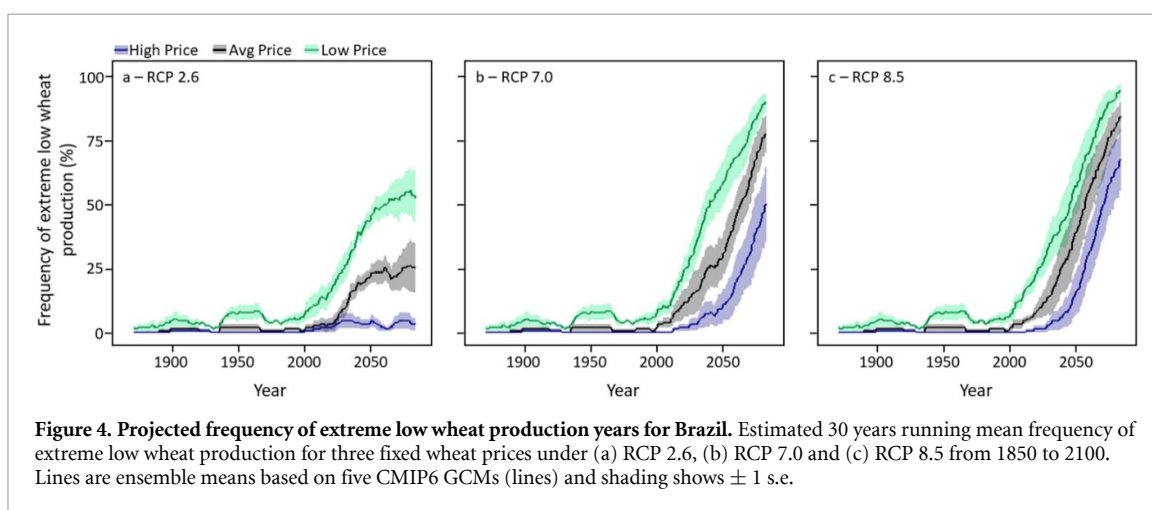


Figure 4. Projected frequency of extreme low wheat production years for Brazil. Estimated 30 years running mean frequency of extreme low wheat production for three fixed wheat prices under (a) RCP 2.6, (b) RCP 7.0 and (c) RCP 8.5 from 1850 to 2100. Lines are ensemble means based on five CMIP6 GCMs (lines) and shading shows ± 1 s.e.

and are magnified by low wheat price, and in northern wheat producing regions, also by a high maize price. For example, in the decades 2070–2100, the projections show the yearly frequency of extreme low wheat production at a national level reaches 70% when wheat prices are high, but reaches 90%, an increase of more than 15-fold, when wheat prices are low under RCP 8.5 (figures 4 and supplementary figure S17).

Extreme low production years are thus projected to become the norm in Brazil by 2100. This has parallels with future projections that extreme heatwaves in Europe (Robine *et al* 2008), as experienced in 2003, will become the norm for Europe by 2100 (Battisti and Naylor 2009). Recently reported extreme low production of wheat in France and Europe, of beans in Brazil and of maize at national to global scales (Trnka *et al* 2014, Ben-Ari *et al* 2018, Zampieri *et al* 2019, Antolin *et al* 2021) are likely to become also more frequent in the future. Indeed, the unprecedented drop in wheat production of over 30% in 2016 in France, the fifth largest wheat producer in the world, came as a total surprise to forecasters because of the unexpected impact of a combination of extreme weather

events, namely warmer early winter temperatures that enabled disease spread, followed by heavy spring rainfall, waterlogging, nutrient leaching and more diseases (Ben-Ari *et al* 2018). A similar compound of extreme events, with increased drought events during the planting season, drought and heat during wheat flowering and grain filling together with high rainfalls during the wheat harvest period, causing production wheat grain losses has been observed and predicted here with the multiple regression models for Brazil, which directly account for the impact of extreme high and low temperature and variations in rainfall, while indirectly considering effects of excess water, nutrient leaching, and disease damage. The magnitude of recently experienced extreme production losses in 2006 in Brazil and the projections of extreme low production years are in stark contrast to previous climate impact studies which have largely focused on average climate change effects, essentially from increased heat and drought, with smaller yield losses and occasionally small increases computed, such as a global mean change of +1.7% for wheat (−4.5% to +3%, lower to upper quartile), of −5.8% for maize (−16%–0%, lower to upper quartile) by 2070–2100 (Rosenzweig

et al 2014), and for Brazil, a national wheat production change of -5% (Liu *et al* 2019).

While the increased frequency of extreme lows in crop production will be a challenge for food supply, our projections further suggest that the magnitude of the shortfalls will increase, that is, the extremes will become more extreme. For example, the projections indicate that the volume of wheat harvested in Brazil in extreme low production years, when the wheat price is low, would decline from 2020 onwards by 44 000 t decade⁻¹ under RCP 2.6, and by 230 000 and 300 000 t decade⁻¹ under RCP 7.0 and RCP 8.5, respectively (supplementary figure S18). That means, the extreme years will become even lower in wheat production than the extreme low production years in the past.

Extreme lows in a country's wheat production, as occurred in 2006 in Brazil, impact national food security and can also have implications for global food security. For example, simultaneous wheat production failures in several exporting countries in 2008 contributed to food riots across the world (IMF 2008). And, the heatwave in Russia in 2010 destroyed one third of its national wheat production, leading to a ban on wheat export to other countries, contributing to a 50% spike in the global wheat price (FAO 2021) that is suggested to as a consequence have sparked unrest in Northern Africa (Perez 2013). A heatwave in Egypt, the largest wheat importer in the world, in the same year experienced depressed national wheat production by 13% (Asseng *et al* 2018) and this decline might also have added to the unrest in Egypt in the following year. These recent food crises demonstrate the sensitivity of global food security to extreme low crop production wherever it occurs. From 1964 to 2007, extreme drought and heat waves reduced global cereal production by up to 10% in some years (Lesk *et al* 2016), mostly affecting poor regions (FAO, IFAD, UNICEF, WFP and WHO 2018, Verschuur *et al* 2021). The per capita gross domestic income of Brazil, as well as that of Central Africa and India, has decreased by almost 20% due to recent global warming, accentuating global economic inequality (Diffenbaugh and Burke 2019). As extreme events from climate change increase, whether single events like heat and drought, or combinations of detrimental impacts from frost, excess water, and disease spread together with heat or drought occur, the frequency of extreme low crop production years will increase in the future. This will threaten Brazil's and many other countries progress toward food security and abolishing hunger.

Our results highlight a steep decline in wheat production in Brazil with a sharp increase with extreme low wheat production years. Alternative crops like sugar-cane, maize and pasture might be better suited to a warmer climate and an increase in these crops has been noted in recent years in south of Brazil (Conab 2020, Zilli *et al* 2020). The introduction of

irrigation could be another adaptation to a changing rainfall pattern and a warmer climate (for crop cooling through increased transpiration), but would be costly or might not be feasible due to lack of water resources in some areas. However, in Central Brazil, recent public and private investments have started to expand wheat production with irrigation (Pereira *et al* 2019). To assist farmers to cope with an increase in extreme low crop production seasons, crop insurance could also become an option, but usually requires government subsidies to be affordable (Mahul and Stutley 2010).

1. Methods

Wheat planted area, non-harvested area, trend-corrected yield and production from 776 municipalities (IBGE 2020) representing 90% of Brazilian wheat production were used in a multi-model regression analysis (supplementary figure S2). Yield anomalies (Y_{ann} , supplementary figure S4) were computed as the percent difference between observed (Y_{obs}) and average (Y_{avg}) trend-corrected yield divide by Y_{avg} :

$$Y_{\text{ann}} = \frac{Y_{\text{obs}} - Y_{\text{avg}}}{Y_{\text{avg}}} \times 100. \quad (1)$$

Using yield anomalies, a hierarchical clustering analysis was performed across the municipalities and the 19 years from 2001 to 2019. As a result, four main wheat regions (Group I–IV) were defined based on their agroclimatic conditions (Scheeren *et al* 2008) (supplementary figure S3). Monthly maximum and minimum temperatures and accumulated rainfall recorded by National Institute of Meteorology (INMET 2021) from weather stations, from each of the four regions (supplementary table S5), thus assuming each group to represent similar climates (Scheeren *et al* 2008). Wheat prices, and for two regions wheat and maize prices, before the wheat cropping season were used to estimate wheat planted area. The commodity price data used were from 2005 to 2019 (CEPEA 2020). Wheat and maize prices for 2001–2004 were reconstructed with a regression relating international to domestic prices.

Statistical models were developed separately for each of the four main wheat-producing regions in Brazil. Statistical models for each region were developed for wheat planted area, non-harvested wheat area and wheat grain trend-corrected yield with municipality-based observations from 2001 to 2019, together with monthly seasonal climate records and commodity prices (before planting) (supplementary table S2). A recently suggested stepwise selection procedure for quantifying extreme crop yields (Ben-Ari *et al* 2018) was applied to identify the best combination of input variables using R (Version 4.0.3) (supplementary figure S1, supplementary figures S8–S11 and supplementary tables S2–S3). Similar results were obtained with the least absolute shrinkage

and operator method suggested by Vogel *et al* (2021) as an alternative statistical approach (supplementary figure S23).

Monthly climate data from five CMIP6 global climate models (GCMs) for 1850–2100 were used to estimate the wheat planted area, non-harvested wheat area and wheat yield for each group, under RCP 2.6, RCP 4.5, and RCP 8.5 future scenarios (CMIP6 2020). A CO₂ growth stimulus effect on yield was included based on Tebaldi and Lobell (2018) (supplementary table S4 and supplementary figure S24). The wheat harvested area was calculated from the difference between planted and non-harvested wheat area. Wheat production was estimated by multiplying the estimated yield with harvested area. Three contrasting wheat price scenarios were applied. The high, average and low wheat prices are from a combination of the highest, average and lowest recorded wheat and wheat/maize ratio price during 2001–2019. All estimated group results were aggregated to estimate national production.

Extreme low national wheat production was estimated for each GCM separately and defined as the 5th percentile (Vogel *et al* 2021) wheat production during 1850–2020 (which as a 5% frequency is equivalent to once every 20 years), a period when all RCPs were similar and using the low national wheat price from the reference period 2001–2020.

Data availability statement

The data that support the findings of this study are available upon reasonable request from the authors.

Author contributions


RSNJ and SA conceptualized the study, all co-authors contributed to the methodology, RSNJ developed the statistical models and analyzed data, ACR assisted with climate data, TBA assisted with statistical models and statistical analysis, RF assisted with economic analysis, all co-authors contributed to data evaluation and interpretation, RSNJ wrote initial draft, all co-authors assisted with writing and reviewed the manuscript.

Conflict of interest


The authors declare no competing interests.

ORCID iDs

Rog6rio de Souza N6ia J6nior 
<https://orcid.org/0000-0002-4096-7588>

Pierre Martre 
<https://orcid.org/0000-0002-7419-6558>

Marijn van der Velde 
<https://orcid.org/0000-0002-9103-7081>

Alex C Ruane 
<https://orcid.org/0000-0002-5582-9217>

Senthold Asseng 
<https://orcid.org/0000-0002-7583-3811>

References

- Antolin L A S, Heinemann A B and Marin F R 2021 Impact assessment of common bean availability in Brazil under climate change scenarios *Agric. Syst.* **191** 103174
- Asseng S, Cammarano D, Basso B, Chung U, Alderman P D, Sonder K, Reynolds M and Lobell D B 2017 Hot spots of wheat yield decline with rising temperatures *Glob. Chang. Biol.* **23** 2464–72
- Asseng S, Kheir A M S, Kassie B T, Hoogenboom G, Abdelaal A I N, Haman D Z and Ruane A C 2018 Can Egypt become self-sufficient in wheat? *Environ. Res. Lett.* **13** 094012
- Battisti D S and Naylor R L 2009 Historical warnings of future food insecurity with unprecedented seasonal heat *Science* **323** 240–4
- Ben-Ari T, Bo6 J, Ciais P, Lecerf R, van der Velde M and Makowski D 2018 Causes and implications of the unforeseen 2016 extreme yield loss in the breadbasket of France *Nat. Commun.* **9** 1627
- CEPEA 2020 Center for Advanced Studies on Applied Economics: *Agric. Ser.* (www.cepea.esalq.usp.br/en) (Accessed 05 November 2020)
- CMIP6 2020 WCRP Coupled Model Intercomparison Project Model output from the coupled model intercomparison project phase 6 (available at: <https://pcmdi.llnl.gov/index.html>) (Accessed 05 July 2020)
- Conab 2020 National supply company Agricultural Information System (available at: <https://portaldeinformacoes.conab.gov.br/index.php/safra/safra-serie-historica>) (Accessed 5 November 2020)
- Diffenbaugh N S and Burke M 2019 Global warming has increased global economic inequality *Proc. Natl Acad. Sci.* **116** 9808–13
- FAO, IFAD, UNICEF, WFP and WHO 2018 *The State of Food Security and Nutrition in the World Building climate resilience for food security and nutrition* (Rome: FAO) 181
- FAO 2021 FAOSTAT FAO statistical databases (available at: www.fao.org/faostat/en/#home) (Accessed 10 February 2021)
- FAO 2021 FAOSTAT Statistical Database
- IBGE 2020 Brazilian Institute of Geography and Statistics: *Munic. Agric. Res.* (<https://sidra.ibge.gov.br/home/ipca/brasil>) (Accessed 01 October 2020)
- IMF 2008 *International Monetary Fund: Food and Fuel Prices: Recent Developments, Macroeconomic Impact, and Policy Responses* (Washington, DC)
- INMET 2021 National Institute of Meteorology: *Weather Stations Data* (<https://mapas.inmet.gov.br/>) (Accessed 13 January 2021)
- Lesk C, Rowhani P and Ramankutty N 2016 Influence of extreme weather disasters on global crop production *Nature* **529** 84–87
- Liu B *et al* 2019 Global wheat production with 1.5 and 2.0 °C above pre-industrial warming *Glob. Chang. Biol.* **25** 1428–44
- Mahul O and Stutley C J 2010 *Government Support to Agricultural Insurance: Challenges and Options for Developing Countries* (Washington, DC: World Bank)
- Pereira J F, da Cunha G R and Moresco E R 2019 Improved drought tolerance in wheat is required to unlock the production potential of the Brazilian Cerrado *Crop Breed. Appl. Biotechnol.* **19** 217–25
- Perez I 2013 *Sci. Am. Sustain.* (<https://www.scientificamerican.com/article/climate-change-and-rising-food-prices-heightened-arab-spring/>) (Accessed 10 February 2021)
- Raymond C *et al* 2020 Understanding and managing connected extreme events *Nat. Clim. Chang.* **10** 611–21

- Robine J-M, Cheung S L K, Le Roy S, van Oyen H, Griffiths C, Michel J-P and Herrmann F R 2008 Death toll exceeded 70 000 in Europe during the summer of 2003 *C.R. Biol* **331** 171–8
- Rosenzweig C et al 2014 Assessing agricultural risks of climate change in the 21st century in a global gridded crop model intercomparison *Proc. Natl Acad. Sci.* **111** 3268–73
- Santi A, Vicari M B, Pandolfo C, Dalmago G A, Massignam A M and Pasinato A 2018 Impacto de cen6rios futuros de clima no zoneamento agroclim6tico do trigo na regi6o Sul do Brasil *Agrometeoros* **25** 303–11
- Scheeren P L et al 2008 Challenges to wheat production in Brazil *Challenges to International Wheat Breeding* (Mexico: CIMMYT) 167–70
- Tebaldi C and Lobell D 2018 Estimated impacts of emission reductions on wheat and maize crops *Clim. Change* **146** 533–45
- Trnka M, R6tter R P, Ruiz-Ramos M, Kersebaum K C, Olesen J E, Źalud Z and Semenov M A 2014 Adverse weather conditions for European wheat production will become more frequent with climate change *Nat. Clim. Chang.* **4** 637–43
- Verschuur J, Li S, Wolski P and Otto F E L 2021 Climate change as a driver of food insecurity in the 2007 Lesotho-South Africa drought *Sci. Rep.* **11** 3852
- Vogel J, Rivoire P, Deidda C, Rahimi L, Sauter C A, Tschumi E, van der Wiel K, Zhang T and Zscheischler J 2021 Identifying meteorological drivers of extreme impacts: an application to simulated crop yields *Earth Syst. Dyn.* **12** 151–72
- Webber H et al 2018 Diverging importance of drought stress for maize and winter wheat in Europe *Nat. Commun.* **9** 4249
- Wheeler T and von Braun J 2013 Climate change impacts on global food security *Science* **341** 508–13
- Zampieri M, Ceglar A, Dentener F, Dosio A, Naumann G, Berg M and Toreti A 2019 When will current climate extremes affecting maize production become the norm? *Earth's Future* **7** 113–22
- Zilli M, Scarabello M, Soterroni A C, Valin H, Mosnier A, Lecl6re D, Havl6k P, Kraxner F, Lopes M A and Ramos F M 2020 The impact of climate change on Brazil's agriculture *Sci. Total Environ.* **740** 139384

Supplementary materials for

Extreme lows of wheat production in Brazil

Rogério de Souza Nóia Júnior, Pierre Martre, Robert Finger, Marijn van der Velde, Tamara Ben-

Ari, Frank Ewert, Heidi Webber, Alex C. Ruane, Senthold Asseng

Table of Contents

Extreme lows of wheat production in Brazil	1
Supplementary Methods	3
Supplementary Text	4
Wheat farming in Brazil	4
Wheat imports and wheat price fluctuation in Brazil.....	4
2017 wheat growing season	4
Possible expansion of wheat production in Brazil	5
Supplementary Tables	6
Table S1. Variables used for modeling wheat planted area, non-harvested area and yield.	6
Table S2. Description of cropping seasons diagnoses in Brazil.	7
Table S3. Multiple linear regression models for estimating planted area, area non-harvested and grain yield in Brazil. Variables are defined in Supplementary Table S1.	8
Table S4. CO2 fertilization effects for C3 crops, according to experiments performed with the DSSAT4 model.	9
Table S5. Geographical coordinates of the weather stations within each group	10
Supplementary Figures	11
Figure S1. Flowchart of the procedures for estimating national wheat production.....	11
Figure S2. Observed spatio-temporal variations of wheat cropping area in Brazil.....	12
Figure S3. Observed spatio-temporal contribution of wheat production regions in Brazil.	13
Figure S4. Observed spatio-temporal pattern of wheat yield anomaly in Brazil.	14
Figure S5. The observed 2006 wheat grain yield anomaly in Brazil.	15
Figure S6. The observed 2017 wheat grain yield anomaly in Brazil.	16
Figure S7. Observed off-season maize and wheat in Brazil.....	17

Figure S8. Multiple linear regression model performance for estimating wheat production in Group I.	18
Figure S9. Multiple linear regression model performance for estimating wheat production in Group II.	19
Figure S10. Multiple linear regression model performance for estimating wheat production in Group III.	20
Figure S11. Multiple linear regression model performance for estimating wheat production in Group IV.	21
Figure S12. Estimated wheat production in Group I.	22
Figure S13. Estimated wheat production in Group II.	23
Figure S14. Estimated wheat production in Group III.	24
Figure S15. Estimated wheat production in Group IV.	25
Figure S16. Projected changes in wheat production over the 1850-2020 historical period in Brazil.....	26
Figure S17. Projected change in frequency of extreme low wheat production over 1850-2020 historical period in Brazil.	27
Figure S18. Projected wheat yield and production over time.....	28
Figure S19. Projected variability of low wheat production in Brazil.	29
Figure S20. Pearson’s correlations for monthly climatic variables and wheat planted area, non-harvested area, yield, production and extreme low production in the different groups.	30
Figure S21. Climate Characterization.....	31
Figure S22. Climatic events.	32
Figure S23. Projected frequency of extreme low national wheat production of Brazil using the Lasso method.....	33
Figure S24. Global atmospheric CO2 concentration projections for RCP 2.6, RCP 7.0 and RCP 8.5.	34
Figure S25. Wheat expansion production towards Central Brazil.....	35
References	36

Supplementary Methods

Brazil's wheat production was divided into three components: wheat planted area, non-harvested area and yield.

The planting area in Brazil is affected by the wheat price, and in two regions by the relation between wheat and maize price (Group II and III, Supplementary Fig S3 and Fig S7). The wheat planted area was estimated by combining two linear equations (Supplementary Table S2). The first one calculated the planted area determined by wheat or wheat/maize ratio price ($Area_{Price}$) as a linear relation between planted area and commodity grain prices in October and November of the previous year. The second one calculates planting area as determined by weather conditions in the previous and during planting months ($Area_{Climate}$) as a multiple linear regression between the residuals of the $Area_{Price}$ equation and the climatic variables of April, May and June (sowing period, Supplementary Table S2). The planted area was estimated by combining the result of both equations (i.e. sum of the results of $Area_{Price}$ and $Area_{Climate}$ equations).

The wheat non-harvested areas and yield, are affected by adverse weather condition during wheat flowering and grain filling (see more details in Supplementary, Table S2). We therefore selected the climatic variables that historically affect the wheat planted area, non-harvested area and yield in Brazil. We used stepwise method for an automatic selection of meteorological variables that are linked with inter-annual variability of wheat planted area, non-harvested area and grain yield in Brazil.

Supplementary Text

Wheat farming in Brazil

Brazil produces less than 1% of the wheat produced in the world, but is the seventh largest importer in the world (1). Wheat cultivation in southern Brazil is rainfed, and characterized by no-till farming. Wheat is preceded by a summer crop, mostly soybean. Wheat is usually sown between April and July. The wheat season from sowing to harvest is about 100 to 170 days, with harvesting usually occurring between August and November. The majority of farmers who cultivate wheat are technically advanced, acquire specific seeds for the region, use fertilizers, and try to control common pest and diseases (2). Average wheat farm size is 47 ha (3). Main challenges include adverse weather, incidence of diseases such as wheat blast and wheat powdery mildew and emerging new pest and diseases, and poor economic returns (2).

Wheat imports and wheat price fluctuation in Brazil

In Brazil, the prevalence of undernourished people has been increasing since 2013, reaching 10 million (~5%) in 2018 (4). Wheat is an important component of the Brazilian diet, but the national wheat production covers <60% of domestic demand (5). The dependence on imported wheat makes the bread price dependent on international currency exchange rate variations. For example, the coronavirus pandemic caused the Brazilian Real to drop in relation to dollar, resulting in the price of bread to increase by 120% in some Brazilian regions exposing parts of the population to additional food insecurity (6).

The increase in wheat price stimulates increasing wheat planted areas as farmers benefit from high wheat prices. However, consumers would experience a simultaneous decline in real wages in the short run, which can lead to food insecurity.

On the other hand, a decline of wheat price before the wheat-cropping season discourages farmers to plant wheat, leading to a reduced wheat planted area. In these years, the wheat production declines, but can in two of the regions lead to an increase in maize production (2) (Supplementary Fig S7).

2017 wheat growing season

Another low national wheat producing year during 2001 and 2020 occurred in Brazil in 2017, when unusually high temperatures combined with a prolonged drought during the grain filling period in spring, reduced the national wheat production by about 30% (Supplementary Fig. S6 and Supplementary Table S2), followed by an increase in wheat imports in the following year (1).

Possible expansion of wheat production in Brazil

To become self-sufficient in wheat, Brazil has directed research and development to expand wheat production to Central Brazil, a region well known for the production of other important commodities such as cotton, soybean and maize. This area expansion could increase the national wheat production by several folds if successful (7). Currently, the largest expansion of wheat production occurs in the state of Minas Gerais, where production has increased by 250% in the last 10 years (Supplementary Fig S25). However, to unlock the wheat production in this area improved wheat cultivars with drought tolerance is needed (8).

Supplementary Tables

Table S1. Variables used for modeling wheat planted area, non-harvested area and yield.

Name	Unit	Description
Rain	mm	Monthly accumulated rainfall
Tmax	°C	Mean monthly maximum air temperature
Tmin	°C	Mean monthly minimum air temperature
Htemp	days	Number of days in a month with maximum air temperature above 32°C
Ltemp	days	Number of days in a month with minimum air temperature below 2°C
Drought	counts	Ten consecutive days with no rainfall; the periods are counted for multiples of 10, i.e. 20 consecutive days with no rainfall is equivalent to 2 drought periods.
HRain	days	Number of days with rainfall above 30 mm
Rainy days	days	Number of days with rainfall above 0.1 mm

Table S2. Description of cropping seasons diagnoses in Brazil. The description is based on technical literature, extension service and expertise magazines. Variables are defined in Supplementary Table S1.

Estimated variables	Variables that are historically involved with wheat production variability in Brazil	Variables selected for statistical models
Planted Area	<p>The decision to sow wheat or not is usually based on wheat price before the soybean cropping season (i.e. September-November), when the farmers buy the inputs for the next cropping season. Also, during this period the farmers are selling part of the wheat harvest, thus low wheat selling price and poor returns can discourage the farmers for the next cropping season.</p> <p>In some locations of Paraná State (i.e. Northern Brazilian wheat producing regions, Groups II and III in this study; Supplementary Fig. S7), the wheat compete for area with the off-season maize. And, in these regions, the decision of which crop will be sown is based on the comparison of wheat and maize prices.</p> <p>The planted area can also be affected by weather conditions in the previous and during planting months:</p> <ul style="list-style-type: none"> • 2006: The national wheat planted area decreased by 15% because of very poor returns of 2005 wheat growing season and low wheat price, and dry conditions at planting that forced many producers to opt for other crops or fallow (9, 10). • 2012: The wheat planted area reduced by 11% because of a drought in the State of Rio Grande do Sul in the South Region (Group I) (11). • 2017: The wheat planted area reduced by 12% because of excessive volume of rainfall in April and May and the low prices of wheat before sowing (12). <p>Also, some farmers wait for the temperature to reach 15-20°C, to plant wheat, consequently temperature out of this range during the planting period can delay planting and make farmers opt other crops (13).</p>	<p>First, the wheat planted area of each group was linearly correlated with wheat price or wheat/maize ratio price.</p> <ul style="list-style-type: none"> • Group I and IV: Wheat price in October of the previous year (*). • Group II and III: Wheat/maize price ratio in November of the previous year (**). <p>The residuals of the above-mentioned relation were correlated with seasonal monthly climate variables (Rain, Tmax, Tmin, Htemp, Ltemp, Hrain, Drought and Rainy days).</p> <ul style="list-style-type: none"> • Group I and IV: The seasonal monthly variables were from May to June. • Group II and III: The seasonal monthly variables were from April to May.
	Non-harvested area	<p>Extreme weather events, particularly frost and drought, can destroy the wheat planted area in Brazil. The crops areas are then not harvested and are named “non-harvested areas”.</p> <ul style="list-style-type: none"> • 2006: The national non-harvested area was about 12% because of a combination of drought and hard frosts at the end of August and September in the major production area of Rio Grande do Sul and Paraná (9, 10) (Groups I, II and III). • 2013: The national non-harvested area was about 7% because of high relative humidity in July favored the development of crop diseases and the crops were then more susceptible to the hard frosts in August. Due to these conditions, some farmers opted to not harvesting more than 90% area planted with wheat, leaving it as straw for the summer crop (14). <p>The drought and frost effects are enhanced when they occur in combination with other events such as extremely heavy rainfall and high temperatures.</p>
Yield	<p>The occurrence of adverse climatic events between June and September are the main cause of wheat yield lost in Brazil.</p> <ul style="list-style-type: none"> • 2006: The national yield dropped by 15% because of a combination of factors. The dry conditions during the planting period, caused the planting of wheat to occur late, which reduced the potential yield of the crop. The yield was also affected by a combination of drought and hard frosts at the end of August and September (9, 10). • 2015: Wheat yield drastically drop in Santa Catarina state and in some parts of Rio Grande do Sul and Paraná (Group IV). The yield drop in Santa Catarina was about 40%. The El Nino phenomenon caused excessive rainfall in the region, increasing the relative humidity. The high relative humidity greatly increased the incidence of foliar diseases, harming the yield. The high relative humidity also increased the production costs due to a 70% increase in fungicide applications (15). • 2017: The national yield dropped by 36% from the country’s 2016 wheat output because of drought and frost conditions during critical development stages of the crop. The drought occurred in June, July, September and October and its effects were magnified by extremely high temperatures (12, 16, 17). 	<p>Seasonal monthly variables used: Rain, Tmax, Tmin, Tmean, Htemp, Ltemp, Hrain, Drought and Rainy days.</p> <ul style="list-style-type: none"> • Group I and IV: The seasonal monthly variables were from June to October. • Group II and III: The seasonal monthly variables were from May to September.

2 (*) and (**) - The month selection was based on the one with the highest correlation coefficient between wheat planted area and commodity price. The
3 selected months were those when farmers are selling the wheat harvest and are preparing soybean plantings, buying the inputs for the entire cropping season.
4 (**) In these regions, wheat competes by area with off-season maize (Supplementary Fig. S7).

Table S3. Multiple linear regression models for estimating planted area, area non-harvested and grain yield in Brazil. Variables are defined in Supplementary Table S1.

Group	Variable	Equation	P-value	RMSE
Group I	Area _{Price}	$531033 + 997 \text{ Wheat}_{\text{Price}}$	0.02	-
	Area _{Climate}	$88359 + 151167 \text{ Drought}_{\text{Jun}} - 8902 \text{ Rainy Days}_{\text{May}}$	0.03	175684 ha (23%)
	Area _{non-harvested}	$-0.01 + 0.16 \text{ Drought}_{\text{Oct}} - 0.08 \text{ Htemp}_{\text{Sep}} + 0.002 \text{ Ltemp}_{\text{Jun}} + 0.01 \text{ Drought}_{\text{Sep}} + 0.003 \text{ Drought}_{\text{Aug}} + 0.002 \text{ Hrain}_{\text{Jun}} + 0.001 \text{ Hrain}_{\text{Sep}}$	< 0.0005	5%
	Yield	$2.1 + 0.04 \text{ Tmax}_{\text{Aug}} + 0.05 \text{ Ltemp}_{\text{Jul}} - 0.4 \text{ Ltemp}_{\text{Oct}} - 0.07 \text{ Tmean}_{\text{Oct}} - 0.0009 \text{ Rain}_{\text{Sep}} + 0.03 \text{ Hrain}_{\text{Aug}} - 0.06 \text{ Hrain}_{\text{Aug}} + 0.009 \text{ Tmin}_{\text{Sep}} - 0.04 \text{ Ltemp}_{\text{May}} - 0.06 \text{ Tmean}_{\text{Jun}} + 0.03 \text{ Hrain}_{\text{May}} - 0.06 \text{ Tmin}_{\text{Aug}} - 0.04 \text{ Htemp}_{\text{Oct}} - 0.01 \text{ Ltemp}_{\text{Jun}} - 0.004 \text{ Rainy Days}_{\text{Sep}}$	< 0.0005	0.4 t ha ⁻¹ (15%)
Group II	Area _{Price}	$251872 + 173992 \text{ Wheat}_{\text{Price}}/\text{Maize}_{\text{Price}}$	0.03	-
	Area _{Climate}	$-142767 + 12279 \text{ Rainy}_{\text{April+May}} - 27781 \text{ Hrain}_{\text{May}}$	< 0.0005	92051 ha (19%)
	Area _{non-harvested}	$-0.04 + 0.04 \text{ Drought}_{\text{May}} + 0.03 \text{ Drought}_{\text{Aug}} - 0.05 \text{ Hrain}_{\text{Jun}} - 0.04 \text{ Hrain}_{\text{Jul}} - 0.02 \text{ Hrain}_{\text{Aug}} + 0.02 \text{ Drought}_{\text{Jun}} + 0.02 \text{ Hrain}_{\text{Sep}} - 0.01 \text{ Htemp}_{\text{Aug}}$	0.005	12%
	Yield	$-0.9 + 0.06 \text{ Drought}_{\text{Sep}} - 0.15 \text{ Ltemp}_{\text{Jul}} + 0.01 * \text{ Rainy Days}_{\text{Jun}} - 0.002 \text{ Rain}_{\text{Oct}} - 0.06 \text{ Drought}_{\text{May}} - 0.25 \text{ Drought}_{\text{Oct}} + 0.1 \text{ Tmean}_{\text{Sep}} + 0.05 \text{ Rainy Days}_{\text{Aug}} - 0.06 \text{ Tmax}_{\text{Aug}} - 0.07 \text{ Ltemp}_{\text{Jun}} + 0.11 \text{ Tmin}_{\text{Jun}} - 0.06 \text{ Drought}_{\text{Jul}} + 0.5 \text{ Ltemp}_{\text{Aug}} - 0.05 \text{ Tmin}_{\text{Oct}}$	< 0.0005	0.3 t ha ⁻¹ (13%)
Group III	Area _{Price}	$209901 + 203836 \text{ Wheat}_{\text{Price}}/\text{Maize}_{\text{Price}}$	0.003	-
	Area _{Climate}	$44311 - 30092 \text{ Hrain}_{\text{April}} - 59847 \text{ Ltemp}_{\text{May}}$	0.014	58955 ha (12%)
	Area _{non-harvested}	$-0.021 + .021 \text{ Hrain}_{\text{June}} + 0.028 \text{ Ltemp}_{\text{Sep}} + 0.011 \text{ Ltemp}_{\text{Aug}}$	< 0.0005	6%
	Yield	$3.34 + 0.024 \text{ Tmin}_{\text{Jun}} - 0.09 \text{ Ltemp}_{\text{Aug}} - 0.028 \text{ Tmin}_{\text{Aug}} - 0.13 \text{ Tmax}_{\text{May}} - 0.014 \text{ Rainy Days}_{\text{May}} - 0.15 \text{ Ltemp}_{\text{Sep}} - 0.057 \text{ Drought}_{\text{Sep}} + 0.22 \text{ Ltemp}_{\text{May}} + 0.02 \text{ Rainy Days}_{\text{Aug}} - 0.019 \text{ Hrain}_{\text{Sep}} + 0.018 \text{ Drought}_{\text{May}} + 0.006 \text{ Rainy Days}_{\text{July}} - 0.008 \text{ Htemp}_{\text{Aug}} - 0.009 \text{ Hrain}_{\text{July}}$	< 0.0005	0.3 t ha ⁻¹ 16%
Group IV	Area _{Price}	$138608 + 916 \text{ Wheat}_{\text{Price}}$	< 0.0005	-
	Area _{Climate}	$-93897 - 21433 \text{ Tmin}_{\text{May}} - 235 \text{ Rain}_{\text{Jun}} + 418 \text{ Rain}_{\text{May}} + 18778 \text{ Tmax}_{\text{May}} - 8292 \text{ Tmin}_{\text{Jun}}$	0.005	80341 ha (23%)
	Area _{non-harvested}	$0.0085 + 0.001 \text{ Htemp}_{\text{Sep}} - 0.005 \text{ Ltemp}_{\text{Aug}} - 0.001 \text{ Drought}_{\text{Aug}}$	0.05	2%
	Yield	$1.8 - 0.05 \text{ Tmin}_{\text{Oct}} + 0.08 \text{ Ltemp}_{\text{Jun}} - 0.04 \text{ Tmin}_{\text{Sep}} - 0.001 \text{ Rain}_{\text{Oct}} - 0.06 \text{ Ltemp}_{\text{Aug}} + 0.02 \text{ Tmax}_{\text{Jun}} - 0.04 \text{ Hrain}_{\text{May}} - 0.07 \text{ Ltemp}_{\text{Sep}} - 0.03 \text{ Tmean}_{\text{May}} - 0.02 \text{ Tmean}_{\text{Aug}} - 0.008 \text{ Hrain}_{\text{Sep}}$	< 0.0005	0.4 t ha ⁻¹ (15%)

Table S4. CO₂ fertilization effects for C3 crops, according to experiments performed with the DSSAT4 model. All values refer to productivity at 393 ppm of atmospheric CO₂ concentration, which is the average CO₂ concentration of the period (2001-2019) used to build the multiple linear regression models used in this study. Reprinted by permission from Springer Nature Customer Service Centre GmbH: Springer Nature, Climatic Change, adapted from Tebaldi and Lobell (18).

CO₂ concentration (ppm)	C3 yield correcting factor
220	0.88
330	0.95
393	1.00
440	1.03
550	1.11
660	1.19
770	1.26
880	1.31
990	1.36

7

8

9

10

11

12

13

14

15

16

17

18

Table S5. Geographical coordinates of the weather stations within each group

Group	Latitude	Longitude
Group I	-28.66	-50.43
Group II	-23.31	-51.13
Group III	-24.05	-52.36
Group IV	-25.09	-50.16

19

20

21

22

23

24

25

26

27

28

29

30

31

32

33

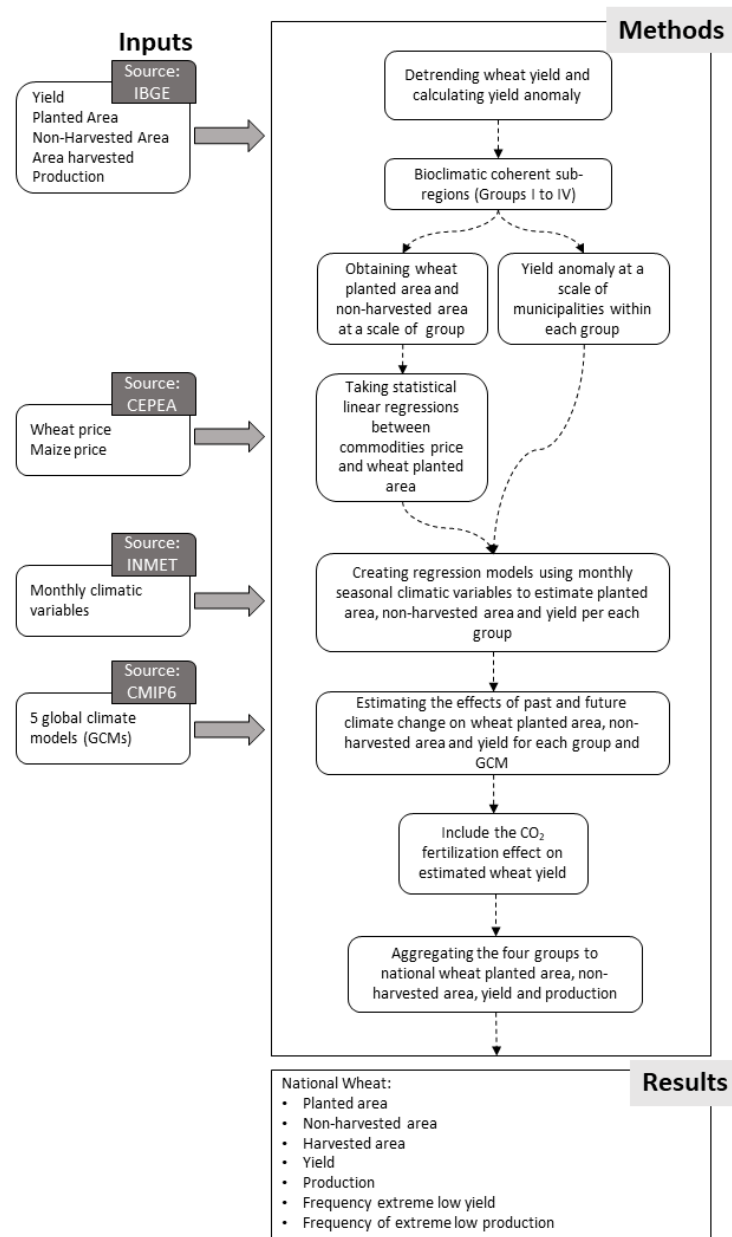
34

35

36

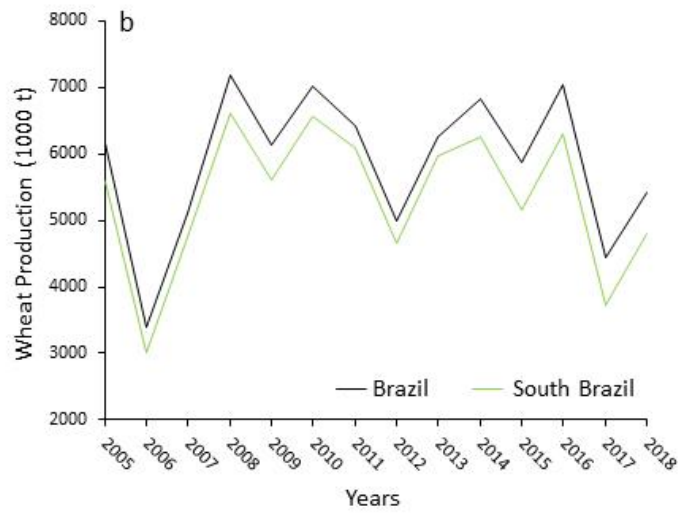
37

Supplementary Figures



39

40 **Figure S1. Flowchart of the procedures for estimating national wheat production.** A group
 41 consists of similar locations in terms of interannual variability in reported wheat yield
 42 (Supplementary, Figure S3).

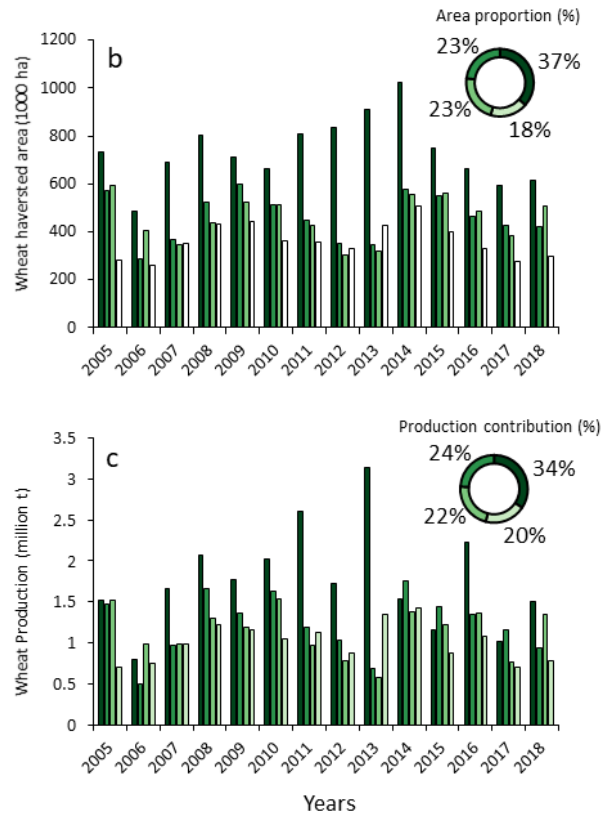
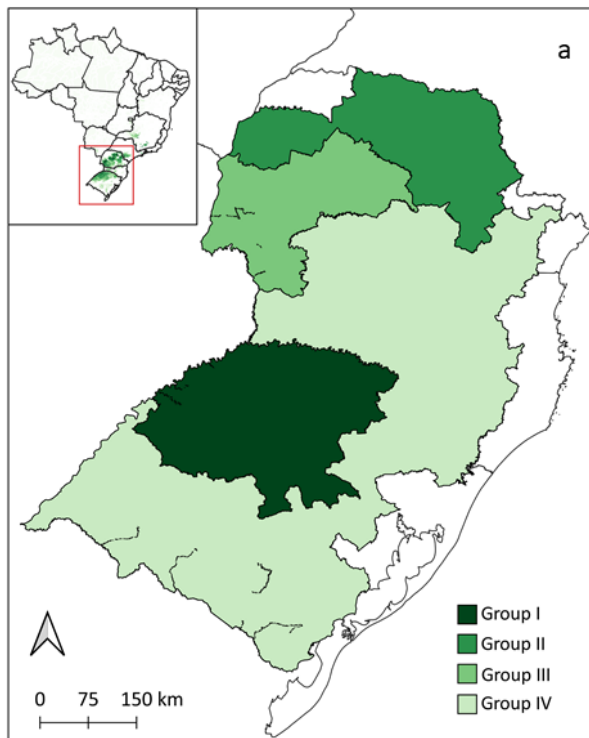


43

44 **Figure S2. Observed spatio-temporal variations of wheat cropping area in Brazil.** (a) observed
 45 percentage of harvested wheat area in 2018 in Brazil. The percentage of harvested area
 46 corresponds to the ratio between wheat harvested area in a location and total area of a
 47 municipality. Main wheat region in Southern Brazil is delineated in bold red contours. (b)
 48 Observed wheat production variation in Brazil and in south Brazil.

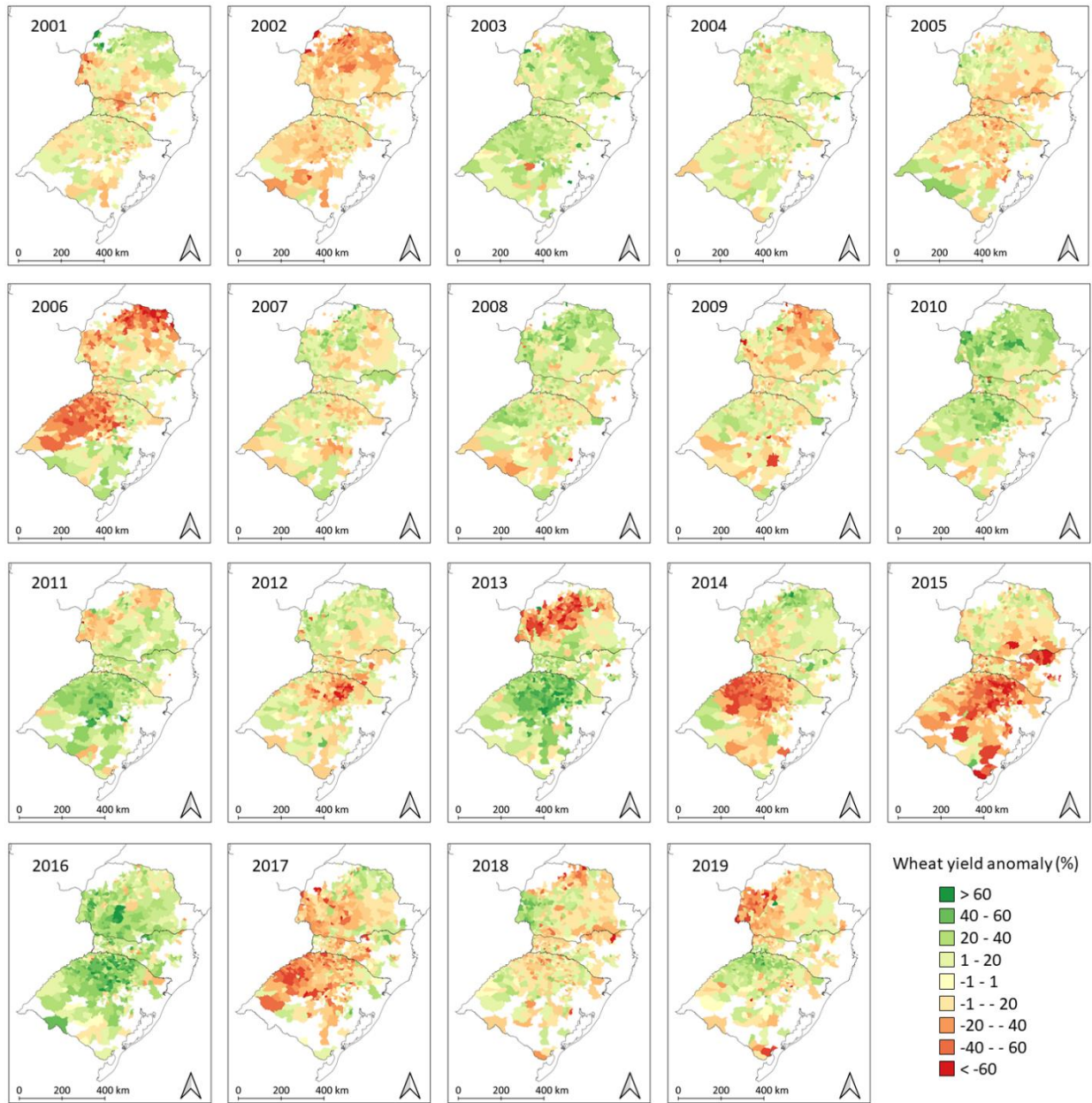
49

50



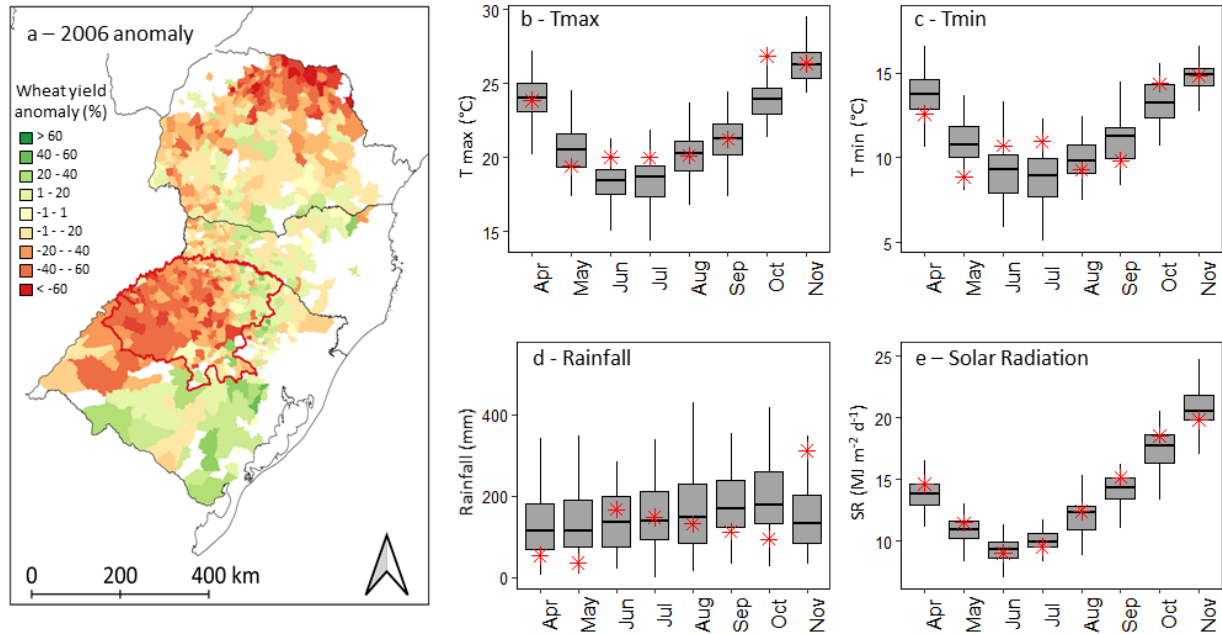
51

52 **Figure S3. Observed spatio-temporal contribution of wheat production regions in Brazil. (a)**
 53 Groups of similar locations in terms of interannual variability in observed wheat yield in Southern
 54 Brazil, and **(b-c)** their area and production contribution. The four groups were obtained through
 55 hierarchical clustering analysis by the nearest neighbor method and by using wheat data from
 56 776 municipalities in Southern Brazil.



57

58 **Figure S4. Observed spatio-temporal pattern of wheat yield anomaly in Brazil.** Observed wheat
 59 yield anomalies relative to average values defined in each municipality (2001-2019).



60

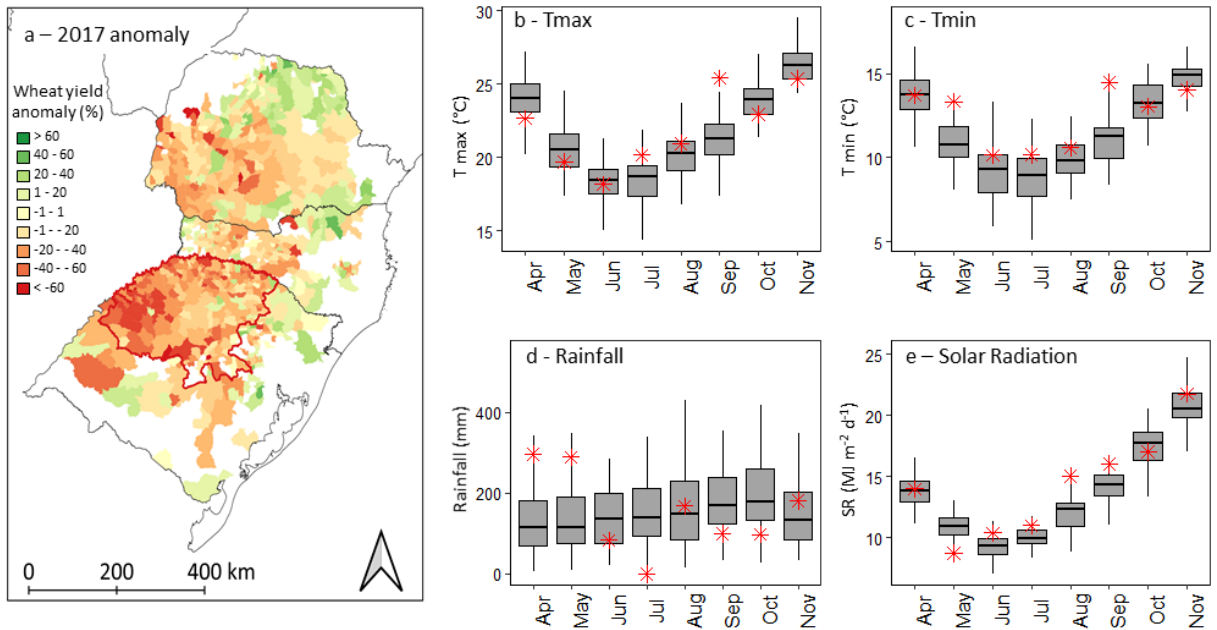
61 **Figure S5. The observed 2006 wheat grain yield anomaly in Brazil.** (a) Spatial-temporal pattern
 62 of the 2006 extreme yield loss. Boxplots for (a) maximum (Tmax), (c) minimum (Tmin) air
 63 temperature, (d) monthly rainfall and (e) global solar radiation (SR) over the 2001–2019 wheat
 64 growing seasons for Group I. Whiskers extend to maximum and minimum values. Values in the
 65 2006 growing season are presented as red asterisk. The Group I is delineated in bold red contours
 66 in (a).

67

68

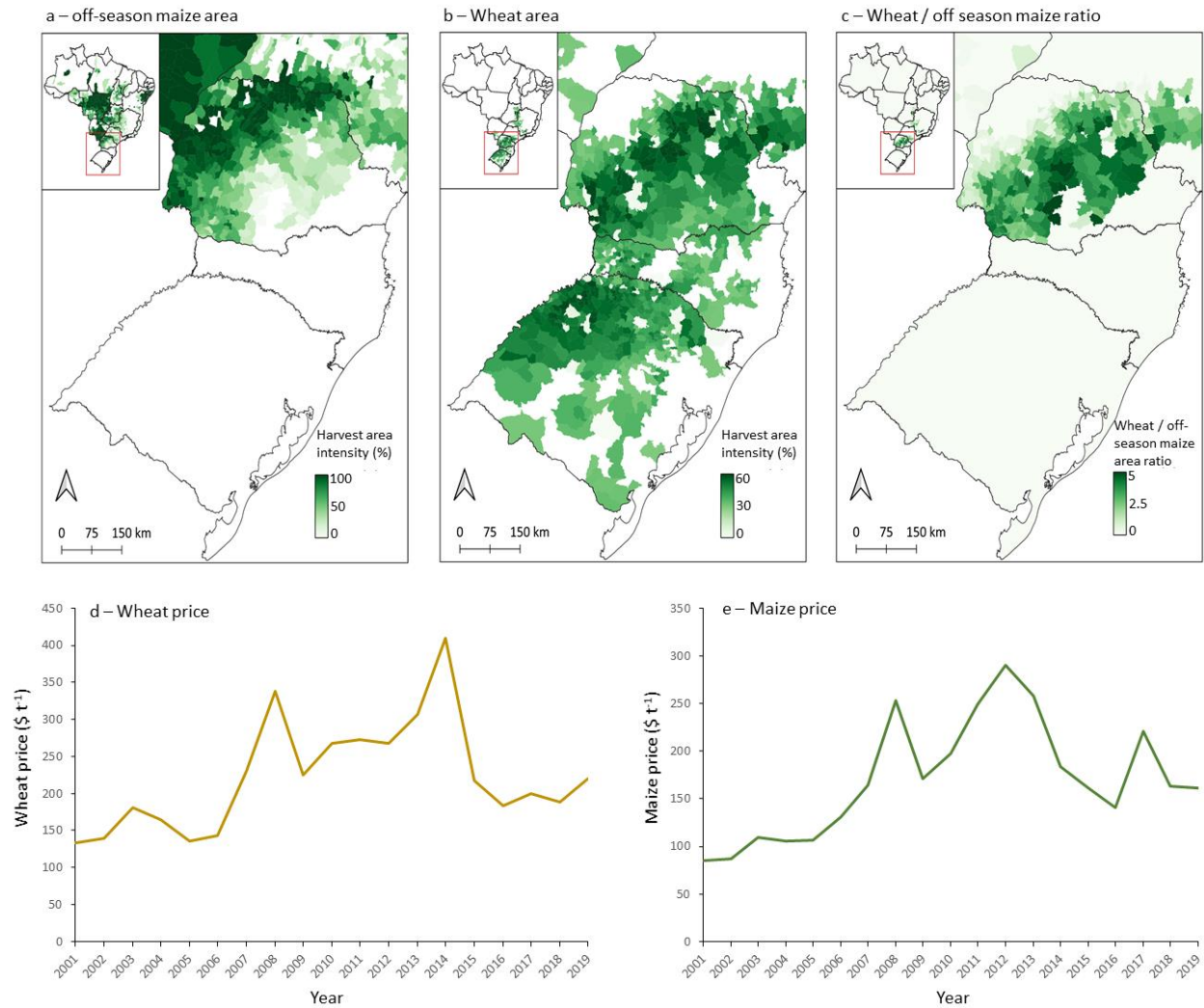
69

70



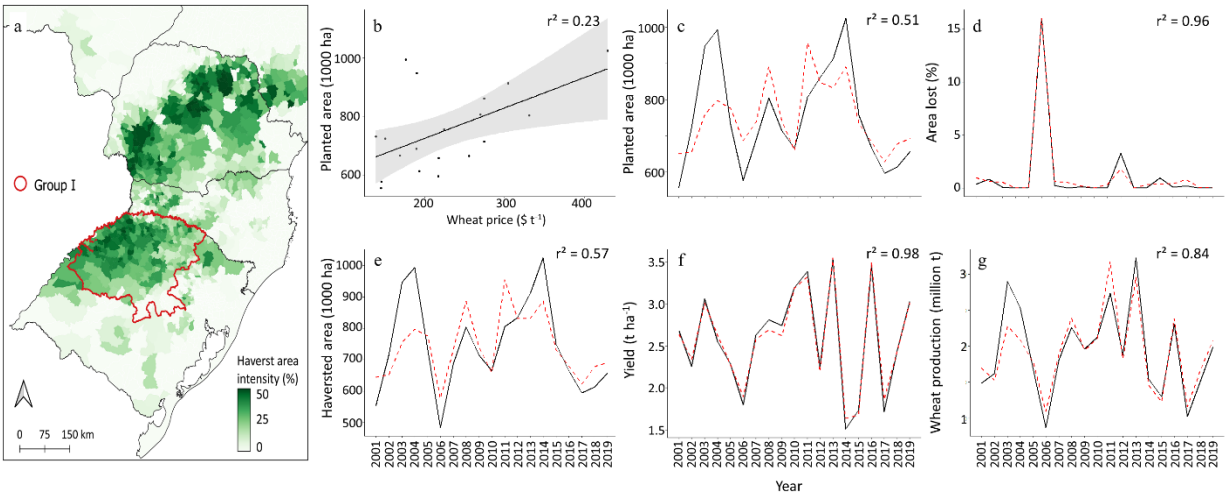
71

72 **Figure S6. The observed 2017 wheat grain yield anomaly in Brazil.** (a) Spatial-temporal pattern
 73 of the 2017 extreme yield loss. Boxplots for (a) maximum (Tmax), (c) minimum (Tmin) air
 74 temperature, (d) monthly rainfall and (e) global solar radiation (SR) over the 2001–2019 wheat
 75 growing seasons for Group I. Whiskers extend to maximum and minimum values. Values in the
 76 2017 growing season are presented as red asterisk. The Group I is delineated in bold red contours
 77 in (a).



78

79 **Figure S7. Observed off-season maize and wheat in Brazil.** Harvested area intensity in 2019 of
 80 (a) off-season maize and (b) wheat in Brazil(4). Harvested area intensity corresponds to the ratio
 81 between wheat-harvested area in the location and total area of the municipality. (c) Ratio
 82 between wheat and off-season maize in Brazil. (d) Wheat and (e) off-season price historical
 83 variation (2001-2019) in Brazil. Wheat and maize price data were used from 2005-2019 (19).
 84 Wheat and maize prices for 2001-2004 were reconstructed with a regression relating
 85 international to domestic prices (1).



86

87 **Figure S8. Multiple linear regression model performance for estimating wheat production in**
 88 **Group I. (a)** Spatial pattern of the harvest area intensity in Brazil (Group I delineated in bold red
 89 contours). **(b)** Relation between wheat price and observed wheat planted area. Estimated and
 90 observed wheat **(c)** planted area, **(d)** area non-harvested, **(e)** harvested area, **(f)** yield, and **(g)**
 91 production, from a multiple linear regression model based on wheat price and climate
 92 projections fitted to the full time series (2001-2019) in southern Brazil.

93

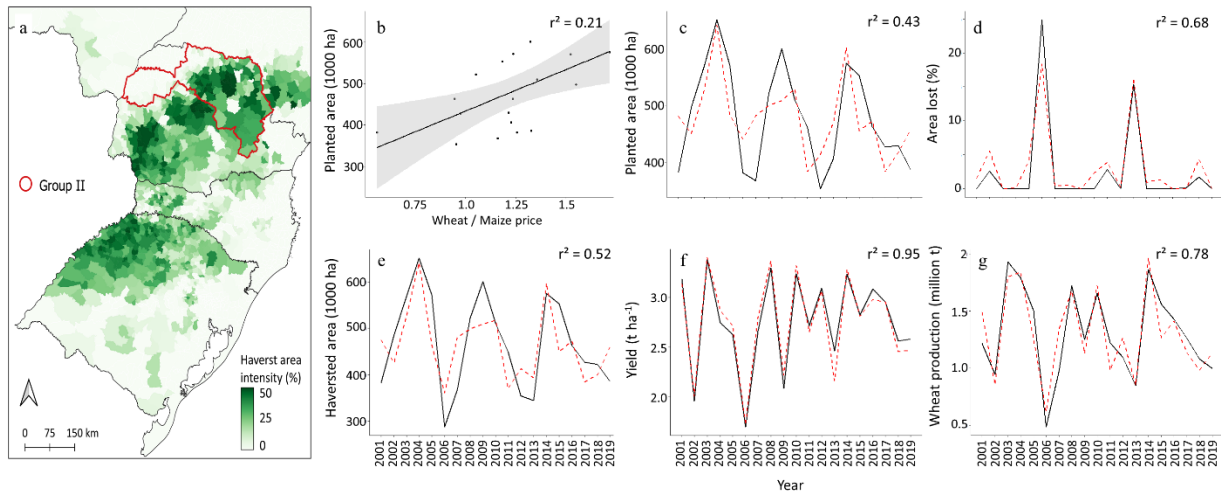
94

95

96

97

98



99

100 **Figure S9. Multiple linear regression model performance for estimating wheat production in**
 101 **Group II.** (a) Spatial pattern of the harvest area intensity in Brazil (Group II delineated in bold red
 102 contours). (b) Relation between wheat price and wheat planted area. Estimated and observed
 103 wheat (c) planted area, (d) area non-harvested, (e) harvested area, (f) yield, and (g) production,
 104 from a multiple linear regression model based on wheat/maize ratio price and climate projections
 105 fitted to the full time series (2001-2019) in southern Brazil.

106
 107

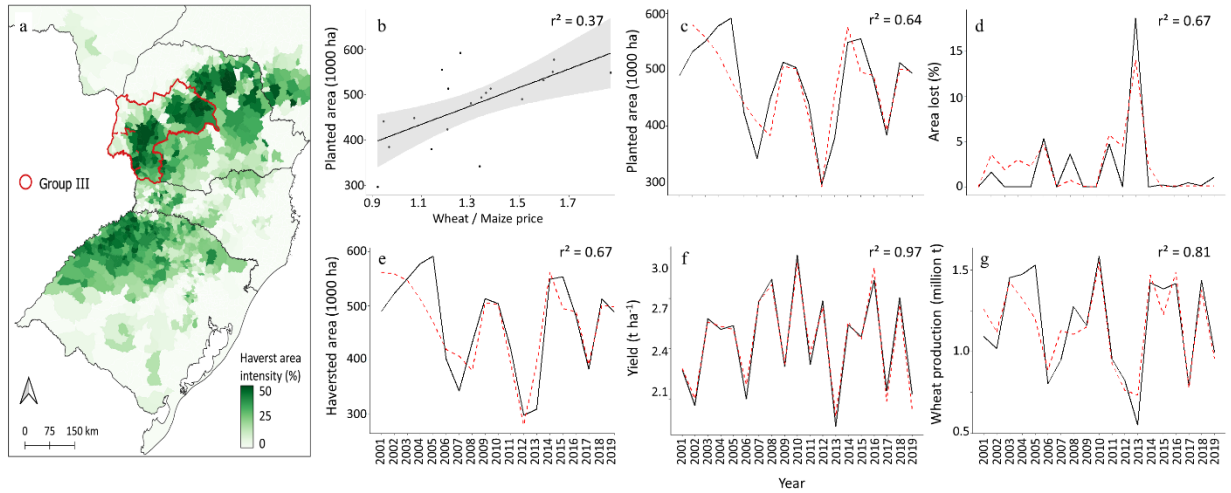
108

109

110

111

112



113

114 **Figure S10. Multiple linear regression model performance for estimating wheat production in**
 115 **Group III.** (a) Spatial pattern of the harvest area intensity in Brazil (Group III delineated in bold
 116 red contours). (b) Relation between wheat price and wheat planted area. Estimated and
 117 observed wheat (c) planted area, (d) area non-harvested, (e) harvested area, (f) yield, and (g)
 118 production, from a multiple linear regression model based on wheat/maize ratio price and
 119 climate projections fitted to the full time series (2001-2019) in southern Brazil.

120

121

122

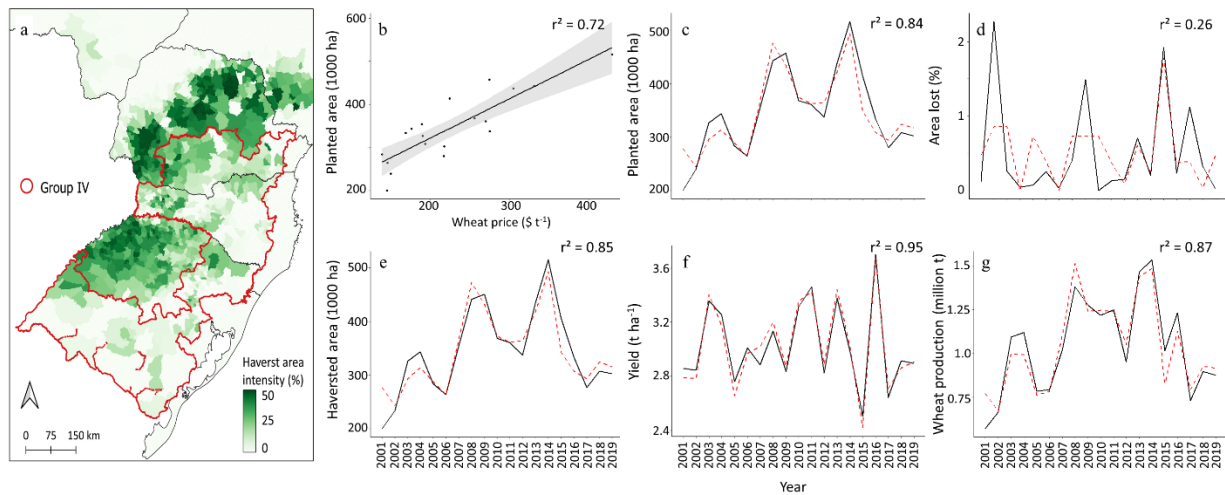
123

124

125

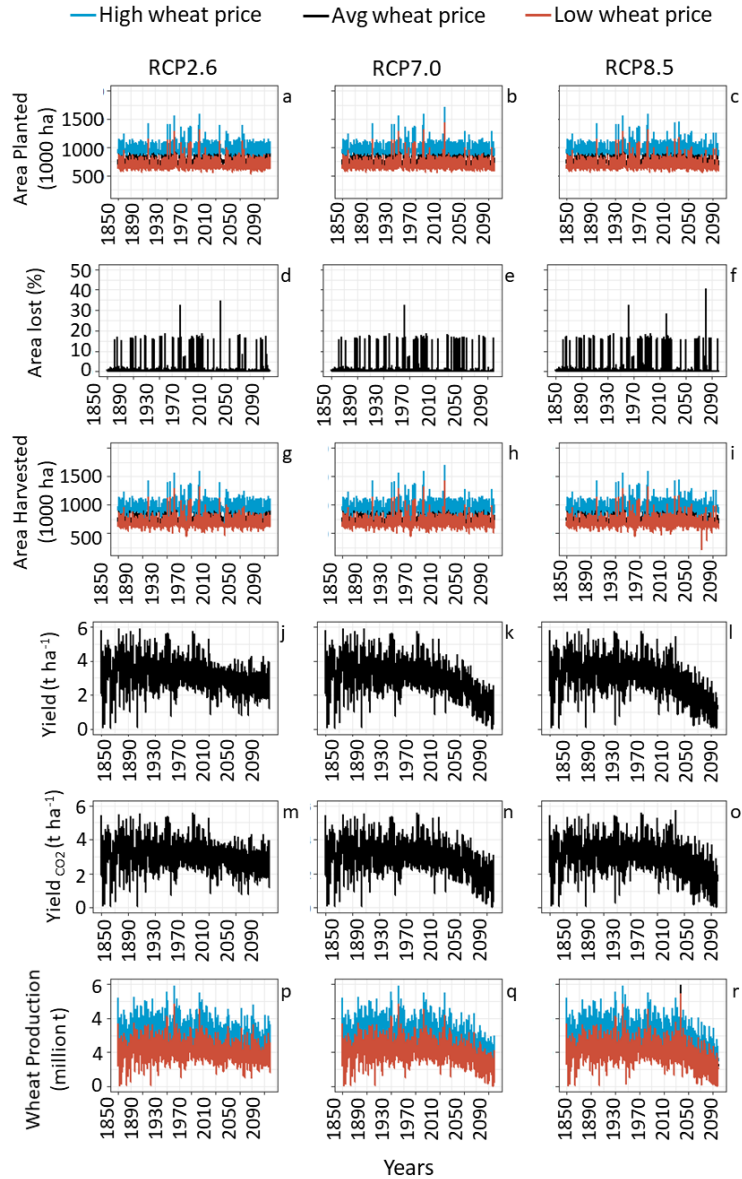
126

127

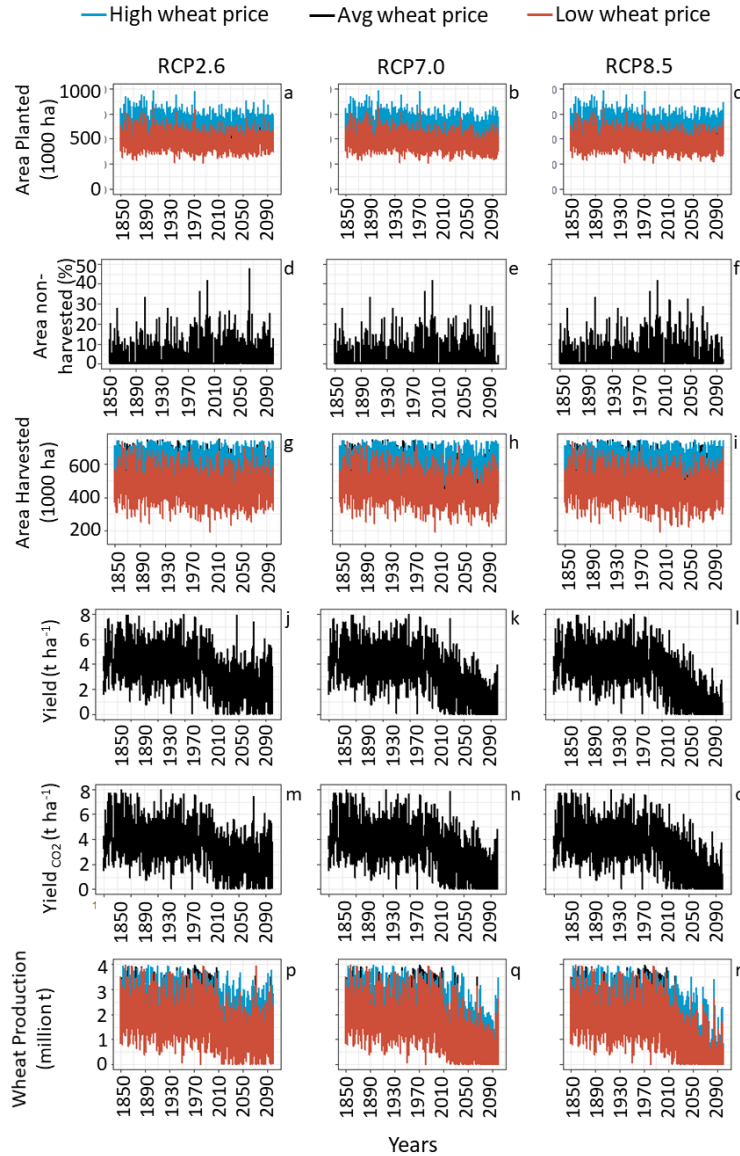


128

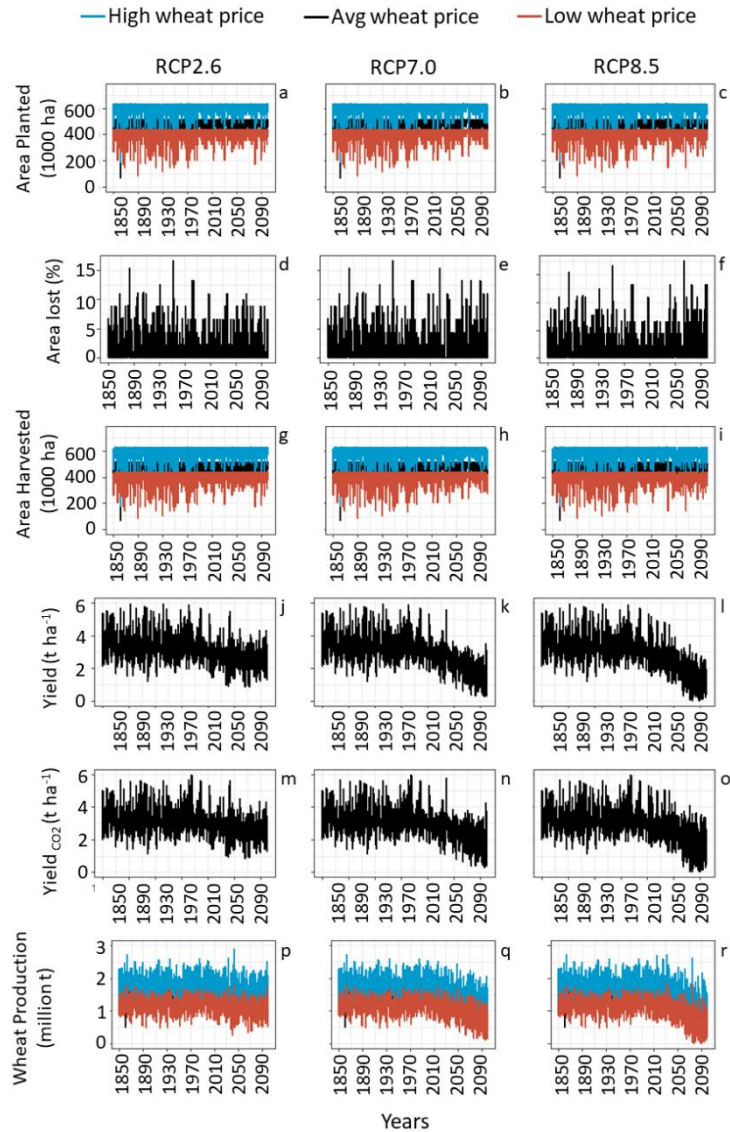
129 **Figure S11. Multiple linear regression model performance for estimating wheat production in**
 130 **Group IV. (a) Spatial pattern of the harvest area intensity in Brazil (Group IV delineated in bold**
 131 **red contours). (b) Relation between wheat price and wheat planted area. Estimated and**
 132 **observed wheat (c) planted area, (d) area non-harvested, (e) harvested area, (f) yield, and (g)**
 133 **production, from a multiple linear regression model based on wheat price and climate**
 134 **projections fitted to the full time series (2001-2019) in southern Brazil.**
 135



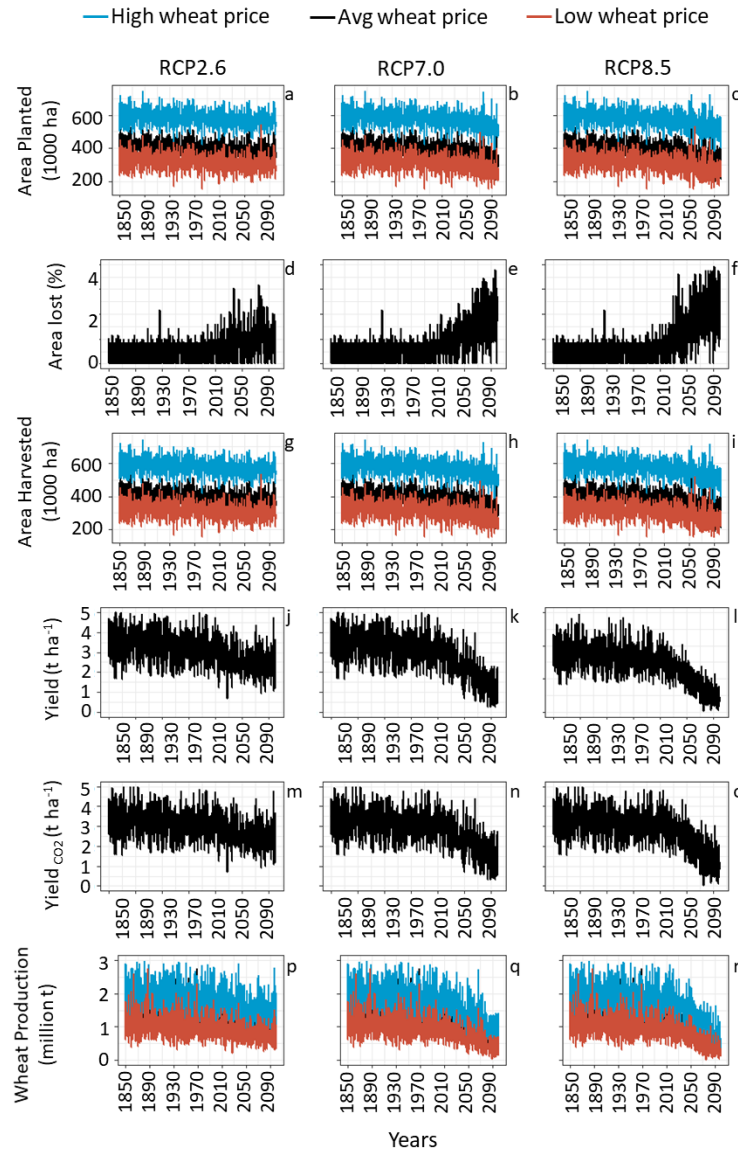
136
 137 **Figure S12. Estimated wheat production in Group I.** Projected area planted for three different
 138 wheat prices and for (a) RCP 2.6, (b) RCP 7.0, and (c) RCP 8.5. Projected area non-harvested for
 139 (d) RCP 2.6, (e) RCP 7.0, and (f) RCP 8.5. Projected area harvested (Area planted – Area non-
 140 harvested) for three different wheat prices and for (g) RCP 2.6, (h) RCP 7.0, and (i) RCP 8.5.
 141 Projected wheat grain yield for (j) RCP 2.6, (k) RCP 7.0, and (l) RCP 8.5. Projected wheat grain
 142 yield corrected by CO₂ fertilization effects for (m) RCP 2.6, (n) RCP 7.0, and (o) RCP 8.5. Projected
 143 wheat grain production (Area Harvested x Yield_{CO₂}) for three different wheat prices and for (p)
 144 RCP 2.6, (q) RCP 7.0, and (r) RCP 8.5. Projections are the ensemble of five CMIP6 global change
 145 models. CO₂ fertilization effects correction is given in Supplementary Table S4 and Figure S24.



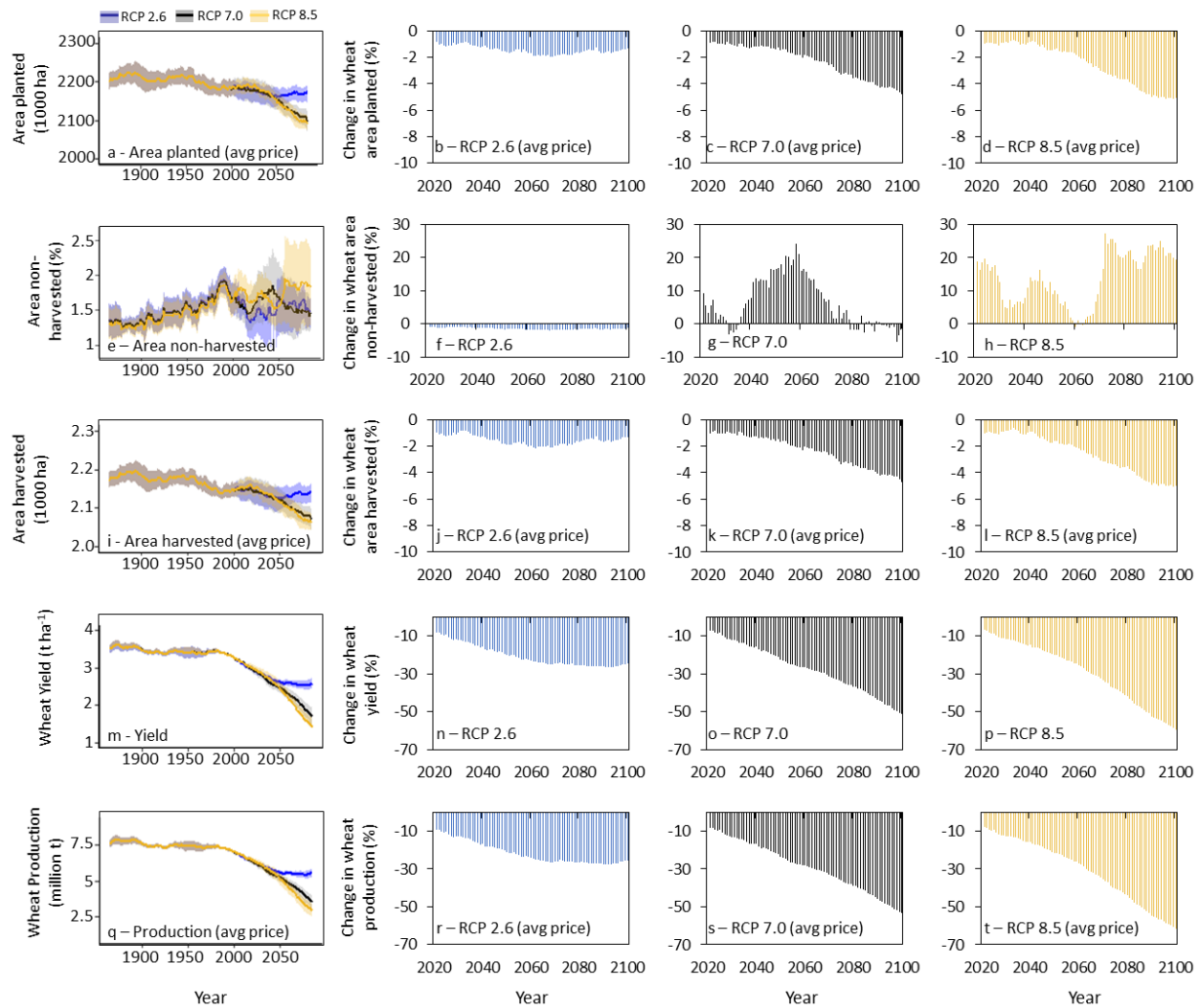
146
 147 **Figure S13. Estimated wheat production in Group II.** Projected area planted for three different
 148 wheat prices and for (a) RCP 2.6, (b) RCP 7.0, and (c) RCP 8.5. Projected area non-harvested for
 149 (d) RCP 2.6, (e) RCP 7.0, and (f) RCP 8.5. Projected area harvested (Area planted – Area non-
 150 harvested) for three different wheat prices and for (g) RCP 2.6, (h) RCP 7.0, and (i) RCP 8.5.
 151 Projected wheat grain yield for (j) RCP 2.6, (k) RCP 7.0, and (l) RCP 8.5. v wheat grain yield
 152 corrected by CO₂ fertilization effects for (m) RCP 2.6, (n) RCP 7.0, and (o) RCP 8.5. Projected wheat
 153 grain production (Area Harvested x Yield_{CO₂}) for three different wheat prices and for (p) RCP 2.6,
 154 (q) RCP 7.0, and (r) RCP 8.5. Projections are the ensemble of five CMIP6 global change models.
 155 CO₂ fertilization effects correction is given in Supplementary Table S4 and Figure S24.



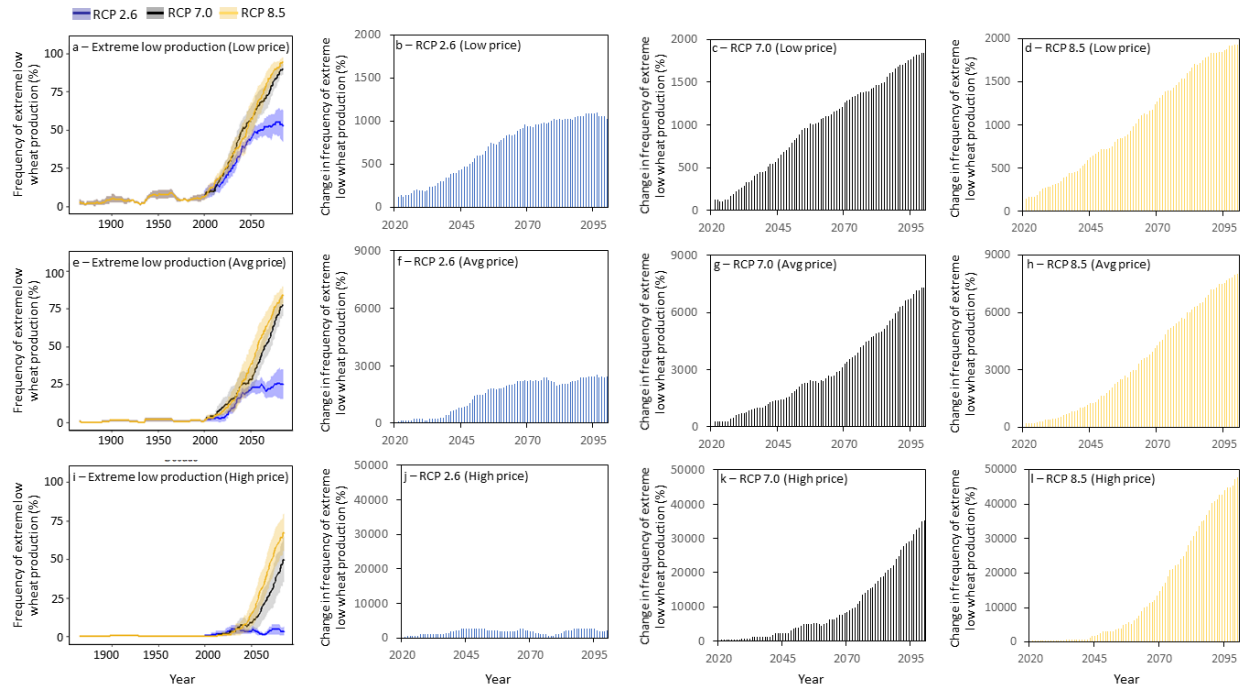
156
 157 **Figure S14. Estimated wheat production in Group III.** Projected area planted for three different
 158 wheat prices and for (a) RCP 2.6, (b) RCP 7.0, and (c) RCP 8.5. Estimated area non-harvested for
 159 (d) RCP 2.6, (e) RCP 7.0, and (f) RCP 8.5. Projected area harvested (Area planted – Area non-
 160 harvested) for three different wheat prices and for (g) RCP 2.6, (h) RCP 7.0, and (i) RCP 8.5.
 161 Projected wheat grain yield for (j) RCP 2.6, (k) RCP 7.0, and (l) RCP 8.5. Projected wheat grain
 162 yield corrected by CO₂ fertilization effects for (m) RCP 2.6, (n) RCP 7.0, and (o) RCP 8.5. Projected
 163 wheat grain production (Area Harvested x Yield_{CO₂}) for three different wheat prices, and for (p)
 164 RCP 2.6, (q) RCP 7.0 and (r) RCP 8.5. Projections are the ensemble of five CMIP6 global change
 165 models. CO₂ fertilization effects correction is given in Supplementary Table S4 and Figure S24.



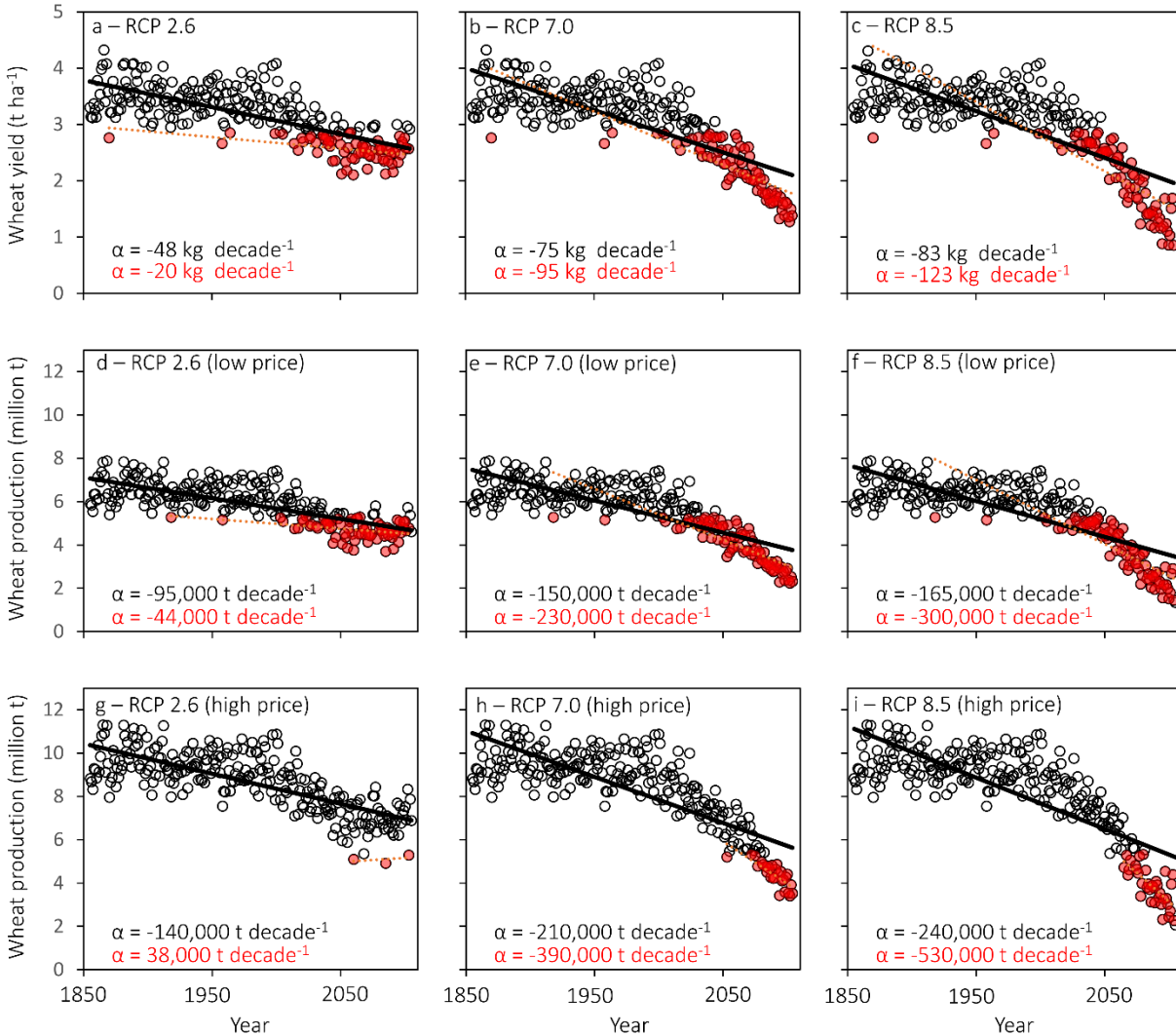
166
 167 **Figure S15. Estimated wheat production in Group IV.** Projected area planted for three different
 168 wheat prices and for (a) RCP 2.6, (b) RCP 7.0, and (c) RCP 8.5. Projected area non-harvested for
 169 (d) RCP 2.6, (e) RCP 7.0, and (f) RCP 8.5. Projected area harvested (Area planted – Area non-
 170 harvested) for three different wheat prices and for (g) RCP 2.6, (h) RCP 7.0, and (i) RCP 8.5.
 171 Projected wheat grain yield for (j) RCP 2.6, (k) RCP 7.0, and (l) RCP 8.5. Projected wheat grain
 172 yield corrected by CO₂ fertilization effects for (m) RCP 2.6, (n) RCP 7.0, and (o) RCP 8.5. Projected
 173 wheat grain production (Area Harvested x Yield_{CO₂}) for three different wheat prices and for (p)
 174 RCP 2.6, (q) RCP 7.0, and (r) RCP 8.5. Projections are the ensemble of five CMIP6 global change
 175 models. CO₂ fertilization effects correction is given in Supplementary Table S4 and Figure S24.



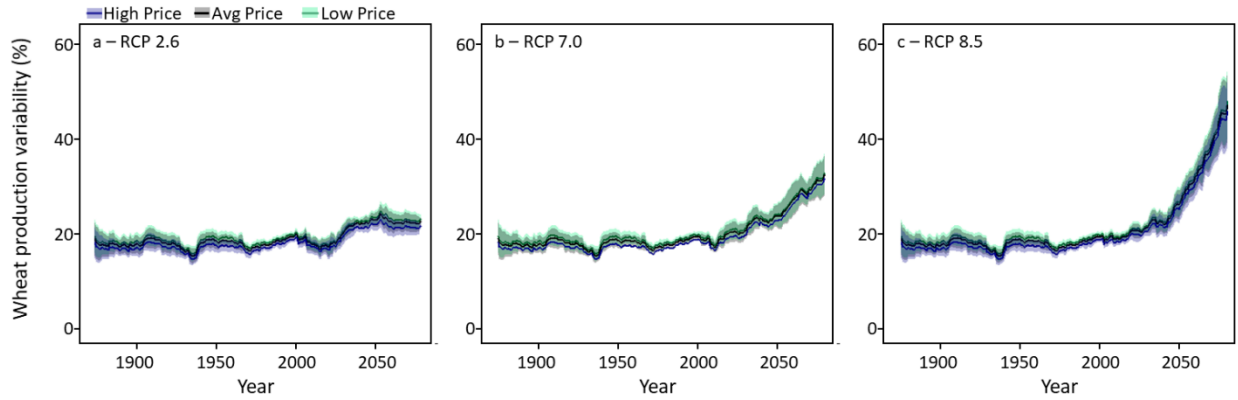
176
 177 **Figure S16. Projected changes in wheat production over the 1850-2020 historical period in**
 178 **Brazil.** Wheat (a) planted area, (e) non-harvested area, (i) harvested area, (m) yield, and (q)
 179 production (30 years running mean) were calculated for three RCP scenarios and low wheat price
 180 for the period of 1850-2100. Percent change in planted area considering average wheat price for
 181 (b) RCP 2.6, (c) RCP 7.0, and (d) RCP 8.5. Percent change in non-harvested area for (f) RCP 2.6, (g)
 182 RCP 7.0, and (h) RCP 8.5. Percent change in harvested area considering average wheat price for
 183 (j) RCP 2.6, (k) RCP 7.0, and (l) RCP 8.5. Percent change in yield for (n) RCP 2.6, (o) RCP 7.0, and
 184 (p) RCP 8.5. Percent change in wheat production considering average wheat price for (r) RCP 2.6,
 185 (s) RCP 7.0, and (t) RCP 8.5. Percent change is calculated considering the 1850-2020 period as
 186 baseline. In (a), (e) and (i) lines are the ensemble mean based on five CMIP6 global climate models
 187 and shaded areas show ± 1 s.e. In (b-d), (f-h), and (j-l) bars are the ensemble mean based on five
 188 CMIP6 global climate models.



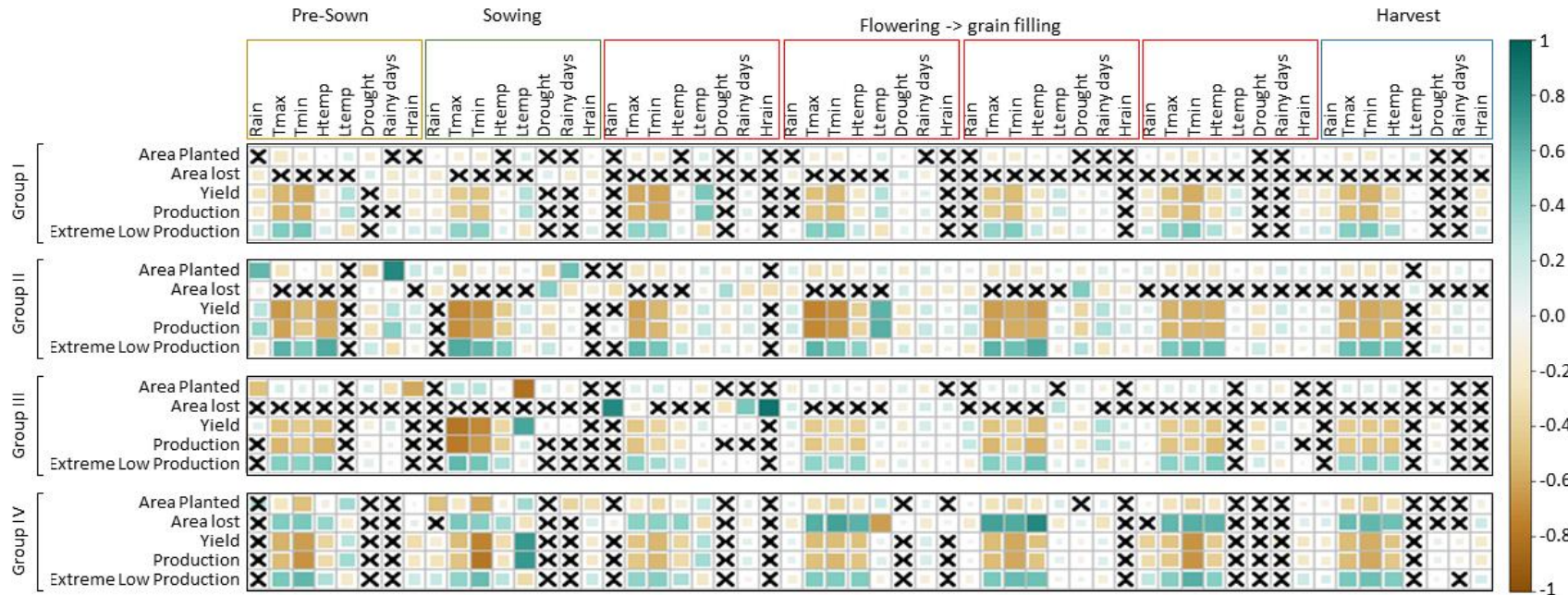
189
 190 **Figure S17. Projected change in frequency of extreme low wheat production over 1850-2020**
 191 **historical period in Brazil.** Frequency of extreme low wheat production (30 years running mean)
 192 for three RCP scenarios and (a) low price, (e) average price and (i) high price, from the periods of
 193 1865 (1850-1880) to 2085 (2070-2100). Change in frequency for (b) for RCP 2.6 and low wheat
 194 price, (c) RCP 7.0 and low wheat price, (d) RCP 8.5 and low wheat price, (f) RCP 2.6 and average
 195 wheat price, (g) RCP 7.0 and average wheat price, (h) RCP 8.5 and average wheat price, (j) RCP
 196 2.6 and high wheat price, (k) RCP 7.0 and high wheat price, and (l) RCP 8.5 and high wheat price.
 197 Percent changes is calculated considering the 1850-2020 historical period as baseline. Extreme
 198 low national wheat productions were defined for each GCM separately as the projected 5th
 199 percentile lowest wheat production during 1850-2020 with the low national wheat price from
 200 the reference period 2001-2020. In (a), (e), and (i) lines are ensemble mean based of five CMIP6
 201 global climate models, shaded areas show ± 1 s.e. In (b-d), (f-h) and (j-i) bars are ensemble mean
 202 based of five CMIP6 global climate models.



203
 204 **Figure S18. Projected wheat yield and production over time.** Projected wheat grain yield for (a)
 205 RCP 2.6, (c) RCP 7.0, and (c) RCP 8.5. Projected wheat grain production with low wheat price and
 206 for (d) RCP 2.6, (e) RCP 7.0, and (f) RCP 8.5. Projected wheat production for average price and for
 207 (g) RCP 2.6, (h) RCP 7.0, and (i) RCP 8.5. Data are ensemble mean based on five CMIP6 global
 208 climate models. α , rate of wheat yield and production change per decade for extreme low
 209 production and yield (red) and for all wheat cropping seasons (black). Rate of decline are
 210 represented by black solid lines for all wheat cropping seasons and red dashed line for extreme
 211 wheat cropping seasons only.



212
 213 **Figure S19. Projected variability of low wheat production in Brazil.** Variability (30 years running
 214 mean) of estimated wheat production for three different wheat prices and (a) RCP 2.6, (b) RCP
 215 7.0, and (c) RCP 8.5 for the period of 1850-2100. Lines are ensemble mean based on five CMIP6
 216 global climate models and shaded areas show ± 1 s.e.



218

219

220

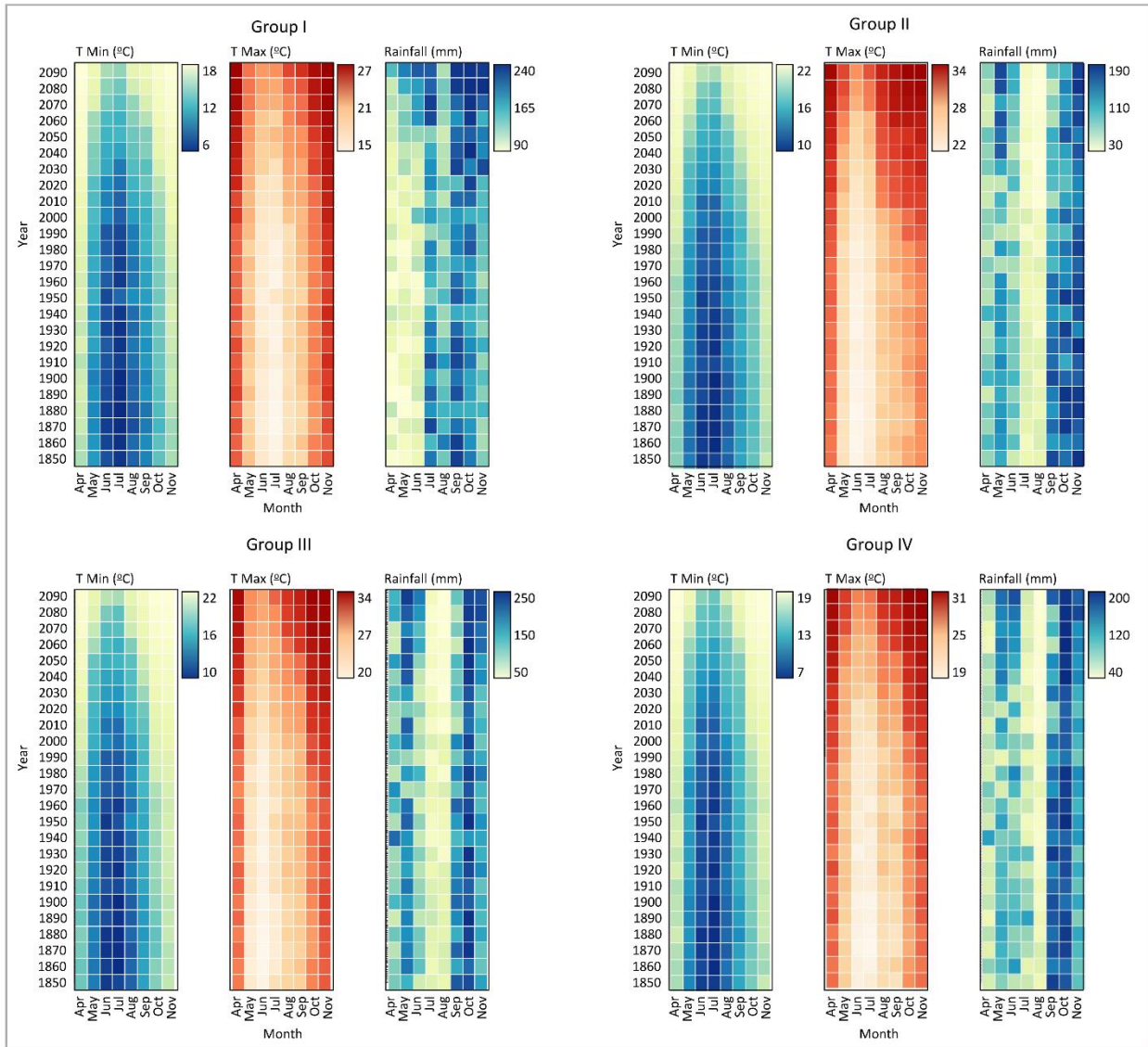
221

222

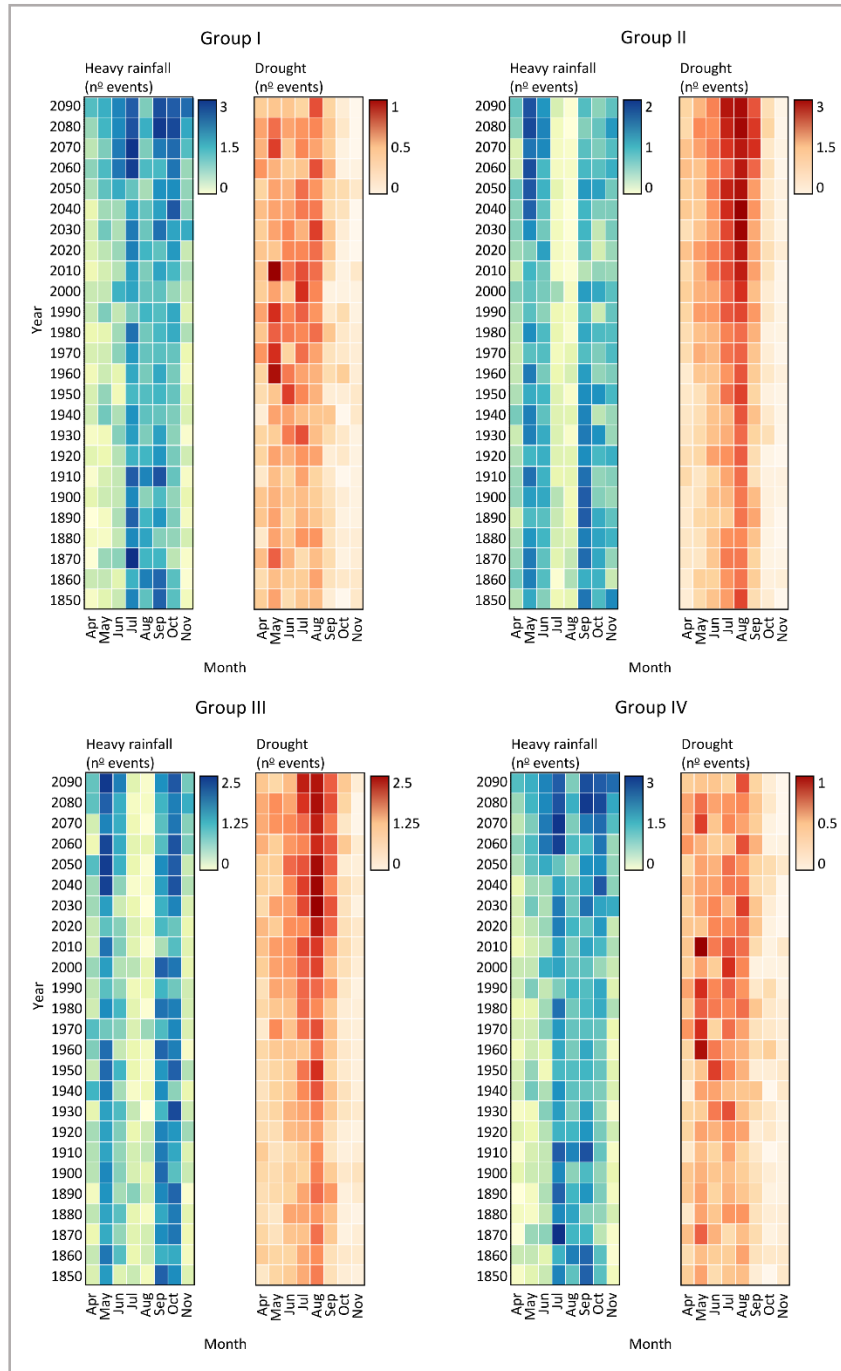
223

224

Figure S20. Pearson’s correlations for monthly climatic variables and wheat planted area, non-harvested area, yield, production and extreme low production in the different groups. Values overlapped with an “X” are not statistically significant at the 0.05 significance level. For Group I and Group IV, the Pre-Sown period occurs in May, Sowing in June, Flowering to Grain filling phenological phases in July, August, September and October, and harvest in November. For Group II and Group III, the Pre-Sown period occurs in April, Sowing in May, Flowering to Grain filling phenological phases in June, July, August and September and harvest in October. Variables are defined in Supplementary Table S1.



226
 227 **Figure S21. Climate Characterization.** Average monthly minimum (TMin), maximum temperature
 228 (TMax), and accumulated rainfall (Rainfall) for the period 1850-2100, in the Groups I, II, III and IV,
 229 and for RCP 7.0. The values presented are the mean of five CMIP6 global change models.



230

231

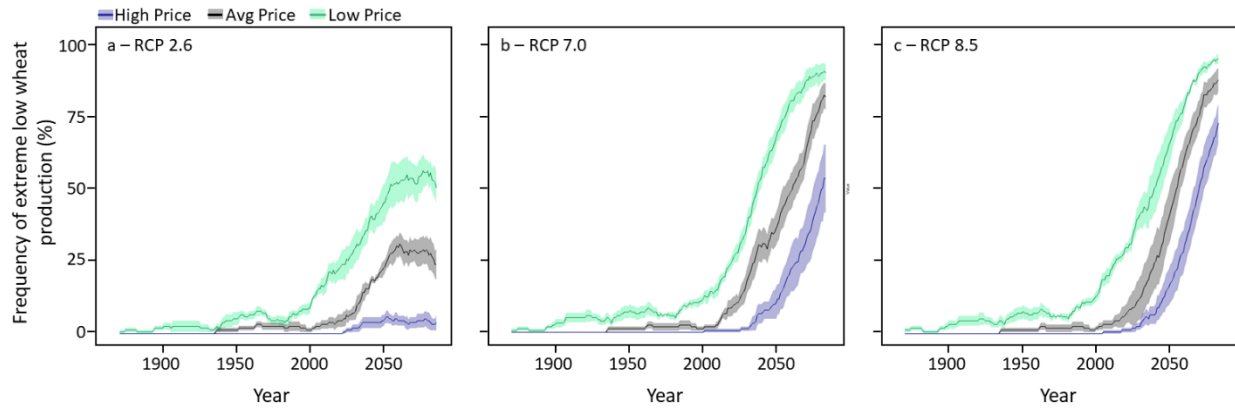
Figure S22. Climatic events. Average number heavy rainfall (>30mm) and Drought events

232

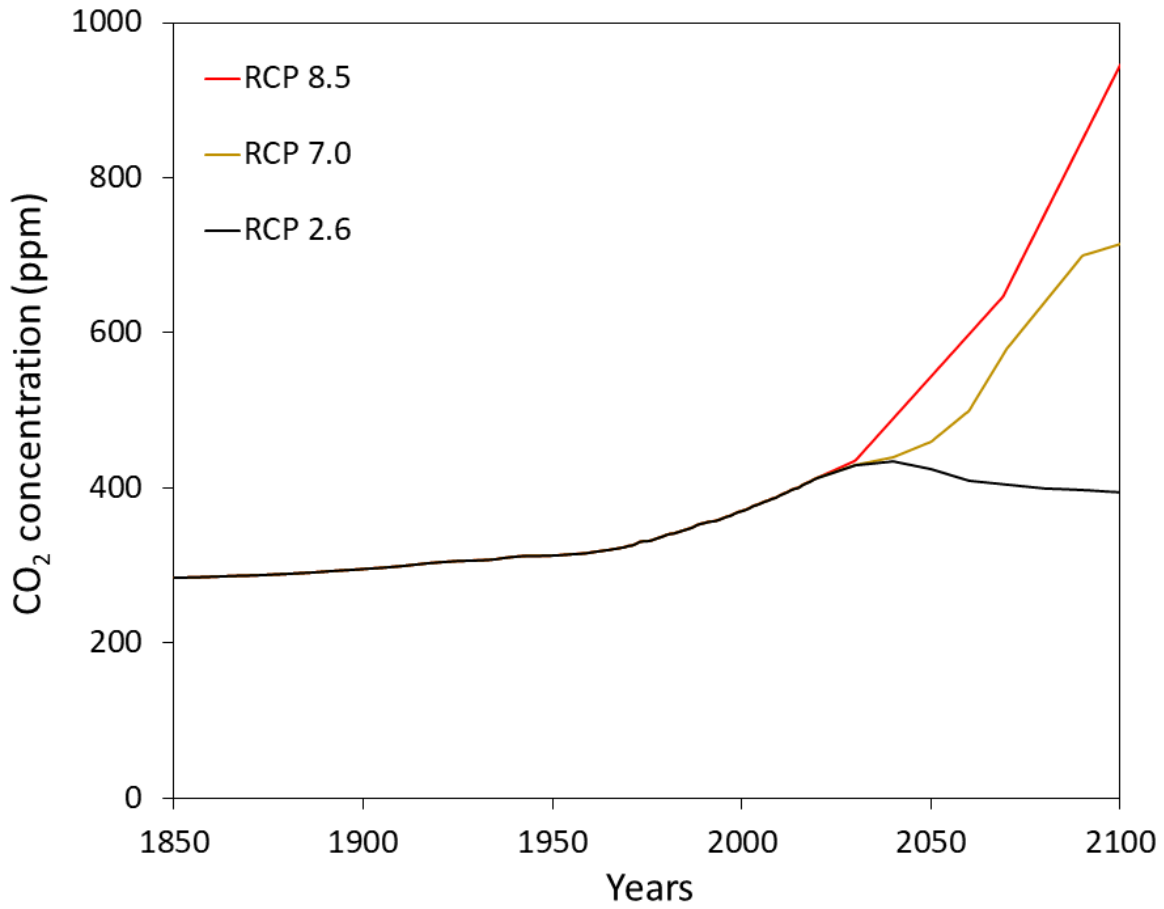
(number of 10 consecutive days with no rainfall) for the period 1850-2100, in the Groups I, II, III

233

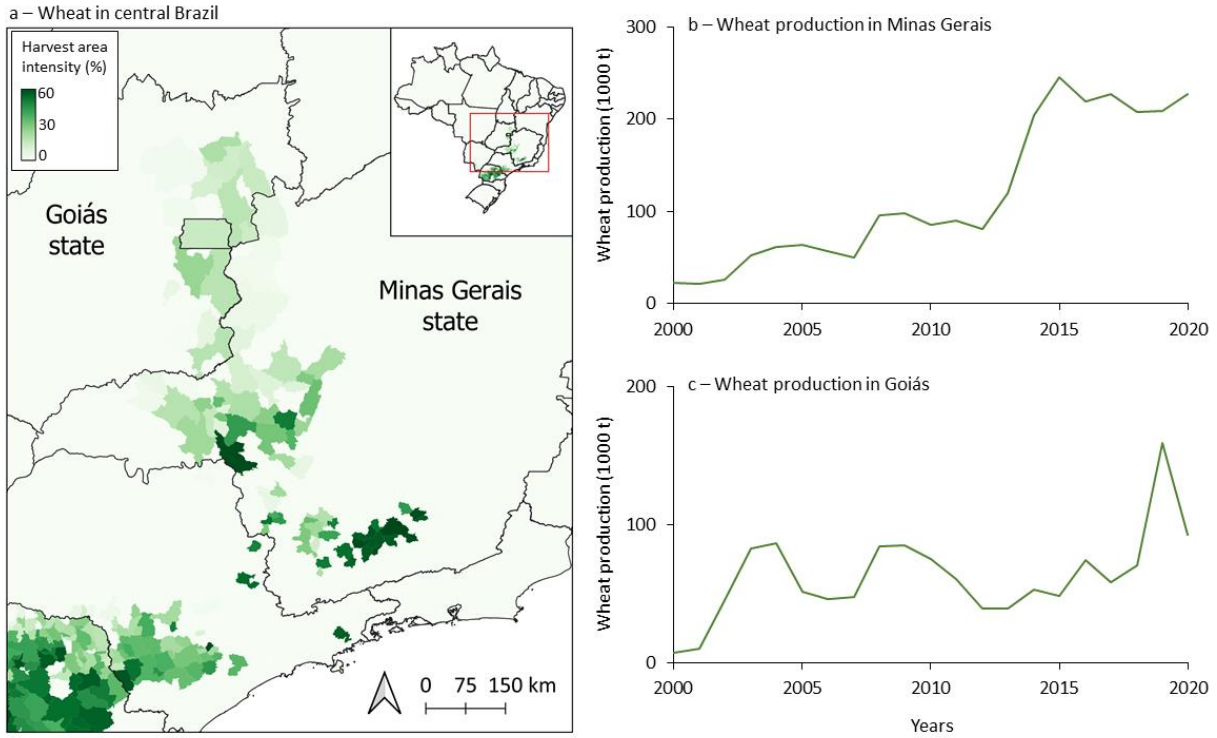
and IV, and for RCP 7.0. The values presented are the mean of five CMIP6 global change models.



234
 235 **Figure S23. Projected frequency of extreme low national wheat production of Brazil using the**
 236 **Lasso method.** Projected 30 year running mean frequency (ensemble mean based on five CMIP6
 237 global climate models (line) with +/- 1 s.e. of the mean (shaded area)) of extreme low wheat
 238 production for three different wheat prices for (a) RCP 2.6, (b) RCP 7.0 and (c) RCP 8.5 for 1850-
 239 2100. An extreme low national wheat production is defined for each GCM separately as the
 240 projected 5th percentile lowest wheat production during 1850-2020, with the lowest national
 241 wheat price from the reference period 2001-2020. The high, average and low wheat prices are
 242 from a combination of the highest, average and lowest recorded wheat and wheat/maize ratio
 243 price during 2001-2019. The Lasso method was used to estimate wheat area planted, non-
 244 harvested area, and yield in each of the groups presented in Fig S3 and results were aggregated
 245 to national level.



246
247 **Figure S24. Global atmospheric CO₂ concentration projections for RCP 2.6, RCP 7.0 and RCP 8.5.**
248 Reprinted by permission from Springer Nature Customer Service Centre GmbH: Springer Nature,
249 Climatic Change, Adapted from van Vuuren et al. (20).



250

251 **Figure S25. Wheat expansion production towards Central Brazil.** Harvested area intensity in
 252 2019 of (a) wheat in central Brazil(4). Historical wheat production in (b) Goiás and (c) Minas
 253 Gerais states.

254

255

256

257

258

259

260

261

262

263

264










265

References

- 267 1. FAO, FAOSTAT: FAO statistical databases (2020) (October 10, 2020).
 268 2. CONAB, *The Wheat Crop* (2017).
 269 3. IBGE, Agricultural Census. *Brazilian Inst. Geogr. Stat.* (2017) (May 10, 2018).
 270 4. IBGE, Brazilian Institute of Geography and Statistics. *Munic. Agric. Res.* (2020) (October 10,
 271 2010).
 272 5. Conab, National Supply Company: Agricultural information system (2020) (October 10,
 273 2018).
 274 6. PROCON, “Bread Price Research” (2020).
 275 7. B. A. R. C. Embrapa, Estimation of the potential for increasing wheat production in Brazil
 276 (2015).
 277 8. J. F. Pereira, G. R. da Cunha, E. R. Moresco, Improved drought tolerance in wheat is
 278 required to unlock the production potential of the Brazilian Cerrado. *Crop Breed. Appl.*
 279 *Biotechnol.* **19**, 217–225 (2019).
 280 9. F. A. S. USDA, “GAIN Report - Brazil Grain and Feed: An Interesting Year Ahead for Wheat
 281 Traders 2006” (2006).
 282 10. F. A. S. USDA, “GAIN Report - Brazil Grain and Feed Winter Crops Update 2006” (2006).
 283 11. A. Estado, Conab estima redução de 11,3% da área plantada de trigo em 2012. *Globo Rural*
 284 (2012).
 285 12. A. F. Nunes, Preço do trigo provoca redução da área plantada com o grão no PR. *Globo*
 286 *Rural* (2017).
 287 13. P. A. Manfron, C. Lazzarotto, S. L. P. Medeiros, TRIGO - Aspectos agrometeorológicos.
 288 *Ciência Rural* **23**, 233–239 (1993).
 289 14. C. for A. S. in A. E. CEPEA, “CUSTOS DE PRODUÇÃO AGRÍCOLA” (2013).
 290 15. G. Paraná, Chuva prejudica produção de trigo, e indústria analisa qualidade do grão.
 291 *Globo.com* (2015).
 292 16. A. Donley, Brazil wheat output to fall in 2017-18. *World-Grain.com* (2018).
 293 17. F. A. S. USDA, “Gain Report - Brazilian Wheat Production, Quality Suffer After Adverse
 294 Weather” (2018).
 295 18. C. Tebaldi, D. Lobell, Estimated impacts of emission reductions on wheat and maize crops.
 296 *Clim. Change* **146**, 533–545 (2018).
 297 19. CEPEA, Center for Advanced Studies in Applied Economics: Commodities prices. *Agric. Ser.*
 298 (2020) (December 17, 2020).
 299 20. D. P. van Vuuren, *et al.*, The representative concentration pathways: an overview. *Clim.*
 300 *Change* **109**, 5 (2011).

RESEARCH ARTICLE

The extreme 2016 wheat yield failure in France

Rogério de S. Nória Júnior¹  | Jean-Charles Deswarte² | Jean-Pierre Cohan³  |
 Pierre Martre⁴  | Marijn van der Velde⁵  | Remi Lecerf⁵ | Heidi Webber^{6,7}  |
 Frank Ewert^{6,8}  | Alex C. Ruane⁹  | Gustavo A. Slafer^{10,11}  | Senthold Asseng¹ 

¹Department of Life Science Engineering, Digital Agriculture, HEF World Agricultural Systems Center, Technical University of Munich, Freising, Germany

²ARVALIS - Institut du Végétal, Villiers-le-Bâcle, France

³ARVALIS - Institut du Végétal, Loireauxence, France

⁴LEPSE, Univ Montpellier, INRAE, Institut Agro Montpellier, Montpellier, France

⁵European Commission, Joint Research Centre, Ispra, Italy

⁶Leibniz-Centre for Agricultural Landscape Research (ZALF), Müncheberg, Germany

⁷Brandenburg Technical University (BTU), Cottbus, Germany

⁸Crop Science Group, INRES, University of Bonn, Bonn, Germany

⁹NASA Goddard Institute for Space Studies, New York, New York, USA

¹⁰Department of Crop and Forest Sciences, University of Lleida - AGROTECNIO Center, Lleida, Spain

¹¹ICREA, Catalanian Institution for Research and Advanced Studies, Barcelona, Spain

Correspondence

Senthold Asseng, Department of Life Science Engineering, Digital Agriculture, HEF World Agricultural Systems Center, Technical University of Munich, Freising, Germany.
 Email: senthold.asseng@tum.de

Abstract

France suffered, in 2016, the most extreme wheat yield decline in recent history, with some districts losing 55% yield. To attribute causes, we combined the largest coherent detailed wheat field experimental dataset with statistical and crop model techniques, climate information, and yield physiology. The 2016 yield was composed of up to 40% fewer grains that were up to 30% lighter than expected across eight research stations in France. The flowering stage was affected by prolonged cloud cover and heavy rainfall when 31% of the loss in grain yield was incurred from reduced solar radiation and 19% from floret damage. Grain filling was also affected as 26% of grain yield loss was caused by soil anoxia, 11% by fungal foliar diseases, and 10% by ear blight. Compounding climate effects caused the extreme yield decline. The likelihood of these compound factors recurring under future climate change is estimated to change with a higher frequency of extremely low wheat yields.

KEYWORDS

compounding factors, extreme weather, food security, grain number, grain size, temporally and multivariate events

1 | INTRODUCTION

The production of wheat, the most important source of food for humans (Igrejas & Branlard, 2020), is increasingly variable due to climatic extremes, which threatens to disrupt global efforts toward

abolishing poverty and ensuring food security and peace (Nória Júnior et al., 2021; Perez, 2013; Shew et al., 2020). Europe is responsible for 35% of global wheat production (FAO stat, 2022). Drought and heatwaves are the main causes of the historical crop failures widespread across the breadbasket regions of the continent,

This is an open access article under the terms of the [Creative Commons Attribution-NonCommercial](https://creativecommons.org/licenses/by-nc/4.0/) License, which permits use, distribution and reproduction in any medium, provided the original work is properly cited and is not used for commercial purposes.

© 2023 The Authors. *Global Change Biology* published by John Wiley & Sons Ltd.

as experienced by northern European countries in 2018 (Beillouin et al., 2020; Webber et al., 2020). Such adverse weather conditions will become more pronounced and widespread with climate change (Battisti & Naylor, 2009; IPCC, 2021; Trnka et al., 2014). For example, in 2010, Russia suffered from the worst heatwave on record according to the Warm Spell Duration Index (Hoag, 2014). Initial attempts have been made to identify the future risk posed by heat and drought to local agriculture (Bailey et al., 2015; Rosenzweig et al., 2013). Several wheat crop modeling approaches have been developed and improved to estimate wheat yield responses to extreme weather conditions (Ceglar et al., 2019; Jägermeyr et al., 2021; Lischeid et al., 2022; Martre et al., 2015; Rötter et al., 2018; Wang et al., 2017; Webber et al., 2017). These studies have helped to identify future regional risks to national and global wheat production directly caused by extreme weather disasters (Asseng et al., 2011; Liu et al., 2019; Webber et al., 2018), and have been incorporated into wheat yield forecast systems to anticipate seasonal food shortages (Bussay et al., 2015; Lecerf et al., 2019; van der Velde & Nisini, 2019).

A major wheat production decline occurred in 2016 in Western Europe, centered around France, the fourth largest wheat-exporting country in the world (Ben-Ari et al., 2018). The national wheat yield of France dropped by 27% in 2016. This was the most extreme wheat yield decline in France since 1960 causing a shortfall of about 2.3 billion USD in the country's trade balance (Ben-Ari et al., 2018). The public European forecasting system failed to anticipate the magnitude of this wheat yield loss until shortly before harvest (van der Velde et al., 2020), which has been explained by the complexity (sequence, timing, or connectedness) of likely yield-determining events in 2016. Indeed, the 2016 yield failure was not caused by a single event. Winter wheat usually remains dormant during the cold of winter, flowering in the drier, warmer spring weather. However, the combination of a warm, wet winter and an extended period of precipitation in the spring of 2016 led to a number of simultaneous or consecutive yield-reducing factors, including heavy rainfall, crop diseases, low solar radiation, and anoxia, affecting both grain set and grain filling (Ben-Ari et al., 2018). Temporal and multivariate compound events (Bevacqua et al., 2021; Zscheischler et al., 2020) caused the extreme 2016 wheat yield failure. Most crop modeling approaches only consider seasonal water shortage and heat stress, thus neglecting the connected or compound nature of many extreme climate- (Lischeid et al., 2022; Raymond et al., 2020) and weather-related events on crop growth and development. For example, heavy rainfall may damage fragile flowers, immediately reducing the potential to set grain, while waterlogging the soil and depriving roots of oxygen, simultaneously creating humid conditions that encourage the spread of plant diseases with detrimental effects on grain yield and quality. By not accounting for the complex effects or concurrence of multiple factors, the predictive ability of crop forecast systems for Europe is limited, especially for extreme weather (Ruane et al., 2021; van der Velde et al., 2020).

The inability of crop and statistical models to predict the extremely low 2016 wheat yield in France suggests that we are potentially underestimating the projected impacts of climate change

on agriculture (van der Velde et al., 2020; Webber et al., 2020). To improve seasonal forecasting systems, we aimed to quantify the impact on yield formation of the possible causes of the poor 2016 yield in France proposed by Ben-Ari et al. (2018). We used a unique detailed dataset from ARVALIS-Institut du végétal, with observations from 3512 experimental unit treatments at eight locations across the French breadbasket region over 6 years spanning the 2016 extreme (2014–2019). Multi-model regressions, process-based crop growth simulation modeling, and observations of yield physiology were used to separate and quantify various climate impacts on the main wheat yield components in 2016, comparing locations and seasons. We then extended the analysis based on long-term climate change scenarios—from the recent Coupled Model Intercomparison Project phase 6 (CMIP6) climate model ensemble for 2020 to 2100—to analyze the frequency of future concurrent or consecutive weather events potentially causing similar compound yield losses in France.

2 | MATERIALS AND METHODS

The breadbasket of France, accounting for around 70% of France's total wheat production, extends over 27 departments, all impacted by the extreme yield losses in 2016 (Figure 1). ARVALIS-Institut du Végétal wheat field trial data from 3512 experimental unit treatments of 221 cultivars for six cropping seasons (2014–2019 harvests) at eight locations across the breadbasket region were used to quantify the individual contribution of nitrogen leaching, plant diseases, low solar radiation, anoxia, and high rainfall to variation in wheat yield in France in 2016.

2.1 | ARVALIS-Institut du Végétal field trial management

The experimental unit treatments in the 2014–2019 field trials designed and performed by ARVALIS-Institut du Végétal for different objectives were useful in analyzing the following specific aspects (Figure 2).

- Growth performance: 3188 experimental unit treatments tested the performance of a total of 221 winter wheat cultivars in eight research stations, here named 1 to 8 according to the magnitude of wheat yield loss (Figure 1). We used 738 of these experimental unit treatments (which included 172 in 2016) to compute yield component anomalies and develop grain number and grain size statistical models. Only cultivars that had experimental unit treatments in 2016 and in at least one additional year were considered to ensure any yield anomaly was independent of the research station and department (Figure S27). The number of experimental unit treatments per research station is shown in Table S1. In addition, we tested the DSSAT-Nwheat (Kassie et al., 2016) crop simulation model with 42 wheat experimental unit treatments for simulating wheat yield of the winter wheat cultivar Rubisko

(Figures S30 and S31). Growth performance experiments had two types of experiments:

- Cultivar comparison: with around 92% of data, and in all research stations. The objective of these experiments is to compare the growth of several commonly used and developing wheat cultivars. Measurements of wheat ear emergence date, grain number per unit area, average single grain size, grain nitrogen concentration, and grain yield were performed. For these experiments, the flowering date was simulated considering a linear relationship with the ear emergence date, as presented in Figure S28.
- Observatory: with around 8% of data, and in all research stations. The objective of these experiments is to perform a detailed performance measurement of the most common cultivars with greater prospects for use. Measurements of wheat ear emergence and flowering date, total aboveground biomass at anthesis and maturity, total aboveground nitrogen at anthesis, ear density, grain number per unit area, grain number per ear, average single grain size, grain nitrogen concentration, and grain yield were performed.
- Nitrogen response: 124 experimental unit treatments testing the response of wheat cultivars to nitrogen fertilizer rates at research stations 3, 5, and 8. Nitrogen fertilizer rates varied from 0 to 350 kg ha⁻¹ (Figure S12). Measurements of wheat ear emergence and flowering date, total aboveground biomass at anthesis and maturity, total aboveground nitrogen at anthesis, ear density, grain number per unit area, grain number per ear, average single grain size, grain nitrogen concentration, and grain yield were performed.
- Plant disease: 2650 experimental unit treatments had records of plant disease types and tests of fungicide efficiency. The efficiency of fungicides was obtained by comparing experimental unit treatments with and without a particular fungicide application. Measurements of wheat yield were performed.

All experimental unit treatments were rainfed and sown from late September to November and harvested between the beginning of July and the end of August. For trials on growth performance and nitrogen response, the crop protection programs were similar to local farm practices which may have included fungicides, herbicides, and insecticides to prevent any damage to the crop. For growth performance and plant disease, nitrogen fertilizer was usually applied in early February, mid-March, and late April, with the total amount applied varying from 175 to 225 kg N ha⁻¹. Phosphorous and potassium fertilizers were applied during autumn if needed to prevent late-season shortage of these nutrients affecting nitrogen uptake, yield, and grain quality.

A single experimental plot was typically 2 m wide and 10 m long, with 11 rows, and the 7 middle rows were harvested. For each experimental unit treatment, we used the average of three single experimental plots, as described by Cohan et al. (Cohan et al., 2019). These field trials sufficiently capture the broader regional impact that occurred in 2016 (Figure S27).

2.2 | Anomalies in wheat yield components

Anomalies in the wheat yield components (WC anomaly) of total aboveground biomass at anthesis and maturity, total aboveground nitrogen at anthesis, ear density, grain number per unit area, average single grain size, grain nitrogen concentration, grain number per ear, and grain yield were calculated based on the 738 growth performance trials. Observed data for grain number per unit area, average single grain size, grain nitrogen concentration, and grain yield were available for all these trials. However, only 40% of the trials had observed data for grain number per ear, and only 10% had observed data for total aboveground biomass at anthesis and maturity, total aboveground nitrogen at anthesis, and ear density.

No WC anomaly was found for total aboveground biomass at anthesis at research stations 2 and 3, or for ear density and grains per ear at research station 2.

For each yield component, the 2016 WC anomaly relative to the 2014–2019 (omitting 2016) reference period was calculated as:

$$\text{WC anomaly}_{(ij)} = \frac{1}{C_{(ij)}} \sum_{k=1}^{C_{(ij)}} \frac{\text{WC}_{2014-2019 (ijk)} - \text{WC}_{2016 (ijk)}}{\text{WC}_{2014-2019 (ijk)}} \quad (1)$$

where $\text{WC}_{2014-2019 (ijk)}$ and $\text{WC}_{2016 (ijk)}$ are the wheat yield components for the i th research station for the 2014–2019 reference period and the year 2016, respectively, j th represents the different wheat yield components, and C is the number of cultivars, each individually represented by k th.

2.3 | Analysis of the causes of the 2016 anomalies of grain number per unit area and average single grain size

To identify the causes of the 2016 wheat yield failure, we first analyzed the climatic anomalies that occurred across the research stations in France, and noticed that a remarkably wet and warm winter was followed by increased rainfall in late spring, around the time of wheat anthesis. We created indices to analyze the effect of excessive rainfall, low solar radiation, and anoxia, as shown in Tables S2 and S3. We also analyzed the possibility that nitrogen leaching may have affected crop nitrogen uptake, as shown in Section 2.3.1. According to the frequency of diseases observed in the plant disease trials, wheat fusarium ear blight (*Microdochium nivale*), septoria leaf blotch (*Zymoseptoria tritici*), and leaf rust (*Puccinia striiformis* f. sp. *tritici*) were the main diseases of the 2016 wheat-cropping season. Oidium (*Blumeria graminis*) was reported in 0.2% of all the experimental unit treatments and considered not significant for the wheat yield losses of 2016.

The potential contribution of plant diseases, anoxia, heavy rainfall, and nitrogen leaching to the poor 2016 wheat yield was individually analyzed, and separated into those that occurred around anthesis (thus affecting wheat grain number per unit area) and those that occurred during grain filling (thus affecting average single grain size).

2.3.1 | Effects of nitrogen leaching on wheat yield

To determine if nitrogen leaching caused nitrogen deficit stress on plants, we analyzed the results of the nitrogen response and growth performance trials. With these data, the nitrogen nutrition index (NNI), proposed by Justes et al. (1994), was calculated at anthesis for each research station and cropping season, as follows:

$$\text{NNI} = \frac{\%N}{\%N_c} \quad (2)$$

where %N ($\text{g N } 100 \text{ g}^{-1} \text{ DM}$) is the nitrogen concentration in the aboveground biomass at anthesis, and %N_c is the critical nitrogen concentration, calculated as:

$$\%N_c = 5.35 \times \text{Biomass}_{\text{ant}}^{-0.442} \quad (3)$$

where Biomass_{ant} (t N ha^{-1}) is the total aboveground biomass at anthesis. The crop nitrogen status (Justes et al., 1994) is considered optimal when NNI equals 1, limiting when <1, and “luxury” when >1.

To assess whether crop nitrogen uptake was affected in 2016, the mass of nitrogen that had been taken up by the crops at anthesis and the mass of nitrogen that was translocated from the aboveground vegetative tissues to grains during the grain-filling period were calculated for the years 2016 to 2019 (Figure S13), based on the nitrogen content in straw and grain measured in the experimental unit treatments during these years. Nitrogen leaching was also simulated with DSSAT-Nwheat (see Section 2.4.3) to verify whether the crop simulation model simulated impacts on yield even under nitrogen leaching conditions (Figure S11).

2.3.2 | Effects of solar radiation, rainfall, plant diseases, and anoxia on grain number per unit area and average single grain size

Wheat grain number per unit area is closely related to growing conditions before and shortly after anthesis (Fischer, 1985), when the number of fertile florets is determined and when fertile florets set grains (Slafer et al., 2015). Therefore, solar radiation, rainfall, and temperature conditions were analyzed together with the modeled impact of plant diseases on grain number per unit area for the period around anthesis for each wheat cultivar and each location. The impact of fungal foliar diseases on grain number was not considered because differences between resistant and non-resistant cultivars were not observed in the field experiments (Figure S15). Plant diseases and anoxia were considered as causes of the average single grain size anomaly, as they mostly occurred during the grain-filling period in June and July. Both, septoria leaf blotch and leaf rust are favored by warm, wet winters and wet springs (te Beest et al., 2009), and their impacts were calculated together here as “fungal foliar diseases.”

Weather-based indices for low solar radiation, heavy rainfall, and anoxia, as well as other indexes, such as a photo-thermal quotient,

were built using daily records of accumulated rainfall (mm), maximum and minimum air temperature (°C), and solar radiation ($\text{MJ m}^{-2} \text{ day}^{-1}$) from weather stations located close to each research stations. These weather-based indices were created considering wheat phenology, and further details on how these indices were developed and their equations are presented in Tables S2 and S3. Relevant plant disease infection rate models were originally developed and tested by te Beest et al. (2009) for fungal foliar diseases, namely septoria leaf blotch and leaf rust, and for ear blight by Madgwick et al. (2011), we used these models to quantify the incidence of these wheat diseases in France between 2014 and 2019 (Figure S32). Equations and further details of the plant disease models are described in Table S3. These equations were fitted as explanatory variables to calculate grain number per unit area and average single grain size anomalies of 2016.

2.4 | Modeling grain number per unit area and average single grain size anomalies of 2016

2.4.1 | Statistical models

Statistical models were built considering the anomalies of grain number per unit area and average grain size (calculated as in Equation 1) as the objective variables. Weather-based indices for heavy rainfall, solar radiation, and air temperature were used as explanatory variables for grain number per unit area anomalies (Table S2). And weather-based indices for fungal foliar diseases, ear blight, and anoxia, as well as solar radiation and temperature, were the explanatory variables for average grain size anomalies (Table S3). With these weather-based indices, the Gini index (Menze et al., 2009) from the random forest machine learning method was calculated to identify the most influential indices determining grain number per unit area and average single grain size anomalies for 2016 and each of the years of the reference period 2014–2019 (excluding 2016).

A stepwise procedure was then used to select the best combination of input variables for quantifying extreme crop yields (Ben-Ari et al., 2018; Nóia Júnior et al., 2021). These stepwise procedures were also performed in R with the command step. Based on the Gini index, an indicator of the relative importance of the weather-related factors in determining the 2016 anomalies, statistical models were built using the explanatory variables of ear blight, low solar radiation, and high rainfall indices for grain number anomaly of 2016, and fungal foliar diseases, ear blight, low solar radiation, and anoxia during grain filling for grain size anomaly of 2016. The statistical models for grain number or grain size (\hat{y}_g) were built as shown in Equation 4:

$$\hat{y}_g = \beta_0 + \beta_1 x_1 + \dots + \beta_D x_D \quad (4)$$

where \hat{y}_g is the objective variable (or grain number per unit area anomaly or average grain size anomaly of 2016), β_0 is the estimate of intercept, and β_1 and β_D are the estimates of coefficient for each of the explanatory variables from x_1 and x_D .

The research stations had different numbers of experimental unit treatments (Table S1), and to capture the spatial distribution of grain number and average single grain size anomalies, the statistical models were built 1000 times with parameter values perturbed through random selections of the variables, keeping two experimental unit treatments per research station (the experimental unit treatment values within the same research station usually correspond to different cultivars). Thus, the statistical models were always trained for two experimental units simultaneously in eight research stations, summing up to 16 values of grain number or grain size anomalies fitting their 16 corresponding values of each explanatory variable. The performance of the models (r^2) was computed in a randomly selected grain number or grain size anomaly of 2016 not included in the trained dataset (out-of-sample analysis). The influential weather-based indices were selected using the Akaike information criterion (AIC) independently for each of the 1000 models for grain number per unit area and average grain size. Thus, the final contribution of each index considered in the grain number per unit area and average single grain size anomaly models was assessed with the mean of an ensemble of 1000 statistical models (quantification of the impacts of different indices is detailed and explained in Section 2.4.2).

Grain number and average single grain size were observed in field experiments from 738 (with 172 in 2016) performance trials. Anomalies were calculated from these observed grain numbers and grain sizes.

2.4.2 | Quantifying the impacts of individual yield-limiting factors in 2016

The 1000 models of grain number and grain size anomalies in the 2016 cropping season were executed by initially taking the 2016 values for each input variable (derived from weather-based indices and plant disease model outputs). The models were executed again, but this time, value of an explanatory variable for 2016 was replaced by that for each of the years in the reference period from 2014 to 2019 except 2016 (Figure S29). This step was repeated, replacing the value of each input variable in turn. Thus, the contribution of each factor to the 2016 wheat yield anomaly was calculated as the difference between the estimated grain number or average single grain size values from running the models with all variables for 2016, and the estimates from running the statistical models with all variables of 2016 except one from a reference year (Figure S29). For example, to calculate the contribution of low solar radiation to the grain number per unit area in 2016, all the 1000 models of grain number were executed with all variables (weather-based indices inputs) from the 2016 cropping season. At the same time, the same 1000 models were executed with all variables for 2016 but low solar radiation index was from 2014 to 2019 (excluding 2016 and individually executed for each year of the reference period). As a result, there were 6000 grain number anomaly estimates (1000 for 2016 with all variables from 2016 and 5000 for 2016 with modified solar radiation from 2014 to 2019 reference period). The difference between the average of the 1000 estimates for 2016 with all variables

from 2016 ("R1: in Figure S29) and the average of the 5000 estimates for 2016 with modified solar radiation from 2014 to 2019 reference period ("R2"–"Rx" in Figure S29) was considered to be the size of the impact of low solar radiation. This procedure was repeated for each input variable (weather-based indices and plant disease model outputs) for grain number per unit area and average grain size. The impacts on yield were computed considering that grain yield is the result of the product of grain number per unit area and average grain size. The calculated impact of each variable was summed up and proportionally divided according to the size of the anomaly of grain number per unit area, average grain size, and grain yield of each location. The residual is considered as the difference between the estimated and observed anomalies (Figures 3h and 4j). Additional details are presented in Text S1.

This is similar to the method proposed by Asseng et al. (2011) for separating the impacts of temperature from other factors on wheat yield. The contribution of each factor calculated with the statistical models was compared with solar radiation impacts simulated by the DSSAT-Nwheat crop simulation model (described in Section 2.4.3, Figure S17) and impact of plant diseases calculated with resistant and sensitive cultivars in the plant disease trials.

Weather-based indices highly correlated as heavy rainfall and anoxia were explanatory variables for different objective variables (heavy rainfall for grain number and anoxia for grain size, as described in Section 2.3.2). The impacts of low solar radiation index (which is correlated with heavy rainfall, both explanatory variables of grain number per unit area) were also quantified with a crop simulation model as an independent analysis.

2.4.3 | DSSAT-Nwheat crop simulation model

The DSSAT-Nwheat process-based crop simulation model used in this study is part of the DSSAT crop modeling framework (<https://dssat.net/>). DSSAT-Nwheat has been widely tested in wheat modeling growth studies across the world (Kassie et al., 2016). The calibration of DSSAT-Nwheat to the breadbasket region of France was done for cultivar Rubisko grown in the 42 experimental unit treatments in 2014, 2015, 2017, and 2019 (Text S1). Although data from 2016 and 2018 were available, they were not used for calibration because of the high incidence of wheat diseases in these years, which is not simulated by the Nwheat model. The root-mean-square error (RMSE) for total aboveground biomass and grain yield was 0.8 kg ha⁻¹ (4%) and 0.6 kg ha⁻¹ (6%), respectively. The precision of Nwheat was satisfactory for total aboveground biomass ($r^2 = .83$) and grain yield ($r^2 = .70$) (Figure S30). After calibrating, Nwheat was tested for 2016 and 2018 with the result that total aboveground biomass and grain yield were both overestimated (Figure S31). This was expected because Nwheat does not account for how the stress factors of heavy rainfall around anthesis, anoxia, and diseases affect plant growth. However, Nwheat was still used to quantify the solar radiation (Figures S16 and S17) and nitrogen leaching (Figure S11) impacts on wheat grain yield. The calibrated coefficients are shown in Table S4. The impact of low solar radiation with DSSAT-Nwheat was calculated by modifying the 2016

seasonal daily solar radiation inputs with the other years in the reference period 2014–2019, the same as the method applied to statistical models (described in Section 2.4.2).

2.5 | Climate change scenarios

Daily climate data for the 1960–2100 period were drawn from the Inter-Sectoral Impacts Model Intercomparison Project (ISIMIP) (Lange, 2019), which provides bias-adjusted and spatially disaggregated climate model outputs from the Coupled Model Intercomparison Project phase 6 (CMIP6) (Eyring et al., 2016). Historical simulations before 2015 are from climate models forced by the historical trends in the main natural and anthropogenic factors. After 2015, simulations follow the Shared Socioeconomic Pathway and Representative Concentration Pathway SSP5-8.5 (O'Neill et al., 2020). The IPCC describes this as a “very high” emissions scenario (IPCC, 2021), and we use it here to illustrate the upper tail of future risk (analysis was also performed for SSP5-2.6 and the results are shown in Figure S21). We considered five CMIP6 models (GFDL-ESM4, IPSL-CM6A-LR, MPI-ESM1-2-HR, MRI-ESM2-0, and UKESM1-0-LL) that include high, medium, and low climate sensitivity models similar to the full CMIP6 distribution (Jägermeyr et al., 2021). We used daily weather data from the ISIMIP downscaled projections for the five selected models to quantify future frequency of ear blight, foliar fungal diseases, heavy rainfall, low solar radiation around anthesis (with anthesis date fixed at 1 June), and anoxia during wheat grain filling (from 1 June to 31 July) using the indices previously described (Tables S2 and S3) for predicting wheat grain number per unit area and average single grain size anomalies of 2016. To minimize uncertainties related to fixed anthesis and grain-filling periods, we carried out an additional analysis considering different fixed dates of anthesis (with anthesis date fixed at 1 May), and anoxia during wheat grain filling (from 1 May to 15 June) (Figures S19–S34).

The extreme 2016 wheat yield failure occurred once in 62 years from 1960 to 2021, with 1.6% frequency. Similarly, extreme low national wheat yield was here estimated for each GCM separately and defined as the 1st percentile of each wheat yield component during 1960–2020 (which as a 1% frequency is equivalent to once every 100 years), with the grain number and grain size anomaly models used for quantifying the impacts of individual yield-limiting factors in 2016. We averaged the simulated grain number and grain size for the eight research stations to scale-up to the regional level, as suggested by Ben-Ari et al. (2018). Individual results for each research station are presented in Figure S19.

With weather-based index used for building the grain number per unit area and average grain size statistical models (Tables S2 and S3), we refitted a new statistical model to estimate grain yield from 1984 to 2020 in the breadbasket of France (Figure S33). This new statistical model for wheat yield was built as described in Section 2.4.1. We applied the new wheat yield model used to project the future frequency of extremely low wheat yield years in the breadbasket of France and the results are shown in Figure S33b. This was performed to reduce uncertainties of projections for future frequency of the extreme 2016 wheat yield failure in the breadbasket of France.

2.6 | Statistical analysis

All data analyses and statistical analyses were carried out using the statistical program software R (R Core Team, 2017). To analyze the yield component anomalies across research stations, the data were submitted to an analysis of variance (ANOVA) and, when significant, the mean values were compared using the Tukey test. The random forest models were fitted to the data by using the function randomForest of the R package “randomForest.” ANOVA (mean of squares) were carried out to determine the degree to which the climatic variables selected by the statistical models could explain wheat grain number per unit area and average single grain size anomalies of 2016 across all the studied research stations (i.e., ANOVA was only computed for 2016 anomaly). Statistically significant differences were judged at $\alpha = .05$. An ANOVA was performed with the function aov. As the statistical models, ANOVA was computed 1000 times. The importance of each variable to explain spatial variation of wheat grain number per unit area and average grain size anomalies in 2016 was calculated as the average of 1000 ANOVA analyses.

3 | RESULTS

3.1 | Extreme yield loss and weather conditions in 2016 in France

The 2015/2016 wheat-growing season in France started with unusually high temperatures, with monthly averages of 3°C above November and December (autumn and early winter) averages for the 2010–2020 period (Figure 1b). Late winter was particularly wet, with accumulated rainfall of 90 mm in March, twice the 2010–2020 average for this month (Figure 1c). After the warm and wet winter, spring 2016 was on average 1.5°C cooler than the average spring temperature of the 2010–2020 period. There was high rainfall from late May to early June in 2016. The accumulated rainfall in this period was the highest recorded in 30 years (Figure S3). Cloud cover associated with the high rainfall led to a 30% decrease in monthly solar radiation in May and June compared to the 2010–2020 average. Low solar radiation and high rainfall continued until early July. The weather conditions in France and other parts of Western Europe in 2016 were similar (Figure 1a; Figures S1 and S2), but the accumulated rainfall in May and June was not uniformly high, as some northwestern areas of France received less rainfall including around research station 8 (Figure S1).

3.2 | Yield components during the wheat-growing season for the 2016 harvest in France

For each of the eight research stations across France, the 2016, anomaly in various wheat growth and yield components was calculated with respect to the 2014–2019 reference period (omitting 2016; Figure 2) from field experiment data. Total aboveground biomass at anthesis (Figure 2a) and ear density (Figure 2b) for 2016 was

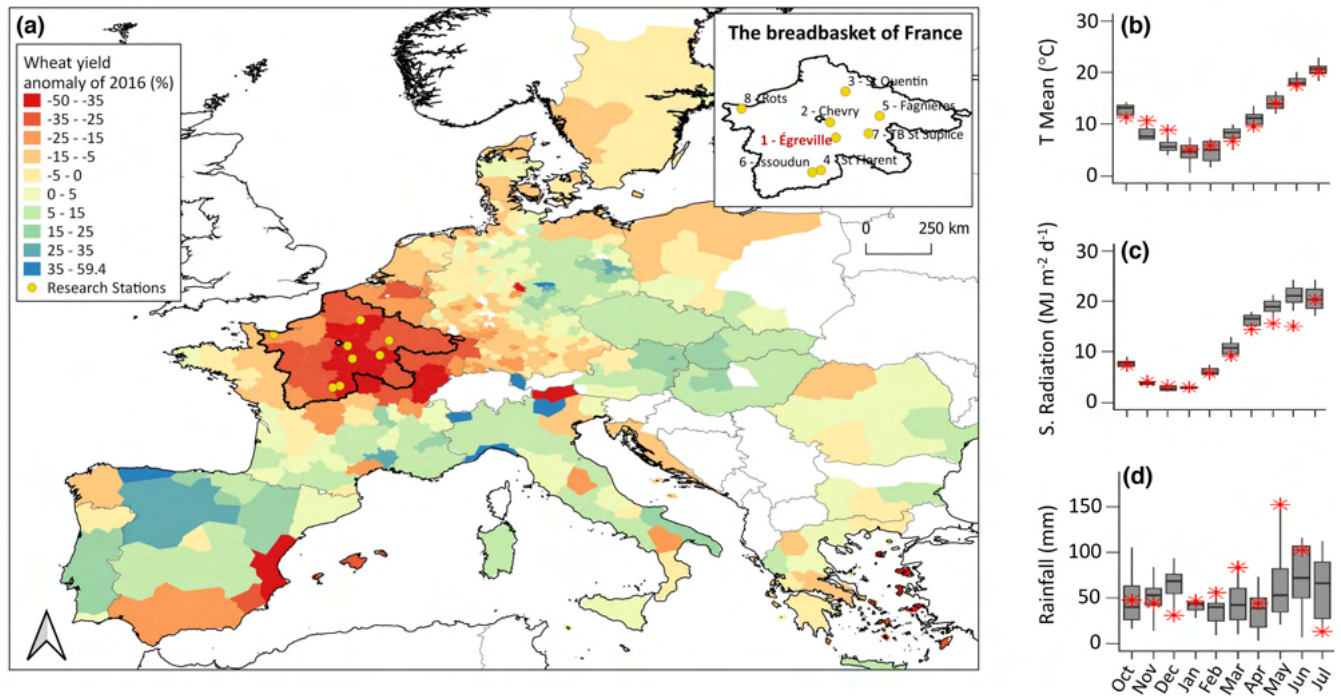


FIGURE 1 Extremely low wheat yields in Western Europe in 2016. (a) Spatial distribution of the observed 2016 trend-corrected wheat yield anomaly. The breadbasket region of France is outlined by bold black contours with locations and names of the research stations (yellow dots) shown also in the inset (upper right). Boxplot of monthly (b) mean temperature (T mean), (c) solar radiation, and (d) rainfall, over the wheat-growing season for 2013–2020 harvest years for the most severely affected region at Égreville, France (research station 1). Lower whiskers extend below the 25% quantile (Q1) and upper whiskers above the 75% quantile (Q3) by 1.5 times the interquartile range (interval between Q3 and Q1). Values for the 2015/2016 growing season are plotted as red asterisks. Weather data for the other field sites studied and across Europe are shown in [Figures S1–S8](#). Map lines delineate study areas and do not necessarily depict accepted national boundaries.

similar to those of the reference period averages, with anomalies varying from -10% to 10% at the different research stations. DSSAT-Nwheat crop growth model simulation results suggest that nitrogen leaching in 2016 occurred between the stem elongation and anthesis ([Figure S11](#)). Despite this, total aboveground nitrogen at anthesis was up to 25% higher ([Figure 2c](#)), and the corresponding nitrogen nutrition index at anthesis was 5%–20% higher in 2016 than during the reference period ([Figure 2f](#)).

Observed total aboveground biomass at maturity dropped by as much as 40% ([Figure 2d](#)), while grain number per ear and per m² fell by as much as 40% and 50%, respectively, in 2016 ([Figure 2e,g](#)). A negative anomaly of about 40% in grain size (i.e., average single grain size) was also found for 2016 ([Figure 2h](#)) compared with the reference period. As a result, the grain yield loss in 2016 compared to 2014–2019 varied from 15% to 72% according to the research station ([Figure 2i](#)), and the greatest loss across a district was 55%.

Wheat yield is the result of wheat grain number and grain size, and their values are indicative of stresses that occur within a season and the timing of those stresses. For example, grain number per unit area is related to growing conditions before and shortly after anthesis (Fischer, 1985), when most fertile florets set grains (Slafer et al., 2015). Therefore, we first identified the growing conditions potentially causing the wheat yield anomaly in 2016, and placed these effects in the phenological context of when they would have occurred.

3.3 | Grain number and extremes of high rainfall and low solar radiation around anthesis

In 2016, anthesis occurred a few days later than usual because the low temperatures of late winter and early spring delayed wheat phenology ([Figure 3a,c](#)). The delayed anthesis coincided with abnormally heavy rainfalls (i.e., daily rainfall >20 mm) and low solar radiation in late May and early June ([Figure 3b,d](#)). In addition to numerous heavy rainfall events, the accumulated rainfall during the 15 days around anthesis, varying from 45 mm to 180 mm depending on the research station, was up to five times more than expected for the period. Indeed, records show that this was the longest period of rainfall in 30 years. Anthesis occurred during 54 h of almost uninterrupted rainfall ([Figure S8](#)) in a week when hourly solar radiation mostly remained below the wheat light compensation point of 50 W m^{-2} (Pang et al., 2018). The 2016 anomaly in grain number per unit area was the most drastic in the research stations receiving more rainfall and less solar radiation around anthesis, and was particularly low for specific cultivars which underwent anthesis just at the time of peak rainfall in this period of maximum daily accumulated rainfall ([Figure 3e](#)). For example, the grain number anomaly was -13% for the cultivar Rubisko in research station 8, which is less extreme than the -45% anomaly for this cultivar in research station 1, but more extreme than the decline seen for cultivar Soissons grown in the same research station but which underwent anthesis earlier ([Figure 3e](#)).

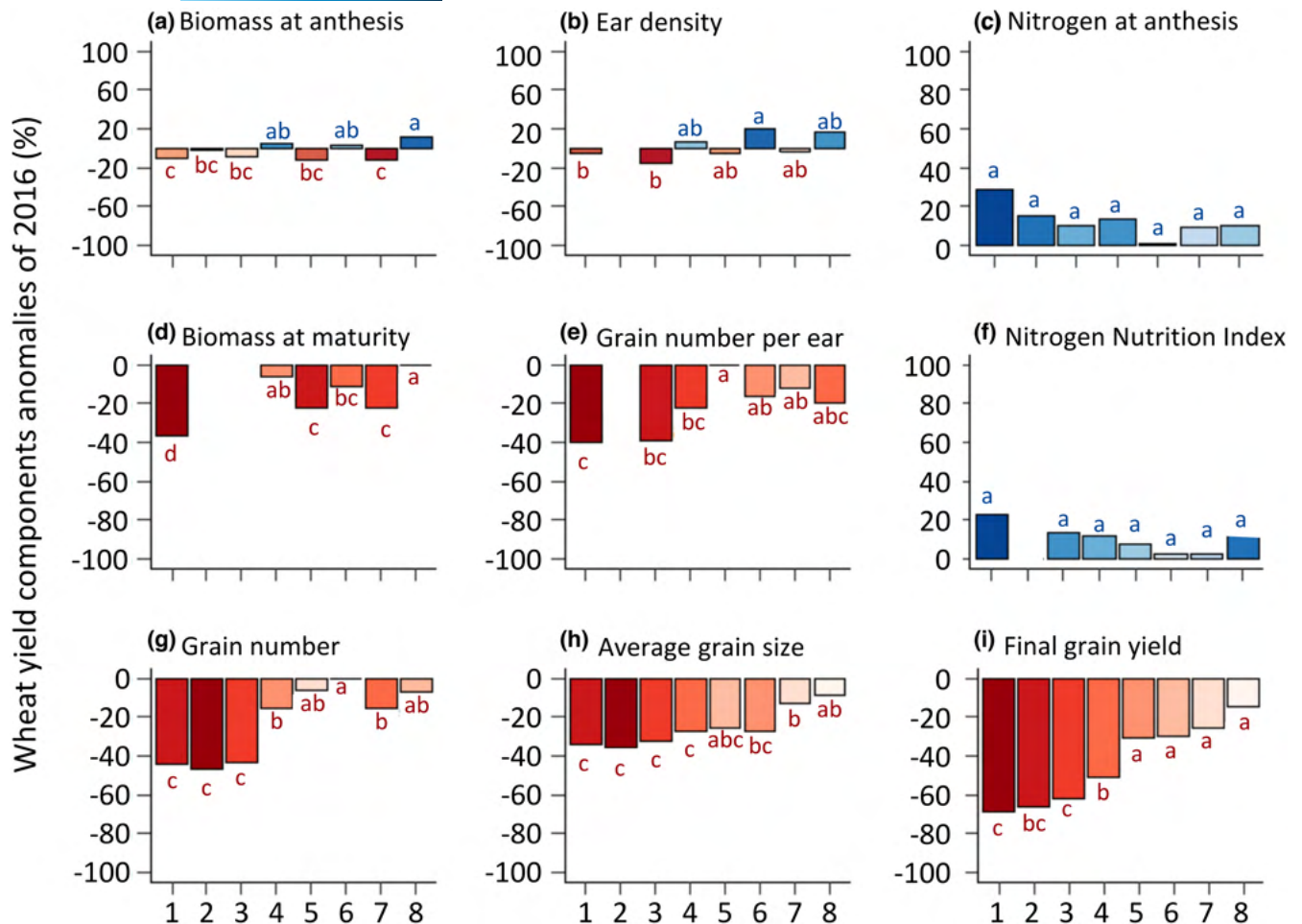


FIGURE 2 Components of 2016 wheat yield anomalies that occurred at eight sites in the main breadbasket of France. Observed positive (blue) and negative (red) anomalies in 2016 in relation to the average for 2014–2019 (omitting 2016) wheat harvests for the growth components, (a) total aboveground biomass at anthesis, (b) ear density (ear number per unit area), (c) total aboveground nitrogen at anthesis, (d) total aboveground biomass at maturity, (e) grain number per ear, (f) nitrogen nutrition index, (g) grain number per unit area, (h) average single grain size, and (i) final grain yield. Different letters within each panel represent statistically significant differences in the component anomaly between the research stations ($p < .05$). For each yield component, bar shading indicates the ranking in magnitude of anomalies (as in i) for each site from the largest (dark) to the smallest (pale). The research stations were numbered from 1 to 8 according to the magnitude of their wheat yield loss in 2016 (as in i, location 1 had the highest yield loss in 2016 and location 8 the lowest): 1, Égreville; 2, Chevry; 3, Saint-Quentin; 4, Saint-Florent; 5, Fagnières; 6, Issoudun; 7, Barbarey-Saint-Sulpice; and 8, Rots.

To assess the impacts of low solar radiation and high rainfall and other possible limiting factors on the 2016 grain number anomaly, we determined the Gini index to show the importance of the variables in a random forest and a multi-model regression model fitted using a stepwise selection procedure. Both the Gini index and the multi-model regressions were calculated 1000 times through random selections of wheat grain number anomalies. Thus, the circular graphs in Figure 3f,g represent the frequency of selection of each limiting factor as the first, second, or third most important variable for explaining wheat grain number in 2016 (Figure 3f) and for the reference period of 2014–2019 (without 2016) (Figure 3g). The photo-thermal quotient (Fischer, 1985) (Table S2) was by far the most important factor for defining wheat grain number per unit area in the 2014–2019 reference period, whereas the variation of grain number among the stations and cultivars in 2016 was explained mainly by the level of solar radiation

and heavy rainfall events, both around anthesis. In the multi-model regression models, these variables together explain most of the 2016 anomaly of grain number per unit across the eight locations representative of the breadbasket region of France (Figure 3h).

3.4 | Grain size and plant diseases and anoxia

The autumn and early winter of 2015 were unusually warm, including several days when the mean temperature was 10°C higher than the 2010–2020 average (Figure 4a,c). This was followed by higher-than-normal amounts of precipitation during late winter and early spring, with a total accumulated rainfall of up to 300 mm (Figure 4b,d). Such warm and moist conditions were propitious to foliar diseases and Septoria leaf blotch was observed in 91% and wheat leaf rust in

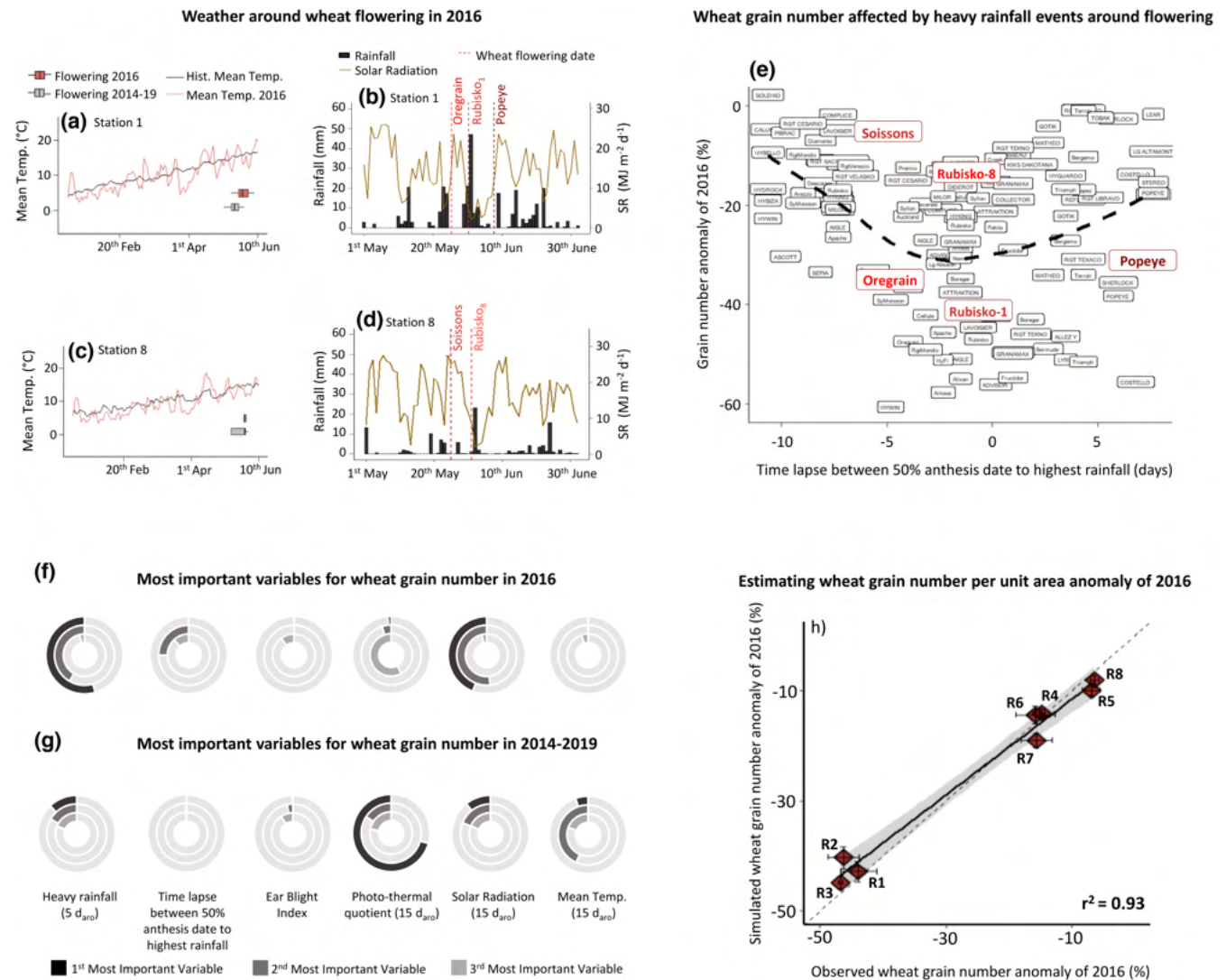


FIGURE 3 Wheat grain number as affected by adverse weather conditions around anthesis. (a–d) Comparison of wheat anthesis date and weather conditions during late winter and spring for 2016 and the mean of 2014–2019 (without 2016) harvests at (a, b) research station 1 and (c, d) research station 8. (a, c) Mean temperature traces with boxplots of anthesis dates of all cultivars grown at each site. (b, d) Daily solar radiation (trace) and accumulated rainfall (bars) with dotted lines indicating the anthesis dates of individual cultivars. (e) Relationship between observed anomaly in grain number of different winter wheat cultivars for the 2016 and 2014–2019 harvests and the time lapse between the date when 50% of individuals had flowered (50% anthesis date) and the day with highest rainfall (see Table S2). (f, g) The three most important variables selected according to the Gini index from 1000 different models estimated from random forest variable selector method for estimating wheat grain number anomalies in France considering (f) only the 2016 harvest, and (g) all harvests from 2014 to 2019 excluding 2016. (h) Comparison between the observed and simulated 2016 wheat grain number per unit area anomaly using a multiple regression linear model, from 1000 different models in an out-of-sample analysis – errors bars show the standard errors from the 1000 simulations (vertical errors bars) and the observed grain number anomaly (horizontal errors bars) in (h). The research stations (R) are as follows: 1, Égreville; 2, Chevry; 3, Saint-Quentin; 4, Saint-Florent; 5, Fagnières; 6, Issoudun; 7, Barbarey-Saint-Sulpice; and 8, Rots.

17% of all experimental unit treatments studied by ARVALIS across the breadbasket region of France (Figure 4g). High rainfall around anthesis led to widespread soil saturation and flooding during the wheat grain-filling period (Figure 4e) and a high incidence of ear blight. Usually marginal, ear blight was observed in 27% of all the experimental unit treatments in 2016 (Figure 4g). Water balance simulations, accounting for the difference between daily reference evapotranspiration and rainfall, indicated an excess of water

of up to 120mm from early June until late July, spanning most of the wheat grain-filling period (Figure 4e). Water was in excess at all the research stations except research station 8, which notably had the smallest yield loss (Figure 4f). The combination of these extreme conditions, plus the stress from disease and anoxia, and limited solar radiation during grain filling, may have affected grain size (Text S1 and Figure S23). The effect of these variables was confirmed by ranking their importance using the Gini index (Figure 4h,i). Overall,

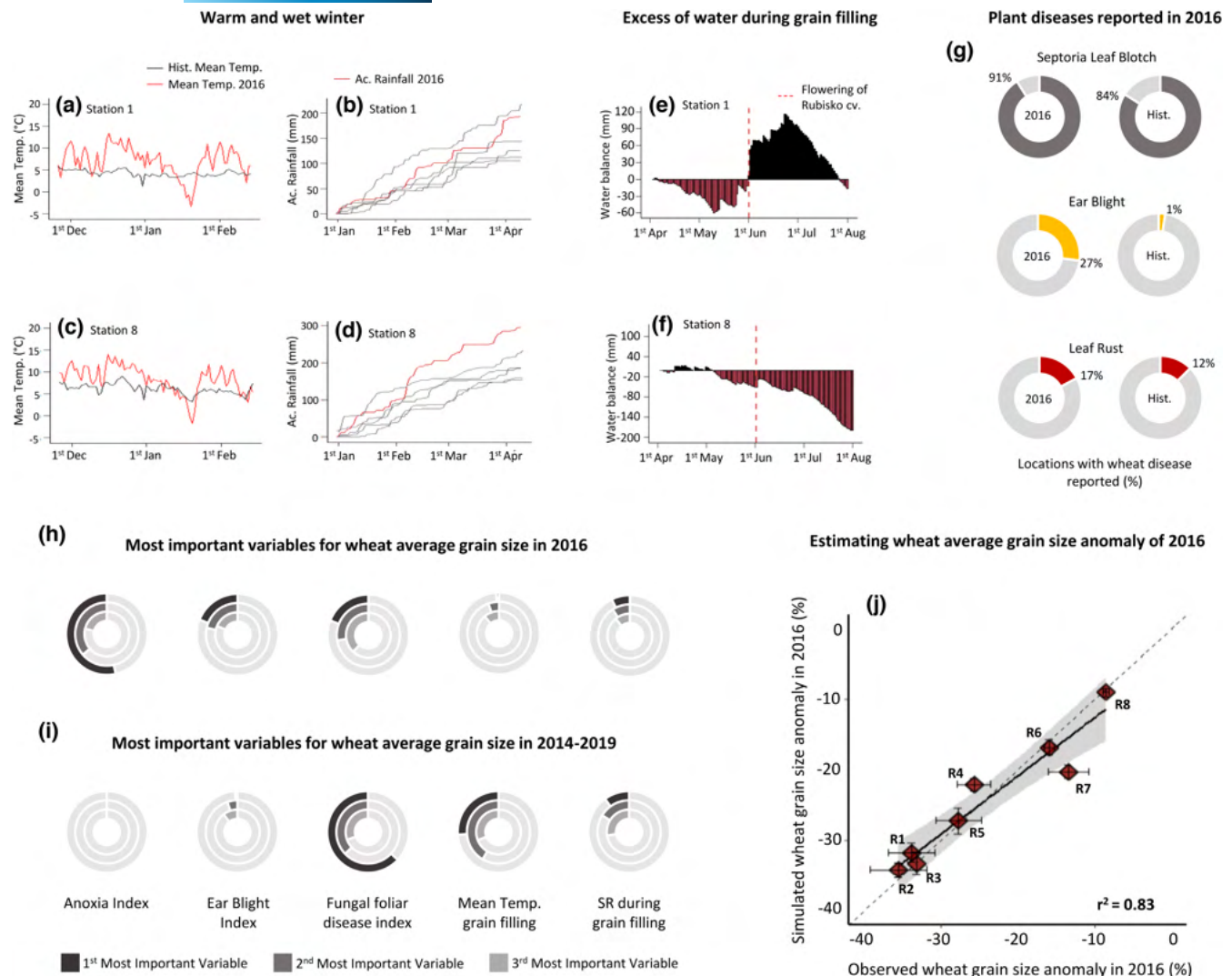


FIGURE 4 Wheat grain size affected by plant diseases and excess water. (a–d) Weather conditions during the 2016 winter at (a, b) research station 1 and (c, d) research station 8. (a, c) Mean temperature in 2016 (red trace) compared to the average (grey trace) for the reference period of 2014–2019 (omitting 2016) and (b, d) daily accumulated rainfall (red trace) compared to other individual years in the reference period of 2014–2019 (grey traces). (e, f) Accumulated daily difference between reference evapotranspiration (ET_o) and rainfall (water balance) around anthesis in 2016 in (e) research station 1 and (f) research station 8. Red bars indicate a positive balance, and black bars indicate a negative balance. The flowering time of the Rubisco cultivar at each site is indicated. (g) Frequency of plant diseases reported in ARVALIS plant disease trials across the breadbasket region of France in 2016 compared to the average (Hist.) of 2014–2019 (omitting 2016). (h, i) The three most important variables selected according to the Gini index from 1000 different models estimated from random forest variable selector for estimating average single grain size anomalies considering (h) only 2016, and (i) all the harvests from 2014 to 2019, excluding 2016. (j) Comparison between the simulated and observed 2016 anomaly in average single grain size with a multiple regression linear model, from 1000 different models in an out-of-sample analysis – errors bars show the standard errors from the 1000 simulations (vertical errors bars) and the observed grain size anomaly (horizontal errors bars) in (j). The research stations are as follows: 1, Égreville; 2, Chevry; 3, Saint-Quentin; 4, Saint-Florent; 5, Fagnières; 5, Issoudun; 7, Barbarey-Saint-Sulpice; and 8, Rots.

in multi-model regressions, fungal foliar diseases, ear blight, anoxia, and low solar radiation could explain most of the 2016 anomaly in grain size (Figure 4j).

3.5 | Causes of wheat yield decline in 2016

Based on the skill of the multi-regression models at estimating grain number and grain size anomalies, we extended the analysis

to quantify the contribution of each of these factors to the 2016 losses in grain number per unit area, grain size, and grain yield at each research stations (Figure 5). ANOVA results indicated that the 2016 grain number per unit area anomaly was mainly caused by low solar radiation (56%) and heavy rainfall (41%) considering data from all research stations, with a 3% residual not explained by these variables. At individual research stations, the impacts of low solar radiation on grain number per unit area varied from 4% to 33%, impacts of heavy rainfall varied from 1% to 15%, and the impact of ear

blight was less than 1%. For grain size, the main causes of decline were anoxia (51%), fungal foliar disease (21%), ear blight (19%), and low solar radiation during grain filling (6%), with 3% not explained by these variables. Apart from research station 8 where there was no waterlogging, the impact of anoxia on the decrease in grain size varied from 2% to 20%. Grain size was also affected by fungal foliar diseases, ear blight, and low solar radiation, which caused grain size decreases of up to 8% at individual research stations. The relatively low impact of low solar radiation on grain size (8% at most) compared to grain number (33% at most) was consistent with simulation results from the DSSAT-Nwheat model (Figures S16 and S17).

The contribution to grain yield of individual limiting factors in 2016 was estimated by combining the contributions to grain number per unit area and grain size. Overall, when ranked by the size of impact, the 2016 yield drop can primarily be explained by reduced solar radiation around anthesis (31%), anoxia during grain filling (26%), heavy rainfall events at anthesis (19%), fungal foliar diseases (11%), and ear blight during grain filling (10%), with 3% of the loss not explained (Figure 5).

3.6 | Increased frequency of adverse weather conditions for wheat yield under future climate

We used bias-adjusted climate projections from the CMIP6 subset to anticipate risks similar to the 2016 impacts over the shared socioeconomic pathway SSP5-8.5 for the 2020–2100 period. We thus assessed whether future climate change trends might change the frequencies of heavy rainfall and solar radiation around wheat anthesis, ear blight, fungal foliar diseases, and anoxia during grain filling, as experienced in 2016 (Figure 6, which shows the average climate projections for eight research station across the breadbasket of France). Results indicate that under the SSP5-8.5 scenario, heavy rainfall around anthesis is projected to become up to 100% more frequent after 2040 (Figure 6a), while small changes are possible in average solar radiation around anthesis, increasing by 5% by 2100 (Figure 6b). Similarly, under the SSP5-8.5 scenario, the frequency of ear blight would increase by 110% and fungal foliar diseases would increase by 50% by 2100 due to warmer winter and spring (Table S3). By contrast, anoxia during June to July, the grain-filling period, is projected to become up to 25% less frequent under the SSP5-8.5 scenario. All factors which caused the large yield drop in 2016 would become more pronounced with future climate change, but low solar radiation and anoxia would be limiting less often. Similar projections are expected in other regions of Europe and for different wheat anthesis dates (Figures S19 and S20). High decadal variability is shown for all projected weather-based index (Figure 6a–e), but particularly for heavy rainfall at anthesis (Figure 6a) and ear blight (Figure 6b), which may be linked to the uncertainties of the ensemble means based on the CMIP6 global climate models.

Extreme low wheat yields are here statistically defined as the <2nd percentile of occurrence of simulated wheat yields during 1960–2020, thus with a probability which occurred once in 60 years

in the past (corresponding to the frequency of the 2016 wheat yield failure). With increasing solar radiation and heavy rainfall during anthesis, the frequency of extreme low wheat grain number due to climatic factors that occurred in 2016 is projected to remain unchanged (Figure 6f). However, with increasing plant disease, extremely low wheat grain size and hence grain yields are projected to become five times more frequent by the end of the century under the SSP5-8.5 scenario (Figure 6g,h). Similar results are expected under the SSP5-2.6 scenario (Figure S21). Yet, these projections may vary according to the modeling approach used (Figure S33).

4 | DISCUSSION

Grain yield in wheat is determined by grain number per unit area and average single grain size. There is a negative relationship between the two components, which suggests that wheat partially compensates during development for variation in grain number per unit area by modifying grain size once grain number is determined (Zhang et al., 2010). However, we showed here that the large and sudden drop in wheat yield in 2016 in France occurred due to simultaneous drops in grain number per unit area and in average single grain size due to a combination of adverse climate events (Figure S22). The low grain number was partly driven by low solar radiation around anthesis in France in spring of 2016. An 18% decrease in grain number due to 65% less solar radiation centered around anthesis was reported by Fischer (1985). A shading experiment by Yang et al. (2020) showed a 58% drop in grain number when two wheat cultivars were 90% shaded during the early microspore stage of flower development when grain number is determined. These reports are in accordance with the estimates from regression and crop simulation models presented here. Broadly compared to other years before and after, only one-fifth of the solar radiation was received during the crucial flowering period with one-third fewer grains formed in some of the experimental locations in 2016 (Figures S4 and S5). High rainfall is often linked to low grain numbers due to its indirect effect on plant disease spread and nitrogen leaching (Mäkinen et al., 2018). From the data presented here, it is more likely that the intense rainfall around anthesis in 2016 in France directly caused flower abortion (Lawson & Rands, 2019) or increased lodging during anthesis (Fischer & Stapper, 1987; Niu et al., 2016).

Waterlogging, simply indicated here by water balance, was a widespread phenomenon in 2016, leading to flooding in wheat fields across the Seine River basin (Ben-Ari et al., 2018). Anoxia probably only occurred during the wheat grain-filling period. Marti et al. (2015) reported a grain yield decline of 20% due to 10–15 days of waterlogging with a high impact on grain number due to the excess of water just before anthesis. The timing of the impact on grain size is therefore different from that reported here. Fungal foliar diseases also reduced average wheat grain size, with ear blight and low solar radiation exacerbating the decrease. Similar effects of low radiation during different growth periods were observed by Shimoda

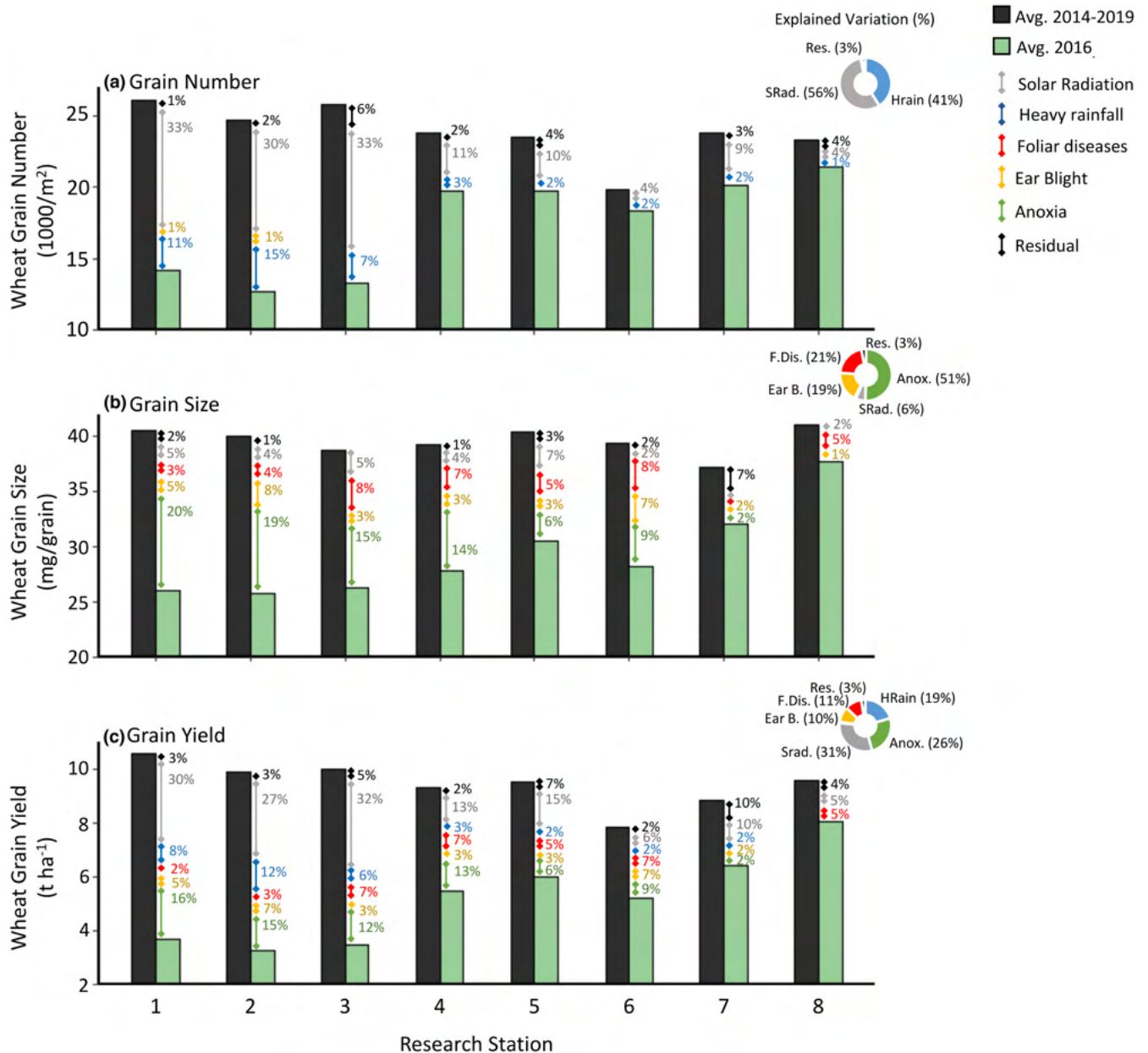


FIGURE 5 Causes of the extremely low wheat yield in France in 2016. Comparison of the observed (a) grain number per unit area, (b) average single grain size, and (c) grain yield reported in 2016 and the average of 2014, 2015, 2017, 2018, and 2019 harvests. The colored arrows represent the different causes of the 2016 decline in grain number, size, and yield, and the length represents the magnitude of each contribution. The donut charts in the right upper corner of each panel show ANOVA (mean of squares) results with the amount of variation in (a) grain number per unit area, (b) average single grain size, and (c) grain yield explained by different factors in 2016 across all research stations: SRad., solar radiation; Hrain, heavy rainfall; F. Dis., foliar diseases; Ear B., ear blight; Anox., anoxia; and Res., residual. The research stations are as follows: 1, Égreville; 2, Chevry; 3, Saint-Quentin; 4, Saint-Florent; 5, Fagnières; 6, Issoudun; 7, Barbarey-Saint-Sulpice; and 8, Rots.

and Sugikawa (2020) and estimated by Asseng et al. (2017) using the same wheat crop model as in this study. In the model, the determination of grain number is source limited while grain growth beyond the onset of grain filling is often sink limited (Asseng et al., 2017). In the absence of any disease control, up to 30% decline in yield may be caused by ear blight (Shah et al., 2018) and up to 50% by septoria blotch (Fones & Gurr, 2015). The impact of plant diseases estimated here using regression models was smaller. However, resistant cultivars or fungicide applications during the growing season

(Fones & Gurr, 2015; Shah et al., 2018) (up to three applications are common practice in Western Europe including the experimental unit treatments in France analyzed here) may have limited the wheat yield decline due to these diseases to between 5% and 10%.

European countries are global hotspots for climate change-driven compound events with the potential to cause severe impacts on agriculture (Ranasinghe et al., 2021; Ridder et al., 2020). Recent studies showed that drought and heat stress during wheat anthesis and grain filling would become more frequent by 2100 with climate change, in

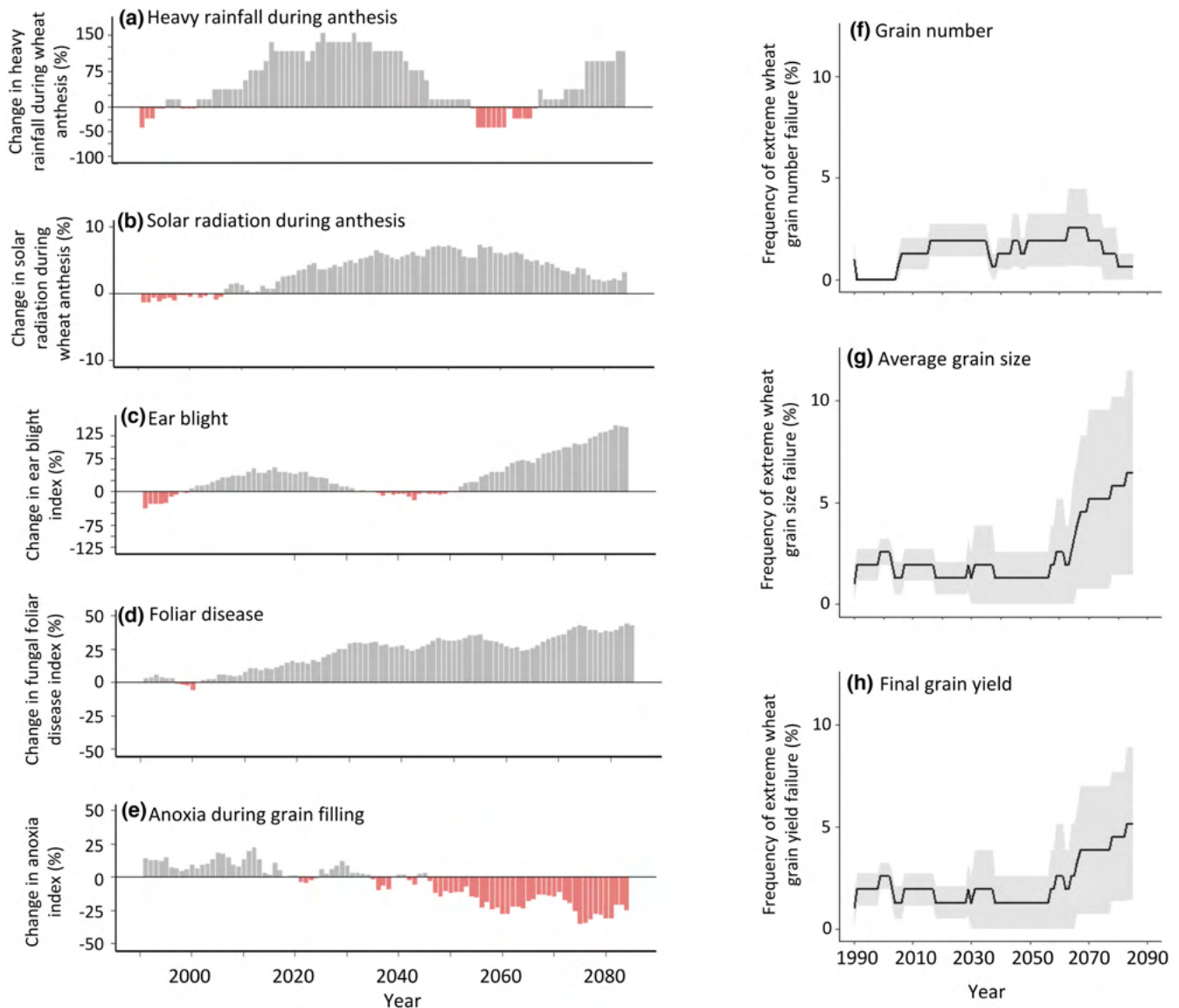


FIGURE 6 Projected future frequency of the extreme weather on the 2016 wheat yield failure in France. Estimated running mean change for future 30 years of (a) heavy rainfall (daily rainfall >20 mm) at ± 5 days around anthesis, (b) solar radiation at ± 15 days around anthesis, (c) ear blight index, (d) fungal foliar disease index, and (e) anoxia index during grain filling in relation to the reference period 1960–2020. Estimated running mean change for future 30 years frequency of extremely low wheat (f) grain number per unit area, (g) average single grain size, and (c) grain yield from 1990 to 2085, with each year as the middle of a 30-year period. (a–e) Bars are ensemble means based on five bias-adjusted CMIP6 global climate models (GCMs) for SSP5-8.5. (f–h) Lines are ensemble means based on five bias-adjusted CMIP6 GCMs for SSP5-8.5 (lines) and shading shows ± 1 SE. In the simulations, anthesis was fixed as 1 June, and the anoxia index was calculated every year from 1 June to 31 July. CMIP6 GCMs for SSP5-8.5 data are an average of climate projections for the following eight research stations: 1, Égreville; 2, Chevry; 3, Saint-Quentin; 4, Saint-Florent; 5, Fagnières; 6, Issoudun; 7, Barbarey-Saint-Sulpice; and 8, Rots. Individual results for these research stations and other locations in Europe, as well as with different anthesis dates, are shown in [Figures S19](#) and [S20](#), respectively. Climate projections for monthly maximum and minimum temperature, solar radiation, and rainfall, are shown in [Figure S18](#). Projected future frequency of the extreme weather on the 2016 wheat yield failure in France for SSP5-2.6 is shown in [Figure S21](#). Thresholds for heavy rainfall (daily rainfall >20 mm) are similar in both observed climate and climate models ([Figure S9](#)), and modeled weather-based indices have similar distribution in both observed climate and climate models ([Figure S10](#)).

many European wheat-growing countries (Trnka et al., 2014, 2019; Webber et al., 2018). This is consistent with our projections of less anoxia from rainfall during wheat grain filling by 2100. However, wheat diseases and heavy rainfall around anthesis, which together caused the majority of the wheat yield decline in 2016 in France, are both projected to become more frequent with climate change

in the region ([Figure 6](#)). Heavy rainfall has already become more intense in Central Europe (Zeder & Fischer, 2020). Therefore, if climate extremes of drought and heat stress during wheat anthesis and grain filling are compounded with elevated pressure from disease and more heavy early rainfall events, future episodes of extremely low wheat production in Western Europe are to be expected. This

parallels recent widespread wheat crop failures in other countries of Europe and the world. For example, in 2018, a combination of a warm, wet winter, with increased wheat disease pressure, followed by a severely hot and dry summer in central-northern Europe (Beillouin et al., 2020; Moravec et al., 2021; Webber et al., 2020) caused the national wheat yield of France to drop by 10%. This was also the lowest wheat-yielding year in the recent history of Germany (after trend correction, Figure S25) and of many northern European countries (Beillouin et al., 2020; Webber et al., 2020), with a total wheat shortfall of 13 million tons in the European Union compared to 2017. These examples of climate change driving extremely low wheat production seasons in other parts of the world demonstrate the risks of simultaneous global breadbasket failures (Gaupp et al., 2020), and have implications for global food security. For example, the simultaneous wheat production failures in several wheat-exporting countries in 2008 contributed to food riots across many countries in the world (IMF, 2008). And, the heatwave in Russia and Ukraine in 2010 decimates 24 million tons of wheat, contributing to a 50% spike in global wheat price this year (FAO stat, 2022).

The simultaneous occurrence of multiple limiting impacts often makes it difficult to forecast extremely low wheat-yielding seasons. Forecasting seasons like 2016 in France are often hampered by the poor representation of waterlogging and plant disease in both crop simulation and statistical models (Ben-Ari et al., 2018). New routines accounting for plant diseases (Berton Ferreira et al., 2021; Bregaglio et al., 2021) and waterlogging impact (Liu et al., 2021) need to be developed and integrated into crop simulation models to capture the extent of such compounding factors. In the meantime, the simple relationships developed here capture some of the physiological impacts of waterlogging and diseases, as first steps toward a more comprehensive cropping systems analysis.

Our modeling approach included some assumptions. Factors affecting grain number per unit area were rather simply separated from those affecting average single grain size, even though potential grain size is also determined during the period when grain number per unit area is set (Acreche & Slafer, 2006; Calderini et al., 2021). Even with the large and detailed dataset studied, the available measurements did not allow us to quantify the impact of climate factors on the potential grain size during anthesis. Also, the anthesis dates and grain-filling duration for the future climate change impact analysis were kept constant, but these timings might change with increasing temperatures or future cultivars. Depending on the direction of the changes in anthesis date and grain-filling period (whether earlier anthesis and shorter grain filling with current cultivars or unaltered or later anthesis with possible future cultivars [Asseng et al., 2019]), the overall impact might vary.

While the data analysis focused on the breadbasket of France, the approach used here could be extended to other countries in Western Europe which suffered similar weather anomalies during the wheat cropping season of 2016 (Figure 1). Our framework provides a basis for future improvement of the prediction capacity of crop simulation models and yields forecast systems, and for developing

wheat cultivars with an increased ecophysiological capacity to grow in complex environments, like those in 2016 in France. Forecasting and planning for such compound yield-reducing events may to some extent mitigate the instability of future grain production under more extreme climates.

ACKNOWLEDGMENTS

The authors thank ARVALIS-Institut du Végétal for performing all the field experiments and for the financial support of this study. R.S.N.J. acknowledges support from the Prince of Albert II of Monaco foundation through the IPCC Scholarship Program. The contents of this manuscript are solely the liability of R.S.N.J. and under no circumstances may be considered a reflection of the position of the Prince Albert II of Monaco Foundation and/or the IPCC. P.M. acknowledges support from the Agriculture and Forestry in the Face of Climate Change: Adaptation and Mitigation (CLIMAE) Metaprogram of the French National Research Institute for Agriculture, Food and Environment (INRAE). Support for A.C.R. was provided by the NASA Earth Sciences Directorate support of the GISS Climate Impacts Group. F.E. acknowledges support from the Deutsche Forschungsgemeinschaft (DFG, German Research Foundation) under Germany's Excellence Strategy – EXC 2070 – 390732324 (PhenoRob). Open Access funding enabled and organized by Projekt DEAL.

CONFLICT OF INTEREST STATEMENT

The authors declare no conflict of interest.

DATA AVAILABILITY STATEMENT

The data that support the findings of this study are available at <https://doi.org/10.5061/dryad.fxpnvx0x1>.

ORCID

Rogério de S. Nóia Júnior  <https://orcid.org/0000-0002-4096-7588>

Jean-Pierre Cohan  <https://orcid.org/0000-0003-2117-7027>

Pierre Martre  <https://orcid.org/0000-0002-7419-6558>

Marijn van der Velde  <https://orcid.org/0000-0002-9103-7081>

Heidi Webber  <https://orcid.org/0000-0001-8301-5424>

Frank Ewert  <https://orcid.org/0000-0002-4392-8154>

Alex C. Ruane  <https://orcid.org/0000-0002-5582-9217>

Gustavo A. Slafer  <https://orcid.org/0000-0002-1766-4247>

Senthold Asseng  <https://orcid.org/0000-0002-7583-3811>

REFERENCES

- Acreche, M. M., & Slafer, G. A. (2006). Grain weight response to increases in number of grains in wheat in a Mediterranean area. *Field Crops Research*, 98(1), 52–59. <https://doi.org/10.1016/j.fcr.2005.12.005>
- Asseng, S., Foster, I., & Turner, N. C. (2011). The impact of temperature variability on wheat yields. *Global Change Biology*, 17(2), 997–1012. <https://doi.org/10.1111/j.1365-2486.2010.02262.x>
- Asseng, S., Kassie, B. T., Labra, M. H., Amador, C., & Calderini, D. F. (2017). Simulating the impact of source-sink manipulations in wheat. *Field Crops Research*, 202, 47–56. <https://doi.org/10.1016/j.fcr.2016.04.031>

- Asseng, S., Martre, P., Maiorano, A., Rötter, R. P., O'Leary, G. J., Fitzgerald, G. J., Girousse, C., Motzo, R., Giunta, F., Babar, M. A., Reynolds, M. P., Kheir, A. M. S., Thorburn, P. J., Waha, K., Ruane, A. C., Aggarwal, P. K., Ahmed, M., Balković, J., Basso, B., ... Ewert, F. (2019). Climate change impact and adaptation for wheat protein. *Global Change Biology*, 25(1), 155–173. <https://doi.org/10.1111/gcb.14481>
- Bailey, R., Benton, T. G., Challinor, A., Elliott, J., & Gustafson, D. (2015). *Extreme weather and resilience of the global food system*. The Global Food Security Programme.
- Battisti, D. S., & Naylor, R. L. (2009). Historical warnings of future food insecurity with unprecedented seasonal heat. *Science*, 323(5911), 240–244. <https://doi.org/10.1126/science.1164363>
- Beillouin, D., Schauburger, B., Bastos, A., Ciais, P., & Makowski, D. (2020). Impact of extreme weather conditions on European crop production in 2018. *Philosophical Transactions of the Royal Society, B: Biological Sciences*, 375(1810), 20190510. <https://doi.org/10.1098/rstb.2019.0510>
- Ben-Ari, T., Boé, J., Ciais, P., Lecerf, R., van der Velde, M., & Makowski, D. (2018). Causes and implications of the unforeseen 2016 extreme yield loss in the breadbasket of France. *Nature Communications*, 9(1), 1627. <https://doi.org/10.1038/s41467-018-04087-x>
- Berton Ferreira, T., Pavan, W., Cunha Fernandes, J. M., Asseng, S., Antunes de Oliveira, F. A., Amaral Ho'lbíg, C., Noletto Luz Pequeno, D., Dalmago, G. A., Lazaretti Zanatta, A., & Hoogenboom, G. (2021). Coupling a Pest and disease damage module with CSM-NWheat—A wheat crop simulation model. *Transactions of the ASABE*, 64, 2061–2071. <https://doi.org/10.13031/trans.14586>
- Bevacqua, E., De Michele, C., Manning, C., Couasnon, A., Ribeiro, A. F. S., Ramos, A. M., Vignotto, E., Bastos, A., Blesić, S., Durante, F., Hillier, J., Oliveira, S. C., Pinto, J. G., Ragno, E., Rivoire, P., Saunders, K., van der Wiel, K., Wu, W., Zhang, T., & Zscheischler, J. (2021). Guidelines for studying diverse types of compound weather and climate events. *Earth's Future*, 9(11), e2021EF002340. <https://doi.org/10.1029/2021EF002340>
- Bregaglio, S., Willcoquet, L., Kersebaum, K. C., Ferrise, R., Stella, T., Ferreira, T. B., Pavan, W., Asseng, S., & Savary, S. (2021). Comparing process-based wheat growth models in their simulation of yield losses caused by plant diseases. *Field Crops Research*, 265, 108108. <https://doi.org/10.1016/j.fcr.2021.108108>
- Bussay, A., van der Velde, M., Fumagalli, D., & Seguin, L. (2015). Improving operational maize yield forecasting in Hungary. *Agricultural Systems*, 141, 94–106. <https://doi.org/10.1016/j.agsy.2015.10.001>
- Calderini, D. F., Castillo, F. M., Arenas-M, A., Molero, G., Reynolds, M. P., Craze, M., Bowden, S., Milner, M. J., Wallington, E. J., Dowle, A., Gomez, L. D., & McQueen-Mason, S. J. (2021). Overcoming the trade-off between grain weight and number in wheat by the ectopic expression of expansin in developing seeds leads to increased yield potential. *New Phytologist*, 230(2), 629–640. <https://doi.org/10.1111/nph.17048>
- Ceglar, A., van der Wijngaart, R., de Wit, A., Lecerf, R., Boogaard, H., Seguin, L., van den Berg, M., Toreti, A., Zampieri, M., Fumagalli, D., & Baruth, B. (2019). Improving WOFOST model to simulate winter wheat phenology in Europe: Evaluation and effects on yield. *Agricultural Systems*, 168, 168–180. <https://doi.org/10.1016/j.agsy.2018.05.002>
- Cohan, J.-P., Le Souder, C., Guicherd, C., Lorgeou, J., Du Cheyron, P., Bonnefoy, M., Decarrier, A., Piraux, F., & Laurent, F. (2019). Combining breeding traits and agronomic indicators to characterize the impact of cultivar on the nitrogen use efficiency of bread wheat. *Field Crops Research*, 242, 107588. <https://doi.org/10.1016/j.fcr.2019.107588>
- Eyring, V., Bony, S., Meehl, G. A., Senior, C. A., Stevens, B., Stouffer, R. J., & Taylor, K. E. (2016). Overview of the coupled model Intercomparison project phase 6 (CMIP6) experimental design and organization. *Geoscientific Model Development*, 9(5), 1937–1958. <https://doi.org/10.5194/gmd-9-1937-2016>
- FAO stat. (2022). *FAOSTAT: FAO statistical databases*. FAO Stat. <http://www.fao.org/faostat/en/#home>
- Fischer, R. A. (1985). Number of kernels in wheat crops and the influence of solar radiation and temperature. *The Journal of Agricultural Science*, 105(2), 447–461. <https://doi.org/10.1017/S0021859600056495>
- Fischer, R. A., & Stapper, M. (1987). Lodging effects on high-yielding crops of irrigated semidwarf wheat. *Field Crops Research*, 17(3), 245–258. [https://doi.org/10.1016/0378-4290\(87\)90038-4](https://doi.org/10.1016/0378-4290(87)90038-4)
- Fones, H., & Gurr, S. (2015). The impact of Septoria tritici blotch disease on wheat: An EU perspective. *Fungal Genetics and Biology*, 79, 3–7. <https://doi.org/10.1016/j.fgb.2015.04.004>
- Gaupp, F., Hall, J., Hochrainer-Stigler, S., & Dadson, S. (2020). Changing risks of simultaneous global breadbasket failure. *Nature Climate Change*, 10(1), 54–57. <https://doi.org/10.1038/s41558-019-0600-z>
- Hoag, H. (2014). Russian summer tops “universal” heatwave index. *Nature*, 16, 250–252. <https://doi.org/10.1038/nature.2014.16250>
- Igrejas, G., & Branlard, G. (2020). The importance of wheat. In G. Igrejas & G. Branlard (Eds.), *Wheat quality for improving processing and human health* (pp. 1–7). Springer International Publishing. https://doi.org/10.1007/978-3-030-34163-3_1
- IMF. (2008). *International Monetary Fund: Food and fuel prices: Recent developments, macroeconomic impact, and policy responses*.
- IPCC. (2021). Technical summary. Contribution of working group I to the sixth assessment report of the intergovernmental panel on climate change. In V. Masson-Delmotte, P. Zhai, A. Pirani, S. L. Connors, C. Péan, S. Berger, N. Caud, Y. Chen, L. Goldfarb, M. I. Gomis, M. Huang, K. Leitzell, E. Lonnoy, J. B. R. Matthews, T. K. Maycock, T. Waterfield, O. Yelekçi, R. Yu, & B. Zhou (Eds.), *Climate Change 2021: The Physical Science Basis*.
- Jägermeyr, J., Müller, C., Ruane, A. C., Elliott, J., Balkovic, J., Castillo, O., Faye, B., Foster, I., Folberth, C., Franke, J. A., Fuchs, K., Guarin, J. R., Heinke, J., Hoogenboom, G., Iizumi, T., Jain, A. K., Kelly, D., Khabarov, N., Lange, S., ... Rosenzweig, C. (2021). Climate impacts on global agriculture emerge earlier in new generation of climate and crop models. *Nature Food*, 2, 873–885. <https://doi.org/10.1038/s43016-021-00400-y>
- Justes, E., Mary, B., Meynard, J.-M., Machet, J.-M., & Thelier-Huche, L. (1994). Determination of a critical nitrogen dilution curve for winter wheat crops. *Annals of Botany*, 74(4), 397–407. <https://doi.org/10.1006/anbo.1994.1133>
- Kassie, B. T., Asseng, S., Porter, C. H., & Royce, F. S. (2016). Performance of DSSAT-Nwheat across a wide range of current and future growing conditions. *European Journal of Agronomy*, 81, 27–36. <https://doi.org/10.1016/j.eja.2016.08.012>
- Lange, S. (2019). Trend-preserving bias adjustment and statistical downscaling with ISIMIP3BASD (v1.0). *Geoscientific Model Development*, 12(7), 3055–3070. <https://doi.org/10.5194/gmd-12-3055-2019>
- Lawson, D. A., & Rands, S. A. (2019). The effects of rainfall on plant-pollinator interactions. *Arthropod-Plant Interactions*, 13(4), 561–569. <https://doi.org/10.1007/s11829-019-09686-z>
- Lecerf, R., Ceglar, A., López-Lozano, R., van der Velde, M., & Baruth, B. (2019). Assessing the information in crop model and meteorological indicators to forecast crop yield over Europe. *Agricultural Systems*, 168, 191–202. <https://doi.org/10.1016/j.agsy.2018.03.002>
- Lischeid, G., Webber, H., Sommer, M., Nendel, C., & Ewert, F. (2022). Machine learning in crop yield modelling: A powerful tool, but no surrogate for science. *Agricultural and Forest Meteorology*, 312, 108698. <https://doi.org/10.1016/j.agrformet.2021.108698>
- Liu, B., Martre, P., Ewert, F., Porter, J. R., Challinor, A. J., Müller, C., Ruane, A. C., Waha, K., Thorburn, P. J., Aggarwal, P. K., Ahmed, M., Balković, J., Basso, B., Biernath, C., Bindi, M., Cammarano, D., De Sanctis, G., Dumont, B., Espadafor, M., ... Asseng, S. (2019). Global wheat production with 1.5 and 2.0°C above pre-industrial warming. *Global Change Biology*, 25(4), 1428–1444. <https://doi.org/10.1111/gcb.14542>

- Liu, K., Harrison, M. T., Archontoulis, S. V., Huth, N., Yang, R., Liu, D. L., Yan, H., Meinke, H., Huber, I., Feng, P., Ibrahim, A., Zhang, Y., Tian, X., & Zhou, M. (2021). Climate change shifts forward flowering and reduces crop waterlogging stress. *Environmental Research Letters*, 16(9), 94017. <https://doi.org/10.1088/1748-9326/ac1b5a>
- Madgwick, J. W., West, J. S., White, R. P., Semenov, M. A., Townsend, J. A., Turner, J. A., & Fitt, B. D. L. (2011). Impacts of climate change on wheat anthesis and fusarium ear blight in the UK. *European Journal of Plant Pathology*, 130(1), 117–131. <https://doi.org/10.1007/s10658-010-9739-1>
- Mäkinen, H., Kaseva, J., Trnka, M., Balek, J., Kersebaum, K. C., Nendel, C., Gobin, A., Olesen, J. E., Bindi, M., Ferrise, R., Moriondo, M., Rodríguez, A., Ruiz-Ramos, M., Takáč, J., Bezák, P., Ventrella, D., Ruget, F., Capellades, G., & Kahiluoto, H. (2018). Sensitivity of European wheat to extreme weather. *Field Crops Research*, 222, 209–217. <https://doi.org/10.1016/j.fcr.2017.11.008>
- Marti, J., Savin, R., & Slafer, G. A. (2015). Wheat yield as affected by length of exposure to waterlogging during stem elongation. *Journal of Agronomy and Crop Science*, 201(6), 473–486. <https://doi.org/10.1111/jac.12118>
- Martre, P., Wallach, D., Asseng, S., Ewert, F., Jones, J. W., Rötter, R. P., Boote, K. J., Ruane, A. C., Thorburn, P. J., Cammarano, D., Hatfield, J. L., Rosenzweig, C., Aggarwal, P. K., Angulo, C., Basso, B., Bertuzzi, P., Biernath, C., Brisson, N., Challinor, A. J., ... Wolf, J. (2015). Multimodel ensembles of wheat growth: Many models are better than one. *Global Change Biology*, 21(2), 911–925. <https://doi.org/10.1111/gcb.12768>
- Menze, B. H., Kelm, B. M., Masuch, R., Himmelreich, U., Bachert, P., Petrich, W., & Hamprecht, F. A. (2009). A comparison of random forest and its Gini importance with standard chemometric methods for the feature selection and classification of spectral data. *BMC Bioinformatics*, 10(1), 213. <https://doi.org/10.1186/1471-2105-10-213>
- Moravec, V., Markonis, Y., Rakovec, O., Svoboda, M., Trnka, M., Kumar, R., & Hanel, M. (2021). Europe under multi-year droughts: How severe was the 2014–2018 drought period? *Environmental Research Letters*, 16(3), 34062. <https://doi.org/10.1088/1748-9326/abe828>
- Niu, L., Feng, S., Ding, W., & Li, G. (2016). Influence of speed and rainfall on large-scale wheat lodging from 2007 to 2014 in China. *PLoS One*, 11(7), e0157677. <https://doi.org/10.1371/journal.pone.0157677>
- Nóia Júnior, R. d. S., Martre, P., Finger, R., van der Velde, M., Ben-Ari, T., Ewert, F., Webber, H., Ruane, A. C., & Asseng, S. (2021). Extreme lows of wheat production in Brazil. *Environmental Research Letters*, 16(10), 104025. <https://doi.org/10.1088/1748-9326/ac26f3>
- O'Neill, B. C., Carter, T. R., Ebi, K., Harrison, P. A., Kemp-Benedict, E., Kok, K., Kriegler, E., Preston, B. L., Riahi, K., Sillmann, J., van Ruijven, B. J., van Vuuren, D., Carlisle, D., Conde, C., Fuglested, J., Green, C., Hasegawa, T., Leininger, J., Monteith, S., & Pichs-Madruga, R. (2020). Achievements and needs for the climate change scenario framework. *Nature Climate Change*, 10(12), 1074–1084. <https://doi.org/10.1038/s41558-020-00952-0>
- Pang, G., Xu, Z., Wang, T., Cong, X., & Wang, H. (2018). Photosynthetic light response characteristics of winter wheat at heading and flowering stages under saline water irrigation. *IOP Conference Series: Earth and Environmental Science*, 170, 52031. <https://doi.org/10.1088/1755-1315/170/5/052031>
- Perez, I. (2013). *Climate change and rising food prices heightened Arab spring*. Scientific American: Sustainability.
- R Core Team. (2017). *R: A language and environment for statistical computing*. R Foundation for Statistical Computing (p. {ISBN} 3-900051-07-0). <http://www.R-project.org/>
- Ranasinghe, R., Ruane, A. C., Vautard, R., Arnell, N., Coppola, E., Cruz, F. A., Dessai, S., Islam, A. S., Rahimi, M., Carrascal, D. R., Sillmann, J., Sylla, M. B., Tebaldi, C., Wang, W., & Zaaboul, R. (2021). Chapter 12: Climate change information for regional impact and for risk assessment. In V. Masson-Delmotte, P. Zhai, A. Pirani, S. L. Connors, C. Péan, S. Berger, N. Caud, Y. Chen, L. Goldfarb, M. I. Gomis, M. Huang, K. Leitzell, E. Lonnoy, J. B. R. Matthews, T. K. Maycock, T. Waterfield, O. Yelekçi, R. Yu, & B. Zhou (Eds.), *Climate change 2021: The physical science basis. Contribution of Working Group I to the Sixth Assessment Report of the Intergovernmental Panel on Climate Change, August 2021* (pp. 351–364).
- Raymond, C., Horton, R. M., Zscheischler, J., Martius, O., AghaKouchak, A., Balch, J., Bowen, S. G., Camargo, S. J., Hess, J., Kornhuber, K., Oppenheimer, M., Ruane, A. C., Wahl, T., & White, K. (2020). Understanding and managing connected extreme events. *Nature Climate Change*, 10(7), 611–621. <https://doi.org/10.1038/s41558-020-0790-4>
- Ridder, N. N., Pitman, A. J., Westra, S., Ukkola, A., Do, H. X., Bador, M., Hirsch, A. L., Evans, J. P., Di Luca, A., & Zscheischler, J. (2020). Global hotspots for the occurrence of compound events. *Nature Communications*, 11(1), 5956. <https://doi.org/10.1038/s41467-020-19639-3>
- Rosenzweig, C., Jones, J. W., Hatfield, J. L., Ruane, A. C., Boote, K. J., Thorburn, P., Antle, J. M., Nelson, G. C., Porter, C., Janssen, S., Asseng, S., Basso, B., Ewert, F., Wallach, D., Baigorría, G., & Winter, J. M. (2013). The agricultural model Intercomparison and improvement project (AgMIP): Protocols and pilot studies. *Agricultural and Forest Meteorology*, 170, 166–182. <https://doi.org/10.1016/j.agrformet.2012.09.011>
- Rötter, R. P., Hoffmann, M. P., Koch, M., & Müller, C. (2018). Progress in modelling agricultural impacts of and adaptations to climate change. *Current Opinion in Plant Biology*, 45, 255–261. <https://doi.org/10.1016/j.pbi.2018.05.009>
- Ruane, A. C., Phillips, M., Müller, C., Elliott, J., Jägermeyr, J., Arneth, A., Balkovic, J., Deryng, D., Folberth, C., Iizumi, T., Izaurralde, R. C., Khabarov, N., Lawrence, P., Liu, W., Olin, S., Pugh, T. A. M., Rosenzweig, C., Sakurai, G., Schmid, E., ... Yang, H. (2021). Strong regional influence of climatic forcing datasets on global crop model ensembles. *Agricultural and Forest Meteorology*, 300, 108313. <https://doi.org/10.1016/j.agrformet.2020.108313>
- Shah, L., Ali, A., Yahya, M., Zhu, Y., Wang, S., Si, H., Rahman, H., & Ma, C. (2018). Integrated control of fusarium head blight and deoxynivalenol mycotoxin in wheat. *Plant Pathology*, 67(3), 532–548. <https://doi.org/10.1111/ppa.12785>
- Shew, A. M., Tack, J. B., Nalley, L. L., & Chaminuka, P. (2020). Yield reduction under climate warming varies among wheat cultivars in South Africa. *Nature Communications*, 11(1), 4408. <https://doi.org/10.1038/s41467-020-18317-8>
- Shimoda, S., & Sugikawa, Y. (2020). Grain-filling response of winter wheat (*Triticum aestivum* L.) to post-anthesis shading in a humid climate. *Journal of Agronomy and Crop Science*, 206(1), 90–100. <https://doi.org/10.1111/jac.12370>
- Slafer, G. A., Elia, M., Savin, R., García, G. A., Terrile, I. I., Ferrante, A., Miralles, D. J., & González, F. G. (2015). Fruiting efficiency: An alternative trait to further rise wheat yield. *Food and Energy Security*, 4(2), 92–109. <https://doi.org/10.1002/fes3.59>
- te Beest, D. E., Shaw, M. W., Pietravalle, S., & van den Bosch, F. (2009). A predictive model for early-warning of Septoria leaf blotch on winter wheat. *European Journal of Plant Pathology*, 124(3), 413–425. <https://doi.org/10.1007/s10658-009-9428-0>
- Trnka, M., Feng, S., Semenov, M. A., Olesen, J. E., Kersebaum, K. C., Rötter, R. P., Semerádová, D., Klem, K., Huang, W., Ruiz-Ramos, M., Hlavinka, P., Meitner, J., Balek, J., Havlík, P., & Büntgen, U. (2019). Mitigation efforts will not fully alleviate the increase in water scarcity occurrence probability in wheat-producing areas. *Science Advances*, 5(9), eaau2406. <https://doi.org/10.1126/sciadv.aau2406>
- Trnka, M., Rötter, R. P., Ruiz-Ramos, M., Kersebaum, K. C., Olesen, J. E., Žalud, Z., & Semenov, M. A. (2014). Adverse weather conditions for European wheat production will become more frequent with climate change. *Nature Climate Change*, 4(7), 637–643. <https://doi.org/10.1038/nclimate2242>

- van der Velde, M., & Nisini, L. (2019). Performance of the MARS-crop yield forecasting system for the European Union: Assessing accuracy, in-season, and year-to-year improvements from 1993 to 2015. *Agricultural Systems*, 168, 203–212. <https://doi.org/10.1016/j.agsy.2018.06.009>
- van der Velde, M., Lecerf, R., d'Andrimont, R., & Ben-Ari, T. (2020). Chapter 8—Assessing the France 2016 extreme wheat production loss—Evaluating our operational capacity to predict complex compound events. In J. Sillmann, S. Sippel, & S. Russo (Eds.), (pp. 139–158). Elsevier. <https://doi.org/10.1016/B978-0-12-814895-2.00009-4>
- Wang, E., Martre, P., Zhao, Z., Ewert, F., Maiorano, A., Rötter, R. P., Kimball, B. A., Ottman, M. J., Wall, G. W., White, J. W., Reynolds, M. P., Alderman, P. D., Aggarwal, P. K., Anothai, J., Basso, B., Biernath, C., Cammarano, D., Challinor, A. J., De Sanctis, G., ... Asseng, S. (2017). The uncertainty of crop yield projections is reduced by improved temperature response functions. *Nature Plants*, 3(8), 17102. <https://doi.org/10.1038/nplants.2017.102>
- Webber, H., Ewert, F., Olesen, J. E., Müller, C., Fronzek, S., Ruane, A. C., Bourgault, M., Martre, P., Ababaei, B., Bindi, M., Ferrise, R., Finger, R., Fodor, N., Gabaldón-Leal, C., Gaiser, T., Jabloun, M., Kersebaum, K.-C., Lizaso, J. I., Lorite, I. J., ... Wallach, D. (2018). Diverging importance of drought stress for maize and winter wheat in Europe. *Nature Communications*, 9(1), 4249. <https://doi.org/10.1038/s41467-018-06525-2>
- Webber, H., Lischeid, G., Sommer, M., Finger, R., Nendel, C., Gaiser, T., & Ewert, F. (2020). No perfect storm for crop yield failure in Germany. *Environmental Research Letters*, 15(10), 104012. <https://doi.org/10.1088/1748-9326/aba2a4>
- Webber, H., Martre, P., Asseng, S., Kimball, B., White, J., Ottman, M., Wall, G. W., De Sanctis, G., Doltra, J., Grant, R., Kassie, B., Maiorano, A., Olesen, J. E., Ripoche, D., Rezaei, E. E., Semenov, M. A., Stratonovitch, P., & Ewert, F. (2017). Canopy temperature for simulation of heat stress in irrigated wheat in a semi-arid environment: A multi-model comparison. *Field Crops Research*, 202, 21–35. <https://doi.org/10.1016/j.fcr.2015.10.009>
- Yang, H., Dong, B., Wang, Y., Qiao, Y., Shi, C., Jin, L., & Liu, M. (2020). Photosynthetic base of reduced grain yield by shading stress during the early reproductive stage of two wheat cultivars. *Scientific Reports*, 10(1), 14353. <https://doi.org/10.1038/s41598-020-71268-4>
- Zeder, J., & Fischer, E. M. (2020). Observed extreme precipitation trends and scaling in Central Europe. *Weather and Climate Extremes*, 29, 100266. <https://doi.org/10.1016/j.wace.2020.100266>
- Zhang, H., Turner, N. C., & Poole, M. L. (2010). Source - sink balance and manipulating sink - source relations of wheat indicate that the yield potential of wheat is sink-limited in high-rainfall zones. *Crop and Pasture Science*, 61(10), 852. <https://doi.org/10.1071/CP10161>
- Zscheischler, J., Martius, O., Westra, S., Bevacqua, E., Raymond, C., Horton, R. M., van den Hurk, B., AghaKouchak, A., Jézéquel, A., Mahecha, M. D., Maraun, D., Ramos, A. M., Ridder, N. N., Thiery, W., & Vignotto, E. (2020). A typology of compound weather and climate events. *Nature Reviews Earth & Environment*, 1(7), 333–347. <https://doi.org/10.1038/s43017-020-0060-z>

SUPPORTING INFORMATION

Additional supporting information can be found online in the Supporting Information section at the end of this article.

How to cite this article: Nóia Júnior, R. d. S., Deswarte, J.-C., Cohan, J.-P., Martre, P., van der Velde, M., Lecerf, R., Webber, H., Ewert, F., Ruane, A. C., Slafer, G. A., & Asseng, S. (2023). The extreme 2016 wheat yield failure in France. *Global Change Biology*, 00, 1–17. <https://doi.org/10.1111/gcb.16662>

Supplementary materials for

The extreme 2016 wheat yield failure in France

Rogério de Souza Nória Júnior, Jean-Charles Deswarte, Jean-Pierre Cohan, Pierre Martre, Marijn Van der Velde, Remi Lacerf, Heidi Webber, Frank Ewert, Alex C. Ruane, Gustavo A. Slafer, Senthold Asseng

Contents

1 Supplementary Text.....	2
1.1 Nwheat crop growth simulation	2
1.2 Nitrogen leaching did not affect total above ground nitrogen in 2016	2
1.3 Causes of wheat grain size and grain number decline of 2016	2
1.4 Heavy rainfall impacts.....	3
2 Supplementary Tables	4
Table S1. Geographical coordinates and the number of experimental unit treatments (with cultivars and years) the research stations used in the study.....	4
Table S2. Description of the weather-based indices calculated to assess the potential impact of climatic factors on grain number.	5
Table S3. Description of the weather-based calculated to assess the potential impact of climate factor on average single grain size.	6
Table S4. Nwheat genetic coefficients of Rubisko wheat cultivar.....	7
Table S5. Research stations soils characteristics.	8
3 Supplementary Figures	9
3.1 Supplementary results	9
3.1.1 Climatic analysis.....	9
3.1.2 Nitrogen leaching and nitrogen wheat uptake.....	19
3.1.3 Plant diseases analysis	22
3.1.4 Solar radiation.....	24
3.1.5 Climatic change.....	26
3.1.6 Wheat growth	30
3.1.7 National wheat yield anomaly	32
3.1 Supplementary methods	34
References	43

1 Supplementary Text

1.1 Nwheat crop growth simulation

This study simulated wheat yield by using the DSSAT-NWheat v. 4.7.5 model (Kassie et al., 2016) available in the Decision Support System for Agrotechnology Transfer – DSSAT platform (Hoogenboom et al., 2019). Calibration of the DSSAT-Nwheat model to simulate wheat yield and wheat total above ground biomass was performed, and the results are shown in Supplementary Fig S. The predominant soil types of each research station were collected by Arvalis-Institute-du-Végetal, and information about the sand, clay and silt contents, pH and organic carbon and nitrogen contents for each soil type is shown in Supplementary Table S5.

1.2 Nitrogen leaching did not affect total above ground nitrogen in 2016

Nitrogen leaching causing nitrogen stress to wheat was not considered a cause of this wheat yield decline in this study for three reasons: (i) grain yield did not increase with high nitrogen inputs in the field experiments testing nitrogen fertilizer application rates, and the total above ground biomass and grain nitrogen concentration was higher than for the other years (Supplementary Fig S12); (ii) Total above ground nitrogen at anthesis and NNI in 2016 was higher than in other years, but it was not remobilized from the shoot to the grain and, consequently reduced grain nitrogen mass (Supplementary Fig S13); (iii) Relatively high nitrogen leaching was simulated by the Nwheat crop simulation model in 2016 but showed no simulated impact on total above ground biomass and grain yield (Supplementary Fig S11).

1.3 Causes of wheat grain size and grain number decline of 2016

The wheat yield decline of 2016 was caused by an unlikely combination of wheat grain number and grain size decline. Wheat grain number is linearly and closely related to growing conditions ± 15 days pre or post anthesis (Ralph A. Fischer, 2009), when most fertile florets set grains (Slafer et al., 2015). Therefore, low solar radiation and the heavy rainfall events occurred around wheat anthesis were considered as affecting wheat grain number. In addition, ear blight was included in the statistical models for grain number decline, because the optimal conditions for the disease's development occurred before or during anthesis. The impact of fungal foliar diseases on grain number were not considered, because this was not observed in the field experiments comparing resistant and non-resistant cultivars (Supplementary Fig S15). Plant diseases, as well as anoxia were considered as causes of the grain size decline, as these occurred mostly during the grain filling period.

Recent studies indicated that several wheat cultivars defoliated after wheat anthesis presented a decrease of about 18% of wheat grain size, compared to the control plants (non-defoliated plants) (Rivera-Amado et al., 2020), indicating that a large amount of carbohydrates during wheat grain filling can come from remobilization from stems. This suggests that the extremely low wheat grain size measured in 2016, came from a combination of poor grain filling condition and low potential grain size set, which is also defined around anthesis simultaneously with setting grain numbers (Calderini et al., 2021). However, the remobilization efficiency of 2016 was extremely low compared to other years (Supplementary Fig S13), which is usually linked to wheat plant diseases (Schierenbeck et al., 2019), and thus we analyzed grain number and grain size anomalies separately.

For each of the yield components: grain number per unit area and average grain size, the impact of each weather based index (WI) was calculated as follows:

$$WI_{ijl} = \frac{1}{1000} \sum_{k=1}^{1000} \left[WC \text{ anomaly } 2016_{ijk} - \frac{1}{5} \sum_{m=2014}^{2019} \text{but } 2016 WC \text{ anomaly } 2016_{mijkl} \right] \quad (1)$$

(1)

where Wl_{ij} is the contribution of i^{th} explanatory variable (weather-based index or plant disease model output) in 2016 to the anomaly of j^{th} yield component (grain number or grain size) at i^{th} research station. $WC\ anomaly\ 2016_{ijk}$ is the simulated anomaly of j^{th} yield component with all the explanatory variables for 2016 at the i^{th} research station, whereas $WC\ anomaly\ 2016_m_{ijkl}$ is the same as $WC\ anomaly\ 2016_{ijk}$ but calculated with l^{th} explanatory variable in a year m between 2014 and 2019 except 2016. The WC anomaly 2016 and $WC\ anomaly\ 2016_m$ was calculated for 1000-times (section 2.5.1) as represented by the subscript k (equation 1).

1.4 Heavy rainfall impacts

Rainfall started in early May 2016, 30 days before wheat anthesis. At the beginning of May, with the episodes of rainfall, the daily solar radiation alternated from around 20 MJ m⁻²d⁻¹ to 10 MJ m⁻²d⁻¹ (which is less than half of the expected value for this period). According to Fischer (1985), the number of grains can be affected by shadow periods from 60 days before anthesis until around 20 days after anthesis, being particularly sensitive 12 days before anthesis. In France, in 2016, the lowest number of grains were observed in experiments where wheat anthesis occurred just before the highest recorded rainfall over this period (Figure 3a), together with the lowest availability of solar radiation. Late cultivars had 50% anthesis occurring up to 10 days after the highest rainfall. The late cultivars received the lowest solar radiation before anthesis (starting 7 days before anthesis, which is a more sensitive period compared to starting at anthesis, according to Fischer (1985)), but still had more grains at harvest than cultivars with anthesis at the highest recorded rainfall (and lowest solar radiation). This, together with the period of almost 52 hours of continuous rain just before anthesis (for most of the cultivars), indicated that heavy rains had an additional physical impact on grain number set. The heavy rainfall index (daily rainfall > 20 mm) was also identified as one of the most important features for grain number by the statistical models

2 Supplementary Tables

Table S1. Geographical coordinates and the number of experimental unit treatments (with cultivars and years) the research stations used in the study. The experimental unit treatments refer to the wheat growth performance experiments.

Research Station	Location	Latitude	Longitude	Number of experimental unit treatments	Number of cultivars	Number of years
1	Égreville	48.18	2.86	96	51	5
2	Chevry	48.72	2.66	12	7	2
3	Saint Quentin	49.87	3.20	5	3	2
4	Saint Florent	47.03	2.33	185	61	5
5	Fagnieres	48.95	4.41	58	28	6
6	Issoudun	46.96	2.03	114	43	6
7	Troyes-Barberey St Suplice	48.32	4.02	201	78	6
8	Rots	49.20	0.47	97	53	5

Table S2. Description of the weather-based indices calculated to assess the potential impact of climatic factors on grain number. The correlation coefficient (r^2) was calculated by regressing the anomaly of wheat grain number per unit area for each cultivar and research station with each of the weather-based indices.

Climate factor	Description in literature	Equation	r^2
Heavy rainfall	Heavy rainfall events are well-known to cause wheat yield losses in Europe (Mäkinen et al., 2018). The impacts of heavy rainfall on wheat yield are usually linked to anoxia and soil nutrient losses (Beillouin et al., 2020; Ben-Ari et al., 2018). However, only few studies indicated possible physical damage due to high rainfall (Li et al., 2019).	<p>Heavy rainfall (5d_{anth}) – number of days with accumulated rainfall >20 mm, during the 5 days period around anthesis (with 50% anthesis occurring on the 3rd day of the period)</p> $\text{Heavy rainfall (5d}_{\text{anth}}) = \sum_{(\text{day of 50\% Flowering})-2}^{(\text{day of 50\% Flowering})+2} \text{Heavy rainfall events}$ <p>Where: heavy rainfall events are days with rainfall > 20 mm.</p> <p>Several combinations of the duration of the period around anthesis (3, 5, 11, 15, and 21 days*) and threshold of daily accumulated rainfall (10, 15, 20, 25, 30, and 40 mm) were correlated with the grain number change in 2016, for each cultivar. The combination of 5 days around anthesis (5d_{anth}) and 20 mm of daily accumulated rainfall was the one with highest r^2 value.</p>	0.11
	In 2016 in France, the various events of heavy rainfall around anthesis is one of the probable causes of the wheat grain number and yield decline. To test it, we have created three different indices and correlated each with grain number reduction of 2016.	<p>Accumulated rainfall (15d_{anth}) – Accumulated rainfall during the 15 days around anthesis (with 50% anthesis occurring on the 8th day).</p> $\text{Accumulated rainfall (15d}_{\text{anth}}) = \sum_{(\text{day of 50\% Flowering})-7}^{(\text{day of 50\% Flowering})+7} \text{Rainfall}$ <p>Where: Rainfall is the daily rainfall in mm.</p> <p>Several combinations of the duration of the period around anthesis were tested (3, 5, 11, 15 and 21 days*). Fifteen days (15d_{anth}) gave the highest r^2 value.</p>	0.15
		<p>Time lapse between 50% anthesis date to highest rainfall – absolute days difference between the date of 50% anthesis and the peak of rainfall during the 21 days period around anthesis.</p> $\text{Time lapse between 50\% anthesis date to highest rainfall} = \text{day of 50\% Anthesis} - \text{Peak of rainfall}_{21\text{d}} $ <p>Where: Peak of rainfall_{21d} is the day with the maximum daily rainfall recorded in the 21 days period around anthesis*.</p>	0.08
Solar radiation and air temperature	In well managed and watered wheat crops, wheat grain number is linearly and closely related to incident solar radiation and temperature in the 30 days or so around anthesis (Ralph A. Fischer, 2009).	<p>Solar Radiation (15d_{anth}) – Mean incident solar radiation during the 15 days period around anthesis (with 50% anthesis occurring on the 8th day).</p> $\text{Solar Radiation (15d}_{\text{anth}}) = \frac{\sum_{(\text{day of 50\% Flowering})-7}^{(\text{day of 50\% Flowering})+7} \text{SR}}{15}$ <p>Where: SR is the daily solar radiation in MJ m⁻² d⁻¹.</p> <p>Several combinations of the duration of the period around anthesis were tested (3, 5, 11, 15 and 21 days*). Fifteen days (15d_{anth}) gave the highest r^2 value.</p>	0.48
	With that, three different indices accounting for the effects of temperature and solar radiation were tested.	<p>Mean Temperature 15d_{anth} – Mean air temperature during the 15 days around anthesis (with 50% anthesis occurring on the 8th day).</p> $\text{Mean Temperature (15d}_{\text{anth}}) = \frac{\sum_{(\text{day of 50\% Flowering})-7}^{(\text{day of 50\% Flowering})+7} T_{\text{mean}}}{15}$ <p>Where: T_{mean} is the daily mean air temperature in °C.</p> <p>Several combinations of the duration of the period around anthesis were tested (3, 5, 11, 15 and 21 days*). Fifteen days (15d_{anth}) gave the highest r^2 value.</p>	0.01
		<p>Photo-thermal quotient 15d_{anth} – average ratio of daily solar radiation to daily mean temperature for the 15 days period around anthesis (with 50% anthesis occurring on the 8th day).</p> $\text{Photothermal (15d}_{\text{anth}}) = \frac{\sum_{(\text{day of 50\% Flowering})-7}^{(\text{day of 50\% Flowering})+7} \left(\frac{\text{SR}}{T_{\text{mean}} - 4.5} \right)}{15}$ <p>Several combinations of the duration of the period around anthesis were tested (3, 5, 11, 15 and 21 days*). Fifteen days (15d_{anth}) gave the highest r^2 value</p>	0.10

*Anthesis date was always considered as the median values of the tested period, i.e. for the test with 15 days around anthesis, the 50% anthesis date was on 8th day. For calculating these indices, anthesis date was required, and for the experimental plots with no anthesis date observed, it was calculated based on ear emergence date (Supplementary Fig S28), which was recorded in all field trials.

Table S3. Description of the weather-based calculated to assess the potential impact of climate factor on average single grain size. The correlation coefficient (r^2) was calculated by regressing the anomaly of average grain size for each cultivar and research station with each of the weather-based indices.

Disease or climate factor	Description	Index	r^2
<p>Fungal foliar diseases:</p> <p>1. Septoria blotch (<i>Zymoseptoria tritici</i>)</p> <p>2. Leaf Yellow Rust (<i>Puccinia striiformis</i>)</p>	<p>The survival of fall infection of winter wheat by Septoria blotch and leaf rust is favored by warm temperatures during the late autumn and winter (Chaloner et al., 2019; te Beest et al., 2009). After it, the development of these foliar fungal diseases depends on wet environments, especially on rain in March and April (El Jarroudi et al., 2016).</p> <p>Weather based model for predicting such diseases, usually have as input, leaf wetness duration. There are no data on relative humidity and/or leaf wetness duration in all the research stations here studied. Thus, in this study, we focus on models that only require precipitation and temperature as an input to be run.</p> <p>Foliar fungal diseases are well-managed by farms in France and are usually easily controlled by fungicides. However, weather conditions in 2016 favored higher foliar disease pressure, causing yield losses.</p> <p>*Both foliar fungal disease indices were used for the model building to assess the potential impact of foliar fungal disease on average single grain size anomaly of 2016, and the impact of foliar fungal disease is considered to be the average of both.</p>	<p>A predictive model for early-warning of Septoria leaf blotch on winter wheat To be expressed with mathematical formulae after te Beest et al. (2009):</p> $\text{Fungal foliar index A} = \sum_{GS1-140d}^{GS1-30d} \text{Max}(0.046 \text{ Rain}_3 + 0.042 \text{ Tmin} - 6.69, 0)$ $\text{Fungal foliar index B} = \sum_{GS1-110d}^{GS1-30d} \text{Max}(0.07 \text{ Rain}_6 - 2.94, 0)$ <p>Where: Rain_x represents daily rainfall greater than x mm and Tmin represents daily minimum air temperature higher than 0 °C. Fungal foliar index A is for all cultivars, whereas Fungal foliar index B is for resistant cultivars after te Beest et al. (2009). Their averages are used in this study.</p>	0.09
<p>Ear blight or Fusarium ear blight (<i>Microdochium nivale</i>, <i>Microdochium majus</i>, <i>Fusarium graminearum</i>, <i>Fusarium culmorum</i>)</p>	<p>The infection of ear blight usually occurs during anthesis, under warm and humid conditions, and high rainfall during summer allows infection to spread (Madgwick et al., 2011; West et al., 2012; Xu, 2003). Ear Blight infections are not common in France (Supplementary Fig S14), and its control is less efficient than foliar fungal diseases.</p>	$\text{Ear blight index} = 100 \frac{\exp(-15.3 + 0.941 T_{mean_{May}} + 0.069 \text{ Rainfall}_{1week-June})}{1 + \exp(-15.3 + 0.941 T_{mean_{May}} + 0.069 \text{ Rainfall}_{1week-June})}$ <p>Where: $T_{mean_{May}}$ is the mean temperature in May and $\text{Rainfall}_{1week-June}$ is the accumulated rainfall in first week of June. Equation from Madgwick et al. (2011). Accumulated rainfall for different weeks of late May and June were tested, and the 1st week of June (which was the week when 50% anthesis occurred in 2016) had the highest correlation with grain size anomaly in 2016 considering all sites.</p>	0.12
Anoxia	<p>In waterlogged soils, roots are exposed to low oxygen concentrations, leading to anoxia. Anoxia reduces accumulation and remobilization of carbohydrates into grains, affecting grain size and grain yield (Hossain et al., 2011). Anoxia is frequently cited as a factor causing crop yield losses in France (van der Velde et al., 2012), especially in the 2016 cropping season (Ben-Ari et al., 2018; van der Velde et al., 2020). In order to quantify anoxia, we have calculated a water balance based only on the accumulation of daily difference between reference evapotranspiration (ETo) and rainfall (Rain). Based on this water balance (Supplementary Fig S2-5), we have considered that anoxia would occur when daily accumulated Rain - ETo > 30 mm.</p>	$\text{Anoxia index} = \sum_{(\text{day of } 50\% \text{ anthesis})}^{(\text{day of } 50\% \text{ anthesis}) + 50} \text{Max}(\text{Rainfall} - \text{ETo}, 30 \text{ mm})$ <p>Where: ETo is the daily reference evapotranspiration (mm) and Rainfall is the daily rainfall (mm). ETo was calculated following the Priestley-Taylor method. The first 50 days after 50% anthesis was considered for this index. Anoxia indices comprising different periods around anthesis and with different lengths were also tested, the 50 days after anthesis had the highest correlation with grain size anomaly in 2016.</p>	0.31
Solar Radiation	<p>Low solar radiation incidence during May and June of 2016, are pointed as one of the main causes of 2016 yield loss (Ben-Ari et al., 2018). To test the direct impact of solar radiation on wheat grain size in 2016, an index considering the mean solar radiation incidence during grain filling was built. To validate our results of solar radiation affecting wheat grain size, the crop growth model NWHEAT (Supplementary Fig S16-S17) was run considering all climatic variables of 2016 cropping season and considering all climatic variables of 2016 cropping season but average daily solar radiations from 2014-2019 period.</p>	$\text{Solar Radiation}_{\text{grain filling}} = \sum_{(\text{day of } 50\% \text{ anthesis})}^{(\text{day of harvest})} \frac{SR}{n}$ <p>Where: SR is the daily solar radiation in MJ m⁻² d⁻¹, and n is the number of days between anthesis and harvest.</p>	0.01
Rainfall	<p>Droughts and extreme rainfall are major factors affecting wheat yield variability in Europe (Moravec et al., 2021). In 2016, the excessive rainfall in late May early June is appointed as one of the main factors causing the wheat yield loss (Ben-Ari et al., 2018). To test the direct impact of rainfall on wheat grain size in 2016, an index considering the accumulated rainfall during grain filling was built.</p>	$\text{Rainfall}_{\text{grain filling}} = \sum_{(\text{day of } 50\% \text{ anthesis})}^{(\text{day of harvest})} \frac{\text{Rainfall}}{n}$ <p>Where: Rainfall is the daily rainfall in mm, and n is the number of days between anthesis and harvest.</p>	0.11
Temperature	<p>Temperature is reported to affect grain yield of wheat crops (Asseng et al., 2011), particularly due to change in cropping season length (Webber et al., 2020). In 2016 in France, high winter temperatures favored the survival and development of fungal foliar diseases. Besides that, the low temperature during the spring lead to delay in anthesis date, coinciding the period of anthesis with heavy rainfall events. However, to test the direct impact of temperature on wheat grain size in 2016, an index considering the mean temperature during grain filling was built.</p>	$\text{Temperature}_{\text{grain filling}} = \sum_{(\text{day of } 50\% \text{ anthesis})}^{(\text{day of harvest})} \frac{T_{mean}}{n}$ <p>Where: T_{mean} is the daily mean temperature in °C, and n is the number of days between anthesis and harvest.</p>	0.05

Table S4. Nwheat genetic coefficients of Rubisko wheat cultivar.

Genetic Coefficient	Definition	Rubisko cv.
VSE	Sensitivity to vernalisation	3.7
PPSEN	Sensitivity to photoperiod	4.0
P1	Thermal time from seedling emergence to the end of the juvenile phase	400
P5	Thermal time (base 0oC) from beginning of grain filling to maturity: range 500 to 700	700.0
PHINT	Phyllochron interval	110.0
GRNO	Coefficient of kernel number per stem weight at the beginning of grain filling	26.5
MXFIL	Potential kernel growth rate	1.9
STMMX	Potential final dry weight of a single tiller	3.0
SLAP1	Ratio of leaf area to mass at emergence	280.0
SLAP2	Ratio of leaf area to mass at end of leaf growth	270.0
P5AF	Power term at af1	3.0
MAXNUP	Max N uptake per day	2.0
INGWT	Initial grain weight	10.0

Table S5. Research stations soils characteristics. Silt (%), clay (%), bulk density (g/cm³), pH in Water, carbon (%), nitrogen contents (%), and simulated soil depth (m) of soils in the 8 research stations used in this study.

Research Station	Silt (%)	Clay (%)	Bulk density (g/cm³)	pH in Water	Carbon (%)	Nitrogen (%)	Soil Depth (m)
1, Égreville	68	12	1.35	7.0	0.7	0.1	2.1
2, Chevry	65	12	1.35	7.0	0.5	0.1	2.1
3, Saint-Quentin	68	22	1.57	6.5	0.4	0.08	2.1
4, Saint-Florent	60	30	1.37	7.0	0.2	0.03	2.3
5, Fagnières	50	20	1.47	7.0	0.25	0.03	1.9
6, Issodun	45	30	1.45	7.5	0.3	0.05	1.9
7, Barbarey-Saint-Sulpice	49	29	1.50	7.8	0.25	0.03	2.3
8, Rots	60	10	1.35	7	0.3	0.05	1.5

3 Supplementary Figures

3.1 Supplementary results

3.1.1 Climatic analysis

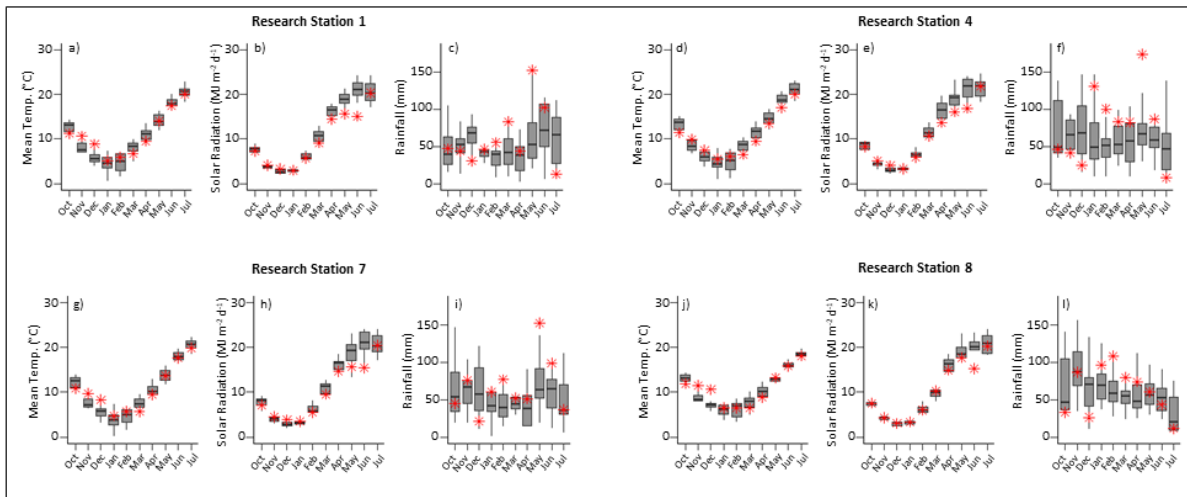


Figure S1. Weather conditions during wheat cropping season in France. Boxplot of monthly (a, d, g and j) mean temperature (Mean Temp), (b, e, h and k) solar radiation and (c, f, i and l) rainfall, over the 2013–2020 wheat growing seasons in France (whisker plots). Weather data are shown for Research Stations 1, 4, 7 and 8. Whiskers extend to maximum and minimum values. Values for the 2015-2016 growing season are presented as red asterisk.

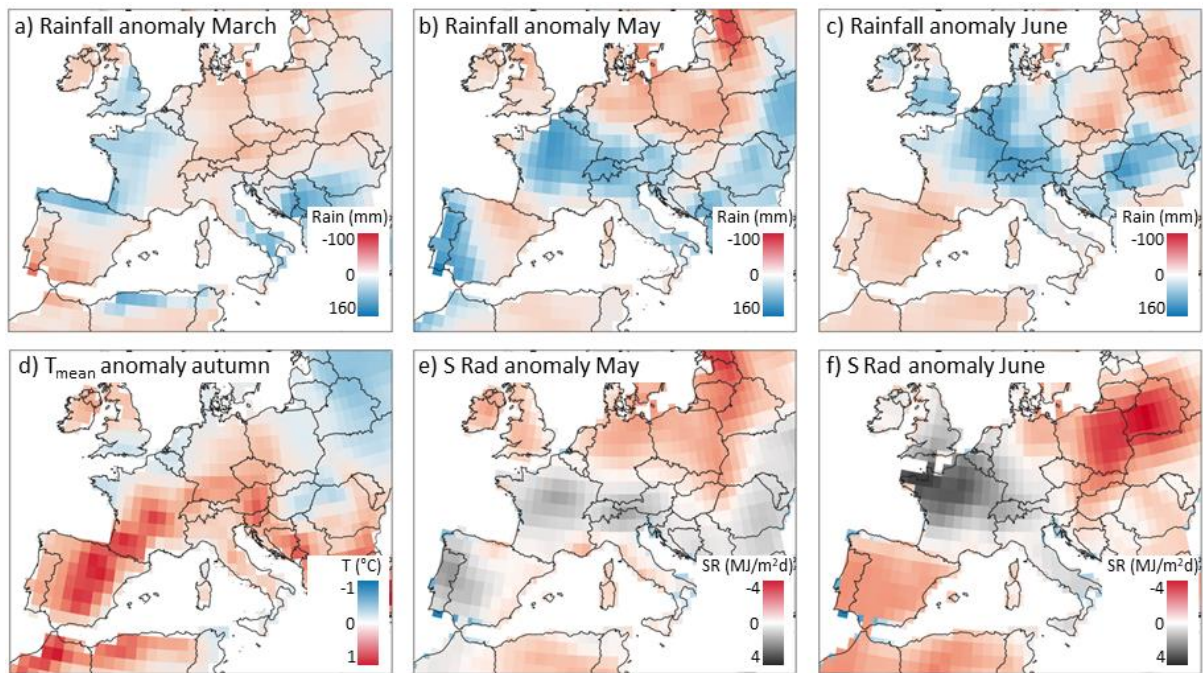


Figure S2. Weather anomaly of 2016 wheat cropping season in Europe. Spatial distribution of the weather anomaly in 2016 of accumulated rainfall (a) in March, (b) May, (c) and in June, (d) monthly mean temperature (T_{mean}) during the autumn of 2015 (October to December), and solar radiation (S Rad) (e) in May and (f) in June, compared to the 30-years historical average for the 1990-2019 period. Climate variables data are from the NASAPower (Team, 2021), with a spatial resolution of 0.5 deg x 0.5 deg.(Team, 2021). Maps lines delineate study areas and do not necessarily depict accepted national boundaries.

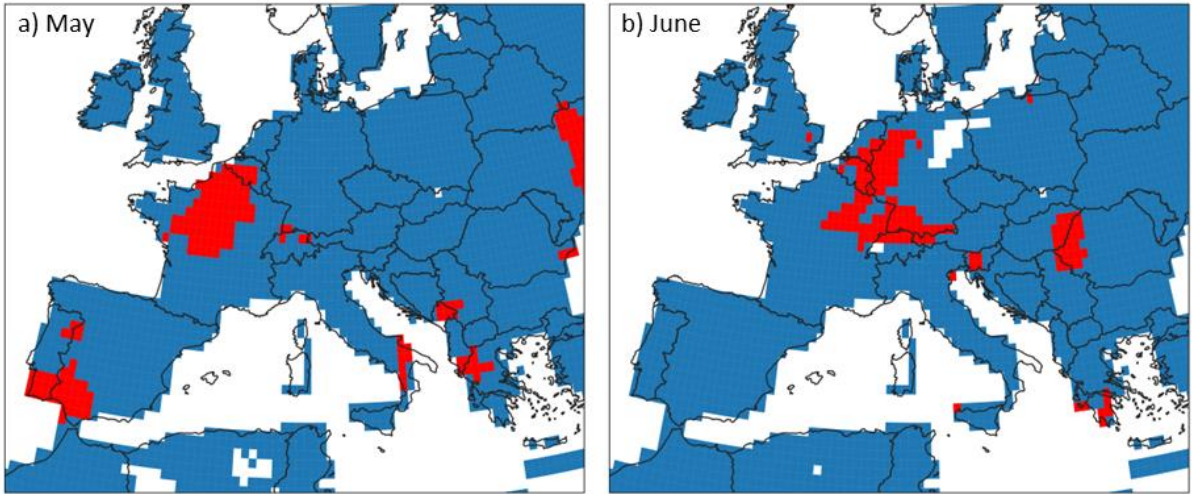


Figure S3. Rainfall anomalies across western Europe in 2016. Red areas indicate the highest accumulated rainfall of the last 30 years, in (a) May and (b) June of 2016. Data are from the NASAPower (Team, 2021), with a spatial resolution of 0.5 deg x 0.5 deg. Maps lines delineate study areas and do not necessarily depict accepted national boundaries.

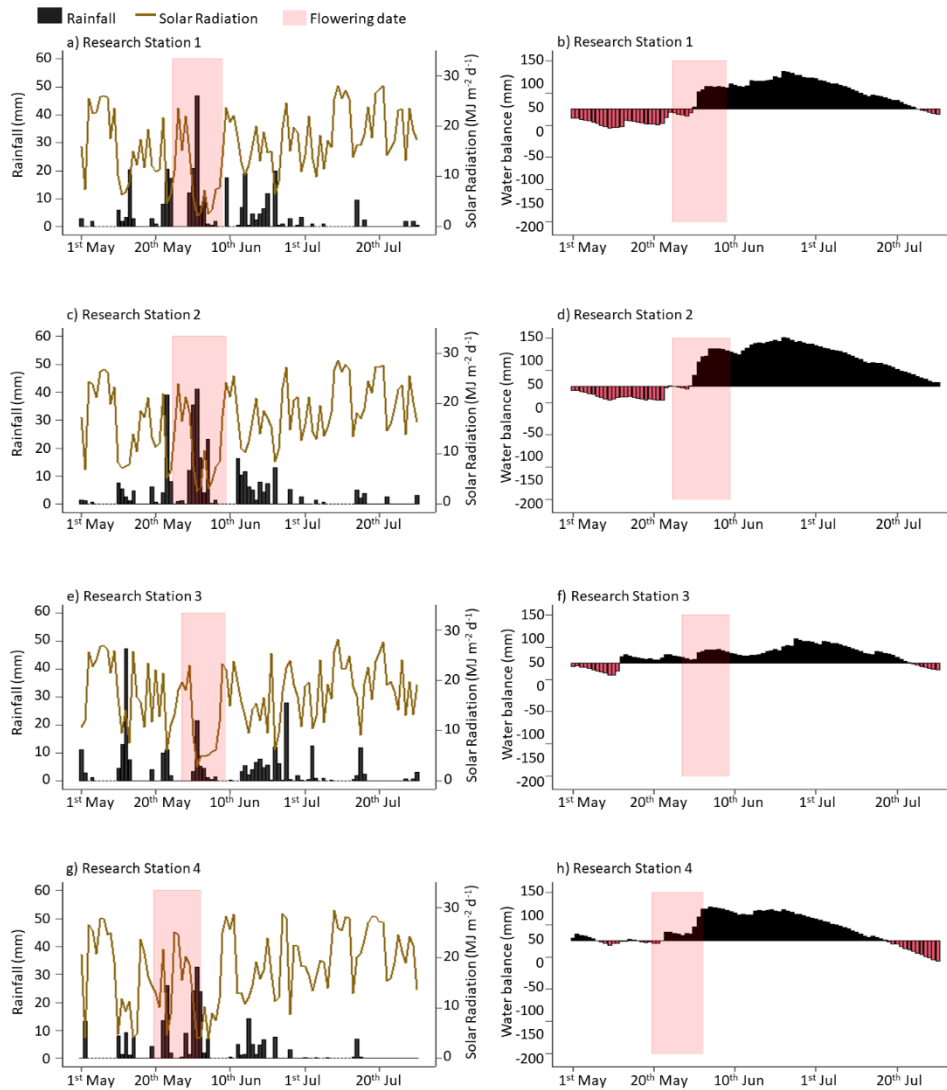


Figure S4. Weather around wheat anthesis in France 2016. (a, c, e and g) Daily rainfall and solar radiation, and (b, d, f and h) water balance based on the accumulation of daily difference between measured rainfall and calculated reference evapotranspiration (ET_o) for the research stations 1, 2, 3 and 4. The area in red demonstrates the period where wheat anthesis occurred for different cultivars.

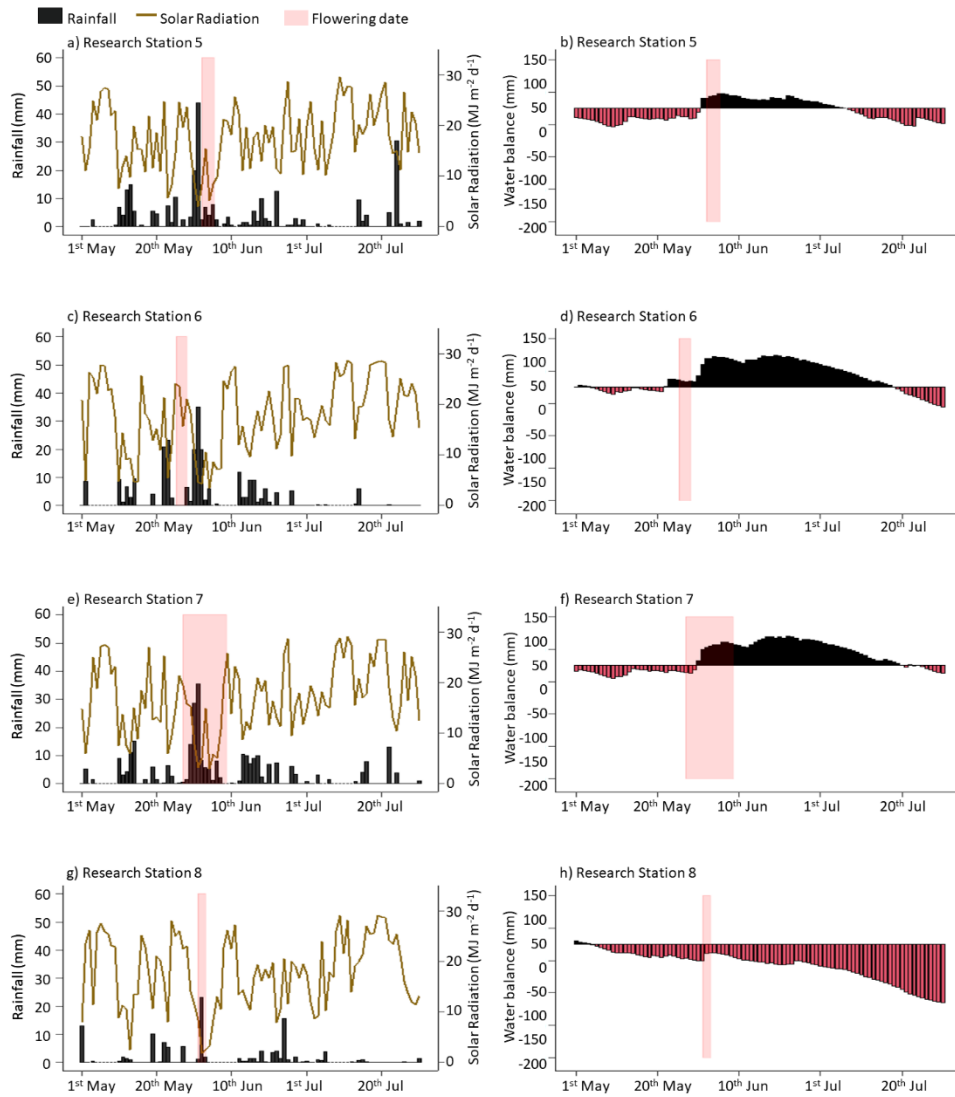


Figure S5. Weather around wheat anthesis in France 2016. Daily rainfall (mm) and solar radiation, (**b**, **d**, **f** and **h**) and water balance based on the accumulation of daily difference between measured rainfall and calculated reference evapotranspiration (ET₀). Shown for research stations 5, 6, 7 and 8. The area in red demonstrates the period where wheat anthesis occurred for different cultivars.

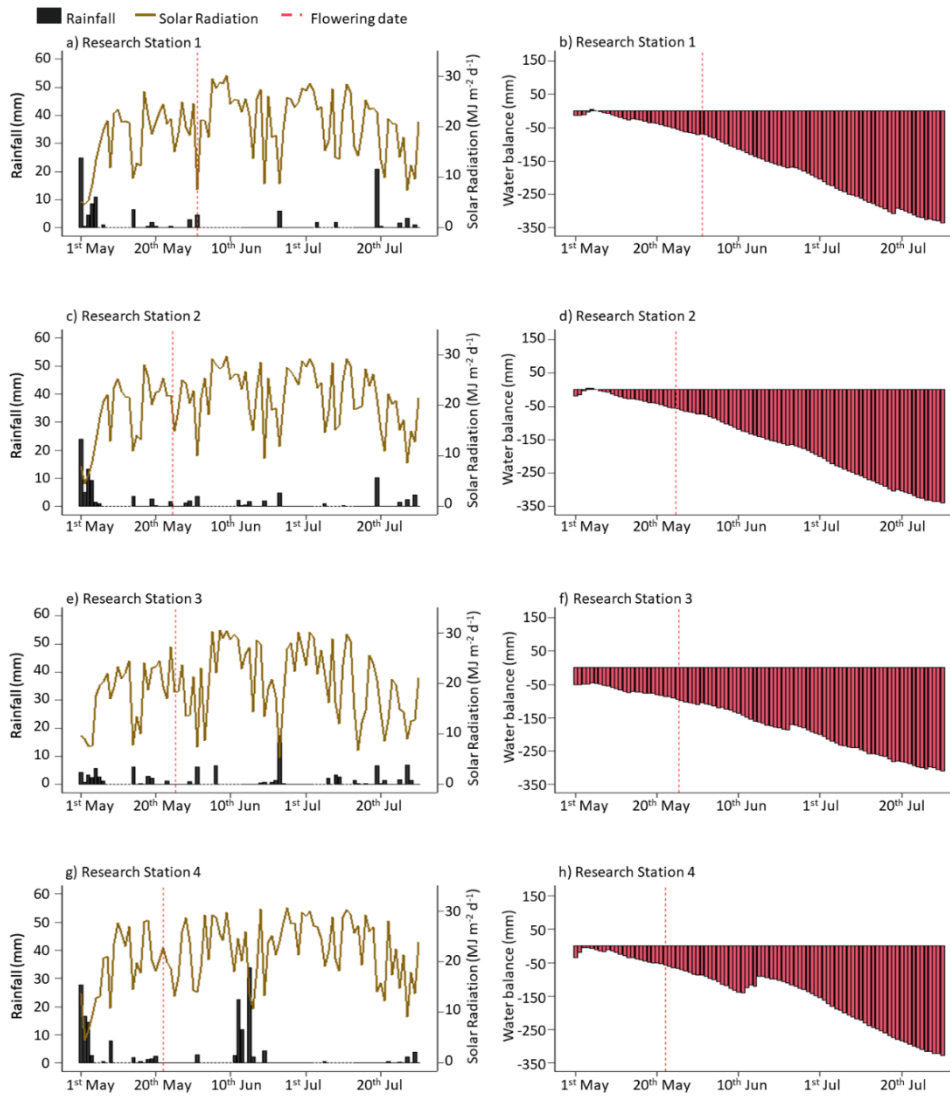


Figure S6. Weather around wheat anthesis in France 2015. (a, c, e and g) Daily rainfall (mm) and solar radiation, (b, d, f and h) and water balance based on the accumulation of daily difference between measured rainfall and calculated reference evapotranspiration (ET₀) for the research stations 1, 2, 3 and 4.

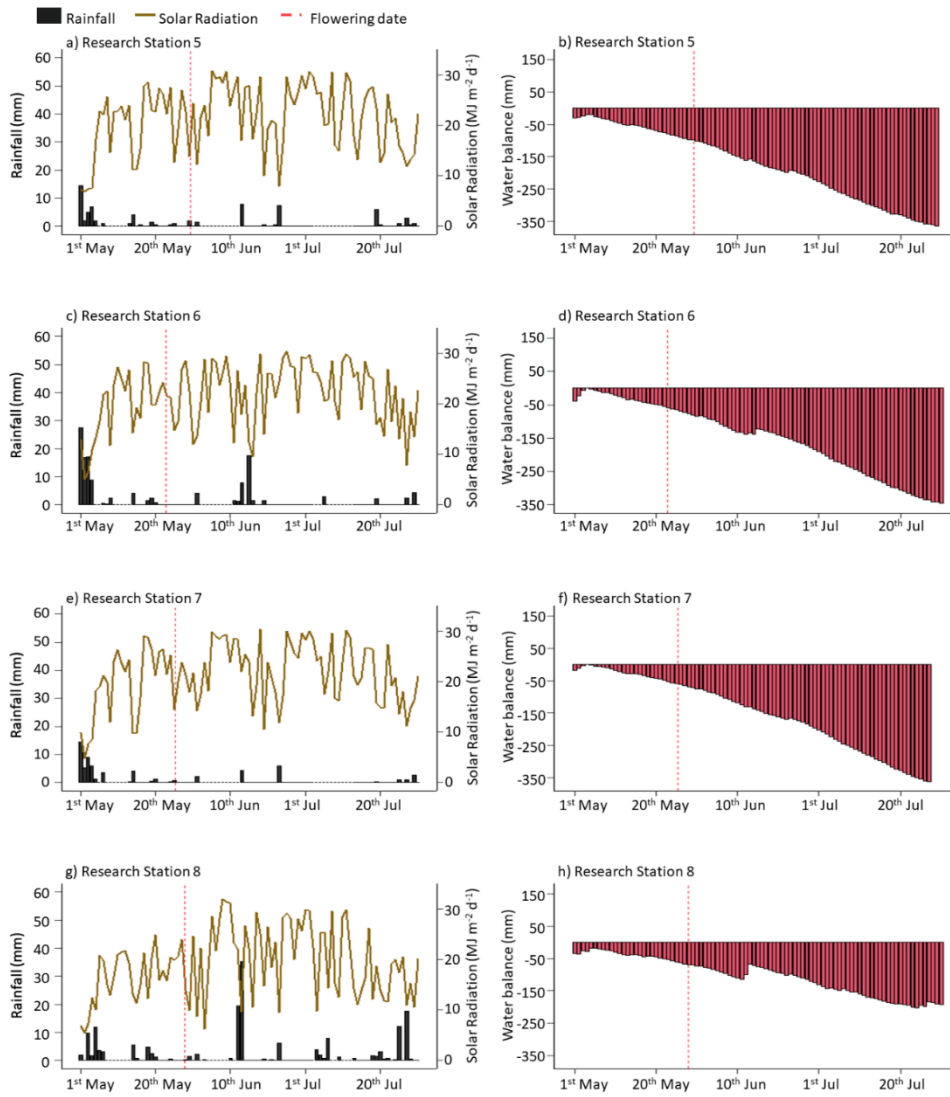


Figure S7. Weather around wheat anthesis in France 2015. (a, c, e and g) Daily rainfall (mm) and solar radiation, (b, d, f and h) and water balance based on the accumulation of daily difference between measured rainfall and calculated reference evapotranspiration (ETo) for the research stations 5, 6, 7 and 8.

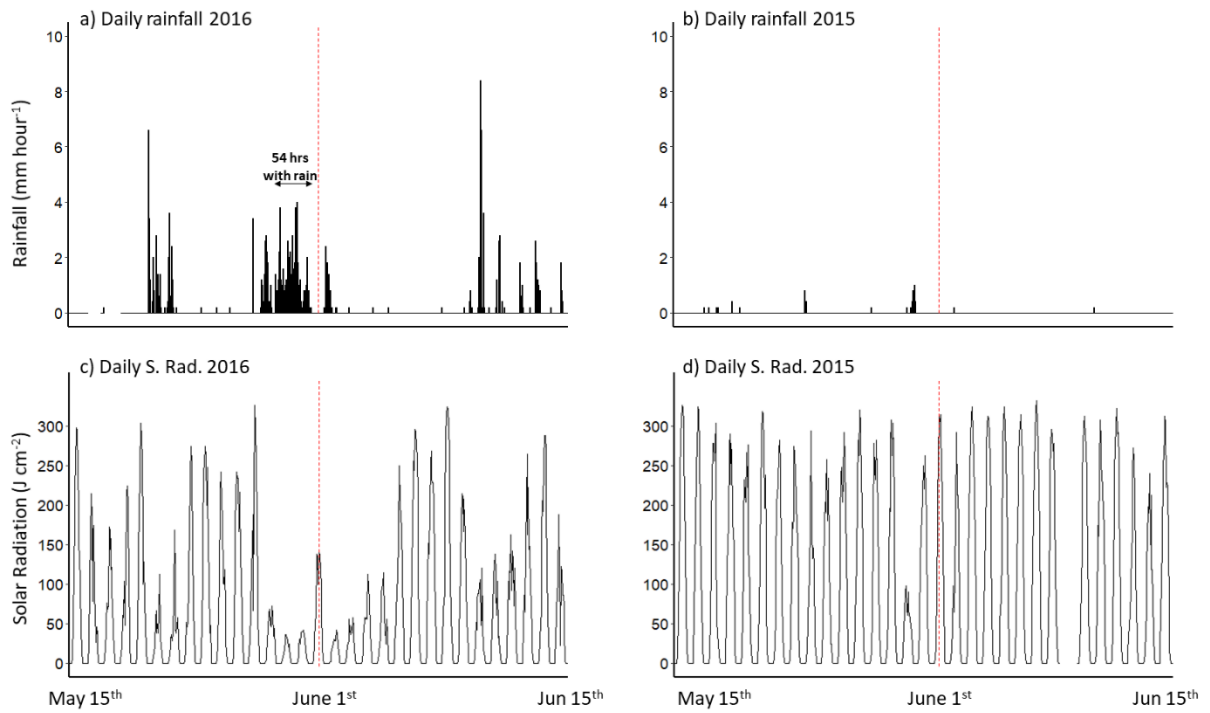


Figure S8. Hourly weather conditions around wheat anthesis. Hourly variation rainfall in (a) 2016 and (b) 2015, and solar radiation in (c) 2016 and (d) 2015. Weather data is shown for Boigneville, France, location near to Research station 1 (Égreville) of this study. Red dashed line is on 1st June, the average date of anthesis for Boigneville.

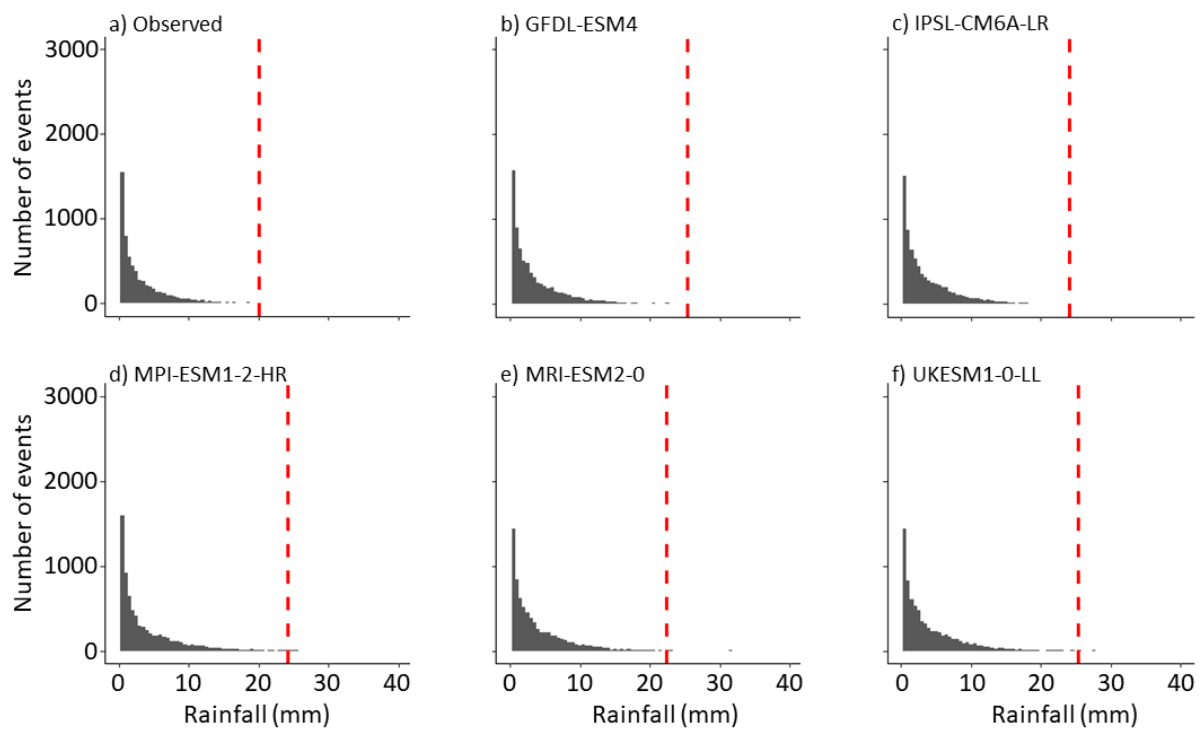


Figure S9. Daily rainfall data from 1981 to 2020 distribution. Distribution is shown for (a) observed and for five CMIP6 models (b) GFDL-ESM4, (c) IPSL-CM6A-LR, (d) MPI-ESM1-2-HR, (e) MRI-ESM2-0 and (f) UKESM1-0-LL. Vertical dashed line shows the 0.995 quantile for observed (rainfall equal 20mm) in (a) and for each of the five CMIP6 models in (b-f).

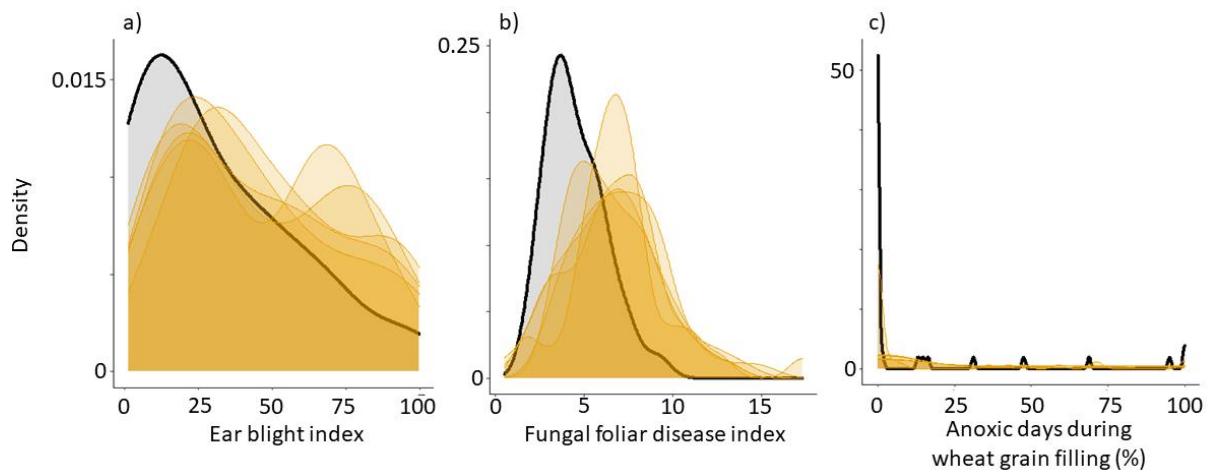


Figure S10. Ear blight, Foliar diseases and anoxic days from 1981 to 2020 distribution. Distribution is shown for (a) ear blight, (b) foliar fungal diseases and (c) number of anoxic days during grain filling for observed climate (gray) with for five CMIP6 models (tons of yellow) GFDL-ESM4, IPSL-CM6A-LR, MPI-ESM1-2-HR, MRI-ESM2-0 and UKESM1-0-LL from 1981 to 2020.

3.1.2 Nitrogen leaching and nitrogen wheat uptake

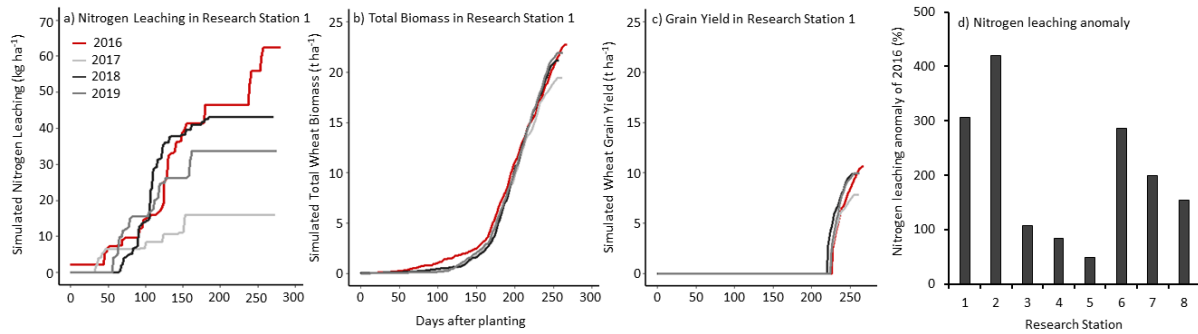


Figure S11. Simulated nitrogen leaching, total above ground biomass and grain yield. (a) Nitrogen leaching, (b) total above ground biomass, and (c) grain yield for the winter wheat cultivar Rubisko grown in Égreville (Research Station 1), France were simulated with the Nwheat crop simulation model. (d) Nitrogen leaching anomaly of 2016 compared to 2017 for all eight research stations here studied. The nitrogen application rates were similar to those applied in the Arvalis field trials. In 2016, 52 kg N ha⁻¹ were applied on 18 Feb, 92 kg N ha⁻¹ on 7 Mar, 41 kg N ha⁻¹ on 20 Apr, and 32 kg N ha⁻¹ on 29 Apr. For the other years, nitrogen was applied in three splits with an average of 52 kg N ha⁻¹ in early February, 85 kg N ha⁻¹ in early March and 60 kg N ha⁻¹ in late April. The soil characteristics are presented in Table S1.

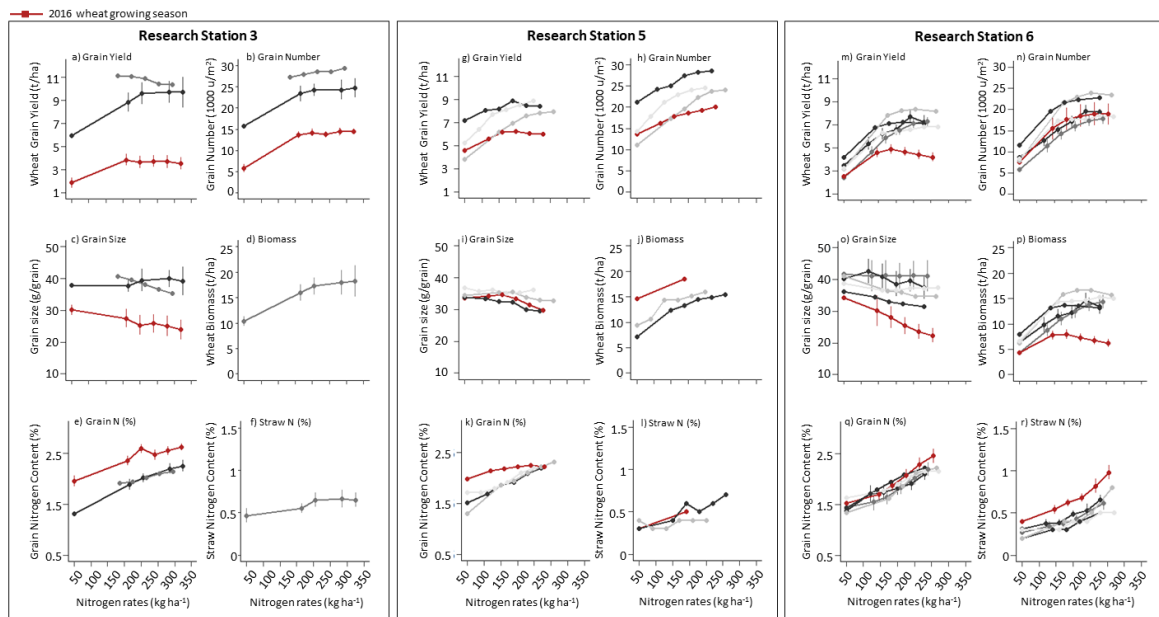


Figure S12. Observed wheat responses to nitrogen fertilizer application rates. (a, g and m) Grain yield, (b, h and n) grain number, (c, i and o) grain size, (d, j and q) nitrogen grain concentration, (e, k and r) total above ground biomass at maturity and (f, l and s) nitrogen straw concentration responses curves to nitrogen fertilizer application rates for the wheat cultivars grown in the field at three research stations. Shades of gray colored lines refer to wheat size responses to nitrogen fertilizer application rates in different years in the 2014 to 2019 growing seasons (excluding 2016).

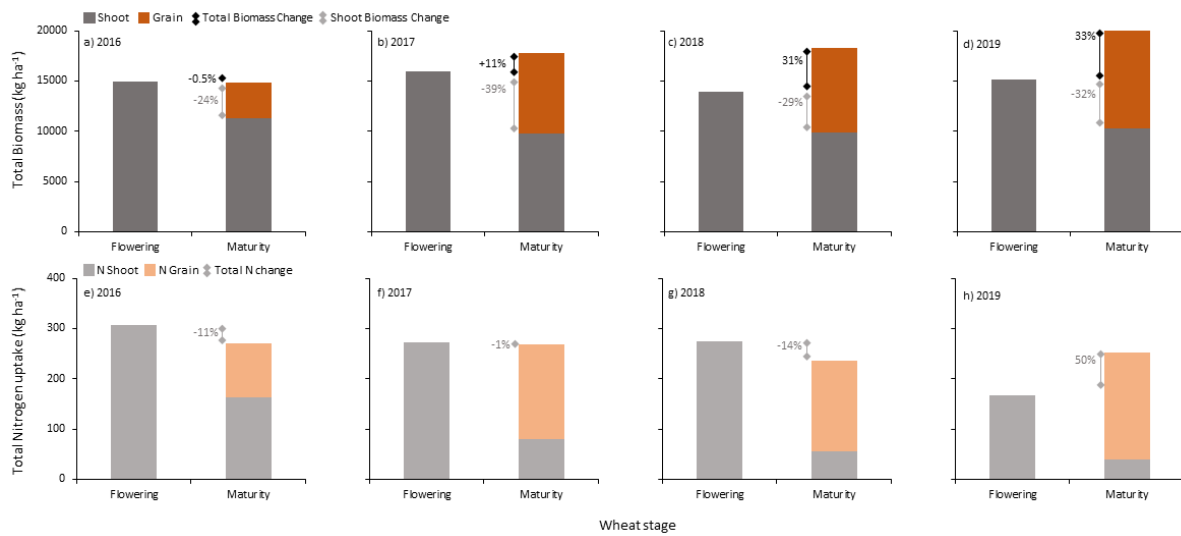


Figure S13. Measured total above ground biomass and nitrogen at anthesis and maturity. Above ground biomass at anthesis and maturity in vegetative tissues and grains for the (a) 2016, (b) 2017, (c) 2018, and (d) 2019 harvest. Above ground nitrogen at anthesis and maturity in vegetative tissues and grains in (e) 2016, (f) 2017, (g) 2018 and (h) 2019. Data for the Rubisko cultivar grown in the field at Égreville (Research Station 1), France.

3.1.3 Plant diseases analysis

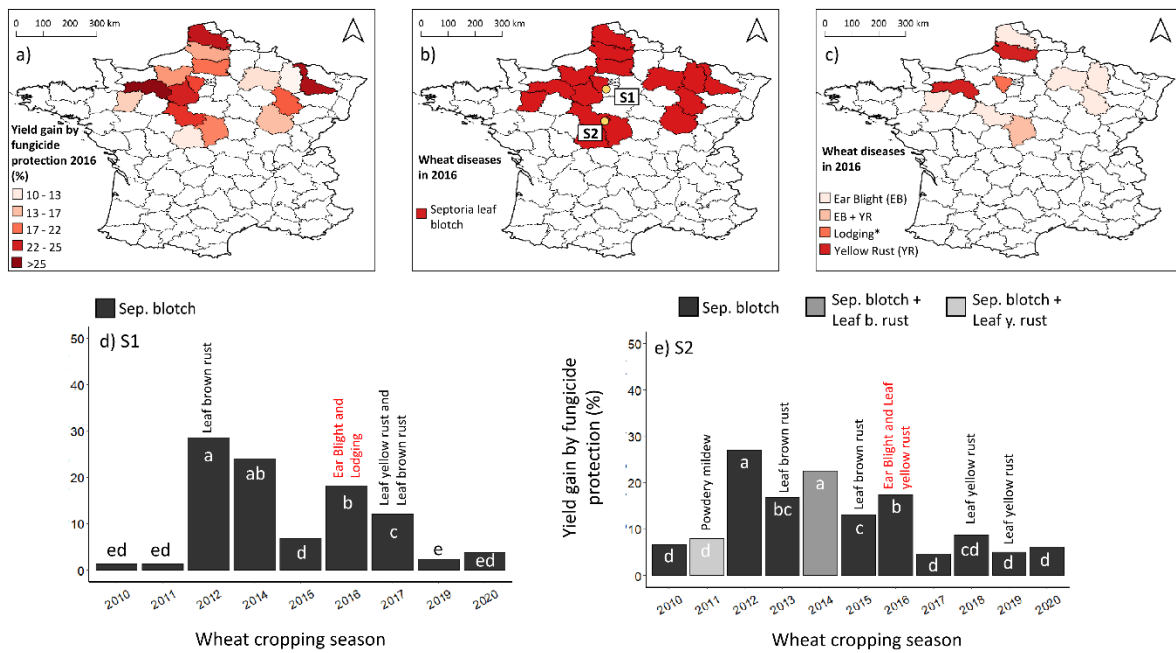


Figure S14. Wheat crop diseases across the breadbasket of France in 2016. Spatial distribution of (a) yield gain by fungicide protection, (b) dominant and (c) secondary wheat disease around the breadbasket of France in 2016. Wheat yield gain by fungicide protection, and the (d) dominant and (e) secondary wheat disease from 2010 to 2020. Maps lines delineate study areas and do not necessarily depict accepted national boundaries.

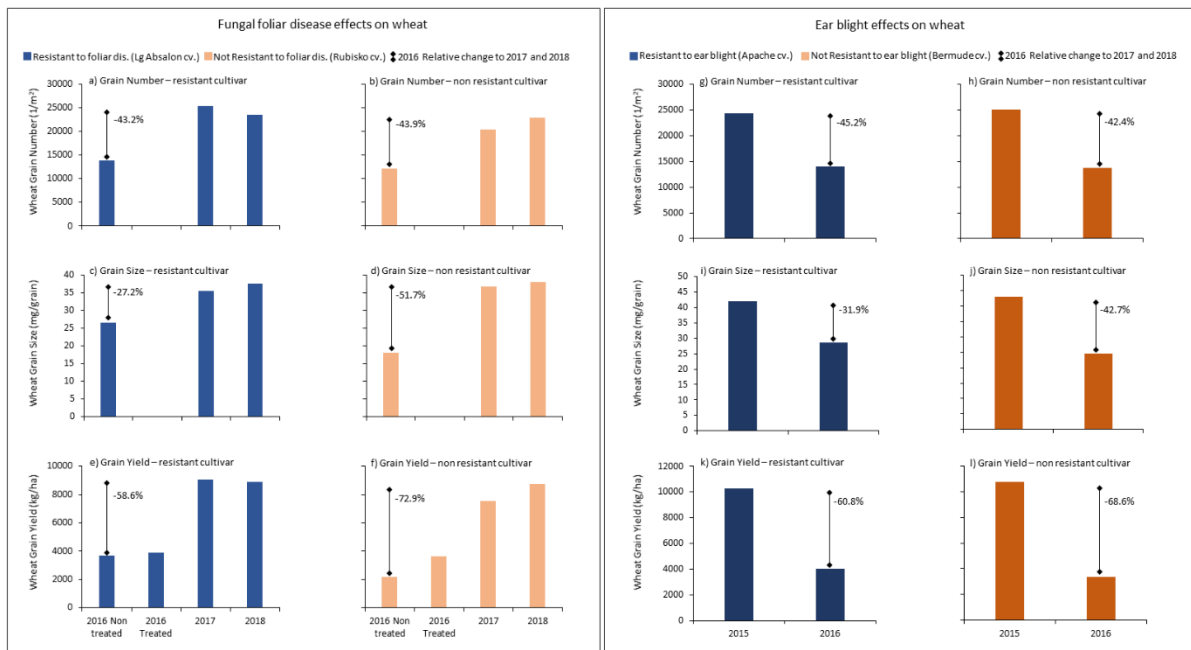


Figure S15. Wheat grain number, grain size and yield for resistant and non-resistant cultivars for plant diseases. Wheat (a-b) grain number, (c-d) grain size and (e-f) yield for the resistant wheat cv. Lg Absalon for fungal foliar diseases in (a, c and e), and for a susceptible wheat cv. Rubisko in (b, d and f). Wheat (g-h) grain number, (i-j) grain size and (k-l) yield for the resistant wheat cv. Apache for ear blight in (g, i and k), and for a susceptible wheat cv. Bermude in (h, j and l). Wheat cultivars were grown in Research station 1, and all wheat cultivars were sown in the same day in 2016 cropping season. For resistant and non-resistant wheat cultivars of foliar fungal diseases, anthesis was also observed in the same day. However, for ear blight Apache cv. Flowered one week after cv Bermude, with more pronounced effects of heavy rainfall and low solar radiation on grain numbers, as presented in Figure 4.

3.1.4 Solar radiation

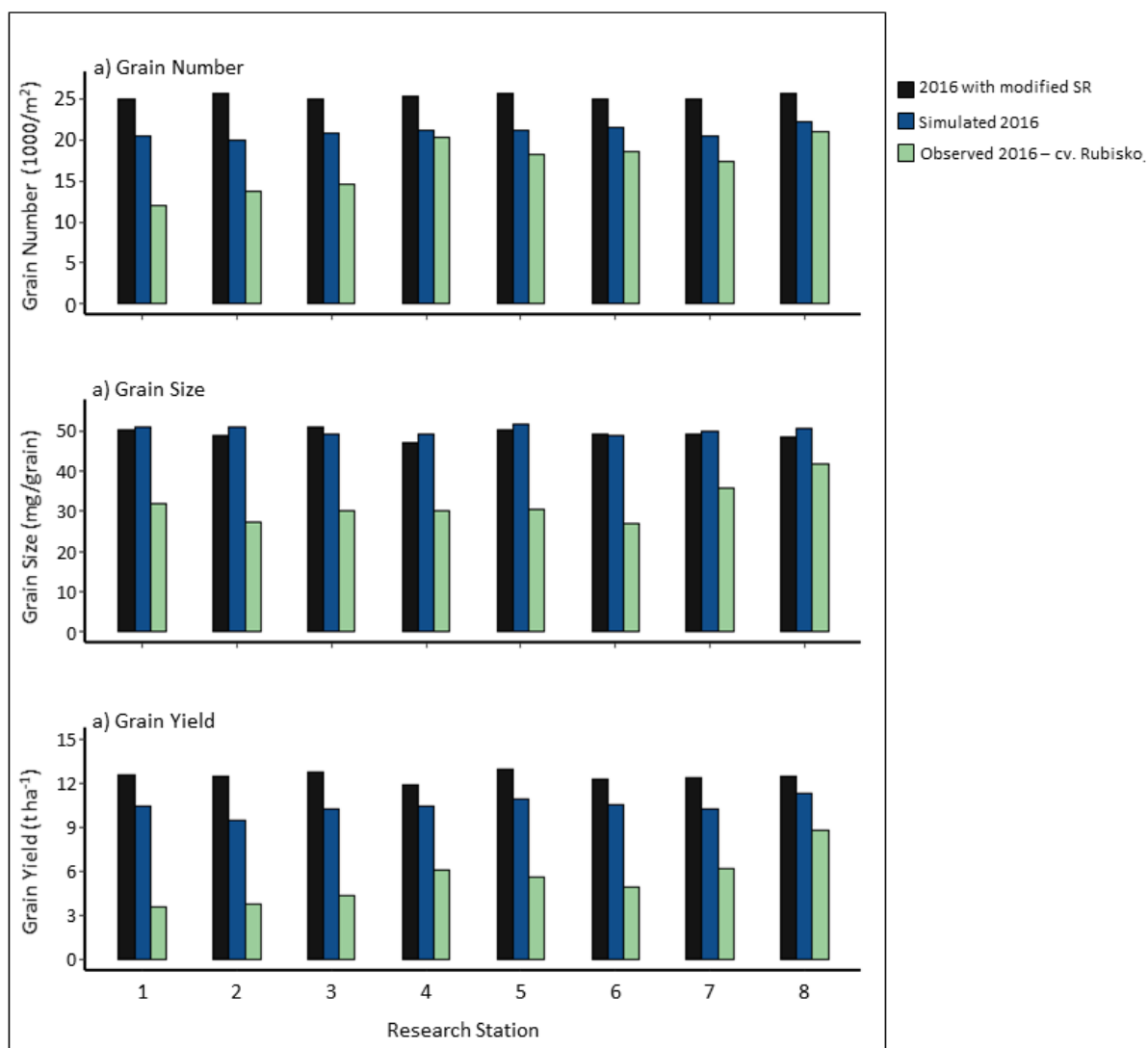


Figure S16. Effect of 2016 solar radiation on wheat grain yield and yield components in 2016. Comparison of (a) grain number, (b) grain size and (c) grain yield for 2016 simulated with using average solar radiation from 2014, 2015, 2017, 2018 and 2019 wheat cropping season (black), simulated with 2016 solar radiation (blue) and observed with cultivar Rubisko in field trials in 2016 (green). The research stations were: 1, Égreville; 2, Chevry; 3, Saint-Quentin; 4, Saint-Florent; 5, Fagnières; 6, Issodun; 7, Barbarey-Saint-Sulpice; and 8, Rots. The black bars (2016 with modified SR) refers to grain number, grain size and yield simulations considering rainfall, maximum and minimum temperature from 2016 but with solar radiation data (SR) from 2014, 2015, 2017, 2018 and 2019 wheat cropping seasons. Thus, wheat growth simulations of 2016 with modified solar radiation were carried out five times, one per each of the cropping seasons from 2014 to 2019, and the black bars represent the average of these simulations.

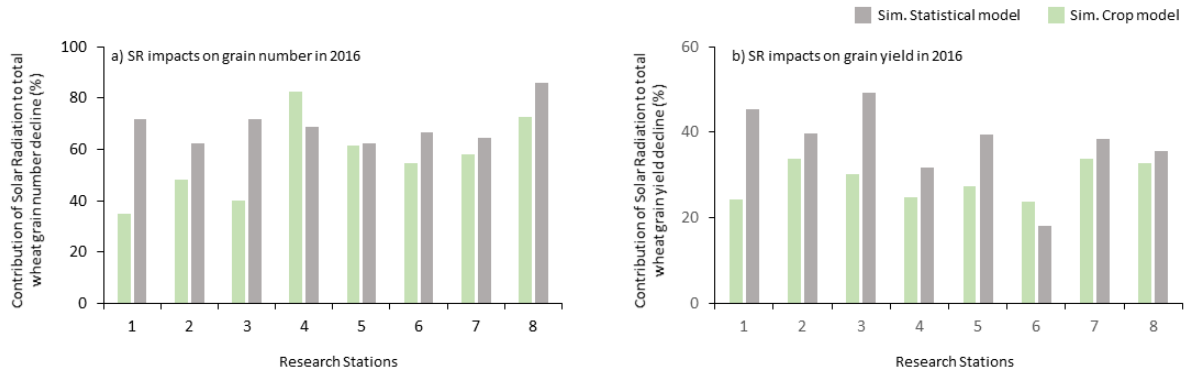


Figure S17. Contribution of solar radiation to total wheat (a) grain number and (b) grain yield decline at eight research stations in the France breadbasket. Simulations were done with the NWheat crop simulation model (green bars) and with multiple regression statistical models (gray bars). Note, solar radiation had no impact on grain size as shown in Fig S11. The research stations were: 1, Égreville; 2, Chevry; 3, Saint-Quentin; 4, Saint-Florent; 5, Fagnières; 6, Issodun; 7, Barbarey-Saint-Sulpice; and 8, Rots.

3.1.5 Climatic change

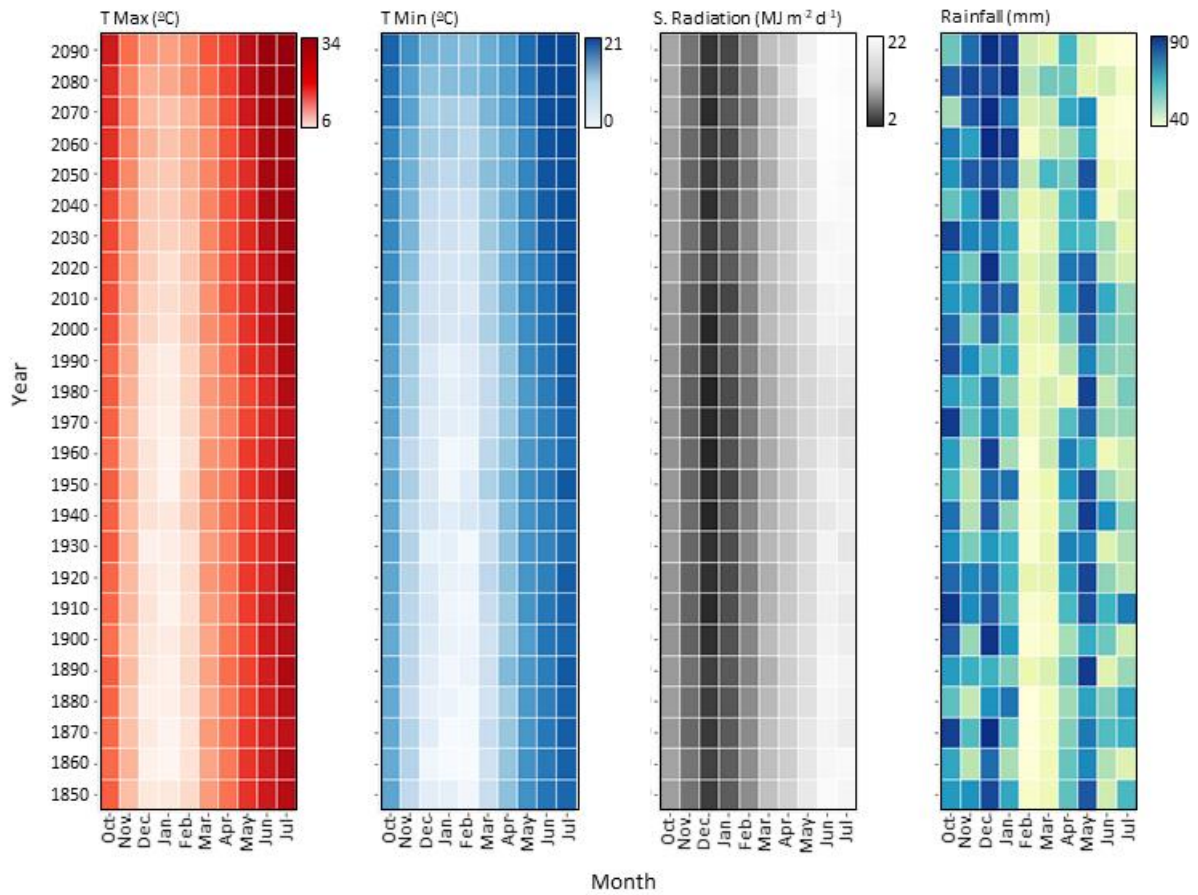


Figure S18. Projected future climate in Égreville, France. Average monthly maximum (T Min), minimum temperature (T Max), solar radiation (S. Radiation), and accumulated rainfall (Rainfall) for the period 1850-2100, in Égreville, France, and for SSP5-8.5. The values presented are the mean of five CMIP6 global change models.

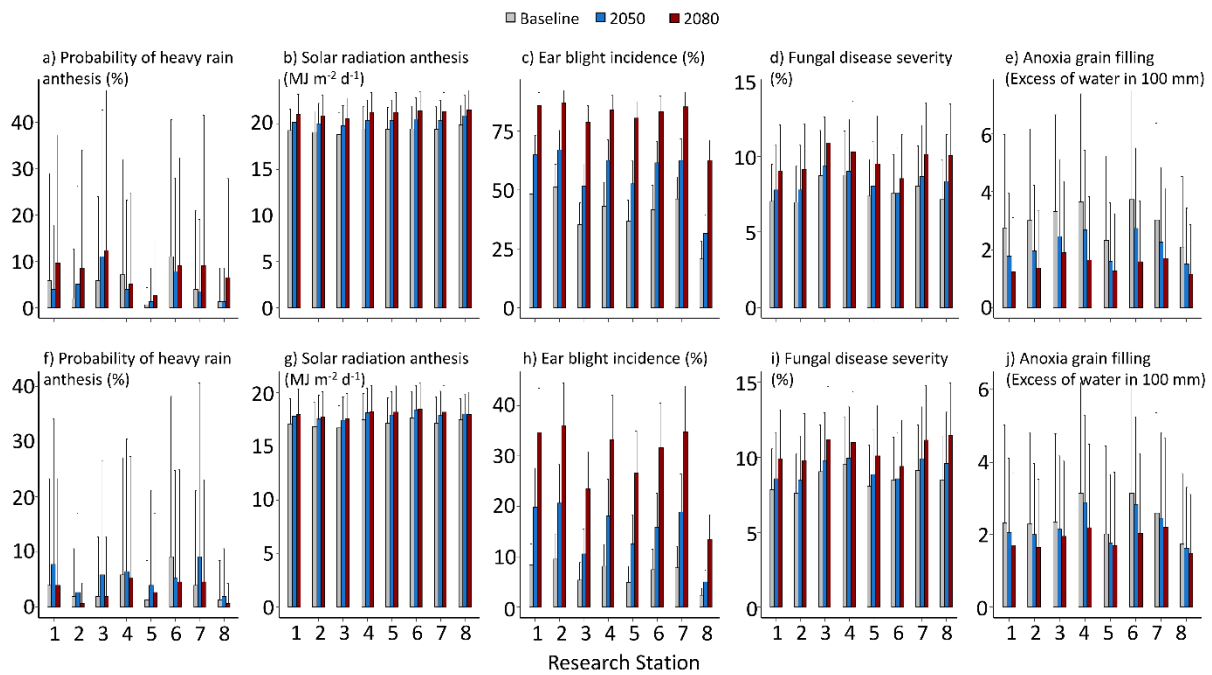


Figure S19. Projected future frequency of the extreme weather on the 2016 wheat yield failure in the breadbasket of France. Estimated indices of (a and f) heavy rainfall (daily rainfall > 20 mm) at ± 5 days around anthesis, (b and g) solar radiation at ± 15 days around anthesis, (c and h) ear blight index, (d and i) fungal foliar disease index and (e and j) anoxia index during grain filling for the baseline (1960-2020), 2050 (average between 2035 and 2065) and 2080 (average between 2070 and 2100) and for two anthesis date according in (a-e) 1 June and (f-j) 1 May. Bars are ensemble means based on five bias-adjusted CMIP6 global climate models (GCMs) for SSP5-8.5. In the simulations, anthesis was fixed as 1 June in (a-e) and 1 May in (f-g), and the anoxia index was calculated every year from (a-e) 1 June to 31 July and (f-g) 1 May to 15 June. The research stations were numbered from 1 to 8 according to the magnitude of their wheat yield loss in 2016 (as in i, location 1 had the highest yield loss in 2016 and location 8 the lowest): 1, Égreville; 2, Chevry; 3, Saint-Quentin; 4, Saint-Florent; 5, Fagnières; 6, Issoudun; 7, Barbarey-Saint-Sulpice; and 8, Rots.

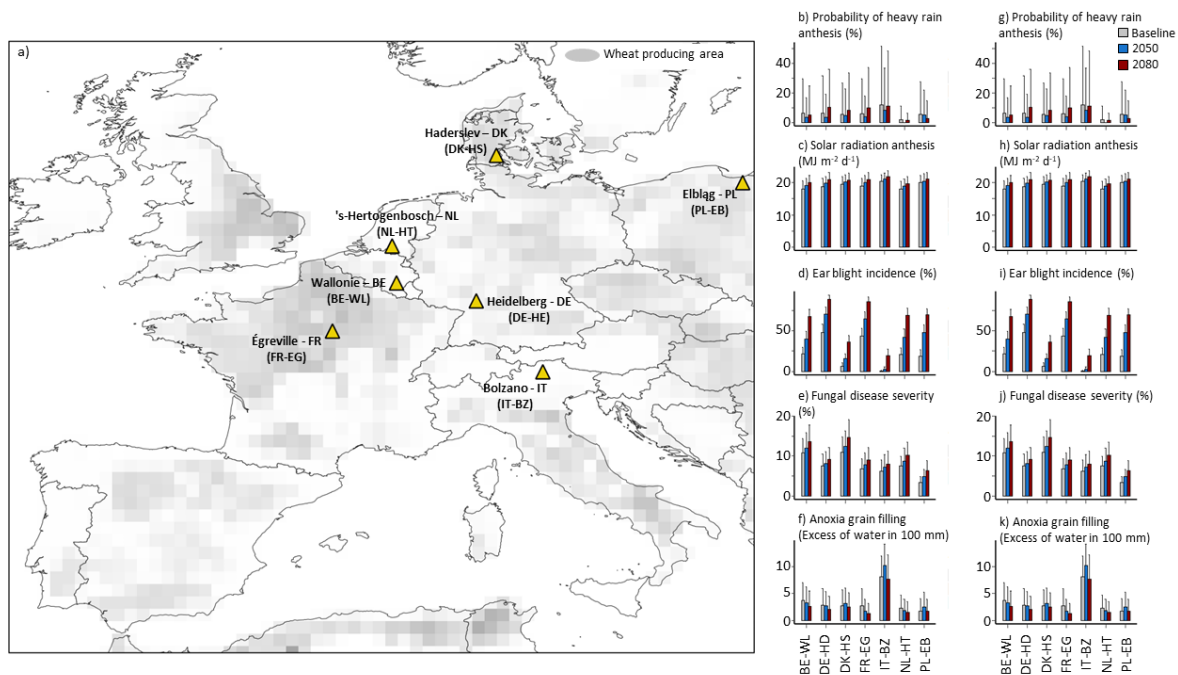


Figure S20. Projected future frequency of the extreme weather on the 2016 wheat yield failure in Western Europe. (a) Spatial distribution of the locations in western Europe studied. Estimated indices of (b and g) heavy rainfall (daily rainfall > 20mm) at ± 5 days around anthesis, (c and h) solar radiation at ± 15 days around anthesis, (d and i) ear blight index, (e and j) fungal foliar disease index and (f and k) anoxia index during grain filling for the baseline (1960-2020), 2050 (average between 2035 and 2065) and 2080 (average between 2070 and 2100) for two anthesis date according in (b-f) 1 June and (g-k) 1 May. Bars are ensemble means based on five bias-adjusted CMIP6 global climate models (GCMs) for SSP5-8.5. In the simulations, anthesis was fixed as 1 June in (b-f) and 1 May in (g-k), and the anoxia index was calculated every year from (b-f) 1 June to 31 July and (g-k) 1 May to 15 June. Map lines delineate study areas and do not necessarily depict accepted national boundaries.

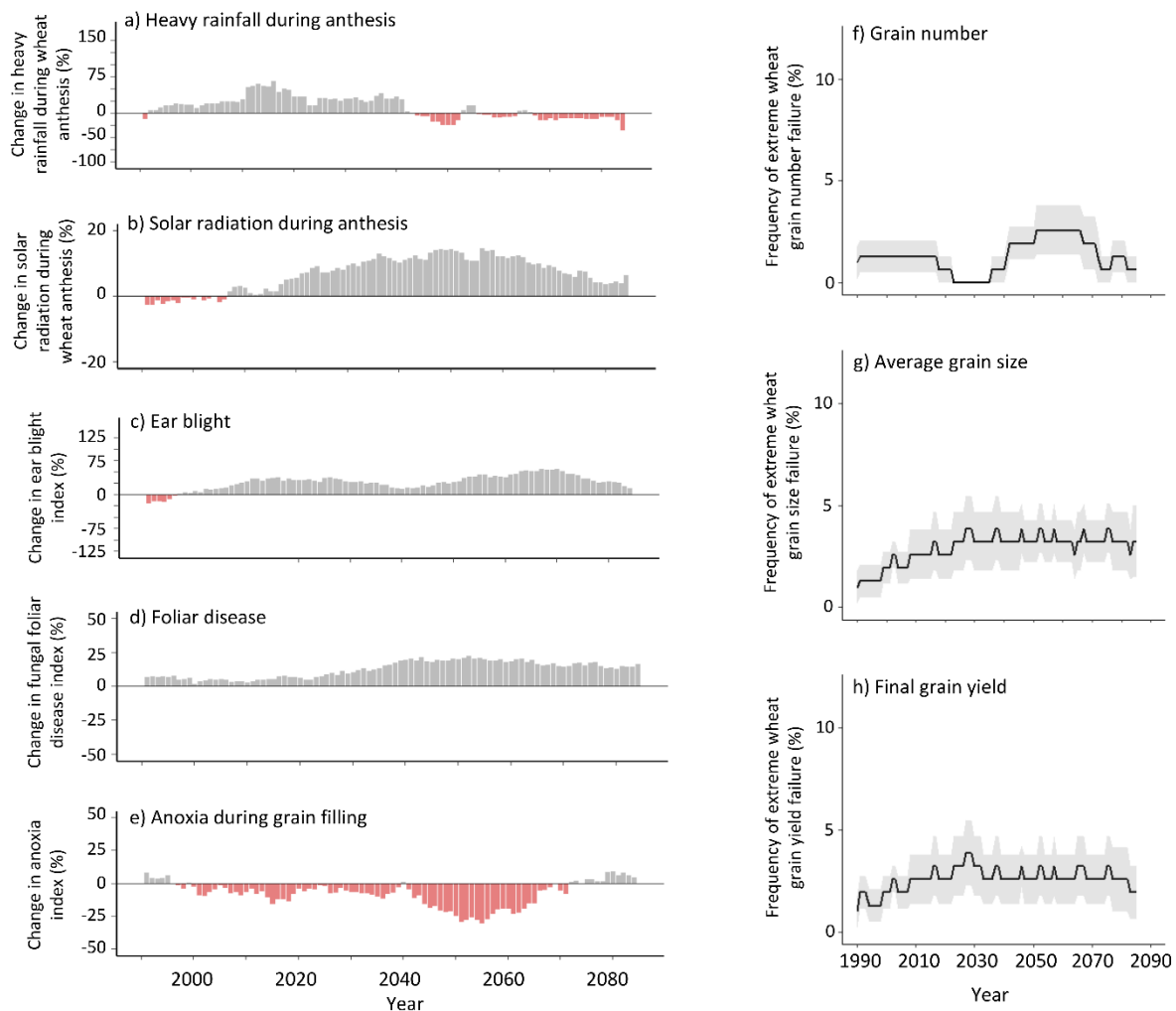


Figure S21. Projected future frequency of the extreme weather on the 2016 wheat yield failure in France with SSP5-2.6. Estimated running mean change for future 30 years of (a) heavy rainfall (daily rainfall > 20 mm) at ± 5 days around anthesis, (b) solar radiation at ± 15 days around anthesis, (c) ear blight index, (d) fungal foliar disease index and (e) anoxia index during grain filling in relation to the reference period 1960-2020. Estimated running mean change for future 30 years frequency of extreme low wheat (f) grain number per unit area, (g) average single grain size and (c) grain yield from 1990 to 2085, with each year as the middle of a 30-years period. (a-e) Bars are ensemble means based on five bias-adjusted CMIP6 global climate models (GCMs) for SSP5-2.6. (f-h) Lines are ensemble means based on five bias-adjusted CMIP6 GCMs for SSP5-2.6 (lines) and shading shows ± 1 s.e. In the simulations, anthesis was fixed as 1 June, and the anoxia index was calculated every year from 1 June to 31 July. CMIP6 GCMs for SSP5-2.6 data are an average of climate projections for the following eight research stations: 1, Égreville; 2, Chevry; 3, Saint-Quentin; 4, Saint-Florent; 5, Fagnières; 6, Issoudun; 7, Barbarey-Saint-Sulpice; and 8, Rots.

3.1.6 Wheat growth

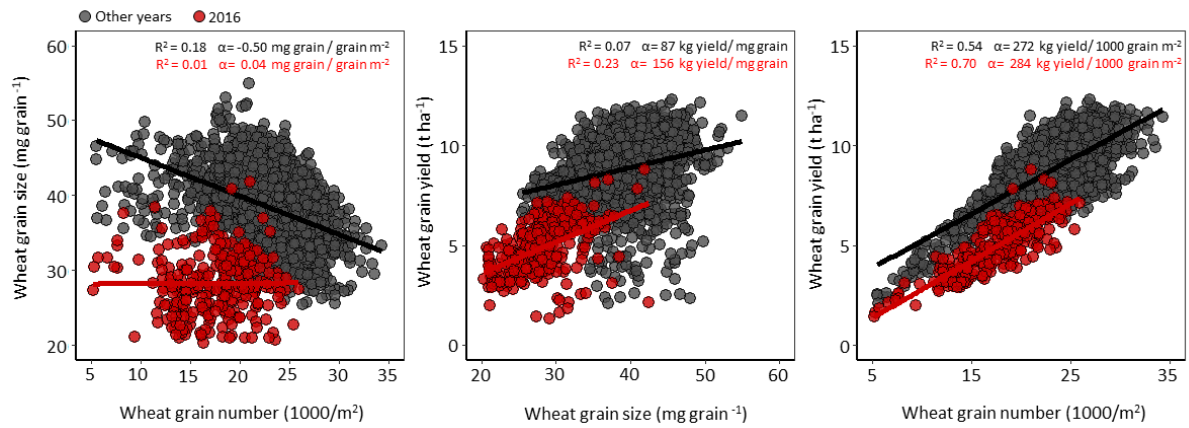


Figure S22. Wheat grain number and grain size relations with grain yield. Relationship between observed wheat (a) grain number and grain size (b) grain size and grain yield (c) grain number and grain yield. Alfa is the rate of wheat grain size change per unit of grain number in (a), and the rate of wheat grain yield change per unit of grain size in (b), and per unit of grain number in (c).

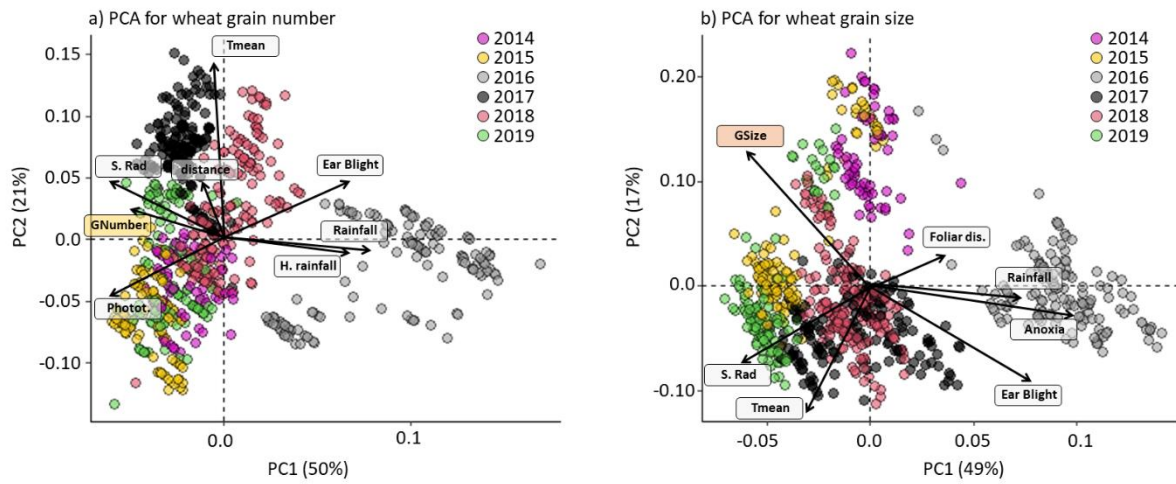


Figure S23. Plant diseases and weather effects on observed wheat grain number and grain size. Bi-plot of the loadings of the original variables in the first two canonical variables for weather and plant diseases effects on observed wheat for (a) grain number and (b) grain size in the breadbasket of France. The percentage of total variance explained by each canonical variable is indicated in parentheses.

3.1.7 National wheat yield anomaly

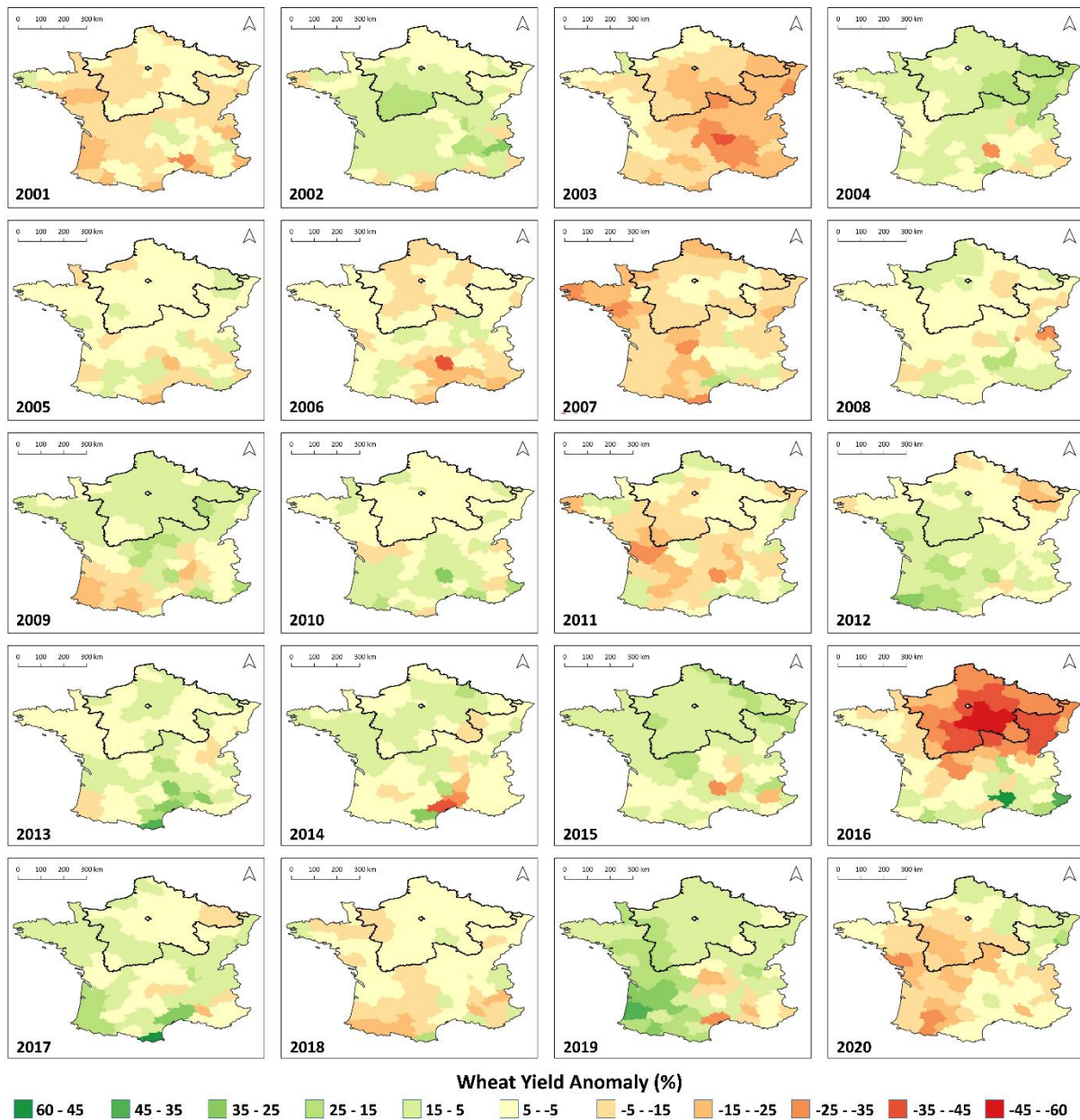


Figure S24. Observed spatial-temporal pattern of trend-corrected wheat yield anomaly in France. Observed wheat yield anomalies relative to average values defined in each French department (2001-2019). Observed winter wheat yield anomaly for the French departments (administrative units known in France as *départements* at NUTS1 spatial scale) were calculated from observed wheat yield collected from the French Ministry of Agriculture official survey data (Agreste, 2022). The French Ministry of Agriculture provides seasonal wheat yield data for all departments that cultivate wheat. Maps lines delineate study areas and do not necessarily depict accepted national boundaries.

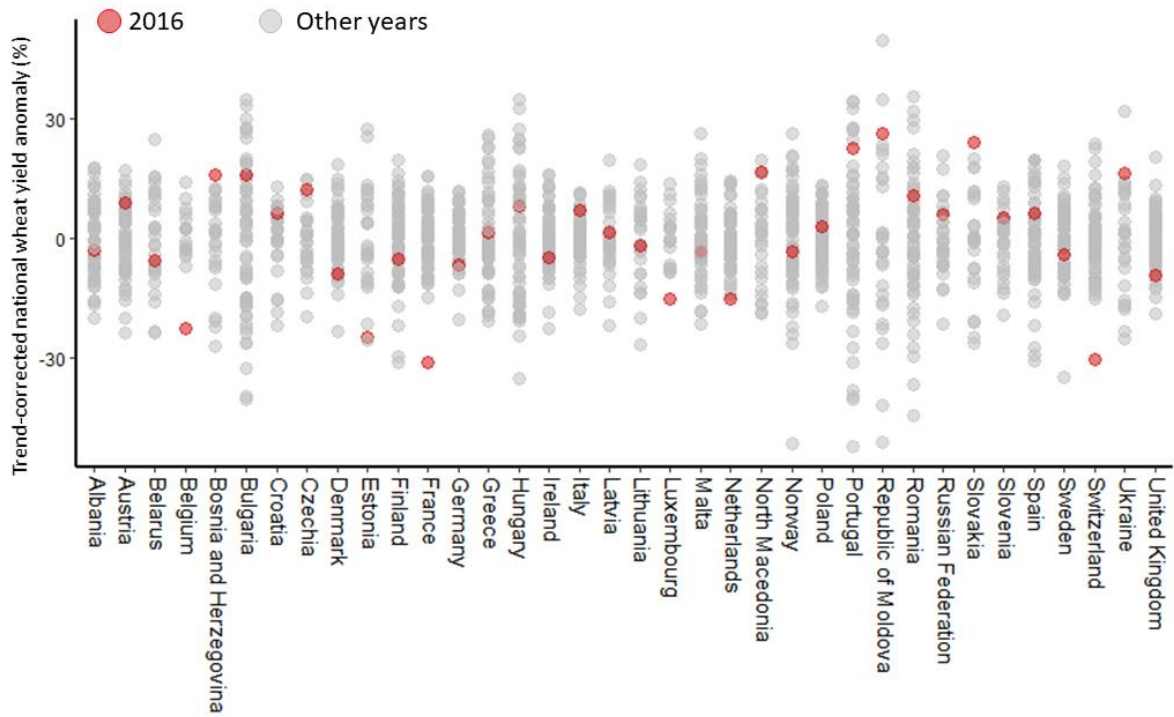


Figure S25. Trend-corrected national wheat yield across Europe for the period 1960-2019. Values in the 2015/16 trend-corrected wheat yield are presented as red dots.

3.1 Supplementary methods

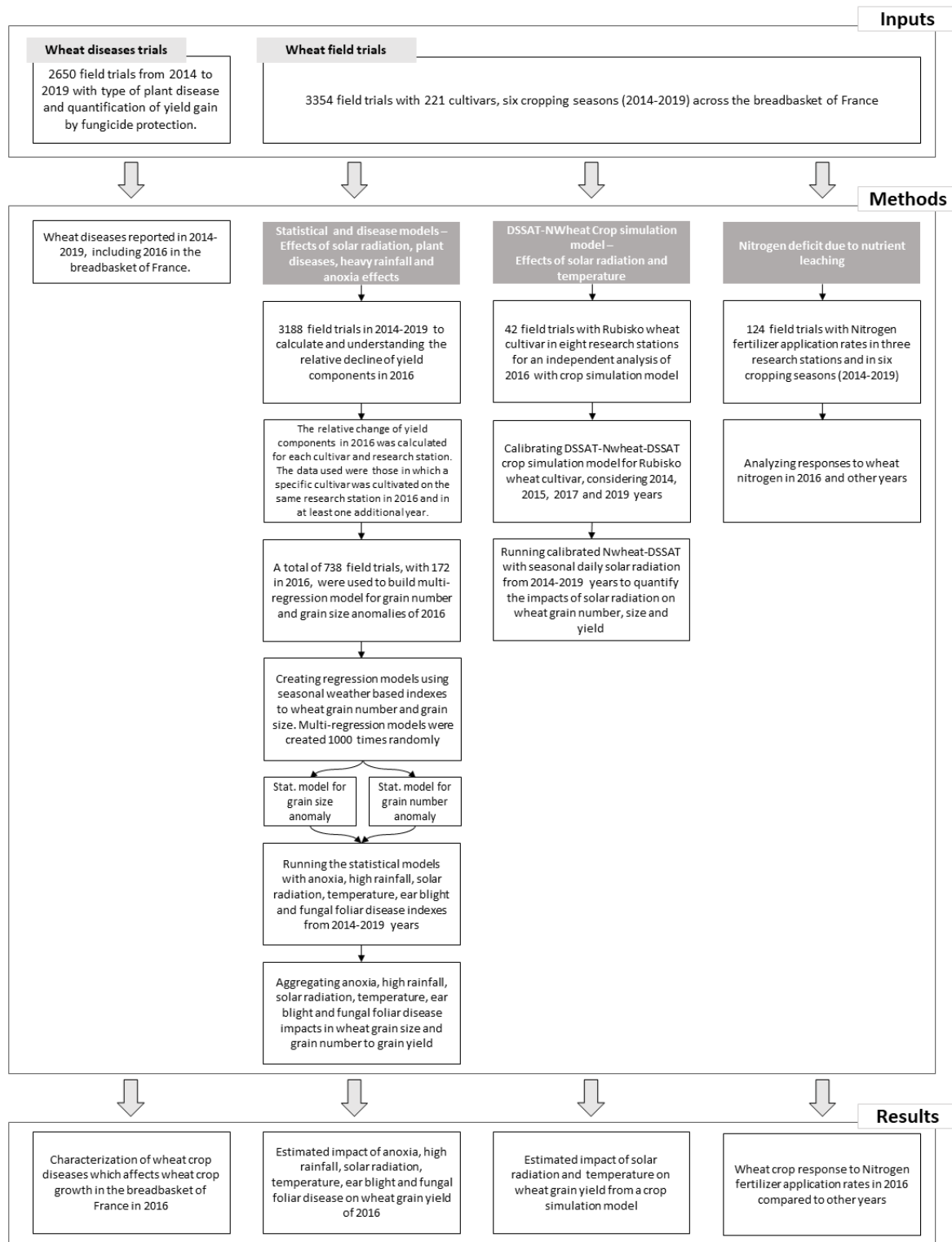


Figure S26. Flowchart of the procedures for quantifying the extreme low wheat yield of 2016 in France.

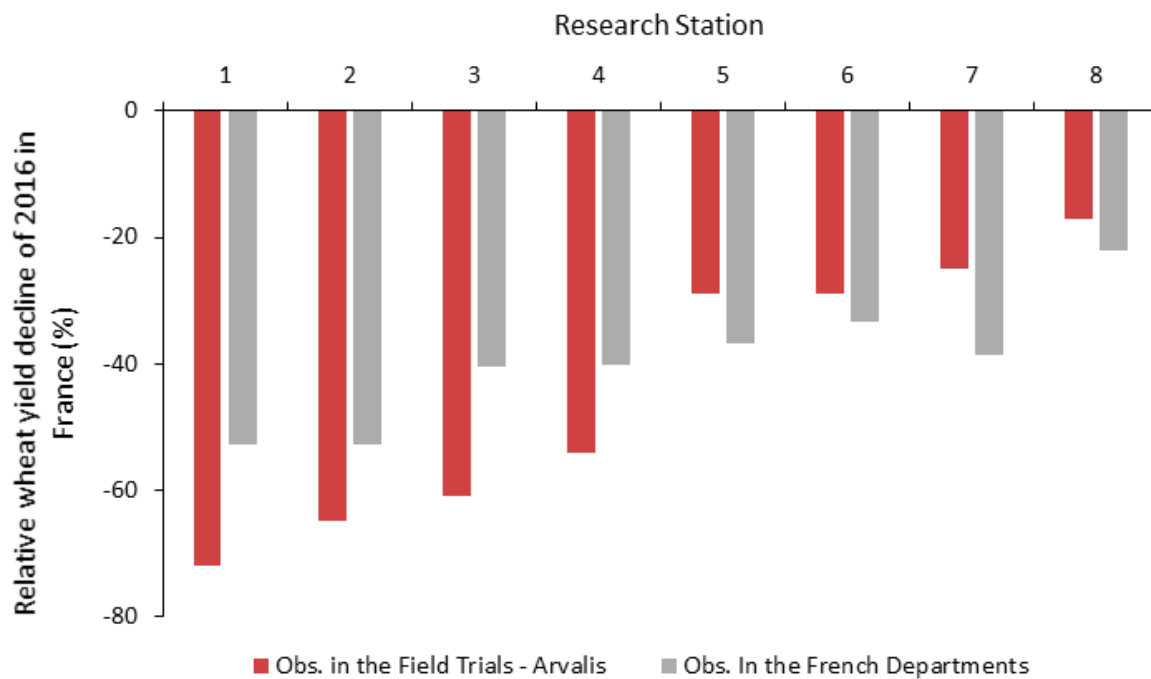


Figure S27. Comparison between observed relative wheat yield anomalies of 2016 calculated based on the Arvalis’ field trials (red) and the yield anomalies observed in the French departments (gray). The reference period for both relative wheat yield decline calculation is 2014-2019. Observed winter wheat yield anomaly for the French departments (administrative units known in France as *départements* at NUTS1 spatial scale) were calculated from observed wheat yield collected from the French Ministry of Agriculture official survey data (Agreste, 2022). The French Ministry of Agriculture provides seasonal wheat yield data for all departments that cultivate wheat.

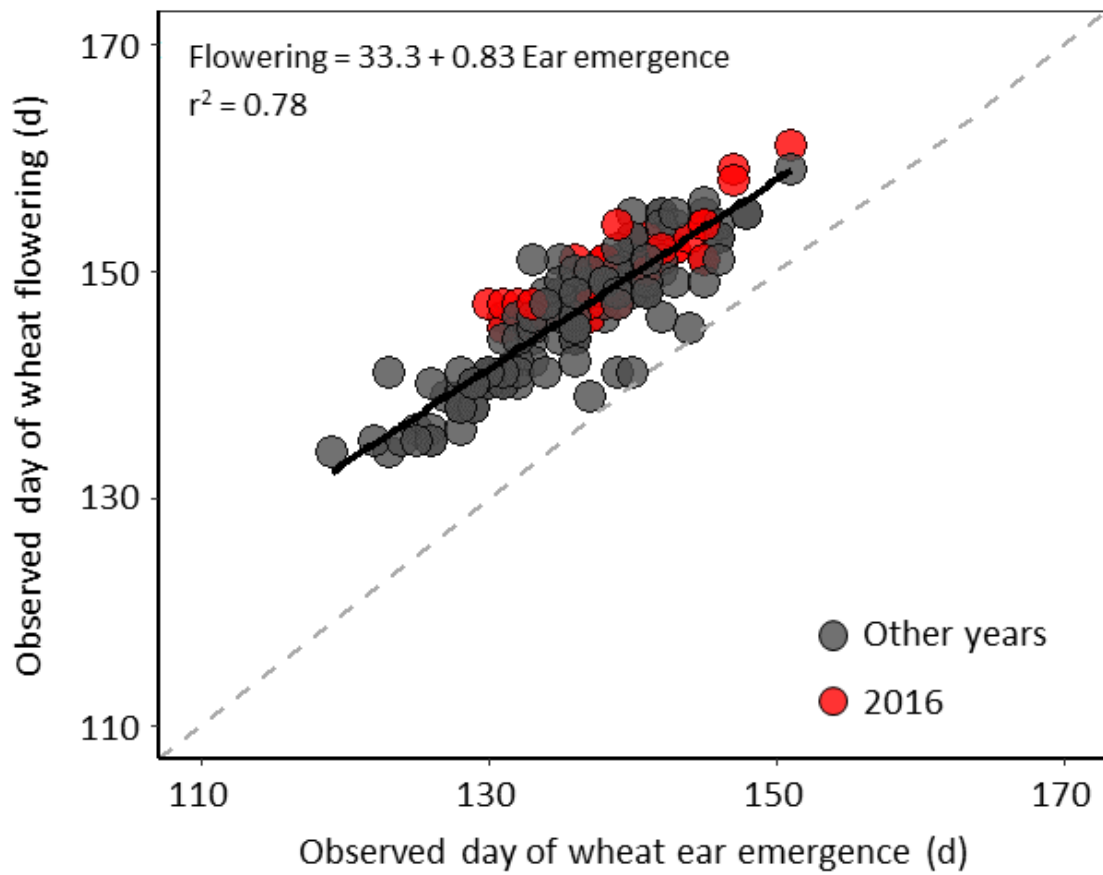


Figure S28. Estimating wheat anthesis day from wheat ear emergence day. The observed days are presented in day of the year (d), where January 1st is the day 1.

Variables selected to compose the statistical model					Model output	Impact of variables
V1 (e.g. S. radiation)	V2 (e.g. P. disease)	V3 (e.g. Rainfall)	V4 (e.g. Anoxia)	... Vx (e.g. F. Disease)	Estimated R1 (e.g. Grain yield)	Estimated Impact
V1 in 2016	V2 in 2016	V3 in 2016	V4 in 2016	Vx in 2016	R1 in 2016	
V1 in 2016	V2 in 2016	V3 in 2016	V4 in 2016	Vx in ref. period	R2	R2 – R1 (Impact of variable Vx)
V1 in 2016	V2 in 2016	V3 in 2016	V4 in ref. period	Vx in 2016	R3	R3 – R1 (Impact of variable V4)
V1 in 2016	V2 in 2016	V3 in ref. period	V4 in 2016	Vx in 2016	R4	R4 – R1 (Impact of variable V3)
V1 in 2016	V2 in ref. period	V3 in 2016	V4 in 2016	Vx in 2016	R5	R5 – R1 (Impact of variable V2)
V1 in ref. period	V2 in 2016	V3 in 2016	V4 in 2016	Vx in 2016	R6	R6 – R1 (Impact of variable V1)

Figure S29. Schematic representation of the procedure to compute the impacts of individual yield limiting factors in 2016. The letter ‘V’ represents the explanatory variables selected by Step Variable selector method. In addition, the letter ‘R’ represents the estimated model output (result) from the statistical model.

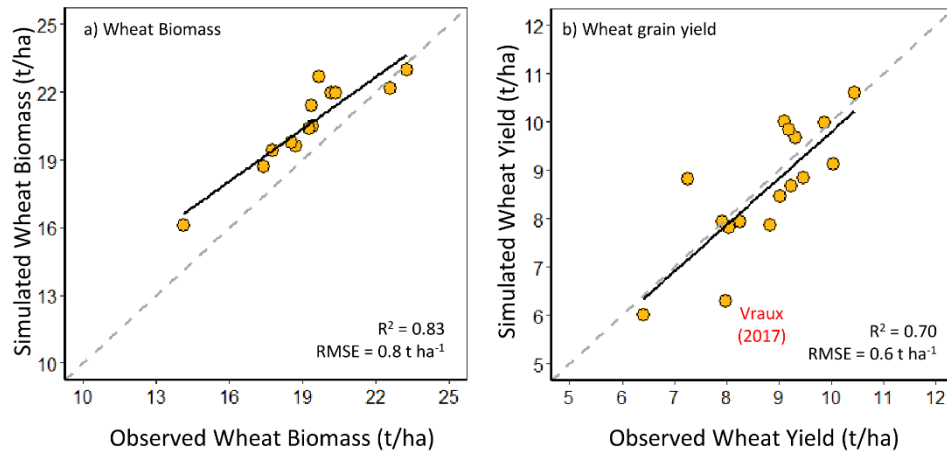


Figure S30. Calibration of NWHEAT crop simulation model. Relationship between observed and simulated wheat (a) biomass at maturity and (b) grain yield in France. Calibration with data from 2014, 2015, 2017 and 2019 years and cultivar Rubisko. In 2017 at Vraux the model simulated a reduction of grain yield due to water stress.

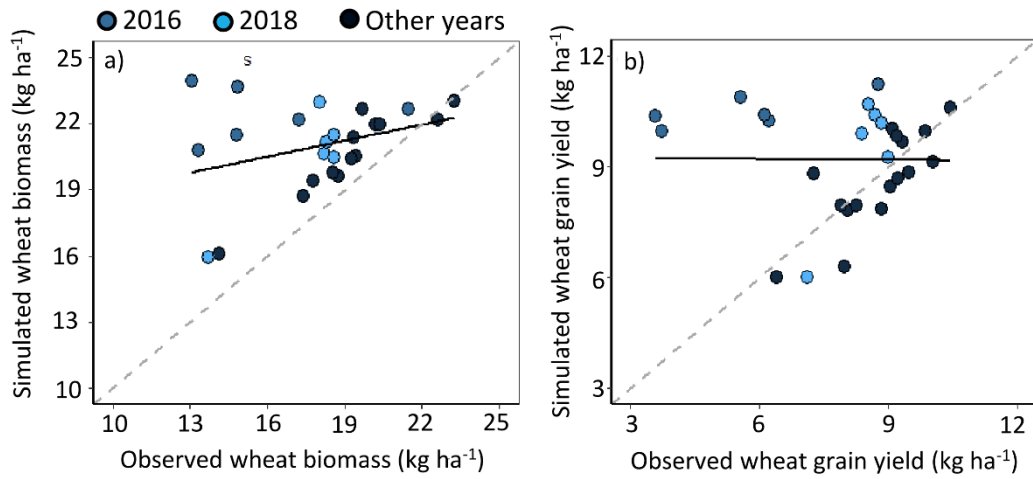


Figure S31. NWHEAT crop simulation for 2014-2019 years, including 2016 and 2016. Relationship between observed and simulated wheat for (a) biomass at maturity and (b) grain yield in France. Observed data are for cultivar Rubisko.

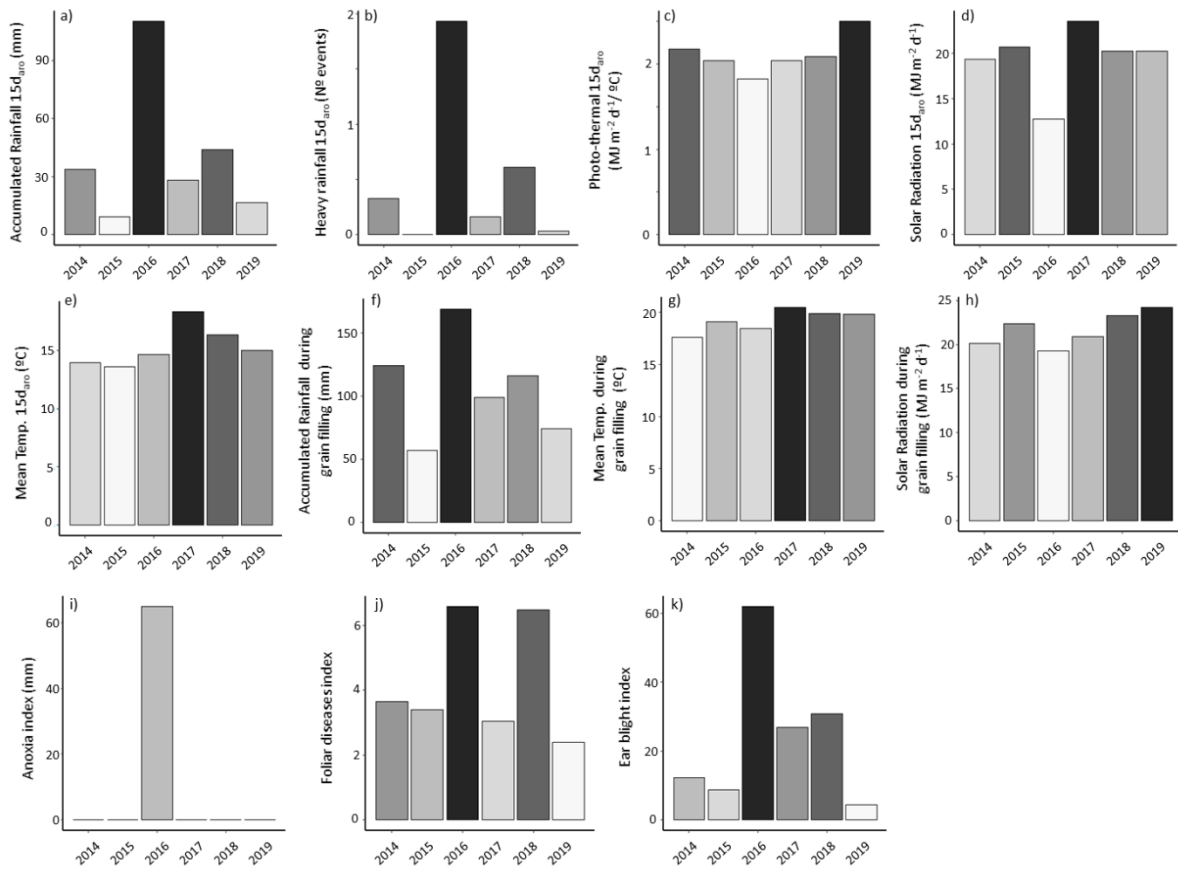


Figure S32. Average values of the weather based index for plant disease and weather from 2014 to 2019 in the breadbasket of France. The average values are from the eight research station selected in the study. The indices definitions and calculations are presented in Supplementary Tables S2 and S3.

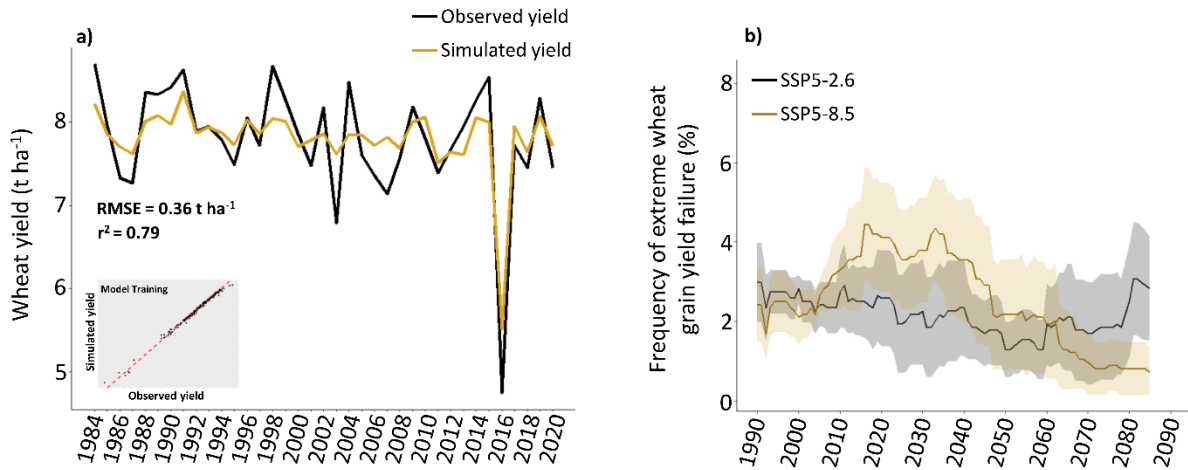


Figure S33. Projected frequency of extreme low wheat yield years in the breadbasket of France. (a) Inter-annual variability from 1984–2020 of observed (black lines) and estimated (yellow lines) wheat trend corrected yield of the breadbasket of France. Estimated results are from a LOOCV validation leaving all years from a location out of the training set. Inset in (a) shows the training set results. Statistical model for wheat yield was built with the same features used for simulate wheat grain number per unit area (features are shown in Supplementary Table S2) and for average grain size (Supplementary Table S3). For this analysis, there was no separation between grain number per unit area and average grain size (as in Fig 3 and 4) so all features were made available to the statistical model to directly simulate trend-corrected wheat yield. (b) Estimated 30 years running mean frequency of extreme low wheat yield under SSP5-2.6 (black trace) and SSP5-8.5 (red trace) from 1990 to 2085 for the breadbasket of France. Lines are ensemble means based on five CMIP6 GCMs (lines) and shading shows ± 1 s.e. These projections consider a fixed wheat anthesis on 1st June. Statistical model in (a) and CMIP6 GCMs for SSP5-2.6 and SSP5-8.5 in (b) data are an average of the following eight research stations: 1, Égreville; 2, Chevry; 3, Saint-Quentin; 4, Saint-Florent; 5, Fagnières; 6, Issoudun; 7, Barbarey-Saint-Sulpice; and 8, Rots.

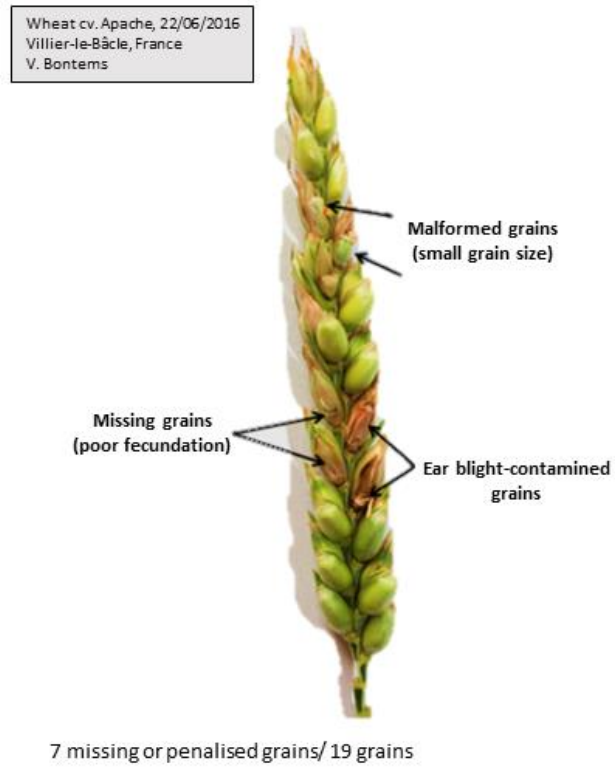


Figure S34. Representative wheat ear from 2016 cropping season from Villier-le-Bâcle, France.

References

- Asseng, S., Foster, I., & Turner, N. C. (2011). The impact of temperature variability on wheat yields. *Global Change Biology*, 17(2), 997–1012. <https://doi.org/https://doi.org/10.1111/j.1365-2486.2010.02262.x>
- Beillouin, D., Schauburger, B., Bastos, A., Ciais, P., & Makowski, D. (2020). Impact of extreme weather conditions on European crop production in 2018. *Philosophical Transactions of the Royal Society B: Biological Sciences*, 375(1810), 20190510. <https://doi.org/10.1098/rstb.2019.0510>
- Ben-Ari, T., Boé, J., Ciais, P., Lecerf, R., Van der Velde, M., & Makowski, D. (2018). Causes and implications of the unforeseen 2016 extreme yield loss in the breadbasket of France. *Nature Communications*, 9(1), 1627. <https://doi.org/10.1038/s41467-018-04087-x>
- Calderini, D. F., Castillo, F. M., Arenas-M, A., Molero, G., Reynolds, M. P., Craze, M., Bowden, S., Milner, M. J., Wallington, E. J., Dowle, A., Gomez, L. D., & McQueen-Mason, S. J. (2021). Overcoming the trade-off between grain weight and number in wheat by the ectopic expression of expansin in developing seeds leads to increased yield potential. *New Phytologist*, 230(2), 629–640. <https://doi.org/https://doi.org/10.1111/nph.17048>
- Chaloner, T. M., Fones, H. N., Varma, V., Bebbler, D. P., & Gurr, S. J. (2019). A new mechanistic model of weather-dependent Septoria tritici blotch disease risk. *Philosophical Transactions of the Royal Society B: Biological Sciences*, 374(1775), 20180266. <https://doi.org/10.1098/rstb.2018.0266>
- El Jarroudi, M., Kouadio, L., Bock, C. H., El Jarroudi, M., Junk, J., Pasquali, M., Maraite, H., & Delfosse, P. (2016). A Threshold-Based Weather Model for Predicting Stripe Rust Infection in Winter Wheat. *Plant Disease*, 101(5), 693–703. <https://doi.org/10.1094/PDIS-12-16-1766-RE>
- Fischer, R. A. (1985). Number of kernels in wheat crops and the influence of solar radiation and temperature. *The Journal of Agricultural Science*, 105(2), 447–461. <https://doi.org/DOI:10.1017/S0021859600056495>
- Fischer, Ralph A. (2009). Farming Systems of Australia. In *Crop Physiology* (pp. 22–54). Elsevier. <https://doi.org/10.1016/B978-0-12-374431-9.00002-5>
- Hoogenboom, G., Porter, C. H., Boote, K. J., Shelia, V., Wilkens, P. W., Singh, U., White, J. W., Asseng, S., Lizaso, J. I., Moreno, L. P., Pavan, W., Ogoshi, R., Hunt, L. A., Tsuji, G. Y., & Jones, J. W. (2019). The DSSAT crop modeling ecosystem. In K. J. Boote (Ed.), *Advances in crop modelling for a sustainable agriculture* (pp. 173–216). Burleigh Dodds Science Publishing. <https://doi.org/10.1201/9780429266591>
- Hossain, M. A., Araki, H., & Takahashi, T. (2011). Poor grain filling induced by waterlogging is similar to that in abnormal early ripening in wheat in Western Japan. *Field Crops Research*, 123(2), 100–108. <https://doi.org/https://doi.org/10.1016/j.fcr.2011.05.005>
- Kassie, B. T., Asseng, S., Porter, C. H., & Royce, F. S. (2016). Performance of DSSAT-Nwheat across a wide range of current and future growing conditions. *European Journal of Agronomy*, 81, 27–36. <https://doi.org/10.1016/j.eja.2016.08.012>
- Li, Y., Guan, K., Schnitkey, G. D., DeLucia, E., & Peng, B. (2019). Excessive rainfall leads to maize yield loss of a comparable magnitude to extreme drought in the United States. *Global Change Biology*, 25(7), 2325–2337. <https://doi.org/https://doi.org/10.1111/gcb.14628>
- Madgwick, J. W., West, J. S., White, R. P., Semenov, M. A., Townsend, J. A., Turner, J. A., & Fitt, B. D. L. (2011). Impacts of climate change on wheat anthesis and fusarium ear blight in the UK. *European Journal of Plant Pathology*, 130(1), 117–131. <https://doi.org/10.1007/s10658-010-9739-1>
- Mäkinen, H., Kaseva, J., Trnka, M., Balek, J., Kersebaum, K. C., Nendel, C., Gobin, A., Olesen, J. E., Bindi, M., Ferrise, R., Moriondo, M., Rodríguez, A., Ruiz-Ramos, M., Takáč, J., Bezák, P., Ventrella, D., Ruget, F., Capellades, G., & Kahiluoto, H. (2018). Sensitivity of European wheat to extreme weather. *Field Crops Research*, 222, 209–217. <https://doi.org/https://doi.org/10.1016/j.fcr.2017.11.008>
- Moravec, V., Markonis, Y., Rakovec, O., Svoboda, M., Trnka, M., Kumar, R., & Hanel, M. (2021). Europe under multi-year droughts: how severe was the 2014–2018 drought period? *Environmental*

- Research Letters*, 16(3), 34062. <https://doi.org/10.1088/1748-9326/abe828>
- Rivera-Amado, C., Molero, G., Trujillo-Negrellos, E., Reynolds, M., & Foulkes, J. (2020). Estimating Organ Contribution to Grain Filling and Potential for Source Upregulation in Wheat Cultivars with a Contrasting Source–Sink Balance. In *Agronomy* (Vol. 10, Issue 10). <https://doi.org/10.3390/agronomy10101527>
- Schierenbeck, M., Fleitas, M. C., Cortese, F., Golik, S. I., & Simón, M. R. (2019). Nitrogen accumulation in grains, remobilization and post-anthesis uptake under tan spot and leaf rust infections on wheat. *Field Crops Research*, 235, 27–37. <https://doi.org/https://doi.org/10.1016/j.fcr.2019.02.016>
- Slafer, G. A., Elia, M., Savin, R., García, G. A., Terrile, I. I., Ferrante, A., Miralles, D. J., & González, F. G. (2015). Fruiting efficiency: an alternative trait to further rise wheat yield. *Food and Energy Security*, 4(2), 92–109. <https://doi.org/https://doi.org/10.1002/fes3.59>
- te Beest, D. E., Shaw, M. W., Pietravalle, S., & van den Bosch, F. (2009). A predictive model for early-warning of Septoria leaf blotch on winter wheat. *European Journal of Plant Pathology*, 124(3), 413–425. <https://doi.org/10.1007/s10658-009-9428-0>
- Team, P. P. (2021). *The POWER Project*. NASA Prediction of Worldwide Energy Resources. <https://power.larc.nasa.gov/>
- van der Velde, M., Lecerf, R., d’Andrimont, R., & Ben-Ari, T. (2020). *Chapter 8 - Assessing the France 2016 extreme wheat production loss—Evaluating our operational capacity to predict complex compound events* (J. Sillmann, S. Sippel, & S. B. T.-C. E. and T. I. for I. and R. A. Russo (eds.); pp. 139–158). Elsevier. <https://doi.org/https://doi.org/10.1016/B978-0-12-814895-2.00009-4>
- van der Velde, M., Tubiello, F. N., Vrieling, A., & Bouraoui, F. (2012). Impacts of extreme weather on wheat and maize in France: evaluating regional crop simulations against observed data. *Climatic Change*, 113(3), 751–765. <https://doi.org/10.1007/s10584-011-0368-2>
- Webber, H., Lischeid, G., Sommer, M., Finger, R., Nendel, C., Gaiser, T., & Ewert, F. (2020). No perfect storm for crop yield failure in Germany. *Environmental Research Letters*, 15(10), 104012. <https://doi.org/10.1088/1748-9326/aba2a4>
- West, J. S., Holdgate, S., Townsend, J. A., Edwards, S. G., Jennings, P., & Fitt, B. D. L. (2012). Impacts of changing climate and agronomic factors on fusarium ear blight of wheat in the UK. *Fungal Ecology*, 5(1), 53–61. <https://doi.org/https://doi.org/10.1016/j.funeco.2011.03.003>
- Xu, X. (2003). *Effects of environmental conditions on the development of Fusarium ear blight BT - Epidemiology of Mycotoxin Producing Fungi: Under the aegis of COST Action 835 ‘Agriculturally Important Toxigenic Fungi 1998–2003’, EU project (QLK 1-CT-1998–01380)* (X. Xu, J. A. Bailey, & B. M. Cooke (eds.); pp. 683–689). Springer Netherlands. https://doi.org/10.1007/978-94-017-1452-5_3

Past and future wheat yield losses in France

Rogério de S. Nória Júnior¹, Pierre Martre², Jean-Charles Deswarte³, Jean-Pierre Cohan⁴, Marijn Van der Velde⁵, Heidi Webber^{6,7}, Frank Ewert^{6,8}, Alex C. Ruane⁹, Tamara Ben-Ari¹⁰, Senthold Asseng^{1*}

¹Technical University of Munich, Department of Life Science Engineering, Freising, Germany

²LEPSE, Univ Montpellier, INRAE, Institut Agro Montpellier, Montpellier, France

³ARVALIS - Institut du Végétal, Villiers-le-Bâcle, France

⁴ARVALIS - Institut du Végétal, Loireauxence, France

⁵European Commission, Joint Research Centre, Ispra, Italy

⁶Leibniz-Centre for Agricultural Landscape Research (ZALF), Müncheberg, Germany

⁷Brandenburg Technical University (BTU), Cottbus, Germany

⁸Crop Science Group, INRES, University of Bonn, Bonn, Germany

⁹NASA Goddard Institute for Space Studies, New York, NY, USA

¹⁰Centre International de Recherche sur l'Environnement et le Développement, Nogent-sur-Marne, France

*Corresponding author: senthold.asseng@tum.de

ABSTRACT

In recent decades, compounding weather extremes and plant diseases have been influencing increased wheat yield variability in France, the largest wheat producer in the European Union. How these might affect future wheat production remains unclear. Based on department wheat yields from the French government, disease, and climate indices from 1984 to 2020 in France, we combined an existing disease model with machine learning algorithms to estimate grain yields. This approach was able to explain around 60% of historical yield variability. Extreme low wheat yields will continue to occur once every 10 years according to projections with five CMIP6 climate models. While flooding related losses are projected to be reduced by over 30%, losses associated with combined extreme drought and heat wave during anthesis, and grain filling will double. Disease damage from ear blight is projected to increase and cause 35% of the 700 kg ha⁻¹ total expected average wheat yield losses. French wheat production systems need to adapt to future droughts and heat waves while dealing with increased disease pressure.

Keywords: Compounding factors; extreme weather; machine learning; plant diseases.

1. Introduction

Climate change may cause increased year-to-year wheat yield variability in many regions around the world (Bezner Kerr et al., 2022; Gaupp et al., 2020; Liu et al., 2021; Schaubberger et al., 2018). Extreme lows of wheat yield, which is usually defined as yields below the 10th percentile of historical period (with 20 years or more) (Guarin et al., 2020; Seneviratne et al., 2012), is also expected to occur more often (Nóia Júnior et al., 2021; Trnka et al., 2014). This could increase global food insecurity.

France accounts for 10% of the world's wheat exports (FAO stat, 2022), and extreme lows of national wheat production have occurred in the past due to adverse climate events (Ben-Ari et al., 2018; van der Velde et al., 2012). In the summer of 2003, France was hit by an unprecedented and prolonged heatwave. This event caused wheat production losses of 17%, or 7 million metric tons (Mt), compared to the previous five year average and left France with its worst wheat harvest since 1960 at this time (Ciais et al., 2005; FAO stat, 2022). Drought and heatwaves were the main causes of other historical crop failures in France and Europe in 2007 and 2018 (Beillouin et al., 2020; Schaubberger et al., 2021; Webber et al., 2020; Zhu et al., 2021), and most recently in 2022, lowering wheat yield by 5% compared to the previous five years average (Baruth et al., 2022). Many studies have quantified the past and potential future impacts of heatwaves and droughts on wheat production across the world (Asseng et al., 2011; Battisti and Naylor, 2009; Lobell et al., 2011; Webber et al., 2020, 2018). On average, regional heatwaves and droughts have reduced national wheat yield by 4% and 7% from 1964 to 2007, respectively (Lesk et al., 2016). Global wheat production is expected to fall by 6% for each 1°C of average temperature increase when CO₂ fertilization effects are not accounted for (Asseng et al., 2015; Liu et al., 2016).

Agricultural risk assessment studies typically only consider one climatic driver at a time and neglect the crop diseases, potentially leading to optimistic assessments as interacting climate and diseases risks are not taken into account (Raymond et al., 2020; Ruane et al., 2022; Zscheischler et al., 2018). Recent national wheat production failures are linked to compound events, involving the co-occurrence of multiple climate extremes and crop diseases, such as in Russia in 2010 (Zscheischler et al., 2018), in France in 2016 (Ben-Ari et al., 2018) and in Europe in 2018 (Beillouin et al., 2020). In 2016, France was struck by an unprecedented sequence of compounding climate extremes with a warm, wet winter and an extended period of precipitation in the spring, which together led to simultaneous yield-reducing factors, including heavy rainfall, high incidence of crop diseases, low solar radiation and anoxia, affecting both grain set and grain filling (Ben-Ari et al., 2018). This mix of interacting climate risks in 2016 saw the national wheat yield of France drop by 25%, compared to the previous five years

average. This was the most extreme wheat yield decline in France since 1960, much more serious than 2003 cropping season (Figure 1) and causing a shortfall of approximately 2.3 billion \$USD in the country's trade balance (Simoes, 2022).

In France, year-to-year wheat yield variability has been driven by many different factors, such as droughts, heatwaves, heavy rainfall, flooding, low solar radiation, and plant diseases (van der Velde et al., 2020, 2012). These drivers affect wheat growth at different stages of development and through various mechanisms. Wheat grain yields are affected by both changes in grain number, which is determined from 30 days before to shortly after anthesis, and grain size which is mostly determined during grain filling. Most year-to-year wheat yield variability is determined in this period before wheat anthesis and until the end of grain filling (Mäkinen et al., 2018; Senapati et al., 2021).

The objective is to quantify the causes of historical wheat yield failures and to analyze how these drivers might affect future wheat production in the breadbasket of France. We use a novel combination of indices accounting for wheat plant diseases, heat, drought, flooding and low solar radiation at both anthesis and during grain filling together with a data-driven machine learning approach to explore the causes of year-to-year variability of wheat yield at a department scale over the past 37 years (1984-2020) in the breadbasket of France.

We extended the analysis based on long-term climate change scenarios for 2020-2100 to identify the main drivers of year-to-year wheat yield variability and project how often extreme lows of wheat yield will occur in the future under advancing climate change in France, provided wheat cropping area distribution production systems and sowing and harvesting dates remain unchanged.

2. Material and Methods

2.1. Sites, weather and wheat yield data

The breadbasket of France is a high wheat yielding region (average wheat yield of 7.4 t ha⁻¹ from 2011 to 2020), which extends over the north and accounts for around 70% of France's total wheat production (Figure 1a) (Ben-Ari et al., 2018). This region is influenced by a temperate climate without particularly dry and warm summers, classified as marine west coast climate type Cfb, according to Köppen-Geiger climatic zone (Peel et al., 2007).

Long term daily weather data (1984-2020) with maximum and minimum temperature, solar radiation and rainfall with a resolution of ½° x 5/8° global grid were used from the Prediction Of World-wide Energy Resources, NASA POWER (Team, 2021). Winter wheat yield data from 1984 to 2020 at

department (Nomenclature of Territorial Units for Statistics [NUTS]1) spatial scale were collected from the French Ministry of Agriculture official survey data (Agreste, 2022).

To represent the breadbasket of France, we selected eight locations representative of the variety of production conditions in the breadbasket of France. These locations were selected following the geographical distribution of research stations from the ARVALIS Institut du Végétal to represent the breadbasket of France, as also suggested by Nória Júnior et al (2023). Thus, the statistical models (described in the subsection 2.4) were based in 8 French locations and 36 years (288 points). From these points, we build the statistical points, correlating their wheat yield anomalies (described in subsection 2.2) from 1984 to 2020 at department spatial scale with climatic indices. We also analyzed the weather conditions in representative locations for the three extreme low yielding wheat cropping seasons of 1987, 2003 and 2016 in the breadbasket of France (Figure 1b), shown in results subsection 3.1.

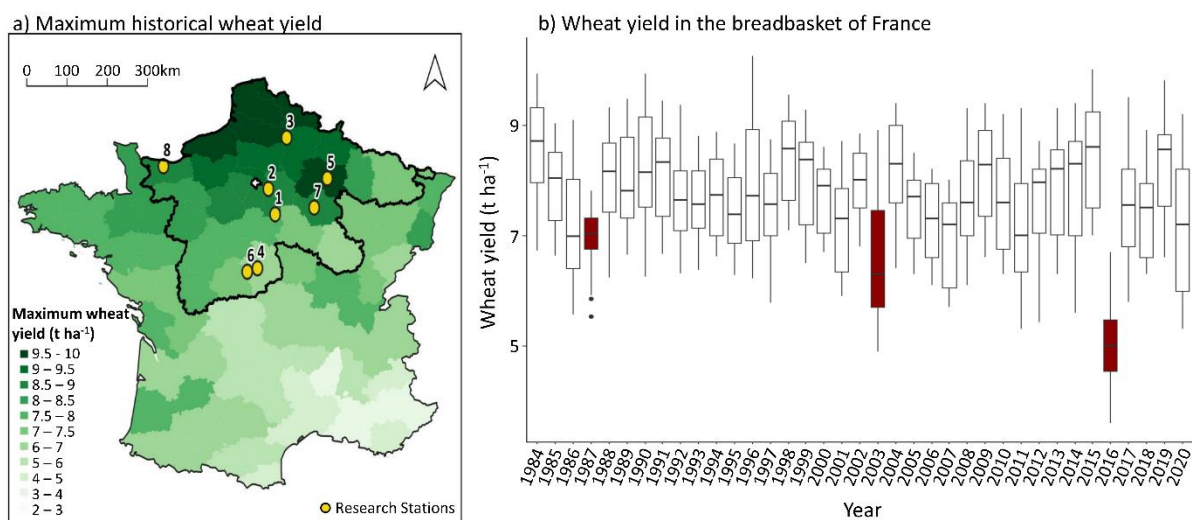


Figure 1. Spatio-temporal pattern of trend-corrected wheat yield in France. (a) Spatial distribution of the highest department level wheat yield observed from 2015 to 2020 (green background), and the studied locations ranked from 1 to 8 according to the magnitude of their wheat yield loss in 2016 (location 1 had the highest yield loss in 2016), in the following order: Égreville (1), Chevry-Cossigny (2), Saint-Quentin (3), Saint-Florent-sur-Cher (4), Fagnières (5), Issodun (6), Barbarey-Saint-Sulpice (7) and Rots (8). The breadbasket region of France is delineated with a bold black contour line. (b) Boxplot of the distribution of trend-corrected wheat yields in the breadbasket of France from 1984 to 2020. Low yielding anomalies in 1987, 2003, and 2016 are highlighted in dark red, which are in the 10th percentile of the historical observed wheat yield from 1984 to 2020. Geographical coordinates of the locations are shown in Supplementary Table S1.

2.2. Wheat yields relative anomaly

We removed wheat yield long-term trends in each department independently, to remove possible effects of technological improvements throughout the study period, as suggested by Guarin et al.

(2020). To remove the long-term trend, we estimated a linear slope through the historical wheat yield series from 1984 to 2000 to identify the average yield increase per year, as suggested by Ben-Ari et al. (2018). Wheat yield of each year from 1984 to 2000 is adjusted to 2000 yield levels by adding the slope for each year difference from 1984 until 2000. Wheat yield from 2001 to 2020 in France presented a plateau, with no positive or negative trend, with no trend correction needed. From the trend-corrected yield (Figure 1b) Yield anomalies (Y_{anm}) were then computed as the percent difference between observed yields (Y_{obs}) and average yields (Y_{avg} , average of the trend-corrected yields) divided by Y_{avg} :

$$Y_{anm}(i, t) = \frac{Y_{obs}(i, t) - Y_{avg}(t)}{Y_{avg}(t)} \times 100 \quad (1)$$

where i indicates the department and t , the harvest calendar year.

2.3. Extreme climate and plant diseases indices

Indices that drive wheat yield loss were identified from the literature (Ben-Ari et al., 2018; Nóia Júnior et al., 2021). We computed diseases indices for ear blight and foliar fungal and climate indices for heavy rainfall at anthesis and of extreme drought, heat, flooding, and low solar radiation for two key phenological stages: (i) wheat anthesis and (ii) grain filling. In total, we calculated 11 indices, being 9 indices for climate and 2 for crop diseases, all used as predictors in the statistical models. We assumed that wheat phenological stages were constant throughout the studied period from 1984 to 2020, with anthesis occurred on 1 June ± 15 days, and the grain filling period lasted from 1 June to 31 July. Current wheat cultivars are expected to have early anthesis and shorter grain filling period due to higher temperatures in future. Asseng et al. (2015) suggested a combination of delayed anthesis with increased grain filling rate as an adaptation for wheat to increased temperature. These traits could boost global wheat production by 7% (Asseng et al., 2019). Considering this, we kept the date of anthesis fixed, assuming that with increasing temperature cultivars with delayed anthesis with increased grain filling will be used in future as an adaptation to increased temperature. However, to reduce uncertainties regarding the fixed anthesis date, additional projection with wheat anthesis fixed on 15th May ± 15 days and grain filling from 15 May to 30 June was performed and results are presented in the Supplementary Fig S13-S21.

To compute drought and flooding indices, we calculate a water balance as the sum of daily rainfall (Rain) minus reference evapotranspiration (ET_o, from Hargreaves and Samani (1985)). Based on this water balance, we considered drought as the number of days during wheat anthesis and grain filling with daily accumulated (Rain – ET_o) < -50 mm. And flooding, as the number of days during wheat anthesis and grain filling in which daily accumulated (ET_o - Rain) > 90 mm. We also considered the

number of days with maximum temperature above 32 °C (heat index) (Nuttall et al., 2018), the number of days with solar radiation below 9 MJ m⁻² d⁻¹ (low solar radiation index), and the number of days with rainfall above 25 mm (heavy rainfall index) (Seneviratne et al., 2021). Extreme thresholds for drought and low solar radiation were defined as the 10th percentile of each climate index probability distribution (for the time baseline period of 1984-2020), considering all locations within the breadbasket region. Similarly, thresholds for flooding, and heat extremes were defined based on the 90th and 99th (for heavy rainfall and heat) percentile of the baseline period 1984-2020. For the thresholds of all indices, a sensitivity analysis was performed to ensure that these indices would cause wheat yield loss (as shown in Fig 4).

Ear blight or fusarium ear blight (*Fusarium graminearum*, *Fusarium culmorum*), usually infects wheat plants during anthesis under warm and humid conditions, and high rainfalls during anthesis. We computed an ear blight index based on the empirical model of Madgwick et al. (2011), as follows:

$$\text{Ear blight index} = 100 \frac{\exp(-15.3 + 0.941 T_{\text{mean}_{\text{May}}} + 0.069 \text{Rainfall}_{1\text{week-June}})}{1 + \exp(-15.3 + 0.941 T_{\text{mean}_{\text{May}}} + 0.069 \text{Rainfall}_{1\text{week-June}})}$$

Where: $T_{\text{mean}_{\text{May}}}$ is the mean temperature in May and $\text{Rainfall}_{1\text{week-June}}$ is the cumulative rainfall in the first week of June, when wheat anthesis occurs.

The survival of fall infection of winter wheat by fungal foliar diseases such as Septoria blotch (*Zymoseptoria tritici*) is favored by warm temperatures during the winter (Ben-Ari et al., 2018; Chaloner et al., 2019; te Beest et al., 2009). The development of these foliar fungal diseases then depends on wet environments, especially on rain in March and April (El Jarroudi et al., 2016). As such, we computed a fungal foliar diseases index based on a previously developed model by te Beest et al. (2009), as follow:

$$\text{Fungal foliar index} = 0.046 \text{Rain}_{(GS31-140) \rightarrow (GS31-30)} + 0.042 T_{\text{min}_{(GS31-140) \rightarrow (GS31-30)}} - 6.69 > 0$$

Where: $\text{Rain}_{(GS31-140) \rightarrow (GS31-30)}$ is the accumulated rainfall (mm) and $T_{\text{min}_{(GS31-140) \rightarrow (GS31-30)}}$ is the mean daily minimum temperature (°C) between 140 and 30 days before growth stage (GS) 31 (ear at 1 cm), fixed as 1st April.

2.4. Modeling wheat yield anomalies with random forest machine learning

A statistical model was developed for wheat yield anomalies using departments observations from 1984 to 2020, together with seasonal climate indices of drought, heat, flooding and low solar radiation

indices calculated around anthesis and during grain filling, as well as heavy rainfall around anthesis and ear blight and foliar fungal diseases indices. Simulated and observed wheat yield anomalies were multiplied by trend-corrected average wheat yield from 1984 to 2020 and converted to trend-corrected wheat yield (used to build the figures). A random forest machine learning approach was applied to identify the best combination of explanatory variables using the function `randomForest` of the R package 'randomForest' (R Core Team, 2017). Random forest was set with 500 trees, with 3 variables tried at each split. The set up of Random Forest followed sensitivity analyzes which indicated where the quality of the predictions plateaued (Supplementary Figure S2). To evaluate the predictive performance of the trend-corrected wheat yield model (or wheat yield model), a leave-one-out cross validation (LOOCV) was performed using the random forest with 7 of the 8 locations to select the best combination of inputs each year, and it was then tested on the excluded location. This process was repeated for each location for a total of 8 interactions. The relative root mean squared error of prediction ($rRMSEP$) (Wallach and Goffinet, 1987), the coefficient of determination (r^2) and the Nash-Sutcliffe model efficiency coefficient (NSE) (McCuen et al., 2006) were then calculated based on the estimated trend-corrected yield (henceforth called estimated wheat yield) at the tested location together with the corresponding observed yield. Statistical indices for model training, leaving one year out cross validation and leaving one location out cross validation are also shown in Supplementary Table S2.

2.5. Quantifying the impacts of individual yield limiting factors

To quantify the impacts of individual yield limiting factors, we used a random forest equation built for all locations during the training phases (Supplementary Table S2). The wheat yield model was executed by initially selecting the climate and plant diseases indices (derived from climate indices and plant disease model outputs) to simulate wheat yield in a target year (Supplementary Figure S1, target year is the cropping season in which losses caused by individual yield limiting factors were quantified, from 1984 to 2020). The models were executed again by modifying one explanatory variable value by replacing the target year value with the corresponding value for each of 1984-2020 (Supplementary Figure S1). This step was repeated, replacing the value of each input variable in turn. Thus, the contribution of each wheat yield limiting factor in each year of the period from 1984 to 2020 was calculated as the difference between the estimated trend-corrected yield from the models with all variables for a target year, and the estimates from the statistical models with all variables of the target year except one from the average of each year from 1984 to 2020 (excluding the target year), as schematically shown in the Supplementary Figure S1 (illustrating 2016 as the target year). This is

similar to the method proposed by Asseng et al. (2011) for separating the impacts of temperature from other factors on wheat yield.

2.6. Climate change scenarios and extreme low wheat yield definition

Daily climate data for the 1985-2100 period were drawn from the Inter-Sectoral Impacts Model Intercomparison Project (ISIMIP; (Lange, 2019)), which provides trend-preserving, bias-adjusted and spatially disaggregated climate model outputs from the Coupled Model Intercomparison Project phase 6 (CMIP6; (Eyring et al., 2016)). Before 2015, these are produced by climate models forced by historical trends of main natural and anthropogenic factors. After 2015, simulations follow the Shared Socioeconomic Pathway (SSP) and Representative Concentration Pathway (RCP) SSP1-2.6 and SSP5-8.5 (O'Neill et al., 2016). The IPCC describe SSP1-2.6 as a “low” and SSP5-8.5 as a “very high” greenhouse gas emissions scenario (IPCC, 2021; O'Neill et al., 2020). We considered five CMIP6 models (GFDL-ESM4, IPSL-CM6A-LR, MPI-ESM1-2-HR, MRI-ESM2-0 and UKESM1-0-LL) that include high, medium and low climate sensitivity models similar to the full CMIP6 distribution (IPCC, 2021), and we use it here to illustrate the bottom and upper tail of future risks. We considered five CMIP6 models (GFDL-ESM4, IPSL-CM6A-LR, MPI-ESM1-2-HR, MRI-ESM2-0 and UKESM1-0-LL) that include high, medium and low climate sensitivity models similar to the full CMIP6 distribution (Jägermeyr et al., 2021). We used daily weather data from the ISIMIP downscaled projections for the five selected models to quantify future frequency of drought, heat, flooding and low solar radiation occurrence both during wheat anthesis (with anthesis fixed on 1 June ± 15 days) and grain filling (from 1 June to 31 July), as well as heavy rainfall during anthesis. These indices together with the indices for ear blight and foliar fungal diseases previously described in subsection 2.1, allow us to estimate wheat grain yield and its losses. To reduce uncertainties regarding the fixed anthesis date, additional projection with wheat anthesis fixed on 15th May ± 15 days and grain filling from 15 May to 30 June was performed and results are presented in the Supplementary Fig S13-S21. Projections for extremely low wheat years frequency and future causes of wheat yield losses are shown as 30 years running mean (i.e. value shown for 2015 is the average from 1986 to 2015, and for 2016 the average from 1987 to 2016). We defined extreme low simulated yields as yields below the 10th percentile (Guarin et al., 2020; Seneviratne et al., 2012) of historical estimated wheat yield during 1984–2020, for each CMIP6 models separately.

3. Results

3.1. Extreme low wheat yield and weather conditions in the breadbasket of France

We analyzed the weather conditions in representative locations for the three extreme low yielding wheat cropping seasons of 1987, 2003 and 2016 in the breadbasket of France (Figure 2). Winter wheat in the breadbasket of France usually has a growing season of 10 months, sown in early October and harvested in late July.

In 1987, the mean temperature from January to March was 3°C below the historical mean temperature for the same period (Figure 2a). After the cold winter and a normal spring, the precipitation of June and July 1987 were more than twice the normal for these months. The average monthly solar radiation from May to July was up to 5 MJ m⁻² d⁻¹ (or 25%) lower than the average (1984-2020), when wheat grain filling occurs.

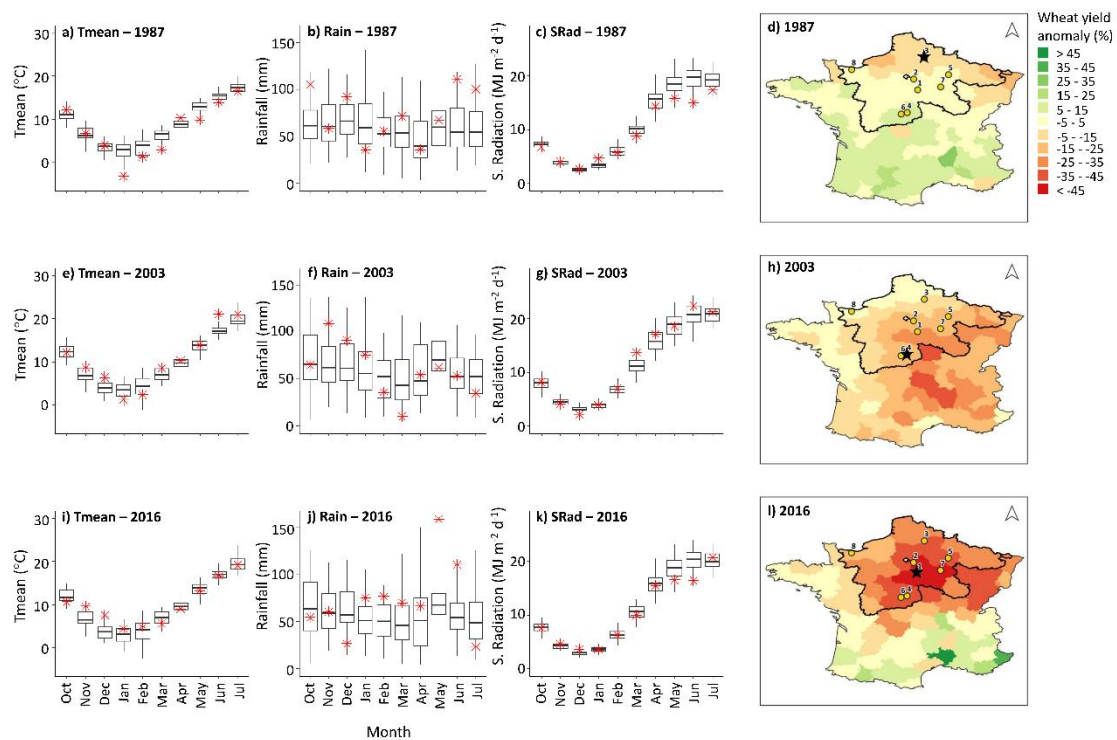


Figure 2. Extreme low yielding wheat cropping seasons in the breadbasket of France. Boxplots for monthly (a, e and i) mean air temperature, (b, f, and j) accumulated rainfall and (c, g, and k) average solar radiation in (a-c) Saint Quentin, (e-g) Saint-Florent and (i-k) Égreville. The red asterisks represent the monthly climatic variables in (a-c) 1987 in Saint Quentin, (e-g) Saint-Florent in 2003 and (i-k) Égreville in 2016. Spatial pattern of the observed wheat yield loss in (d) 1987, (h) 2007 and (l) 2016.

In 2003, the wheat cropping season started with a warm and wet winter, with rainfall in November about 50 mm above the historical average (1984-2020) to the month. Between February and March of 2003, rainfall was below the average, particularly in March with 10 mm of accumulated rainfall observed, or 20% of that expected. The accumulated rainfall was normal from April until July. The

mean temperature recorded in June was about 3°C higher than average, and the temperature remained high in July.

The wheat cropping season of 2016 started with a prolonged warm and wet winter, with warm temperature from November to January and high precipitation from January to April. The accumulated rainfall in May was three times greater than the monthly historical average, and it continued high in June. With the high rainfalls, the solar radiation was about 3 MJ m⁻² d⁻¹ lower than the historical average in May and June, during anthesis and early grain filling.

3.2. Modeling wheat yield in the breadbasket of France

We used wheat plant diseases for ear blight and foliar fungal diseases indices together with climatic indices for heat, drought, flooding, and solar radiation at both anthesis and grain filling with a random-forest machine learning approach to estimate historical wheat yield in eight locations across the breadbasket of France over 37 years, from 1984 to 2020. The *rRMSEp* between estimated and observed wheat yield, during the cross-validation analysis of the wheat yield model, varied from 5% to 8%. The *r*² varied from 0.11 to 0.84. The NSE varied from -2.7 to 0.40. For most of the locations, the cross-validation indicated that the random-forest machine learning for wheat yield showed a satisfactory precision (*r*² > 0.6), efficiency (NSE > 0) and small error (*rRMSEp* < 8%). However, in Rots in the northwestern France, the yield model performed poorly compared to the other locations, with *rRMSEp* of 8% and *r*² of 11%. Notably, the extremely low yield of 2016 was well captured by the model in all other locations, but not in Rots.

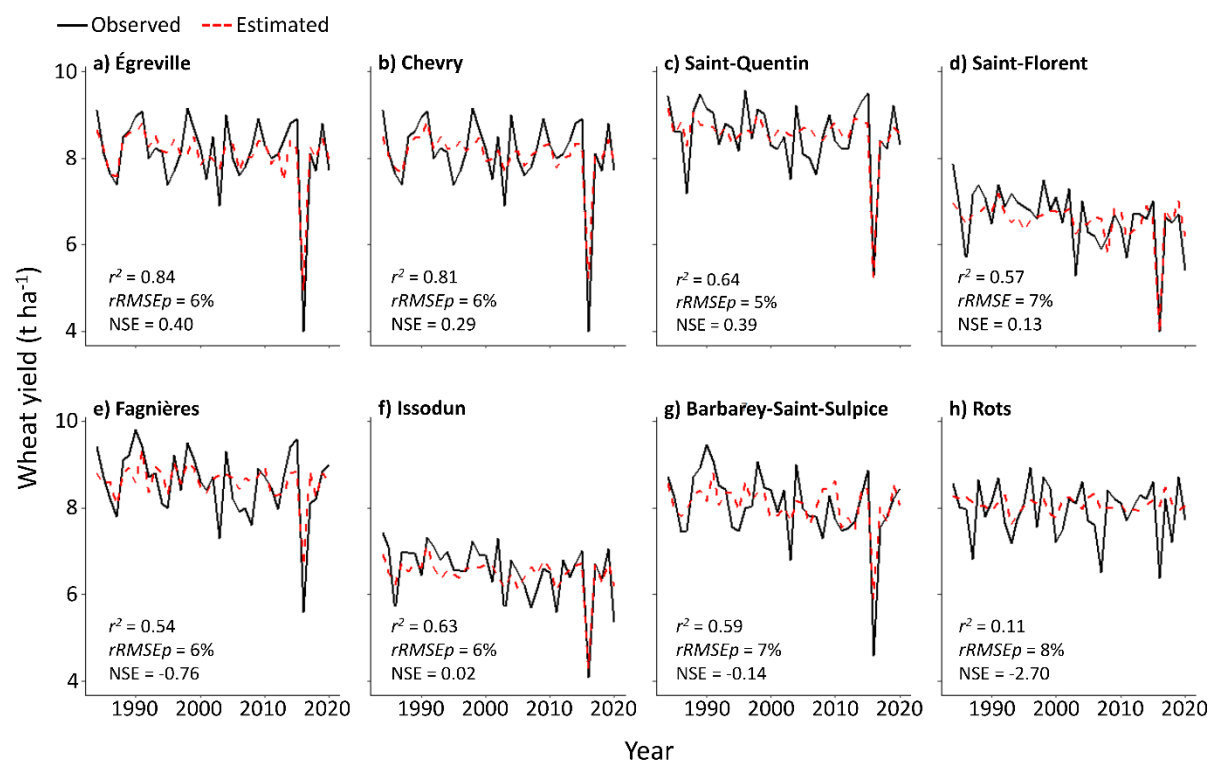


Figure 3. Estimated and observed trend corrected wheat yields in the breadbasket of France. Year-to-year variability from 1984 to 2020 of observed (black solid lines) and estimated (red dashed lines) wheat trend corrected yield at (a) Égreville, (b) Chevry-Cossigny, (c) Saint-Quentin, (d) Saint-Florent-sur-Cher, (e) Fagnières, (f) Issodun, (g) Barbarey-Saint-Sulpice, and (h) Rots. Estimated results are from a LOOCV validation leaving all years from a location out of the training set with a random forest machine learning approach. Training model results are shown in Supplementary Figure S3. Statistical indices for model training, leaving one year out cross validation and leaving one location out cross validation are shown in Supplementary Table S2. The relative root mean squared error of prediction ($rRMSEp$), coefficient of determination (r^2) and Nash-Sutcliffe model efficiency coefficient (NSE) are shown.

3.3. Quantified causes of wheat yield losses

Given the ability of the random-forest machine learning model to estimate wheat yield and wheat yields anomalies, we extended the analysis to quantify the contribution of a series of possible causes for wheat yield losses between 1984 and 2020 in the breadbasket region (Figure 4). The results indicate that the causes of the wheat yield decline of the 1987 and 2016 cropping season varied according to the location but were mainly caused by a combination of ear blight and fungal foliar diseases (causing seasonal wheat yield losses of up to 80%, Supplementary Fig S22), together with high rainfall around anthesis (up to 20%), low solar radiation (up to 75%) and flooding (up to 75%) during wheat grain filling. Heat and drought explained about a third of the wheat yield decline of 2003 and 2011 in Saint-Florent and Issodun (Figures 4d and 4f), in the south of the breadbasket region. In 2007 drought accounted for about 50% of the wheat yield decline in Égreville, Chevry and Fagnières (Figures 4a, 4b and 4e), in the center-east, and flooding accounted for 50 and 30% of the low yields in

Saint-Florent and Rots (Figures 4d and 4h), in the south and west of the breadbasket region, respectively.

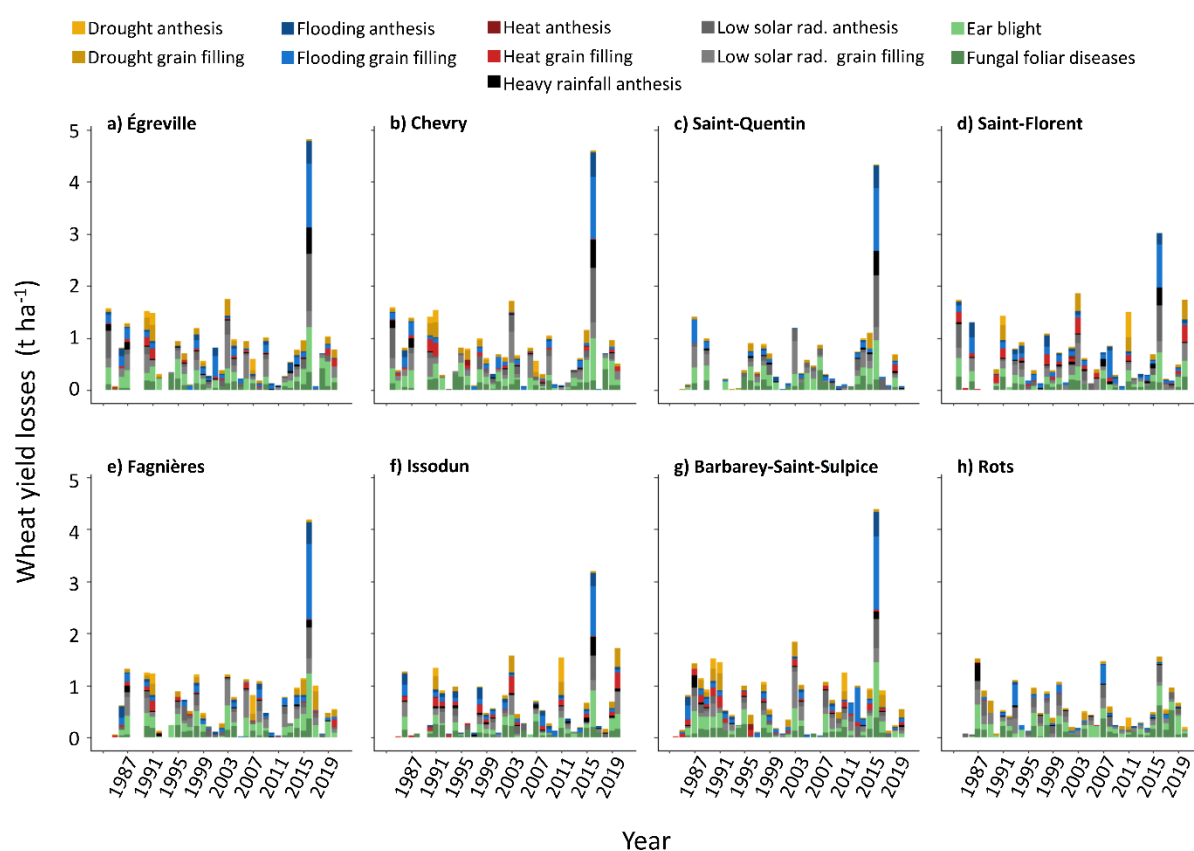


Figure 4. Decomposed wheat yield losses causes in the breadbasket of France. The yield losses are relative to the average of estimated trend-corrected wheat for 37 cropping seasons from 1984 to 2020 in each of the locations of (a) Égreville, (b) Chevry-Cossigny, (c) Saint-Quentin, (d) Saint-Florent-sur-Cher, (e) Fagnières, (f) Issodun, (g) Barbarey-Saint-Sulpice, and (h) Rots

3.4. Future frequency of extremely low wheat yield years

The future frequency of extremely low wheat yield years (that is yields below the 10th percentile of historical estimated wheat yield during 1984–2020) varies according to the climatic scenario (SSP5 2.6 or SSP5 8.5) and location in the breadbasket of France (Figure 5). For most of the locations, our results show no evidence for increased or decreased frequency of extreme low wheat yields by 2100. However, in Fagnières and in Rots the frequency of extreme low wheat yield years varies from the current 10% to more than 30% by the end of the century, with the SSP5-8.5. In Issodun, the frequency of extreme low wheat yield would drop from current 10% to 5% by 2100, in both SSP5 scenarios. These results are calculated considering a fixed wheat anthesis on 1st June, which is currently the case. However, more extreme low wheat yield years are expected to occur if the anthesis date is brought forward to May 15th (Supplementary Figure S13).

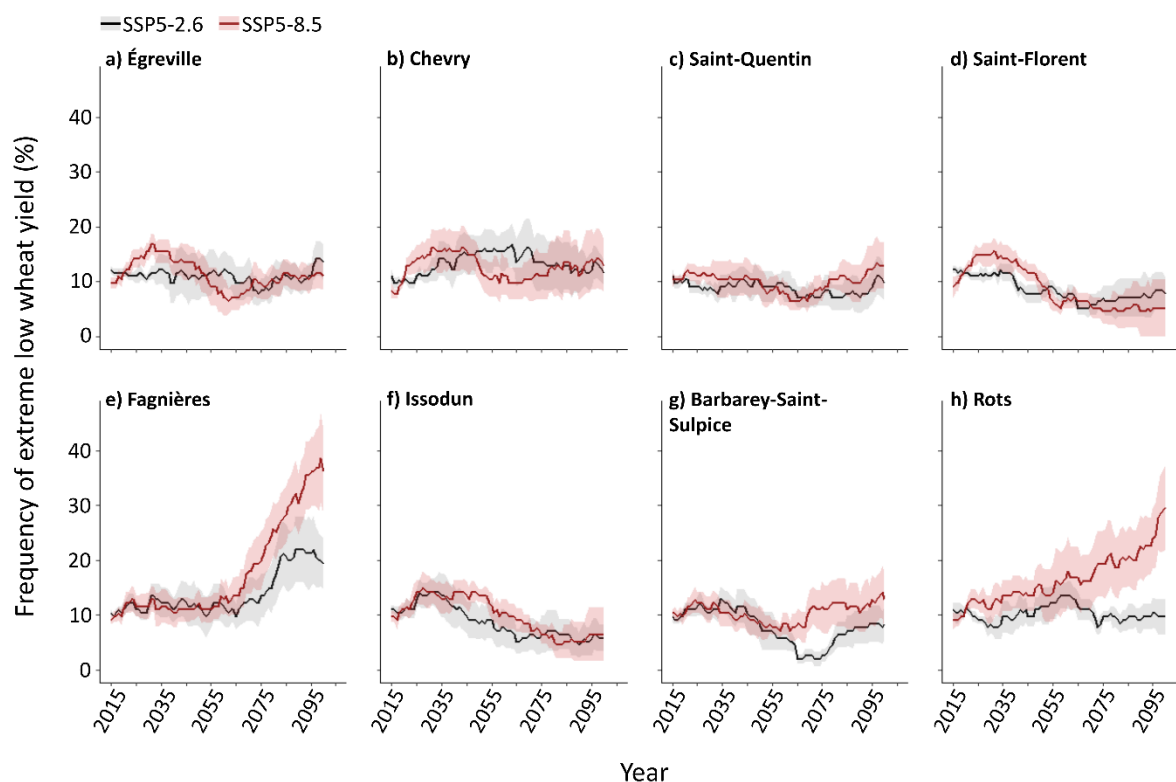


Figure 5. Projected frequency of extreme low wheat yield years in the breadbasket of France. Estimated 30 years running mean frequency of extreme low wheat production under SSP5-2.6 (black trace) and SSP5-8.5 (red trace) from 2015 to 2100, for (a) Égreville, (b) Chevry-Cossigny, (c) Saint-Quentin, (d) Saint-Florent-sur-Cher, (e) Fagnières, (f) Issodun, (g) Barbarey-Saint-Sulpice, and (h) Rots. Lines are ensemble means based on five CMIP6 GCMs (lines) and shading shows ± 1 s.e. These projections consider a fixed wheat anthesis on 1st June.

3.5. Future causes of wheat yield losses

Wheat yield in France is expected to change slightly in future with climate change (Supplementary Fig S5) but the causes of wheat yield losses in France are expected to change in France by 2100 (Figure 6). The wheat yield losses caused by flooding at both anthesis, and grain filling are expected to decrease by the end of the century. We estimate that flooding during grain filling currently causes an average loss of wheat yield of about 150 kg ha^{-1} per season, which may decrease to 100 kg ha^{-1} by the end of the century (Figure 6 and Supplementary Fig S9, each color in each bar in Figure 6 indicates an average 30 years running mean, with the year in each tick mark representing the average of the previous 30 years).

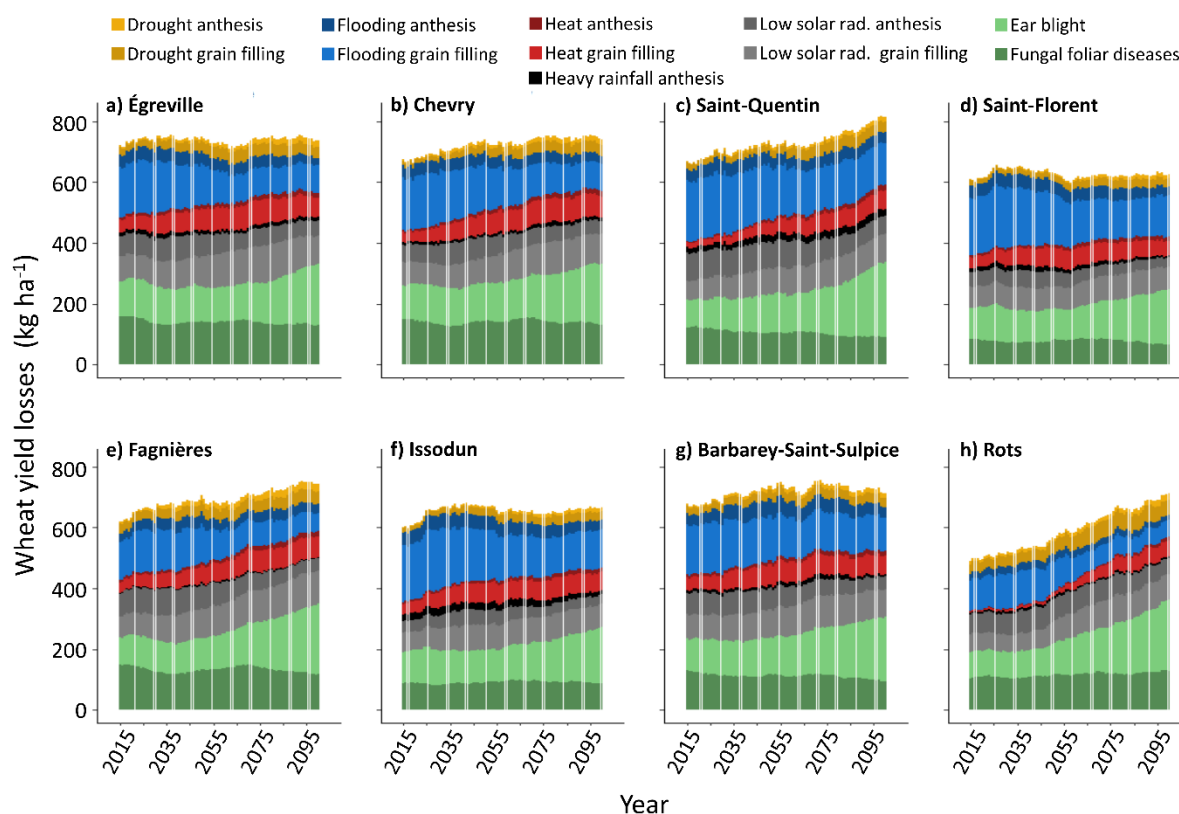


Figure 6. Future causes of wheat yield losses in the breadbasket of France. Projected 30 years running mean wheat yield losses causes from 2015 to 2100 for ((a) Égreville, (b) Chevry-Cossigny, (c) Saint-Quentin, (d) Saint-Florent-sur-Cher, (e) Fagnières, (f) Issodun, (g) Barbarey-Saint-Sulpice, and (h) Rots. Bars are ensemble means based on five bias-adjusted CMIP6 global climate models (GCMs) for SSP5-8.5, with a fixed wheat anthesis on 1st June and grain filling in June and July. Results for SSP5-2.6 are shown in Supplementary Figure S6, and for an early anthesis date (15th May) are shown in Supplementary Figure S14 and 15. Climate projections for monthly maximum and minimum temperature, solar radiation, and rainfall, are shown in Supplementary Figure S4. The projected wheat yield losses are relative to the average of estimated trend-corrected wheat from 2015 to 2100 in each of the locations.

Wheat yield losses by heat and drought are expected to double by the end of the century (Figure 6 and Supplementary Figures S7-S9). Wheat yield losses caused by heat during grain filling may increase from current average of 30 kg ha⁻¹ to up to 60 kg ha⁻¹ by 2100 (Figure 6 and Supplementary Figure S7). In addition to increased heat and drought, ear blight is projected to be the main cause of wheat yield losses in the future of French breadbasket, leading to an average of 35% of total wheat yield losses by 2100 (Figure 6). The projected yield losses by heavy rainfall during anthesis, fungal foliar diseases and low solar radiation fluctuate widely without a clear trend from 2015 to 2100 (Figure 6 and Supplementary Figure S10-S12). The causes of yield losses vary slightly with wheat anthesis date fixed on 15 May (Supplementary Figure S14-S21).

4. Discussion

To separate the historical and future impact of single climatic events on wheat in France, we combined department wheat yields, disease damage, climate indices, and existing disease models with machine learning algorithms for estimating grain yield changes. Our model presents similar performance ($rRMSEp$ varying from 5% to 8% from LOOCV one location out or from 8 to 12% from LOOCV one year out in Supplementary Table S2) in estimating wheat yield in France to other recent studies ($rRMSEp$ varying from 10% to 18% (Paudel et al., 2022)).

Projections with five CMIP6 climate models under low and very high emissions scenarios suggest that current extreme low wheat yields historically occurring once every 10 years, will occur with a somewhat similar frequency in the future. Other studies have also indicated no historical or future evidence for increased volatility of wheat production in most of France (Liu et al., 2019; Schauburger et al., 2021), with the exception of a few regions such as the northwest, as indicated here and by Pequeno et al. (2021). Yet, in France climate extremes can induce national wheat yield losses of one third, with some departments losing more than half the expected grain yield in some years. These events have consequences for France and other main wheat importing countries. Algeria, the main importer of French wheat, has recently stepped-up wheat exports from Russia after excessive rainfall affecting the quality of wheat of France in 2021 (Muftuoglu, 2021). While similar future frequency is expected for extremely low wheat yield events, the causes of wheat yield losses in France are expected to change by 2100.

Wheat production in France can be affected by excess water, causing flooding, reduced solar radiation and plant diseases. These factors historically caused more yield losses than droughts and high temperatures (Figure 6), as occurred in the 2016 cropping season (Ben-Ari et al., 2018; van der Velde et al., 2020). Excessive precipitation was found to be the main factor influencing wheat yields in France since the first half of the 20th Century (Ceglar et al., 2020), and drained areas account for 9% of all arable soils in France (Jeantet et al., 2021). However, due to the recent increased heat and drought events in spring and summer (as in 2003, 2007, 2011, 2020 and 2022), excess rainfall has already shown a lower correlation with wheat yield in the last two decades, compared to previous periods (Ceglar et al., 2020). Despite this, we indicated that heavy rainfall during anthesis fluctuate widely without a clear negative or positive trend from 2015 to 2100. And, extreme rainfall is projected to occur more frequently throughout the year at other wheat phenological stages (Fischer and Knutti, 2015). We emphasize that the water balance used here does not consider possible accumulations of water on the soil surface after heavy rains (due to the speed of infiltration of water into the soil, sometimes being lower than the intensity of the rain). This adds uncertainties to our projections.

Heat and drought, as well as ear blight, may become increasingly damaging to wheat yield in France (Figure 6). This is mostly due to the projected future increase of up to 3°C of maximum monthly mean temperature combined with a decrease in monthly precipitation during wheat flowering and grain filling during May to July (Supplementary Figure S4), further increasing heat and drought stress. These results are in agreement with previous climate change impact studies, which have largely focused on heat, with national wheat yield losses of -4.6% (varying from -4.2% to 5.2%) in France (Liu et al., 2016; Zhao et al., 2017). Summer droughts are expected to become 11 to 28 times more frequent in Europe, compared to current levels (Grillakis, 2019). In addition, winter and spring are expected to become warmer and wetter by the end of the century in the breadbasket of France (Supplementary Figure S4) (Ben-Ari et al., 2018; Ranasinghe et al., 2021), which contributes to wheat ear blight infection spread (Madgwick et al., 2011; West et al., 2012; Xu, 2003). Ear blight is related to rainfall during anthesis and temperature during the preceding weeks (Madgwick et al., 2011). We project that ear blight will cause twice as much wheat yield losses than currently (Figure 6), even if the wheat anthesis date moves forward to mid-May (Supplementary Figure S13 and Figure S21). The incidence of ear blight in wheat is also projected to double by 2050 in southern England, a region with similar edaphoclimatic conditions to the breadbasket in France (Madgwick et al., 2011). Yet, the ear blight model here used does not consider the initial inoculum but correlates it to the high temperatures at spring as stimulants for its increased incidence. Although the initial inoculum benefits from high temperatures (Madgwick et al., 2011), factors such as the pre-crop in rotation with wheat (which also affects the initial inoculum) are neglected by the disease model, which adds uncertainty to the projections and could cause an overestimate of the disease's impact in some years. Estimated ear blight impacts on wheat yield are probably higher than foliar fungal diseases because of its less efficient control (Zhang et al., 2020).

With warmer and wetter summers, the average amount of solar radiation reaching a wheat canopy in France will increase (Supplementary Figure S4). However, due to the continued frequency of heavy rainfall (daily rainfall > 25mm) impacting wheat yield in the future compared to current levels (Supplementary Figure S11), low solar radiation events are expected to continue to impact wheat yield in the future (Supplementary Figure S12). Here, we define a low solar radiation index as the number of days with solar radiation below $9 \text{ MJ m}^{-2} \text{ d}^{-1}$ during wheat anthesis and grain filling, which is a third of the radiation usually received from May to July. Chances of heavy rainfall occurrence in France will increase by 50% to 80% if global average temperatures reach 3°C above pre-industrial conditions (Fischer and Knutti, 2015).

Climate change is driven by the increase in atmospheric concentration of CO₂, increasing global average air temperature. With ample water and nutrient, it has been shown that wheat yields increase can reach about 19% with elevated CO₂ in FACE experiments (from a CO₂ mixing ratio of 353 ppm to 550 ppm) (Kimball, 2016). The same experiments showed that due to low stomatal conductance, wheat transpiration decreases by 15% and canopy temperature increased by 0.6 °C (Kimball, 2016). Decreased transpiration conserves soil moisture, which may reduce the impacts of drought in wheat. However, increased canopy temperature may cause more damage from heat stress. Additionally, the interaction between elevated CO₂ and other factors such as plant diseases, flooding, heavy rainfall and low solar radiation is still understudied (Toreti et al., 2020). A unique study in a controlled environment indicated that high CO₂ may further increase the impacts of ear blight and Septoria blotch on wheat (Váry et al., 2015), but the implications of this study for wheat fields are still unclear. Although the average yield levels may increase with elevated CO₂ provided adequate nitrogen and water (Webber et al., 2018), there are uncertainties about the interactions with yield reducing factors under extreme weather conditions. Due to these uncertainties, we did not consider the potential impacts of elevated CO₂ in this study.

Here, we isolated the effects of individual climate-based factors on wheat yield losses, as changes in different factors may require different adaptation strategies. Our results indicate that wheat yield in France is expected to slightly change in future with climate change in France, but it may face more frequent droughts and heat in the future, which were less common in the past. In addition, our results suggest more attention and study should be given to an understanding how ear blight disease pressure will increase. This calls for an increased need for wheat breeding programs for new cultivars more tolerant to drought, heat, and resistant to plant diseases.

5. Acknowledgements

The authors thank ARVALIS Institut du Végétal for the financial support of this study. R.S.N.J. acknowledges support from the Prince of Albert II of Monaco foundation through the IPCC Scholarship Program. The contents of this manuscript are solely the liability of R.S.N.J. and under no circumstances may be considered as a reflection of the position of the Prince Albert II of Monaco Foundation and/or the IPCC. P.M. acknowledges support from the Agriculture and Forestry in the Face of Climate Change: Adaptation and Mitigation (CLIMAE) Meta-program of the French National Research Institute for Agriculture, Food and Environment (INRAE). Support for A.C.R. was provided by the NASA Earth Sciences Directorate support of the GISS Climate Impacts Group and the Agricultural Model

Intercomparison and Improvement Project (AgMIP). F.E. acknowledges support from the Deutsche Forschungsgemeinschaft (DFG, German Research Foundation) under Germany's Excellence Strategy – EXC 2070 – 390732324 (PhenoRob).

6. References

- Agreste., 2022. Ministère de l'agriculture de l'agroalimentaire et de la forêt. [WWW Document]. 2022. URL <https://stats.agriculture.gouv.fr/disar/> (accessed 2.2.22).
- Asseng, S., Ewert, F., Martre, P., Rötter, R.P., Lobell, D.B., Cammarano, D., Kimball, B.A., Ottman, M.J., Wall, G.W., White, J.W., Reynolds, M.P., Alderman, P.D., Prasad, P.V. V., Aggarwal, P.K., Anothai, J., Basso, B., Biernath, C., Challinor, A.J., De Sanctis, G., Doltra, J., Fereres, E., Garcia-Vila, M., Gayler, S., Hoogenboom, G., Hunt, L.A., Izaurrealde, R.C., Jabloun, M., Jones, C.D., Kersebaum, K.C., Koehler, A.-K., Müller, C., Naresh Kumar, S., Nendel, C., O'Leary, G., Olesen, J.E., Palosuo, T., Priesack, E., Eyshi Rezaei, E., Ruane, A.C., Semenov, M.A., Shcherbak, I., Stöckle, C., Stratonovitch, P., Streck, T., Supit, I., Tao, F., Thorburn, P.J., Waha, K., Wang, E., Wallach, D., Wolf, J., Zhao, Z., Zhu, Y., 2015. Rising temperatures reduce global wheat production. *Nature Climate Change* 5, 143–147. <https://doi.org/10.1038/nclimate2470>
- Asseng, S., Foster, I., Turner, N.C., 2011. The impact of temperature variability on wheat yields. *Global Change Biology* 17, 997–1012. <https://doi.org/https://doi.org/10.1111/j.1365-2486.2010.02262.x>
- Asseng, S., Martre, P., Maiorano, A., Rötter, R.P., O'Leary, G.J., Fitzgerald, G.J., Girousse, C., Motzo, R., Giunta, F., Babar, M.A., Reynolds, M.P., Kheir, A.M.S., Thorburn, P.J., Waha, K., Ruane, A.C., Aggarwal, P.K., Ahmed, M., Balkovič, J., Basso, B., Biernath, C., Bindi, M., Cammarano, D., Challinor, A.J., De Sanctis, G., Dumont, B., Eyshi Rezaei, E., Fereres, E., Ferrise, R., Garcia-Vila, M., Gayler, S., Gao, Y., Horan, H., Hoogenboom, G., Izaurrealde, R.C., Jabloun, M., Jones, C.D., Kassie, B.T., Kersebaum, K.-C., Klein, C., Koehler, A.-K., Liu, B., Minoli, S., Montesino San Martin, M., Müller, C., Naresh Kumar, S., Nendel, C., Olesen, J.E., Palosuo, T., Porter, J.R., Priesack, E., Ripoché, D., Semenov, M.A., Stöckle, C., Stratonovitch, P., Streck, T., Supit, I., Tao, F., Van der Velde, M., Wallach, D., Wang, E., Webber, H., Wolf, J., Xiao, L., Zhang, Z., Zhao, Z., Zhu, Y., Ewert, F., 2019. Climate change impact and adaptation for wheat protein. *Global Change Biology* 25, 155–173. <https://doi.org/https://doi.org/10.1111/gcb.14481>
- Baruth, B., Bassu, S., Ben Aoun, W., Biavetti, I., Bratu, M., Cerrani, I., Chemin, Y., Claverie, M., P, D.P., D, F., G, M., J, M., L, N.S., L, P., G, R., L, S., E, T., M, V.D.B., Z, Z., A, Z., M, V.D.B., S, N., 2022. JRC MARS Bulletin - Crop monitoring in Europe - July 2022 - Vol. 30 No 7. Publications Office of the European Union, Luxembourg (Luxembourg). <https://doi.org/10.2760/577529> (online)
- Battisti, D.S., Naylor, R.L., 2009. Historical Warnings of Future Food Insecurity with Unprecedented Seasonal Heat. *Science* 323, 240–244. <https://doi.org/10.1126/science.1164363>
- Beillouin, D., Schauburger, B., Bastos, A., Ciais, P., Makowski, D., 2020. Impact of extreme weather conditions on European crop production in 2018. *Philosophical Transactions of the Royal Society B: Biological Sciences* 375, 20190510. <https://doi.org/10.1098/rstb.2019.0510>
- Ben-Ari, T., Boé, J., Ciais, P., Lecerf, R., Van der Velde, M., Makowski, D., 2018. Causes and implications of the unforeseen 2016 extreme yield loss in the breadbasket of France. *Nature Communications* 9, 1627. <https://doi.org/10.1038/s41467-018-04087-x>
- Bezner Kerr, R., Naess, L.O., Allen-O'Neil, B., Totin, E., Nyantakyi-Frimpong, H., Risvoll, C., Rivera Ferre, M.G., López-i-Gelats, F., Eriksen, S., 2022. Interplays between changing biophysical and social dynamics under climate change: Implications for limits to sustainable adaptation in food

- systems. *Global Change Biology* 28, 3580–3604. <https://doi.org/https://doi.org/10.1111/gcb.16124>
- Ceglar, A., Zampieri, M., Gonzalez-Reviriego, N., Ciais, P., Schauburger, B., Van der Velde, M., 2020. Time-varying impact of climate on maize and wheat yields in France since 1900. *Environmental Research Letters* 15, 094039. <https://doi.org/10.1088/1748-9326/aba1be>
- Chaloner, T.M., Fones, H.N., Varma, V., Bebbler, D.P., Gurr, S.J., 2019. A new mechanistic model of weather-dependent *Septoria tritici* blotch disease risk. *Philosophical Transactions of the Royal Society B: Biological Sciences* 374, 20180266. <https://doi.org/10.1098/rstb.2018.0266>
- Ciais, P., Reichstein, M., Viovy, N., Granier, A., Ogée, J., Allard, V., Aubinet, M., Buchmann, N., Bernhofer, C., Carrara, A., Chevallier, F., De Noblet, N., Friend, A.D., Friedlingstein, P., Grünwald, T., Heinesch, B., Keronen, P., Knohl, A., Krinner, G., Loustau, D., Manca, G., Matteucci, G., Miglietta, F., Ourcival, J.M., Papale, D., Pilegaard, K., Rambal, S., Seufert, G., Soussana, J.F., Sanz, M.J., Schulze, E.D., Vesala, T., Valentini, R., 2005. Europe-wide reduction in primary productivity caused by the heat and drought in 2003. *Nature* 437, 529–533. <https://doi.org/10.1038/nature03972>
- El Jarroudi, Moussa, Kouadio, L., Bock, C.H., El Jarroudi, Mustapha, Junk, J., Pasquali, M., Maraite, H., Delfosse, P., 2016. A Threshold-Based Weather Model for Predicting Stripe Rust Infection in Winter Wheat. *Plant Disease* 101, 693–703. <https://doi.org/10.1094/PDIS-12-16-1766-RE>
- Eyring, V., Bony, S., Meehl, G.A., Senior, C.A., Stevens, B., Stouffer, R.J., Taylor, K.E., 2016. Overview of the Coupled Model Intercomparison Project Phase 6 (CMIP6) experimental design and organization. *Geoscientific Model Development* 9, 1937–1958. <https://doi.org/10.5194/gmd-9-1937-2016>
- FAO stat, 2022. FAOSTAT: FAO statistical databases [WWW Document]. URL <http://www.fao.org/faostat/en/#home> (accessed 6.6.22).
- Fischer, E.M., Knutti, R., 2015. Anthropogenic contribution to global occurrence of heavy-precipitation and high-temperature extremes. *Nature Climate Change* 5, 560–564. <https://doi.org/10.1038/nclimate2617>
- Gaupp, F., Hall, J., Hochrainer-Stigler, S., Dadson, S., 2020. Changing risks of simultaneous global breadbasket failure. *Nature Climate Change* 10, 54–57. <https://doi.org/10.1038/s41558-019-0600-z>
- Grillakis, M.G., 2019. Increase in severe and extreme soil moisture droughts for Europe under climate change. *Science of The Total Environment* 660, 1245–1255. <https://doi.org/https://doi.org/10.1016/j.scitotenv.2019.01.001>
- Guarin, J.R., Asseng, S., Martre, P., Bliznyuk, N., 2020. Testing a crop model with extreme low yields from historical district records. *Field Crops Research* 249, 107269. <https://doi.org/10.1016/j.fcr.2018.03.006>
- Hargreaves, G.H., Samani, Z.A., 1985. Reference Crop Evapotranspiration from Temperature. *Applied Engineering in Agriculture* 1, 96–99. <https://doi.org/10.13031/2013.26773>
- IPCC, 2021. Technical Summary. Contribution of Working Group I to the Sixth Assessment Report of the Intergovernmental Panel on Climate Change, *Climate Change 2021: The Physical Science Basis*.
- Jägermeyr, J., Müller, C., Ruane, A.C., Elliott, J., Balkovic, J., Castillo, O., Faye, B., Foster, I., Folberth, C., Franke, J.A., Fuchs, K., Guarin, J.R., Heinke, J., Hoogenboom, G., Iizumi, T., Jain, A.K., Kelly, D., Khabarov, N., Lange, S., Lin, T.-S., Liu, W., Mialyk, O., Minoli, S., Moyer, E.J., Okada, M., Phillips, M., Porter, C., Rabin, S.S., Scheer, C., Schneider, J.M., Schyns, J.F., Skalsky, R., Smerald, A., Stella, T., Stephens, H., Webber, H., Zabel, F., Rosenzweig, C., 2021. Climate impacts on global

- agriculture emerge earlier in new generation of climate and crop models. *Nature Food*. <https://doi.org/10.1038/s43016-021-00400-y>
- Jeantet, A., Henine, H., Chaumont, C., Collet, L., Thirel, G., Tournebize, J., 2021. Robustness of a parsimonious subsurface drainage model at the French national scale. *Hydrology and Earth System Sciences* 25, 5447–5471. <https://doi.org/10.5194/hess-25-5447-2021>
- Kimball, B.A., 2016. Crop responses to elevated CO₂ and interactions with H₂O, N, and temperature. *Current Opinion in Plant Biology* 31, 36–43. <https://doi.org/https://doi.org/10.1016/j.pbi.2016.03.006>
- Lange, S., 2019. Trend-preserving bias adjustment and statistical downscaling with ISIMIP3BASD (v1.0). *Geoscientific Model Development* 12, 3055–3070. <https://doi.org/10.5194/gmd-12-3055-2019>
- Lesk, C., Rowhani, P., Ramankutty, N., 2016. Influence of extreme weather disasters on global crop production. *Nature* 529, 84–87. <https://doi.org/10.1038/nature16467>
- Liu, B., Asseng, S., Müller, C., Ewert, F., Elliott, J., Lobell, D.B., Martre, P., Ruane, A.C., Wallach, D., Jones, J.W., Rosenzweig, C., Aggarwal, P.K., Alderman, P.D., Anothai, J., Basso, B., Biernath, C., Cammarano, D., Challinor, A., Deryng, D., Sanctis, G.D., Doltra, J., Fereres, E., Folberth, C., Garcia-Vila, M., Gayler, S., Hoogenboom, G., Hunt, L.A., Izaurrealde, R.C., Jabloun, M., Jones, C.D., Kersebaum, K.C., Kimball, B.A., Koehler, A.-K., Kumar, S.N., Nendel, C., O’Leary, G.J., Olesen, J.E., Ottman, M.J., Palosuo, T., Prasad, P.V.V., Priesack, E., Pugh, T.A.M., Reynolds, M., Rezaei, E.E., Rötter, R.P., Schmid, E., Semenov, M.A., Shcherbak, I., Stehfest, E., Stöckle, C.O., Stratonovitch, P., Streck, T., Supit, I., Tao, F., Thorburn, P., Waha, K., Wall, G.W., Wang, E., White, J.W., Wolf, J., Zhao, Z., Zhu, Y., 2016. Similar estimates of temperature impacts on global wheat yield by three independent methods. *Nature Climate Change* 6, 1130–1136. <https://doi.org/10.1038/nclimate3115>
- Liu, B., Martre, P., Ewert, F., Porter, J.R., Challinor, A.J., Müller, C., Ruane, A.C., Waha, K., Thorburn, P.J., Aggarwal, P.K., Ahmed, M., Balkovič, J., Basso, B., Biernath, C., Bindi, M., Cammarano, D., De Sanctis, G., Dumont, B., Espadafor, M., Eyshi Rezaei, E., Ferrise, R., Garcia-Vila, M., Gayler, S., Gao, Y., Horan, H., Hoogenboom, G., Izaurrealde, R.C., Jones, C.D., Kassie, B.T., Kersebaum, K.C., Klein, C., Koehler, A.-K., Maiorano, A., Minoli, S., Montesino San Martin, M., Naresh Kumar, S., Nendel, C., O’Leary, G.J., Palosuo, T., Priesack, E., Ripoche, D., Rötter, R.P., Semenov, M.A., Stöckle, C., Streck, T., Supit, I., Tao, F., Van der Velde, M., Wallach, D., Wang, E., Webber, H., Wolf, J., Xiao, L., Zhang, Z., Zhao, Z., Zhu, Y., Asseng, S., 2019. Global wheat production with 1.5 and 2.0°C above pre-industrial warming. *Global Change Biology* 25, 1428–1444. <https://doi.org/https://doi.org/10.1111/gcb.14542>
- Liu, W., Ye, T., Jägermeyr, J., Müller, C., Chen, S., Liu, X., Shi, P., 2021. Future climate change significantly alters interannual wheat yield variability over half of harvested areas. *Environmental Research Letters* 16, 94045. <https://doi.org/10.1088/1748-9326/ac1fbb>
- Lobell, D.B., Schlenker, W., Costa-Roberts, J., 2011. Climate Trends and Global Crop Production Since 1980. *Science* 333.
- Madgwick, J.W., West, J.S., White, R.P., Semenov, M.A., Townsend, J.A., Turner, J.A., Fitt, B.D.L., 2011. Impacts of climate change on wheat anthesis and fusarium ear blight in the UK. *European Journal of Plant Pathology* 130, 117–131. <https://doi.org/10.1007/s10658-010-9739-1>
- Mäkinen, H., Kaseva, J., Trnka, M., Balek, J., Kersebaum, K.C., Nendel, C., Gobin, A., Olesen, J.E., Bindi, M., Ferrise, R., Moriondo, M., Rodríguez, A., Ruiz-Ramos, M., Takáč, J., Bezák, P., Ventrella, D., Ruget, F., Capellades, G., Kahiluoto, H., 2018. Sensitivity of European wheat to extreme weather. *Field Crops Research* 222, 209–217. <https://doi.org/https://doi.org/10.1016/j.fcr.2017.11.008>
- McCuen, R., Zachary, K., Gillian, C.A., 2006. Evaluation of the Nash–Sutcliffe Efficiency Index. *Journal*

- of Hydrologic Engineering 11, 597–602. [https://doi.org/10.1061/\(ASCE\)1084-0699\(2006\)11:6\(597\)](https://doi.org/10.1061/(ASCE)1084-0699(2006)11:6(597))
- Muftuoglu, B., 2021. Russia steps up wheat exports to Algeria. Argus.
- Nóia Júnior, R. de S., Martre, P., Finger, R., van der Velde, M., Ben-Ari, T., Ewert, F., Webber, H., Ruane, A.C., Asseng, S., 2021. Extreme lows of wheat production in Brazil. Environmental Research Letters 16, 104025. <https://doi.org/10.1088/1748-9326/ac26f3>
- Nuttall, J.G., Barlow, K.M., Delahunty, A.J., Christy, B.P., O’Leary, G.J., 2018. Acute High Temperature Response in Wheat. Agronomy Journal 110, 1296–1308. <https://doi.org/https://doi.org/10.2134/agronj2017.07.0392>
- O’Neill, B.C., Carter, T.R., Ebi, K., Harrison, P.A., Kemp-Benedict, E., Kok, K., Kriegler, E., Preston, B.L., Riahi, K., Sillmann, J., van Ruijven, B.J., van Vuuren, D., Carlisle, D., Conde, C., Fuglestvedt, J., Green, C., Hasegawa, T., Leininger, J., Monteith, S., Pichs-Madruga, R., 2020. Achievements and needs for the climate change scenario framework. Nature Climate Change 10, 1074–1084. <https://doi.org/10.1038/s41558-020-00952-0>
- O’Neill, B.C., Tebaldi, C., van Vuuren, D.P., Eyring, V., Friedlingstein, P., Hurtt, G., Knutti, R., Kriegler, E., Lamarque, J.-F., Lowe, J., Meehl, G.A., Moss, R., Riahi, K., Sanderson, B.M., 2016. The Scenario Model Intercomparison Project (ScenarioMIP) for CMIP6. Geoscientific Model Development 9, 3461–3482. <https://doi.org/10.5194/gmd-9-3461-2016>
- Paudel, D., Boogaard, H., de Wit, A., van der Velde, M., Claverie, M., Nisini, L., Janssen, S., Osinga, S., Athanasiadis, I.N., 2022. Machine learning for regional crop yield forecasting in Europe. Field Crops Research 276, 108377. <https://doi.org/https://doi.org/10.1016/j.fcr.2021.108377>
- Peel, M.C., Finlayson, B.L., McMahon, T.A., 2007. Updated world map of the Köppen-Geiger climate classification. Hydrology and Earth System Sciences 11, 1633–1644. <https://doi.org/10.5194/hess-11-1633-2007>
- Pequeno, D.N.L., Hernández-Ochoa, I.M., Reynolds, M., Sonder, K., MoleroMilan, A., Robertson, R.D., Lopes, M.S., Xiong, W., Kropff, M., Asseng, S., 2021. Climate impact and adaptation to heat and drought stress of regional and global wheat production. Environmental Research Letters 16, 54070. <https://doi.org/10.1088/1748-9326/abd970>
- R Core Team, 2017. R: A Language and Environment for Statistical Computing. R Foundation for Statistical Computing, Vienna, Austria. <https://doi.org/http://www.R-project.org/>
- Ranasinghe, R., Ruane, A.C., Vautard, R., Arnell, N., Coppola, E., Cruz, F.A., Dessai, S., Islam, A.S., Rahimi, M., Carrascal, D.R., Sillmann, J., M.B. Sylla, C., Tebaldi, W., Wang, Zaaboul, R., 2021. Chapter 12: Climate change information for regional impact and for risk assessment. Climate Change 2021: The Physical Science Basis. Contribution of Working Group I to the Sixth Assessment Report of the Intergovernmental Panel on Climate Change 351–364.
- Raymond, C., Horton, R.M., Zscheischler, J., Martius, O., AghaKouchak, A., Balch, J., Bowen, S.G., Camargo, S.J., Hess, J., Kornhuber, K., Oppenheimer, M., Ruane, A.C., Wahl, T., White, K., 2020. Understanding and managing connected extreme events. Nature Climate Change 10, 611–621. <https://doi.org/10.1038/s41558-020-0790-4>
- Ruane, A.C., Vautard, R., Ranasinghe, R., Sillmann, J., Coppola, E., Arnell, N., F.A. Cruz, S.D., Iles, C.E., Islam, A.K.M.S., Jones, R.G., Rahimi, M., Carrascal, D.R., Seneviratne, S.I., Servonnat, J., Sörensson, A.A., Sylla, M.B., Tebaldi, C., Wang, W., Zaaboul, R., 2022. The Climatic Impact-Driver Framework for assessment of risk-relevant climate information. Earth’s Future.
- Schauberger, B., Ben-Ari, T., Makowski, D., Kato, T., Kato, H., Ciais, P., 2018. Yield trends, variability and stagnation analysis of major crops in France over more than a century. Scientific Reports 8, 16865. <https://doi.org/10.1038/s41598-018-35351-1>

- Schauberger, B., Makowski, D., Ben-Ari, T., Boé, J., Ciais, P., 2021. No historical evidence for increased vulnerability of French crop production to climatic hazards. *Agricultural and Forest Meteorology* 306, 108453. <https://doi.org/https://doi.org/10.1016/j.agrformet.2021.108453>
- Senapati, N., Halford, N.G., Semenov, M.A., 2021. Vulnerability of European wheat to extreme heat and drought around flowering under future climate. *Environmental Research Letters* 16, 24052. <https://doi.org/10.1088/1748-9326/abdcb3>
- Seneviratne, S., Zhang, X., Adnan, M., Badi, W., Dereczynski, C., Luca, A. Di, Ghosh, S., Iskandar, I., Kossin, J., Lewis, S., Otto, F., Pinto, I., Satoh, M., Vicente-Serrano, S.M., Wehner, M., Zhou, B., 2021. The Physical Science Basis, in: Press, C.U. (Ed.), *Sixth Assessment Report of the Intergovernmental Panel on Climate Change*.
- Seneviratne, S.I., Nicholls, N., Easterling, D., Goodess, C.M., Kanae, S., Kossin, J., Luo, Y., Marengo, J., Mc Innes, K., Rahimi, M., Reichstein, M., Sorteberg, A., Vera, C., Zhang, X., Rusticucci, M., Semenov, V., Alexander, L. V., Allen, S., Benito, G., Cavazos, T., Clague, J., Conway, D., Della-Marta, P.M., Gerber, M., Gong, S., Goswami, B.N., Hemer, M., Huggel, C., Van den Hurk, B., Khari, V. V., Kitoh, A., Klein Tank, A.M.G., Li, G., Mason, S., Mc Guire, W., Van Oldenborgh, G.J., Orlovsky, B., Smith, S., Thiaw, W., Velegakis, A., Yiou, P., Zhang, T., Zhou, T., Zwiers, F.W., 2012. Changes in climate extremes and their impacts on the natural physical environment. *Managing the Risks of Extreme Events and Disasters to Advance Climate Change Adaptation: Special Report of the Intergovernmental Panel on Climate Change* 9781107025, 109–230. <https://doi.org/10.1017/CBO9781139177245.006>
- Simoës, A., 2022. The economic complexity observatory [WWW Document]. Workshops at the twenty-fifth AAAI conference on artificial intelligence. URL <https://atlas.media.mit.edu/en/> (accessed 9.21.22).
- te Beest, D.E., Shaw, M.W., Pietravalle, S., van den Bosch, F., 2009. A predictive model for early-warning of Septoria leaf blotch on winter wheat. *European Journal of Plant Pathology* 124, 413–425. <https://doi.org/10.1007/s10658-009-9428-0>
- Team, P.P., 2021. The POWER Project [WWW Document]. NASA Prediction of Worldwide Energy Resources. URL <https://power.larc.nasa.gov/>
- Toreti, A., Deryng, D., Tubiello, F.N., Müller, C., Kimball, B.A., Moser, G., Boote, K., Asseng, S., Pugh, T.A.M., Vanuytrecht, E., Pleijel, H., Webber, H., Durand, J.-L., Dentener, F., Ceglar, A., Wang, X., Badeck, F., Lecerf, R., Wall, G.W., van den Berg, M., Hoegy, P., Lopez-Lozano, R., Zampieri, M., Galmarini, S., O’Leary, G.J., Manderscheid, R., Mencos Contreras, E., Rosenzweig, C., 2020. Narrowing uncertainties in the effects of elevated CO₂ on crops. *Nature Food* 1, 775–782. <https://doi.org/10.1038/s43016-020-00195-4>
- Trnka, M., Rötter, R.P., Ruiz-Ramos, M., Kersebaum, K.C., Olesen, J.E., Žalud, Z., Semenov, M.A., 2014. Adverse weather conditions for European wheat production will become more frequent with climate change. *Nature Climate Change* 4, 637–643. <https://doi.org/10.1038/nclimate2242>
- van der Velde, M., Lecerf, R., d’Andrimont, R., Ben-Ari, T., 2020. Chapter 8 - Assessing the France 2016 extreme wheat production loss—Evaluating our operational capacity to predict complex compound events, in: Sillmann, J., Sippel, S., Russo, S.B.T.-C.E. and T.I. for I. and R.A. (Eds.), . Elsevier, pp. 139–158. <https://doi.org/https://doi.org/10.1016/B978-0-12-814895-2.00009-4>
- van der Velde, M., Tubiello, F.N., Vrieling, A., Bouraoui, F., 2012. Impacts of extreme weather on wheat and maize in France: evaluating regional crop simulations against observed data. *Climatic Change* 113, 751–765. <https://doi.org/10.1007/s10584-011-0368-2>
- Váry, Z., Mullins, E., McElwain, J.C., Doohan, F.M., 2015. The severity of wheat diseases increases when plants and pathogens are acclimatized to elevated carbon dioxide. *Global change biology* 21, 2661–2669. <https://doi.org/10.1111/gcb.12899>

- Wallach, D., Goffinet, B., 1987. Mean Squared Error of Prediction in Models for Studying Ecological and Agronomic Systems. *Biometrics* 43, 561–573. <https://doi.org/10.2307/2531995>
- Webber, H., Ewert, F., Olesen, J.E., Müller, C., Fronzek, S., Ruane, A.C., Bourgault, M., Martre, P., Ababaei, B., Bindi, M., Ferrise, R., Finger, R., Fodor, N., Gabaldón-Leal, C., Gaiser, T., Jabloun, M., Kersebaum, K.-C., Lizaso, J.I., Lorite, I.J., Manceau, L., Moriondo, M., Nendel, C., Rodríguez, A., Ruiz-Ramos, M., Semenov, M.A., Siebert, S., Stella, T., Stratonovitch, P., Trombi, G., Wallach, D., 2018. Diverging importance of drought stress for maize and winter wheat in Europe. *Nature Communications* 9, 4249. <https://doi.org/10.1038/s41467-018-06525-2>
- Webber, H., Lischeid, G., Sommer, M., Finger, R., Nendel, C., Gaiser, T., Ewert, F., 2020. No perfect storm for crop yield failure in Germany. *Environmental Research Letters* 15, 104012. <https://doi.org/10.1088/1748-9326/aba2a4>
- West, J.S., Holdgate, S., Townsend, J.A., Edwards, S.G., Jennings, P., Fitt, B.D.L., 2012. Impacts of changing climate and agronomic factors on fusarium ear blight of wheat in the UK. *Fungal Ecology* 5, 53–61. <https://doi.org/https://doi.org/10.1016/j.funeco.2011.03.003>
- Xu, X., 2003. Effects of environmental conditions on the development of Fusarium ear blight BT - Epidemiology of Mycotoxin Producing Fungi: Under the aegis of COST Action 835 'Agriculturally Important Toxigenic Fungi 1998–2003', EU project (QLK 1-CT-1998–01380), in: Xu, X., Bailey, J.A., Cooke, B.M. (Eds.), . Springer Netherlands, Dordrecht, pp. 683–689. https://doi.org/10.1007/978-94-017-1452-5_3
- Zhang, D., Wang, Z., Jin, N., Gu, C., Chen, Y., Huang, Y., 2020. Evaluation of Efficacy of Fungicides for Control of Wheat Fusarium Head Blight Based on Digital Imaging. *IEEE Access* 8, 109876–109890. <https://doi.org/10.1109/ACCESS.2020.3001652>
- Zhao, C., Liu, B., Piao, S., Wang, X., Lobell, D.B., Huang, Y., Huang, M., Yao, Y., Bassu, S., Ciais, P., Durand, J.-L., Elliott, J., Ewert, F., Janssens, I.A., Li, T., Lin, E., Liu, Q., Martre, P., Müller, C., Peng, S., Peñuelas, J., Ruane, A.C., Wallach, D., Wang, T., Wu, D., Liu, Z., Zhu, Y., Zhu, Z., Asseng, S., 2017. Temperature increase reduces global yields of major crops in four independent estimates. *Proceedings of the National Academy of Sciences* 114, 9326 LP – 9331. <https://doi.org/10.1073/pnas.1701762114>
- Zhu, P., Abramoff, R., Makowski, D., Ciais, P., 2021. Uncovering the Past and Future Climate Drivers of Wheat Yield Shocks in Europe With Machine Learning. *Earth's Future* 9, e2020EF001815. <https://doi.org/https://doi.org/10.1029/2020EF001815>
- Zscheischler, J., Westra, S., van den Hurk, B.J.J.M., Seneviratne, S.I., Ward, P.J., Pitman, A., AghaKouchak, A., Bresch, D.N., Leonard, M., Wahl, T., Zhang, X., 2018. Future climate risk from compound events. *Nature Climate Change* 8, 469–477. <https://doi.org/10.1038/s41558-018-0156-3>

Supplementary Material for

Past and future wheat yield variability in France

Rogério de Souza Nória Júnior, Pierre Martre, Jean-Charles Deswarte, Jean-Pierre Cohan, Marijn Van der Velde⁵, Heidi Webber, Frank Ewert, Alex C. Ruane, Senthold Asseng

Contents

1 Supplementary Methods	3
Figure S1. Schematic representation of the procedure to compute the impacts of individual yield limiting factors in each year of the historical period used for creating the statistical model estimating wheat yield and under climate change scenarios.....	3
2 Supplementary Results	4
Table S1. Geographical coordinates and the departments of locations used in the study.	4
Table S2. Performance of the random forest machine approach to estimate year-to-year wheat yield variability.	5
Figure S2. Estimated wheat yield in the breadbasket of France.	7
Figure S3. Projected future climate in Égreville, France for SSP5-8.5.	8
2.1 Supplementary Results - Wheat anthesis date on 1st June	9
Figure S4. Projected future causes of wheat yield losses in the breadbasket of France for SSP5-2.6, with fixed wheat anthesis on 1 st June.	10
Figure S5. Projected wheat yield losses due to heat at anthesis and grain filling.	11
Figure S6. Projected wheat yield losses due to drought at anthesis and grain filling.	12
Figure S7. Projected wheat yield losses due to flooding at anthesis and grain filling.	13
Figure S9. Projected wheat yield losses due to low solar radiation at anthesis and grain filling.	15
Figure S10. Projected wheat yield losses due to ear blight and fungal foliar diseases.	16
2.2 Supplementary Results - Wheat anthesis date on 15th May	17
Figure S11. Projected frequency of extreme low wheat yield years in the breadbasket of France with fixed wheat anthesis on 15 th May.....	17
Figure S12. Projected future causes of wheat yield losses in the breadbasket of France for SSP5-2.6, with fixed wheat anthesis on 15 th May.....	18

Figure S13. Projected future causes of wheat yield losses in the breadbasket of France for SSP5-8.5, with fixed wheat anthesis on 15 th May.....	19
Figure S14. Projected wheat yield losses due to heat at anthesis and grain filling, with wheat anthesis on 15 th May.....	20
Figure S15. Projected wheat yield losses due to drought at anthesis and grain filling, with wheat anthesis on 15 th May.....	21
Figure S16. Projected wheat yield losses due to flooding at anthesis and grain filling, with wheat anthesis on 15 th May.....	22
Figure S17.....	23
Figure S18.....	24
Figure S19. Projected wheat yield losses due to ear blight and fungal foliar diseases, with wheat anthesis on 15 th May.....	25

1 Supplementary Methods

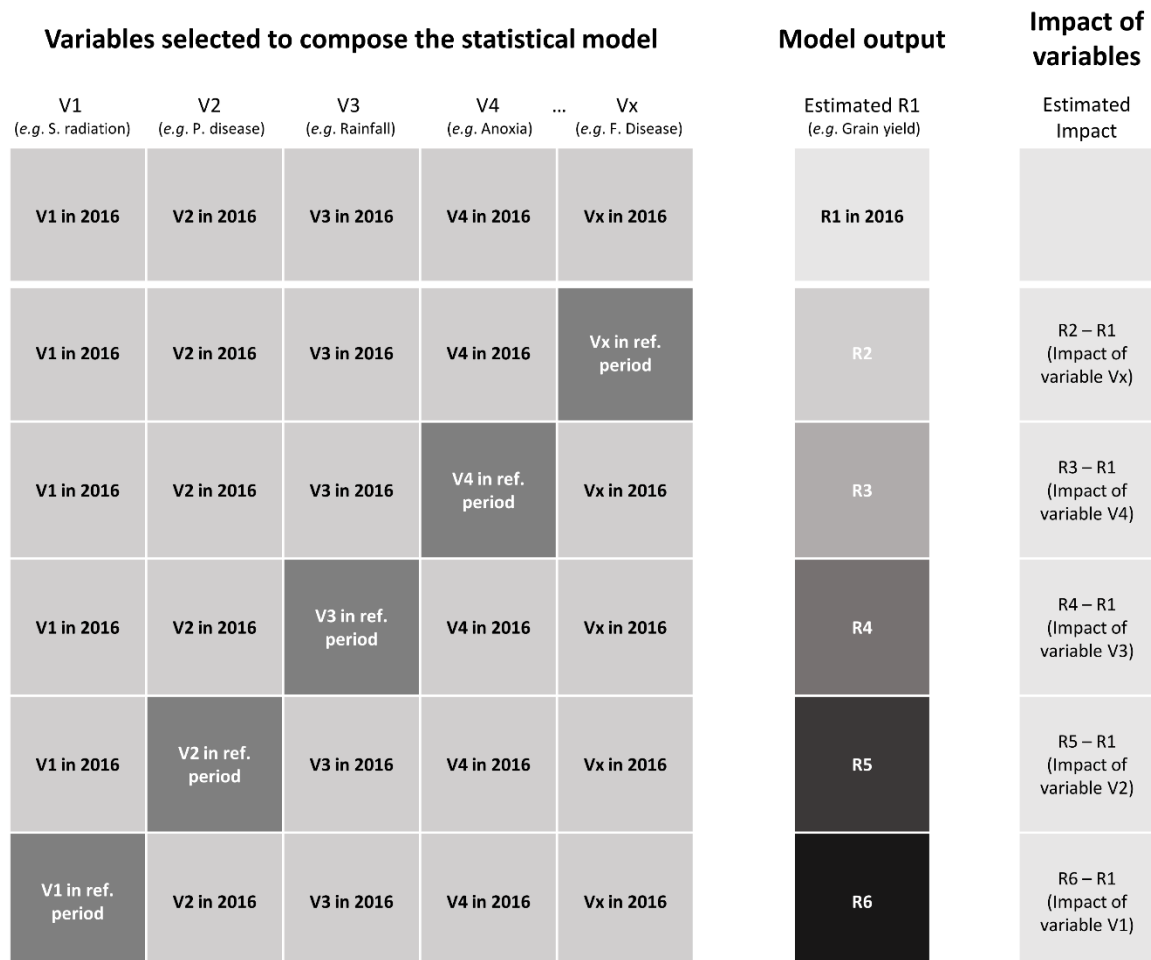


Figure S1. Schematic representation of the procedure to compute the impacts of individual yield limiting factors in each year of the historical period used for creating the statistical model estimating wheat yield and under climate change scenarios. The letter 'V' represents the explanatory variables selected by random forest machine learning method. In addition, the letter 'R' represents the estimated model output (result) from the statistical model. '2016' is representing the target year.

2 Supplementary Results

Table S1. Geographical coordinates and the departments of locations used in the study.

Location	Departments	Latitude	Longitude
Égreville	Seine-et-Marne	48.18	2.86
Chevry-Cossigny	Seine-et-Marne	48.72	2.66
Saint-Quentin	Aisne	49.87	3.20
Saint-Florent-sur-Cher	Cher	47.03	2.33
Fagnières	Marne	48.95	4.41
Issodun	Indre	46.96	2.03
Barbarey-Saint-Sulpice	Aube	48.32	4.02
Rots	Calvados	49.20	0.47

Table S2. Performance of the random forest machine approach to estimate year-to-year wheat yield variability. The performance was calculated during the model training and in two different methods of cross validation (lean one location out and leaving one year out). The relative root mean squared error of prediction (*rRMSEp*), coefficient of determination (r^2) and Nash-Sutcliffe model efficiency coefficient (NSE) are shown.

Locations	r^2	rRMSEp (%)	Nash Sutcliffe
Model training			
Égreville	0.93	3	0.85
Chevry-Cossigny	0.95	3	0.86
Saint-Quentin	0.90	3	0.85
Saint-Florent-sur-Cher	0.90	4	0.81
Fagnières	0.91	3	0.78
Issodun	0.92	3	0.81
Barbarey-Saint-Sulpice	0.91	4	0.75
Rots	0.89	4	0.31
Leaving one location out cross validation			
Égreville	0.84	6	0.40
Chevry-Cossigny	0.81	6	0.29
Saint-Quentin	0.64	5	0.39
Saint-Florent-sur-Cher	0.57	7	0.13
Fagnières	0.54	6	-0.76
Issodun	0.63	6	0.02
Barbarey-Saint-Sulpice	0.59	7	-0.14
Rots	0.11	8	-2.70
Leaving one year out cross validation			
Égreville	0.06	12	-4.6
Chevry-Cossigny	0.02	11	-6.5
Saint-Quentin	0.10	9	-2.7
Saint-Florent-sur-Cher	0.01	12	-4.5
Fagnières	0.01	10	-3.6
Issodun	0.01	11	-8.4
Barbarey-Saint-Sulpice	0.01	12	-3.5
Rots	0.03	8	-3.4

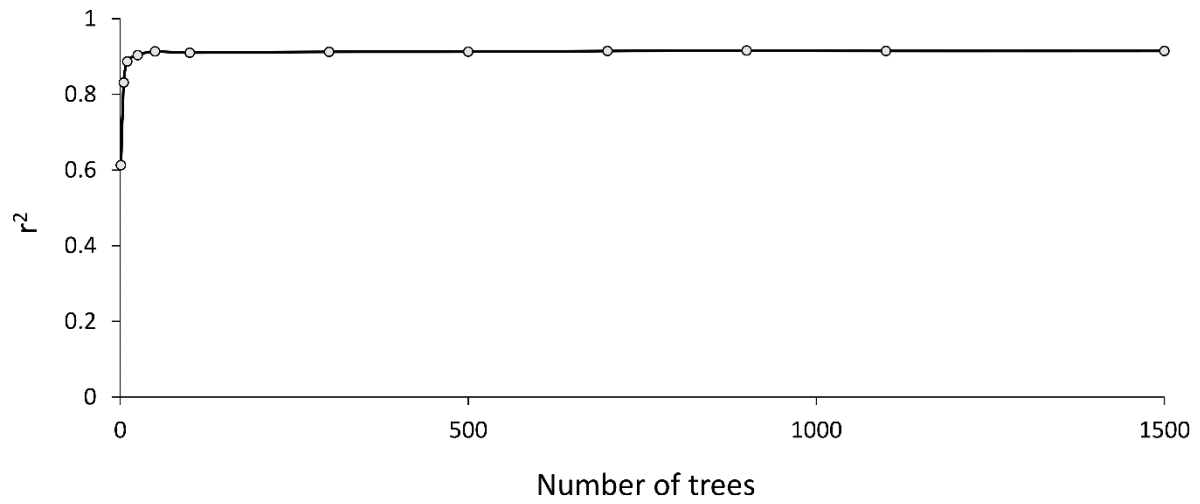


Figure S2. Performance of random forest to estimate wheat yield in the breadbasket of France according to the number of trees used.

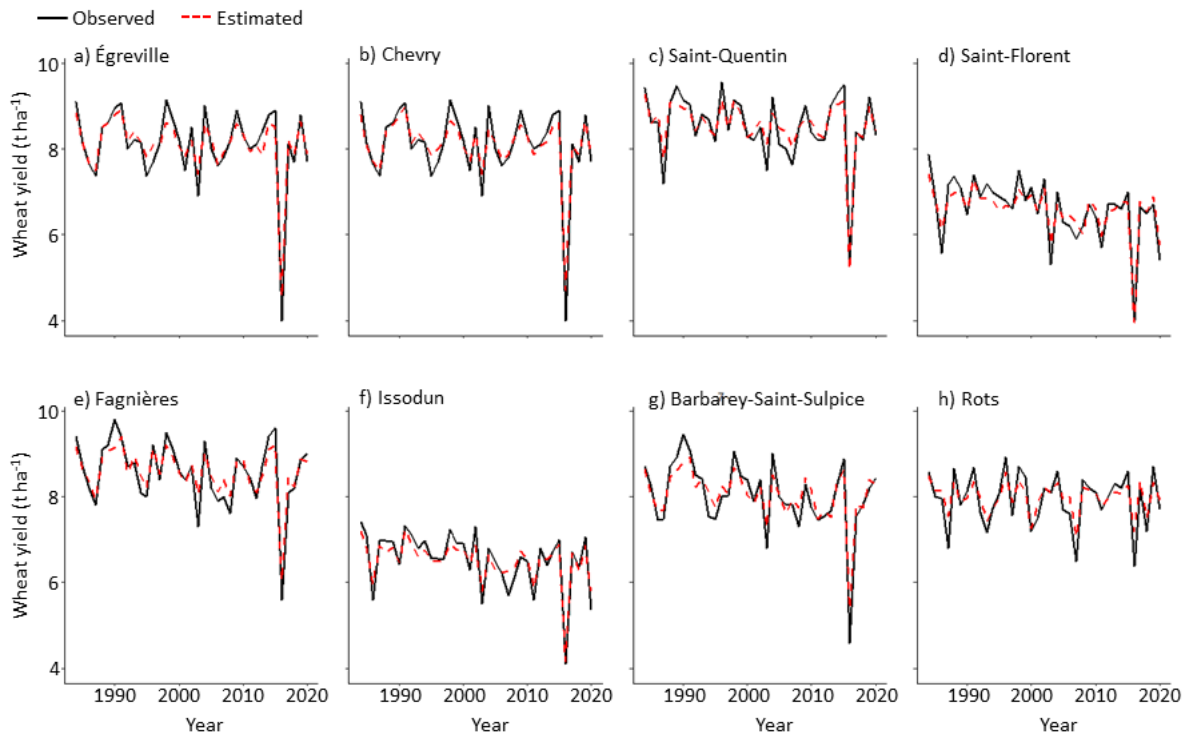


Figure S3. Estimated wheat yield in the breadbasket of France. Interannual variability from 1984–2020 of observed (black solid lines) and estimated (red dashed lines) wheat trend corrected yield of (a) Égreville, (b) Chevry, (c) Saint Quentin, (d) Saint Florent, (e) Fagnières, (f) Issodun, (g) Troyes Barbarey Saint Sulpice and (h) Rots. Estimated results are from a training set results.

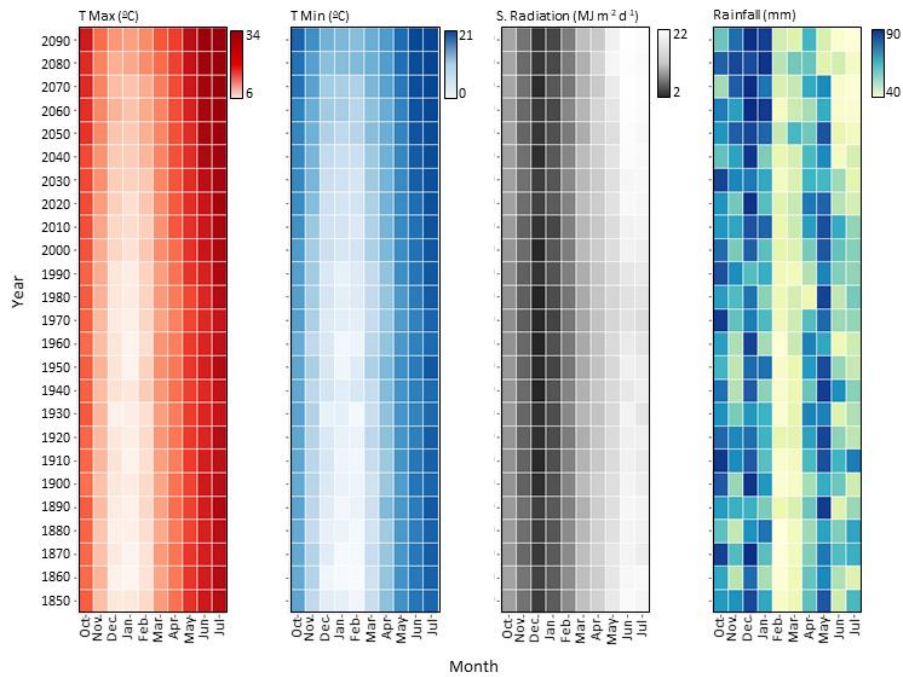


Figure S4. Projected future climate in Égreville, France for SSP5-8.5. Average monthly maximum (T Min), minimum temperature (T Max), solar radiation (S. Radiation), and accumulated rainfall (Rainfall) for the period 1850-2100, in Égreville, France, and for SSP5-8.5. The values presented are the mean of five CMIP6 global change models.

2.1 Supplementary Results - Wheat anthesis date on 1st June

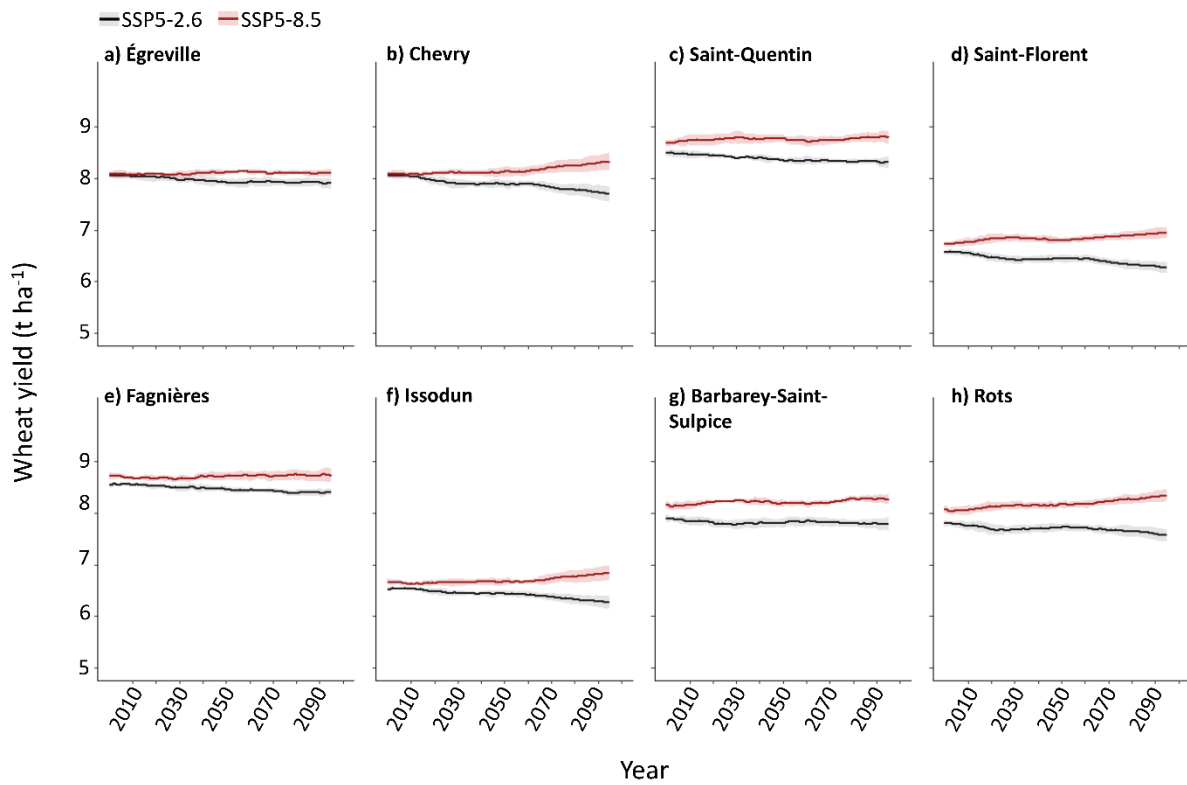


Figure S5. Projected wheat yield in the breadbasket of France. Estimated 30 years running mean frequency of wheat yield SSP5-2.6 (black trace) and SSP5-8.5 (red trace) from 2015 to 2100, for (a) Égreville, (b) Chevry, (c) Saint Quentin, (d) Saint Florent, (e) Fagnières, (f) Issodun, (g) Troyes Barbarey Saint Sulpice and (h) Rots. Lines are ensemble means based on five CMIP6 GCMs (lines) and shading shows ± 1 s.e.

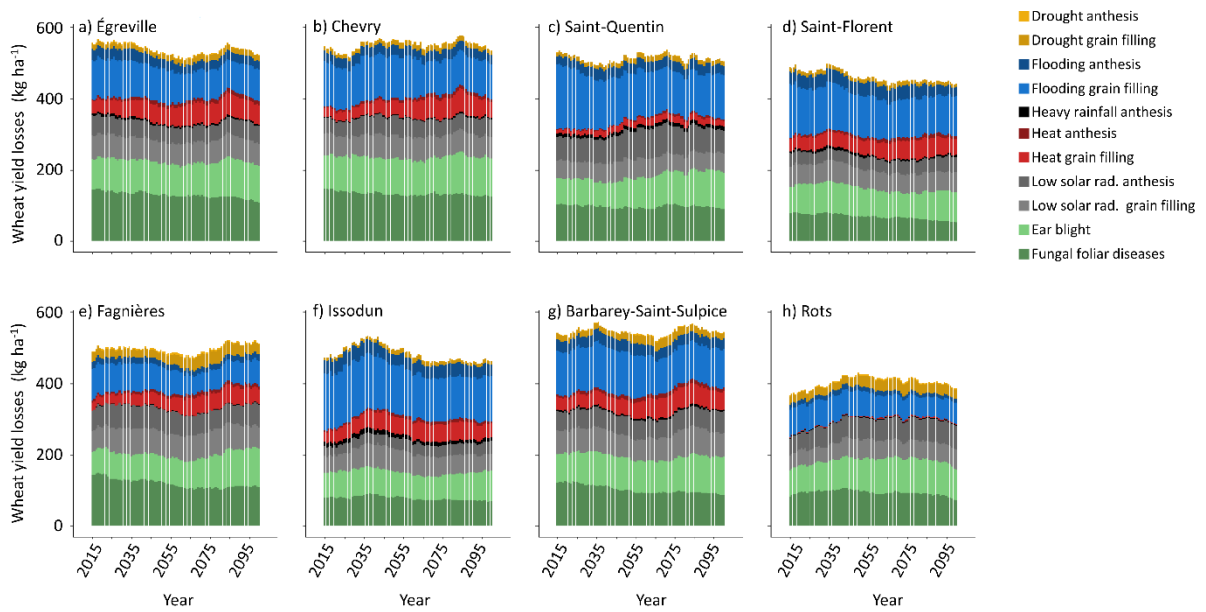


Figure S6. Projected future causes of wheat yield losses in the breadbasket of France for SSP5-2.6, with fixed wheat anthesis on 1st June. Projected wheat yield losses causes from 2015 to 2100 for (a) Égreville, (b) Chevry, (c) Saint Quentin, (d) Saint Florent, (e) Fagnières, (f) Issodun, (g) Troyes Barbarey Saint Sulpice and (h) Rots. Bars are ensemble means based on five bias-adjusted CMIP6 global climate models (GCMs) for SSP5-2.6, with a fixed wheat anthesis on 1st June and grain filling in June and July.

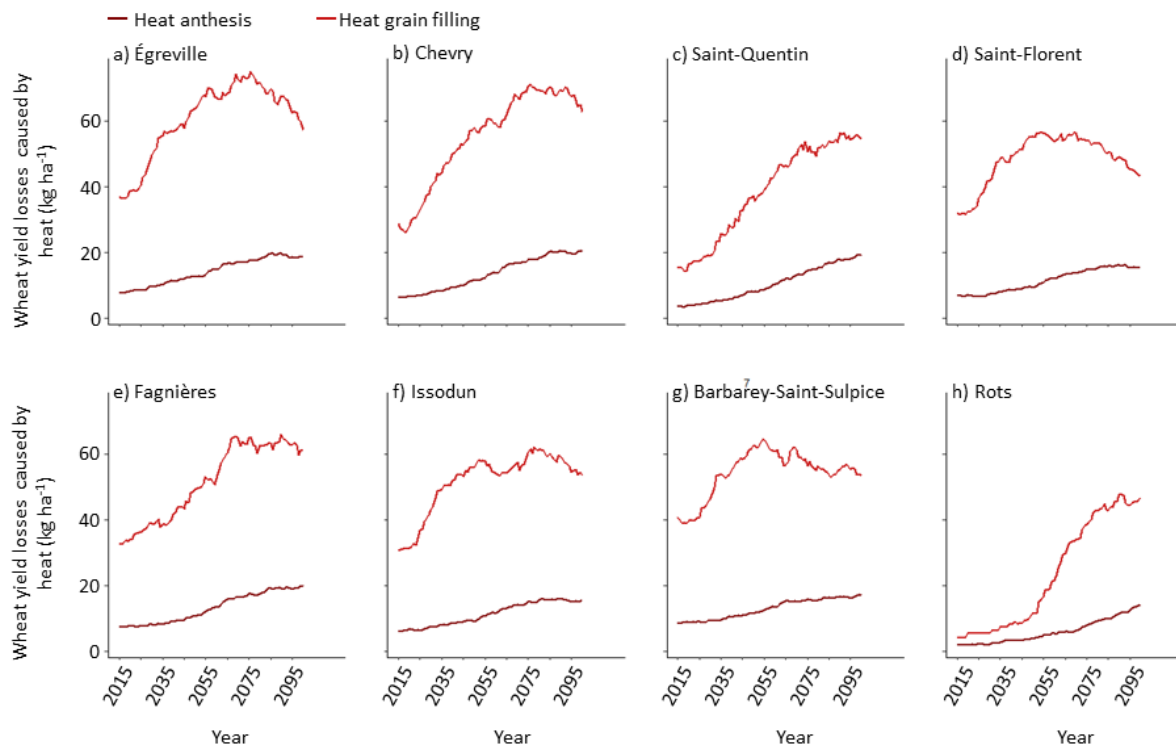


Figure S7. Projected wheat yield losses due to heat at anthesis and grain filling. Projected wheat yield losses due to heat from 2015 to 2100 for (a) Égreville, (b) Chevry, (c) Saint Quentin, (d) Saint Florent, (e) Fagnières, (f) Issodun, (g) Troyes Barbarey Saint Sulpice and (h) Rots. Lines are ensemble means based on five bias-adjusted CMIP6 global climate models (GCMs) for SSP5-8.5, with a fixed wheat anthesis in 1st June and grain filling in June and July.

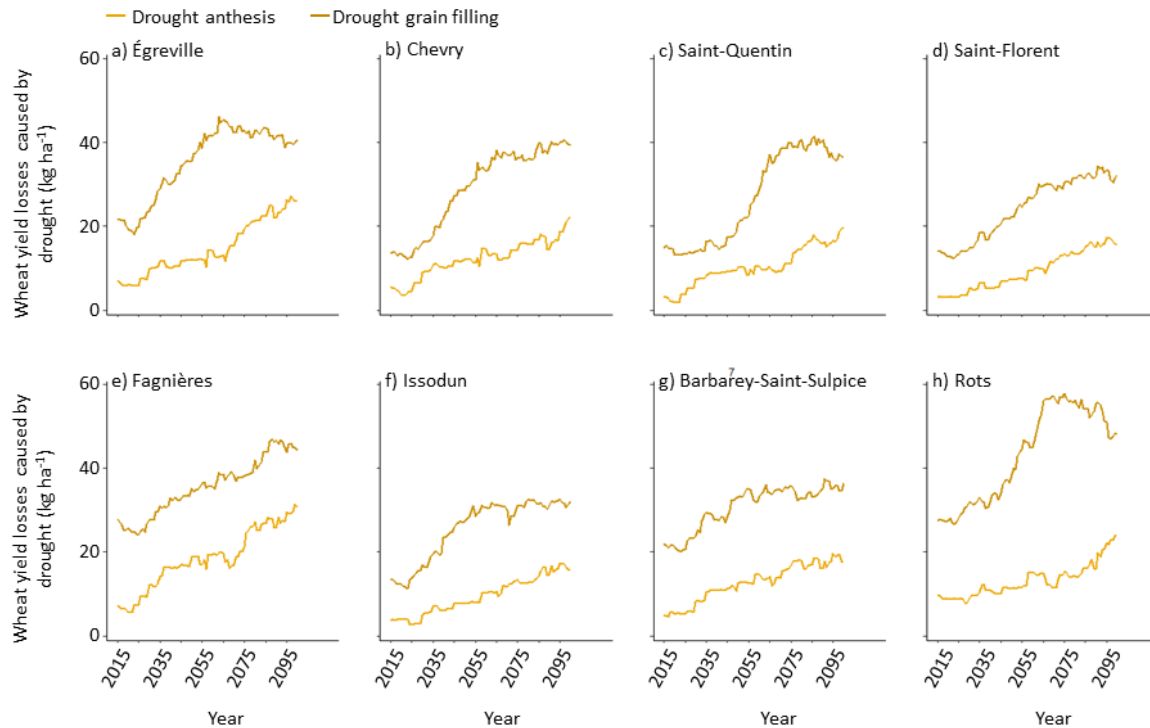


Figure S8. Projected wheat yield losses due to drought at anthesis and grain filling. Projected wheat yield losses due to drought from 2015 to 2100 for (a) Égreville, (b) Chevry, (c) Saint Quentin, (d) Saint Florent, (e) Fagnières, (f) Issodun, (g) Troyes Barbarey Saint Sulpice and (h) Rots. Lines are ensemble means based on five bias-adjusted CMIP6 global climate models (GCMs) for SSP5-8.5, with a fixed wheat anthesis in 1st June and grain filling in June and July.

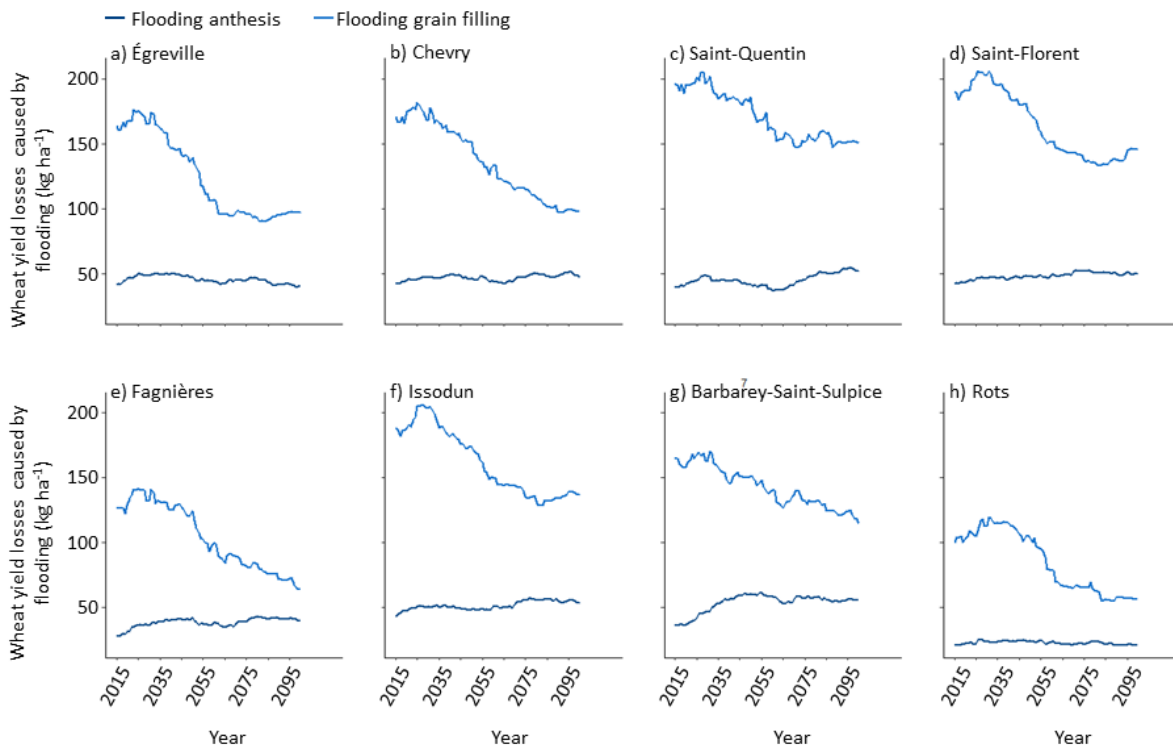


Figure S9. Projected wheat yield losses due to flooding at anthesis and grain filling. Projected wheat yield losses due to flooding from 2015 to 2100 for (a) Égreville, (b) Chevry, (c) Saint Quentin, (d) Saint Florent, (e) Fagnières, (f) Issodun, (g) Troyes Barbarey Saint Sulpice and (h) Rots. Lines are ensemble means based on five bias-adjusted CMIP6 global climate models (GCMs) for SSP5-8.5, with a fixed wheat anthesis in 1st June and grain filling in June and July.

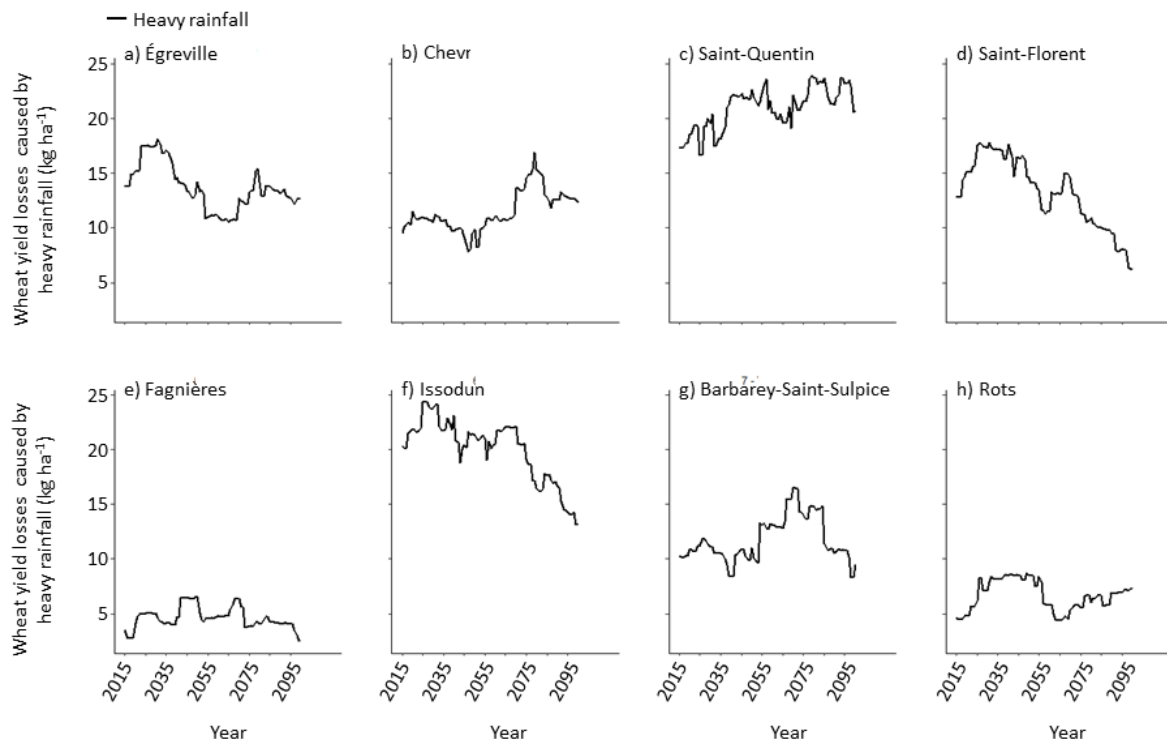


Figure S10. Projected wheat yield losses due to heavy rainfall at anthesis. Projected wheat yield losses due to heavy rainfall from 2015 to 2100 for (a) Égreville, (b) Chevry, (c) Saint Quentin, (d) Saint Florent, (e) Fagnieres, (f) Issodun, (g) Troyes Barbarey Saint Sulpice and (h) Rots. Lines are ensemble means based on five bias-adjusted CMIP6 global climate models (GCMs) for SSP5-8.5, with a fixed wheat anthesis in 1st June.

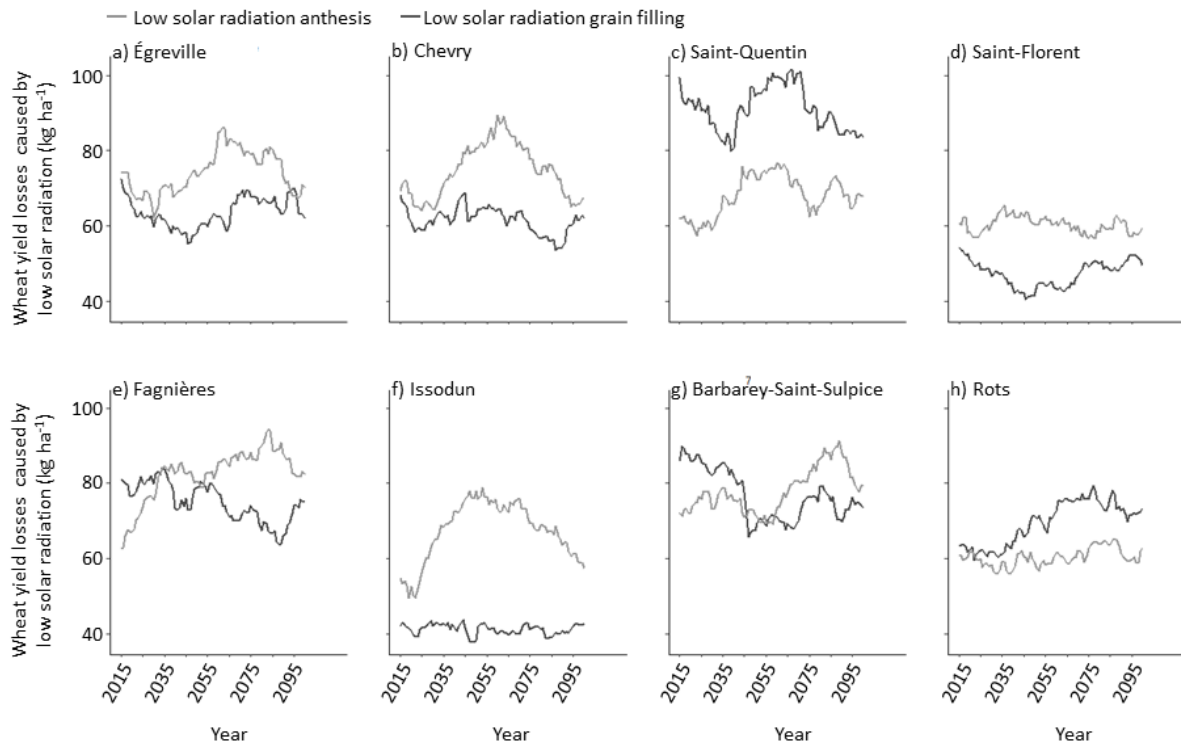


Figure S11. Projected wheat yield losses due to low solar radiation at anthesis and grain filling. Projected wheat yield losses due to low solar radiation from 2015 to 2100 for (a) Égreville, (b) Chevry, (c) Saint Quentin, (d) Saint Florent, (e) Fagnières, (f) Issodun, (g) Troyes Barbarey Saint Sulpice and (h) Rots. Lines are ensemble means based on five bias-adjusted CMIP6 global climate models (GCMs) for SSP5-8.5, with a fixed wheat anthesis in 1st June and grain filling in June and July.

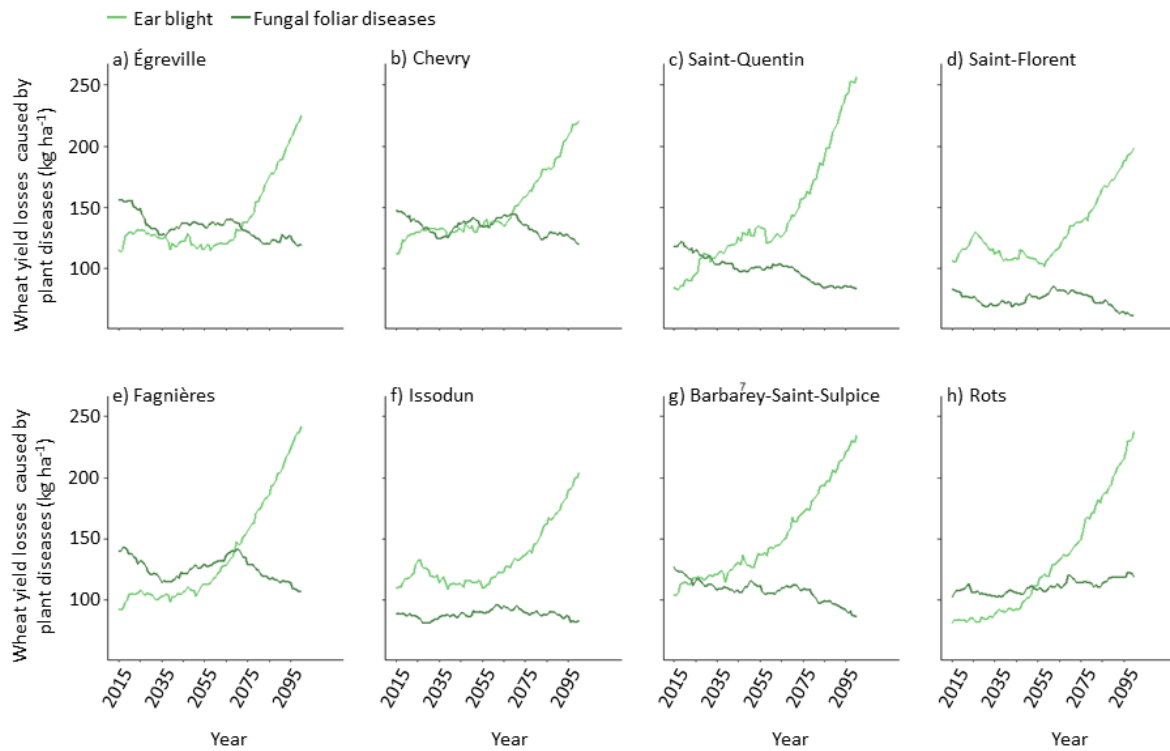


Figure S12. Projected wheat yield losses due to ear blight and fungal foliar diseases. Projected wheat yield losses due to ear blight and fungal foliar diseases from 2015 to 2100 for (a) Égreville, (b) Chevry, (c) Saint Quentin, (d) Saint Florent, (e) Fagnières, (f) Issodun, (g) Troyes Barbarey Saint Sulpice and (h) Rots. Lines are ensemble means based on five bias-adjusted CMIP6 global climate models (GCMs) for SSP5-8.5, with a fixed wheat anthesis in 1st June and grain filling in June and July.

2.2 Supplementary Results - Wheat anthesis date on 15th May

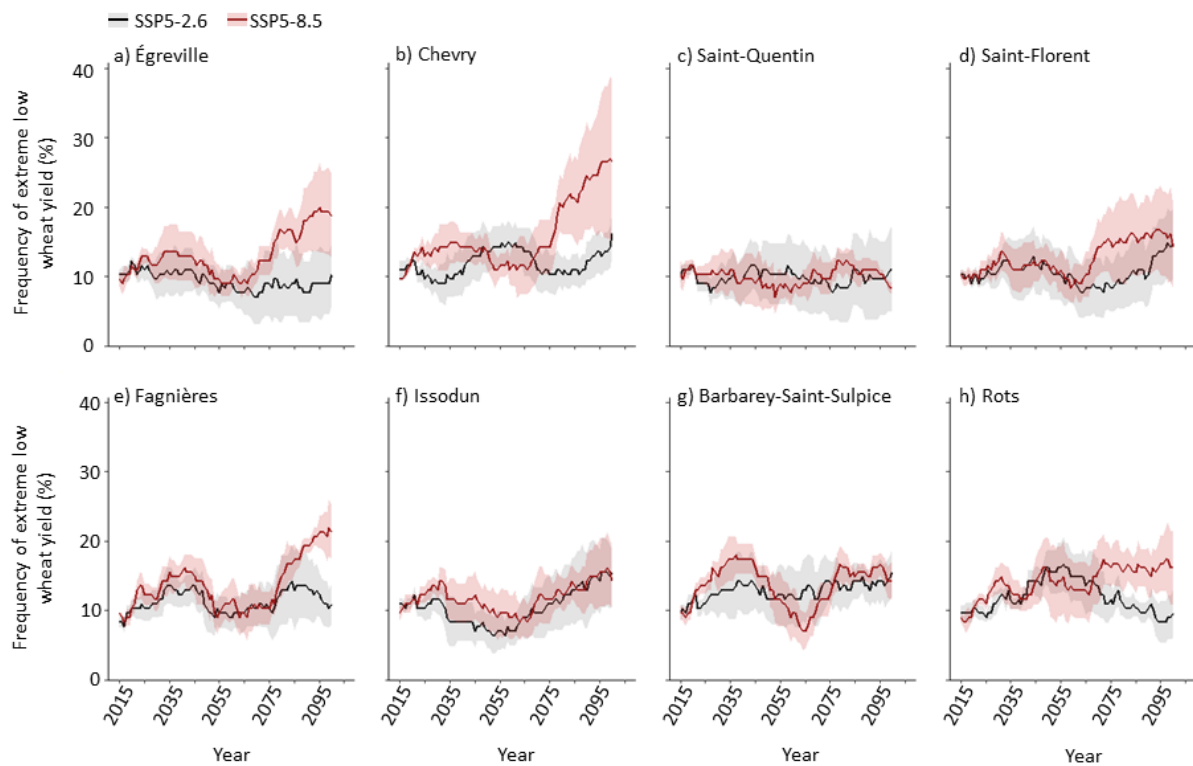


Figure S13. Projected frequency of extreme low wheat yield years in the breadbasket of France with fixed wheat anthesis on 15th May. Estimated 30 years running mean frequency of extreme low wheat production under SSP5-2.6 (black trace) and SSP5-8.5 (red trace) from 2015 to 2100, for (a) Égreville, (b) Chevry, (c) Saint Quentin, (d) Saint Florent, (e) Fagnieres, (f) Issodun, (g) Troyes Barbarey Saint Sulpice and (h) Rots. Lines are ensemble means based on five CMIP6 GCMs (lines) and shading shows ± 1 s.e.

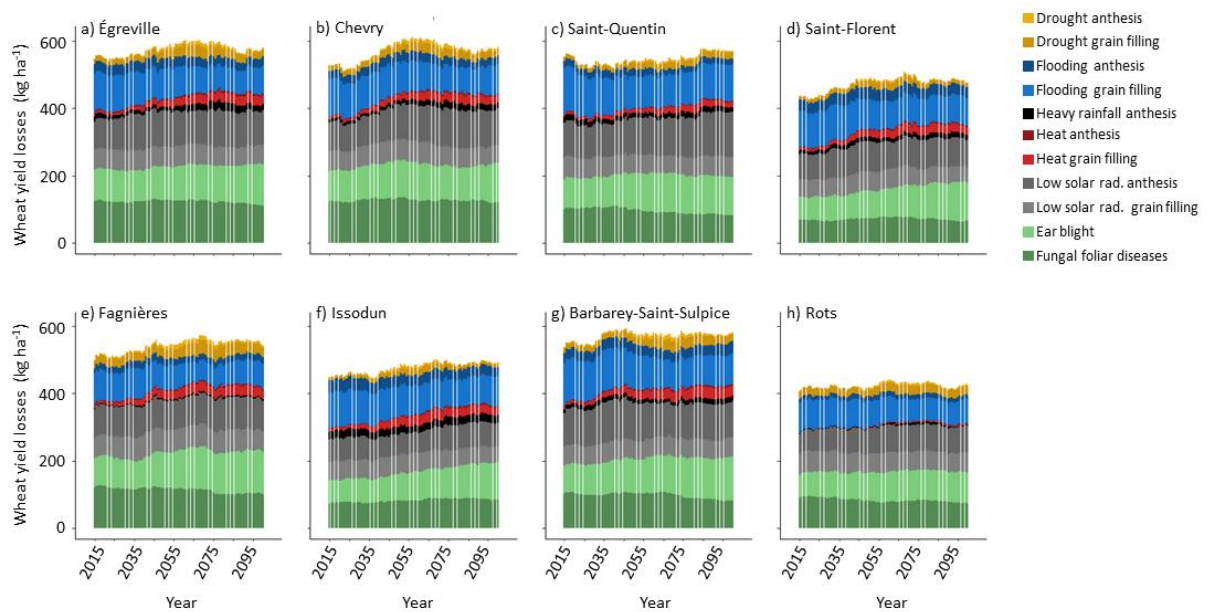


Figure S14. Projected future causes of wheat yield losses in the breadbasket of France for SSP5-2.6, with fixed wheat anthesis on 15th May. Projected wheat yield losses causes from 2015 to 2100 for (a) Égreville, (b) Chevry, (c) Saint Quentin, (d) Saint Florent, (e) Fagnieres, (f) Issodun, (g) Troyes Barbarey Saint Sulpice and (h) Rots. Bars are ensemble means based on five bias-adjusted CMIP6 global climate models (GCMs) for SSP5-2.6, with a fixed wheat anthesis on 15th May and grain filling from 15th May to 31st June.

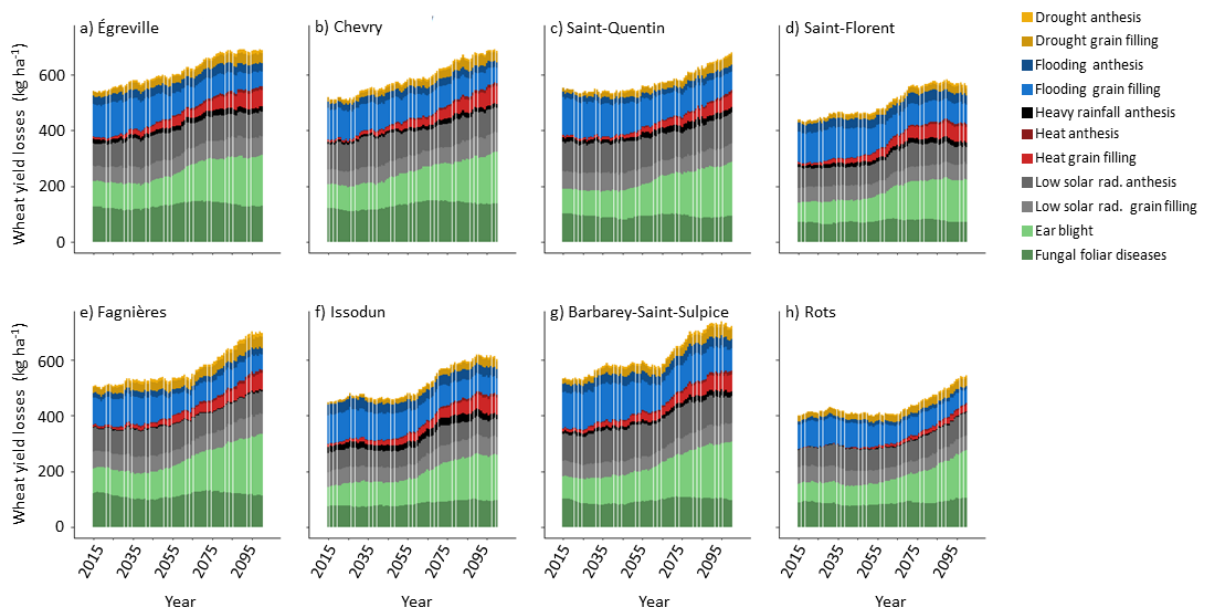


Figure S15. Projected future causes of wheat yield losses in the breadbasket of France for SSP5-8.5, with fixed wheat anthesis on 15th May. Projected wheat yield losses causes from 2015 to 2100 for (a) Égreville, (b) Chevry, (c) Saint Quentin, (d) Saint Florent, (e) Fagnieres, (f) Issodun, (g) Troyes Barbarey Saint Sulpice and (h) Rots. Bars are ensemble means based on five bias-adjusted CMIP6 global climate models (GCMs) for SSP5-8.5, with a fixed wheat anthesis on 15th May and grain filling from 15th May to 31st June.

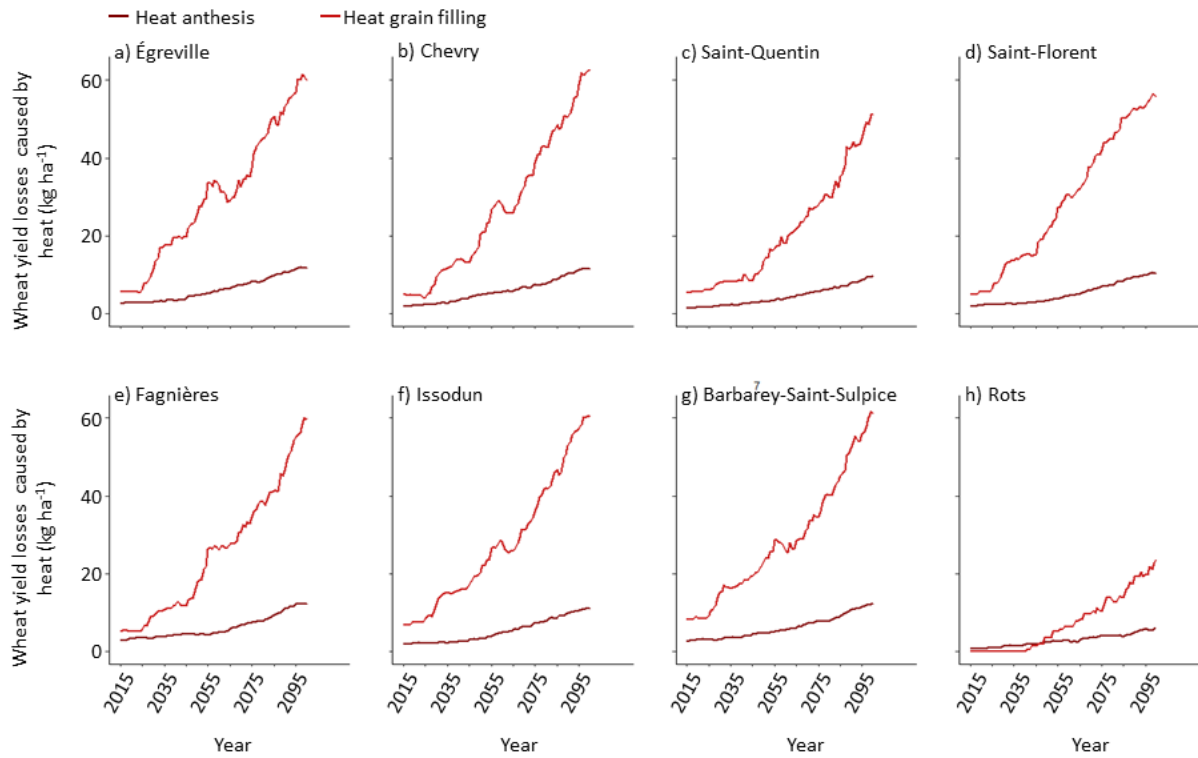


Figure S16. Projected wheat yield losses due to heat at anthesis and grain filling, with wheat anthesis on 15th May. Projected wheat yield losses due to heat from 2015 to 2100 for (a) Égreville, (b) Chevry, (c) Saint Quentin, (d) Saint Florent, (e) Fagnieres, (f) Issodun, (g) Troyes Barbarey Saint Sulpice and (h) Rots. Lines are ensemble means based on five bias-adjusted CMIP6 global climate models (GCMs) for SSP5-8.5, with a fixed wheat anthesis on 15th May and grain filling from 15th May to 31st June.

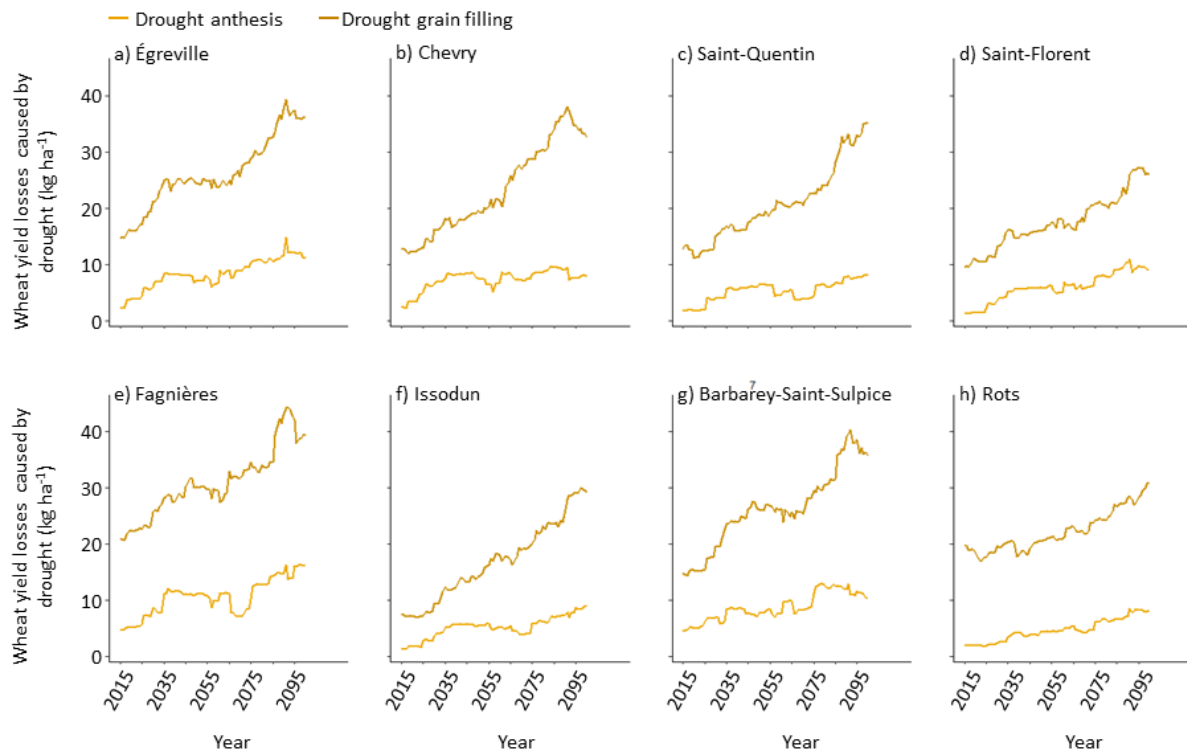


Figure S17. Projected wheat yield losses due to drought at anthesis and grain filling, with wheat anthesis on 15th May. Projected wheat yield losses due to drought from 2015 to 2100 for (a) Égreville, (b) Chevry, (c) Saint Quentin, (d) Saint Florent, (e) Fagnieres, (f) Issodun, (g) Troyes Barbarey Saint Sulpice and (h) Rots. Lines are ensemble means based on five bias-adjusted CMIP6 global climate models (GCMs) for SSP5-8.5, with a fixed wheat anthesis on 15th May and grain filling from 15th May to 31st June.

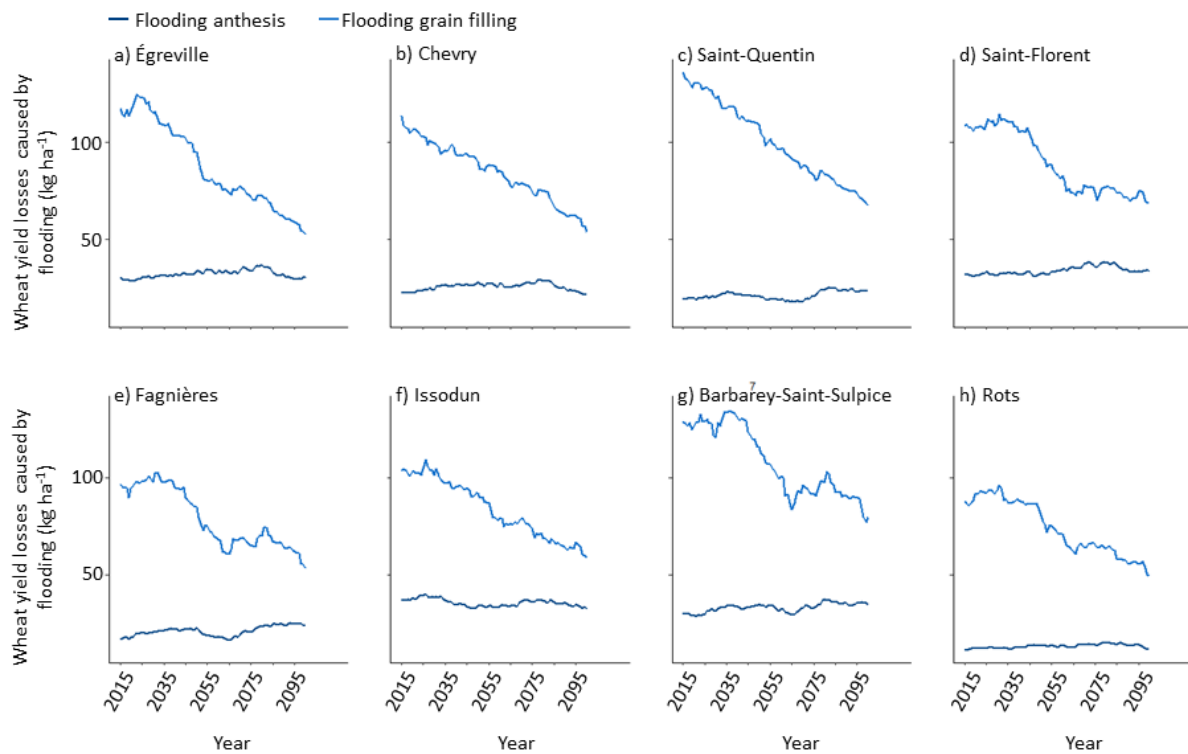


Figure S18. Projected wheat yield losses due to flooding at anthesis and grain filling, with wheat anthesis on 15th May. Projected wheat yield losses due to flooding from 2015 to 2100 for (a) Égreville, (b) Chevry, (c) Saint Quentin, (d) Saint Florent, (e) Fagnieres, (f) Issodun, (g) Troyes Barbarey Saint Sulpice and (h) Rots. Lines are ensemble means based on five bias-adjusted CMIP6 global climate models (GCMs) for SSP5-8.5, with a fixed wheat anthesis on 15th May and grain filling from 15th May to 31st June.

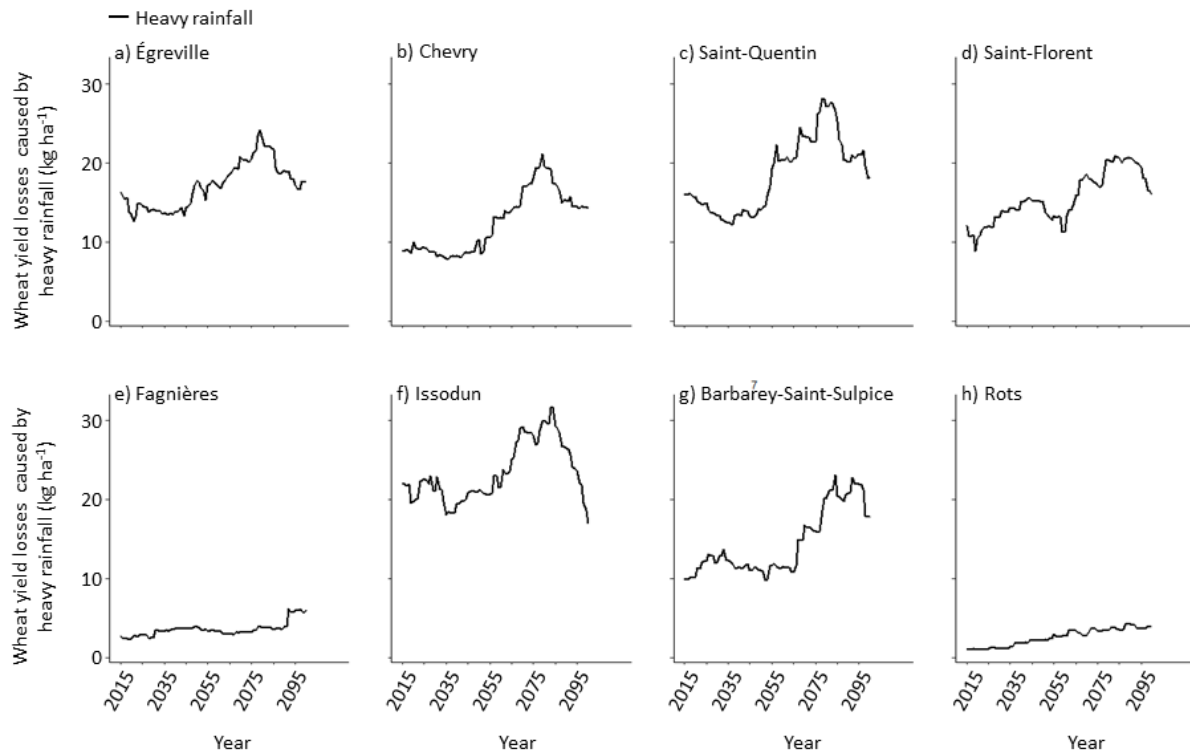


Figure S19. Projected wheat yield losses due to heavy rainfall at anthesis, considering anthesis on 15th May. Projected wheat yield losses due to heat from 2015 to 2100 for (a) Égreville, (b) Chevry, (c) Saint Quentin, (d) Saint Florent, (e) Fagnieres, (f) Issodun, (g) Troyes Barbarey Saint Sulpice and (h) Rots. Lines are ensemble means based on five bias-adjusted CMIP6 global climate models (GCMs) for SSP5-8.5, with a fixed wheat anthesis on 15th May.

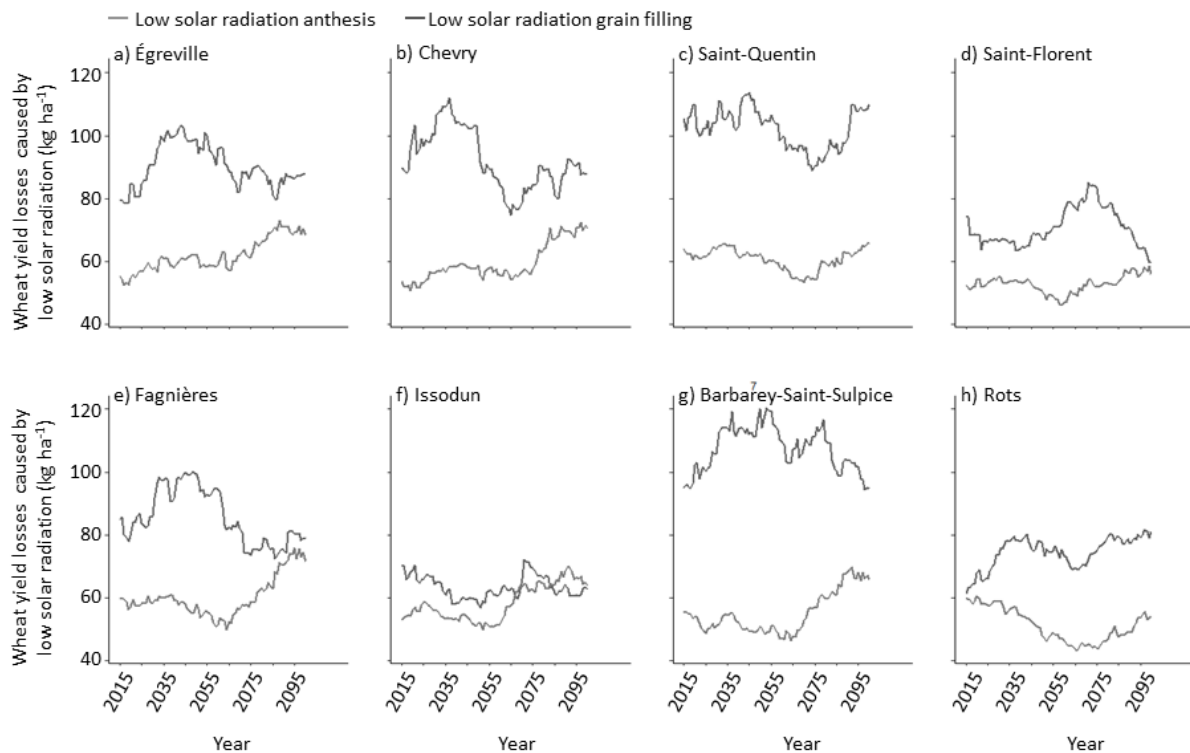


Figure S20. Projected wheat yield losses due to low solar radiation at anthesis and grain filling, with wheat anthesis on 15th May. Projected wheat yield losses due to low solar radiation from 2015 to 2100 for (a) Égreville, (b) Chevry, (c) Saint Quentin, (d) Saint Florent, (e) Fagnieres, (f) Issodun, (g) Troyes Barbarey Saint Sulpice and (h) Rots. Lines are ensemble means based on five bias-adjusted CMIP6 global climate models (GCMs) for SSP5-8.5, with a fixed wheat anthesis on 15th May and grain filling from 15th May to 31st June.

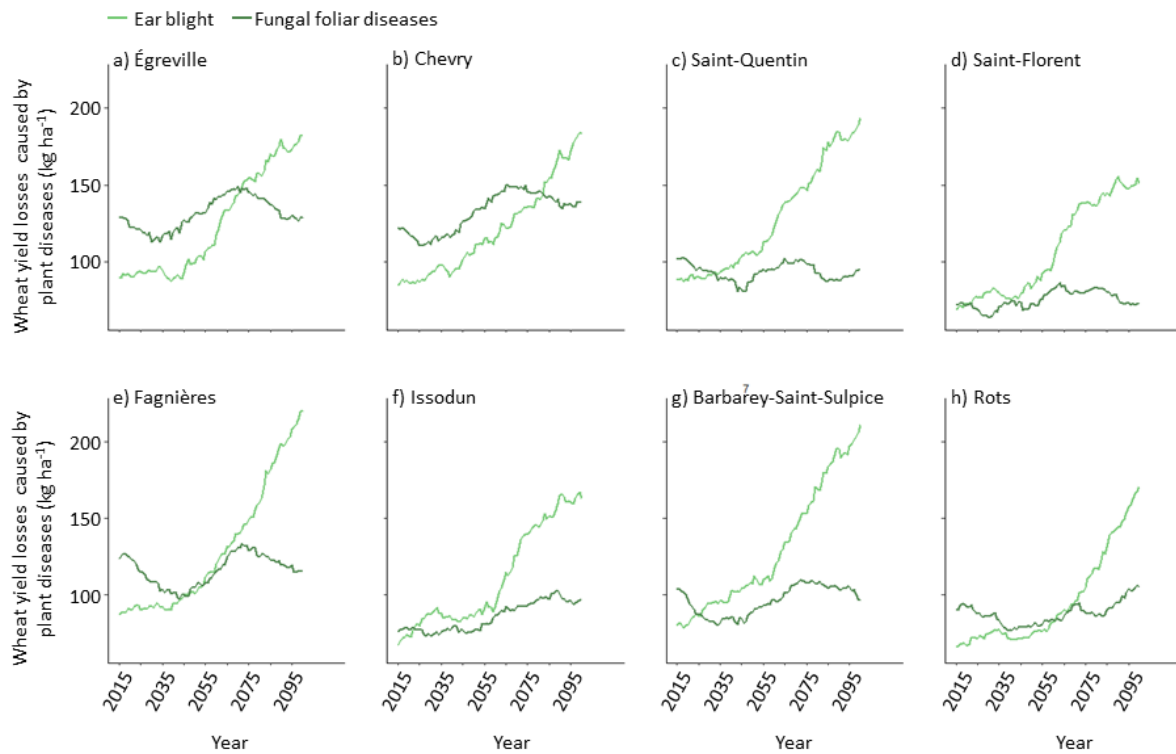


Figure S21. Projected wheat yield losses due to ear blight and fungal foliar diseases, with wheat anthesis on 15th May. Projected wheat yield losses due to ear blight and fungal foliar diseases from 2015 to 2100 for (a) Égreville, (b) Chevry, (c) Saint Quentin, (d) Saint Florent, (e) Fagnieres, (f) Issodun, (g) Troyes Barbarey Saint Sulpice and (h) Rots. Lines are ensemble means based on five bias-adjusted CMIP6 global climate models (GCMs) for SSP5-8.5, with a fixed wheat anthesis on 15th May and grain filling from 15th May to 31st June.

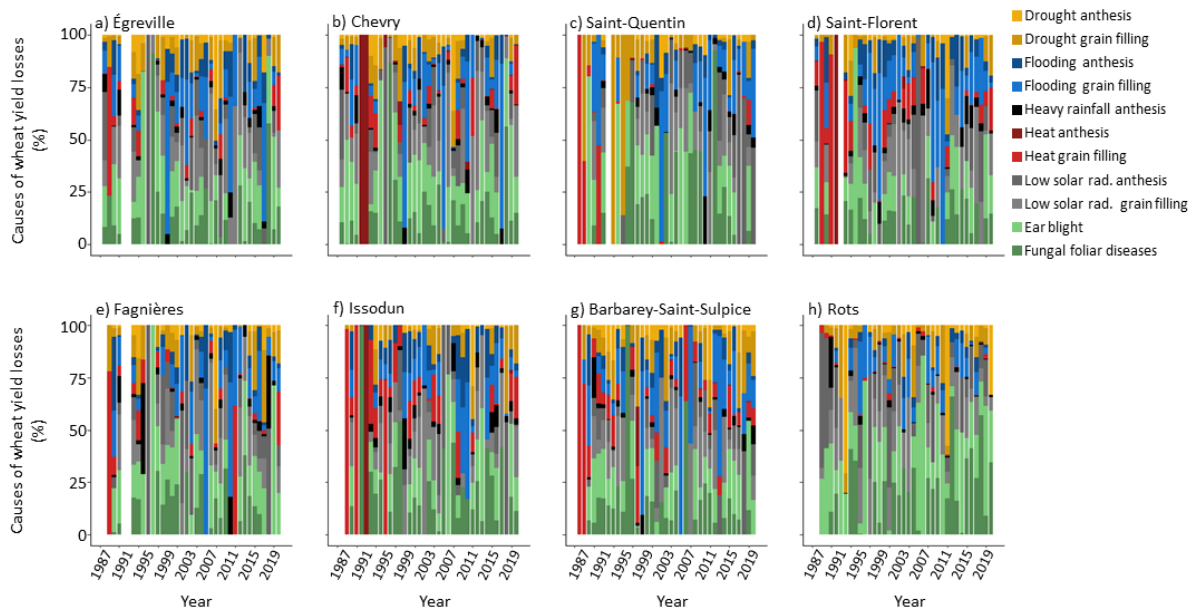
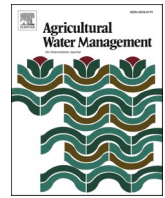


Figure S22. Decomposed wheat yield losses cause in the breadbasket of France in percentage. The yield losses are relative to the average of estimated trend-corrected wheat for 37 cropping seasons from 1984 to 2020 in each of the locations of (a) Égreville, (b) Chevry, (c) Saint Quentin, (d) Saint Florent, (e) Fagnières, (f) Issodun, (g) Troyes Barbarey Saint Sulpice and (h) Rots. The percentage is calculated by dividing the estimated yield losses by each of the factors by their sum.



Short communication

A call to action for global research on the implications of waterlogging for wheat growth and yield

Rogério de S. Nóia Júnior^{a,*}, Senthold Asseng^a, Margarita García-Vila^b, Ke Liu^{c,d},
Valentina Stocca^a, Murilo dos Santos Vianna^e, Tobias K.D. Weber^f, Jin Zhao^g, Taru Palosuo^h,
Matthew Tom Harrison^d

^a Technical University of Munich, Department of Life Science Engineering, Digital Agriculture, HEF World Agricultural Systems Center, Freising, Germany

^b Instituto de Agricultura Sostenible, CSIC, Córdoba, Spain

^c MARA Key Laboratory of Sustainable Crop Production in the Middle Reaches of the Yangtze River (Co-construction by Ministry and Province) /School of Agriculture, Yangtze University, Jingzhou, China

^d Tasmanian Institute of Agriculture, University of Tasmania, Newnham, Launceston, Tasmania 7248, Australia

^e Institute of Crop Science and Resource Conservation (INRES), University of Bonn, Bonn, Germany

^f Section of Soil Science, University of Kassel, Witzenhausen, Germany

^g College of Resources and Environmental Sciences, China Agricultural University, Beijing, China

^h Natural Resources Institute Finland (Luke), Helsinki, Finland

ARTICLE INFO

Handling Editor: Dr. B.E. Clothier

Keywords:

Climate extremes
Crop simulation models
Flooding
Soil water
Waterlogging

ABSTRACT

Waterlogging affects millions of hectares traditionally used for food production every year. Despite this, existing literature and process-based frameworks enabling simulation of waterlogging are sparse. Here, we reveal a lack of field experiments that have enumerated effects of waterlogging on plant growth. We call for more research on waterlogging, particularly in controlled field conditions with quantified soil properties and continuous monitoring of soil moisture. We opine that future experiments should explicitly focus on the impact of waterlogging on phenology, root development, and water and nutrient uptake, including interactions with atmospheric CO₂ concentration, temperature and other biotic/abiotic stresses. Such experimental data could then be used to develop waterlogging algorithms for crop models. Greater understanding of how waterlogging impacts on plant physiology will be conducive to more robust projections of how climate change will impact on global food security.

1. Wheat and waterlogging

Global annual consumption of wheat is over 780 million tonnes (Mt) of which 79% is used for seed, food and industry (human consumption) (USDA PSD, 2022). Wheat production failures (whether local or wide-spread) may provoke increasing wheat commodity prices. Shortages in wheat production have been caused by high costs or low commodity prices (Nóia Júnior et al., 2021; Snow et al., 2021), wars (Nóia Júnior et al., 2022), and increasingly by extreme weather events (Ben-Ari et al., 2018; Nóia Júnior et al., 2023; Webber et al., 2020, 2018). Waterlogging due to heavy rainfall and flooding is one of the main causes of wheat production losses (Zampieri et al., 2017).

Waterlogging is caused by intense or sustained rainfall or irrigation, poor soil hydraulic conductivity or drainage, lateral water flows or rising

water tables, and may lead to direct and indirect negative impacts on crop productivity (Liu et al., 2020a). Waterlogging results in anoxic soil conditions, and anoxia or hypoxia in the plant roots (Colmer and Greenway, 2011; Kotula et al., 2015), inhibiting root growth and thus subsequent absorption and transport of nutrients to the shoot (Colmer and Voesenek, 2009). In extreme cases, anoxia may induce (partial) root death (Herzog et al., 2016). Reduction of root front velocity (Ebrahimi-Mollabashi et al., 2019) together with increased nutrient leaching (due to excessive soil water drainage) may cause nutrient deficit stress (Kaur et al., 2020; Salazar et al., 2014). Even under non-nutrient deficit conditions, waterlogging limits root water conductivity causing stomatal closure and reducing CO₂ within the leaves, ultimately restricting photosynthesis and crop growth (Else et al., 2001; Jitsuyama, 2017). Waterlogging favors occurrence of plant diseases and plant lodging

* Corresponding author.

E-mail address: rogerio.noia@tum.de (R.S. Nóia Júnior).

(Hamada et al., 2011; Nguyen et al., 2016). Globally, the impacts from waterlogging are estimated to affect 15–20% of global wheat cropping regions each year (Kaur et al., 2020; Sayre et al., 1994).

Recent studies have shown that waterlogging could be catastrophic with the changing climate in some regions (Liu et al., 2023). For example, many wheat cropping regions in southern Asia and western Europe are more prone to waterlogging than to drought (Zampieri et al., 2017). High incidences of localized extreme rainfall increased waterlogging intensity and occurrence in the Indus river basins, which accounts for 96% of crop production in Pakistan and 26% in India (Kulkarni et al., 2021). The yield of wheat crops grown in central China has been declining due to increased frequencies of extreme weather events driven by current climate change, including flash flooding and seasonal waterlogging stresses (Liu et al., 2022b; Yan et al., 2022). In

fact, extreme events cause a 10% wheat yield loss every two years in central China (Yan et al., 2022). In France, the fourth largest wheat-exporting country in the world, waterlogging caused by excessive precipitation during spring has been identified as the main factor influencing wheat yields since the first half of the 20th Century (Ceglar et al., 2020). In 2016, France experienced the biggest wheat production failure since 1960. This was caused, in addition to other effects, by an extended period of precipitation during the winter and spring, leading to the simultaneous occurrence of yield-reducing factors (Ben-Ari et al., 2018), including heavy rainfall, crop diseases, low solar radiation and waterlogging (Ben-Ari et al., 2018; N6ia J6nior et al., 2023). High winter and spring rainfalls leading to the increased duration and spatial coverage of waterlogging caused significant wheat production failures also in the Netherlands, Belgium, Switzerland and some parts of

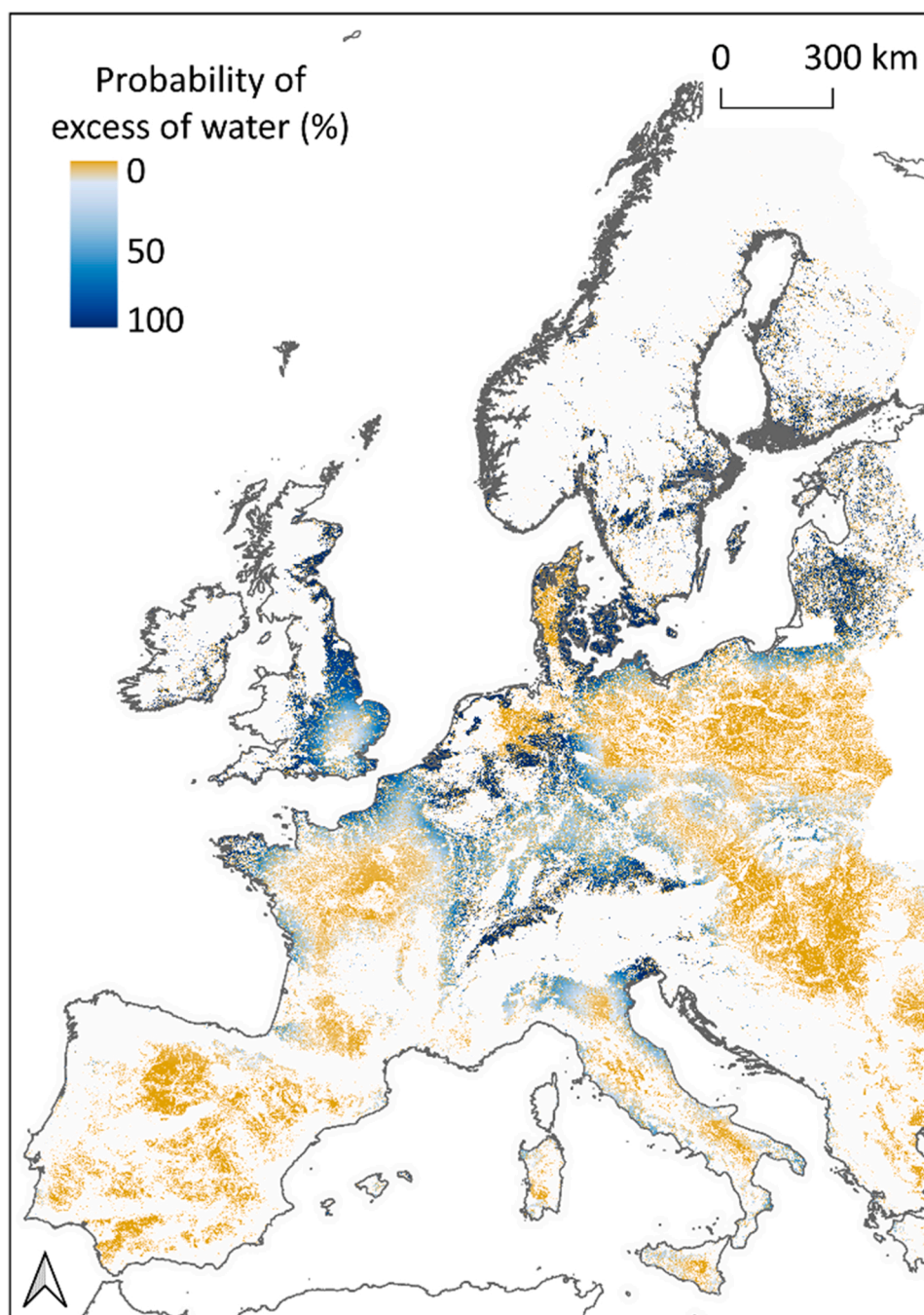


Fig. 1. Probability of excess water during spring in non-irrigated arable lands in Europe. The probability of excess water is the relation between the number of days from April to June (period of wheat anthesis and grain filling in central-southern Europe and wheat establishment in northern Europe) in which cumulative daily Rainfall - ETo is > 30 mm, with ETo being the reference evapotranspiration (Supplementary Fig S1). The probability of excess water was calculated for daily time steps from April to June from 1984 to 2022, and the average of this period is shown. No excess water occurrence is considered for locations where sand content is $\geq 70\%$ in soils (Supplementary Fig S2 and Fig S3). Climate data are from the NASAPower (Team, 2021), with a spatial resolution of 0.5 deg \times 0.625 deg (Team, 2021). The arable land mask is based on CORINE Land Cover 2020 (CLC, 2020) (Supplementary Fig S4).

Germany and England in 2016 (Nóia Júnior et al., 2023). In Europe, overall, central and northern regions have the highest chance of excess water occurrence in spring, during wheat anthesis and grain filling (Fig. 1).

Effects of the climate change crisis on crop production have been documented increasingly (Battisti and Naylor, 2009; Liu et al., 2016; Lobell and Field, 2007; Zhao et al., 2017), particularly after the first IPCC Assessment Report in 1990 (IPCC, 1990). The evidence for changes in frequencies and intensities of extremes such as heatwaves, heavy precipitation, droughts and tropical cyclones has strengthened over the past decade. Over the past 15 years (2008–2023) more than 56000 studies with the term “wheat” and “heat”, and over 26000 with “wheat and drought” have been published on ScienceDirect. In contrast, 2000 studies have been reported on wheat and waterlogging (our search considered all articles that have these terms in the abstract, title, keywords, or the main text including experimental and modeling studies). Compared with drought and heat stress, the negative impacts of waterlogging on wheat growth have received less scientific attention, although it may lead to comparable yield losses (International Food Policy Research Institute, 2022; Liu et al., 2022a). In addition, the state of the art of modeling waterlogging in the soil-plant system is rudimentary and simplistic (Liu et al., 2020b). Here, using wheat crop models as an example, we present a brief overview of how different process-based wheat crop simulation models (CSM) simulate waterlogging impacts on wheat growth and recent experimental studies for waterlogging on wheat growth. We outline the gaps associated with controlled experiments regarding the impact of waterlogging on wheat that may support crop model development and improvement for a more comprehensive assessment of waterlogging impacts on wheat under climate change.

2. Wheat crop simulation models and waterlogging

Some CSMs were built to first simulate the potential yield of crops (i.e. the yield of a crop when grown without water, nutrient and biotic stress (van Ittersum and Cassman, 2013)). Thus, yield potential is primarily driven by solar radiation, temperature and atmospheric CO₂ concentration (van Ittersum and Cassman, 2013). Simultaneously with the simulation of yield potential, CSMs compute stress factors (mainly non-optimal temperature, water and nitrogen deficit) based on the observed weather, soil data, crop management, and the current stage of crop development (Webber et al., 2022). These computed stress factors

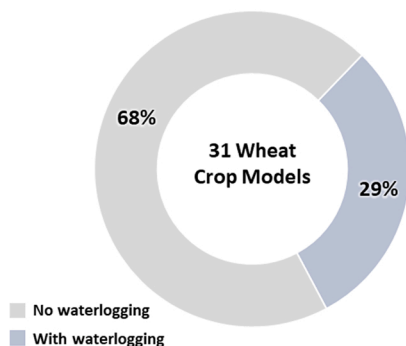
are used to reduce the potential rates of crop growth and development, leading to the simulation of crop yields limited by water and nutrient (van Ittersum and Cassman, 2013). Reducing factors such as biotic stresses due to pests and diseases, frost, hail, high windspeeds and waterlogging are generally not included in CSMs.

We assessed 31 CSMs that have been extensively studied in the AgMIP (Agricultural Model Intercomparison and Improvement Project (Rosenzweig et al., 2013)) wheat projects (Asseng et al., 2013). Only one-third (29%, i.e. 9 out of 31) of the wheat CSMs consider the effects of waterlogging on simulated wheat growth (Fig. 2). Of the nine wheat crop models that consider waterlogging impacts on wheat, five have approaches to reduce wheat transpiration under waterlogged conditions, which indirectly limits root water conductivity and affects water supply to the canopy (Shaw et al., 2013). In addition, waterlogging is also considered to directly reduce photosynthesis (or dry biomass accumulation) in four CSMs, leaf area index (LAI) and root growth in three CSMs and dry biomass partitioning in two CSM (Fig. 2b).

The APSIM-Wheat (Asseng et al., 1997) and the DSSAT-Nwheat (Kassie et al., 2016) crop models cover waterlogging impacts on the wheat LAI and root activity. Recently, a new mechanism that directly affects wheat photosynthesis in response to waterlogging was added to APSIM-Wheat (Liu et al., 2021b; Yan et al., 2022) (Table 1). The AQUACROP (Raes et al., 2018) model, as well as Infocrop (Aggarwal et al., 2006), GLAM (Li et al., 2016) and WOFOST (Githui et al., 2022; Liu et al., 2020b) crop models, represent yield impacts by waterlogging using an indirect effect of reduced transpiration. Similarly, the Hermes crop model (Kersebaum, 2007) considers a reduction of transpiration but together with a direct reduction of photosynthesis due to waterlogging. The EPIC (Githui et al., 2022) model considers wheat growth being affected by waterlogging via reduced photosynthesis and LAI, whereas the WheatGrow model only considers waterlogging impacts on biomass partitioning (Lv et al., 2017). Wheat phenological stage directly determines the effect waterlogging has on wheat growth in four CSMs, APSIM-Wheat, DSSAT-NWheat, Infocrop, AQUACROP and WOFOST. Indirect impacts of waterlogging on crop growth due to nitrogen deficiencies caused by nitrogen leaching from water excess are captured in some (Nóia Júnior et al., 2023).

We demonstrate that only one third of CSMs consider the impact of waterlogging on wheat, and while waterlogging impacts are simulated in different ways, there are few comparisons of which algorithms best reflect biophysical reality. Differences across CSMs in terms of processes that are modeled in waterlogged fields, indicate that observed

a) Crop models and waterlogging



b) Waterlogging impacts on wheat processes by crop models

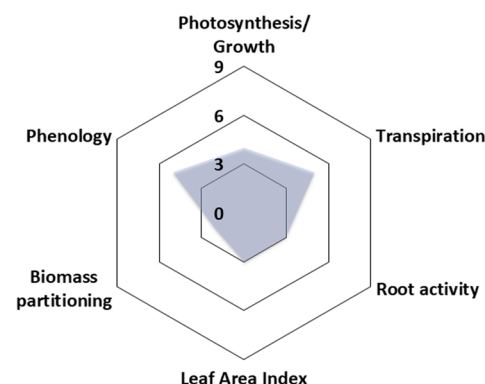


Fig. 2. Capability of wheat crop simulation models in relation to ability to simulate waterlogging. (a) Percentage of crop models with deliberate equations for accounting for the impacts of waterlogging in wheat. (b) Wheat growth processes are directly affected by waterlogging in crop simulation models. Processes of 31 crop simulation models were reviewed (from which 9 had direct routines for accounting for the impacts of waterlogging in wheat, shown in Table 1), namely APSIM-Wheat (Zheng et al., 2015), AQUACROP (Raes et al., 2018), CropSyst (Stockle et al., 1994), DAISY (Hansen, n.d.), DSSAT-CERES (Godwin et al., 1990), DSSAT-CropSim (Thorp et al., 2010), DSSAT-Nwheat (Kassie et al., 2016), EPIC (Sharpley, Villiams, 1990), EXPERT-N-CERES (Priesack, 2019), EXPERT-N-CropSim (Priesack, 2019), EXPERT-N-SPASS (Priesack, 2019),

EXPERT-N-SUCROS (Priesack, 2019), FASSET (Mette Laegdsmand, 2011), GLAM (Challinor et al., 2004), HERMES (Kersebaum, 2011), InfroCrop (Krishnan et al., 2016), LINTUL (Wolf, 2011), LPJmL (Schaphoff et al., 2018), MCWLA-Wheat (Tao et al., 2009), MONICA (Nendel et al., 2022), SALUS (Dzotsi et al., 2013), SIMPLACE (Gaiser et al., 2013), Sirius (Jamieson et al., 1998), Sirius-Quality (Martre et al., 2006), STICS (Brisson et al., 2003), WheatGrow (Guo et al., 2018), WOFOST (Wit, 2022), SIMPLE (Zhao et al., 2019), JULES-Crop (Osborne et al., 2015), AFRCWHEAT2-O3 (Porter, 1993) and BioMA (JRC, 2022).

Table 1

Wheat growth processes are directly affected by waterlogging in the eight crop simulation models that consider waterlogging effects on wheat. (-) indicates that the process is not affected by waterlogging in the crop simulation model.

Crop simulation models	Photosynthesis - Growth	Transpiration	Root activity	LAI	Biomass partitioning	Phenology	Reference
APSIM-Wheat	Yes	-	Yes	Yes	-	Yes	(Yan et al., 2022)
AQUACROP	-	Yes	Yes	-	Yes	Yes	(Raes et al., 2018)
DSSAT-NWheat	-	-	Yes	Yes	-	-	(Shelia et al., 2019)
EPIC	Yes	-	-	Yes	-	-	(Githui et al., 2022)
GLAM	-	Yes	-	-	-	-	(Li et al., 2016)
HERMES	Yes	Yes	-	-	-	-	(Kersebaum, 2007)
INFOCROP	-	Yes	-	-	-	Yes	(Aggarwal et al., 2006)
WHEATGROW	-	-	-	-	Yes	-	(Lv et al., 2017)
WOFOST	Yes	Yes	-	-	-	Yes	(Githui et al., 2022; Liu et al., 2020b)

phenomena in field experiments, so far, have yet to be adequately reflected in CSMs. It is still unclear which physiological processes are most sensitive to waterlogging and impact growth. For example, controlled experiments have shown that elevated CO₂ increases the rate of photosynthesis and reduces water loss through transpiration due to regulation of stomatal opening (Taub, 2010). From these experiments, CSMs were improved to simulate altered photosynthetic and transpiration rates due to CO₂. This model-data learning cycle is yet to be adequately conducted for waterlogging, perhaps because waterlogging involves a range of connected yet complex processes, including impacts on soil oxygen and nutrients, plant responses and recovery. Waterlogging as a phenomenon in the field is also difficult to measure and quantify and there is considerable spatial variation in its prevalence. To better understand such limitations and indicate how new experiments may be performed to guide CSMs improvements, we describe below the current status of wheat-waterlogging experiments.

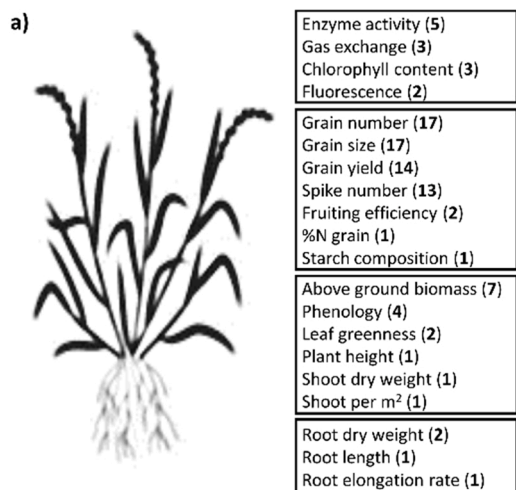
3. Controlled experiments of waterlogging impacts on wheat

Controlled experiments are the most reliable method to understand the linkage between single environmental variables (e.g. waterlogging) and crop growth. Significant relationships between wheat growth and waterlogging have been reported in the literature (Dickin and Wright, 2008; Marti et al., 2015; Olgun et al., 2008). We assessed 17 peer-reviewed published articles from 2008 to 2021 which quantified the impacts of waterlogging on wheat grain yield, grain number or grain

size in 21 controlled experiments (Supplementary Table S1). Relevant articles were found by using keywords ‘waterlogging’, ‘flooding’ or ‘excess of water’ and ‘wheat’ in Google Scholar Database (searches occurred in November 2022). In the assessed articles, waterlogging was applied in different wheat phenological stages, from seedling to grain filling with duration varying from 2 to 58 days with fully waterlogged soil (i.e. soil filled with water, with water 2 cm above the soil surface). Half of these waterlogging experiments were carried out in plastic pots (Fig. 3c). About a quarter of the experiments were performed in PVC tubes and 9% (n = 2) in field plots. One experiment was conducted in lysimeters and rhizotrons. Of all those experiments, 56% were performed in open field conditions (with no control of temperature or rainfall), 26% in greenhouses (full control of temperature and rainfall) and 9% in semi-controlled environment (with controlled rainfall). Nine percent (n = 2) of the assessed articles did not report the environmental conditions.

Wheat growth responses to waterlogging vary according to the phenological stage in which the waterlogging occurred (Liu et al., 2021a). In the assessed articles, around 20% of the experiments tested waterlogging impact on wheat growth at the beginning of wheat stem elongation or anthesis (Fig. 3). These are phenological stages highly correlated with final wheat grain yield, particularly because of the importance of stem elongation stage in defining the number of fertile florets and grain number per unit area (Fischer, 1985; Marti et al., 2015; Miralles et al., 2000), and of the period after anthesis in defining wheat grain size (Hossain et al., 2011). However, losses of grain number per

Measured growth variables in waterlogging experiments



Waterlogging treatments – phenological stages

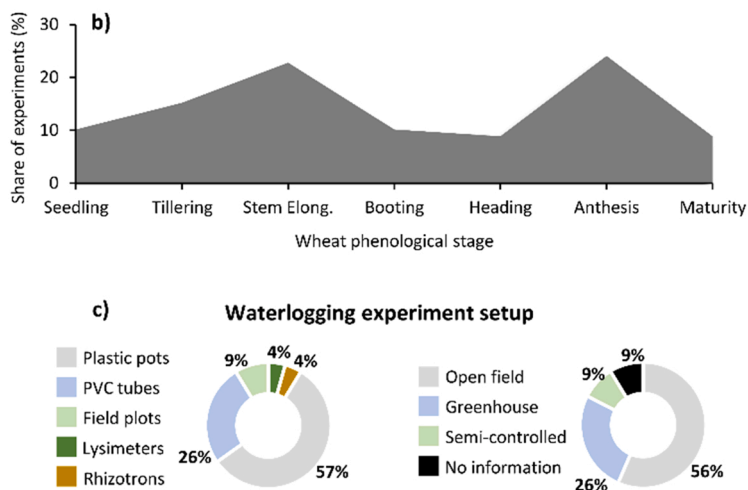


Fig. 3. Published peer-reviewed experiments on waterlogging with wheat. (a) Number of studies that reported the respectively measured wheat growth variable in waterlogging experiments (the number is shown in parentheses). (b) Percentage of experiments according to wheat phenological stages in which waterlogging treatments started. (c) Percentage of experiments with waterlogging treatments applied under different growing conditions. The data are from a total of 23 experiments reported in 17 peer-reviewed articles on the impacts of waterlogging on wheat growth, published from 2008 to 2021 (Supplementary Table S1 and Supplementary Fig S1). All experiments are in disturbed soil conditions, and with the soil completely waterlogged for a period of 4–58 days.

unit area due to waterlogging tends to be the highest before anthesis around heading (de San Celedonio et al., 2014), the phenological stage with less waterlogging experiments in the last 15 years (Fig. 3b). During emergence, tillering and maturity, wheat is less sensitive to the effects of waterlogging (de San Celedonio et al., 2014). San Celedonio et al. (2014) reported a 5% wheat yield loss due to waterlogging during seedling (due to formation of few grains) in contrast to up to 90% yield loss due to waterlogging starting at anthesis and continuing during grain filling (due to few and light grains).

Grain yield in wheat is determined by grain number per unit area and average single grain size (average grain dry mass or grain weight). These are the most measured wheat growth variables among the assessed experiments (Fig. 3a). There are a small number of experiments with measurements of indicating crop growth processes, such as gas exchange, chlorophyll content and enzyme activity. Due to the difficulty of measuring, root components are rarely measured. Above-ground biomass, which is an important indicator of wheat photosynthesis, was measured in one-third of the assessed experiments. All experiments tracked wheat phenology to start waterlogging treatments, but only one-fifth reported the impact of waterlogging on wheat phenology.

Crop waterlogging experiments are few and their experimental setups and observed variables covered do not optimally support the development of waterlogging modules of CSMs. For example, experimental studies indicate that crop phenology is delayed by waterlogging. CSMs, for the most part, simulate wheat phenology considering photo-thermal or degree-days indices, assuming driving variables of temperature and photoperiod. Thus, modifications to CSMs to correctly simulate crop delays in phenology associated with waterlogging require experiments that investigate how waterlogging interacts with phenology (particularly with the photo-thermal or degree-days indices). For this, it would be necessary to carry out experiments with waterlogging occurring at several phenological stages, with time series of the observed phenological stages, photothermal and degree-days indices. To our knowledge however, no controlled experiments have been conducted with such aims, delaying potential model-data learning cycles improving broader understanding of how plants respond to and recover from waterlogging. There thus an urgent need to describe the fundamental mechanisms between waterlogging and plant growth, so that crop modelers have a clear understanding of which mechanisms need to be prioritized. We indicate that experiments used to guide the improvement of CSMs should first provide bases for the critical testing of existing model structures and contemporary processes embedded in CSMs. Thereafter, also the experimental setups and variables measured should be assessed and modified so that they best serve effective model improvements. Additional challenges and future research needs are described in the following subsection.

4. Challenges and future research needs

The implementation and improvement of waterlogging modules in CSMs are constrained by the availability of adequate and representative data in response to waterlogging, and lack of information on critical interactions of plant growth, waterlogging and weather variables such as temperature, solar radiation, atmospheric CO₂, and others. On the other hand, controlled experiments are usually time consuming and expensive. For waterlogging experiments, more complex structures (with better soil water control) are required to keep the soil waterlogged. To overcome this, it is needed to design specific greenhouse and field experiments to derive more comprehensive understanding on which simulated processes by CSM should be improved or included to properly simulate the detrimental impacts of waterlogging on crops.

In the following, we list the identified knowledge gaps regarding the impact of waterlogging on wheat at the plant and field scales, which can be closed by dedicated controlled experiments:

(1) How does the root morphology change under waterlogging stress? Although effects such as partial root death to waterlogging are

demonstrated in the literature (Herzog et al., 2016), further research is essential to improve the representation of waterlogging impacts on roots in CSMs. For instance, the number of days under waterlogging after which root death occurs, or the maximum proportion of roots having died (with respect to the total amount of roots), or that become inactive due to different periods of exposure (in different phenological stages) to waterlogging need to be known. This is essential not only to simulate the direct effects of waterlogging more accurately but also its legacy effect of subsequent droughts whose effects may be more severe after a period of waterlogging having had an impact on the roots (e.g. root length density, depth distribution and others).

(2) How does waterlogging support the evolution of other biotic and abiotic stresses? It is unclear whether waterlogging combined with other stress factors [both occurring in sequence (one stress after other, e.g. waterlogging and drought) or simultaneously (e.g. waterlogging and frost or heavy rainfalls)] will have an additive, multiplicative or even compensatory impact on crop growth.

(3) How does atmospheric CO₂ and temperature interact with the effects of waterlogging? Increasing atmospheric CO₂ concentration due to climate change favors growth of C3 plants, such as wheat and barley. Elevated CO₂ increases the rate of photosynthetic carbon dioxide uptake by leaves and reduces water loss via transpiration due to the regulation of stomatal opening (Taub, 2010). However, waterlogging limits root water conductivity, causing stomatal closure and reducing CO₂ concentration within the leaves, antagonizing CO₂ effects on crops (Else et al., 2001; Jitsuyama, 2017). Therefore, it is necessary to investigate the combined effect of CO₂ and waterlogging on wheat growth, to understand in what conditions the combination may have positive or negative impacts on crop growth, photosynthetic activity and stomatal opening.

(4) What is the effect of partial waterlogging on crop growth? Waterlogging does not necessarily occur uniformly over the soil profile, but depending on soil hydraulic properties and groundwater levels and dynamics are expected to lead to different effects on the dynamic plant growth and require a strong focus on the correct representation of soil hydraulic properties. Examples are that the water table may only strongly affect the deepest soil layers or instantaneous heavy rainfalls affecting only the shallowest soil layers). Waterlogging is generally transient rather than chronic and enduring. To robustly capture such phenomena, field experiments must reflect reality, which could include partial wetting and drying in the season/s with which waterlogging occurs (typically winter and spring). This also emphasizes the importance of continuous and spatially explicit measurement data from the experiments. Such experiments could be performed with sensors that measure soil moisture at different depths (covering the entire root depth) as well as visual crop responses (e.g. through spectroscopy). Continuous measurements of photosynthetic rate and stomatal conductance would also be helpful. Roots are the interface over which the crop perceives waterlogging, thus, root activity should also be measured when possible.

(5) How resilient are different cultivars? A more systematic comparison of waterlogging responses across cultivars is required to understand the cultivars sensitivity to waterlogging and how different cultivar traits support the resilience of cultivars to waterlogging (Liu et al., 2020b).

(6) What are the spatial implications of waterlogging? Severe waterlogging may have minor implications for field-scale production if the extent of waterlogging at the field scale is minor. Spatio-temporal quantification of waterlogging (similar to the study conducted by Chen et al., 2021 at the field scale for pastures) would be valuable as a research endeavor and in scaling the extent of waterlogging from the field to higher scales (Chen et al., 2021).

(7) How does waterlogging affect the availability of plant nutrients? Waterlogging can lead to leaching of nutrients and altered biochemical processes reducing uptake (Rawnsley et al., 2019) and associated greenhouse gas emissions, such as nitrous oxide and methane.

(8) How soil waterlogging responses to engineering management practices across environments?

Engineering practices such as drainage systems, raised beds, and controlled farming tillage are expected to alleviate the negative impacts of waterlogging on wheat plants (Manik et al., 2019). Conducting research to assess the efficacy of various management practices in diverse waterlogging environments can aid farmers and agronomists in making informed decisions about the most suitable engineering practices to adopt for their wheat production systems, considering factors such as cost-effectiveness, feasibility, and local environmental conditions.

Future research on waterlogging proposed here should be done under controlled conditions, such as a greenhouse and in the field, but to better guide agricultural production practices, field validation experiments are needed. These experiments should be performed in fields with well-described physical soil profiles, such as small areas and survey pits. Soil moisture measurements, in different soil depths, are particularly important to improve the computation of waterlogged soils by CSMs. We also encourage measurements of greenhouse gases from waterlogged soil, as soil net greenhouse gas emissions tend to increase under these conditions (Liu et al., 2011). The data resulted from these potential experiments should be strongly encouraged to be made available to the scientific community via cloud-based repositories or open data journals. Only with open access to this cropping, climate, soil and management (sowing date, planting density, fertilizer and irrigation amount and date) data can be tested and used to improve CSMs.

We identified that about one third of the wheat CSMs consider the effects of waterlogging on simulated wheat growth (Fig. 3). Several multi-model ensemble and model comparison studies, such as those implemented under the AgMIP network (Rosenzweig et al., 2013), have evaluated models for a range of crops and regions by comparing outputs with observed growth and yield data, including responses to atmospheric CO₂ concentration, temperature, water shortage and water excess. Models embed different processes and when a range of models are compared using the same initialization and calibration data, insights can be gained as to which models more closely reflect the observed data, and why such results occur. In this way, deeper insight can be gained into processes that are necessary in simulating impacts of waterlogging in crops, as well as those processes that are superfluous and could be simplified or removed completely. In addition, the uncertainty due to missing processes relevant for describing waterlogging and its impacts remains unclear. These are topics that should be emphasized in future research which addresses crop simulation model development for improved representation of waterlogging. Moreover, waterlogging should be included in crop simulation models, especially those to forecast in-season wheat yield in regions where waterlogging occurs, or when assessing the impacts of climate change. To reduce uncertainty in climate impact projections and their impact on future crop production, crop models need to include the simulation the waterlogging and its impact on crop growth and yield. With this, cropping models will be able to give better indications of how to adapt to a future with more extremes arising from climate change. Due to the relevance of waterlogging impacts and the deficiencies identified in state of the art in waterlogging research, this manuscript is a call for boosting wheat waterlogging research around the world.

Declaration of Competing Interest

The authors declare that they have no known competing financial interests or personal relationships that could have appeared to influence the work reported in this paper.

Data availability

Data will be made available on request.

Acknowledgements

This study was implemented as a co-operative project under the umbrella of the Agricultural Model Intercomparison and Improvement Project (AgMIP). R.S.N.J. acknowledges support from the Prince of Albert II of Monaco foundation through the IPCC Scholarship Program. The contents of this manuscript are solely the liability of R.S.N.J. and under no circumstances may be considered as a reflection of the position of the Prince Albert II of Monaco Foundation and/or the IPCC. The time of MTH and KL were supported by the Grains Research and Development Corporation (GRDC), Project Number UOT1906–002RTX. J.Z. was supported by the Henan Key Laboratory of Agrometeorological Ensuring and Applied Technique, China Meteorological Administration, Project Number AMF202304.

Author contributions

All co-authors conceptualized the study. RSNJ performed the formal analysis. SA, TP and MTH supervised the study. RSNJ wrote initial draft, all co-authors assisted with writing and reviewed the manuscript.

Appendix A. Supporting information

Supplementary data associated with this article can be found in the online version at doi:10.1016/j.agwat.2023.108334.

References

- Aggarwal, P.K., Kalra, N., Chander, S., Pathak, H., 2006. InfoCrop: A dynamic simulation model for the assessment of crop yields, losses due to pests, and environmental impact of agro-ecosystems in tropical environments. I. Model description. *Agric. Syst.* 89, 1–25. <https://doi.org/10.1016/j.agsy.2005.08.001>.
- Asseng, S., Keating, B.A., Huth, N.I., Easthan, J., 1997. Simulation of perched water tables in a duplex soil, in: *international congress on modelling and simulation proceedings. the modelling and simulation society of Australia, Hobart, Tasmania* 538–543.
- Asseng, S., Ewert, F., Rosenzweig, C., Jones, J.W., Hatfield, J.L., Ruane, A.C., Boote, K.J., Thorburn, P.J., Rötter, R.P., Cammarano, D., Brisson, N., Basso, B., Martre, P., Aggarwal, P.K., Angulo, C., Bertuzzi, P., Biernath, C., Challinor, A.J., Doltra, J., Gayler, S., Goldberg, R., Grant, R., Heng, L., Hooker, J., Hunt, L.A., Ingwersen, J., Izaurralde, R.C., Kersebaum, K.C., Müller, C., Naresh Kumar, S., Nendel, C., O'Leary, G., Olesen, J.E., Osborne, T.M., Palosuo, T., Priesack, E., Ripoche, D., Semenov, M.A., Shcherbak, I., Steduto, P., Stöckle, C., Stratonovitch, P., Streck, T., Supit, I., Tao, F., Travasso, M., Waha, K., Wallach, D., White, J.W., Williams, J.R., Wolf, J., 2013. Uncertainty in simulating wheat yields under climate change. *Nat. Clim. Change* 3 827–832. <https://doi.org/10.1038/nclimate1916>.
- Battisti, D.S., Naylor, R.L., 2009. Historical warnings of future food insecurity with unprecedented seasonal heat. *Science* 323, 240–244. <https://doi.org/10.1126/science.1164363>.
- Ben-Ari, T., Boé, J., Ciais, P., Lecerf, R., Van der Velde, M., Makowski, D., 2018. Causes and implications of the unforeseen 2016 extreme yield loss in the breadbasket of France. *Nat. Commun.* 9, 1627. <https://doi.org/10.1038/s41467-018-04087-x>.
- Brisson, N., Gary, C., Justes, E., Roche, R., Mary, B., Ripoche, D., Zimmer, D., Sierra, J., Bertuzzi, P., Burger, P., Bussi re, F., Cabidoche, Y.M., Cellier, P., Debaeke, P., Gaudill re, J.P., H nault, C., Maraux, F., Seguin, B., Sinoquet, H., 2003. An overview of the crop model stics. *Eur. J. Agron.* 18, 309–332. [https://doi.org/10.1016/S1161-0301\(02\)00110-7](https://doi.org/10.1016/S1161-0301(02)00110-7).
- Ceglar, A., Zampieri, M., Gonzalez-Reviriego, N., Ciais, P., Schauburger, B., Van der Velde, M., 2020. Time-varying impact of climate on maize and wheat yields in France since 1900. *Environ. Res. Lett.* 15, 094039. <https://doi.org/10.1088/1748-9326/aba1be>.
- Challinor, A.J., Wheeler, T.R., Craufurd, P.Q., Slingo, J.M., Grimes, D.I.F., 2004. Design and optimisation of a large-area process-based model for annual crops. *Agric. For. Meteorol.* 124, 99–120. <https://doi.org/10.1016/j.agrformet.2004.01.002>.
- Chen, Y., Guerschman, J., Shendryk, Y., Henry, D., Harrison, M.T., 2021. Estimating pasture biomass using sentinel-2 imagery and machine learning. *Remote Sens.* <https://doi.org/10.3390/rs13040603>.
- CLC, 2020. Copernicus Land Monitoring Service [WWW Document]. CORINE Land Cover. URL <https://land.copernicus.eu/pan-european/corine-land-cover/clc-2000> (accessed 10.10.22).
- Colmer, T.D., Greenway, H., 2011. Ion transport in seminal and adventitious roots of cereals during O₂ deficiency. *J. Exp. Bot.* 62, 39–57. <https://doi.org/10.1093/jxb/erq271>.
- Colmer, T.D., Voisenek, L.A.C.J., 2009. Flooding tolerance: suites of plant traits in variable environments. *Funct. Plant Biol.* 36, 665–681.
- Dickin, E., Wright, D., 2008. The effects of winter waterlogging and summer drought on the growth and yield of winter wheat (*Triticum aestivum* L.). *Eur. J. Agron.* 28, 234–244. <https://doi.org/10.1016/j.eja.2007.07.010>.

- Dzotsi, K.A., Basso, B., Jones, J.W., 2013. Development, uncertainty and sensitivity analysis of the simple SALUS crop model in DSSAT. *Ecol. Model.* 260, 62–76. <https://doi.org/10.1016/j.ecolmodel.2013.03.017>.
- Ebrahimi-Mollabashi, E., Huth, N.I., Holzworth, D.P., Ordóñez, R.A., Hatfield, J.L., Huber, I., Castellano, M.J., Archontoulis, S.V., 2019. Enhancing APSIM to simulate excessive moisture effects on root growth. *Field Crops Res.* 236, 58–67. <https://doi.org/10.1016/j.fcr.2019.03.014>.
- Else, M.A., Coupland, D., Dutton, L., Jackson, M.B., 2001. Decreased root hydraulic conductivity reduces leaf water potential, initiates stomatal closure and slows leaf expansion in flooded plants of castor oil (*Ricinus communis*) despite diminished delivery of ABA from the roots to shoots in xylem sap. *Physiol. Plant.* 111, 46–54. <https://doi.org/10.1034/j.1399-3054.2001.1110107.x>.
- Fischer, R.A., 1985. Number of kernels in wheat crops and the influence of solar radiation and temperature. *J. Agric. Sci.* 105, 447–461 <https://doi.org/DOI:10.1017/S0021859600056495>.
- Gaiser, T., Perkons, U., Küpper, P.M., Kautz, T., Uteau-Puschmann, D., Ewert, F., Enders, A., Krauss, G., 2013. Modeling biopore effects on root growth and biomass production on soils with pronounced sub-soil clay accumulation. *Ecol. Model.* 256, 6–15. <https://doi.org/10.1016/j.ecolmodel.2013.02.016>.
- Githui, F., Beverly, C., Aiad, M., McCaskill, M., Liu, K., Harrison, M.T., 2022. Modelling waterlogging impacts on crop growth: a review of aeration stress definition in crop models and sensitivity analysis of APSIM. *Int. J. Plant Biol.* 13, 180–200. <https://doi.org/10.3390/ijpb13030017>.
- Godwin, D., Ritchie, J., Singh, U., Hunt, L., 1990. A User's Guide to CERES[®].
- Guo, C., Zhang, L., Zhou, X., Zhu, Y., Cao, W., Qiu, X., Cheng, T., Tian, Y., 2018. Integrating remote sensing information with crop model to monitor wheat growth and yield based on simulation zone partitioning. *Precis. Agric.* 19, 55–78. <https://doi.org/10.1007/s11119-017-9498-5>.
- Hamada, M.S., Yin, Y., Chen, H., Ma, Z., 2011. The escalating threat of Rhizoctonia cerealis, the causal agent of sharp eyespot in wheat. *Pest Manag. Sci.* 67, 1411–1419. <https://doi.org/10.1002/ps.2236>.
- Hansen, S., n.d. Daisy, a flexible Soil-Plant-Atmosphere system Model.
- Herzog, M., Striker, G.G., Colmer, T.D., Pedersen, O., 2016. Mechanisms of waterlogging tolerance in wheat – a review of root and shoot physiology. *Plant. Cell Environ.* 39, 1068–1086. <https://doi.org/10.1111/pce.12676>.
- Hossain, M.A., Araki, H., Takahashi, T., 2011. Poor grain filling induced by waterlogging is similar to that in abnormal early ripening in wheat in Western Japan. *Field Crops Res.* 123, 100–108. <https://doi.org/10.1016/j.fcr.2011.05.005>.
- International Food Policy Research Institute, 2022. 2022 Global food policy report: Climate change and food systems. Washington, DC. <https://doi.org/10.2499/9780896294257>.
- IPCC, 1990. Policymaker Summary of Working Group II (Potential Impacts of Climate Change).
- Jamieson, P.D., Semenov, M.A., Brooking, I.R., Francis, G.S., 1998. Sirius: a mechanistic model of wheat response to environmental variation. *Eur. J. Agron.* 8, 161–179. [https://doi.org/10.1016/S1161-0301\(98\)00020-3](https://doi.org/10.1016/S1161-0301(98)00020-3).
- Jitsuyama, Y., 2017. Hypoxia-responsive root hydraulic conductivity influences soybean cultivar-specific waterlogging tolerance. *Am. J. Plant Sci.* 08, 770–790. <https://doi.org/10.4236/ajps.2017.84054>.
- 2022 JRC, 2022. BioMA Framework [WWW Document]. SOFTWARE RESOURCES. URL <https://agri4cast.jrc.ec.europa.eu/DataPortal/Index.aspx?o=s> (accessed 9.20.22).
- Kassie, B.T., Asseng, S., Porter, C.H., Royce, F.S., 2016. Performance of DSSAT-Nwheat across a wide range of current and future growing conditions. *Eur. J. Agron.* 81, 27–36. <https://doi.org/10.1016/j.eja.2016.08.012>.
- Kaur, G., Singh, G., Motavalli, P.P., Nelson, K.A., Orlowski, J.M., Golden, B.R., 2020. Impacts and management strategies for crop production in waterlogged or flooded soils: A review. *Agron. J.* 112, 1475–1501. <https://doi.org/10.1002/agj2.20093>.
- Kersebaum, K.C., 2007. Modelling nitrogen dynamics in soil–crop systems with HERMES. *Nutr. Cycl. Agroecosystems* 77, 39–52. <https://doi.org/10.1007/s10705-006-9044-8>.
- Kersebaum, K.C., 2011. Special Features of the HERMES Model and Additional Procedures for Parameterization, Calibration, Validation, and Applications, in: *Methods of Introducing System Models into Agricultural Research, Advances in Agricultural Systems Modeling*, pp. 65–94. <https://doi.org/https://doi.org/10.2134/advagricsystemmodel2.c2>.
- Kotula, L., Clode, P.L., Striker, G.G., Pedersen, O., Läuchli, A., Shabala, S., Colmer, T.D., 2015. Oxygen deficiency and salinity affect cell-specific ion concentrations in adventitious roots of barley (*Hordeum vulgare*). *N. Phytol.* 208, 1114–1125. <https://doi.org/10.1111/nph.13535>.
- Krishnan, P., Sharma, R.K., Dass, A., Kukreja, A., Srivastav, R., Singhal, R.J., Bandyopadhyay, K.K., Lal, K., Manjiaah, K.M., Chhokar, R.S., Gill, S.C., 2016. Web-based crop model: Web InfoCrop – Wheat to simulate the growth and yield of wheat. *Comput. Electron. Agric.* 127, 324–335. <https://doi.org/10.1016/j.compag.2016.06.008>.
- Kulkarni, Anil V., Shirsat, T.S., Kulkarni, Ashutosh, Negi, H.S., Bahuguna, I.M., Thamban, M., 2021. State of Himalayan cryosphere and implications for water security. *Water Secur.* 14, 100101 <https://doi.org/10.1016/j.wasec.2021.100101>.
- Mette Laegdsmand, 2011. FASSET - Crop Simulation Model.
- Li, S., Tompkins, A.M., Lin, E., Ju, H., 2016. Simulating the impact of flooding on wheat yield – Case study in East China. *Agric. For. Meteorol.* 216, 221–231. <https://doi.org/10.1016/j.agrformet.2015.10.014>.
- Liu, B., Asseng, S., Müller, C., Ewert, F., Elliott, J., Lobell, D.B., Martre, P., Ruane, A.C., Wallach, D., Jones, J.W., Rosenzweig, C., Aggarwal, P.K., Alderman, P.D., Anothai, J., Basso, B., Biernath, C., Cammarano, D., Challinor, A., Deryng, D., Sanctis, G.D., Doltra, J., Fereres, E., Polberth, C., Garcia-Vila, M., Gayler, S., Hoogenboom, G., Hunt, L.A., Izaurralde, R.C., Jabloun, M., Jones, C.D., Kersebaum, K.C., Kimball, B.A., Koehler, A.-K., Kumar, S.N., Nendel, C., O'Leary, G. J., Olesen, J.E., Ottman, M.J., Palosuo, T., Prasad, P.V.V., Priesack, E., Pugh, T.A.M., Reynolds, M., Rezaei, E.E., Rötter, R.P., Schmid, E., Semenov, M.A., Scherbak, I., Stehfest, E., Stöckle, C.O., Stratonovitch, P., Streck, T., Supit, I., Tao, F., Thorburn, P., Waha, K., Wall, G.W., Wang, E., White, J.W., Wolf, J., Zhao, Z., Zhu, Y., 2016. Similar estimates of temperature impacts on global wheat yield by three independent methods. *Nat. Clim. Change* 6, 1130–1136. <https://doi.org/10.1038/nclimate3115>.
- Liu, K., Harrison, M.T., Shabala, S., Meinke, H., Ahmed, I., Zhang, Y., Tian, X., Zhou, M., 2020a. The state of the art in modeling waterlogging impacts on plants: what do we know and what do we need to know. *e2020EF001801 Earth's Future* 8. <https://doi.org/10.1029/2020EF001801>.
- Liu, K., Harrison, M.T., Shabala, S., Meinke, H., Ahmed, I., Zhang, Y., Tian, X., Zhou, M., 2020b. The state of the art in modeling waterlogging impacts on plants: what do we know and what do we need to know. *Earth's Future* 8. <https://doi.org/10.1029/2020EF001801>.
- Liu, K., Harrison, M.T., Archontoulis, S.V., Huth, N., Yang, R., Liu, D.L., Yan, H., Meinke, H., Huber, I., Feng, P., Ibrahim, A., Zhang, Y., Tian, X., Zhou, M., 2021a. Climate change shifts forward flowering and reduces crop waterlogging stress. *Environ. Res. Lett.* 16. <https://doi.org/10.1088/1748-9326/ac1b5a>.
- Liu, K., Harrison, M.T., Archontoulis, S.V., Huth, N., Yang, R., Liu, D.L., Yan, H., Meinke, H., Huber, I., Feng, P., Ibrahim, A., Zhang, Y., Tian, X., Zhou, M., 2021b. Climate change shifts forward flowering and reduces crop waterlogging stress. *Environ. Res. Lett.* 16, 94017. <https://doi.org/10.1088/1748-9326/ac1b5a>.
- Liu, K., Harrison, M.T., Wang, B., Yang, R., Yan, H., Zou, J., Liu, D.L., Meinke, H., Tian, X., Ma, S., Zhang, Y., Man, J., Wang, X., Zhou, M., 2022b. Designing high-yielding wheat crops under late sowing: a case study in southern China. *Agron. Sustain. Dev.* 42, 29. <https://doi.org/10.1007/s13593-022-00764-w>.
- Liu, K., Harrison, M.T., Yan, H., Liu, D.L., Meinke, H., Hoogenboom, G., Wang, B., Peng, B., Guan, K., Jaegermeyr, J., Wang, E., Zhang, F., Yin, X., Archontoulis, S., Nie, L., Badae, A., Man, J., Wallach, D., Zhao, J., Benjumea, A.B., Fahad, S., Tian, X., Wang, W., Tao, F., Zhang, Z., Rötter, R., Yuan, Y., Zhu, M., Dai, P., Nie, J., Yang, Y., Zhang, Y., Zhou, M., 2023. Silver lining to a climate crisis in multiple prospects for alleviating crop waterlogging under future climates. *Nat. Commun.* 14, 765. <https://doi.org/10.1038/s41467-023-36129-4>.
- Liu, Y., Yang, M., Wu, Y., Wang, H., Chen, Y., Wu, W., 2011. Reducing CH4 and CO2 emissions from waterlogged paddy soil with biochar. *J. Soils Sediment.* 11, 930–939. <https://doi.org/10.1007/s11368-011-0376-x>.
- Lobell, D.B., Field, C.B., 2007. Global scale climate–crop yield relationships and the impacts of recent warming. *Environ. Res. Lett.* 2, 014002 <https://doi.org/10.1088/1748-9326/2/1/014002>.
- Lv, Z., Liu, X., Cao, W., Zhu, Y., 2017. A model-based estimate of regional wheat yield gaps and water use efficiency in main winter wheat production regions of China. *Sci. Rep.* 7, 6081. <https://doi.org/10.1038/s41598-017-06312-x>.
- Manik, S.M.N., Pengilly, G., Dean, G., Field, B., Shabala, S., Zhou, M., 2019. Soil and crop management practices to minimize the impact of waterlogging on crop productivity. *Front. Plant Sci.* 10. <https://doi.org/10.3389/fpls.2019.00140>.
- Marti, J., Savin, R., Slafer, G.A., 2015. Wheat yield as affected by length of exposure to waterlogging during stem elongation. *J. Agron. Crop Sci.* 201, 473–486. <https://doi.org/10.1111/jac.12118>.
- Martre, P., Jamieson, P.D., Semenov, M.A., Zyskowski, R.F., Porter, J.R., Triboui, E., 2006. Modelling protein content and composition in relation to crop nitrogen dynamics for wheat. *Eur. J. Agron.* 25, 138–154. <https://doi.org/10.1016/j.eja.2006.04.007>.
- Miralles, D.J., Richards, R.A., Slafer, G.A., 2000. Duration of the stem elongation period influences the number of fertile florets in wheat and barley. *Funct. Plant Biol.* 27, 931–940.
- Nendel, C., Specka, X., Berg, M., 2022. MONICA [WWW Document]. International Soil Modeling Consortium. URL <https://soil-modeling.org/resources-links/model-portal/monica> (accessed 9.20.22).
- Nguyen, T.-N., Son, S., Jordan, M.C., Levin, D.B., Ayele, B.T., 2016. Lignin biosynthesis in wheat (*Triticum aestivum* L.): its response to waterlogging and association with hormonal levels. *BMC Plant Biol.* 16, 28. <https://doi.org/10.1186/s12870-016-0714-4>.
- Nôia Júnior, R., de, S., Martre, P., Finger, R., van der Velde, M., Ben-Ari, T., Ewert, F., Webber, H., Ruane, A.C., Asseng, S., 2021. Extreme lows of wheat production in Brazil. *Environ. Res. Lett.* 16, 104025 <https://doi.org/10.1088/1748-9326/ac26f3>.
- Nôia Júnior, R., de, S., Ewert, F., Webber, H., Martre, P., Hertel, T.W., van Ittersum, M.K., Asseng, S., 2022. Needed global wheat stock and crop management in response to the war in Ukraine. *Glob. Food Secur.* 35, 100662 <https://doi.org/10.1016/j.gfs.2022.100662>.
- Nôia Júnior, R., de, S., Deswarte, J.-C., Cohan, J.-P., Martre, P., van der Velde, M., Lecerf, R., Webber, H., Ewert, F., Ruane, A.C., Slafer, G.A., Asseng, S., 2023. The extreme 2016 wheat yield failure in France. *Glob. Change Biol. N/a*. <https://doi.org/10.1111/gcb.16662>.
- Olgun, M., Metin Kumlay, A., Cemal Adiguzel, M., Caglar, A., 2008. The effect of waterlogging in wheat (*T. aestivum* L.). *Acta Agriculturae Scandinavica, Section B – Soil & Plant Science* 58, 193–198. <https://doi.org/10.1080/09064710701794024>.

- Osborne, T., Gornall, J., Hooker, J., Williams, K., Wiltshire, A., Betts, R., Wheeler, T., 2015. JULES-crop: a parametrisation of crops in the Joint UK Land Environment Simulator. *Geosci. Model Dev.* 8, 1139–1155. <https://doi.org/10.5194/gmd-8-1139-2015>.
- Porter, J.R., 1993. AFRCWHEAT2: A model of the growth and development of wheat incorporating responses to water and nitrogen. *Eur. J. Agron.* 2, 69–82. [https://doi.org/10.1016/S1161-0301\(14\)80136-6](https://doi.org/10.1016/S1161-0301(14)80136-6).
- Priesack, E., 2019. EXPERT-N Model Library Documentation. Munich.
- Raes, D., Steduto, P., Hsiao, T.C., Fereres, E., 2018. AquaCrop - Reference manual. Rome.
- Rawnsley, R.P., Smith, A.P., Christie, K.M., Harrison, M.T., Eckard, R.J., 2019. Current and future direction of nitrogen fertiliser use in Australian grazing systems. *Crop and Pasture Science* 70, 1034–1043.
- Rosenzweig, C., Jones, J.W., Hatfield, J.L., Ruane, A.C., Boote, K.J., Thorburn, P., Antle, J.M., Nelson, G.C., Porter, C., Janssen, S., Asseng, S., Basso, B., Ewert, F., Wallach, D., Baigorría, G., Winter, J.M., 2013. The Agricultural Model Intercomparison and Improvement Project (AgMIP): Protocols and pilot studies. *Agric. For. Meteorol.* 170, 166–182. <https://doi.org/10.1016/j.agrformet.2012.09.011>.
- Salazar, O., Vargas, J., Nájera, F., Seguel, O., Casanova, M., 2014. Monitoring of nitrate leaching during flush flooding events in a coarse-textured floodplain soil. *Agric. Water Manag.* 146, 218–227. <https://doi.org/10.1016/j.agwat.2014.08.014>.
- de San Celedonio, R.P., Abeledo, L.G., Miralles, D.J., 2014. Identifying the critical period for waterlogging on yield and its components in wheat and barley. *Plant Soil* 378, 265–277. <https://doi.org/10.1007/s11104-014-2028-6>.
- Sayre, K.D., Van Ginkel, M., Rajaram, S., Ortiz-Monasterio, I., 1994. Tolerance to waterlogging losses in spring bread wheat: effect of time of onset on expression. *Annu. Wheat Newsl.* 40, 165–171.
- Schaphoff, S., von Bloh, W., Rammig, A., Thonicke, K., Biemans, H., Forkel, M., Gerten, D., Heinke, J., Jägermeyr, J., Knauer, J., Langerwisch, F., Lucht, W., Müller, C., Rolinski, S., Waha, K., 2018. LPJmL4 – a dynamic global vegetation model with managed land – Part~1: Model description. *Geosci. Model Dev.* 11, 1343–1375. <https://doi.org/10.5194/gmd-11-1343-2018>.
- Sharpley, A., J.R. Williams, 1990. EPIC — Erosion / Productivity.
- Shaw, R.E., Meyer, W.S., McNeill, A., Tyerman, S.D., 2013. Waterlogging in Australian agricultural landscapes: a review of plant responses and crop models. *Crop and Pasture Science* 64, 549–562.
- Shelia, V., Asseng, S., Porter, C., Hoogenboom, G., 2019. SIMULATION OF A PERCHED WATER TABLE WITH IMPACT ON WHEAT CROP GROWTH, in: *Agricultural and Biological Engineering University of Florida*. Gainesville.
- Snow, V., Rodriguez, D., Dynes, R., Kaye-Blake, W., Mallawaarachchi, T., Zydenbos, S., Cong, L., Obadovic, I., Agnew, R., Amery, N., Bell, L., Benson, C., Clinton, P., Dreccer, M.F., Dunningham, A., Gleeson, M., Harrison, M., Hayward, A., Holzworth, D., Johnstone, P., Meinke, H., Mitter, N., Muger, A., Pannell, D., Silva, L.F.P., Roura, E., Siddharth, P., Siddique, K.H.M., Stevens, D., 2021. Resilience achieved via multiple compensating subsystems: the immediate impacts of COVID-19 control measures on the agri-food systems of Australia and New Zealand. *Agric. Syst.* 187, 103025 <https://doi.org/10.1016/j.agsy.2020.103025>.
- Stockle, C.O., Martin, S.A., Campbell, G.S., 1994. CropSyst, a cropping systems simulation model: Water/nitrogen budgets and crop yield. *Agric. Syst.* 46, 335–359. [https://doi.org/10.1016/0308-521X\(94\)90006-2](https://doi.org/10.1016/0308-521X(94)90006-2).
- Tao, F., Yokozawa, M., Zhang, Z., 2009. Modelling the impacts of weather and climate variability on crop productivity over a large area: a new process-based model development, optimization, and uncertainties analysis. *Agric. For. Meteorol.* 149, 831–850. <https://doi.org/10.1016/j.agrformet.2008.11.004>.
- Taub, D.R., 2010. Effects of rising atmospheric concentrations of carbon dioxide on plants. *Nat. Educ.* 3, 21.
- Team, P.P., 2021. The POWER Project [WWW Document]. NASA Prediction of Worldwide Energy Resources. URL <https://power.larc.nasa.gov/>.
- Thorp, K.R., Hunsaker, D.J., French, A.N., White, J.W., Clarke, T.R., 2010. Evaluation of the csm-cropsim-cheres wheat model as a tool for crop water management. *Trans. ASABE* 53, 87–102.
- USDA PSD, 2022. Trade Data Monitor [WWW Document]. URL <https://apps.fas.usda.gov/psdonline/app/index.html#/app/home> (accessed 6.6.22).
- van Ittersum, M.K., Cassman, K.G., 2013. Yield gap analysis—Rationale, methods and applications—Introduction to the Special Issue. *Field Crops Res.* 143, 1–3. <https://doi.org/10.1016/j.fcr.2012.12.012>.
- Webber, H., Ewert, F., Olesen, J.E., Müller, C., Fronzek, S., Ruane, A.C., Bourgault, M., Martre, P., Ababaei, B., Bindi, M., Ferrise, R., Finger, R., Fodor, N., Gabaldón-Leal, C., Gaiser, T., Jabloun, M., Kersebaum, K.-C., Lizaso, J.L., Lorite, I.J., Manceau, L., Moriondo, M., Nendel, C., Rodríguez, A., Ruiz-Ramos, M., Semenov, M. A., Siebert, S., Stella, T., Stratonovitch, P., Trombi, G., Wallach, D., 2018. Diverging importance of drought stress for maize and winter wheat in Europe. *Nat. Commun.* 9, 4249. <https://doi.org/10.1038/s41467-018-06525-2>.
- Webber, H., Lischeid, G., Sommer, M., Finger, R., Nendel, C., Gaiser, T., Ewert, F., 2020. No perfect storm for crop yield failure in Germany. *Environ. Res. Lett.* 15, 104012 <https://doi.org/10.1088/1748-9326/aba2a4>.
- Webber, H., Rezaei, E.E., Ryo, M., Ewert, F., 2022. Framework to guide modeling single and multiple abiotic stresses in arable crops. *Agric., Ecosyst. Environ.* 340, 108179 <https://doi.org/10.1016/j.agee.2022.108179>.
- Wit, A. de, 2022. Principles of WOFOST [WWW Document]. URL <https://www.wur.nl/en/research-results/research-institutes/environmental-research/facilities-tools/software-models-and-databases/wofost/principles-of-wofost.htm> (accessed 9.20.22).
- Wolf, J., 2011. LINTUL-3, a simple crop growth model for both potential, water limited and nitrogen limited growing conditions [WWW Document]. Models and Data Library. URL <https://models.pps.wur.nl/lintul-3-simple-crop-growth-model-both-potential-water-limited-and-nitrogen-limited-growing> (accessed 9.20.22).
- Yan, H., Harrison, M.T., Liu, K., Wang, B., Feng, P., Fahad, S., Meinke, H., Yang, R., Liu, D.L., Archontoulis, S., Huber, I., Tian, X., Man, J., Zhang, Y., Zhou, M., 2022. Crop traits enabling yield gains under more frequent extreme climatic events. *Sci. Total Environ.* 808, 152170 <https://doi.org/10.1016/j.scitotenv.2021.152170>.
- Zampieri, M., Ceglari, A., Dentener, F., Toreti, A., 2017. Wheat yield loss attributable to heat waves, drought and water excess at the global, national and subnational scales. *Environ. Res. Lett.* 12, 64008. <https://doi.org/10.1088/1748-9326/aa723b>.
- Zhao, C., Liu, B., Piao, S., Wang, X., Lobell, D.B., Huang, Y., Huang, M., Yao, Y., Bassu, S., Ciais, P., Durand, J.-L., Elliott, J., Ewert, F., Janssens, I.A., Li, T., Lin, E., Liu, Q., Martre, P., Müller, C., Peng, S., Peñuelas, J., Ruane, A.C., Wallach, D., Wang, T., Wu, D., Liu, Z., Zhu, Y., Zhu, Z., Asseng, S., 2017. Temperature increase reduces global yields of major crops in four independent estimates. *Proceedings of the National Academy of Sciences* 114, 9326 LP – 9331. <https://doi.org/10.1073/pnas.1701762114>.
- Zhao, C., Liu, B., Xiao, L., Hoogenboom, G., Boote, K.J., Kassie, B.T., Pavan, W., Shelia, V., Kim, K.S., Hernandez-Ochoa, I.M., Wallach, D., Porter, C.H., Stockle, C.O., Zhu, Y., Asseng, S., 2019. A SIMPLE crop model. *Eur. J. Agron.* 104, 97–106. <https://doi.org/10.1016/j.eja.2019.01.009>.
- Zheng, B., Chenu, K., Doherty, A., Chapman, S., 2015. The APSIM-Wheat Module (7.5 R3008).

Supplementary Material for

A call to action for global research on the implications of waterlogging on wheat growth and yields

Rogério de S. Nória Júnior, Senthold Asseng, Margarita García-Vila, Ke Liu, Valentina Stocca, Murilo dos Santos Vianna, Tobias K. D. Weber, Jin Zhao, Taru Palosuo, Matthew Tom Harrison

Table S1. Published peer reviewed manuscripts on the effects of waterlogging on wheat. Growth stages from the Zadoks growth stages scale.

ID	Growth stage	Duration of waterlogging (days)	References	Web-link
1	25	47, 58	[1]	here
2	71	30, 5	[2]	here
3	71, 20	4, 7	[3]	here
4	37	7	[4]	here
5	50, 68	14	[5]	here
6	71,39	7, 2	[6]	here
7	71	15	[7]	here
8	61	5, 10, 15, 20, 25, 50	[8]	here
9	31, 39, 45, 50, 58, 64	4, 8, 12, 16, 20, 24	[9]	here
10	10, 20, 30, 40	15, 20	[10]	here
11	32, 50	12	[11]	here
12	14	12	[12]	here
13	61	14	[13]	here
14	30, 50, 60	5, 10, 15	[14]	here
15	33, 45, 65	10	[15]	here
16	10, 20, 25, 40, 50, 60, 71	15, 20	[16]	here
17	20, 30, 40, 61	14, 28, 35	[17]	here

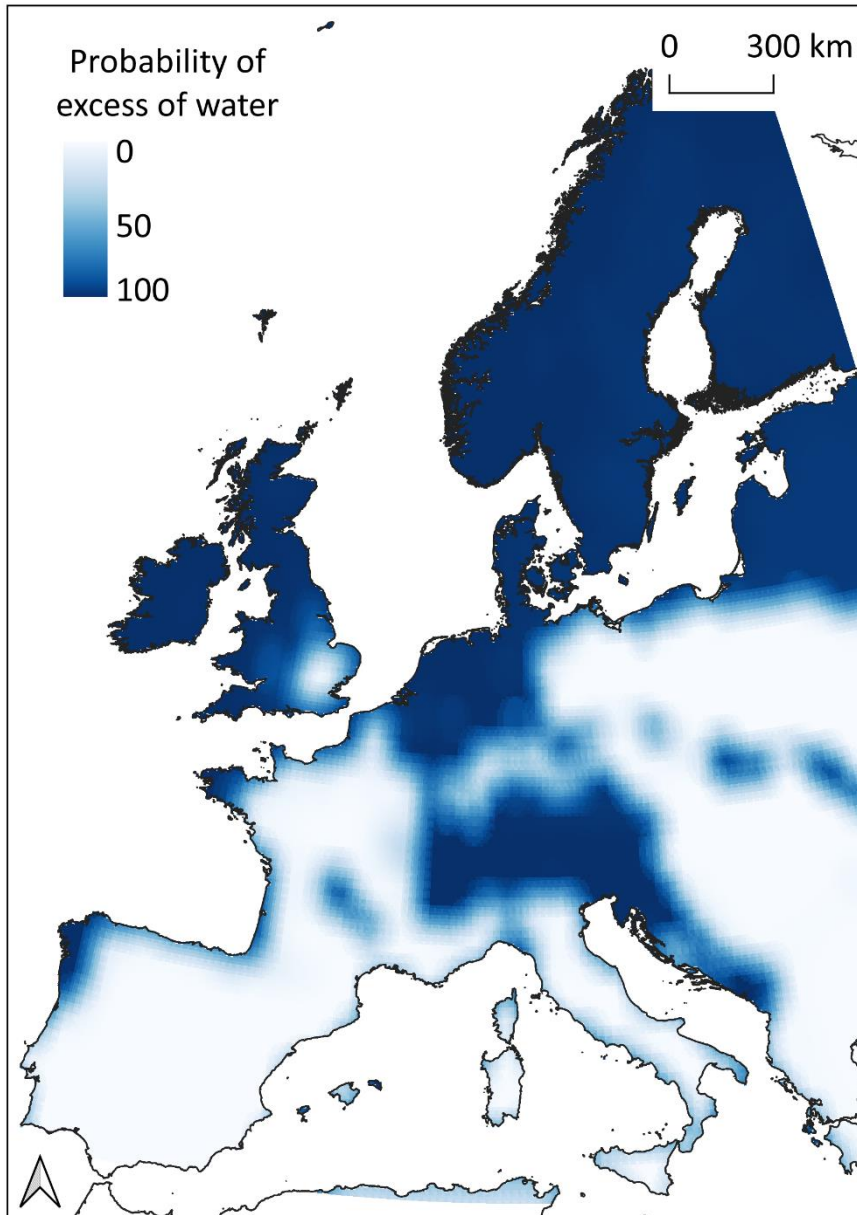


Figure S1. Probability of excess of water during summer in Europe. The probability of excess of water is the relation between the number of days from April to June (wheat anthesis and grain filling) in which daily accumulated Rain - Eto > 30 mm and the total number of days in that same period, being reference evapotranspiration (ETo).

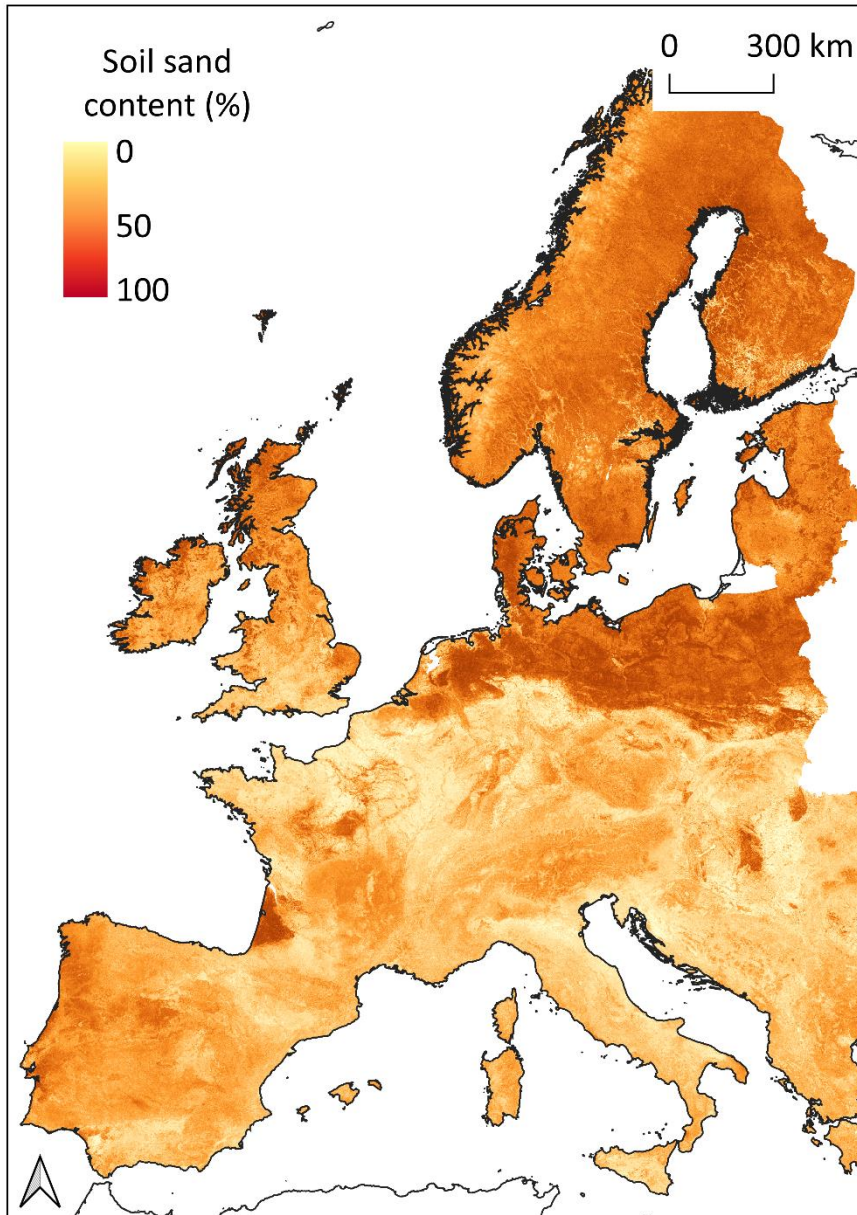


Figure S2. Soil sand content in Europe. Soil data from the European Soil Data Centre 2.0 [19,20].

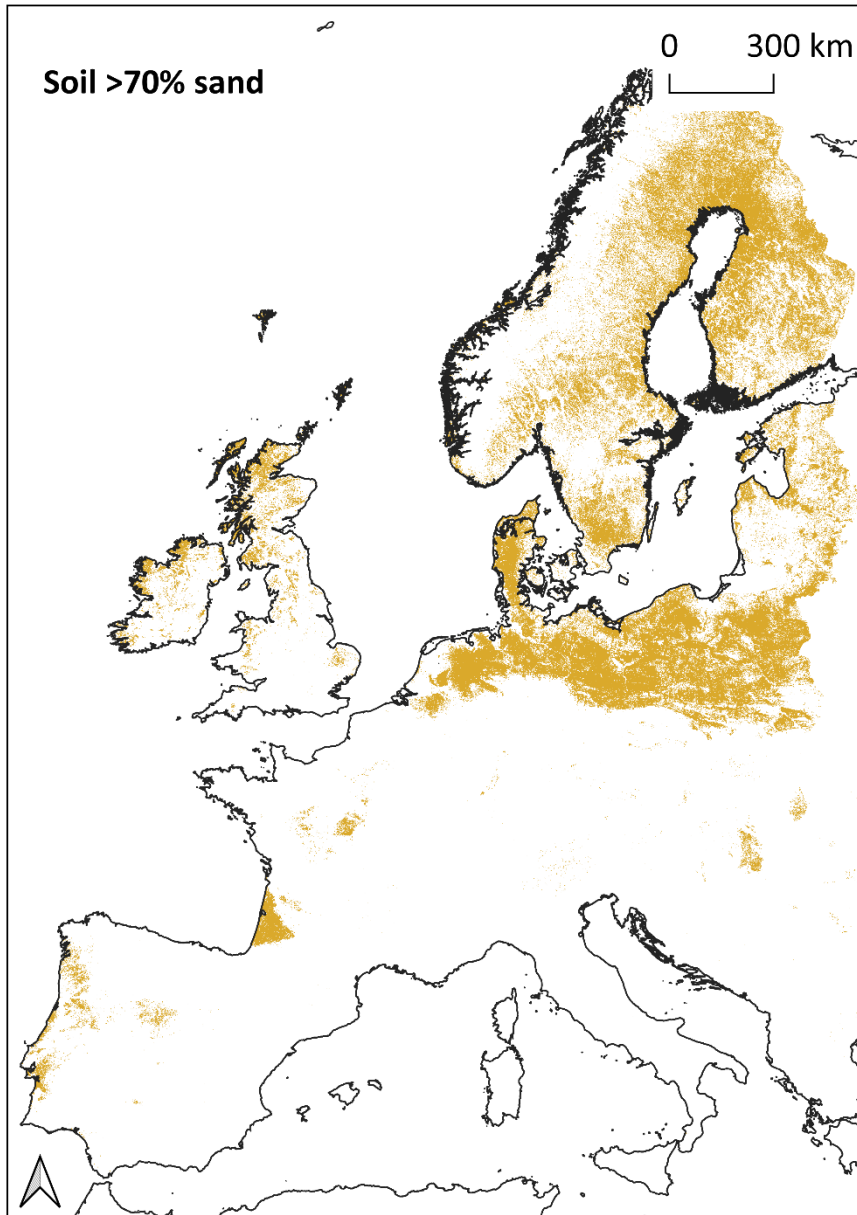


Figure S3. locations with soil sand content above 70%. Calculated using the Soil data from the European Soil Data Centre 2.0 [19,20].

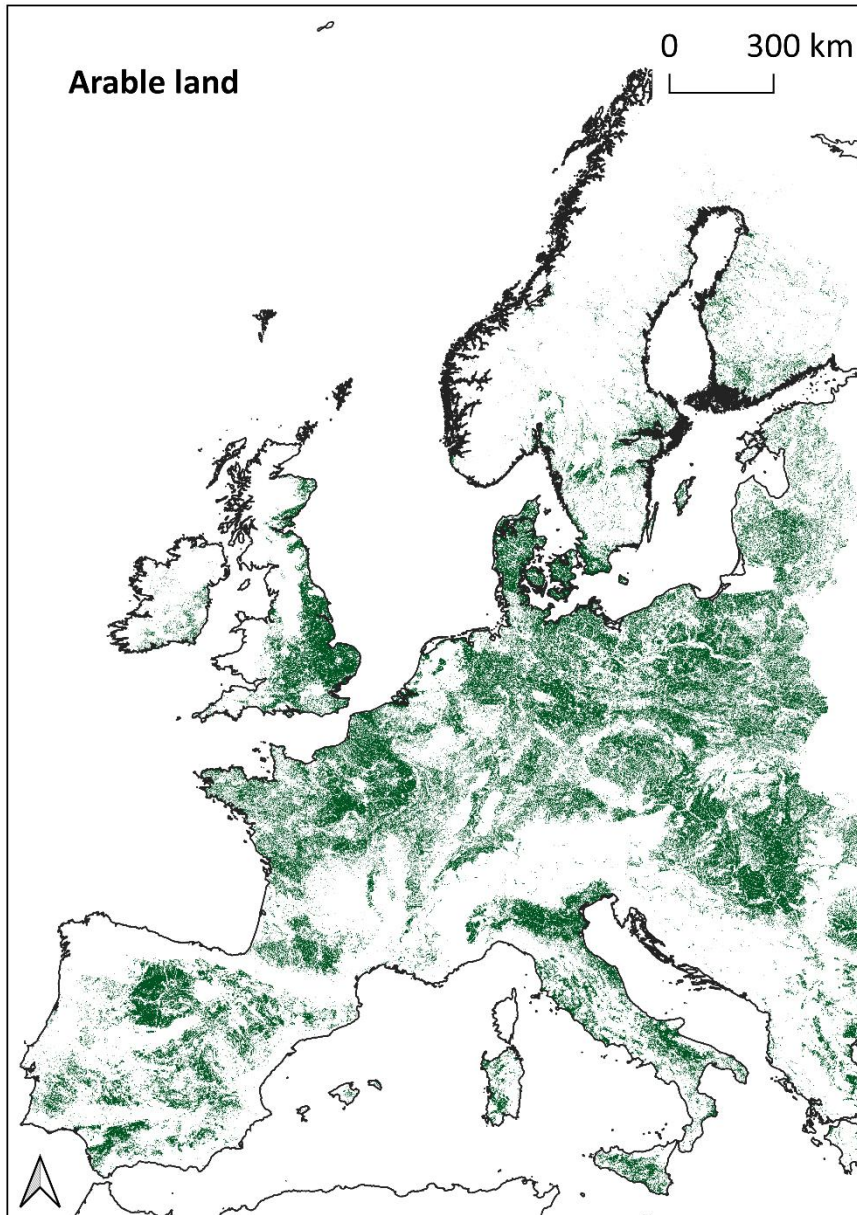


Figure S4. Non-irrigated arable lands in Europe. The arable land mask is based on CORINE Land Cover 2020 [18].

References

1. Dickin E, Wright D: **The effects of winter waterlogging and summer drought on the growth and yield of winter wheat (*Triticum aestivum* L.)**. *European Journal of Agronomy* 2008, **28**:234–244.
2. Zhou Q, Huang M, Huang X, Liu J, Wang X, Cai J, Dai T, Cao W, Jiang D: **Effect of post-anthesis waterlogging on biosynthesis and granule size distribution of starch in wheat grains**. *Plant Physiology and Biochemistry* 2018, **132**:222–228.
3. Wang X, Huang M, Zhou Q, Cai J, Dai T, Cao W, Jiang D: **Physiological and proteomic mechanisms of waterlogging priming improves tolerance to waterlogging stress in wheat (*Triticum aestivum* L.)**. *Environmental and Experimental Botany* 2016, **132**:175–182.
4. Gao J, Su Y, Yu M, Huang Y, Wang F, Shen A: **Potassium Alleviates Post-anthesis Photosynthetic Reductions in Winter Wheat Caused by Waterlogging at the Stem Elongation Stage**. *Frontiers in Plant Science* 2021, **11**.
5. Ploschuk RA, Miralles DJ, Colmer TD, Striker GG: **Waterlogging differentially affects yield and its components in wheat, barley, rapeseed and field pea depending on the timing of occurrence**. *Journal of Agronomy and Crop Science* 2020, **206**:363–375.
6. Li C, Jiang D, Wollenweber B, Li Y, Dai T, Cao W: **Waterlogging pretreatment during vegetative growth improves tolerance to waterlogging after anthesis in wheat**. *Plant Science* 2011, **180**:672–678.
7. Tan W, Liu J, Dai T, Jing Q, Cao W, Jiang D: **Alterations in photosynthesis and antioxidant enzyme activity in winter wheat subjected to post-anthesis water-logging**. *Photosynthetica* 2008, **46**:21–27.
8. Olgun M, Metin Kumlay A, Cemal Adiguzel M, Caglar A: **The effect of waterlogging in wheat (*T. aestivum* L.)**. *Acta Agriculturae Scandinavica, Section B — Soil & Plant Science* 2008, **58**:193–198.
9. Marti J, Savin R, Slafer GA: **Wheat Yield as Affected by Length of Exposure to Waterlogging During Stem Elongation**. *Journal of Agronomy and Crop Science* 2015, **201**:473–486.
10. de San Celedonio RP, Abeledo LG, Miralles DJ: **Physiological traits associated with reductions in grain number in wheat and barley under waterlogging**. *Plant and Soil* 2018, **429**:469–481.
11. Ding J, Huang Z, Zhu M, Li C, Zhu X, Guo W: **Does cyclic water stress damage wheat yield more than a single stress?** *PLOS ONE* 2018, **13**:e0195535.
12. Farkas Z, Varga-László E, Anda A, Veisz O, Varga B: **Effects of Waterlogging, Drought and Their Combination on Yield and Water-Use Efficiency of Five Hungarian Winter Wheat Varieties**. *Water* 2020, **12**.
13. Zhou Q, Wu X, Xin L, Jiang H, Wang X, Cai J, Jiang D: **Waterlogging and simulated acid rain after anthesis deteriorate starch quality in wheat grain**. *Plant Growth Regulation* 2018, **85**:257–265.
14. Martínez M, Arata AF, Lázaro L, Stenglein SA, Dinolfo MI: **Effects of waterlogging stress on plant-pathogen interaction between *Fusarium poae* and wheat/ barley**. *Acta Scientiarum - Agronomy* 2019, **41**:1–9.
15. Ding J, Liang P, Wu P, Zhu M, Li C, Zhu X, Guo W: **Identifying the Critical Stage Near Anthesis for Waterlogging on Wheat Yield and Its Components in the Yangtze River Basin, China**. *Agronomy* 2020, **10**.
16. de San Celedonio RP, Abeledo LG, Miralles DJ: **Identifying the critical period for waterlogging on yield and its components in wheat and barley**. *Plant and Soil* 2014, **378**:265–277.
17. Wu X, Tang Y, Li C, McHugh AD, Li Z, Wu C: **Individual and combined effects of soil waterlogging and compaction on physiological characteristics of wheat in southwestern China**. *Field Crops Research* 2018, **215**:163–172.
18. CLC: **Copernicus Land Monitoring Service**. *CORINE Land Cover* 2020,
19. Panagos P, Van Liedekerke M, Borrelli P, Köninger J, Ballabio C, Orgiazzi A, Lugato E, Liakos L,

- Hervas J, Jones A, et al.: **European Soil Data Centre 2.0: Soil data and knowledge in support of the <scp>EU</scp> policies.** *European Journal of Soil Science* 2022, **73**.
20. Panagos P, Van Liedekerke M, Jones A, Montanarella L: **European Soil Data Centre: Response to European policy support and public data requirements.** *Land Use Policy* 2012, **29**:329–338.

Enabling modeling of waterlogging impact on wheat

Rogério de S. Nória Júnior¹, Valentina Stocca¹, Vakhtang Shelia², Pierre Martre³, Jean-Charles Deswarte⁴, Jean-Pierre Cohan⁵, Benoît Piquemal⁵, Alain Dutertre⁵, Gustavo A. Slafer^{6,7}, Marijn Van der Velde⁸, Yean-Uk Kim⁹, Heidi Webber^{9,10}, Frank Ewert^{9,11}, Taru Palosuo¹², Matthew Tom Harrison¹³, Gerrit Hoogenboom², Senthold Asseng^{1*}

¹Technical University of Munich, Department of Life Science Engineering, Digital Agriculture, HEF World Agricultural Systems Center, Freising, Germany

²Department of Agricultural and Biological Engineering, University of Florida, Gainesville, FL, USA

³LEPSE, Univ Montpellier, INRAE, Institut Agro Montpellier, Montpellier, France

⁴ARVALIS - Institut du Végétal, Villiers-le-Bâcle, France

⁵ARVALIS - Institut du Végétal, Loireauxence, France

⁶Department of Agricultural and Forest Sciences and Engineering, University of Lleida – AGROTECNIO-CERCA Center, Lleida, Spain

⁷ICREA, Catalanian Institution for Research and Advanced Studies, Barcelona, Spain

⁸European Commission, Joint Research Centre, Ispra, Italy

⁹Leibniz-Centre for Agricultural Landscape Research (ZALF), Müncheberg, Germany

¹⁰Brandenburg Technical University (BTU), Cottbus, Germany

¹¹Crop Science Group, INRES, University of Bonn, Bonn, Germany

¹²Natural Resources Institute Finland (Luke), Helsinki, Finland

¹³Tasmanian Institute of Agriculture, University of Tasmania, Newnham, Launceston, Tasmania, Australia

*Corresponding author: senthold.asseng@tum.de

Abstract (max 200 words)

Most crop simulation models do not consider the effect of waterlogging despite being important for crop performance. Here, we reviewed the impact of waterlogging in different wheat phenological stages on grain number per unit area, average grain size, and grain yield. Episodes of waterlogging from the onset of tillering to anthesis result in fewer, and during grain filling in lighter grains. To simulate such impact, we implemented a new waterlogging module into the wheat crop simulation model DSSAT-NWheat, accounting for the effects of waterlogging on wheat root growth, carbohydrate accumulation and potential average grain size. The module was tested with data from a controlled experiment and showed reasonable wheat yield. A sensitivity analysis showed that the simulated impact of waterlogging on above ground biomass and roots, as well as leaf area index, grain number and grain yield varied with phenological stages. The simulated crop was most sensitive to waterlogging shortly before anthesis, as shown in experimental studies. In conclusion, the new waterlogging-enabled crop model simulates reasonably well the impact of excess rainfall and waterlogging on crop growth and final grain yield and could reduce model uncertainties to project studies climate change impact with increasing rainfall intensity.

Keywords: NWheat, DSSAT, excess of water, grain number, grain size.

1. Introduction

Waterlogging could be defined as the phenomenon in which prolonged saturation of a soil with water inhibits or entirely negates oxygen availability to plant roots (Liu *et al.*, 2021a). All direct and indirect impacts of waterlogging together are a major cause of crop yield losses across the world, estimated to affect 15-20% of the global wheat cropping area each year (Sayre *et al.*, 1994; Kaur *et al.*, 2020). Crop production in southern Asia, Europe, Russia, China and southern Brazil may be more sensitive to waterlogging than to drought (Zampieri *et al.*, 2017; Liu *et al.*, 2023). Waterlogging from high rainfall has damaged 33.9 million hectares (Mha) of India's arable area between 2015 to 2022 (Kulkarni *et al.*, 2021). Excessive precipitation causing waterlogging was found to be the main factor influencing wheat yield since the first half of the 20th century in France (Ceglar *et al.*, 2020), where only 9% of the arable has man-made drainage systems installed to reduce the impact of waterlogging (Jeantet *et al.*, 2021). In southern Brazil, a 40% drop in wheat yield was reported in 2017 cropping season due to excessive rainfall causing waterlogging and increased plant diseases (Nóia Júnior *et al.*, 2021). More than 30% of the Pampas Region of Argentina was waterlogged over the last two decades (Kuppel *et al.*, 2015). Despite the large worldwide damage of waterlogging on crops, studies on waterlogging impact on grain production are scarce.

The process of adapting agricultural crops to extreme weather events, such as waterlogging, demands sophisticated understanding of how crop genotypes respond to different weather conditions, at different phenological stages for different management options (Liu *et al.*, 2020a; Githui *et al.*, 2022). For this, it is necessary to have controlled experiments in greenhouse and field conditions, with physiological, morphological and growth measurements. These experiments may be repeated in different years and locations, making them costly and often unfeasible, particularly if a thorough

insight into the solution space is sought (Liu *et al.*, 2020b, 2023; Githui *et al.*, 2022). Such experiments are sparse for waterlogging, and the review of their results are shown here.

Crop models synthesize the gathered knowledge and understanding on crop growth processes and contribute to the understanding of the physiological mechanisms of plant response to abiotic stresses. They are widely applied for simulating crop growth and physiology in different environments, locations and years including climate change scenarios, extreme weather impacts (Kassie *et al.*, 2016; Yan *et al.*, 2022). Indeed, many studies that project the impacts of climate change on agriculture used crop simulation models (Asseng *et al.*, 2013, 2015, 2019; Liu *et al.*, 2016, 2019; Zhao *et al.*, 2017). However, the majority of crop models do not consider yet the impact of waterlogging on crop growth (Liu *et al.*, 2020b; Githui *et al.*, 2022).

Only in few crop models waterlogging is considered and usually are covered only its effects on carbohydrate accumulation, radiation use efficiency, transpiration, root activity and leaf area index (LAI) (Liu *et al.*, 2020c; Githui *et al.*, 2022). In some crop models, the magnitude of simulated impact varies according to the phenological phase in which the waterlogging occurs (e.g., (de San Celedonio *et al.*, 2014)). The wheat crop model in APSIM, for example, considers that the highest photosynthetic and roots activity reduction due to waterlogging occurs before wheat grain filling, with no impact during grain filling (Liu *et al.*, 2021b). The EPIC model considers direct waterlogging effects only on photosynthesis and LAI (Githui *et al.*, 2022), with indirect impacts on other growth mechanisms. In these crop models, wheat growth is penalized via lower photosynthesis due to its direct reduction or lower light capture from decreased leaf area with waterlogging. There could also be a simulated yield penalty via indirect reduced nitrogen uptake due to root reduction from waterlogging. However, these models have only been tested in a few situations with waterlogged wheat, and it is not clear how waterlogging affects yield and its components, and by extension, yield. Some wheat crop models do

not correctly simulate the relationship between number of grains per unit area and average grain size (or grain unit weight), resulting in overestimation of simulated yields, particularly in seasons with poor grain setting (causing low grain number per unit area) and grain filling (causing low average grain size) (Nóia Júnior *et al.*, 2023). The relationship between number of grains per unit area and average grain size is usually studied in controlled environments with few measured data (Fischer, 1985; Calderini *et al.*, 2001; Asseng *et al.*, 2017), making it difficult to improve wheat crop models.

The inability of most crop models to simulate waterlogged wheat growth potentially underestimates the projected impacts of climate change on agriculture (van der Velde *et al.*, 2020; Webber *et al.*, 2020). To improve the representation of waterlogging in crop models, in this study we aimed to improve the waterlogging module in the wheat crop simulation model DSSAT-NWheat. For this, we reviewed published articles from 2008 to 2021 that studied the impacts of waterlogging during different wheat phenological stages on grain number per unit area, average grain size, and grain yield. Based on the general relationships of crop performance and waterlogging, a new waterlogging module was developed and tested in a controlled waterlogging experiment in Lleida, Spain. To better understand the relationship between wheat average grain size and grain number per unit area, we also used a detailed dataset from ARVALIS with observations from 3,512 experimental treatments across the French breadbasket region over six years from 2014 to 2019, as described by Nóia Júnior *et al.* (2023).

2. Material and Methods

2.1. Review of waterlogging impacts on wheat grain number, average grain size and grain yield

We assessed 17 peer-reviewed articles published between 2008 and 2021 which quantified the impacts of waterlogging on wheat grain yield, grain number or grain size in controlled waterlogging

treatments ([SUPPLEMENTARY TABLE S1](#)). Relevant articles were found by using keywords ‘waterlogging’, ‘flooding’ or ‘excess of water’ and ‘wheat’ in Web of Science and Google Scholar Databases. In the assessed articles, waterlogging was happening in different wheat phenological stages, from seedling emergence to onset of grain filling and with waterlogging duration varying from 2 to 58 days ([FIGURE 3D](#)) with fully waterlogged soil (i.e., no variations in soil moisture along the soil profile depth). From the assessed articles, we collected the average grain yield, average grain size (or grain unit dry mass or thousand grain dry mass) and grain number per unit area per each waterlogging treatments and their control. With these values, we calculated the relative change of each treatment in relation to the control and averaged according to the wheat phenological stage. Experiments with waterlogging starting at seven different wheat phenological stages were computed, namely at wheat seedling emergence, onset of tillering, jointing, booting, heading, anthesis and onset grain filling. The experiments were conducted in seven countries from three continents ([FIGURE 1](#)).

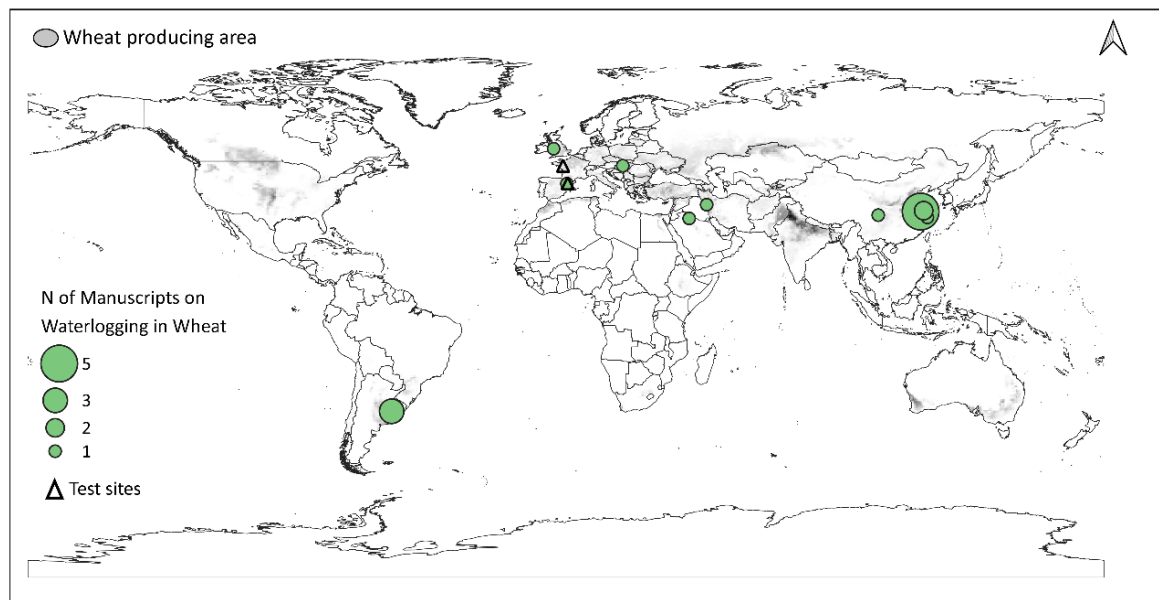


Figure 1. Waterlogging experiments with wheat. Spatial distribution of reviewed experiments on waterlogging impact for wheat (green circles). A total of 17 published studies were used here to summarize how waterlogging affects wheat. A list of all studies is shown in [SUPPLEMENTARY TABLE S1](#).

The black triangles represent experiments that were used to test the new waterlogging module for DSSAT-NWheat.

2.2. Modeling waterlogging on wheat with DSSAT-NWheat

The DSSAT-NWheat model has been evaluated and used to simulate wheat growth and development across many environments around the world, including different seasonal ranges of air temperatures, soil water, nitrogen and CO₂ concentrations (Kassie *et al.*, 2016). Here, we further-developed the waterlogging module of DSSAT-NWheat (Shelia *et al.*, 2020) by adding the soil waterlogging direct impact on carbohydrate accumulation and potential grain size in addition to the already existing impact to root growth. The previously implemented module version was originally developed for APSIM Wheat (Asseng *et al.*, 1997). The waterlogging module is now described. The waterlogging module was built in the DSSAT-Nwheat version 4.7. The waterlogging module of DSSAT-NWheat implemented by Shelia *et al.* (2019) is not available in the latest DSSAT versions (4.7 or 4.8), which are free for download. Thus, the default DSSAT-Nwheat available to the users has no module that accounts for the impacts of waterlogging on wheat growth.

2.2.1. Modeling soil waterlogging

The water flow module of DSSAT-NWheat was described in detail by Asseng *et al.* (1997) and was not further-modified in this study. The vertical water flow in a soil at or near to saturation (when soil water content is in between soil drained upper limit (or soil field capacity) and saturated soil water content) is controlled by soil saturated hydraulic conductivity (SSKS) and the soil saturated macro-flow water conductivity, which is defined as the saturated drainage rate (SLDR) in DSSAT-SBuild ([SUPPLEMENTARY FIGURE S2](#), DSSAT-SBuild is the software to build soil profile in DSSAT). SSKS (with unit of cm h⁻¹) is a quantitative measure of soil's ability to transmit water between soil layers in a multi-layer cascading

approach, with a hydraulic gradient (in short, SSKS describes the speed of vertical water flow in a saturated soil). In DSSAT only a proportion of water can vertically move in a day from a soil layer to the next deeper one. This proportion of water is defined by SLDR. The SLDR varies from 0 to 1 indicating the proportion of the water that flows to the next layer in one day. Thus, the SSKS index that defines the ability of the soil to transmit water is applied only to the proportion of water (defined by SLDR) that can move vertically in a day from one soil layer to the next deeper layer. The remaining water fills the current soil layer up to saturation (*e.g.* with SLDR = 0.95, only 5% of the water above soil drained upper limit in a day remains in the current soil layer). In DSSAT-SBuild the SLDR is defined based on soil drainage classes, varying from soils with very excessive drainage (soil drainage = 0.95) to very poor drainage (0.01). The drainage classes and their respective SLDR value are shown in [SUPPLEMENTARY TABLE S2](#).

Waterlogging is indicated with an aeration deficit factor (AF) which is calculated daily for each rooted soil layer. The aeration deficit factor is calculated based on assumptions of experiments and crop models simulating its impacts on root and crop growth (Lizaso, 1993; Asseng *et al.*, 1997). The AF is calculated as follows:

$$AF_i = \frac{SAT_i - SWC_i}{SAT_i - DUL_i} \quad (1)$$

Where, SAT_i is saturated soil water content, SWC is the soil water content and DUL is the soil drained upper limit (or soil field capacity), in a soil rooted layer i . AF_i is only calculated when soil layer is at or near to saturation, i.e. $SWC > DUL$.

2.2.2. Waterlogging impacts on roots

Waterlogging inhibits root growth and functioning (Colmer and Voesenek, 2009), which may lead to root death (Herzog *et al.*, 2016). The module that accounts for the waterlogging impacts on roots, was

previously implemented by Shelia *et al.* (2019). When AF_i in a rooted layer is below to a default threshold of 0.6 for three consecutive days, the rooting depth is reduced to 5 cm below the deepest non-saturated layer (below the first waterlogged layer, all roots become 'inactive', remaining only 5 cm of 'active' root - 'active' roots are those considered in the DSSAT-NWheat for water and nitrogen uptake), regardless of the soil layer depth. Therefore, it is recommended that the soil layers are set with a depth between 10 (more sensible to waterlogging) and 15 cm (less sensible to waterlogging) when creating soil profile in DSSAT-SBuild. The thresholds for impacting roots are default in the DSSAT-NWheat, not cultivar specific parameters. Although in the module the waterlogging affects the 'active' root system, the root depth before waterlogging (maximum root depth) is still considered in the effect of waterlogging on carbohydrate accumulation, described in detail the next subsection.

2.2.3. Waterlogging impact on carbohydrate accumulation

The waterlogging effect on carbohydrate accumulation is based on a wheat roots aeration index (AF_{root}), calculated as follows:

$$AF_{root} = \left[\frac{\sum_{i=1}^m (AF_i \times \text{Root density}_i)}{\text{Total root density}_{\text{max depth}}} \right]^{P_{AF}} \quad (2)$$

Where, P_{AF} (Parameter of roots aeration index) is set to 3.0 (default), m is the deepest soil layer with roots (considering the maximum root depth before waterlogging), i is the rooted layer and $\text{Total root density}_{\text{max depth}}$ is the root density considering the maximum root depth before the root system was shortened by waterlogging (or total root density applying the maximum rooting depth achieved during the growing season). The AF_{root} is always computed considering the $\text{Total root density}_{\text{max depth}}$ to avoid an abrupt decline of the AF_{root} when the roots are reduced to 5 cm below the top of the shallower waterlogged soil layer after three days of waterlogging. For example, in a case that simulated wheat with roots in four soil layers with 10 cm each (summing 40 cm) and waterlogging occurred for four

days in the two deepest layers (with 20 cm). In the first three days, before the roots are shortened the AF_{root} was calculated considering root density in a 40 cm deep root system (20 cm not waterlogged and 20 cm waterlogged). However, without considering the *Total root density*_{max depth} in the fourth day (after the roots are shortened in the third day) the AF_{root} would be calculated considering a root depth of 25 cm (20 cm not waterlogged and 5 cm waterlogged). As on the fourth day, waterlogging would only continue in this last 5 cm layer, the new AF_{root} would drop abruptly. To avoid this, the AF_{root} continues to be calculated considering the maximum root depth before waterlogging. The *Total root density*_{max} is considered until new roots grow and become deeper than the root depth before waterlogging.

Waterlogging affects daily carbohydrate accumulation in DSSAT-NWheat according to two new wheat cultivar parameters. First, the cultivar sensitivity to AF_{root} , considering the AF_{root} threshold value at which waterlogging impacts starts to affect carbohydrate accumulation (WLSI). Second, the maximum reduction of carbohydrate accumulation under waterlogging (WLMI). Both WLSI and WLMI vary from 0 to 1. A wheat cultivar has maximum sensitivity to waterlogging when WLSI is 1 and WLMI is 0, and maximum tolerance when WLSI is 0 and WLMI is 1 (FIGURE 2). The default values of WLSI and WLMI in the DSSAT-NWheat ecotype parameters file are 0.2 and 0.1, respectively (FIGURE 2).

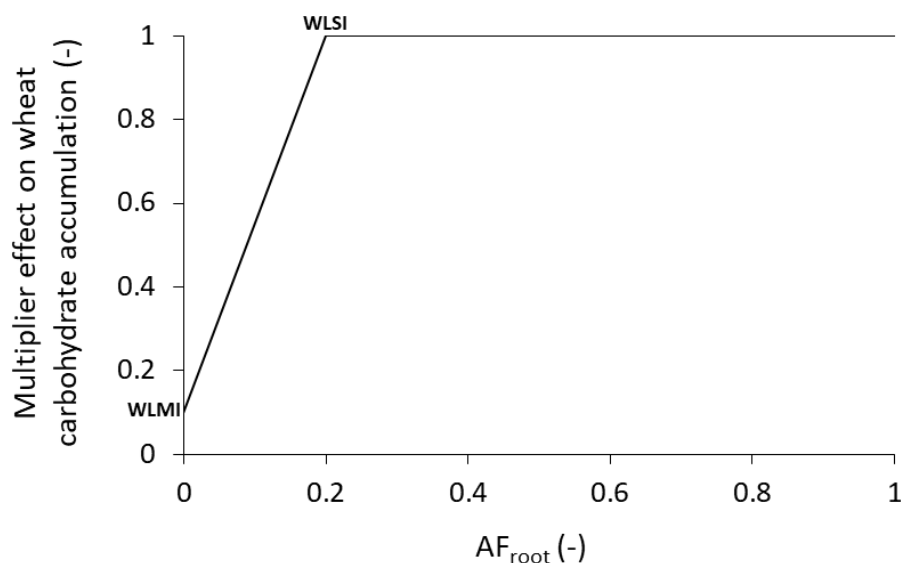


Figure 2. Reduction of carbohydrate accumulation as a function of root aeration factor (AF_{root}) in DSSAT-NWheat. WLSI and WLMI are two new wheat cultivar parameters in DSSAT-NWheat, representing when waterlogging impacts starts to affect wheat carbohydrate accumulation (WLSI – *Water Logging Impact Start*), and the maximum reduction of carbohydrate accumulation under waterlogging (WLMI – *Water Logging Maximum Impact*). The values shown are the default in the code, but they may be parameterized according to the wheat cultivar.

2.2.4. Waterlogging impact on potential grain size

Waterlogging before and during anthesis affects the potential grain size (Marti *et al.*, 2015). In wheat, average grain size is most sensitive to biotic or abiotic stress between booting and the beginning of effective grain filling (Calderini *et al.*, 2001, 2021) (SUPPLEMENTARY FIGURE S3). DSSAT-NWheat, computes daily a water deficit, nitrogen, heat and waterlogging stress factor, which impact potential growth, according to equations 3 and 4.

$$Plant\ stress = \min (water\ deficit_{stress}, nitrogen_{stress}, ozone_{stress}, waterlogging_{stress}) \times heat_{stress} \quad (3)$$

$$Daily\ wheat\ accumulation\ of\ carbohydrate = Potential\ carbohydrate\ accumulation \times plant\ stress \quad (4)$$

Wheat grain number per unit area is closely related to growing conditions before and shortly after anthesis (Fischer, 1985), when the number of fertile florets is determined and when fertile florets set grains (Slafer *et al.*, 2015). This is also the period when potential grain size is set (Acreche and Slafer, 2006; Calderini *et al.*, 2021). DSSAT-NWheat estimates grain number in the first day of grain filling (phenological stage 5 in DSSAT-NWheat), based on the stem (above-ground biomass not considering leaves) growth from start-of-stem-growth (phenological stage 2) to anthesis (phenological stage 4). We added a waterlogging stress factor for potential grain size. In DSSAT-NWheat, the original potential average grain size is set to 55 mg of dry mass per grain (mg grain^{-1} , this is a model parameter named MXGWT in the wheat ecotype file of DSSAT-NWheat). In our new approach, the potential wheat grain size is now based on a weighted crop stress factor between phenological stage 2 to 4, as defined in equations 5 and 6, after Calderini *et al.* (2001):

$$\text{Potential grain size}_{\text{stress}} = 0.25 \times \text{Plant stress}_{\text{stage 2}} + 0.35 \times \text{Plant stress}_{\text{stage 3}} + 0.40 \times \text{Plant stress}_{\text{stage 4}} \quad (5)$$

$$\text{Potential grain size} = 55 \times \text{Potential grain size}_{\text{stress}} \quad (6)$$

Minimum potential grain size is set to 20 mg grain^{-1} , as shown in Figure 4. The weighting factors in equation 5, are defined according to the function proposed by Calderini *et al.* (2001).

2.3. Relationship between wheat grain number per unit area and average grain size

We analyzed the relationship between wheat grain number per unit area and wheat grain size with data from 3,188 experimental treatments with 221 winter wheat cultivars performed by ARVALIS from 2014 to 2019 in different research stations in the breadbasket of France. Detailed experimental setup of this data are described in Nória Júnior *et al.* (2023). The experiments were distributed across the breadbasket of France, which is a high wheat yielding region with average wheat yield of 7.4 t ha^{-1} .

From the relationship between grain number per unit area and average grain size, 4 groups of the relationship between wheat grain number per unit area and average grain size were formed, as follows:

- Potential grain yield: Group I with highest yields obtained by each cultivar across the breadbasket of France from 2014 to 2019.
- Limited grain set: Group II with highest yields obtained by each cultivar, but with a grain number per unit area lower than 21,000 grains m⁻². This threshold of 21,000 grains m⁻² was selected because this was the lowest value of grain number per unit area in the potential grain yield Group I.
- Limited grain filling: Group III with lowest yields obtained by each cultivar, but with a grain number per unit area higher than 21,000 grains m⁻².
- Limited grain set and grain filling: Group IV with lowest yields obtained by each cultivar, but with a grain number per unit area lower than 21,000 grains m⁻².

2.4. Evaluation of the adapted waterlogging module

2.4.1. Outdoor controlled waterlogging experiment in Lleida, Spain

To test the performance of the new waterlogging module we simulated with DSSAT-NWheat the waterlogging experimental setup of Marti et al. (2015). This experiment was conducted with wheat plants grown outdoors in the campus of University of Lleida, Spain (Latitude 41°37'47", Longitude 0°35'47") in columns (84 mm of diameter and 1.25 m deep) filled with a loamy sand soil with 81% sand content. The soil was waterlogged through the blocking of the bottom of the columns, to prevent water drainage. Waterlogging condition was imposed by saturating the soil with water 1 cm above the soil surface. The waterlogging treatments were applied before anthesis, during 4 to 24 days

([SUPPLEMENTARY FIGURE S1](#)). The experiments were free from nutritional and water deficit stress and pests and diseases.

To simulate this experiment, we used the default soil parameter values for loamy sand soil in DSSAT version 4.8 (Hoogenboom et al., 2019), with 1.25 m depth divided in layers of 10 cm thickness. To create the waterlogging condition of the experiment, we set SSKS of the bottom layer at 1 cm h^{-1} , which remains unchanged for the whole growing season. This resulted in undrained of excess water from the bottom of the soil and caused excess water to slowly return to top layers of soil surface. In the simulation setup, the water lost by evapotranspiration was added daily through irrigation, and in the phenological phase when waterlogging was applied ([SUPPLEMENTARY FIGURE S1](#)), excess irrigation was applied to saturate the entire soil profile. The cultivar parameters were calibrated for simulating the observed phenology and wheat yield in the control treatment without waterlogging ([TABLE 1](#)).

2.4.2. Sensitivity analysis

To determine the potential impact of waterlogging on simulated wheat growth with the waterlogging module in DSSAT-NWheat, we conducted a sensitivity analysis. The sensitivity analysis was carried out by simulating waterlogging starting in different phenological stages and with six different waterlogging durations, from 4 to 24 days. This analysis was carried out under the same soil and climate and management conditions as the outdoor controlled waterlogging experiment in Lleida, Spain described in the subsection 2.4.1. The waterlogging conditions were created by setting SSKS of the bottom soil layer at 1 cm h^{-1} , which prevents water from draining from the soil and causes excess water to return to topsoil layers in the surface. In the simulation setup, the water lost by evapotranspiration was added daily through irrigation, and in the phenological phase when waterlogging was applied, excess irrigation was applied to saturate the entire soil profile. Simulated waterlogging was applied during

the following phenological stages: seedling emergence, 2-leaves, 3-leaves, onset of tillering, onset of stem elongation, anthesis, and onset of grain filling.

2.5. Data analysis

Data and statistical analyses were conducted using the statistical software program R (R Core Team, 2017). To evaluate the predictive performance of the waterlogging module in DSSAT-NWheat we computed the relative root mean squared error (rRMSE), the coefficient of determination (r^2) and the Willmott agreement index (d) (Willmott *et al.*, 1985), based on the estimated wheat yield at the tested location together with the corresponding observed yield. The equations for the indices used to evaluate the model performance are presented in [TABLE 2](#).

Table 2. Statistical indexes and errors used for evaluating the DSSAT-NWheat performance.

Statistical indexes and errors	Formula*
Willmott agreement index (d)	$d = 1 - \frac{\sum_{i=1}^n (Sim_i - Obs_i)}{\sum_{i=1}^n (Sim_i - \overline{Obs} + Sim_i - \overline{Obs})^2}$
Root mean squared error (rRMSE)	$rRMSE = \sqrt{\frac{1}{n} \times \sum_{i=1}^n (Sim_i - Obs_i)^2} \bigg/ \frac{\overline{Obs}}{\overline{Est}} \times 100$

* Sim_i and Obs_i are the simulated and observed wheat yield; n is the number of observations; and \overline{Obs} and \overline{Est} are the average of Obs_i and Est_i , respectively.

3. Results

3.1. Review of waterlogging impacts on wheat yield components

Waterlogging from the onset of tillering to anthesis results in a $25 \pm 10\%$ decrease in grain number per unit area in the 17 reviewed articles reporting wheat waterlogging experiments ([FIGURE 3](#)). The highest variation in waterlogging impacts on wheat grain number per unit area (i.e., highest s.d.) are shown when waterlogging occurred at the onset of tillering and heading ([FIGURE 3A](#)). Grain number was less affected when waterlogging occurred at the onset of grain filling, with a $5 \pm 5\%$ decrease.

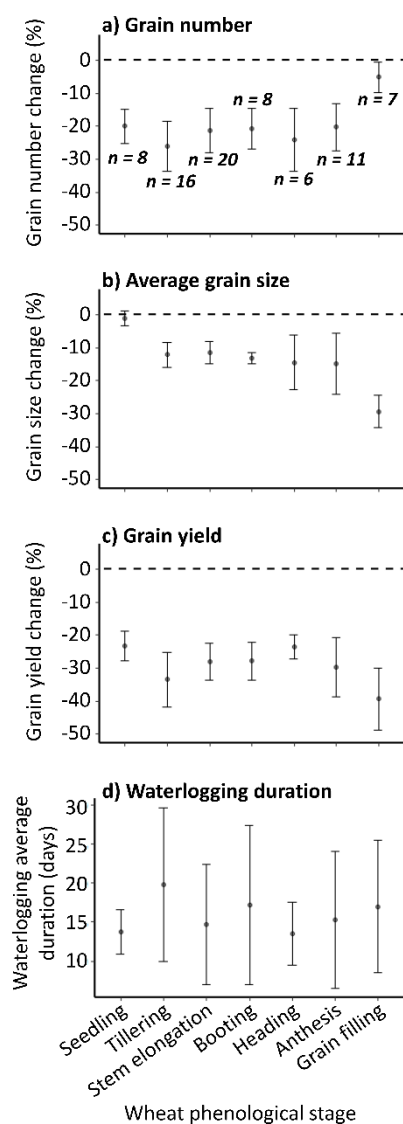


Figure 3. Waterlogging impact on wheat grain number, average grain size, and grain yield. The impacts of waterlogging applied in different phenological stages on (a) grain number per unit area, (b) average grain size, and (c) grain yield. (d) Waterlogging average duration in each phenological phase. The 17 peer-reviewed articles are shown in [SUPPLEMENTARY TABLE S1](#). The number of experiments (n) per for each phenological stage is shown in (a). Points are means \pm 1 s.d.

Episodes of waterlogging resulted in lower average grain size compared with the control treatments with no waterlogging ([FIGURE 3B](#)). Differently from the wheat grain number, the average grain size was more sensitive to waterlogging when it occurred during the onset of grain filling, with a $30\pm 5\%$

decrease. Waterlogging during seedling emergence had almost no impact on average grain size. With the combined effect of waterlogging on average grain number and grain size per unit area, grain yield was more sensitive to waterlogging when it occurred during the onset of tillering, anthesis and the onset of grain filling, with on average $37\pm 10\%$. Waterlogging impacts on grain yield were lower during seedling emergence.

3.2. Relation between wheat grain number per unit area and average grain size

The relation between wheat grain number per unit area and average grain size is shown here to demonstrate the limitations of wheat yield, either by a few grains per unit area or low grain size. In addition, this analysis is further evidence of the definition of the potential grain size in limited grain set conditions (Group II), which was used to improve the simulations of wheat growth in DSSAT-NWheat.

The potential wheat grain yield, with average yields above 10 t ha^{-1} , presented an inverse linear relationship between grain number per unit area and average grain size in a wide experimental dataset from France with more than 200 winter wheat cultivars (FIGURE 4). In this case of potential yield, the average grain size varied from 33 mg grain^{-1} to 50 mg grain^{-1} and the grain number per unit area varied from 22,000 to 34,000 grains m^{-2} . However, the highest values of grain number per unit area occurred simultaneously to the lowest values of grain size, as well as the highest values of average grain size occurred simultaneously to the lowest values of grain number per unit area.

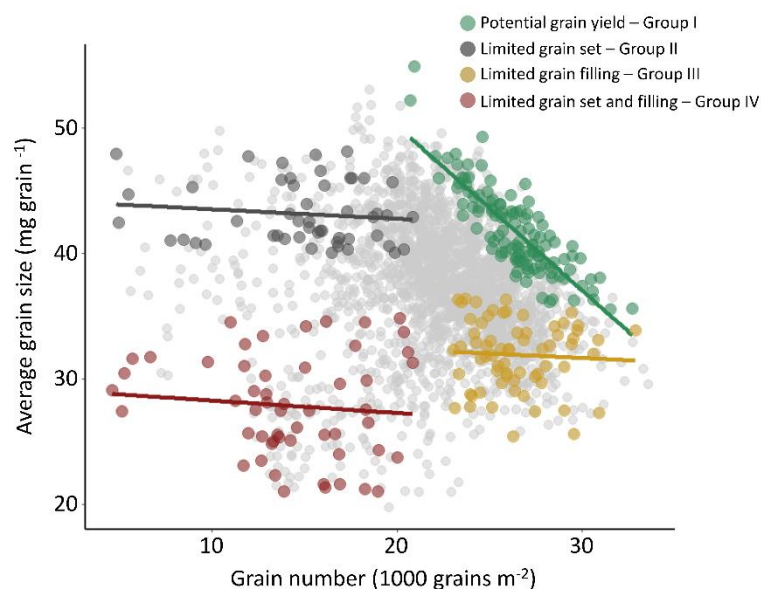


Figure 4. Relationships between wheat grain number and average grain size. The potential grain yield (Group I) highlighted in green represents the highest recorded yields from 221 different cultivars for the period 2014 to 2019. Limited grain set (Group II) highlighted in black represents lowest recorded yields with highest grain size from 221 different cultivars for the period 2014 to 2019. Limited grain filling (Group III) highlighted in yellow represents lowest recorded yields with highest grain number from different cultivars for the period 2014 to 2019. Limited grain set and filling (Group IV) highlighted in red represents lowest recorded yields size from 221 different cultivars for the period 2014 to 2019. Data are from 3,188 experimental treatments with 221 winter wheat cultivars performed by ARVALIS from 2014 to 2019 in different research stations in the breadbasket of France. Circles refer to the observations and lines to linear regression for the data with the same color.

Wheat yields between 3 and 10 t ha⁻¹ occurred in two situations, with limited grain set or limited grain filling. With limited grain set, the grain number per unit area varied from 2,000 to 23,000 grains m⁻², whereas the average grain size was 41 to 48 mg grain⁻¹. With limited grain filling, the grain number per unit area varied from 24,000 to 34,000 grains m⁻², whereas the average grain size was 25 to 37 mg grain⁻¹. In these cases, the linear relationship between grain number and grain size is not as strong as was for the potential grain yields. The lowest yields (< 4 t ha⁻¹) occurred with both, limited grain number and grain filling (Group IV). This combination resulted in average grain size with 20 mg grain⁻¹, and grain number per unit area as low as 2,000 grains m⁻².

Average grain size showed an average value of 44 mg grain⁻¹ for the limited grain set group. A limited grain set results in fewer grains per unit area, but the average grain size also becomes limited, not exceeding 48 mg grain⁻¹, with an average of 44 mg grain⁻¹.

3.3. DSSAT-NWheat performance to simulate the impacts of waterlogging on wheat yield components.

We tested the improved DSSAT-NWheat to simulate the impacts of waterlogging on yield and yield components, with an outdoor controlled waterlogging experiment. First, the simulations were done with the default DSSAT-NWheat without any improvements to simulate waterlogging impacts. As part of this, the simulated wheat yield was 9.3 t ha⁻¹, regardless of the duration of pre-anthesis waterlogging (FIGURE 5). Second, the simulations were performed with DSSAT-NWheat with added modules for simulating the impacts of waterlogging on wheat roots (R) and carbohydrate accumulation (CA). In this case, the simulated wheat yield shows a decline due to pre-anthesis waterlogging, of almost 3 t ha⁻¹ with 24 days long waterlogging period (FIGURE 5A). This yield decline is mainly due to the decreased simulated grain number (FIGURE 5B), with increased grain size compensating for it (FIGURE 5C). The simulated grain size increased up to 57% compared to the simulations with DSSAT-Wheat without any improvements to simulate waterlogging impacts. To better simulate the impacts of waterlogging on yield components, we added an impact of waterlogging on potential grain size (GS). Considering decreased rooting depth, carbohydrate accumulation and potential grain size under waterlogging conditions, the new improved DSSAT-NWheat satisfactorily simulated wheat yield loss due to waterlogging, with lower grain number and grain size (FIGURE 5).

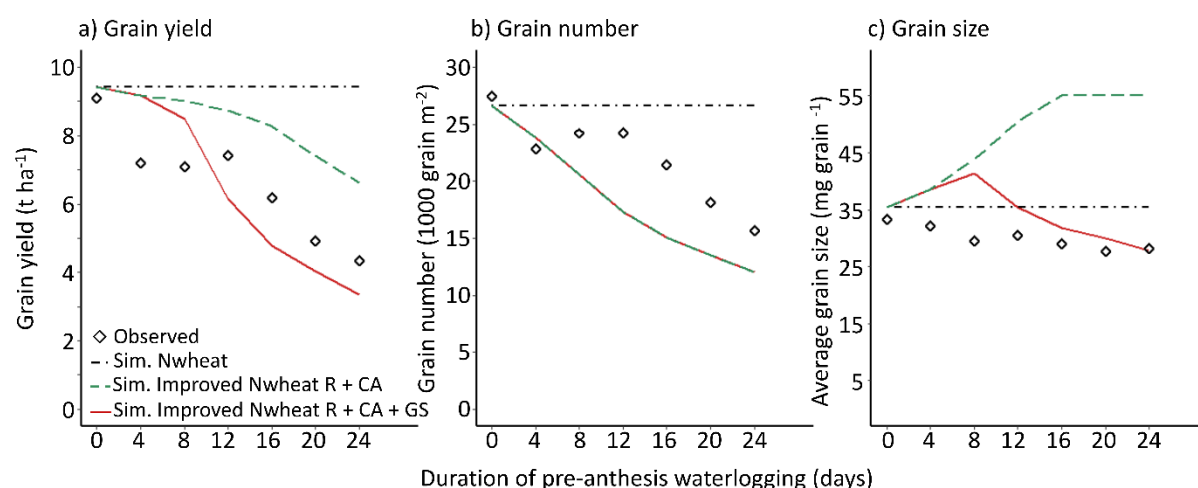


Figure 5. Performance of the improved DSSAT-NWheat in simulating pre-anthesis waterlogging impacts on wheat. Performance of DSSAT-NWheat in simulating pre-anthesis waterlogging impacts on wheat (a) grain yield (b) grain number and (c) grain size. Data (points) are from an outdoor controlled experiment where wheat plants were waterlogged for 0 to 24 days before anthesis (Marti et al., 2015). Simulations (lines) were done with DSSAT-NWheat with no waterlogging module (Sim. NWheat), with the waterlogging module accounting only for the impacts of waterlogging on wheat roots and carbohydrate accumulation (Sim. NWheat improved R + CA) and with the waterlogging module accounting for the impacts of waterlogging on wheat roots, carbohydrate accumulation and potential grain size (Sim. NWheat improved R + CA + GS). The acronyms R represents the waterlogging module with impacts on wheat roots, CA in carbohydrate accumulation and GS in potential grain size.

With the new improved DSSAT-NWheat the rRMSE between simulated and observed waterlogged grain yield, grain number per unit area and grain size was 18% (TABLE 3). For grain yield and grain number r^2 was 0.68, and for average grain size r^2 was 0.30. The accuracy of the model, represented by the index d , was 0.86 for grain yield, 0.79 for grain number per unit area and 0.38 for average grain size. Even with the improvements, the DSSAT-NWheat tends to underestimate the average grain number and to overestimate the average grain size, particularly when waterlogging occurred from 4 to 12 days (FIGURE 5c).

Table 3 Performance of the improved DSSAT-NWheat in simulating pre-anthesis waterlogging impacts on wheat. Data are from an outdoor controlled experiment where wheat plants were waterlogged for 0 to 24 days before anthesis (Marti et al., 2015) with the DSSAT model with a waterlogging module affecting wheat roots, carbohydrate accumulation potential grain size. Statistical

indices are the relative root mean square error (rRMSE), the coefficient of determination (r^2) and the Willmott agreement index (d) (Willmott *et al.*, 1985).

Wheat yield components	rRMSE (%)	r^2	d
Grain yield	18	0.69	0.86
Grain number	18	0.68	0.79
Grain size	18	0.30	0.38

3.4. Sensitivity analyses

The capacity of the model to simulate the impacts of waterlogging on wheat growth variables and yield components is shown through the sensitivity analysis, with waterlogging occurring at different phenological stages and with different durations (**FIGURE 6**). For winter wheat (cultivar Soisson), simulated waterlogging starts to impact yield components during the onset of tillering, except for root biomass. Simulated root biomass is less impacted by waterlogging when it occurred in the early phenological stages (**FIGURE 6B**). The highest impacts on root biomass occur during the onset of grain filling, with a reduction of up to 60% after 24 days of waterlogging compared to control treatment with no waterlogging. The biomass at maturity and the grain number per unit area are affected from the onset of tillering to the onset of grain filling, with the highest impact occurring at the onset of stem elongation (**FIGURE 6A AND 6D**). At this stage, both biomass at maturity and grain number per unit area decrease by 50% with 24 days of waterlogging.

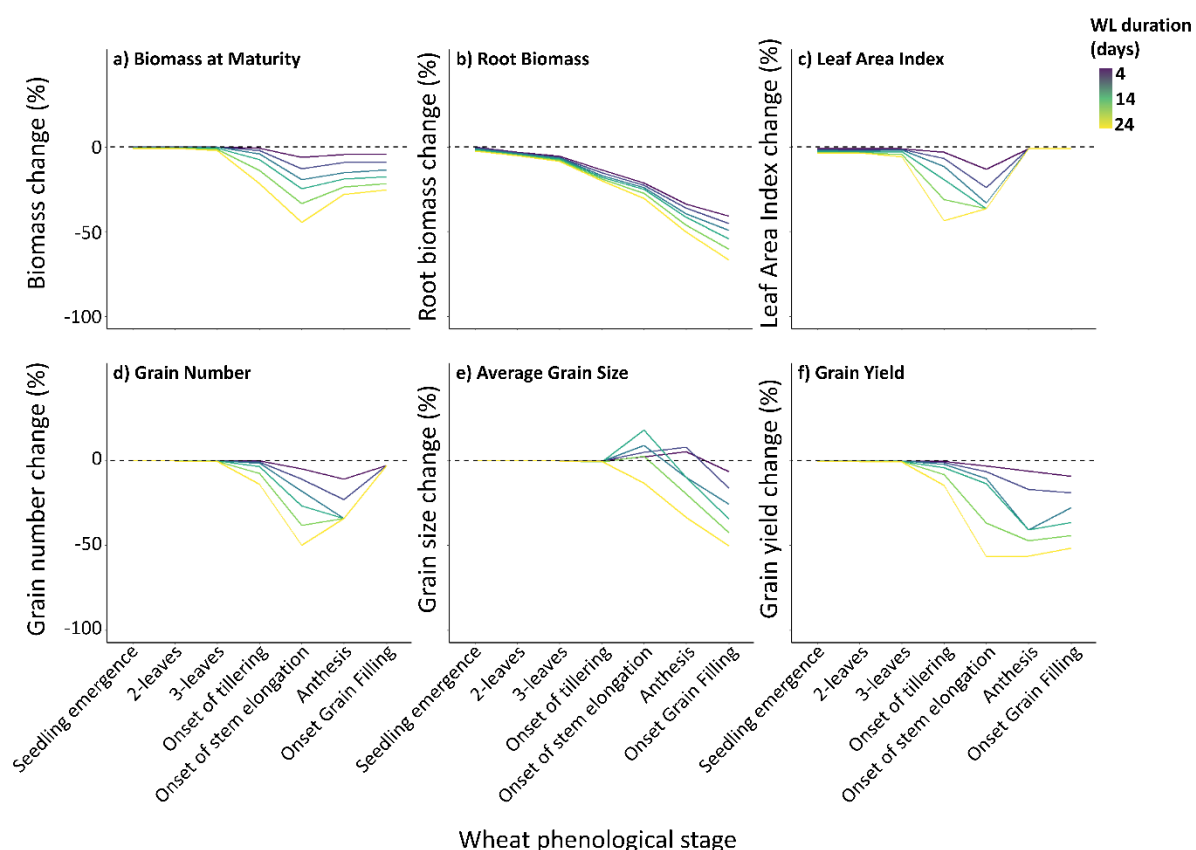


Figure 6. Sensitivity analysis of the impacts of waterlogging on winter wheat growth simulated by DSSAT-NWheat. Impacts of simulated waterlogging on wheat (a) biomass at maturity, (b) root biomass, (c) leaf area index, (d) grain number per unit area, (e) average grain size and (f) grain yield. The sensitivity analysis was carried out by simulating waterlogging starting in different phenological stages, from wheat seedling emergence to the onset of grain filling, with six different durations varying from 4 to 24 days as schematically shown in [SUPPLEMENTARY FIGURE S1](#). Sensitivity analysis of the impacts of waterlogging on spring wheat are shown in [SUPPLEMENTARY FIGURE S4](#).

Leaf area index is impacted by waterlogging from 3-leave-stage to the onset of stem elongation, with the highest sensitivity at the onset of tillering. The average grain size decreased with waterlogging from the onset of stem elongation to the onset of grain filling, and it declines more than 50% with 24 days of waterlogging in the onset of grain filling. As a result of the decline of all wheat yield components under waterlogging conditions, grain yield can decrease by up to 65% compared to the

control (with no waterlogging), with waterlogging occurring from the onset of stem elongation to the onset of grain filling.

4. Discussion

4.1. Modeling performance of the new waterlogging module in DSSAT-NWheat

Oxygen availability is restricted in waterlogged soils, suppressing roots respiration and causing decreased root activity (van Veen *et al.*, 2014). Plants can temporarily maintain energy production during waterlogging via glycolysis and ethanol fermentation, but prolonged waterlogging leads to accumulation of toxic metabolites and increased reactive oxygen species leading to cell death (Pan *et al.*, 2021). This causes inhibition of root growth and malfunctioning in transport of nutrients and water to shoots, and death of roots (Herzog *et al.*, 2016). Reduction of root functioning together with increased nutrient leaching (due to excessive soil water drainage) may cause nutrient deficit stress (Salazar *et al.*, 2014; Kaur *et al.*, 2020). Even under non-nutrient deficit conditions, waterlogging limits root water conductivity causing stomatal closure, reducing carbohydrate accumulation and crop growth (Else *et al.*, 2001; Jitsuyama, 2017). We demonstrated the ability of a new waterlogging module in DSSAT-NWheat to simulate yield in response to waterlogging in an outdoor controlled waterlogging experiment. For an outdoor controlled experiment, the improved version of DSSAT-NWheat presented similar performance with r^2 of 0.69 and rRMSE 18%. For a different controlled experiment, the APSIM crop model improved for simulating the impacts of waterlogging on wheat carbohydrate accumulation, presented r^2 of 0.70 and rRMSE 11% to simulate wheat yield losses to waterlogging (Liu *et al.*, 2023).

4.2. Simulated impacts of waterlogging on wheat yield components

The DSSAT-NWheat model simulates grain number per unit area as a function of the stem weight in the first day of grain filling, considering a crop parameter, ADD parameter name/acronym, which varied from 20 to 32 grain per grams of stem dry mass. After the grain number per unit area simulation, the DSSAT-NWheat simulates the carbohydrate accumulation in grains. The maximum grain size is limited with the parameter name/acronym MXGWT. With few grains, all the carbohydrate assimilated during grain filling plus the carbohydrate remobilized from the shoot is distributed to the few grains, causing the simulation of heavy grains (*i.e.* high average grain size). High average grain size may also be caused due to the non-development and growth of potential grains close to the labile florets, positioned more distally and with constitutively low grain size, which usually occur during limited grain set situations. In this case, these potential grains with low grain size would not succeed (would not grow and become grains), resulting in an increase in the average grain size of harvested grains (because only the bigger grains would be harvested) (Beral *et al.*, 2022). Waterlogging may also accelerate the flag leaf senescence (Li *et al.*, 2012), which alters post-anthesis biomass production and translocation to grain, impairing the filling of small grains, that would not grow to the point of being harvested.

This relation between grain number per unit area and grain size was here demonstrated for waterlogging simulations before wheat anthesis, which resulted in few but heavier grains on average. To minimize the overestimation of grain size, we implemented an equation to limit the potential grain size when abiotic stress occurs before anthesis similar to observations made experimentally (Liu *et al.*, 2020a). This also improved the simulation of waterlogging impact on grain size. Grain volume enlargement involves the coordinated expansion of the pericarp of maternal origin and the endosperm of the seed, and is almost complete when grain filling begins (Asseng *et al.*, 2019; Calderini *et al.*, 2021). The expansion of these tissues determines the grain carbohydrates and proteins storage

capacity and therefore the potential grain size (Herrera and Calderini, 2020). The growing conditions around anthesis are therefore critical for potential grain size determination, a time when simultaneously also grain number per unit area is set (Acreche and Slafer, 2006; Calderini *et al.*, 2021; Slafer *et al.*, 2023). In addition to the impacts of waterlogging on the potential grain size, grain size may also be affected by any other abiotic constraints at this developmental stage, like heat, drought, ozone and nitrogen deficit, all factors considered in DSSAT-NWheat. The combined impact of these factors on grain size determination still needs to be tested with field data.

4.3. Factors that affect the intensity of waterlogging impacts on wheat growth

The impacts of waterlogging on wheat growth varies particularly according to its duration and crop phenological stage. We showed that wheat may be less affected by waterlogging during the seedling emergence stage, and can drop drastically during anthesis and grain filling, either due to lower grain numbers or grain size (FIGURE 3), which was also simulated with the DSSAT-NWheat (FIGURE 6). In addition, waterlogging impacts on wheat and on any crop also vary according to its depth, air temperature, soil type, mineral nutrition management and genotype, factors that were not considered in this study (Herzog *et al.*, 2016). For example, lower air temperatures results in slower soil oxygen depletion making less severe the impacts of waterlogging on crop growth (Trought and Drew, 1982). These factors influencing the impact of waterlogging on wheat growth should be addressed in future studies.

5. Conclusions

The lack of waterlogging modules in crop simulation models causes concern about underestimation of projected negative impacts of climate change on crop productivity (van der Velde *et al.*, 2020;

Webber *et al.*, 2020). The new DSSAT-NWheat model with a coupled waterlogging module may reduce uncertainties in future impact studies. Reduced wheat yields due to excess of rainfall, which so far have not been simulated correctly on most crop models, can now be addressed with the model proposed in this study. For example, waterlogging in 2016 is estimated to have caused 26% of the France's biggest yield decline since 1960 (Nóia Júnior *et al.*, 2023), an unforeseen event for seasonal forecasting systems including crop simulation models (Ben-Ari *et al.*, 2018). This extreme event caused partly by excessive rainfall, may also involve yield loss from increased crop diseases and heavy rainfall which are also usually neglected by crop simulation models. Only with continuous improvements of crop models to simulate the impacts of extreme climate events on crop growth, more robust simulations will be possible in the future. With these improvements, crop models will become capable to assist in understanding how the complexity of climate change will impact future crop production as a prerequisite to develop adaptation strategies.

6. Author contributions

All co-authors conceptualized the study. JCD, JPC, PM and SA supervised the study. VSt and VSh implemented the waterlogging module in DSSAT-NWheat. GS made available the data from the outdoor controlled waterlogging experiment in Lleida in Spain. The grain number per unit area and average grain size data in France, was made available by JCD and JPC. RSNJ and Vst performed the formal analysis. RSNJ wrote initial draft, all co-authors assisted with writing and reviewed the manuscript.

7. Acknowledgements

The authors thank ARVALIS for the financial support of this study. R.S.N.J. acknowledges support from the Prince of Albert II of Monaco foundation through the IPCC Scholarship Program. The contents of this manuscript are solely the liability of R.S.N.J. and under no circumstances may be considered as a reflection of the position of the Prince Albert II of Monaco Foundation and/or the IPCC. P.M. acknowledges support from the Agriculture and Forestry in the Face of Climate Change: Adaptation and Mitigation (CLIMAE) Meta-program of the French National Research Institute for Agriculture, Food and Environment (INRAE). F.E. acknowledges support from the Deutsche Forschungsgemeinschaft (DFG, German Research Foundation) under Germany's Excellence Strategy – EXC 2070 – 390732324 (PhenoRob).

8. References

- Acreche MM, Slafer GA.** 2006. Grain weight response to increases in number of grains in wheat in a Mediterranean area. *Field Crops Research* **98**, 52–59.
- Asseng S, Ewert F, Martre P, et al.** 2015. Rising temperatures reduce global wheat production. *Nature Climate Change* **5**, 143–147.
- Asseng S, Ewert F, Rosenzweig C, et al.** 2013. Uncertainty in simulating wheat yields under climate change. *Nature Climate Change* **3**, 827–832.
- Asseng S, Kassie BT, Labra MH, Amador C, Calderini DF.** 2017. Simulating the impact of source-sink manipulations in wheat. *Field Crops Research* **202**, 47–56.
- Asseng S, Keating BA, Huth NI, Easthan J.** 1997. Simulation of Perched Watertables in a Duplex Soil. *International Congress on Modelling and Simulation Proceedings*. Hobart, Tasmania: The Modelling and Simulation Society of Australia, 538–543.
- Asseng S, Martre P, Maiorano A, et al.** 2019. Climate change impact and adaptation for wheat protein. *Global Change Biology* **25**, 155–173.
- Ben-Ari T, Boé J, Ciais P, Lecerf R, Van der Velde M, Makowski D.** 2018. Causes and implications of the unforeseen 2016 extreme yield loss in the breadbasket of France. *Nature Communications* **9**, 1627.
- Beral A, Girousse C, Le Gouis J, Allard V, Slafer GA.** 2022. Physiological bases of cultivar differences in average grain weight in wheat: Scaling down from plot to individual grain in elite material. *Field Crops Research* **289**, 108713.
- Calderini DF, Castillo FM, Arenas-M A, et al.** 2021. Overcoming the trade-off between grain weight and number in wheat by the ectopic expression of expansin in developing seeds leads to increased yield potential. *New Phytologist* **230**, 629–640.

- Calderini DF, Savin R, Abeledo LG, Reynolds MP, Slafer GA.** 2001. The importance of the period immediately preceding anthesis for grain weight determination in wheat. *Euphytica* **119**, 199–204.
- Ceglar A, Zampieri M, Gonzalez-Reviriego N, Ciais P, Schauburger B, Van der Velde M.** 2020. Time-varying impact of climate on maize and wheat yields in France since 1900. *Environmental Research Letters* **15**, 094039.
- Colmer TD, Voeselek LACJ.** 2009. Flooding tolerance: suites of plant traits in variable environments. *Functional Plant Biology* **36**, 665–681.
- Else MA, Coupland D, Dutton L, Jackson MB.** 2001. Decreased root hydraulic conductivity reduces leaf water potential, initiates stomatal closure and slows leaf expansion in flooded plants of castor oil (*Ricinus communis*) despite diminished delivery of ABA from the roots to shoots in xylem sap. *Physiologia Plantarum* **111**, 46–54.
- Fischer RA.** 1985. Number of kernels in wheat crops and the influence of solar radiation and temperature. *The Journal of Agricultural Science* **105**, 447–461.
- Githui F, Beverly C, Aiad M, McCaskill M, Liu K, Harrison MT.** 2022. Modelling Waterlogging Impacts on Crop Growth: A Review of Aeration Stress Definition in Crop Models and Sensitivity Analysis of APSIM. *International Journal of Plant Biology* **13**, 180–200.
- Herrera J, Calderini DF.** 2020. Pericarp growth dynamics associate with final grain weight in wheat under contrasting plant densities and increased night temperature. *Annals of Botany* **126**, 1063–1076.
- Herzog M, Striker GG, Colmer TD, Pedersen O.** 2016. Mechanisms of waterlogging tolerance in wheat – a review of root and shoot physiology. *Plant, Cell & Environment* **39**, 1068–1086.
- Hoogenboom G, Porter CH, Boote KJ, et al.** 2019. The DSSAT crop modeling ecosystem. *Advances in crop modelling for a sustainable agriculture*. 173–216.
- Jeantet A, Henine H, Chaumont C, Collet L, Thirel G, Tournebize J.** 2021. Robustness of a parsimonious subsurface drainage model at the French national scale. *Hydrology and Earth System Sciences* **25**, 5447–5471.
- Jitsuyama Y.** 2017. Hypoxia-Responsive Root Hydraulic Conductivity Influences Soybean Cultivar-Specific Waterlogging Tolerance. *American Journal of Plant Sciences* **08**, 770–790.
- Jones J., Hoogenboom G, Porter C., Boote K., Batchelor W., Hunt L., Wilkens P., Singh U, Gijssman A., Ritchie J.** 2003. The DSSAT cropping system model. *European Journal of Agronomy* **18**, 235–265.
- Kassie BT, Asseng S, Porter CH, Royce FS.** 2016. Performance of DSSAT-Nwheat across a wide range of current and future growing conditions. *European Journal of Agronomy* **81**, 27–36.
- Kaur G, Singh G, Motavalli PP, Nelson KA, Orlowski JM, Golden BR.** 2020. Impacts and management strategies for crop production in waterlogged or flooded soils: A review. *Agronomy Journal* **112**, 1475–1501.
- Kulkarni A V, Shirsat TS, Kulkarni A, Negi HS, Bahuguna IM, Thamban M.** 2021. State of Himalayan cryosphere and implications for water security. *Water Security* **14**, 100101.
- Kuppel S, Houspanossian J, Noretto MD, Jobbágy EG.** 2015. What does it take to flood the Pampas?: Lessons from a decade of strong hydrological fluctuations. *Water Resources Research* **51**, 2937–2950.
- Li H, Cai J, Liu F, Jiang D, Dai T, Cao W.** 2012. Generation and scavenging of reactive oxygen species in

wheat flag leaves under combined shading and waterlogging stress. *Functional Plant Biology* **39**, 71–81.

Liu B, Asseng S, Müller C, et al. 2016. Similar estimates of temperature impacts on global wheat yield by three independent methods. *Nature Climate Change* **6**, 1130–1136.

Liu K, Harrison MT, Archontoulis S V., et al. 2021a. Climate change shifts forward flowering and reduces crop waterlogging stress. *Environmental Research Letters* **16**.

Liu K, Harrison MT, Archontoulis S V, et al. 2021b. Climate change shifts forward flowering and reduces crop waterlogging stress. *Environmental Research Letters* **16**, 94017.

Liu K, Harrison MT, Ibrahim A, Manik SMN, Johnson P, Tian X, Meinke H, Zhou M. 2020a. Genetic factors increasing barley grain yields under soil waterlogging. *Food and Energy Security* **9**, e238.

Liu K, Harrison MT, Shabala S, Meinke H, Ahmed I, Zhang Y, Tian X, Zhou M. 2020b. The State of the Art in Modeling Waterlogging Impacts on Plants: What Do We Know and What Do We Need to Know. *Earth's Future* **8**.

Liu K, Harrison MT, Shabala S, Meinke H, Ahmed I, Zhang Y, Tian X, Zhou M. 2020c. The State of the Art in Modeling Waterlogging Impacts on Plants: What Do We Know and What Do We Need to Know. *Earth's Future* **8**, e2020EF001801.

Liu K, Harrison MT, Yan H, et al. 2023. Silver lining to a climate crisis in multiple prospects for alleviating crop waterlogging under future climates. *Nature Communications* **14**, 765.

Liu B, Martre P, Ewert F, et al. 2019. Global wheat production with 1.5 and 2.0°C above pre-industrial warming. *Global Change Biology* **25**, 1428–1444.

Lizaso JI. 1993. Flooding and field grown maize : above- and below-ground responses and a simulation model.

Marti J, Savin R, Slafer GA. 2015. Wheat Yield as Affected by Length of Exposure to Waterlogging During Stem Elongation. *Journal of Agronomy and Crop Science* **201**, 473–486.

Nóia Júnior R de S, Deswarte J-C, Cohan J-P, et al. 2023. The extreme 2016 wheat yield failure in France. *Global Change Biology* n/a.

Nóia Júnior R de S, Martre P, Finger R, van der Velde M, Ben-Ari T, Ewert F, Webber H, Ruane AC, Asseng S. 2021. Extreme lows of wheat production in Brazil. *Environmental Research Letters* **16**, 104025.

Pan J, Sharif R, Xu X, Chen X. 2021. Mechanisms of Waterlogging Tolerance in Plants: Research Progress and Prospects . *Frontiers in Plant Science* **11**.

R Core Team. 2017. R: A Language and Environment for Statistical Computing. R Foundation for Statistical Computing, Vienna, Austria, {ISBN} 3-900051-07-0.

Röll G, Memic E, Graeff-Hönninger S. 2020. Implementation of an automatic time-series calibration method for the DSSAT wheat models to enhance multi-model approaches. *Agronomy Journal* **112**, 3891–3912.

Salazar O, Vargas J, Nájera F, Seguel O, Casanova M. 2014. Monitoring of nitrate leaching during flush flooding events in a coarse-textured floodplain soil. *Agricultural Water Management* **146**, 218–227.

de San Celedonio RP, Abeledo LG, Miralles DJ. 2014. Identifying the critical period for waterlogging

on yield and its components in wheat and barley. *Plant and Soil* **378**, 265–277.

Sayre KD, Van Ginkel M, Rajaram S, Ortiz-Monasterio I. 1994. Tolerance to waterlogging losses in spring bread wheat: effect of time of onset on expression. *Annual Wheat Newsletter* **40**, 165–171.

Shelia V, Asseng S, Porter C, Hoogenboom G. 2020. SIMULATION OF A PERCHED WATER TABLE WITH IMPACT ON WHEAT CROP GROWTH. ASA, CSSA and SSSA International Annual Meetings, ASA Section: Climatology and Modeling. November 8-11, Phoenix, AZ .

Slafer GA, Elia M, Savin R, García GA, Terrile II, Ferrante A, Miralles DJ, González FG. 2015. Fruiting efficiency: an alternative trait to further rise wheat yield. *Food and Energy Security* **4**, 92–109.

Slafer GA, Foulkes MJ, Reynolds MP, Murchie EH, Carmo-Silva E, Flavell R, Gwyn J, Sawkins M, Griffiths S. 2023. A ‘wiring diagram’ for sink strength traits impacting wheat yield potential. *Journal of Experimental Botany* **74**, 40–71.

Trought MCT, Drew MC. 1982. Effects of waterlogging on young wheat plants (*Triticum aestivum* L.) and on soil solutes at different soil temperatures. *Plant and Soil* **69**, 311–326.

van Veen H, AKMAN M, JAMAR DCL, VREUGDENHIL D, KOOIKER M, van TIENDEREN P, VOESENEK LACJ, SCHRANZ ME, SASIDHARAN R. 2014. Group VII Ethylene Response Factor diversification and regulation in four species from flood-prone environments. *Plant, Cell & Environment* **37**, 2421–2432.

van der Velde M, Lecerf R, d’Andrimont R, Ben-Ari T. 2020. Chapter 8 - Assessing the France 2016 extreme wheat production loss—Evaluating our operational capacity to predict complex compound events. In: Sillmann J,, In: Sippel S,, In: Russo SBT-CE and TI for I and RA, eds. Elsevier, 139–158.

Webber H, Lischeid G, Sommer M, Finger R, Nendel C, Gaiser T, Ewert F. 2020. No perfect storm for crop yield failure in Germany. *Environmental Research Letters* **15**, 104012.

Willmott CJ, Ackleson SG, Davis RE, Feddema JJ, Klink KM, Legates DR, O’Donnell J, Rowe CM. 1985. Statistics for the evaluation and comparison of models. *Journal of Geophysical Research* **90**, 8995.

Yan H, Harrison MT, Liu K, et al. 2022. Crop traits enabling yield gains under more frequent extreme climatic events. *Science of The Total Environment* **808**, 152170.

Zampieri M, Ceglar A, Dentener F, Toreti A. 2017. Wheat yield loss attributable to heat waves, drought and water excess at the global, national and subnational scales. *Environmental Research Letters* **12**, 64008.

Zhao C, Liu B, Piao S, et al. 2017. Temperature increase reduces global yields of major crops in four independent estimates. *Proceedings of the National Academy of Sciences* **114**, 9326 LP – 9331.

Supplementary Materials for

Enabling modeling of waterlogging impact on wheat

Rogério de S. Nóia Júnior, Valentina Stocca, Vakhtang Shelia, Pierre Martre, Jean-Charles Deswarte, Jean-Pierre Cohan, Benoît Piquemal, Alain Dutertre, Gustavo A. Slafer, Marijn Van der Velde, Yean-Uk Kim, Heidi Webber^{8,9}, Frank Ewert, Taru Palosuo, Matthew Tom Harrison, Gerrit Hoogenboom, Senthold Asseng

Contents

1. Supplementary Tables	2
2. Experiments characterization.....	4
2.1. Controlled experiment of waterlogging on wheat.....	4
3. DSSAT-Nwheat with waterlogging routine.....	5
3.1. DSSAT-Sbuild.....	5
3.2. Wheat average potential grain size	6
3.3. Waterlogging module comparison	8
4. References	9

1. Supplementary Tables

Table S1. Published peer-reviewed articles on the effects of waterlogging on wheat growth. Growth stages from the Zadoks growth stages scale (ZADOKS et al., 1974).

ID	Growth stage	Duration of waterlogging (days)	References	Web-link
1	25	47, 58	(Dickin and Wright, 2008)	here
2	71	30, 5	(Zhou et al., 2018a)	here
3	71, 20	4, 7	(Wang et al., 2016)	here
4	37	7	(Gao et al., 2021)	here
5	50, 68	14	(Ploschuk et al., 2020)	here
6	71,39	7, 2	(Li et al., 2011)	here
7	71	15	(Tan et al., 2008)	here
8	61	5, 10, 15, 20, 25, 50	(Olgun et al., 2008)	here
9	31, 39, 45, 50, 58, 64	4, 8, 12, 16, 20, 24	(Marti et al., 2015)	here
10	10, 20, 30, 40	15, 20	(de San Celedonio et al., 2018)	here
11	32, 50	12	(Ding et al., 2018)	here
12	14	12	(Farkas et al., 2020)	here
13	61	14	(Zhou et al., 2018b)	here
14	30, 50, 60	5, 10, 15	(Martinez et al., 2019)	here
15	33, 45, 65	10	(Ding et al., 2020)	here
16	10, 20, 25, 40, 50, 60, 71	15, 20	(de San Celedonio et al., 2014)	here
17	20, 30, 40, 61	14, 28, 35	(Wu et al., 2018)	here

Table S2. Soil drainage classes in DSSAT-SBuilt and their respective soil drainage rate (SLDR).

Soil drainage classes in DSSAT	SLDR
Very Poorly	0.01
Poorly	0.05
Somewhat poorly	0.25
Moderately well	0.4
Well	0.6
Somewhat excessive	0.75
Excessive	0.85
Very excessive	0.95

2. Experiments characterization

2.1. Controlled experiment of waterlogging on wheat in Spain

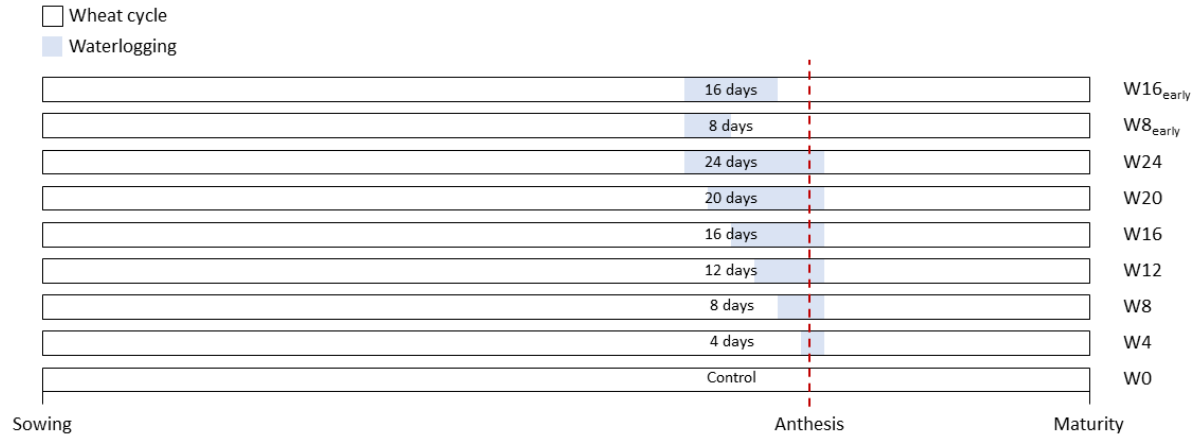


Figure S1. Schematic representation of the controlled experiment of waterlogging on wheat done by Marti et al. (2015). This experiment was performed in Lleida, Spain with the winter wheat cultivar Soissons.

3. DSSAT-Nwheat with waterlogging routine

3.1. DSSAT-Sbuild

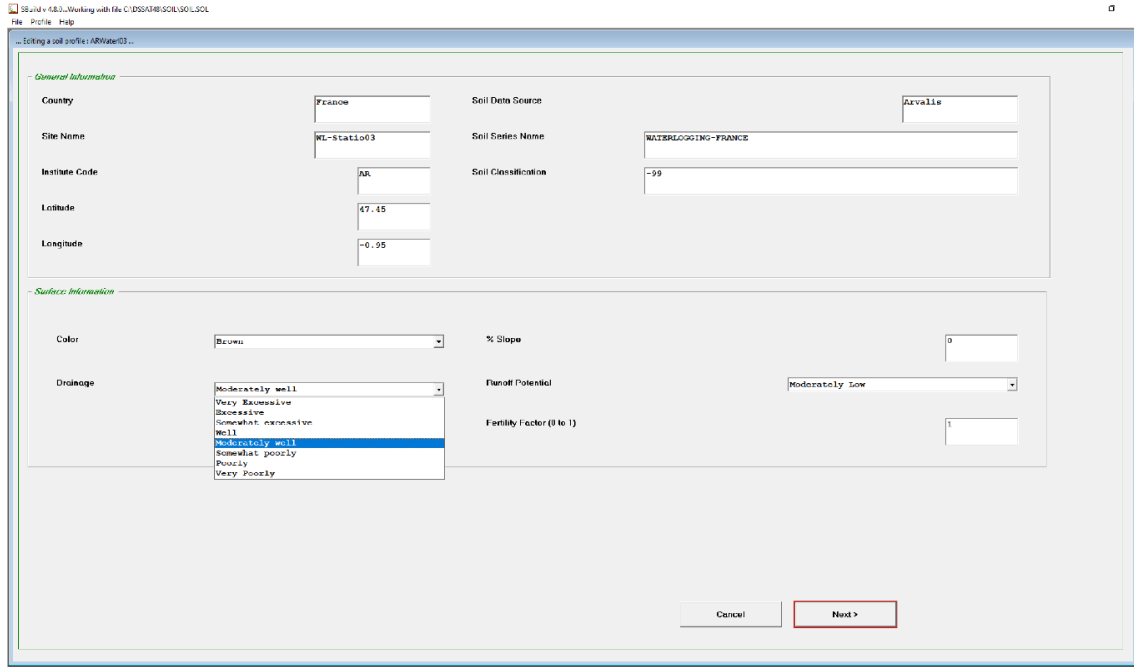


Figure S3. Screenshot of the DSSAT-SBuild graphical user interface. The user selection of the soil drainage rate (SLDR) is highlighted. The correspondent values for each of the drainage classes are shown in [TABLE S2](#).

3.2. Wheat average potential grain size

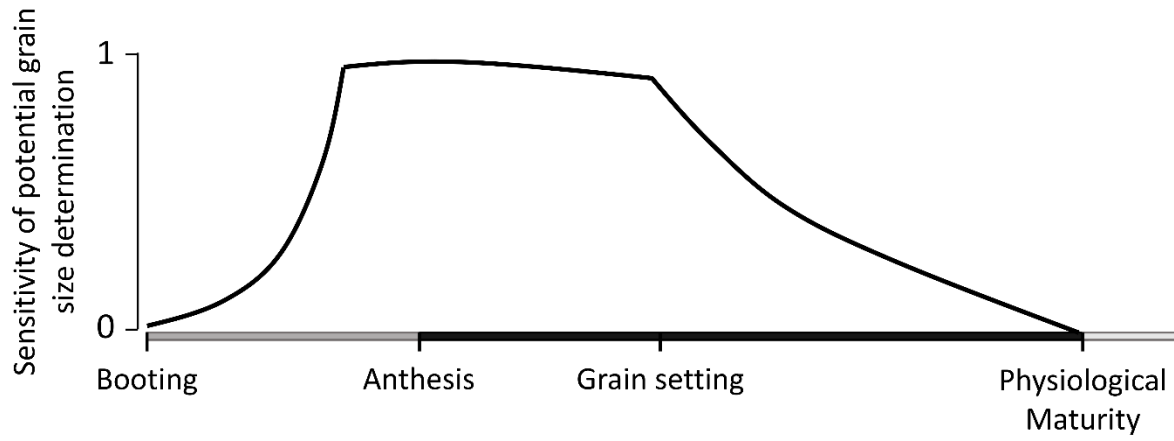


Figure S3. Schematic diagram of the sensitivity of average grain dry mass in wheat during the crop growth cycle. Adapted from Calderini et al. (2001).

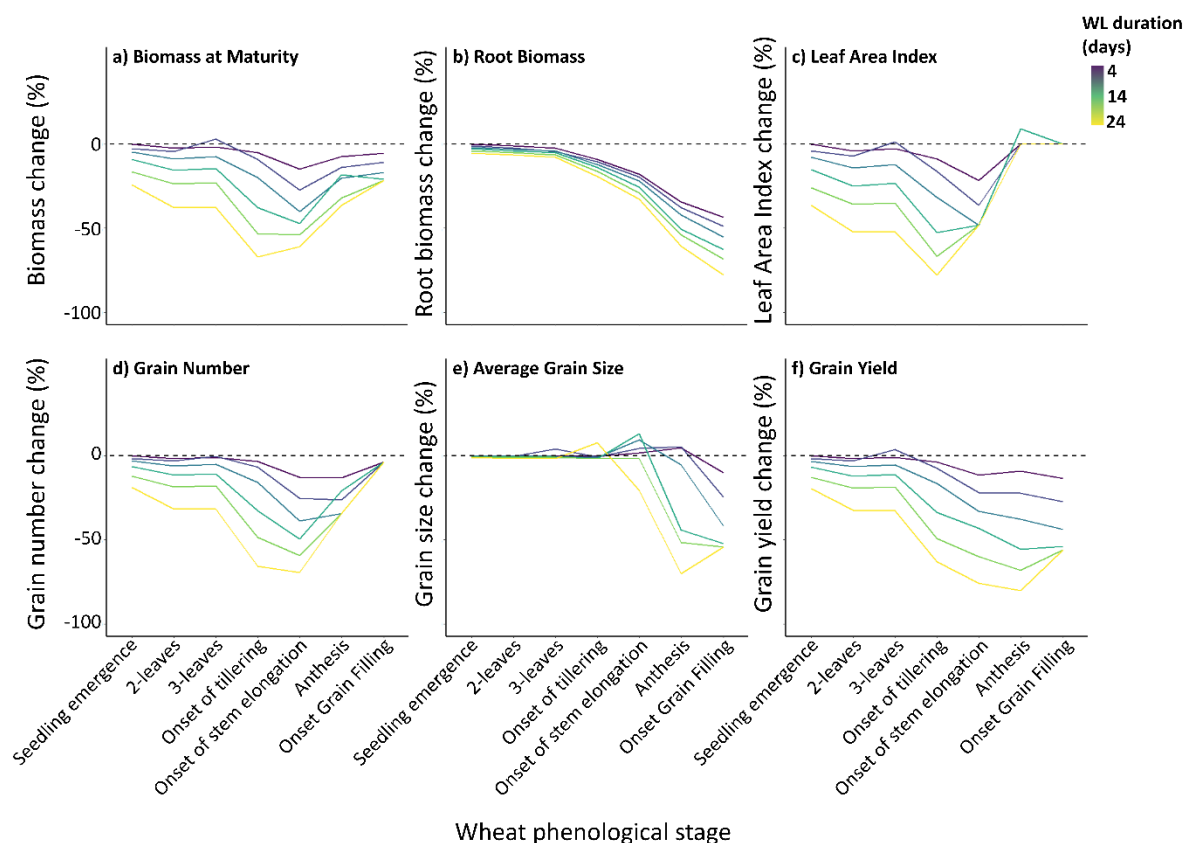


Figure S4. Sensitivity analysis of the impacts of waterlogging on spring wheat growth simulated by CSM-NWheat. Impacts of simulated waterlogging on wheat (a) biomass at maturity, (b) root biomass, (c) leaf area index, (d) grain number per unit area, (e) average grain size and (f) grain yield. The sensitivity analysis was carried out by simulating waterlogging starting in different phenological stages, from wheat seedling emergence to the onset of grain filling, with six different durations varying from 4 to 24 days as schematically shown in [SUPPLEMENTARY FIGURE S2](#).

3.3. Waterlogging module comparison

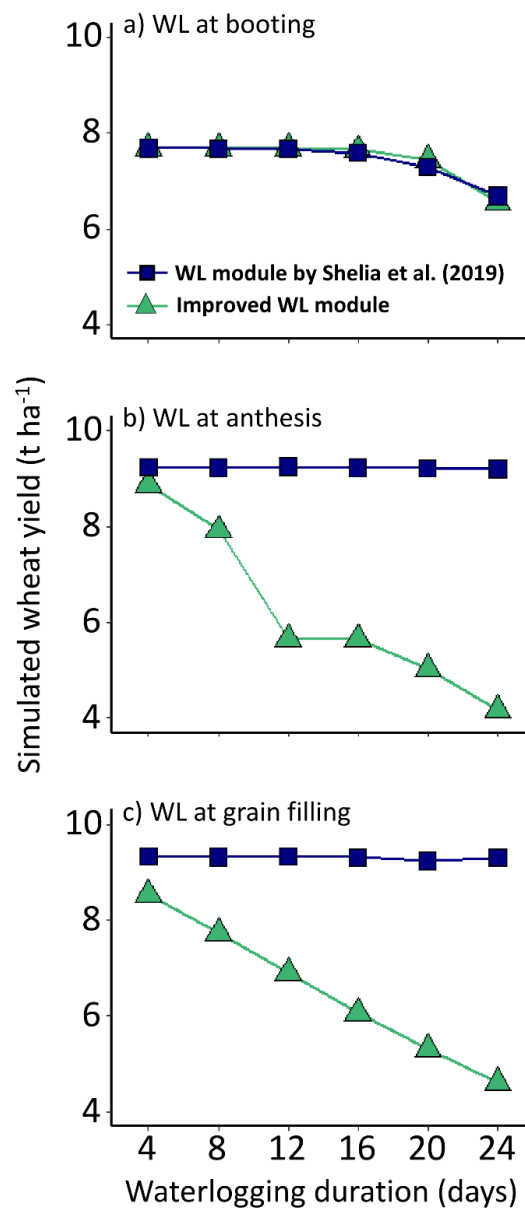


Figure S5. Waterlogging impacts on wheat with different waterlogging modules approaches. Impacts of waterlogging applied during (a) booting (b) anthesis and (c) grain filling on grain yield simulated using a waterlogging module implemented by Shelia et al (2019) in DSSAT-Nwheat and the improved waterlogging module for DSSAT-Nwheat proposed in this study.

4. References

- Calderini, D.F., Savin, R., Abeledo, L.G., Reynolds, M.P., Slafer, G.A., 2001. The importance of the period immediately preceding anthesis for grain weight determination in wheat. *Euphytica* 119, 199–204. <https://doi.org/10.1023/A:1017597923568>
- de San Celedonio, R.P., Abeledo, L.G., Miralles, D.J., 2018. Physiological traits associated with reductions in grain number in wheat and barley under waterlogging. *Plant and Soil* 429, 469–481. <https://doi.org/10.1007/s11104-018-3708-4>
- de San Celedonio, R.P., Abeledo, L.G., Miralles, D.J., 2014. Identifying the critical period for waterlogging on yield and its components in wheat and barley. *Plant and Soil* 378, 265–277. <https://doi.org/10.1007/s11104-014-2028-6>
- Dickin, E., Wright, D., 2008. The effects of winter waterlogging and summer drought on the growth and yield of winter wheat (*Triticum aestivum* L.). *European Journal of Agronomy* 28, 234–244. <https://doi.org/https://doi.org/10.1016/j.eja.2007.07.010>
- Ding, J., Huang, Z., Zhu, M., Li, C., Zhu, X., Guo, W., 2018. Does cyclic water stress damage wheat yield more than a single stress? *PLOS ONE* 13, e0195535.
- Ding, J., Liang, P., Wu, P., Zhu, M., Li, C., Zhu, X., Guo, W., 2020. Identifying the Critical Stage Near Anthesis for Waterlogging on Wheat Yield and Its Components in the Yangtze River Basin, China. *Agronomy* . <https://doi.org/10.3390/agronomy10010130>
- Farkas, Z., Varga-László, E., Anda, A., Veisz, O., Varga, B., 2020. Effects of Waterlogging, Drought and Their Combination on Yield and Water-Use Efficiency of Five Hungarian Winter Wheat Varieties. *Water* . <https://doi.org/10.3390/w12051318>
- Gao, J., Su, Y., Yu, M., Huang, Y., Wang, F., Shen, A., 2021. Potassium Alleviates Post-anthesis Photosynthetic Reductions in Winter Wheat Caused by Waterlogging at the Stem Elongation Stage . *Frontiers in Plant Science* .
- Li, C., Jiang, D., Wollenweber, B., Li, Y., Dai, T., Cao, W., 2011. Waterlogging pretreatment during vegetative growth improves tolerance to waterlogging after anthesis in wheat. *Plant Science* 180, 672–678. <https://doi.org/https://doi.org/10.1016/j.plantsci.2011.01.009>
- Marti, J., Savin, R., Slafer, G.A., 2015. Wheat Yield as Affected by Length of Exposure to Waterlogging During Stem Elongation. *Journal of Agronomy and Crop Science* 201, 473–486. <https://doi.org/https://doi.org/10.1111/jac.12118>
- Martínez, M., Arata, A.F., Lázaro, L., Stenglein, S.A., Dinolfo, M.I., 2019. Effects of waterlogging stress on plant-pathogen interaction between *Fusarium poae* and wheat/ barley. *Acta Scientiarum - Agronomy* 41, 1–9. <https://doi.org/10.4025/actasciagron.v41i1.42629>
- Olgun, M., Metin Kumlay, A., Cemal Adiguzel, M., Caglar, A., 2008. The effect of waterlogging in wheat (*T. aestivum* L.). *Acta Agriculturae Scandinavica, Section B — Soil & Plant Science* 58, 193–198. <https://doi.org/10.1080/09064710701794024>
- Ploschuk, R.A., Miralles, D.J., Colmer, T.D., Striker, G.G., 2020. Waterlogging differentially affects yield and its components in wheat, barley, rapeseed and field pea depending on the timing of occurrence. *Journal of Agronomy and Crop Science* 206, 363–375. <https://doi.org/https://doi.org/10.1111/jac.12396>

- Shelia, V., Asseng, S., Porter, C., Hoogenboom, G., 2019. SIMULATION OF A PERCHED WATER TABLE WITH IMPACT ON WHEAT CROP GROWTH, in: Agricultural and Biological Engineering University of Florida. Gainesville.
- Tan, W., Liu, J., Dai, T., Jing, Q., Cao, W., Jiang, D., 2008. Alterations in photosynthesis and antioxidant enzyme activity in winter wheat subjected to post-anthesis water-logging. *Photosynthetica* 46, 21–27. <https://doi.org/10.1007/s11099-008-0005-0>
- Wang, X., Huang, M., Zhou, Q., Cai, J., Dai, T., Cao, W., Jiang, D., 2016. Physiological and proteomic mechanisms of waterlogging priming improves tolerance to waterlogging stress in wheat (*Triticum aestivum* L.). *Environmental and Experimental Botany* 132, 175–182. <https://doi.org/https://doi.org/10.1016/j.envexpbot.2016.09.003>
- Wu, X., Tang, Y., Li, C., McHugh, A.D., Li, Z., Wu, C., 2018. Individual and combined effects of soil waterlogging and compaction on physiological characteristics of wheat in southwestern China. *Field Crops Research* 215, 163–172. <https://doi.org/https://doi.org/10.1016/j.fcr.2017.10.016>
- ZADOKS, J.C., CHANG, T.T., KONZAK, C.F., 1974. A decimal code for the growth stages of cereals. *Weed Research* 14, 415–421. <https://doi.org/https://doi.org/10.1111/j.1365-3180.1974.tb01084.x>
- Zhou, Q., Huang, M., Huang, X., Liu, J., Wang, X., Cai, J., Dai, T., Cao, W., Jiang, D., 2018a. Effect of post-anthesis waterlogging on biosynthesis and granule size distribution of starch in wheat grains. *Plant Physiology and Biochemistry* 132, 222–228. <https://doi.org/https://doi.org/10.1016/j.plaphy.2018.08.035>
- Zhou, Q., Wu, X., Xin, L., Jiang, H., Wang, X., Cai, J., Jiang, D., 2018b. Waterlogging and simulated acid rain after anthesis deteriorate starch quality in wheat grain. *Plant Growth Regulation* 85, 257–265. <https://doi.org/10.1007/s10725-018-0390-8>



A simple procedure for a national wheat yield forecast

Rogério de S. Nóia Júnior^{a,1}, Luc Olivier^{b,1}, Daniel Wallach^c, Esther Mullens^d,
Clyde W. Fraisse^b, Senthold Asseng^{a,*}

^a Technical University of Munich, Department of Life Science Engineering, Digital Agriculture, HEF World Agricultural Systems Center, Freising, Germany

^b University of Florida, Agricultural and Biological Engineering Department, Gainesville, FL, USA

^c National Institute of Agricultural Research and Environment (INRAE), UMR 1248 Agroecology, Innovations & Territories (AGIR), Castanet-Tolosan, France

^d University of Florida, Department of Geography, Gainesville, FL, USA

ARTICLE INFO

Keywords:

Crop yield estimation
Yield variability
National yields
Statistical crop model

ABSTRACT

National crop yields are difficult to estimate during a crop season and are usually only known after crop harvest. The goal of this study was to develop a simple methodology to estimate national wheat yields that could be easily applied to any country and crop. Twenty years of readily available global gridded monthly climate data (0.5°) across wheat cultivated areas of a country were correlated with national wheat production-weighted mean climate indices to determine the single most representative climate grid cell for the entire wheat region. The same 20 years of monthly climate data from this most representative grid cell were then used to build statistical models to estimate trend-corrected national wheat yields, including a Stepwise Regression function (Stepwise) set with the Bayesian information criterion (BIC), a least absolute shrinkage and selection operator algorithm (Lasso), and a Random Forest machine-learning algorithm (Random Forest). The best of the three models estimated trend-corrected national yield variability from 1998 to 2021 for Brazil with an rRMSE of 9.1%. In an additional validation, the same approach was then applied to national wheat yields in France and Russia resulting in an rRMSE from a Leave One Out Cross Validation (LOOCV) of 6.7% and 6.4%, respectively. As the statistical models employed monthly climate data from within a season, national yield predictions are possible during a cropping season before crop harvest by using the best performing model with the predictability of a national yield further improving towards harvest. This approach should be applicable to any crop and nation.

1. Introduction

National crop yield estimating approaches are vital for policy makers and agricultural commodity traders to plan ahead and adjust strategies to expected national crop production. In particularly low yielding seasons, an early national crop yield estimation before harvest can assist to minimize possible disruptions in food supply (Abel et al., 2019). However, national crop yields are difficult to estimate during the crop season and are usually only known after crop harvest. In addition, an increased variability in weather patterns in recent years has made national crop yield forecasts even more difficult (van der Velde et al., 2020).

There are several techniques for yield forecasting with the traditional methods based on field surveys with observations and measurements made by crop experts throughout the growing season (Basso and Liu, 2019). This method is time consuming and subject to sample bias. Other methods include the use of remote sensing and crop simulation models

(Jones et al., 2003; Keating et al., 2003) and statistical models (Lobell and Burke, 2010). Remoting sensing methods often rely on calibrated relationships between vegetation indices and yield, which are specific to a year and location, frequently requiring ground measurements (Lobell et al., 2015). Crop simulation models can predict growth and development for many crops, but require detailed information for initial conditions, soils, cultivars and crop management (Boote et al., 2013), often hindering their use at national level. In addition, some crop models do not consider pest, diseases, excess water and frost damage. Statistical models can be built by using historical yield and climatic variables and may include other important factors for crop yield, such as frost damage and climate-induced pest and disease damage (Lobell and Asseng, 2017). The drawbacks of the statistical models for estimating national crop yield are related to the large amount of climate data required to build and run such a model, considering that agricultural systems are highly variable across a country.

* Corresponding author.

E-mail address: senthold.asseng@tum.de (S. Asseng).

¹ Authors contributed equally to the study

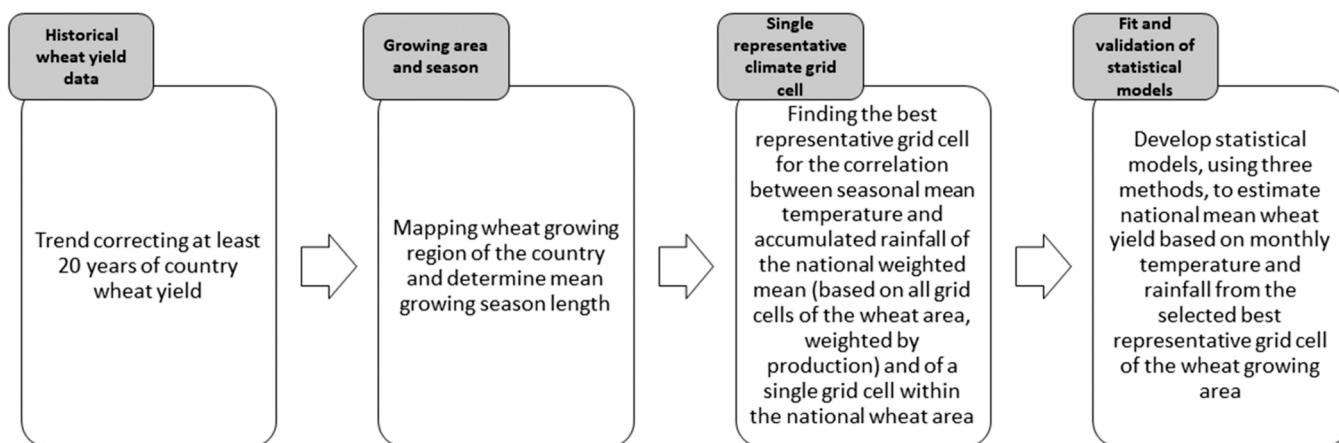


Fig. 1. Flowchart to derive statistical models based on monthly and seasonal climate data from a single grid cell of a cropping area to estimate a country wheat yield.

While numerous sophisticated yield estimation methods exist, the complexity of their implementation can be an impediment to growers, traders and policy makers, particularly in less resourced countries. Thus, a simple national crop yield estimating system should be accurate, precise, and easily replicable for any country of the world. For this, the estimating system must be based on few and accessible inputs, such as few locations and monthly climatic variables. Some studies have

suggested monitoring small representative agricultural regions within a country to estimate national crops yield by remote sensing (Petersen, 2018; Kastens et al., 2005), but the climatic representativeness of these regions to national climate has not been tested. The concept of collecting data of small samples representing a whole is widely applied for political and demographic census (Zahnd et al., 2019; Wardrop et al., 2018; Schug et al., 2021), but with few applications in agriculture.

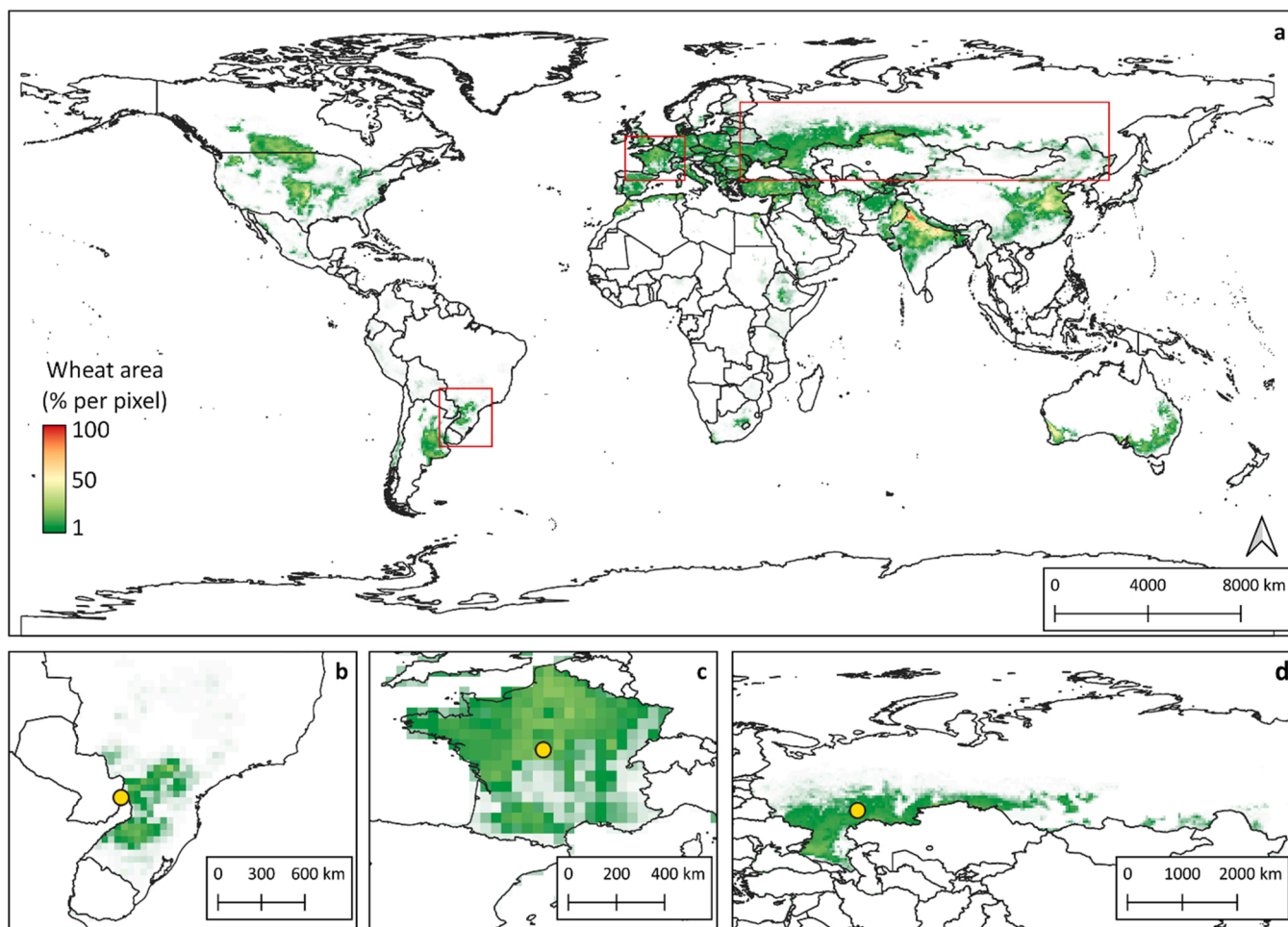


Fig. 2. Wheat production areas of (a) the world (b) for Brazil, (c) for France, and (d) for Russia after Monfreda et al. (2008). Yellow circles in b-d indicate the center of the grid cell for the best correlation between seasonal mean temperature and rainfall of the national mean (based on all grid cells of the wheat area) and a single grid cell within the national wheat area.

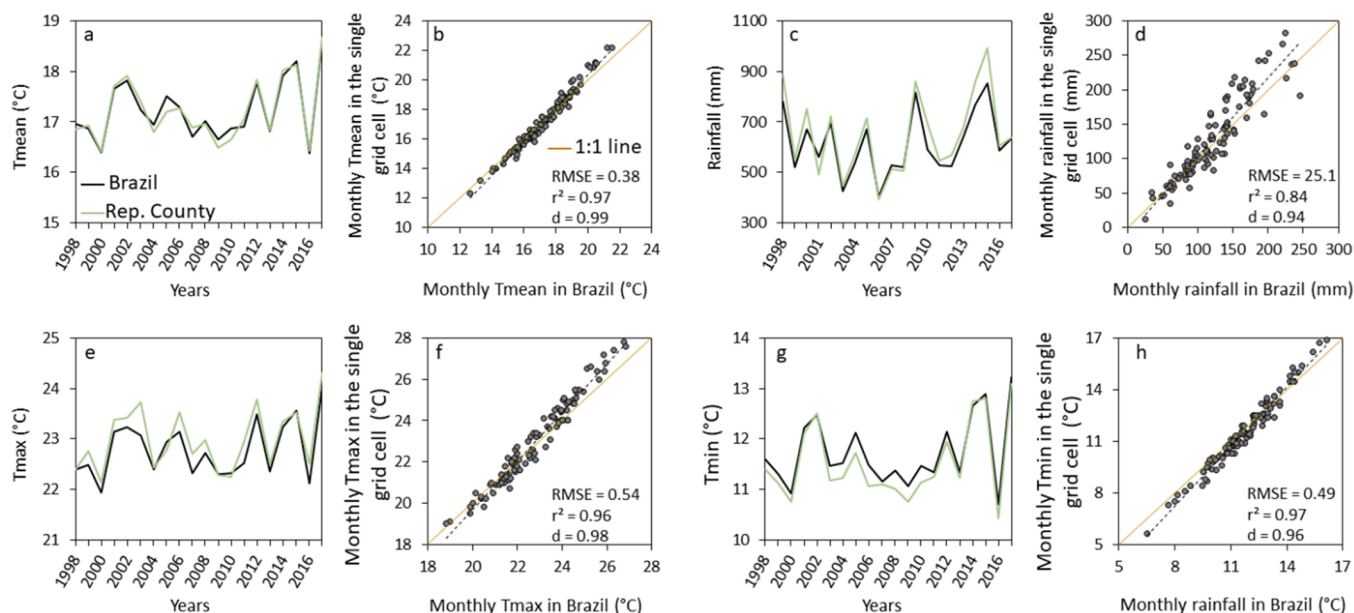


Fig. 3. Comparison between the historical seasonal (a, c, e and g) and monthly (b, d, f and h) mean, maximum and minimum temperature and rainfall (1998–2017) in average of the entire wheat area of Brazil and for the most representative location within this area. RMSE (Root mean squarer error), r^2 (coefficient of determination) and d (Willmott index of agreement).

Accordingly, the objective of this study was to develop a method for estimating national yields from a single representative point within a national crop area, developed and tested in three wheat-producing countries.

Brazil’s wheat yield is about 2.6 t/ha and the crop in southern part of the country is planted in April/May, flowers in July/August and is harvested in September/October. It has a slightly shorter growing season towards the warmer north (Paraná state) and a slightly longer growing season towards the cooler south of the Brazilian wheat growing region (highlands of Santa Catarina and Rio Grande do Sul states). France is a high-yielding country with yields of about 6.9 t/ha; planting occurs from September to November with winter dormancy in the main wheat area in the cooler north. There is less winter dormancy towards the warmer south, which has less wheat, and harvesting starts in June, whereas the northern regions delay harvesting until August. Wheat yields in Russia are about 2.7 t/ha; the crop is planted in October, followed by dormancy over winter, and regrow in March/April and harvest in July. Spring wheat is planted in the north of Russia in May, flowers in July and is harvested in August/September (USDA F A S, 2020). A simple method for national yield forecasting from a single representative point within the national cropping area was developed for wheat in Brazil and then evaluated for wheat in France and Russia, countries with contrasting wheat production systems and growing conditions.

2. Materials and Methods

2.1. Study steps

The estimation of wheat yield at a national level was carried out for three countries, following several steps (Fig. 1). First, national country wheat yields for Brazil using 20 growing seasons (1998–2017) were detrended to remove the trend of increased yield due to the implementation of new technologies, as suggested by Guarin et al. (2020). Second, the country wheat cultivated area for Brazil and its correspondent wheat growing season was obtained. Third, a single grid cell within the country’s wheat growing region which best correlates with the country seasonal mean temperature and rainfall across the wheat growing seasons for the same 20-year period was identified. Fourth, a statistical regression model for national wheat yields in Brazil was

developed using national wheat yields and statistically significant monthly and seasonal climate variables for this one single grid cell with three Variables Selector Methods, including: Stepwise Regression, Lasso

Table 1

Historical monthly and seasonal average of mean, maximum and minimum temperature, and rainfall; and Pearson’s correlation coefficient for the monthly and seasonal climatic variables and national wheat yield of Brazil. The data were normalized by dividing the difference between each data point and the arithmetic mean of the variable of interest by the standard deviation of the variable.

Climatic variables	Historical average (1998 – 2017)	Pearson’s correlations with wheat yield
T _{mean-May} (°C)	17.0	-0.4 *
T _{max-May} (°C)	22.2	-0.4 *
T _{min-May} (°C)	11.8	-0.4 *
Rainfall _{May} (mm)	168.4	-0.2 *
TR _{May}	-	-0.4 *
T _{mean-June} (°C)	15.9	-0.3
T _{max-June} (°C)	21.1	-0.2
T _{min-June} (°C)	10.7	-0.3
Rainfall _{June} (mm)	127.6	-0.2 *
TR _{June}	-	-0.3 *
T _{mean-July} (°C)	15.8	0.0
T _{max-July} (°C)	21.9	0.0
T _{min-July} (°C)	9.8	0.0
Rainfall _{July} (mm)	115.4	-0.2
TR _{July}	-	-0.2
T _{mean-August} (°C)	17.6	-0.5 *
T _{max-August} (°C)	24.0	-0.4 *
T _{min-August} (°C)	11.2	-0.5 *
Rainfall _{August} (mm)	101.0	-0.3
TR _{August}	-	-0.5 *
T _{mean-September} (°C)	19.7	-0.1
T _{max-September} (°C)	25.5	0.0
T _{min-September} (°C)	13.9	-0.2
Rainfall _{September} (mm)	136.4	-0.2
TR _{September}	-	-0.3
T _{mean-Season} (°C)	17.2	-0.5 *
T _{max-Season} (°C)	22.9	-0.4 *
T _{min-Season} (°C)	11.5	-0.6 *
Rainfall _{Season} (mm)	648.9	-0.4 *
TR _{Season}	-	-0.6 *

An “*” indicates statistically significant at the 0.05 significance level.

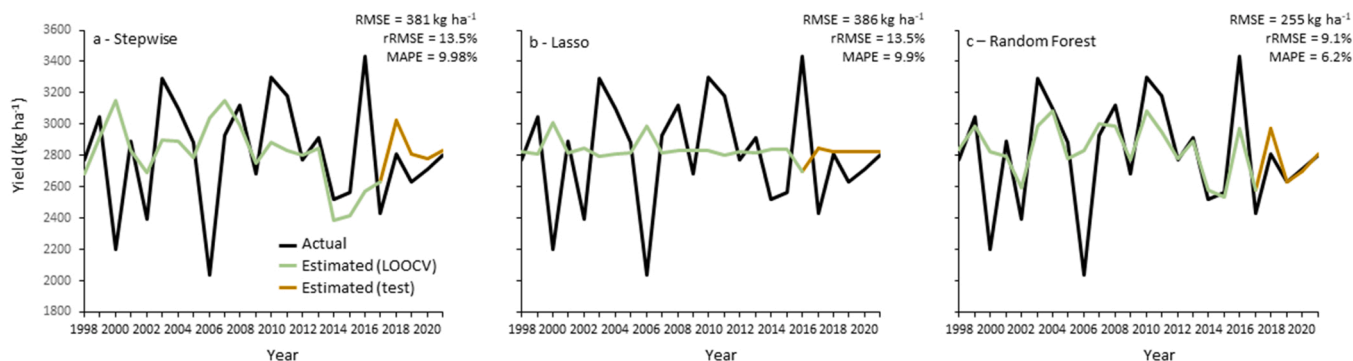


Fig. 4. Trend-corrected observed wheat yield (black line) (IBGE, 2022) and estimated from LOOCV (green line) and from unseen validation test (brown line) wheat yield from the regression model based on climate variables at one grid cell of the wheat growing region in Brazil (1998–2017), with (a) Stepwise, (b) Lasso and (c) Random Forest Variables Selector Methods. The RMSE (Root Mean Squared Error), rRMSE (relative Root Mean Squared Error) and the mean absolute percentage error (MAPE) are from LOOCV and unseen validation test.

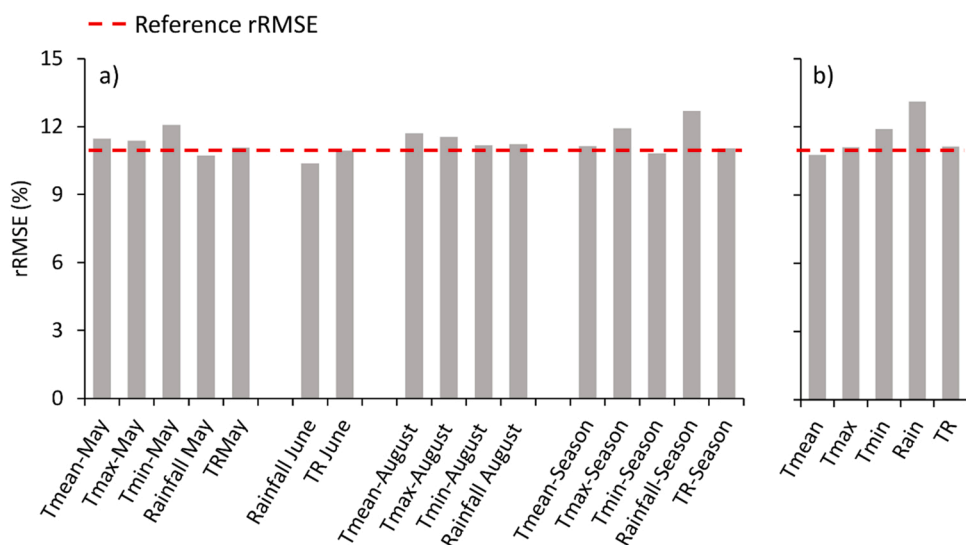


Fig. 5. Sensitivity analysis for monthly and seasonal climatic variables used to predict wheat yield in Brazil with Random Forest Method. A sensitivity analysis was performed by removing individually each of the (a) monthly and seasonal climatic variables available for Random Forest selection, as well as, (b) all seasonal and monthly individual climatic variables. The red dashed line corresponds to the reference rRMSE, when all climatic and seasonal variables were used. To perform the sensitivity analysis, the variables were individually removed from the set of variables available for Random Forest selection, before model training.

Regression, and Random Forest. After the models were developed and analyzed for Brazil, the procedure was evaluated by applying it to two independent additional national wheat crops in France and Russia.

2.2. Climate and wheat yield data

Historical climate data were taken from the Climate Research Unit (CRU) Time-Series (TS) version 4.02 database (Harris et al., 2020). The dataset was derived from statistically interpolating monthly observations from weather stations across the globe and consisted of gridded (0.5°x 0.5° resolution) monthly mean minimum, maximum, and mean temperature, and precipitation data were from 1998 to 2020. Since solar radiation is less variable among years and is correlated with rainfall, this variable was not considered. National historical observed wheat yield data were obtained from the Food and Agricultural Organization Corporate Statistical Database (FAO stat, 2022). Yield data from 1998 to 2017 were trend-corrected by removing a linear technology trend. Although wheat yield data prior to 1998 are available, they were not used due to uncertainties when removing historical wheat yield technology trend longer than 20 years (Guarin et al., 2020). The global geographic distribution of wheat was from a global gridded dataset with weighted cells, in m², for the wheat growing regions within each country (Monfreda et al., 2008) as shown in Fig. 2.

2.3. Aggregating climate national data during the wheat growing season

A growing season is the time frame between average planting and harvesting dates for a location. It extended from the first day of the planting month to the last day of the harvesting month. Information about planting and harvest month were from United States Department of Agriculture Crop Calendars (USDA F A S, 2020). Planting and harvesting months for Brazil are May and September, for Russia October and July for winter wheat and May and September for spring wheat, and for France October and July, respectively. Using the geographical distribution of wheat within a country, the wheat area per grid cell and growing season period, national production-weighted average minimum, maximum, and mean temperatures, and average total precipitation were calculated. The grid cells within each country were weighted using the production of wheat per grid cell, and divided by the combined wheat production of the country.

2.4. Finding the representative location and model building

The seasonal climate data for each grid cell within Brazil were correlated with the country average seasonal mean temperature and accumulated seasonal rainfall climate data across the growing seasons (1998–2017), weighted by production. The country weighted seasonal climate data were calculated considering the contribution of each grid

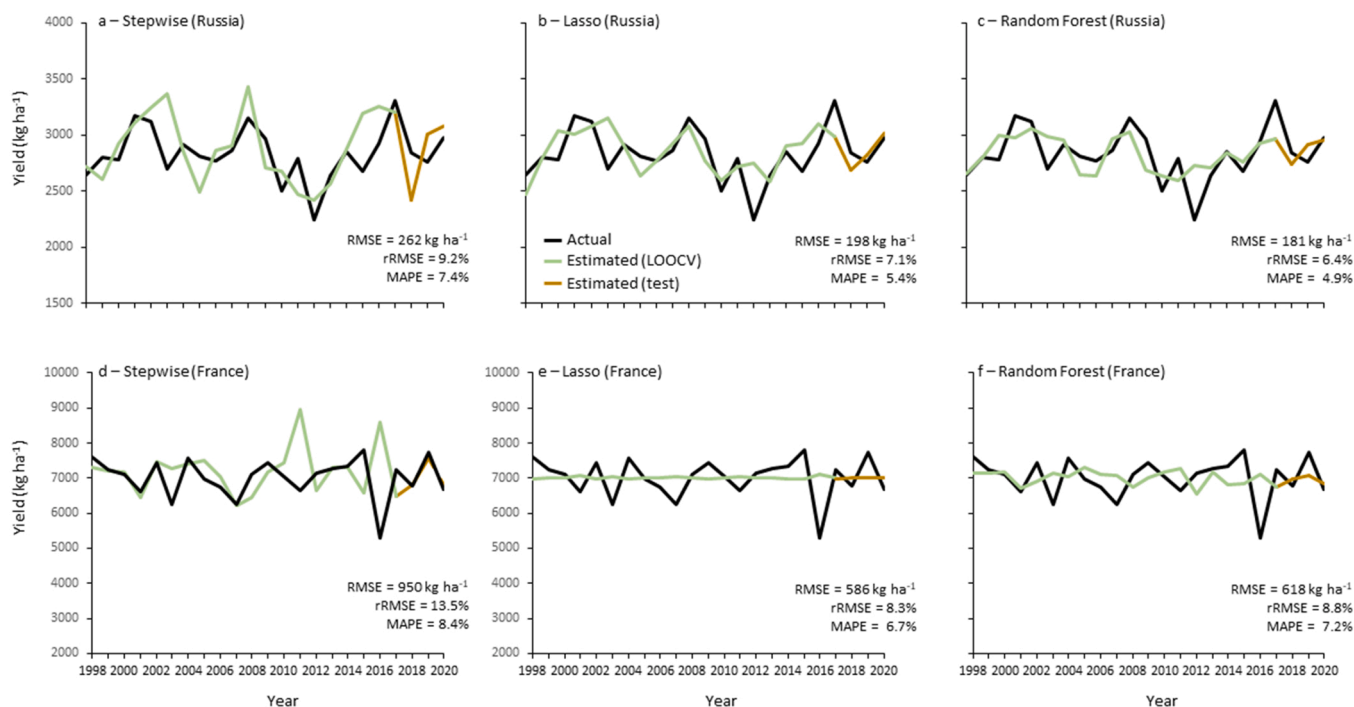


Fig. 6. Trend-corrected observed national wheat yield (black line) (IBGE, 2022) and estimated national wheat yield from LOOCV (green line) and from unseen validation test (brown line) from three regression models based on climate variables at one grid cell of the wheat growing region in (a-c) Russia and (d-f) France, using (a and d) Stepwise, (b and e) Lasso and (c and f) Random Forest for 1998–2017. The RMSE (Root Mean Squared Error), rRMSE (relative Root Mean Squared Error) and the mean absolute percentage error (MAPE) are from LOOCV and unseen validation test.

cell to the national wheat production, *i.e.* seasonal climate of high wheat producing grid cells had the highest weight in the country seasonal climate. The root mean square error (RMSE) for temperature and precipitation was calculated by comparing the seasonal single grid cell values with the country weighted seasonal climate. The obtained RMSE for temperature and precipitation was divided by the average country weighted seasonal temperature and precipitation, resulting in the relative RMSE for each climate variable. The single grid cell with the lowest average relative root mean square error (rRMSE) in comparison to the country average seasonal temperature and precipitation was selected as the most representative grid cell. This grid cell for a country was then used to build a multiple regression model based on monthly and seasonal climate data to estimate trend-corrected national wheat yields. Two additional variables were added: TR and $\text{Rainfall}_{\text{season}}$, representing the average of the standardized rainfall over the standardized T_{mean} and average seasonal rainfall, respectively. We first computed the Pearson's correlation for each independently variable and selected a subset of the variables which were statistically significant at $\alpha = 0.05$. A subset of monthly and seasonal climate variables was then selected using three methods: a Stepwise Regression (Stepwise) function step() set with the Bayesian information criterion (BIC), least absolute shrinkage and selection operator algorithm (Lasso), and a Random Forest machine-learning algorithm (Random Forest) being all performed in RStudio (R Core Team, 2017; Team Rs, 2020). The Stepwise Regression with a forward regression allowed for automated variable selection by choosing the best subset of variables that minimizes the BIC when building the regression equation. It does so by building multiple models based on variations of the input variables, calculating the BIC for each model, and then selecting the model with the lowest BIC. This method was based on recent studies with the objective of estimating national wheat yield (Nóia Júnior et al., 2021; Ben-Ari et al., 2018). The Lasso Regression reduces estimated coefficients toward zero and so reduces likelihood of overfitting data, and the number of features. The Random Forest is an ensemble learner based on randomized decision trees and

does not make underlying assumptions of data and so can deal with collinearity, being less influenced by outliers (Strobl et al., 2008; Svetnik et al., 2003). However, Random Forest does not have equations similar to other regression methods and the Gini index is a general indicator of feature relevance (Menze et al., 2009). The original model building approach, using each of the three methods was first performed with wheat data from Brazil. The same approach was then repeated as a validation for wheat and independent data from France and Russia.

2.5. Statistical and sensitivity analysis and in-season forecasting

The climatic representability of the single grid cell of Brazil, as well the ability of the simple country crop wheat yield model to estimate national yield for each country, were determined by the coefficient of determination (r^2), as a measure of precision, and by the agreement index (d) (Willmott et al., 1985), as a measure of accuracy. The performance of the wheat yield forecasting models for each country was tested with a leave-one-out cross validation (LOOCV). First a model was built using each of the three Variables Selector Methods tested, with 19 of the 20 years (from 1998 to 2017) to select the best subset of variables, and then it was tested on the excluded year (Cross-validation). This process was repeated for each year for a total of 20 interactions. In addition, the model was validated with four unseen years in Brazil (from 2018 to 2021) and three unseen years in Russia and France (from 2018 to 2020) (Wheat yield data for the 2021 cropping season was not available in FAOstat for Russia and France). The mean absolute percentage error (MAPE) and RMSE were then calculated based on the predicted yield of the test year and the corresponding observed national wheat yield. The relative root mean square error (rRMSE) was also calculated, as the RMSE divided by the average observed trend correct yield in each country.

A sensitivity analysis with the seasonal and monthly climatic variables available for building the statistical wheat yield models for Brazil, was performed with Random Forest Variable Selector Method. To do so,

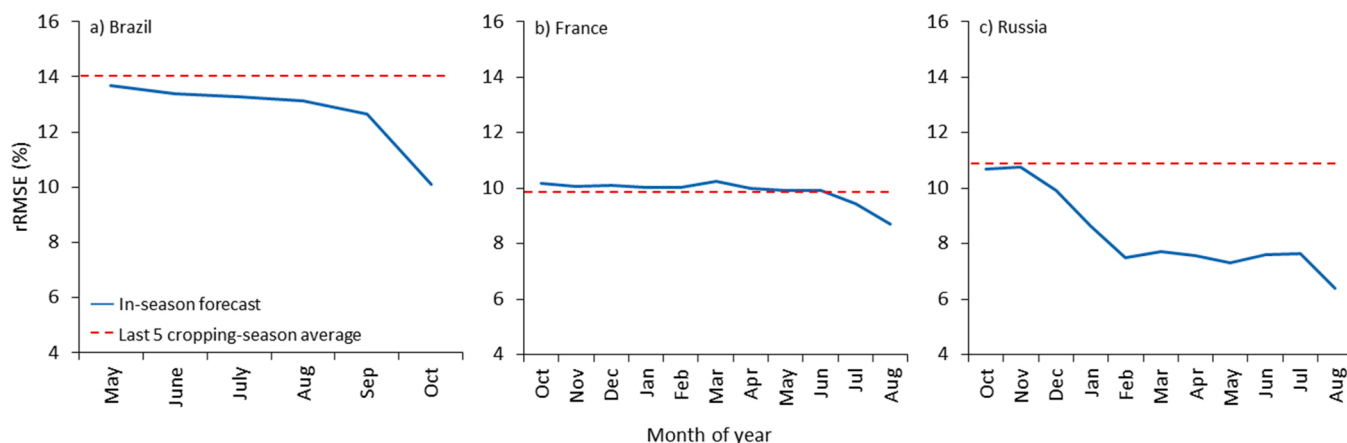


Fig. 7. Relative Root Mean Squared Error (rRMSE) of an in-season wheat yield forecast (blue dashed line) (average of 20 years, 1998–2017) for (a) Brazil, (b) France and (c) Russia. The forecasts were made with a Random Forest model in the beginning of each month, considering past observed monthly and seasonal climate data. The red dashed line shows the rRMSE when using the last five years average yield as predicted yield for the following year. The wheat yield forecasts are made on the first day of each month presented on the x-axis. Thus, the forecast in the month of August (performed on the 1st August) reflects what happened in all of July and not in August.

the statistical model building process was computed several times, always leaving one single climatic variable out, in two different ways: leaving out of the analysis (i) individual seasonal and monthly climatic variables, and (ii) a specific climatic variables in all months, *i.e.* leaving out rainfall (or minimum, or maximum, or mean temperature), of the season and all months. The relative root mean square error (rRMSE) from LOOCV was calculated each time the sensitivity analysis was carried out, to identify the importance of each climate variable for the statistical model built.

An in-season analysis was performed to identify the wheat yield forecast performance of the statistical model during the wheat season in Brazil, France and Russia. This was carried out at the beginning of each month during the wheat cropping-season for each country, considering past observed monthly climatic data for the season, and the five-last year average of monthly climate data as expected climate until the end of the season. With the same approach, seasonal climatic variables were also updated during the season. Because the forecasts are made on the first day of each month during the wheat cropping-season, the estimate in the month of August (which is performed on the 1st August) for example, reflects what happened in all of July and not in August. The rRMSE from LOOCV was calculated during the season (*i.e.* the models were re-trained with 19 of the 20 years (from 1998 to 2017) and then it was tested with forecasting the excluded year. This process was repeated for each year for a total of 20 interactions, and the rRMSE was calculated considering the excluded year and averaged over the 20 tests and average over the 20 tests) and compared to the rRMSE of the average wheat yield of the last five cropping-season as another simple benchmark for yield expected for the next cropping season. And, spring and winter wheat were not considered separately for simplicity of the approach.

3. Results

3.1. Performance of a single location to represent the country climate inter-annual variability in Brazil

In Brazil, the most representative climatic grid cell was in the central-western part of the wheat cropping area (Fig. 2b). We were able to determine the climatic grid cell performance by comparing it to the country-wide climatic averages. A single grid cell was able to capture the inter-annual monthly mean temperature (Fig. 3a), monthly mean maximum temperature (Fig. 3e) and monthly mean minimum temperature (Fig. 3g), and monthly accumulated rainfall (Fig. 2c). The RMSE

was 0.38 °C, 0.54 °C and 0.49 °C for the mean (Fig. 3b), maximum (Fig. 3f) and minimum temperature (Fig. 3h), respectively. For monthly rainfall, the RMSE was 25.1 mm (Fig. 3d). The RMSE was 2% of the average monthly mean and maximum temperature, 4% of the average monthly minimum temperature and around 20% of the monthly accumulated rainfall. The precision (r^2) and accuracy (d) of the single grid cell to represent the national inter-annual climate variability of monthly mean, maximum and minimum temperature was 0.97, for rainfall, r^2 was 0.84, and the d index was 0.94.

3.2. A simple country wheat yield model and its performance for Brazil

Using climate data from a representative single grid cell for the Brazil wheat cropping area, the historical series of monthly climatic variables were plotted against the historical national trend-corrected yields. Among the variables with a significant Pearson's correlation with wheat yield, the $T_{\min\text{-season}}$ and TR_{season} index presented values of -0.6 , being the ones with the highest Pearson's correlation (Table 1). These significant variables were used to build national wheat yield estimation models based on three different Variables Selector Methods, the Stepwise, Lasso and Random Forest Approaches, and their performance is presented in Fig. 4.

The accuracy and precision of the wheat yield estimation approach varied with the Variables Selector Method. The Stepwise, Lasso, and Random Forest methods yielded a RMSE of 381, 386, 255 kg ha⁻¹, and MAPE of 9.98%, 9.9%, 6.2%, respectively from the LOOCV.

3.3. Sensitivity analysis of monthly and seasonal climatic variables with Random Forest Method

A sensitivity analysis of monthly and seasonal climatic variables was carried out for the Random Forest Method, which presented the highest performance for estimating wheat yield in Brazil (Fig. 4). The rRMSE from LOOCV for the Random Forest model, using all the climatic and seasonal variables is 11% (red dashed line in Fig. 5), but it can drop to 10.4% or increase to 12.2%, with the removal of monthly and seasonal climatic variables of the set of variables available for Random Forest selection (Fig. 5). The removal of the variable $R_{\text{rainfall}_{\text{season}}}$ increased rRMSE to 12.2%. The removal of the variable $R_{\text{rainfall}_{\text{June}}}$, decreased rRMSE to 10.4% (Fig. 5a).

In addition, a sensitivity analysis for the climate variables was also performed. In this analysis, all monthly and seasonal climatic variables,

e.g. T_{mean} , were removed from the set of variables available for Random Forest selection. The rRMSE increased to 13.1% when removing rainfall, and decreased to 10.7% when removing T_{mean} (Fig. 5b).

3.4. Applying the method to France and Russia

As an independent validation of the method developed for wheat forecasting in Brazil, the same approach was repeated for forecasting national wheat yield for France and Russia. The most representative single grid cell in France was located in the central part of the country (Fig. 1c), and for Russia in the Volga region (Fig. 1d). After finding the most representative grid cell, the Pearson's correlation between climatic monthly variables and wheat yield in Russia and France was performed, selecting the ones with a significant correlation (Supplementary Table S1 and S2). These significant variables were then used to build a national wheat yield forecast with Stepwise, Lasso, and Random Forest methods. The statistical models were able to estimate some of the wheat yield inter-annual variability in France and Russia, but also missed some of the more extreme high and low yields (Fig. 6). In Russia, the Stepwise method resulted in a RMSE of 262 kg ha⁻¹, with a rRMSE and MAPE of 9.2% and 7.4%, respectively. When using the Lasso method, the RMSE was 198 kg ha⁻¹, and rRMSE 7.1%. The best performance for estimating national yields of Russia was obtained with the Random Forest method, with a rRMSE of 6.4% and MAPE of 4.9%, and in for France with rRMSE of 8.8% and MAPE of 7.2%. For France the rRMSE from Stepwise, Lasso and Random Forest were 13.9%, 8.5% and 6.7% respectively. We also test the model ensemble of the three Variables Selector Methods, but individual models performed as well or slightly better than their mean ensemble (Supplementary Fig S2).

3.5. In-season national wheat yield forecasting

After creating a simple national wheat yield estimation model based on a single representative location within the wheat area for Brazil and repeating the approach for France and Russia as a validation, we performed an in-season forecasting analysis, using the LOOCV procedure of Random Forest, the method with the best performance (Figs. 4 and 6). The results of this analysis were compared with the average of the last 5 years as the forecast for the next crop (used as the benchmark). In all three countries, the rRMSE of our forecast decreased (i.e. the yield forecast improved) as the wheat cropping-season progressed. In Brazil, as well as in Russia our simple national wheat yield estimation model performed better than using the average yield of the last five cropping-seasons as a forecast. In France, one month before harvesting, in early July, our simple model achieved a better prediction than a five-year yield average. In Russia, the rRMSE became smaller after November with Random Forest model, and rRMSE was 7.5% in February, seven months before harvesting in September.

4. Discussion

A simple country wheat yield estimation approach was developed based on monthly weather data from a single, representative grid cell within a nation-wide wheat cropping area for one country and then applied for another two contrasting countries. We demonstrated the ability of this new modeling approach to estimate some of the national wheat yield variability, although it misses some of the more extreme high and low yields. In contrast to other crop yield estimations, this simple method requires relatively few, publicly, readily available input information.

In Brazil and in France, the rRMSE was lower than 10% (from LOOCV and unseen test), when using Random Forest Variables Selector Method. The Random Forest outperformed Lasso and Stepwise. For Brazil, Lasso and Stepwise presented a rRMSE of 13%, but Random Forest presented an rRMSE of 9.1%. The performance of Random Forest in estimating crop yields has been extensively tested at regional, national and global

levels (Prasad et al., 2021), and many of these studies have shown a better performance of Random Forest than other methods. However, in some studies Random Forest performed poorer than other methods in estimating yield (Jeong et al., 2016).

Our modeling approach applies a well-known concept of small representative samples in political and demographic census (Zahnd et al., 2019; Wardrop et al., 2018; Schug et al., 2021) to yield forecasting. This approach allows building simple forecast models based on a simple representative location, avoiding massive data collection across an entire country. Our proposed method presents similar results with others that estimate national wheat yield by an aggregation of estimated yield for each wheat-producing county. A recent method to estimate national wheat yield in Germany used an extensive weather, soil and crop phenology dataset at county level (Srivastava et al., 2021) and obtained a r^2 of 0.9 and RMSE of 390 kg ha⁻¹, corresponding to 6% of the country average yield. Another method using county wheat yield and vegetation indices for estimating national winter wheat yield in the U.S., obtained a RMSE of 700 kg ha⁻¹ (Feng et al., 2021). Although our method presents results similar to other published models of wheat yield estimation, it still misses some extreme low wheat yields as e.g. in 2006 in Brazil, in 2012 in Russia and in 2016 in France. The low frequency of occurrence of these extreme events makes it difficult for machine learning to recognize them. For example, the extreme low yield in 2016 in France was caused by an unprecedented combination of excessive rainfall and plant diseases which our statistical models failed to forecast. Also the European forecasting system, using crop simulation modeling, failed to anticipate the magnitude of this wheat yield loss (van der Velde et al., 2020).

The wheat yield estimation with the most representative national climate data cell presented similar results to estimates using the average climate data of the wheat growing area (Supplementary Fig S1). However, the use of one grid cell is more advantageous because it avoids the annual calculation of the production-weighted mean climate for every cropping-season. This single point also has disadvantages and can generate erroneous estimates in some years, due to the spatial variability of extreme weather events, particularly due to the territorial extension of some countries such as Russia and Brazil (Fig. 4). Choosing a single representative point within these large countries might lead to over or underestimation of yield in some years. However, the single point selected in Brazil represented satisfactorily (r^2 of 0.96 for seasonal temperature and 0.84 for rainfall) the positive and negative variations of seasonal temperature and rainfall of the entire wheat area of Brazil across the country from 1998 to 2017 (Fig. 3). To reduce the uncertainties of the proposed method with only a single representative point, homogeneous crop production zones within a country could be used to delimit the selection of additional representative points (one representative point per zone) within the country, such as the homogeneous zones for wheat and soybean in Brazil (Nóia Júnior et al., 2021; Battisti and Sentelhas, 2019). A recent study has shown that dividing the country into homogeneous climatic zones and choosing one representative location per zone (instead of one per country), may lead to better predictive models (Nóia Júnior et al., 2021). In Brazil, for example, statistical models reproduced trend-corrected national wheat yields satisfactorily from four locations of four homogeneous agro-climatic zones (Nóia Júnior et al., 2021). However, the statistical models proposed by Nóia Júnior et al. (2021) were built using wheat yield of > 700 wheat producing municipalities combined with 4 meteorological stations (one for each of the four homogeneous zone).

The presented modeling approach could also be combined with other yield estimation and forecasting approaches, to improve predictability, similar to combining various temperature impact estimation methods (Zhao et al., 2017). Also, remote sensing data could be combined with the new approach using soil water and crop canopy status as additional inputs for the regression using any of the three methods applied here. Our method could be used to indicate which location or sub-regions should be monitored by remoting sensing, in an approach that works

with representative regions to monitor national crops yield (Kastens et al., 2005; Petersen, 2018). The representative grid cell could also be used with a crop simulation model to estimate wheat yields of a country. However, to apply a crop model like DSSAT (Jones et al., 2003), daily weather data will be required for this grid cell, plus information about a representative soils, initial soil conditions and crop management.

An advantage of the presented simple approach is that if the statistically significant variables selected in the model occur before harvest, the model can therefore provide a yield forecast before harvest. For example, minimum temperature in August ($T_{\text{min-Aug}}$) presented one of the highest Pearson's correlation with yield (Table 1), which indicates that wheat yield could be forecasted two months prior the harvest in Brazil, using this variable. The uncertainty of this prediction can be quantified with the established error of the model. To demonstrate this, we have performed an in-season analysis and showed that the proposed approach could be used to estimate wheat yield before harvesting, but model performance over a season depends on the country. In Russia, the model had a rRMSE of about 7% in February, seven months before local wheat harvesting, while in France the rRMSE was close to 10% in July, which is just before harvesting in this region. The climatic variables used to build the models were chosen by a statistical Variables Selector Methods but also have physiological explanations. For example, for Brazil the variables TR_{Season} and $T_{\text{mean-August}}$ also presented a high Pearson's correlation with wheat yield. Since Brazil's wheat crops are primarily rainfed and grow in a relative warm environment, a higher temperature together with low rainfall during the growing season are indicated by a high TR_{Season} , usually resulting in low wheat grain yields. The mean and minimum temperature for August, $T_{\text{mean-August}}$ and $T_{\text{min-August}}$, occur during flowering and early grain filling, when heat or frost can severely damage flowers and hasten grain filling, both resulting in reduced grain yields (Farooq et al., 2011). Episodes of frost occurred in August of 2012 destroyed 14% of Brazilian wheat yield (CONAB, 2022; Caier6o, 2013) and required additional wheat imports into the country. Because of this extreme event, Brazil was the second largest importer of wheat in the world in 2012 and 2013 (FAO stat, 2022). In the same years, the wheat selling price in Brazil was 80% higher than the world average price (CEPEA, 2022; FAO stat, 2022).

For France, temperature in December ($T_{\text{mean-Dec}}$, $T_{\text{max-Dec}}$ and $T_{\text{min-Dec}}$), and rainfall in May may be relevant variables for the wheat yield estimating according to the Pearson's correlation (Supplementary Table S1). High temperature during the late French autumn and winter stimulates early growth and crops are often prone to disease infections (Ben-Ari et al., 2018). Excessive rainfall in May during flowering, a period of high crop growth rates, can reduce crop growth and grain yield through water logging, disease spread, N leaching and low solar radiation. A combination of high temperatures in December and excessive rainfall in May are indicated as the main causes of the extreme low wheat yield of 2016 in France (N6ia J6nior et al., 2023; Ben-Ari et al., 2018). Very high precipitation occurred in May leading to excessive soil moisture, local flooding, favoring plant diseases causing wheat yield drop of 2016 in France (van der Velde et al., 2012).

For Russia, the TR_{October} was a variable correlated with wheat yield (Pearson's correlation in Supplementary Table S2). In the southern part of Russia where winter wheat is grown, this is likely due to too much growth before dormancy, negatively affecting winter survival, impacting regrowth in spring and consequently grain yield (Nyachiro et al., 2002). The statistical importance (high Pearson's correlation value) of climatic indexes occurring early in the wheat season, such as TR_{October} , $T_{\text{mean-February}}$ and $T_{\text{mean-March}}$ explains the drop of rRMSE during the in-season wheat yield forecasting for Russia in February (Fig. 7). Several climate variables in May/June also presented a high correlation with wheat yield in Russia (Supplementary Table S2), as these are high-growth-rate months for spring and winter wheat in Russia. A high $T_{\text{mean-June}}$, $T_{\text{mean-May}}$ and high $T_{\text{max-May}}$ reduces final grain yield by shortening growth duration. For winter wheat, the crops are likely in the grain filling period in June, which is susceptible to heat stress and can

reduce grain yields. Hence, while statistical models do not include many of the systems functionality of a dynamic crop simulation model, variables chosen in a statistical model can also have biological meaning. Other factors important for crop yields particularly at national scale like pest and diseases, which are usually not considered in crop models, are indirectly considered in statistical models, if driven by climate variability, and can make statistical models more suitable at such a scale (Lobell and Asseng, 2017). Although we discussed the physiological importance of each weather variable, other additional variables could be considered since these are not the only factors causing year-to-year variability in wheat yield.

The Stepwise method set with the Bayesian information criterion (BIC) test a range of linear models (with different selected variables) and selects the one with the lowest BIC value. The BIC penalizes a model for its complexity, meaning that models with high numbers of variables selected will have a lower BIC. The Lasso method uses a shrinkage estimator technique, shrinking those variables with little or no predictive power to zero and using the remaining shrunken coefficients for prediction (Knaus et al., 2021). Stepwise and Lasso try to select fewer variables, and can generate null models (*i.e.* containing only the intercept value), as resulted in the Lasso Variable Selector Method for France (Fig. 6). A Random Forest method is a decision tree-based method based on the concept of building multiple trees combining effects to produce a single consensus (in the case of this study, wheat yield) and tends to creating models with all the variables available (Knaus et al., 2021). Thus, the input of features with less predictive power, such as $Rainfall_{\text{June}}$ for wheat in Brazil (Fig. 5), can make the Random Forest methods less accurate. This demonstrates the importance of performing a sensitivity analysis before creating a multi-regression model with the Random Forest methods. In addition, statistical models such as linear and decision trees models usually benefit from large datasets, and it is important that models are continually updated after each cropping season. Constant updating assist machine learning to be trained on how wheat yield interacts with climate variables, particularly in the case of new combinations of extreme weather events or adoption of new cultivars and crop management techniques.

5. Conclusion

A simple national yield forecast model has been introduced using readily available climate data of a single representative climate grid cell per country. There is the potential to combine this method with other forecasting methods including crop models and remote sensing to improve predictability of national yields. The new approach could be applied to any national crop yield in any country in the world.

CRedit authorship contribution statement

RSNJ, LO and SA conceptualized the study, all co-authors contributed to the methodology, RSNJ and LO developed the statistical models and analyzed data, DW assisted with statistical models and statistical analysis, all co-authors contributed to data evaluation and interpretation, RSNJ and LO wrote initial draft, all co-authors assisted with writing and reviewed the manuscript.

Declaration of Competing Interest

The authors declare that they have no known competing financial interests or personal relationships that could have appeared to influence the work reported in this paper.

Data Availability

Data will be made available on request.

Acknowledgements

L.O. is currently employed by the Federal Energy Regulatory Commission, and the opinions expressed in this article do not represent the views of the Federal Energy Regulatory Commission. R.S.N.J. acknowledges support from the Prince of Albert II of Monaco foundation through the IPCC Scholarship Program. The contents of this manuscript are solely the liability of R.S.N.J. and under no circumstances may be considered as a reflection of the position of the Prince Albert II of Monaco Foundation and/or the IPCC.

Appendix A. Supporting information

Supplementary data associated with this article can be found in the online version at [doi:10.1016/j.eja.2023.126868](https://doi.org/10.1016/j.eja.2023.126868).

References

- Abel, G.J., Brottrager, M., Crespo Cuaresma, J., Muttarak, R., 2019. Climate, conflict and forced migration. *Glob. Environ. Change* 54, 239–249 (Online). <https://www.sciencedirect.com/science/article/pii/S0959378018301596>.
- Basso, B., Liu, L., 2019. Chapter Four - Seasonal crop yield forecast: Methods, applications, and accuracies vol 154, ed D L B T-A. A Sparks. Academic Press, pp. 201–255 (Online). <https://www.sciencedirect.com/science/article/pii/S0065211318300944>.
- Battisti, R., Sentelhas, P.C., 2019. Characterizing Brazilian soybean-growing regions by water deficit patterns. *Field Crops Res.* 240, 95–105 (Online). <https://linkinghub.elsevier.com/retrieve/pii/S0378429018315715>.
- Ben-Ari, T., Boé, J., Ciaïa, P., Lecerf, R., Van der Velde, M., Makowski, D., 2018. Causes and implications of the unforeseen 2016 extreme yield loss in the breadbasket of France. *Nat. Commun.* 9, 1627 (Online). <http://www.nature.com/articles/s41467-018-04087-x>.
- Boote, K.J., Jones, J.W., White, J.W., Asseng, S., Lizaso, J., 2013. Putting mechanisms into crop production models (Online). *Plant, Cell Environ.* 36, 1658–1672. <https://doi.org/10.1111/pce.12119>.
- Caieraó E. 2013 Wheat in Brazil - 2012 crop year.
- CEPEA 2022 Center for Advanced Studies in Applied Economics: Commodities prices *Agricultural series* Online: <https://www.cepea.esalq.usp.br/en>.
- CONAB 2022 National Supply Company: Agricultural information system Online: <http://portaldeinformacoes.conab.gov.br/index.php/safra/safra-serie-historica>.
- FAO stat 2022 FAOSTAT: FAO statistical databases Online: <http://www.fao.org/faostat/en/#home>.
- Farooq, M., Bramley, H., Palta, J.A., Siddique, K.H.M., 2011. Heat Stress in Wheat during Reproductive and Grain-Filling Phases (Online). *Crit. Rev. Plant Sci.* 30, 491–507. <https://doi.org/10.1080/07352689.2011.615687>.
- Feng, L., Wang, Y., Zhang, Z., Du, Q., 2021. Geographically and temporally weighted neural network for winter wheat yield prediction. *Remote Sens. Environ.* 262, 112514 (Online). <https://www.sciencedirect.com/science/article/pii/S00344257211002340>.
- Guarin, J.R., Asseng, S., Martre, P., Bliznyuk, N., 2020. Testing a crop model with extreme low yields from historical district records. *Field Crops Res.* 249, 107269 (Online). <https://linkinghub.elsevier.com/retrieve/pii/S0378429017314971>.
- IBGE 2022 Brazilian Institute of Geography and Statistics *Municipal agricultural research* Online: <https://sidra.ibge.gov.br/home/ipca/brasil>.
- Jeong, J.H., Resop, J.P., Mueller, N.D., Fleisher, D.H., Yun, K., Butler, E.E., Timlin, D.J., Shim, K.-M., Gerber, J.S., Reddy, V.R., Kim, S.-H., 2016. Random Forests for Global and Regional Crop Yield Predictions (Online). *PLOS ONE* 11, e0156571. <https://doi.org/10.1371/journal.pone.0156571>.
- Jones, J., Hoogenboom, G., Porter, C., Boote, K., Batchelor, W., Hunt, L., Wilkens, P., Singh, U., Gijssman, A., Ritchie, J., 2003. The DSSAT cropping system model. *Eur. J. Agron.* 18, 235–265 (Online). <http://linkinghub.elsevier.com/retrieve/pii/S1161030102001077>.
- Kastens, J.H., Kastens, T.L., Kastens, D.L.A., Price, K.P., Martinko, E.A., Lee, R.-Y., 2005. Image masking for crop yield forecasting using AVHRR NDVI time series imagery. *Remote Sens. Environ.* 99, 341–356 (Online). <https://www.sciencedirect.com/science/article/pii/S0034425705003056>.
- Keating, B.A., Carberry, P.S., Hammer, G.L., Probert, M.E., Robertson, M.J., Holzworth, D., Huth, N.I., Hargreaves, J.N.G., Meinke, H., Hochman, Z., McLean, G., Verburg, K., Snow, V., Dimes, J.P., Silburn, M., Wang, E., Brown, S., Bristow, K.L., Asseng, S., Chapman, S., McCown, R.L., Freebairn, D.M., Smith, C.J., 2003. An overview of APSIM, a model designed for farming systems simulation. *Eur. J. Agron.* 18, 267–288.
- Knaus, M.C., Lechner, M., Strittmatter, A., 2021. Machine learning estimation of heterogeneous causal effects: Empirical Monte Carlo evidence. *Econ. J.* 24, 134–161.
- Lobell, D.B., Burke, M.B., 2010. On the use of statistical models to predict crop yield responses to climate change. *Agric. For. Meteorol.* 150, 1443–1452 (Online). <https://www.sciencedirect.com/science/article/pii/S0168192310001978>.
- Lobell, D.B., Asseng, S., 2017. Comparing estimates of climate change impacts from process-based and statistical crop models (Online). *Environ. Res. Lett.* 12, 15001. <https://doi.org/10.1088/1748-9326/aa518a>.
- Lobell, D.B., Thau, D., Seifert, C., Engle, E., Little, B., 2015. A scalable satellite-based crop yield mapper. *Remote Sens. Environ.* 164, 324–333 (Online). <https://www.sciencedirect.com/science/article/pii/S0034425715001637>.
- Menze, B.H., Kelm, B.M., Masuch, R., Himmelreich, U., Bachert, P., Petrich, W., Hamprecht, F.A., 2009. A comparison of random forest and its Gini importance with standard chemometric methods for the feature selection and classification of spectral data (Online). *BMC Bioinforma.* 10, 213. <https://doi.org/10.1186/1471-2105-10-213>.
- Monfreda, C., Ramankutty, N., Foley, J.A., 2008. Farming the planet: 2. Geographic distribution of crop areas, yields, physiological types, and net primary production in the year 2000 (Online). *Glob. Biogeochem. Cycles* 22. <https://doi.org/10.1029/2007GB002947>.
- Nóia Júnior, R., de, S., Martre, P., Finger, R., van der Velde, M., Ben-Ari, T., Ewert, F., Webber, H., Ruane, A.C., Asseng, S., 2021. Extreme lows of wheat production in Brazil (Online). *Environ. Res. Lett.* 16, 104025. <https://doi.org/10.1088/1748-9326/ac26f3>.
- Nóia Júnior, R., de, S., Deswarte, J.-C., Cohan, J.-P., Martre, P., van der Velde, M., Lecerf, R., Webber, H., Ewert, F., Ruane, A.C., Slafer, G.A., Asseng, S., 2023. The extreme 2016 wheat yield failure in France. *Glob. Change Biol.* <https://doi.org/10.1111/gcb.16662> n/a.
- Nyachiro, J.M., Clarke, F.R., DePauw, R.M., Knox, R.E., Armstrong, K.C., 2002. Temperature effects on seed germination and expression of seed dormancy in wheat (Online). *Euphytica* 126, 123–127. <https://doi.org/10.1023/A:1019694800066>.
- Petersen, L.K., 2018. Real-time prediction of crop yields from MODIS relative vegetation health: a continent-wide analysis of Africa. *Remote Sens.* 10.
- Prasad, N.R., Patel, N.R., Danodia, A., 2021. Crop yield prediction in cotton for regional level using random forest approach (Online). *Spat. Inf. Res.* 29, 195–206. <https://doi.org/10.1007/s41324-020-00346-6>.
- R Core Team 2017 R: A Language and Environment for Statistical Computing R *Foundation for Statistical Computing, Vienna, Austria* {ISBN} 3–900051-07–0.
- Schug, F., Frantz, D., van der Linden, S., Hostert, P., 2021. Gridded population mapping for Germany based on building density, height and type from Earth Observation data using census disaggregation and bottom-up estimates (Online). *PLOS ONE* 16, e0249044. <https://doi.org/10.1371/journal.pone.0249044>.
- Srivastava A.K., Safaei N., Khaki S., Lopez G., Zeng W., Ewert F., Gaiser T. and Rahimi J. 2021 Comparison of Machine Learning Methods for Predicting Winter Wheat Yield in Germany *arXiv e-prints* arXiv:2105.01282 Online: <https://ui.adsabs.harvard.edu/abs/2021arXiv210501282S>.
- Strobl, C., Boulesteix, A.-L., Kneib, T., Augustin, T., Zeileis, A., 2008. Conditional variable importance for random forests (Online). *BMC Bioinforma.* 9, e0249307. <https://doi.org/10.1186/1471-2105-9-307>.
- Svetnik, V., Liaw, A., Tong, C., Culbertson, J.C., Sheridan, R.P., Feuston, B.P., 2003. Random forest: a classification and regression tool for compound classification and QSAR modeling (Online). *J. Chem. Inf. Comput. Sci.* 43, 1947–1958. <https://doi.org/10.1021/ci304160g>.
- Team Rs 2020 RStudio: Integrated Development for R Online: <http://www.rstudio.com/>.
- USDA F A S 2020 Crop Calendar Charts *Crop Calendar Charts* Online: <https://ipad.fas.usda.gov/ogamaps/cropcalendar.aspx>.
- van der Velde, M., Tubiello, F.N., Vrieling, A., Bouraoui, F., 2012. Impacts of extreme weather on wheat and maize in France: evaluating regional crop simulations against observed data (Online). *Clim. Change* 113, 751–765. <https://doi.org/10.1007/s10584-011-0368-2>.
- van der Velde, M., Lecerf, R., d'Andrimont, R., Ben-Ari, T., 2020. In: Sillmann, J., Sippel, S., T-C E, S.B., for I, T.I., Russo, R.A. (Eds.), Chapter 8 - Assessing the France 2016 extreme wheat production loss—Evaluating our operational capacity to predict complex compound events. Elsevier, pp. 139–158 (Online). <https://www.sciencedirect.com/science/article/pii/B9780128148952000094>.
- Wardrop, A., Jochem, C., Bird, J., Chamberlain, R., Clarke, D., Kerr, D., Bengtsson, L., Juran, S., Seaman, V., Tatem, J., 2018. Spatially disaggregated population estimates in the absence of national population and housing census data (Online). *Proc. Natl. Acad. Sci.* 115, 3529–3537. <https://doi.org/10.1073/pnas.1715305115>.
- Willmott, C.J., Ackleson, S.G., Davis, R.E., Feddema, J.J., Klink, K.M., Legates, D.R., O'Donnell, J., Rowe, C.M., 1985. Statistics for the evaluation and comparison of models. *J. Geophys. Res.* 90, 8995 (Online). <http://doi.wiley.com/10.1029/JC090iC05p08995>.
- Zahnd, W.E., Askelson, N., Vanderpool, R.C., Stradtman, L., Edward, J., Farris, P.E., Petermann, V., Eberth, J.M., 2019. Challenges of using nationally representative, population-based surveys to assess rural cancer disparities. *Prev. Med.* 129, 105812 (Online). <https://www.sciencedirect.com/science/article/pii/S0091743519302889>.
- Zhao, C., Liu, B., Piao, S., Wang, X., Lobell, D.B., Huang, Y., Huang, M., Yao, Y., Bassu, S., Ciaïa, P., Durand, J.-L., Elliott, J., Ewert, F., Janssens, I.A., Li, T., Lin, E., Liu, Q., Martre, P., Müller, C., Peng, S., Peñuelas, J., Ruane, A.C., Wallach, D., Wang, T., Wu, D., Liu, Z., Zhu, Y., Zhu, Z., Asseng, S., 2017. Temperature increase reduces global yields of major crops in four independent estimates. *Proc. Natl. Acad. Sci.* 114, 9326–9331 (Online). <http://www.pnas.org/content/114/35/9326.abstract>.

Supplementary Material for:

A simple procedure for a national wheat yield forecast

Rogério de Souza Nóia Júnior, Luc Olivier, Daniel Wallach, Esther Mullens, Clyde Fraisse,
Senthold Asseng

Table S1. Historical monthly and seasonal average of mean, maximum and minimum temperature, and rainfall; and Pearson's correlation coefficient for the monthly and seasonal climatic variables and national wheat yield of France. An "*" indicates statistical significance at the 0.05 significance level. The data were normalized by dividing the difference between each data point and the arithmetic mean of the variable of interest by standard deviation of the variable.

Climatic variables	Historical average (1998 – 2017)	Pearson's correlations with wheat yield
T _{mean-October} (°C)	13.3	0.1*
T _{max-October} (°C)	18.3	0.1
T _{min-October} (°C)	8.4	0.1
Rainfall _{October} (mm)	49.9	0.2*
TR _{October}	-	0.2*
T _{mean-November} (°C)	5.7	-0.2*
T _{max-November} (°C)	9.1	-0.3*
T _{min-November} (°C)	2.2	-0.2
Rainfall _{November} (mm)	44.8	0.0
TR _{November}	-	-0.1
T _{mean-December} (°C)	-2.2	-0.3*
T _{max-December} (°C)	0.0	-0.3*
T _{min-December} (°C)	-4.5	-0.3*
Rainfall _{December} (mm)	41.7	0.2*
TR _{December}	-	-0.1
T _{mean-January} (°C)	-7.9	-0.1
T _{max-January} (°C)	-5.4	-0.1
T _{min-January} (°C)	-10.5	-0.1
Rainfall _{January} (mm)	41.1	-0.1
TR _{January}	-	-0.1
T _{mean-February} (°C)	-10.4	-0.2*
T _{max-February} (°C)	-7.5	-0.1*
T _{min-February} (°C)	-13.3	-0.2*
Rainfall _{February} (mm)	38.8	-0.2*
TR _{February}	-	-0.2*
T _{mean-March} (°C)	-9.6	0.0
T _{max-March} (°C)	-6.3	0.0
T _{min-March} (°C)	-12.9	-0.1
Rainfall _{March} (mm)	30.6	-0.4*
TR _{March}	-	-0.3*

T _{mean-April} (°C)	-3.0	-0.1
T _{max-April} (°C)	0.6	-0.2
T _{min-April} (°C)	-6.6	0.1
Rainfall _{April} (mm)	33.4	0.3
TR _{April}	-	0.2
T _{mean-May} (°C)	6.9	-0.1
T _{max-May} (°C)	11.7	-0.1
T _{min-May} (°C)	2.1	-0.1
Rainfall _{May} (mm)	34.2	-0.5*
TR _{May}	-	-0.5*
T _{mean-June} (°C)	15.1	0.1
T _{max-June} (°C)	20.6	0.1
T _{min-June} (°C)	9.6	-0.1
Rainfall _{June} (mm)	39.0	-0.4*
TR _{June}	-	-0.3*
T _{mean-July} (°C)	19.1	0.0
T _{max-July} (°C)	24.6	0.0
T _{min-July} (°C)	13.7	0.0
Rainfall _{July} (mm)	58.4	0.0
TR _{July}	-	0.0
T _{mean-Season} (°C)	21.5	-0.3*
T _{max-Season} (°C)	27.0	-0.3*
T _{min-Season} (°C)	16.1	-0.3*
Rainfall _{Season} (mm)	52.3	-0.3
TR _{Season}	-	0.0

Table S2. Historical monthly and seasonal average of mean, maximum and minimum temperature, and rainfall; and Pearson’s correlation coefficient for the monthly and seasonal climatic variables and national wheat yield of Russia. An “*” indicates statistical significance at the 0.05 significance level. The data were normalized by dividing the difference between each data point and the arithmetic mean of the variable of interest by standard deviation of the variable.

Climatic variables	Historical average (1998 – 2017)	Pearson’s correlations with wheat yield
T _{mean-September} (°C)	13.1	-0.3*
T _{max-September} (°C)	17.6	-0.2*
T _{min-September} (°C)	8.7	-0.3*
Rainfall _{September} (mm)	70.7	0.1
TR _{September}	-	-0.1*
T _{mean-October} (°C)	13.1	-0.4*
T _{max-October} (°C)	17.6	-0.3*
T _{min-October} (°C)	8.7	-0.3*
Rainfall _{October} (mm)	70.7	-0.3
TR _{October}	-	-0.5*
T _{mean-November} (°C)	8.0	0.1*
T _{max-November} (°C)	11.4	0.0*
T _{min-November} (°C)	4.6	0.0*
Rainfall _{November} (mm)	69.4	0.1*
TR _{November}	-	0.1
T _{mean-December} (°C)	4.9	0.0
T _{max-December} (°C)	8.0	0.0
T _{min-December} (°C)	1.9	0.0
Rainfall _{December} (mm)	68.3	-0.1
TR _{December}	-	-0.1
T _{mean-January} (°C)	4.6	0.3*
T _{max-January} (°C)	7.6	0.3*
T _{min-January} (°C)	1.6	0.3*
Rainfall _{January} (mm)	59.5	0.2*
TR _{January}	-	0.3*
T _{mean-February} (°C)	5.3	0.5*
T _{max-February} (°C)	9.1	0.5*
T _{min-February} (°C)	1.5	0.5*
Rainfall _{February} (mm)	49.6	0.4*
TR _{February}	-	0.5*
T _{mean-March} (°C)	8.4	0.7*
T _{max-March} (°C)	13.2	0.7*
T _{min-March} (°C)	3.5	0.6*
Rainfall _{March} (mm)	56.4	0.0*
TR _{March}	-	0.5*
T _{mean-April} (°C)	10.9	-0.1
T _{max-April} (°C)	16.3	-0.1
T _{min-April} (°C)	5.7	-0.2
Rainfall _{April} (mm)	67.5	-0.1

TR _{April}	-	-0.2
T _{mean-May} (°C)	14.7	-0.5*
T _{max-May} (°C)	20.2	-0.5*
T _{min-May} (°C)	9.4	-0.5*
Rainfall _{May} (mm)	75.6	0.4*
TR _{May}	-	-0.1*
T _{mean-June} (°C)	18.3	-0.6*
T _{max-June} (°C)	24.2	-0.6*
T _{min-June} (°C)	12.5	-0.6*
Rainfall _{June} (mm)	58.7	0.4*
TR _{June}	-	-0.3*
T _{mean-July} (°C)	20.1	-0.2
T _{max-July} (°C)	26.2	-0.2
T _{min-July} (°C)	14.0	-0.1
Rainfall _{July} (mm)	61.2	0.1
TR _{July}	-	-0.1
T _{mean-Season} (°C)	10.8	0.1*
T _{max-Season} (°C)	15.4	0.1*
T _{min-Season} (°C)	6.3	0.2*
Rainfall _{Season} (mm)	70.7	0.4*
TR _{Season}	-	-0.3*

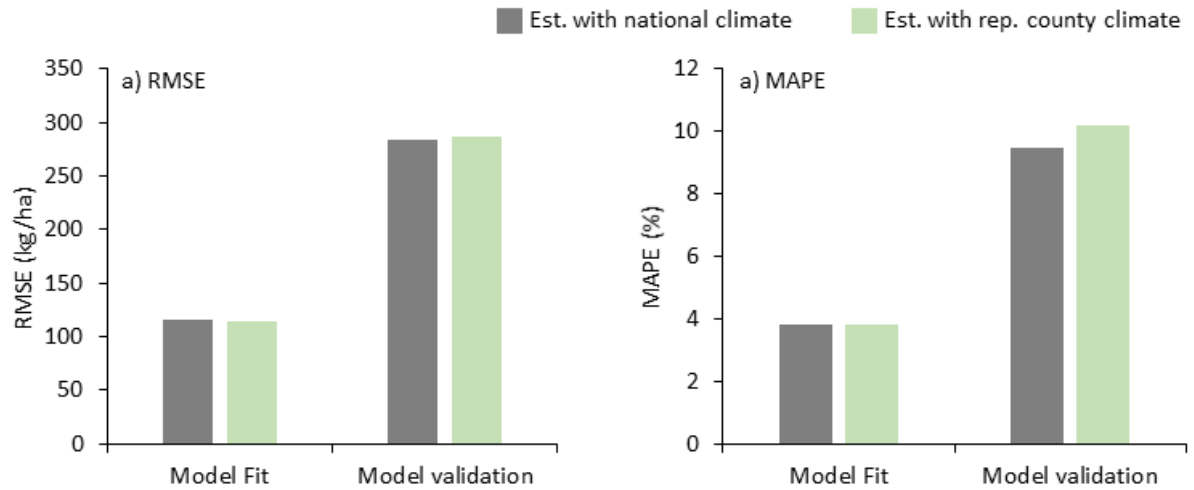


Fig S1. (a) Root mean square error (RMSE) and (b) mean absolute percentage error (MAPE) of national wheat yield of Brazil simulated with seasonal and monthly maximum, minimum and minimum temperature and rainfall in average of the entire wheat area of Brazil (grey) and for the most representative location within this area (green).

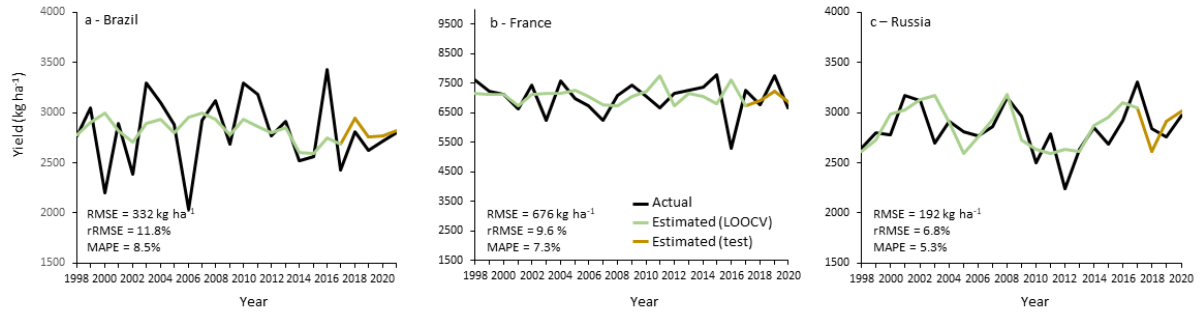


Fig S2. Trend-corrected observed wheat yield (black line) and estimated and estimated national wheat yield from LOOCV (green line) and from unseen validation test (brown line) based on climate variables at one grid cell of the wheat growing region in Brazil (1998-2017), with the ensembles of the three models (Stepwise, Lasso and Random Forest), for (a) Brazil, (b) France and (c) Russia. The RMSE (Root Mean Squared Error), rRMSE (relative Root Mean Squared Error) and the mean absolute percentage error (MAPE) are from LOOCV and unseen validation test. Ensembles are the mean of the tree models.